

CANADIAN THESES ON MICROFICHE

THÈSES CANADIENNES SUR MICROFICHE



National Library of Canada
Collections Development Branch

Canadian Theses on
Microfiche Service

Ottawa, Canada
K1A 0N4

Bibliothèque nationale du Canada
Direction du développement des collections

Service des thèses canadiennes
sur microfiche

NOTICE

The quality of this microfiche is heavily dependent upon the quality of the original thesis submitted for microfilming. Every effort has been made to ensure the highest quality of reproduction possible.

If pages are missing, contact the university which granted the degree.

Some pages may have indistinct print especially if the original pages were typed with a poor typewriter ribbon or if the university sent us an inferior photocopy.

Previously copyrighted materials (journal articles, published tests, etc.) are not filmed.

Reproduction in full or in part of this film is governed by the Canadian Copyright Act, R.S.C. 1970, c. C-30. Please read the authorization forms which accompany this thesis.

THIS DISSERTATION
HAS BEEN MICROFILMED
EXACTLY AS RECEIVED

AVIS

La qualité de cette microfiche dépend grandement de la qualité de la thèse soumise au microfilmage. Nous avons tout fait pour assurer une qualité supérieure de reproduction.

S'il manque des pages, veuillez communiquer avec l'université qui a conféré le grade.

La qualité d'impression de certaines pages peut laisser à désirer, surtout si les pages originales ont été dactylographiées à l'aide d'un ruban usé ou si l'université nous a fait parvenir une photocopie de qualité inférieure.

Les documents qui font déjà l'objet d'un droit d'auteur (articles de revue, examens publiés, etc.) ne sont pas microfilmés.

La reproduction, même partielle, de ce microfilm est soumise à la Loi canadienne sur le droit d'auteur, SRC 1970, c. C-30. Veuillez prendre connaissance des formules d'autorisation qui accompagnent cette thèse.

LA THÈSE A ÉTÉ
MICROFILMÉE TELLE QUE
NOUS L'AVONS REÇUE

Canada



National Library
of Canada

Bibliothèque nationale
du Canada

0-315-19555-X

Canadian Theses Division / Division des thèses canadiennes

Ottawa, Canada
K1A 0N4

674631

PERMISSION TO MICROFILM — AUTORISATION DE MICROFILMER

Please print or type — Écrire en lettres moulées ou dactylographier

Full Name of Author — Nom complet de l'auteur

MINOO RAZZAGHI

Date of Birth — Date de naissance

23 AUG 1951

Country of Birth — Lieu de naissance

IRAN

Permanent Address — Résidence fixe

C/O Dr. S. Manouchehri, Dept. of Economics, Univ. of Winnipeg,
Winnipeg, Manitoba

Title of Thesis — Titre de la thèse

Modelling of the Catalytic Claus Process

University — Université

University of Alberta

Degree for which thesis was presented — Grade pour lequel cette thèse fut présentée

Ph. D.

Year this degree conferred — Année d'obtention de ce grade

1985

Name of Supervisor — Nom du directeur de thèse

Dr. J. G. Dalla Lana

Permission is hereby granted to the NATIONAL LIBRARY OF CANADA to microfilm this thesis and to lend or sell copies of the film.

The author reserves other publication rights, and neither the thesis nor extensive extracts from it may be printed or otherwise reproduced without the author's written permission.

L'autorisation est, par la présente, accordée à la BIBLIOTHÈQUE NATIONALE DU CANADA de microfilmer cette thèse et de prêter ou de vendre des exemplaires du film.

L'auteur se réserve les autres droits de publication; ni la thèse ni de longs extraits de celle-ci ne doivent être imprimés ou autrement reproduits sans l'autorisation écrite de l'auteur.

Date

Jan / 12 / 1985

Signature

Minoo Razzaghi

THE UNIVERSITY OF ALBERTA

MODELLING OF THE CATALYTIC CLAUS PROCESS

by

MINOO RAZZAGHI

A THESIS

SUBMITTED TO THE FACULTY OF GRADUATE STUDIES AND RESEARCH
IN PARTIAL FULFILMENT OF THE REQUIREMENTS FOR THE DEGREE
OF DOCTOR OF PHILOSOPHY

DEPARTMENT OF CHEMICAL ENGINEERING

EDMONTON, ALBERTA

SPRING 1985

THE UNIVERSITY OF ALBERTA

RELEASE FORM

NAME OF AUTHOR MINOO RAZZAGHI
TITLE OF THESIS MODELLING OF THE CATALYTIC CLAUS PROCESS
DEGREE FOR WHICH THESIS WAS PRESENTED DOCTOR OF PHILOSOPHY
YEAR THIS DEGREE GRANTED SPRING 1985

Permission is hereby granted to THE UNIVERSITY OF ALBERTA LIBRARY to reproduce single copies of this thesis and to lend or sell such copies for private, scholarly or scientific research purposes only.

The author reserves other publication rights, and neither the thesis nor extensive extracts from it may be printed or otherwise reproduced without the author's written permission.

(SIGNED) *Minoo Razzaghi*

PERMANENT ADDRESS:

*1079 K.I. Kenny Dr.
Winnipeg, Manitoba
R3T 4R7*

DATED *Apr 15* 1985

THE UNIVERSITY OF ALBERTA
FACULTY OF GRADUATE STUDIES AND RESEARCH

The undersigned certify that they have read, and
recommend to the Faculty of Graduate Studies and Research,
for acceptance, a thesis entitled MODELLING OF THE CATALYTIC
CLAUS PROCESS submitted by MINOO RAZZAGHI in partial
fulfilment of the requirements for the degree of DOCTOR OF
PHILOSOPHY in CHEMICAL ENGINEERING.

W. Della Lora.....

Supervisor

Richard W. Jones.....

David T. Lynch.....

Bruce L. Clarke.....

R. R. Hudgins.....

External Examiner

Date..... 1985-04-12

ABSTRACT

The industrially important, modified Claus process was studied using a fundamental approach. The major emphasis of this work was to develop a Claus reactor modelling procedure for predicting the performance of such a convertor under a wide variety of operating conditions.

The modelling of the Claus process introduces multiple reactions, sulfur vapor equilibria, non-linear kinetics and limiting thermodynamic conversions. The diffusional transport limitations in the Claus catalytic convertors also introduces further complexities in the calculation procedure.

First, the role of an individual Claus catalyst pellet was studied, where the effect of the transport of the different species into the pores of the catalyst pellet coupled with the Claus chemical reaction was represented by an effectiveness factor. This analysis demonstrated a means for generating a local effectiveness factor, η , as a function of a modified Thiele parameter for spherical particles.

Next, both one-dimensional and two-dimensional numerical models of the Claus convertor were considered. The results showed that the one-dimensional model describes the behaviour of the Claus convertor, under industrial conditions reasonably well.

In a Claus catalytic reactor operated below the dew-point temperature of the elemental sulfur vapor being

produced, the catalytic activity of the pellets gradually declines. This results in a deactivation profile which moves along the bed axis, and which eventually breaks through the bed at excessive times on the stream. A kinetic model was adopted to this process and combined with the model used to simulate the behaviour of such a stirred reactor. The simulation predicts low rates of deactivation and a breakthrough capacity for a typical bed of the order on several days.

ACKNOWLEDGEMENTS

My sincere thanks are due to my supervisor, Professor I. G. Dalla Lana without whose sympathetic advise and acute criticisms, this thesis would not have been completed.

I also wish to extend my gratitude to Professor D. Lynch who provided me with ready advice during the course of this study. The financial assistance provided by the University of Alberta is also gratefully acknowledged.

Further, I owe an everlasting gratitude to Mrs. C. Deperez and L. Navarro for their invaluable motherly care of my son.

I wish to record here my deep appreciations to my loving and encouraging husband and parents. I would also like to thank my parents-in-law for their understanding and support. Special thanks are due to my sister, Maryam, for patiently typing this thesis.

My biggest debt of gratitude is to my sons, Eghtedar and Namdar, on whom the burden of writing this thesis has mostly fallen, and with whom I have much to make up. To them, with my warmest love and appreciations, I dedicate this thesis.

Table of Contents

Chapter	Page
1. INTRODUCTION	1
1.1 Status of <i>a priori</i> Design of Claus Catalytic Reactors	1
1.2 Anticipated Complexities in the Modelling of a Claus Process Reactor	2
1.3 Objectives of This Work	3
2. LITERATURE REVIEW	4
2.1 Introduction	4
2.2 Claus Process	4
2.3 Sulfur Vapor and Equilibrium Conversion	7
2.4 Kinetics of the Claus Reaction	9
2.5 Claus Catalyst Deactivation	15
2.6 Claus Catalytic Converter	19
2.7 Modelling of Fixed Bed Catalytic Reactors	21
2.7.1 Pseudo-Homogeneous Models	22
2.7.1.1 Plug Flow Model	22
2.7.1.2 Pseudo-Homogenous Model with Axial Mixing	23
2.7.1.3 Pseudo-Homogenous Model with Radial Mixing	25
2.7.1.4 Pseudo-Homogenous Model with Axial and Radial Mixing	28
2.7.1.5 Approximate Two-Dimensional Pseudo-Homogenous Model	30
2.7.2 Heterogeneous Models	31
2.7.2.1 1-Dimensional Heterogeneous Model: Interparticle Resistances ..	32
2.7.2.2 2-Dimensional Heterogeneous model: Interparticle Resistances ..	33

2.7.2.3	Heterogeneous Model with Inter and Intraparticle Resistances	33
2.7.3	Reaction Rate in Heterogeneous Models	36
2.7.3.1	Interparticle Transport Resistances	36
2.7.3.2	Intraparticle Transport Resistances	37
2.7.3.3	Diffusivity in the Catalyst Pores ..	41
2.7.3.4	Numerical Method for Prediction of Catalyst Effectiveness Factor ..	43
2.7.4	Modelling of the Claus Converter	44
2.8	Catalyst Deactivation Modelling	47
2.8.1	Deactivation Kinetics	48
2.8.2	Deactivation of Single Pellet	51
2.8.3	Deactivation of the Catalyst Reactor Beds ..	61
3.	KINETICS AND EQUILIBRIUM ASPECTS OF THE CLAUS PROCESS	65
3.1	Free Energy Minimization	65
3.2	Claus Process Equilibrium in the Presence of Liquid Sulfur	67
3.2.1	Mathematical Analysis of the Method A.	67
3.2.2	Trial and Error Method - Method B.	74
3.2.3	Results of the Analysis of the Claus Process Equilibria in the Presence of Liquid Sulfur	74
3.3	Claus Reaction as a Set of Parallel Reactions ...	76
3.4	Sulfur Vapor Composition for Nonequilibrium Conversion Levels.	78
3.5	Heat of Claus Reaction	80
3.6	Thermodynamically Consistent Claus Rate Expression	85
4.	MODELS OF CLAUS CATALYST PELLET	91

4.1	Introduction	91
4.2	Nonisothermal Claus Pellets	93
4.2.1	Computational Scheme	97
4.2.2	Nonisothermal Claus Pellet Modelling Results	99
4.3	Isothermal Claus Pellets	103
4.3.1	Computational Scheme for Isothermal Claus Pellets	107
4.3.2	Isothermal Claus Pellet Modelling Results	108
4.4	Simplified Local Effectiveness Factor	115
5.	HIGH TEMPERATURE CLAUS REACTOR MODEL	121
5.1	Introduction	121
5.2	Model Development	122
5.3	Adiabatic 1-Dimensional Claus Process Model	125
5.3.1	Computational Scheme	130
5.3.2	Numerical Results of One-Dimensional Claus Model	131
5.4	2-Dimensional Claus Process Model	152
5.4.1	Introduction	152
5.4.2	Model Formulation	154
5.4.3	Computational Scheme	159
5.4.4	Numerical Results of Two-Dimensional Claus Model	160
5.5	Comparison of 1- and 2-Dimensional Models	163
6.	COLDBED CLAUS REACTOR MODEL	173
6.1	Introduction	173
6.2	Reaction Chemistry at Low Temperature	177
6.3	Analysis of Deactivation Rate	180
6.4	Coldbed Reactor Model	182

6.4.1 Global Reaction Rate in Coldbed Reactor ..	183
6.4.2 Deactivation Rate in Coldbed Reactor	189
6.5 Computational Scheme	189
6.6 Numerical Results of Coldbed Simulation	190
6.7 Application of the Model to Coldbed Reactors ...	194
7. CONCLUSIONS AND RECOMMENDATIONS	213
7.1 Conclusions	213
7.2 Recommendations	216
NOMENCLATURE	218
BIBLIOGRAPHY	225
APPENDIX A: Claus Equilibria	241
APPENDIX B: Gas Composition at a Given H ₂ S Conversion ...	279
APPENDIX C: Nonisothermal Claus Pellet	294
APPENDIX D: Isothermal Claus Pellet	313
APPENDIX E: Claus Converter Model	358
APPENDIX F: Coldbed Reactor	419
APPENDIX G: Physical Properties of Claus Catalytic Process.	462

List of Tables

Table	page
2.1 Rate Expressions for the Claus Reaction	11
3.1 Comparison of equilibrium conversion of H_2S obtained by free energy minimization and equilibrium constant methods.	72
3.2 Claus Equilibrium in the Presence of Liquid Sulfur	75
3.3 Heat of Claus Reaction	87
5.1 Scheme for Development of Models for High Temperature Claus Reactor	123
B.1 Composition of the Claus gas for different conversion levels of H_2S	288
D.1 Effective Reaction Zone with 2 Interior Points	324
D.2 A and B Matrices for Spherical Coordinates	338
E.1 A and B Matrices for Cylindrical Coordinates	395

List of Figures

Figure		Page
3.1	Sulfur Species Stoichiometric Numbers	82
3.2	Sulfur Vapor Composition	84
3.3	Heat of Claus Reaction	86
4.1	Nonisothermal Claus Pellet Effectiveness Factor at $T_s=500$ K	101
4.2	Nonisothermal Claus Pellet Effectiveness Factor at $T_s=600$ K	102
4.3	Comparison Between Runge-Kutta-Fehlberg and Orthogonal Collocation Numerical Methods	109
4.4	Effectiveness Factor Versus Thiele Modulus at Varying Conversion Levels of H_2S at Pellet Exterior Surface.....	111
4.5	Local Thiele Modulus in the Claus Reactor	113
4.6	Effectiveness Factor Versus Thiele Modulus at Varying Exterior Surface Temperatures	114
4.7	Effectiveness Factor Versus Modified Thiele Modulus at Varying Conversion Levels of H_2S at Pellet Exterior Surface	118
4.8	Effectiveness Factor Versus Modified Thiele Modulus at Varying Exterior Surface Temperatures	119
5.1	H_2S Conversion Profile Along the Catalyst Bed	132
5.2	Temperature Profile Along the Catalyst Bed	133
5.3	Local Effectiveness Factor in the Catalytic	

Claus Converter	134
5.4 Effect of Film Mass Transport Limitation	136
5.5 Effect of Film Heat Transport Limitation	137
5.6 Effect of Accuracy of Thermodynamic Properties of Sulfur Species on the Predicted Performance of Claus Converter	139
5.7 Effect of Inlet Temperature on the Performance of Claus Converter	142
5.8 Effect of Inlet Temperature on the Adiabatic Reaction Path	143
5.9 Effect of Space Velocity on the Performance of Claus Converter	145
5.10 Comparison Between Novel and Commercial Catalysts	146
5.11 H ₂ S Conversion along Novel and Alumina Catalyst Beds	148
5.12 Efficiency of Alumina and Novel Catalysts	150
5.13 Space Velocity for Utilizing 1-meter depth of Novel and Alumina Catalysts	151
5.14 Axial Profile of the Radial Mean Temperature	161
5.15 Axial Profile of the Radial Mean Conversion of H ₂ S	162
5.16 Radial Temperature Profile	164
5.17 Radial Profile of H ₂ S Conversion	165
5.18 Temperature Profile by One-and Two-Dimensional Models	166

5.19	Conversion Profile by One-and Two-Dimensional Models	167
5.20	Radial Temperature Profile at Different Axial Positions	168
5.21	Temperature Profile by One- and Two-Dimensional Models in Industrial Size Claus Reactor	170
5.22	Conversion Profile by One- and Two-Dimensional Models in Industrial Size Claus Reactor	171
6.1	Flow-chart of MCRC Process	174
6.2	Flow-chart of Amoco CBA Process	175
6.3	Sulfur Vapor Composition at its Vapor Pressure	179
6.4	Axial Profile of Partial Pressure at Short Residence Times	191
6.5	Deactivation at Short Residence Times	192
6.6	Temperature Profile at Short Residence Times in the 2nd-Stage Convertor	195
6.7	Axial profile of Partial Pressure in the 2nd-Stage Convertor	196
6.8	Temperature Profiles in the 2nd-Stage Convertor	198
6.9	Deactivation of the 2nd-Stage "sub-dew" Convertor	199
6.10	Axial Profile of Partial Pressure in the 3rd-Stage Convertor	200

6.11	Temperature Profiles in the 3rd-Stage Convertor	201
6.12	Deactivation in the 3rd-Stage Convertor	202
6.13	Temperature Profile at Times (<1 hr) in the Amoco CBA Convertor	203
6.14	Axial Profile of Partial Pressure of H_2S in the Amoco CBA Convertor	204
6.15	Deactivation in the Amoco CBA Convertor	205
6.16	Temperature Profile in Amoco CBA Convertor	206
6.17	Temperature Profile After Flow Reversal in 2nd-Stage Convertor	209
6.18	Partial Pressure Profile After Flow Reversal in the 2nd-Stage Convertor	210
6.19	Deactivation After Flow Reversal in the 2nd-Stage Convertor	211
C.1	Flow-chart of "NONISOEFF" Program	300
D.1	Flow-chart of "ORTEFF" Program	344
E.1	Flow-chart of "ADONEDIMBED" Program	372
E.2	Flow-chart of "BEDTWO" Program	397
F.1	Flow-chart of "COLDBED" Program	436

1. INTRODUCTION

1.1 Status of *a priori* Design of Claus Catalytic Reactors

Hydrogen sulfide, a major by-product of the processing of sour crude oils, sour natural gases, and sulfur-containing bitumen, is usually converted to elemental sulfur by the modified Claus process.

In the modified Claus process, $1/3$ of the H_2S is initially reacted homogeneously with air in a furnace to form SO_2 , and then the remaining $2/3$ is reacted with the SO_2 produced in the combustion step, in a catalytic convertor.

In spite of the industrial importance of the Claus process, only sparse fundamental information is available on this process. The available design procedures are based on the assumption of the attainment of thermodynamic equilibrium conversion of H_2S in each process stage.

The customary design approach is to assume an outlet conversion of H_2S corresponding to the intersection of the adiabatic reaction path with the equilibrium line (44,55,197). This approach is not adequate for the prediction of performance of such plants under a wide variety of operating conditions. It also fails to utilize any known information with regard to the efficiency of different catalysts under the same operating conditions.

The development of a more fundamental approach to the design of the catalytic Claus process is needed for predicting the performance of existing or novel Claus processes.

processes.

1.2 Anticipated Complexities in the Modelling of a Claus Process Reactor

The elemental sulfur which is a product of the Claus reaction can exist in several molecular forms. The dynamics of formation and equilibration of the different sulfur species are not fully known (to be discussed in chapter 2). Furthermore, the coexistence of different sulfur polymers introduces multiple reactions into the chemistry of the catalytic Claus process. This chemistry will be developed in chapter 3.

The actual limiting conversion of H_2S attainable in a finite bed of catalyst along the reaction path is a rate problem. To predict the performance of such a reactor, information concerning the behaviour of both the reactor and the catalytic rate of the reaction is required in some mathematical form. The intrinsic rate of the Claus reaction is represented by non-linear kinetics and is discussed in chapter 3. Furthermore, the Claus reaction can be limited by the rate of diffusion of the species in the catalyst pores (23,29,44,93,94). This effect will complicate the analysis of the Claus catalytic bed by superimposing the diffusional transport rates on the chemical reaction rate.

Thus the prediction of the performance of catalytic Claus reactors involves multiple reactions, sulfur vapor equilibria, non-linear kinetics, diffusional transport

limitations and limiting thermodynamic conversions.

1.3 Objectives of This Work

The main objective of the present work is to study the Claus reaction using a fundamental approach. This thesis will be divided into four main chapters, each dealing with one aspect of the modelling of the $\text{H}_2\text{S}/\text{SO}_2$ reaction in a catalytic Claus convertor.

Chapter 3 considers the thermodynamic equilibrium conversion calculation and basic chemistry of the Claus process. Possible models of an individual Claus catalyst pellet are considered in chapter 4, while chapters 5 and 6 present the models of the Claus catalytic convertors for the high and low operating temperatures, respectively. At low operating temperatures, i.e. below the sulfur vapor dew-point, condensation of the product sulfur in the pores of the Claus catalyst pellet results in catalyst deactivation. Nonetheless, the low temperature operation has become popular in recent years due to the favourable thermodynamic conversions possible at low temperatures. Furthermore, condensation of the product sulfur removes the product of the reaction from the reaction gaseous phase, facilitating the forward reaction rate.

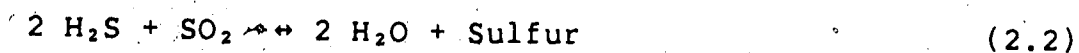
2. LITERATURE REVIEW

2.1 Introduction

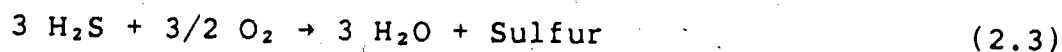
Different aspects of sulfur recovery processes, and the Claus process in particular, have been extensively reviewed in the literature. Noteworthy are the reviews by Cho (44), Crynes (52), Goar (88,89), Grancher (93), Liu (135), McCulloch (145), Stecher (192), and Truong (199). "The Gas Processing Handbook" issue of Hydrocarbon Processing (84) has summarized the different sulfur recovery processes, their commercial installations and their licensors. This survey will mostly emphasize the kinetics of the catalytic Claus reaction, catalyst deactivation processes, and models of both catalytic and deactivating fixed-bed reactors.

2.2 Claus Process

Oxidation of hydrogen sulfide, and its reaction with the formed sulfur dioxide over a suitable catalyst has been used commercially since late nineteenth century. C.F. Claus's Patent of 1882 describes the process for recovery of elemental sulfur from hydrogen sulfide after being produced by calcium sulfide. The original Claus process comprised oxidation of hydrogen sulfide with air over a number of catalysts: iron ore, manganese oxide, aluminium hydroxide, zinc oxide, limestone, and bauxite. The major reactions involved are:



which makes the overall reaction:



The oxidation reaction is highly exothermic. The resulting high temperature also limits the hydrogen sulfide conversion to a low value. A significant advance was made about 1937 by I.G. Farbenindustrie (8). Instead of burning the hydrogen sulfide directly over the catalyst, one-third of it was burned completely to form sulfur dioxide in the boiler. The reaction was then completed by combination of the remaining hydrogen sulfide and sulfur dioxide over the catalyst at 600 K. In this way, the large heat of reaction could be dissipated without causing damage to the catalyst. The high temperature in the boiler also results in the homogeneous reaction between hydrogen sulfide and the combustion product SO_2 to the extent of 50 - 70 % conversion. This is now known as the modified Claus Process and is the most widely used sulfur production process. It is applicable to the production of sulfur from acid gas streams containing from about 15% to 100% H_2S (88).

The reactions which occur in a Claus unit are not as simple as represented by equations (2.1) and (2.2). Hyne

(108), and Cullis (53) have reported on the possibility of nineteen reactions that may occur in the sulfur burner with the admission of only hydrogen sulfide and air to the burner. An additional complicating factor is the presence of appreciable quantities of carbon dioxide and light hydrocarbons in the acid gases fed to the burner. The high temperature combustion of such an acid gas may give rise to the production of COS and CS₂ (34). Pearson (165, 166), Opekar and Goar (160), and Grancher (93, 94) have listed several reactions that can lead to the production of these components in the combustion zone. Nabor and Smith (156) have studied the formation of CS₂ from methane and sulfur over a silica catalyst. Their results suggest the possibility of the formation of CS₂ in the catalytic convertors of sulfur plants. However, plant data have not been released to substantiate the catalytic activity of alumina toward this reaction. Furthermore, kinetic considerations indicate that the reaction rate is very slow even on silica catalyst at the Claus convertor temperatures (156).

Yet another complexity arises from the fact that several molecular forms of sulfur can co-exist. At low temperatures, S₈ makes up a large fraction of the vapor; while at high temperatures, S₂ may be the dominant species. This shift in molecular form of sulfur leads to the exothermic - endothermic behaviour for the Claus reaction. The Claus reaction is exothermic in the low operating

temperatures of catalytic convertors, and is endothermic at high furnace temperatures. The minimum in the equilibrium hydrogen sulfide conversion occurs between 800 and 1000 K (14).

2.3 Sulfur Vapor and Equilibrium Conversion

The molecular composition of sulfur vapor has been a controversial topic for many years. Different investigators (28, 169, 171) have reported different sulfur vapor compositions and different thermodynamic data. This controversy has been reviewed in detail by Truong (199) and examined by Chao (42). Berkowitz (15) and Opekar and Goar (160) suggest that the vapor contains all forms of the molecule, S_n , where $2 < n < 10$. However, reliable thermodynamic data for S_3 , S_5 are not available (42). Furthermore, the effect of S_3 , S_5 , S_7 is believed to be negligible in the temperature ranges normally encountered in either the thermal or catalytic stages of the Claus process (140, 219).

Commonly it has been observed that experimentally measured hydrogen sulfide conversions are somewhat higher than the corresponding equilibrium values predicted using selected thermodynamic properties published in the literature (4, 14, 25, 44, 83). This discrepancy has been attributed to the inaccuracy of the thermodynamic data. Hence, the properties of sulfur species have been adjusted empirically to increase the predicted values for equilibrium conversions of hydrogen sulfide. Using such adjusted

properties, a more realistic value for the equilibrium composition should, in principle, be predicted. Such generated adjusted thermodynamic data are usually proprietary information (23).

Truong (199) could predict higher conversions than those observed by Cho (44) and Gamson and Elkins (83), by considering the sulfur vapor model of $S_2 - S_6 - S_7 - S_8$ and adjusting the thermodynamic data of all the species including H_2O , H_2S , SO_2 and N_2 , in the direction of more favorable conversions at the catalytic convertor temperatures.

Bennett and Meisen (14) produced a perfect match between theoretical and experimental conversion data at a high furnace temperature of 1300 K by decreasing the free energies of H_2S and SO_2 and increasing them for H_2O and S_2 by 2.57%, 2.88%, 1.55% and 5.13%, respectively.

The thermodynamic properties of H_2S , SO_2 , H_2O , and N_2 (144, 193) have, however, been obtained by well established experimental methods and the results obtained by different workers are consistent (219). Hence, Yung (219) adjusted only the free energies of S_2 , S_6 , and S_8 , which have a high degree of uncertainty. Using 10%, 15%, and 20% increases in the free energies of S_2 , S_6 , and S_8 respectively, the best overall adjusted predictions resulted for the temperature range spanning both the catalytic convertor temperatures and high temperature furnace region (219).

McCulloch (145) studied the kinetics of the reverse Claus reaction step (equation 2.2). He observed that the predicted equilibrium conversion of sulfur and water to H_2S and SO_2 was consistently below the experimentally determined equilibrium. This is the same trend in discrepancy that was noted for the approach to the equilibrium for the forward reaction step. This observation appears to be inconsistent in explaining the discrepancy between the equilibria in terms of the free energies of the sulfur species being too low or too high. However, the experimental data of McCulloch were not accurate, and were greatly scattered.

2.4 Kinetics of the Claus Reaction

The kinetics of Claus reaction has been studied quantitatively as early as 1927 (195). However, the early studies often were empirical in formulating rate expressions and varied in the catalysts employed.

The Claus reaction does not proceed homogeneously (44, 85, 86, 113, 148, 179), at temperatures less than 880 K. This reaction can be catalyzed by various substances such as glass surface, iron, condensed water, and liquid sulfur, (30, 113, 126, 148, 178).

The Claus reaction can be limited by the rate of diffusion of the species in the catalytic process (23, 29, 44, 85, 86, 94, 95). However, the work of Hammer (96) and of McGregor (148) presented limited qualitative experimental evidence that only the external area of the catalyst was

involved in catalyzing reaction. McGregor concluded that neither pore diffusion nor film diffusion were important in the Claus reaction, presumably all pores were filled by condensed elemental sulfur. Hence he expressed the pre-exponential factor in his rate expression as a simple linear function of the external pellet surface area.

Blanc et al. (23) did not discard the pore diffusion limitation, but expressed its overall effect empirically. Their pre-exponential factor was expressed exponentially as a function of pellet diameter.

The analytical rate expressions for the Claus reaction are summarized in Table 2.1. The subscript 1, 2, and 3 in table 2.1 denotes H_2S , SO_2 , and H_2O , respectively. Kerr's (116) rate expression is restricted in the sense that, the complexities of film and pore diffusion have been neglected without justification. Furthermore, the equilibrium term does not contain stoichiometric coefficients and is thermodynamically inconsistent.

The rate expressions of Dalla Lana et al. (56) and Dalla Lana et al. (57) were nearly identical, except for the exponent of the denominator. Liu (135) has however shown, that the Dalla Lana (56) expression can also well be represented using the exponent of unity in the denominator because of the correlation between the exponent and the water absorption term. Blanc et al. (23) also concluded that the power of the denominator term could be varied over a large range without the sum of the squared deviation between

Table 2.1 RATE EXPRESSIONS FOR THE CLAUS REACTION

(R, mol/g h P, mm Hg)

Subscript 1, 2, and 3 represents H_2S , SO_2 , and H_2O respectively.

Investigator	Catalyst
Taylor and Wesley (195)	Pyrex glass
$-R_1 = k P_1^{1/5} P_2 \quad (2.4)$	

McGregor (148)	Porocel
$-R_1 = 2.198 \exp\{-3819/T\} P_1^{0.63} P_2^{0.359} \quad (2.5)$	
$-R_1 = 1.292 \exp\{-3573/T\} (P_1^{0.904} P_2^{0.474} - 0.504 P_3^{0.982}) \quad (2.6)$	

Dalla Lana et al. (57)	Porocel
$-R_1 = 1.124 \exp\{-3744/T\} \frac{P_1 P_2^{0.5}}{1 + 0.00423 P_3} \quad (2.7)$	

George (85)	Co-Mo- γ alumina
$-R_1 = \frac{k_0 \exp\{-2768/T\} P_1}{(1 + 0.1 P_3)} \quad (2.8)$	

Kerr et al. (116)	bauxite and γ -alumina
$-R_1 = k_0 \exp\{-2527/T\}$	
$([H_2S][SO_2] - \frac{[H_2S][SO_2]}{[H_2O][Sn]} [H_2O][Sn]) \quad (2.9)$	

Table 2.1 continued

Dalla Lana et al. (56)

 γ -alumina

$$-R_1 = 0.92 \exp\{-3700/T\} \frac{P_1 P_2^{0.5}}{(1+0.006P_3)^2} \quad (2.10)$$

Liu (135)

 γ -alumina

$$-R_1 = 0.7 \exp\{-3509/T\} \frac{P_1 P_2^{0.5}}{[1+1.15 \cdot 10^{-5} \exp(3157/T) P_3]^2 P_n^{1/2n}} \quad (2.11)$$

Blanc et al. (23)

activated alumina

$$-R_1 = k_0 \exp\{1938/T\} \frac{P_1 P_2^{0.5} - (1/\sqrt{K}) P_3 P_1^{0.5}}{(1+0.0842P_3)^{0.5}} \quad (2.12)$$

$$\text{where } K = \left(\frac{P_1^2 P_3}{P_1^2 P_2} \right)$$

McCulloch (145)

Kaiser S201 alumina

$$R_1 = \frac{k_0 \exp(-7995/T) P_3^{0.88} P_1^{0.39}}{(1+0.0037P_3)^2} \quad (2.13)$$

the experimental and computed values changing greatly.

The rate expressions (2.4), (2.5), (2.7), (2.8), (2.10) and (2.11) are expressed without the reverse reaction term. The reverse reaction rate term in equation (2.6) was chosen to account for the retarding influence of water. Dalla Lana et al. (57) have shown statistically that the reverse reaction contribution was negligible for those experimental conditions and the retarding effect likely originated from interactions between water molecules and active sites on the surface (as shown by equations (2.7), (2.8), (2.10), (2.11), (2.12) and (2.13)).

Liu (135) did not detect SO_2 as a product when Claus reaction products, sulfur and water, were introduced to his reactor at different temperatures and comparable or even higher partial pressures than used in any of his measurements.

The Blanc et al. (23) rate expression is based on the rate of forward reaction. The reverse reaction rate was constructed to meet the criterion of thermodynamic consistency. However, the sulfur partial pressure in their equation (2.12) has been defined somewhat arbitrarily. Equation (2.12) shows a small activation energy compared to those in equations (2.7) and (2.10). The Dalla Lana (56) expression is believed to be free of film and pore diffusion limitations, while the pore diffusion effect has not been eliminated in developing the rate expression (2.12). This could partly be responsible for their low value of

activation energy, because in the diffusion-limited region, the observed activation energy should be less than the intrinsic one (181).

The reverse reaction expression (2.13) has been obtained by initial rate studies. The units of pressure used in the original McCulloch (145) rate expression was the Pascal. The parameters of the McCulloch expression as shown in table 2.1 have been adjusted to mm Hg unit for pressure. This facilitates the comparison between equations (2.10) and (2.13). The absorption equilibrium constant for water in equation (2.13) is of the same order of magnitude as those in equations (2.7) and (2.10). The activation energy for the reverse Claus reaction is almost twice that of the forward reaction and implies the endothermicity of the reverse reaction. The order of reaction with respect to water (0.89) is almost in agreement with the order required for thermodynamic consistency (unity). This is not however the case with the sulfur term which requires an exponent of 0.1875.

With the exception of equation (2.11), the rate expressions in table 2.1 are empirical. The reliability of the rate expressions would be expected to improve when they are based on surface chemistry studies. Liu's (135) rate expression has been developed using the infrared spectroscopic results. He constructed various reaction mechanisms and their corresponding kinetic models consistent with the chemical observations. The expression (2.11) was

the kinetic model which best correlated his measured reaction rate data.

Dalla Lana (56) states that the similarities between expressions (2.7) and (2.10) implies that these kinetic expressions are more generally applicable, since they are based on different alumina catalysts. Then, the principal characteristics observed for the forward term of Claus rate expressions (23, 93, 94) are:

1. order of unity with respect to H_2S ,
2. order of 0.5 with respect to SO_2 ,
3. inhibition by water.

2.5 Claus Catalyst Deactivation

The deactivation of a Claus catalyst is a complex phenomenon which may be divided into two categories: irreversible aging and reversible aging (i.e., the activity can be recovered through an appropriate regeneration).

Mechanisms involving alteration of the catalyst structure, e.g., modification in the texture (specific area, porosity) due to sintering, attrition, thermal aging or recrystallization and phase changes (94, 95, 116) are irreversible aging processes. In general, the Claus catalyst, gamma-alumina, transforms and loses part of its activity when the temperature exceeds 873 K (95, 116). Kerr et al. (116) observed that the surface area decreases in proportion to the temperature and attributed the surface area reduction to the collapse of the small pores. This

thermal transformation is to be avoided during the regeneration of the catalyst and sulfur desorption on the occasion of shut downs. The thermal aging of gamma-alumina is however, limited. The catalyst after three to four years of service retains a surface area of about $150 \text{ m}^2/\text{g}$ (95), which is high enough for good conversion of hydrogen sulfide.

The deposition or formation of a foreign substance on the catalyst surface, e.g., by sulfation, coking, or sulfur condensation could deactivate the catalyst but the activity can be recovered through an appropriate regeneration.

The sulfur deposition on the Claus catalyst is believed to arise from two mechanisms: adsorption and condensation (116). The quantity of elemental sulfur adsorbed by the catalyst is a function of the catalyst temperature and the concentration of the sulfur in the gas phase. Typical catalyst contents of adsorbed sulfur in the first and second convertors lie between 3 to 10 weight percent (116). McGregor (148) and Karren (113) detected 10 and 2 weight percent sulfur on their used bauxite catalyst, respectively. Boldingh (24) could reduce the sulfur content of an artificially loaded alumina catalyst to a minimum value of 4 weight percent, after heating the sample for 500 hours at 413 K.

Elemental sulfur condensed on the catalyst surface is a severe deactivating agent, and is generally the result of operation of convertors at low temperatures. The condensed

elemental sulfur can be present up to levels of thirty weight percent which then can completely deactivate the catalyst (98, 116). Pearson (167), however found that a 50 weight percent sulfur loading can be achieved on activated alumina S-201 type. A 30 to 35 weight percent sulfur loading produced only a minor loss in H_2S/SO_2 conversion efficiency of his catalyst (167). The deactivation due to condensed sulfur from sub-dew-point operation can, however, be corrected by the simple expedient of increasing the convertor temperature (90, 91, 99, 173).

The thermal decomposition of hydrocarbon impurities of an acid gas in the furnace of the Claus plant forms carbon. Carbon can exist in the forms of coke, a finely dispersed powder, or glossy carbon, or hydrocarbon-sulfur complexes. Both deactivate the Claus catalyst by blocking the pores (116). Coking is an upstream phenomenon, i.e. the coke content of the catalyst is higher in the first convertor compared to that in the second convertor.

The major deactivation agent for the Claus catalyst is believed to be from sulfation (29, 94, 95, 116, 170). The sulfation has generally been regarded as the consequence of oxidation of SO_2 on the catalyst surface (95, 116, 135, 166). The adsorption of SO_3 vapor is the most effective way of forming sulfate on alumina (95, 135, 166). It is not known whether the formation of sulfate from SO_2 and O_2 proceeds directly or via formation of SO_3 (135).

Kerr et al. (117) concluded from their experimental work that in the absence of SO_2 or O_2 , sulfation rates are very small. They assumed that the chief poisoning agent was FeSO_4 and showed that it may be produced from FeS , a reaction favorable over the temperature range found in the Claus plants. The enhancement of sulfation in the presence of H_2S was explained to be the resultant of the formation of FeS (117).

Hyne and Ho (109) have shown that the reverse Claus reaction can generate sulphuric acid capable of sulphating the alumina catalyst.

According to Quet et al. (170), the sulfates, from the presence of H_2S and SO_2 without oxygen, or from the presence of sulfur vapor without oxygen, do not affect the activity of Claus catalyst significantly. Their catalyst remained at nearly constant activity for a long time under the above mentioned conditions. These sulfates are named "neutral" compared to the "bad" sulfates which contribute to fast deactivation and are formed by the presence of O_2 and/or SO_3 (170).

The extent of sulfation depends on the temperature and concentrations of H_2S , SO_2 , SO_3 , O_2 , and elemental sulfur through the establishment of equilibrium (94). Sulfation increases with low H_2S concentration, high SO_3 , and O_2 concentrations and low temperatures (94). Kerr et al. (117) found that under process conditions, sulfate concentrations on the catalyst increased downstream in the convertor beds.

This can be explained by considering that there are lower temperatures and lower H_2S concentrations in the second and third convertors compared to those in the first convertor.

There are commercially advertised promoted alumina catalysts available that are claimed to resist sulfation and to be insensitive to oxygen in concentrations up to 2000 ppm (67, 170).

2.6 Claus Catalytic Convertor

In the modern Claus sulfur plants a number of catalytic stages, usually three or four with in-between sulfur condensers are used to increase the yield of the elemental sulfur, since the high temperature of a single reactor would limit the conversion of hydrogen sulfide to the low equilibrium values. Recoveries of 94% to 96% sulfur in the feed can usually be attained with three catalytic reactors (59).

The catalytic convertors of the Claus plants operate at temperatures below 700 K where the reaction between H_2S and SO_2 is exothermic, thus equilibrium conversion is favored by decreasing the reaction temperature. The reaction can also be pushed to higher conversions of H_2S by removal of the product sulfur from the reaction phase. These principles have been used in the development of operation of the Claus convertors at temperatures below the dew point of sulfur vapor (52, 91, 99, 173). During sub-dew point operation, the product sulfur condenses in the pores of the catalyst and as

a result, the catalyst loses its activity. This will necessitate catalyst regeneration.

The first commercial sub-dew point Claus convertor, the "Sulfreen Process", was developed by Lurgi Apparate- Technik and S.N.P.A. (52). Activated carbon was used as the catalyst in the first commercial Sulfreen plant. In more recently installed Sulfreen plants, activated alumina is used as the catalyst (167). The overall removal efficiency of two Claus convertors plus a Sulfreen plant has been reported to reach 99% (138).

The Amoco Coldbed Adsorption (CBA) units are also based on sub-dew point temperature operation. It is similar to the Sulfreen process except that it uses process gas for regeneration and cooling. The overall conversion for the two Claus convertor and two CBA convertors, one CBA in regeneration mode, and the other in adsorption mode, is from 98 to 99.3% (157).

The MCRC sulfur recovery process (99) also employs sub-dew point operation. This process is designed with either three or four catalytic convertors. Its difference with the Amoco (CBA) process is that it operates the second stage Claus convertor at sub-dew point temperatures. The MCRC overall sulfur yield has also been reported to about 99% (99).

The catalytic convertors in the Claus unit are designed for a space velocity of about 1000 SCFH of reactant gas mixture per cubic foot of catalyst bed volume. The beds are

shallow, wide and insulated. The catalyst is contained in horizontal drums about eighteen meters long and four meters in diameter with flow downward through the bed which is packed to a depth of one meter.

2.7 Modelling of Fixed Bed Catalytic Reactors

Various kinds of models have been proposed for the heterogeneous catalytic reactions, ranging from the very simple ones to some recently proposed very sophisticated ones. The degree of sophistication used in the modelling depends on the process, i.e., the reaction scheme and its sensitivity in the operating conditions. However, the degree of accuracy of any model would depend on the accuracy of kinetic and transport parameters. Froment (82) has reviewed the models of the catalytic fixed bed reactors up to 1979. This survey will employ the same categories of the models as was used by Froment (82).

The models of fixed-bed catalytic reactors can be divided into two main categories; pseudo-homogeneous models which do not account explicitly for the presence of catalyst, and heterogeneous models which do by separate conservation equations for fluid and catalyst phases. Within each group the models are classified in order of increasing complexity.

2.7.1 Pseudo-Homogeneous Models

These models consider only the macroscopic temperature and concentration gradients. The most general model in this category is the one which accounts for both radial and axial mixing. The steady state conservation equations for this model are:

$$(1/r)\partial(r D_r \partial C/\partial r)/\partial r + \partial(-V_r C + D_z \partial C/\partial z)/\partial z - R = 0 \quad (2.14)$$

$$(1/r)\partial(r K_r \partial T/\partial r)/\partial r + \partial/\partial z (K_z \partial T/\partial z) - G\partial(C_p T)/\partial z + (-\Delta H)R = 0 \quad (2.15)$$

where the rate, R is expressed per unit volume of the catalytic bed.

2.7.1.1 Plug Flow Model

The simplest model in the pseudo-homogenous category is the ideal model which neglects radial and axial mixing and considers the overall flow as the only transport mechanism. In this model velocity could be still a function of reactor depth because of

1. changes in the number of moles due to the reaction;
2. pressure changes with z ;
3. temperature changes with z .

Bilous and Amundson (17), and Van Welsenaere and Froment (202) have considered this simplest model in the modelling of the nonadiabatic convertors. They have found hot spots in the bed, which is typical for

strongly exothermic processes. The magnitude of the hot spots depends on the enthalpy change on reaction, the rate of the reaction, the heat transfer coefficient and transfer areas. Its location depends on the flow velocity. This model has also been used in optimization in case of multibed processes (137).

2.7.1.2 Pseudo-Homogenous Model with Axial Mixing

The second model in this group is the one-dimensional model with axial mixing. Due to the turbulence and presence of packing, mixing in the axial direction occurs, which is accounted for by superimposing effective transport on the overall transport by plug flow. In principle the effect of the axial mixing is to reduce concentration and temperature gradients and results in lower conversion. Danckwerts (58) has proposed the following boundary conditions for models with axial mixing:

$$V_s (C - C^0) = -D_z \partial C / \partial z \quad \text{at } z=0 \quad (2.16)$$

$$\rho V_s C_p (T^0 - T) = -K_z \partial T / \partial z$$

$$\partial C / \partial z = \partial T / \partial z = 0 \quad \text{at } z=L \quad (2.17)$$

Validity of this set of boundary conditions has been reexamined from various point of view and approaches (20, 72, 106, 164, 200, 207). Wehner and

Wilhelm (207) showed that the role of the catalyst support does not enter in the results of the part of the bed in which reaction takes place and hence justified the Danckwerts relations for the first-order reactions. Pearson (164) has also reached the same conclusion. Bischoff (20) showed that the conclusion of Wehner and Wilhelm is correct for reactions of any order. The Danckwerts boundary conditions hold for the unsteady state systems if no diffusion occurs in the support section of the catalyst bed (200).

The axial dispersion model has been used frequently, more particularly for adiabatic beds, because it might lead to the possibility of more than one steady state (103, 104, 105, 172).

The effect of axial mixing on conversion, for the flow velocities encountered in industrial practice, is not important when the bed depth exceeds about fifty particle diameters (112, 40). Hlavecek and Hofmann (104) have shown that multiplicity can occur even for high Peclet number, i.e. long beds, for strongly exothermic reactions with high activation energy. However, the range is rather narrow and the profiles in the multiple steady state range are very close. Usually through the entire range of axial coordinates the profiles coincide; the great difference exists in the immediate neighborhood of the reactor outlet only.

Young and Finlayson (218) have questioned the conclusion reached by Carberry (40) that the axial dispersion is unimportant when $L/D_p > 50$. They have shown that the importance of axial dispersion is primarily dependent on the magnitude of the maximum temperature and conversion gradients. If axial dispersion is to be negligible, then the maximum absolute value of the conversion gradient should be less than or equal to the ratio of the velocity to the axial diffusion coefficient; and the maximum absolute value of the temperature gradient should be less than or equal to $(\rho V, C_p/K_z)$ (218). To check Young's criterion, the magnitude of conversion and temperature gradients can be obtained either from experimental data or may be approximated from numerical computations using the mathematical models which neglect axial dispersion.

2.7.1.3 Pseudo-Homogenous Model with Radial Mixing

For nonadiabatic reactors, it is necessary to develop a two dimensional model because of a non-uniform temperature profile in the cross section of the bed. This leads to the third class of pseudo-homogeneous models, the models which consider radial heat and mass dispersion in equation (2.14) and (2.15) but neglect axial dispersion terms.

Several investigators (2, 74, 77) have studied pseudo-homogeneous reactor models with radial dispersion. Such a two dimensional model was solved by

means of the finite difference method (77), and orthogonal collocation (2, 74).

According to Ahmed and Fahien (2), in the conventional orthogonal collocation method, the temperature and concentration at the center of the packed bed convertor are not obtained accurately since there is no collocation point at the center. Thus, they used central differencing in the vicinity of the convertor center line.

Finlayson (74) concluded that the orthogonal collocation method is an efficient numerical method for solving the equations governing packed bed reactors with radial gradients.

One of the modifications in the area of modelling a fixed-bed reactor is the consideration of radial velocity profiles. In a packed bed, the velocity profile is flat near the center, rises to a peak near the wall and falls rapidly right at the wall (32, 66, 155, 182, 185). Leron and Froment (132) found out that the velocity profile that is inversely proportional to the porosity profile leads to a correct prediction of the radial temperature profile, which is comparable to the experimental data in beds without chemical reaction.

The velocity profile induces a radial variation in effective radial thermal conductivity and diffusivity (2, 74, 125, 132, 182). There are two methods for incorporating effective radial thermal conductivity. One

is, to assume a uniform radial thermal conductivity, and introduce a heat transfer coefficient at the wall to account for the higher resistance at the wall. The other is to vary the effective radial thermal conductivity with radius (82).

The two dimensional pseudo-homogeneous model which incorporates radial velocity profile has been investigated by Finlayson (74), Ahmed and Fahien (2), and Lerou and Froment (132).

Finlayson (74) used the isothermal velocity profile data of Schwartz and Smith (185), and the effective radial thermal conductivity correlation of Baddour and Smith (7). He concluded from his modelling results that the velocity profile model could predict a wall heat transfer coefficient which when used in the plug flow model could give similar temperature and concentration predictions.

The Lerou and Froment (132) velocity profile model of the catalyst reactor predicts more sensitivity to variation in the inlet and wall temperatures relative to the uniform velocity model. It also predicts runaway where the model without the velocity profile still predicts a safe operation.

Ahmed and Fahien (2) have used the velocity profile correlation of Fahien and Stankovich (71). They also allowed for the radial variation of effective diffusivity and thermal conductivity. Their model was

tested against the experimental data from the laboratory reactor of Schuler et al. (184) for oxidation of sulfur dioxide to sulfur trioxide over a platinum catalyst in the presence of air. Throughout the length of the reactor the conversion obtained from their model agreed quite well with the experimental values. Their model predicted the temperature at the hot spots and the hot spot location very well. The calculated center line temperature agreed reasonably well with the experimental measurements, except towards the end of the reactor.

2.7.1.4 Pseudo-Homogenous Model with Axial and Radial Mixing

The fourth class of models in the pseudo-homogeneous category is the two dimensional model which also include axial mixing. Feick and Quon (73) used the Danckwerts boundary conditions while, Young and Finlayson (218) considered radial dispersion in their boundary conditions. Both investigators used a uniform velocity profile:

Feick and Quon (73) used a finite difference approach to solve the axial-radial dispersion nonadiabatic reactor model. They presented the modelling results for a highly exothermic reaction with first-order Langmuir-Hinshelwood kinetics. Their reactor has the length of 50 and diameter of 10 catalyst particle diameters. Their results showed that most of the reaction occurs in the first half of the reactor and

in the area of the center line. Feick and Quon (73) observed a hot spot along the center line and a minimum concentration at various radial positions except at the wall. These observations are the result of direct coupling of the radial diffusion of heat toward the reactor wall and a counter diffusion of reactants in the opposite direction toward the reactor center (73). The authors indicated that the reactants would diffuse axially backward against the convective flow direction in the second half of the reactor. This happens as the result of radial diffusion of reactants and the fact that the temperature is not high enough to maintain a high rate of reaction in the second half of the reactor (73). Thus due to both axial and radial diffusion, the high reaction zone near the front of the reactor is supplied with the reactant from the low reaction, higher concentration, areas of the reactor. Hence, Feick and Quon (73) concluded that a model which does not account for radial and axial diffusion gives a rather conservative estimate of conversion.

Young and Finlayson (218) used a general two dimensional model with axial mixing, to simulate experimental results of Schuler et al. (184). They assumed constant thermal conductivity over the cross section and accounted for the higher wall resistance by using a constant transfer coefficient at the wall. However, instead of predicting the heat transfer

parameters *a priori*; they were obliged to adjust them until they obtained the desired results. Their results were found to be in a good agreement with the experimental results. Only the temperatures near the hot spots depart significantly from the experimental values. They concluded that both the axial and radial dispersions are important in the experimental SO_2 oxidation reactor of Schuler et al. (184).

Ahmed and Fahien (2) used the same SO_2 oxidation data to evaluate the performance of their model which neglected axial dispersion, but accounted for the radial velocity, thermal conductivity and diffusivity profiles. Ahmed and Fahien (2) used a different SO_2 oxidation rate expression than Young and Finlayson (218). Thus a comparison of the performance and goodness of the fit of the two reactor models is difficult to make.

2.7.1.5 Approximate Two-Dimensional Pseudo-Homogenous Model

To reduce the computational time without loss of much accuracy, modified one-dimensional models have been developed (3, 147). In this model the radial temperature and conversion profiles are approximated by polynomials, and axial dispersion is neglected. Ahmed and Fahien (3) have used polynomials of variable degree which are calculated at each axial position and no parameters needed to be obtained empirically or assumed. Their method, however, requires the simultaneous solution of

five ordinary differential equations at each axial position. The Ahmed and Fahien method is believed to be applicable to a wide range of reaction kinetics (3).

The McGreavy and Turner (147) method is based on a third order polynomial curve fit of the conversion profile and an eleventh order polynomial for temperature profile. They used an empirical equation to improve the variation of concentration and temperature with axial position. Three parameters in this expression were empirically determined. Their results were given for first-order Arrhenius kinetics. The McGreavy and Turner (147) method requires the solution of two ordinary differential equations at each axial position along with a number of algebraic equations.

2.7.2 Heterogeneous Models

These models distinguish between conditions in the fluid and on the catalyst surface. They are divided further into two groups; a group accounting for intraparticle gradients; and another neglecting intraparticle gradients. Each group can then be divided into one dimensional and two dimensional models.

In the heterogeneous models, the complex behaviour in the reactor is concentrated in two homogeneous phases; in the flowing fluid and in the fixed catalyst, or in the number of cells behaving like a non-isothermal CSTR.

2.7.2.1 1-Dimensional Heterogeneous Model: Interparticle Resistances

Liu and Amundson (134) developed a continuous two-phase model for the analysis of packed bed reactors without intraparticle resistances to heat and mass flow. Their model is one dimensional and assumes that the reaction is controlled by interphase effects.

The distinction between the conditions in the fluid and on the solid leads to the problem of stability and multiple steady state solutions. The heat produced on the catalyst surface is a sigmoidal curve when plotted as a function of the particle temperature, and the heat removed by the fluid film surrounding the particle is a straight line (133, 134). The steady state is given by the intersection of both lines, three intersections, therefore three steady states are possible (133, 134). The instability of a single catalyst pellet, then through the continuity of the mathematical model can result in a large number of multiple solutions for the axial profile of temperature (133, 134). Liu and Amundson (134) have neglected the axial coupling between the particles.

Eigenberger (69) has modified the Liu and Amundson (134) model by including the effect of heat conduction in the catalyst phase. He has concluded that the infinite multiplicity of steady state solutions of Liu and Amundson is reduced to a few by the effect of axial

heat conduction in the catalyst phase. Eigenberger (69) has also investigated the effect of different boundary conditions in the frontal surface of the catalyst bed. According to his results, a radiation boundary condition should be considered, when a high temperature can occur in the catalyst phase can occur.

2.7.2.2 2-Dimensional Heterogeneous model: Interparticle Resistances

Feick and Quon (73) developed a two dimensional, two phase nonadiabatic model which neglected the intraparticle resistance. Their model predicted much less conversion for a highly exothermic second order reaction compared to the two dimensional pseudo-homogeneous model. They have pointed out that, this significant difference in conversion is due to the resistance to the heat and mass transfer between the particles and the bulk fluid.

2.7.2.3 Heterogeneous Model with Inter and Intraparticle Resistances

Several investigators have considered the effect of both interphase and intraphase transport resistances (35, 63, 64, 73, 127, 128, 147). The role of intraparticle gradients is frequently reduced to an algebraic term to simplify the analysis, namely the so-called effectiveness factor. In its classical sense, the effectiveness factor is a factor that multiplies the

reaction rate evaluated at the condition at the external surface of the pellet to yield the rate actually experienced by the particle (82).

Cappelli et al. (35) simulated the methanol synthesis reactor, using the one-dimensional two-phase model. They considered interphase and intraphase gradients but neglected axial diffusion and conduction. Their results are in good agreement with the industrial results. The film transport resistances were found to be negligible.

The two phase, two dimensional models which include both interphase and intraphase resistances have been developed by Feick and Quon (73), McGreavy and Cresswell (147) and De Wasch and Froment (63). The difficulty encountered with the two dimensional two phase models arises from the heat transfer, which in contrast with mass transfer, occurs through both the fluid and the solid phase (82). Thus, De Wasch and Froment (63) developed their two-dimensional, two-phase model taking into account the radial dispersion of heat through the solid phase. They claim that the models which do not account for radial heat transfer through the solid phase are not realistic, because up to twenty-five percent of the radial heat transfer occurs through the solid (63); and the temperature and concentration profiles are very sensitive to effective thermal conductivity. The De Wasch and Froment model consists of a two-dimensional

fluid mass and temperature balance, and also a balance on a thin layer of the solid. They introduced the intraparticle effects by an effectiveness factor.

The Feick and Quon (73), and McGreavy and Cresswell (147) models have implicitly assumed that heat is only transferred through the fluid phase.

De Wasch and Froment showed that when the McGreavy and Cresswell model predicts runaway, their model predicts safe operation.

Finally Lee (127) proposed an approximate approach for the design and analysis of fixed-bed catalytic reactors in which the intraphase diffusion is important.

Lee (127) transformed a heterogeneous, two-dimensional phase reactor problem into a pseudo-homogeneous reactor problem by use of a generalized effectiveness factor which is expressed solely in terms of bulk fluid temperature and concentration. The approximations of Lee's method are: isothermality of the catalyst pellet; negligible interphase mass transfer resistance; approximation of the concentration at the pellet center by the concentration corresponding to a pseudo-first-order reaction; and approximation of a rate constant ratio by the first-order term in Taylor series expansion. Lee (127) checked the above approximations and concluded that for most reactions under realistic conditions they are valid.

2.7.3 Reaction Rate in Heterogeneous Models

The heterogeneous models of section 2.7.2 account explicitly for the presence of catalyst pellets. In these models the observed (global) reaction rate may be influenced by the transport process: heat and mass transfer between the fluid and the solid (interparticle resistances), or inside the porous catalyst pellets (intraparticle resistances).

2.7.3.1 Interparticle Transport Resistances

Film transport resistances between the catalyst pellet surface and the flowing stream may not be significant in cases where the catalyst is only moderately active, but become important if the catalyst is highly active. In the latter case the temperature and concentration on the catalyst surface differ from the observed bulk quantities.

The significance of film resistances to mass and heat transfer is expressed in terms of heat and mass transfer coefficients. There have been many experimental studies of mass and heat transfer coefficients in packed bed. Sherwood et al. (187), Froment (79), Whitaker (212), and Dwivedi (68) have summarized the results and the correlations.

For Reynolds number greater than 10, Dwivedi reports:

$$J_m = 0.458/\epsilon (Re)^{-0.407} \quad (2.18)$$

where

$$J_m = k_m \rho / G (Sc)^{2/3} \quad (2.19)$$

There have been correlation other than (2.18) for $J_h (= h / CpG Pr^{2/3})$, (60, 97). However, Smith (189) points out that the validity of the difference between correlations of J_h and J_m in the absence of radiation is uncertain, and recommends use of relation (2.18) for J_h .

Paspek and Verma (161) have argued that the reported correlation were obtained from experiments involving the determination of transport phenomena in the absence of reaction. Hence, the gradients involved are not as severe as those encountered in a reacting system (161). They applied a least squares analysis of the mass and heat transfer for the experimental data of oxidation of ethylene in an adiabatic fixed-bed reactor. Their J factors are almost five times greater than given by the above correlations. However, the Reynolds number dependence is about the same as equation (2.18).

2.7.3.2 Intraparticle Transport Resistances

In heterogeneously catalyzed reactions, the catalyst usually comes in the form of a porous pellet and the reacting fluid has to diffuse into the interior of the pellet where the reaction takes place. If the potential rate of reaction is small compared to the potential rate of diffusion, the size of the pellet is not important since the concentration of the reacting species at the center of the pellet is not very much

different than its value at the external surface. Otherwise, the concentration of reactant is depleted by reaction before it has a chance to diffuse within the pellet, and the reaction is said to be diffusion limited. The modelling of these processes will lead to a rather complicated system of nonlinear two-point boundary value differential equations.

Comprehensive reviews and discussion on intraparticle transport resistances are available by Aris (6), Satterfield (180) and Wheeler (211).

The first theoretical treatment of simultaneous chemical reaction and diffusion in porous isothermal pellets was reported simultaneously by (197) and Zeldowitsch (220). For nonisothermal pellets, Weisz and Hicks (208) have reported a full set of computation on chemical reaction with mass and heat transfer through the pellets. For nonisothermal pellets, the problem is complicated since both reactant concentration and rate constant, which generally is exponentially dependent on temperature, will be functions of position in the particle.

The effect of intraparticle transport limitation is frequently reduced to a lumped parameter, "effectiveness factor", η , introduced by Thiele. It is defined as the ratio of observed rate of reaction to the rate evaluated at the condition of the external surface of the catalyst pellet.

An important result of Thiele's analysis was that the effectiveness factor does not depend on the individual absolute values of radius of pores, rate constant, diffusivity through the pores, or the size of the pellet, but on their ratios as they appear in the dimensionless parameter, called the "Thiele modulus ϕ ";

$$\phi^2 = L^2 \left(\frac{\text{reaction rate at the surface condition}}{D C_s} \right) \quad (2.20)$$

which for first-order reaction reduces to:

$$\phi^2 = \frac{L^2 k}{D} \quad (2.21)$$

For most reactions in an isothermal pellet, the effectiveness factor is less than or equal to unity. Certain reaction rate forms lead to effectiveness factors greater than unity or even multivalued in an isothermal pellets. These reaction rate forms exhibit approximate negative order behavior. This effect was first reported by Roberts et al. (176) for Langmuir-Hinshelwood kinetics and later Smith et al. (190) for CO-oxidation.

For nonisothermal pellets, effectiveness factors greater than unity and multivalued have been reported for n-th order and Langmuir-Hinshelwood reaction kinetics (37, 100, 102, 190, 198, 208).

Hlavacek et al. (100,101) have shown that there is only small possibility that multiplicity in porous catalyst could occur in practical situations in the absence of film transport resistances. However, McGreavy and Cresswell (146) have shown that "multiplicity for the effectiveness factor may be expected for practical situations if external transport limitations are considered.

McGreavy and Cresswell (146) used the estimated values of the external transport coefficients (36) and reached the conclusion that the major mass transfer resistance is in the pellet but that there is an appreciable resistance to heat transfer across the film. Carberry (38) concluded that the catalyst pellets behave isothermally and that the resistance to heat transfer can be lumped at the surface.

Aris (5) has shown that the asymptotes of the effectiveness factor versus Thiele modulus curves for various pellet shapes may be brought together using the ratio of pellet volume to pellet external surface area as the characteristic dimension of the particle in the definition of the Thiele modulus. The maximum deviation between different shapes is in the order of 16% which occurs in the Thiele modulus range of 1.3 to 1.7 (174).

Bischoff (22) derived a generalized effectiveness factor for reactions with a general rate form in the absence of the external transport resistance. His

formula is an integral formula. Lee (127) used Bischoff's result and extended the generalized effectiveness factor to include the mass and heat transfer across the pellet-fluid interface.

Gottiferedi et al. (92) have used perturbation method and obtained analytical expression for the effectiveness factor in an isothermal pellet for n -th order reactions. Their method assumes that the asymptotic expressions for effectiveness factor, valid at small and large Thiele modulus values, can be matched with a unique and simple algebraic expression with three coefficients. These coefficients must satisfy a set of three algebraic equations. Their results are valid provided the order of the reaction is greater than 0.5.

2.7.3.3 Diffusivity in the Catalyst Pores

The analysis of intraparticle transport resistances contains the diffusivity parameter to which an absolute value can't easily be assigned. Theoretical models of gas diffusion in porous catalyst pellets are well developed (110, 143, 206, 211). The simplest one is based on Wheeler's parallel pore model which empirically accounts for the tortuous nature of pores through a factor called the "tortuosity or labyrinth factor", τ . In this model the diffusivity through pores is multiplied by the ratio of porosity to tortuosity.

Pore may occur by bulk diffusion or Knudsen diffusion. If the pores are large and the pressure is

high then the diffusion process is that of bulk diffusion, while Kundsén diffusion occurs for low and moderate pressures in small pores. For the transition region Bosanquet (26) has given an additive resistance relation of the form:

$$\frac{1}{D} = \frac{1}{D_b} + \frac{1}{D_k} \quad (2.22)$$

According to Wheeler (211), Kundsén diffusion is the predominate diffusion mechanism in pores of 10 nm or less, which is encountered in activated aluminas, up to gas pressures of about ten atmospheres.

The diffusion flux equations of the species in the multicomponent system, through catalyst pores are unsolvable only when the diffusion mechanism is of Kundsén type. In the transition and bulk diffusion region, the diffusional flux relations for the species are strongly coupled and the problem of solving the combined equations of diffusion and chemical reaction to predict the composition profiles and effectiveness factor appears much more formidable. Nevertheless, the case of a single reaction of the bulk diffusion limit was treated by Hugo (107) and for the intermediate diffusion regime by Abed and Rinker (1) and by Wong and Denny (214). The general problem of multicomponent diffusion accompanied by multiple reactions in the intermediate diffusion regime has been considered by

Kaza et al. (114,115), and by Sorenden and Stewart (191).

The problem of diffusional flux in the intermediate and bulk diffusion regime can be simplified by the evaluation of the mixture bulk diffusivity at some average composition. Kubota et al. (124) used this method and compared the effectiveness factor results with the exact solution for the bulk diffusion regime. They found that the relative error is about 2% for average for first-order reactions.

2.7.3.4 Numerical Method for Prediction of Catalyst Effectiveness Factor

In the last decade the orthogonal collocation method which was introduced by Villadsen and Stewart (203) has become popular for solution of the effectiveness factor problem (19, 41, 115, 162, 201). The prime advantage of orthogonal collocation method is its accuracy and simplicity. For example, for isothermal pellets with an effectiveness factor greater than 0.2, a two-term orthogonal collocation solution predicted the effectiveness factor within 1% of the exact solution (76).

For large Thiele modulus, when the solution has a steep gradient near the pellet surface, the orthogonal collocation method with a large number of collocation points is needed in order to have points near the pellet surface.

Paterson and Cresswell (162) developed the effective reaction zone method for large values of the Thiele modulus and applied the orthogonal collocation method in that zone. Van Den Bosch and Padmanabhan (201) have recommended the collocation point of $1/\sqrt{2}$ to be used in the Paterson and Cresswell method of effective reaction zone. Villadsen and Michelsen (204) have shown that the correct choice for first-order reactions is $1/\sqrt{2}$. However, they concluded that as the order of reaction increases, the collocation point should be increased toward one.

Carey and Finlayson (41), and Birnbaum and Lapidus (19) have introduced the method of orthogonal collocation on finite elements for situations corresponding to high Thiele modulus. This method yields accurate results, though the programming task is difficult.

2.7.4 Modelling of the Claus Convertor

The literature on the design of catalytic convertors for Claus process is sparse. Opekar and Goar (160) used the Gamson and Elkins method (83) to calculate adiabatic convertor equilibrium conversions used in material and energy balance equations. They, however, provided no information regarding the convertor size, geometry, reaction kinetics, global reaction control mechanism, or the catalyst. It is suspected that their method is only the

equilibrium conversion calculation based on the expected temperature rise of the convertor.

Burns et al. (29) used a first-order kinetic model for the Claus reaction and expressed the extent of reaction E with z , the depth of catalyst from the top of the bed for an isothermal reactor. Their extent of reaction formula is:

$$E = K(1 - e^{-z/m}) \quad (2.23)$$

where " m " is V_1/k , and " k " is the first-order rate constant for the Claus reaction. The parameter " K " represents an equilibrium condition and depends on the thermodynamic properties of the gas, and " m " is a function only of catalyst properties and temperature under steady state conditions (29). Equation (2.23) has been obtained by integration of the first-order reaction rate expression, substitution of z/V_1 for time (t), and use of the two boundary conditions for $t=0$ and $t=\infty$ at which times the reaction is uninitiated, $E=0$, and complete, $E=K$, respectively.

Burns et al. (29) fitted their experimental data to equation (2.23) and obtained different values of " m " and " K " for different catalysts under the same gas flow condition. The smaller value of " m " which implies a higher value of k , indicates the higher catalyst activity (29). Burns et al. (29) compared the " m " value for bauxite and activated alumina and claimed that bauxite has a distinctly higher

activity for the Claus reaction. They also found different "K" values for different catalysts. This is surprising, since by definition "K" represents an equilibrium condition and depends on the thermodynamic properties of the gas which was the same for the different catalysts.

The results of the Burns et al. (29) on the modelling of Claus reaction can be regarded as purely empirical, since they approached the problem by assuming a first-order reaction; ignoring the pellet diffusion limitation - although they were aware of it, in the integration of the rate expression; and finally obtained different values of "K" for the same gas composition for different catalysts.

Cho (44) modelled the Claus convertor as a one-dimensional, two-homogeneous phases, adiabatic reactor. He considered film transport resistances and used a constant value of 0.2 for the catalyst effectiveness factor. He modelled the sulfur vapor as $S_2-S_8-S_8$, and evaluated the sulfur vapor composition at each axial position and temperature at the total pressure of the reactor, using the free energy minimization. The sulfur vapor composition was then used in the evaluation of the heat of reaction.

Cho (44) simplified the mass balance equation by introduction of conversion which was defined as $(C-C^0)/C^0$, where C^0 is the feed concentration of the reactant. This definition of conversion ignores the volume expansion by either temperature rise or by change of the number of moles due to the reaction progress. He used equation (2.10) as the

rate of reaction which ignores the reverse reaction term.

His results show that a bed depth of one meter would provide the necessary contact time for high H_2S conversion when the Claus process alone is considered.

2.8 Catalyst Deactivation Modelling

Deactivation of catalysts involves sintering, poisoning or fouling. Catalyst deactivation by fouling agents is the result of deposition of substances on the catalyst and masking of active sites, while catalyst poisons cause deactivation by very strong adsorption on the catalyst surface. Reviews of modelling of catalyst deactivation by fouling agents and/or poisons have been given by Butt (31) and Froment (80).

Prior to the 1960's, the deactivation of the catalyst has been empirically expressed as a function of process time without any consideration to the effect of the concentration of the reactants. Szepe and Levenspiel (194) have summarized these experimentally determined deactivation equations.

Froment and Bischoff (81) questioned such an approach. They proposed the mechanisms of deactivation process and considered the production of the catalyst fouling compound either from the reactant or from the product. If the fouling compound is formed as the result of the side reaction of the reactant, the mechanism is called "parallel" fouling. In the "series" deactivation mechanism, the fouling compound is assumed to be formed by a reaction consecutive to the main

reaction. The deactivation by the presence of impurities in the feed is termed the "independent" mechanism.

2.8.1 Deactivation Kinetics

In general under varying operating conditions, the reaction rate on the deactivating catalyst at a given moment will be a function of the entire past history of the catalyst. In the terminology of Szepe and Levenspiel, a complete rate equation is of the form:

$$R = R\{\text{present condition, past condition}\} \quad (2.24)$$

The simplest possible form of equation (2.24) is the product of two terms.

$$R = R^0\{\text{present condition}\} \quad a\{\text{past condition}\} \quad (2.25)$$

This is the "separable deactivation rate expression", introduced by Szepe and Levenspiel. In this form, deactivation would only affect the reaction rate constant, and does not affect the adsorption equilibrium constants of reactants or products.

The nonseparable reaction rate expression is reported for deactivation caused by impurities in the feed, i.e., poisoning deactivation (31). Bakshi and Gavalas (9) studied dehydration of methanol and ethanol on silica/alumina, poisoned by n-butylamine. In contrast to the assumption of

separability, they found out that the adsorption equilibrium constants varied with the extent of deactivation.

Lowe (139) has proposed a method to test whether a reaction obeys separable kinetics by measurement of the ratio,

$$\frac{R\{C^{\circ}, T^{\circ}, a\}}{R\{C^{\circ}, T^{\circ}, a^{\circ}\}} \quad (2.26)$$

in different activity states "a" of a catalyst. If this ratio is independent of the reference conditions, C° and T° , then at least within the investigated region of C, T, and activity, the kinetics may be treated as separable (139).

The deactivation of a catalyst by fouling substances is generally expressed in the separable form. The activity function "a" (sometimes called deactivation function) is then, the ratio of the rate of a given reaction at a given fouling substance content (and time) to the rate at zero fouling substance content but otherwise identical reaction conditions (11,80). The activity of the catalyst for the main reaction of the reactant (1) is (11, 80)

$$a_1 = \frac{R_1}{R_1^0} \quad (2.27)$$

with

$$R_1^0 = k f_1\{C_1, C_2, \dots, K_1, K_2, \dots\} \quad (2.28)$$

where k the rate constant, is a multiple of the total number of active sites, s , raised to the power n_1 . The number, n_1 , being the number of sites involved in the surface reaction. It is equal to one for a single-site and two for a dual site surface reaction (11, 80).

The activity function for the production of fouling substances is defined similarly by (11, 80)

$$a_d = \frac{R_d}{R_d^0} \quad (2.29)$$

with

$$R_d^0 = k_d f_2(C_1, C_2, \dots, K_1, K_2, \dots) \quad (2.30)$$

here k_d is also assumed to be a multiple of s^{n_d} , where n_d is the number of sites involved in the deactivation reaction.

When deactivation occurs by site coverage only, a_1 and a_d will be defined by,

$$a_1 = \left(1 - \frac{s_d}{s} \right)^{n_1} \quad (2.31)$$

$$a_d = \left(1 - \frac{s_d}{s} \right)^{n_d} \quad (2.32)$$

where s_d is the number of sites deactivated. The values for a_1 and a_d are equal if $n_1 = n_d$, i.e. if the same number of sites are involved in the reaction kinetics of the main and

fouling reactions.

The rate of fouling of the active sites is, on the other hand, proportional to the rate of production of the fouling substance (11, 80). That is

$$\frac{d(s_f/s)}{dt} = \frac{d\gamma}{dt} = \frac{a_s R_s}{Q} \quad (2.33)$$

where, Q is the maximum catalyst capacity of the fouling substance at which value the deactivation is complete, and γ is the fraction of sites which have been deactivated.

When sites can not participate in the reaction because access to a fraction of the pore has been blocked by the fouling substance, equations (2.31) and (2.32) no longer satisfy the definition of a_s and a_s given in (2.27) and (2.29) (11, 80). In that case, a_s and a_s must be experimentally correlated with the fouling substance content of the catalyst. Froment and Bischoff (81) and De Pauw and Froment (62) have proposed the use of hyperbolic or exponential correlations between the activity function and the fouling substance content of the catalyst.

2.8.2 Deactivation of Single Pellet

The first development of quantitative effects of deactivation in a catalyst pore is due to Wheeler (211). He considered "uniform" and "pore-mouth" poisoning.

In uniform deactivation, the poisoning substance is assumed to be evenly distributed along the wall of a typical

pore. In the terminology of Froment (80), Wheeler assumed a single-site mechanism and defined the activity function as $(1 - \gamma)$ for uniform poisoning.

Wheeler also concluded that for uniform poisoning, the activity of the whole pellet, or the whole pore, is not directly proportional to $(1 - \gamma)$ for a fast reaction. For example for a first-order reaction in a single pore, the ratio of rate observed in a poisoned pore to that observed in an unpoisoned pore would be

$$F = \frac{R(\text{poisoned})}{R(\text{unpoisoned})} = [\sqrt{(1-\gamma)}] \frac{\tanh[\phi\sqrt{(1-\gamma)}]}{\tanh \phi} \quad (2.34)$$

where $\phi = L \sqrt{[2k/(rD)]}$ is the Thiele modulus. When ϕ is small (surface completely available), this ratio becomes $(1-\gamma)$, since the hyperbolic tangent terms become equal to their arguments. This effect is termed by Wheeler as non-selective poisoning. That is, the activity of the whole pore is proportional to its fraction of the surface which has remained active.

When ϕ is very large, the hyperbolic tangent terms approach unity and

$$F = \sqrt{(1-\gamma)} \quad (2.35)$$

This equation shows that for a fast reaction in which a poison is distributed homogeneously, activity of the whole pore falls less than linearly with fraction of surface

poisoned, γ .

In the pore-mouth poisoning analysis of Wheeler (211), it is assumed that the fraction γ of the surface which is deactivated is located near the mouth. Then the length (γL) nearest to the mouth is completely deactivated, and a length ($L(1-\gamma)$) beyond this will be fully active. In this case, F will be (211)

$$F = \left\{ \frac{\tanh \phi(1-\gamma)}{\tanh \phi} \right\} \left\{ \frac{1}{1 + \gamma\phi} \right\} \quad (2.36)$$

If ϕ is large then,

$$F = \frac{1}{1 + \gamma\phi} \quad (2.37)$$

which shows that a very large drop in the activity of the pore can be caused by a small amount of poisoned section γ , compared to the case of uniform poisoning.

The pore-mouth deactivation model of Wheeler, has been extended to pellets by several investigators (39, 142, 158, 163). This model is called "shell-progressive" fouling when applied to pellets.

In the shell progressive model the position of deactivated portion of the catalyst depends on the fouling mechanism. For series type fouling, the central core of the pellet is assumed to be completely deactivated in the shell model. This is due to a high concentration of the main

reaction product, upon which in the series type, the fouling depends. For parallel fouling, deposition of fouling agent is most severe in the outer layer. This would be equivalent to a shell near the external surface of the pellet which is completely deactivated in the shell model. The same kind of deactivation near the pellet exterior is expected for independent fouling.

In the shell model, time is not an inherent property of the model (142). The variation of the position of the boundary between completely fouled and fresh catalyst with time is related to the amount of disappearance of reactant in the parallel type, or the amount of formation of product in the series type, by the fouling reaction (142).

Masamune and Smith (142) investigated the behavior of an individual catalyst pellet fouled by parallel, series, and impurity mechanisms without resorting to assumptions regarding the distribution of fouled surface (uniform or shell model) within the pellet. They illustrated the method for a first-order reaction in an isothermal pellet. They used a point activity function, $(1-\gamma)$, and assumed a linear relationship between activity and the amount of fouling agent deposited on the catalyst. That is, if Q is the concentration of fouling agent on the surface when deactivation is complete, the activity function would be

$$1 - \gamma = 1 - \frac{q}{Q} \quad (2.38)$$

where q is the instantaneous fouling agent content of the catalyst. The differentiation of (2.38) when dq/dt is replaced by the corresponding rate expression, yields equation (2.33).

The mass balance conservation equation for reactant(1) with a first-order reaction within a spherical pellet is (142)

$$De \nabla^2 C_1 - \epsilon \partial C_1 / \partial t - k C_1 (1-\gamma) = 0 \quad (2.39)$$

$$\partial \gamma / \partial t = (k_d / Q) C_d (1-\gamma) \quad (2.40)$$

where C_d in (2.40) refers to reactant, product, or impurity concentration for parallel, series, or independent fouling mechanisms.

Masamune and Smith neglected the second term in equation (2.39). This is justified when the time necessary to reach steady state with respect to the accumulation of mass in the void space of the pellet is negligible with respect to the time required for the catalyst activity $(1-\gamma)$ to change significantly. This assumption is termed "pseudo-steady state" hypothesis which for all practical purposes is a valid assumption, otherwise, the catalyst could not be useful in the form of a pellet since it would be deactivated too fast to be interesting for an industrial use (42, 129). The pseudo-steady state assumption has been extensively used in the literature (45, 118, 120, 121, 127,

129, 142, 163).

Masamune and Smith solved equations (2.39) and (2.40) numerically. They evaluated the performance of the model in terms of a pellet effectiveness factor, defined as the ratio of actual rate of reaction at any particular time to the rate of reaction at zero time if the interior of the catalyst pellet were equally available for the reaction. Their numerical results show that for series fouling, activity of the catalyst is an ascending function of the pellet coordinate r , except for negligible diffusion resistance ($\phi \approx 0$). Conversely the descending activity function was observed for parallel and independent fouling mechanisms.

For series fouling, the extent of deactivation increases with diffusion resistance (ϕ) (142). This is true regardless of time, so that the preferred catalyst is one with the least diffusion resistance.

For parallel fouling, the fresh catalyst (small times) effectiveness factor decreases as diffusion resistance increases, however at large times, the effectiveness factor increases with (ϕ) (142). Hence Masamune and Smith concluded that, for parallel fouling, a catalyst with some diffusion resistance is more stable for long process times.

The method of Masamune and Smith although simple and flexible enough to treat a variety of kinetic expressions, is time consuming and the lengthy numerical procedure is its disadvantage. Hence, Masamune and Smith obtained a simple

solution by supposing that the shell-progressive model represents the deposition of the fouling material in the pellet. Based on the catalyst effectiveness factor, the authors showed that, for parallel and independent type fouling, the shell model gives results within 15% of the numerical method. For series fouling the limitation of the shell model are more serious and large deviations from the numerical solution can occur (142).

Petersen (163) used the average pellet activity versus the amount of fouling agent on the catalyst as the criterion for the comparison of the numerical results with the simpler shell model results. The average pellet activity is defined as the ratio of rate of reaction at any particular time to the reaction rate at zero time. In this definition the reaction at zero time is the observed rate which includes the diffusional resistance in the pellet.

Petersen (163) concluded that there is a significant difference between the numerical results and the shell model results for all three fouling mechanisms. That is, the observed reaction rate is sensitive to the distribution as well as the amount of fouling agent on the surface (163).

Chu (45) studied the catalyst pellet deactivation for a Langmuir-Hinshelwood single-site mechanism kinetic. His numerical results show that the distribution of the activity with pellet radius does not conform with, or even approach the shell model for any fouling mechanism.

Khang and Levenspiel (118) tested the validity of using simple rate forms to describe complex pore diffusion-deactivation interaction. With first-order main reaction, they considered the validity of

$$-R = kC_s \eta a \quad (2.41)$$

$$-\frac{da}{dt} = k_d C_s a^m \quad (2.42)$$

where η is the effectiveness factor for a reaction with a fresh catalyst. C_s refers to the concentration of reactant, product, or impurity for parallel, series, or impurity fouling mechanisms, respectively, and a is the overall or average pellet activity. The exponent m is called "the order of deactivation".

Khang's analysis shows that, for series deactivation equation (2.42) with $m=1$ satisfactorily represents the deactivating pellet for all values of ϕ as long as there is some product in the main gas stream surrounding the pellet. However, for parallel deactivation, equation (2.42) with a constant m does not adequately represent the changing pellet. The order of deactivation (m) is a function of ϕ and changes from unity to three for the extremes of no diffusional resistance to very strong diffusional resistance.

In certain reactions, such as isomerization and cracking, deactivation may be caused both by reactant and

product (118). In that case since the total concentration of product and reactant remains constant, the deactivation rate becomes independent of concentration. Krishnaswamy and Kittrell (120, 121) have considered this concentration independent deactivation mechanism.

Lee and Butt (130) and Lee (129) have considered deactivation of the catalyst pellet for a reaction with arbitrary kinetics. Lee and Butt (130) considered the limiting cases of uniform and pore-mouth deactivation, and developed an expression for pellet effectiveness factor which is suitable for direct inclusion in reactor bed conservation equations. Their pellet effectiveness factor is defined as the ratio of observed rate for the deactivated catalyst to the intrinsic rate evaluated for fresh catalyst at the pellet surface condition.

Lee (128) considered a catalyst pellet with a general nonuniform activity function. The nonuniformity of activity may be the result of deliberate design as in the case of a partially impregnated pellet, or may be due to the catalyst deactivation process. Lee's analysis resulted in a rather simple generalized approximate equation for the flux of reactant at the outer surface of the catalyst pellet. It is generalized in the sense that it is applicable to arbitrary, non-negative order kinetics and an arbitrary, spatial activity distribution function in the pellet. Lee's equation

at $r=D_p/2$ is

$$-De \frac{dC}{dr} = [2(1-\gamma_s) R^0(C) dC]^{1/2} \quad (2.43)$$

The parameter, $(1-\gamma_s)$, denotes the evaluation of the activity at the surface conditions of the pellet and C_s and C_0 are the surface and pellet center concentration of the reacting species, respectively.

According to Lee (129), the equation (2.43) is applicable to series deactivation mechanism in which case the local activity monotonically increases toward the catalyst surface as predicted by Masamune and Smith (142). For parallel fouling, this equation is applicable when the differential of activity with respect to pellet coordinate r , evaluated at the pellet surface, is not steep. That is, when the deactivation is intermediate between uniform and shell progressive deactivation.

Lee's development of equation (2.43) was based on slab geometry. However, in view of an analogy with the results of shape normalization known for pellets with uniform activity distribution (174), he recommends use of equation (2.43) for any geometry with characteristic length defined as the ratio of volume to surface area.

Do and Bailey (65) have also given a similar equation for flux at the catalyst surface with nonuniform activity function. According to Do and Bailey, equation (2.43) is valid as long as the pellet surface activity is not zero.

2.8.3 Deactivation of the Catalyst Reactor Beds

Froment and Bischoff (81) modelled an isothermal deactivating fixed-bed reactor in the absence of inter and intra-particle transport resistances. The activity function of the catalyst was expressed as an exponential and hyperbolic function of catalyst fouling agent content. These forms of deactivation functions are believed to be the result of catalyst pore blockage (11, 80).

Froment and Bischoff's results show that the bed deactivates in a descending fashion with reactor length for the parallel mechanism. The converse is true for a series mechanism. These observations are consistent with the results of Masamune and Smith (142) for a single pellet.

Froment and Bischoff found that in the descending deactivation profile, the locus of maximum reaction rate would travel down the bed as time progresses; for large times, the entire reaction, although of plug flow type, would operate at a nearly uniform reaction rate.

For nonisothermal beds, the maximum reaction rate would be reflected as the maximum temperature rise for exothermic reactions. Menon et al. (150) observed such a moving maximum temperature loci experimentally for the air-oxidation of H_2S on activated carbon. There, the sulfur formed as the product progressively covered the catalyst surface.

Weng et al. (210) modelled a nonisothermal, nonadiabatic deactivating fixed-bed reactor using benzene hydrogenation as the model reaction poisoned by thiophene.

They considered a one-dimensional pseudo-steady state model, and neglected inter and intra-particle transport resistances but included the axial dispersion in their model. They, however, found that the axial mass dispersion had only a very small effect on the computed temperature profile.

Weng et al. (210) observed that the rate of migration of the hot spot obtained experimentally is more rapid than that predicted from the model. The calculation was found to be sensitive to the value of Q , the maximum adsorption capacity for thiophene. The authors had to set Q at 0.4 of the experimentally determined value to obtain a good correlation between theory and experiment. This effect has been attributed to the possibility of activity of only 40% of total sites available for thiophene chemisorption toward benzene hydrogenation.

Billimoria and Butt (18) investigated the transients involved in the start-up or ignition of the reaction in both a fresh and a partially deactivated bed. They also employed poisoning hydrogenation of benzene by thiophene as the model of the deactivating reaction. Their model is the same as that of Weng et al. (210), but does not assume pseudo-steady state.

Billimoria and Butt (18) have shown that there are three distinct time zones for temperature and concentration profiles. During the first, termed the fast motion (FM) zone, the concentration profile develops rapidly with no change in the temperature profile. Subsequently, another

zone called the first slow motion (SM(I)) zone, arises during which the temperature profile evolves to its final shape with concomitant changes in the concentration profile. During the third zone (SM(II)), the profiles retain their shape and migrate down the bed.

The author's results indicate that the time necessary to reach pseudo-steady state (end of SM(I) zone), ranges between half an hour to two hours depending on the inlet temperature, concentration, and catalyst diluent.

Bhatia and Hlavacek (16) also modelled a pseudo-steady state nonadaibatic packed bed reactor for poisoning of hydrogenation of benzene by thiophene. Their reactor is of industrial size and in that respect is different from the one used by Weng and Billimoria. The authors ignored the intrusions of interphase, intraparticle gradients, and axial dispersion processes. Their major purpose was to compare the one and two-dimensional models of the deactivating beds.

Bhatia and Hlavacek (16) results show that there is a very good agreement between the one and two-dimensional models. There is small difference in the vicinity of the hot spots. The concentration profiles are however identical for both models. The radial activity profile is found to be a simple parabola-like function with a minimum in the center of the reactor. However if the activation energy for the poisoning reaction is increased to a very high number (30,000 cal/mol) then, the activity would be very sensitive to the temperature profile and the prediction of the one and

two dimensional models could differ. The activity profile can also be affected by the concentration profile in wide beds (16). The complex interaction of the effect of temperature and concentration on the activity then, may result in radial profiles of activity with a minimum outside the reactor axis (16).

The high activation energy of the deactivation kinetics causes a different deactivation process than the expected "travelling wave" profile (16). In this case a "standing wave" of activity in the reactor results which propagates slowly toward the inlet as well as the exit of the reactor (16). The temperature profile then will also show a standing wave profile. The position of the hot spot is not then very sensitive to the degree of the deactivation and decreases in value as time increases (16).

Bhatia and Hlavacek (16) concluded that the pseudo-steady state model without dispersion can satisfactorily describe the majority of deactivation processes taking place in industrial packed bed reactors. They recommend use of two-dimensional model only for a high-activation-energy deactivation processes in large diameter reactors.

3. KINETICS AND EQUILIBRIUM ASPECTS OF THE CLAUS PROCESS

3.1 Free Energy Minimization

In systems of chemical reactions, it is desirable to know the distribution of products that is expected at thermodynamic equilibrium. This will represent the maximum obtainable conversion, or a distribution that is to be avoided by the use of a selective catalyst or a short contact time.

One of the methods of predicting the thermodynamic equilibrium composition in a system of multiple equilibrium reactions is free energy minimization. This procedure does not consider the individual equilibrium reactions, rather a general mathematical technique is used to predict a minimum free energy for the system.

The free energy minimization method was introduced by White et al. (213) for the gaseous species and extended by Oliver et al. (159) to include condensed phases.

The method of White et al. and the corresponding computer program for prediction of equilibria in a system of multiple equilibrium reactions has been reviewed by McGregor (148). In his program the free energy of the species is expressed as a polynomial function of temperature, where the coefficients of the polynomial function should be provided as the input.

Liu (135) modified McGregor's program to accommodate the condensed species. However, as in the original program,

the coefficients of the free energy polynomial should be read in for both gaseous and condensed species. Truon's (199) version of free energy minimization is that of Liu's but it evaluates the free energy of the species from the standard heat of formation, entropy, and the heat capacity correlations.

The reading in of the coefficients of the free energy polynomials of each species is a nuisance, especially for frequent use of the program in a system which contains many chemical species such as in the Claus process. Here, Liu's program has been modified to read the coefficients of the free energy polynomial from the data file. The data file is general in a sense that it contains the data necessary for all the species encountered in the Claus process. The data file defines each species in terms of the elements H, C, O, S, and N.

The coefficient matrix of the elemental mass balance equations becomes singular for systems of chemical species which lack one of the above mentioned five elements. The system of H_2S , SO_2 , H_2O , N_2 , and sulfur species, for example lack species with carbon elements. The singularity problem due to use of the general data file has been dealt with in the program. The program checks for the presence of a column of zeros in the coefficient matrix of the elemental mass balance equations and eliminates it. Then it proceeds to find the minimum free energy by the same procedure as used by McGregor and by Liu.

The program code and the data file have been presented in Appendix A.

3.2 Claus Process Equilibrium in the Presence of Liquid Sulfur

During this study, the equilibrium composition and conversion in the presence of liquid sulfur were determined by imposing the constraint, that the partial pressure of sulfur in the vapor may not exceed the vapor pressure of sulfur at the given temperature. This constraint implied that the condensed sulfur is pure. Truong (199) has also used the vapor pressure constraint for the equilibrium analysis in the presence of liquid sulfur. She, however, has not given any information on the mathematical procedure whereby this constraint was implemented.

In this thesis two methods have been used for the equilibrium calculation in the presence of the liquid sulfur. The first method is intuitively logical, while the second method is basically a trial and error method. The basic assumption in both methods requires that the gases behave ideally.

3.2.1 Mathematical Analysis of the Method A.

The total dimensionless free energy of a mixture of gaseous species is expressed as,

$$G(x) = \sum_{i=1}^N g_i \quad (3.1)$$

The free energy contributed by the gaseous species is given by:

$$g_i = x_i \{ g f_i + \ln x_i / x \} \quad (3.2)$$

$$g f_i = \left(\frac{G^\circ}{Rg - T} \right)_i + \ln \Pi \quad (3.3)$$

The determination of the equilibrium composition requires finding a non-negative set of mole number, x_i , which will minimize $G(x)$. In the presence of liquid sulfur this set must satisfy the mass balance consideration for all chemical elements present except sulfur. Due to condensation of some of the sulfur, the mass balance equation for sulfur in the gas phase is not satisfied. Instead, the vapor pressure constraint should be satisfied. In mathematical terms the mass balances are represented by the equations,

$$\sum_{i=1}^{N_1} a_{ij} x_i = b_j \quad (3.4)$$

$$j = 1, \dots, m-1$$

and the vapor pressure constraint by,

$$\beta \sum_{i=1}^{N_1} x_i = \sum_{i=N_1+1}^N x_i \quad (3.5)$$

where, a_{ij} is the number of atoms of element j in a molecule

of species i , and b_j is the total number of atomic weights of element j originally present in the mixture. The species numbers 1 to N , are the species other than sulfur species. The number, N , is the total number of species, and m is the number of chemical elements present with S as the m -th element. The parameter, β , is the ratio $P_v/(\Pi - P_v)$.

The method of solution is that of White et al. (213) which is reviewed by McGregor (148). However, it is necessary to present the mathematical steps because of the peculiarities introduced by constraint (3.5).

Let $y = (y_1, y_2, \dots, y_N)$ be an initial guess for the mole numbers of the gaseous species. The vector y should be chosen as a positive set that satisfies the constraints (3.4) and (3.5). The free energy of the system is then,

$$G(y) = \sum_{i=1}^N y_i \{gf_i + \ln y_i / \bar{y}\} \quad (3.6)$$

where

$$\bar{y} = \sum_{i=1}^N y_i \quad (3.7)$$

let

$$\begin{aligned} \Delta_i &= x_i - y_i \\ \Delta' &= x - \bar{y} \\ f_i &= gf_i + \ln y_i / \bar{y} \end{aligned}$$

An expression, $Q(x)$ is obtained as an approximation for $G(x)$ by using a Taylor expansion about the initial guess, y :

$$Q(x) = G(y) + \sum_{i=1}^N f_i \Delta_i + \frac{1}{2} \sum_{i=1}^N y_i (\Delta_i / y_i - \Delta' / y)^2 \quad (3.8)$$

In the original paper of White et al. (213) which is the basis of the free energy minimization method since 1958, a term in the first derivative of $G(x)$ has been neglected. The correct first derivative of $G(x)$ is

$$\partial G(x) / \partial x_i = [g f_i + \ln (x_i / x)] + [1 - x_i / x] \quad (3.9)$$

If $[1 - x_i / x]$ in equation (3.9) is neglected, equation (3.8) would be obtained for the quadratic approximation of $G(x)$. Otherwise the correct quadratic approximation of $G(x)$ is,

$$Q'(x) = Q(x) + \sum_{i=1}^N (1 - y_i / y - 0.5 \Delta' / y) \Delta_i + 0.5 \sum_{i=1}^N (y_i / y^2 - 1.5 / y) \Delta_i^2 + 0.75 \Delta'^2 / y \quad (3.10)$$

Table 3.1 compares the equilibrium prediction of the Claus mixture by equilibrium constant method and by free energy minimization method employing equation (3.8). The data in table 3.1 cover the range of gas phase up to approximately saturation point for sulfur. It is apparent that in the gaseous phase the two methods predict the same equilibrium conversion. Thus the term $(1 - x_i / x)$ in equation

Table 3.1 Comparison of equilibrium conversion prediction by free energy minimization and equilibrium constant method.

Pressure atm(10^3) ; Temperature K

T	Pv	Ps(Eq.)	X(Eq.) ¹	X(Eq.) ²
700	762.7	7.6	0.30588	0.30587
600	122.7	10.2	0.66427	0.66575
550	36.2	11.8	0.80901	0.80964
515	12.8	12.7	0.88247	0.88246

1 Free energy minimization method.

2 Equilibrium constant method.

(3.9) seems to be unimportant, at least for the Claus gas. In the derivation of method A which follows, equation (3.8) is used for approximation of $G(x)$.

The equation (3.2) is based on the assumption that the gases form an ideal gas mixture, which would only be the case if there were no attractive or repulsive forces between the molecules. Since sulfur is condensing, the attractive forces must be considered. In that case the term $(x_i \ln \phi_i')$ has to be added to equation (3.2). The fugacity coefficient of the sulfur species is 0.00013 at 450 K as shown in table A.2. Thus g_i for sulfur species will be lower than obtained from equation (3.2). A lower g_i for sulfur species will cause the equilibrium point of the Claus reaction to lie further to the right. Considering the above, the equilibrium

conversion calculation based on ideal gas mixture approximation will introduce some error and predicts a conservative equilibrium conversion.

In order to find a better approximation to the desired solution, $Q(x)$ is minimized subject to the mass balance coefficients. It is first required to define $G_1(x)$ as,

$$G_1(x) = Q(x) + \sum_{j=1}^{m-1} \pi_j (b_j - \sum_{i=1}^{N_1} a_{ij} x_i) +$$

$$\lambda \left(\beta \sum_{i=1}^{N_1} x_i - \sum_{i=N_1+1}^N x_i \right) \quad (3.11)$$

where, π_j and λ are Lagrange multipliers. To get a new estimate of composition, $\partial G_1 / \partial x_i$ is set equal to zero and x_i is calculated from its solution as,

$$x_i = \sum_{j=1}^{m-1} \pi_j a_{ij} y_i + (x/y) y_i - y_i f_i - \lambda \beta y_i \quad \text{for } i=1, 2, \dots, N_1 \quad (3.12)$$

$$x_i = \lambda y_i + (x/y) y_i - y_i f_i \quad \text{for } i=N_1+1, \dots, N \quad (3.13)$$

Summing (3.12) over $i=1, \dots, N_1$ and (3.13) over $i=N_1+1, \dots, N$, adding the results, and using equations (3.4), (3.6), and (3.7) yields,

$$\sum_{j=1}^{m-1} \pi_j b_j = G(y) \quad (3.14)$$

Substitution of (3.12) into (3.4) yields $(m-1)$ equations in the unknown π_1, \dots, π_{m-1} , x/y , and λ as follows,

$$\begin{aligned} \pi_1 r_{k1} + \pi_2 r_{k2} + \dots + \pi_{m-1} r_{k(m-1)} + (x/y) b_k - \lambda \beta b_k \\ = b_k + \sum_{i=1}^{N_1} a_{ik} y_i f_i \quad \text{for } k=1, 2, \dots, (m-1). \end{aligned} \quad (3.15)$$

where

$$r_{kj} = r_{jk} = \sum_{i=1}^{N_1} a_{ij} a_{ik} y_i \quad (3.16)$$

Substitution of (3.12) and (3.13) into (3.5) yields,

$$\begin{aligned} \sum_{j=1}^{m-1} b_j \pi_j - \lambda \beta \sum_{i=1}^{N_1} y_i - (\lambda \beta) (1/\beta^2) \sum_{i=N_1+1}^N y_i \\ = \sum_{i=1}^{N_1} y_i f_i - 1/\beta \sum_{i=N_1+1}^N y_i f_i \end{aligned} \quad (3.17)$$

Solution of the system of equation (3.12) to (3.17) yields the Lagrange multipliers, π_1 to π_{m-1} , the product, $(\lambda\beta)$, and the ratio, (x/y) . The product $(\lambda\beta)$ has been used as the unknown rather than λ (β is known), to reduce the condition number of the coefficient matrix in the system of equations (3.12) to (3.17).

The determined values of the Lagrange multipliers, $(\lambda\beta)$, and x/y are then substituted in equations (3.12) and

(3.13) to find the new estimate of the composition. The procedure is repeated until the difference between subsequent iterations is small enough to satisfy some arbitrary convergence criterion.

3.2.2 Trial and Error Method - Method I

This method minimizes the free energy of the gaseous species under the constraint of the mass balance equation (3.4) for all of the chemical elements present including sulfur at each trial.

In the first trial the condensation of the sulfur is ignored i.e., the total number of atom equivalent of sulfur originally present in the mixture, b_m , is assumed to be present in the gas phase. The free energy minimization using the above assumption yields the equilibrium composition from which the partial pressure of the sulfur species is calculated and is compared with the vapor pressure of sulfur. If it exceeds the vapor pressure, then the atom equivalent of sulfur in the gas phase is reduced and the new equilibrium composition is predicted. The procedure is continued until the sulfur partial pressure matches its vapor pressure within the acceptable accuracy limit.

3.2.3 Results of the Analysis of the Claus Process

Equilibria in the Presence of Liquid Sulfur

The results of the above two methods are given in Appendix A. Table 3.2 compares the results.

Table 3.2 Equilibrium in the Presence of Liquid Sulfur. $T=450\text{ K}$, $\Pi=1\text{ atm}$

Method	% H_2S Conversion	Free Energy
A	10.5	-42.232
B	98.3	-42.094
Ignoring Condensation ($P_s > P_v$)	97.4	-42.636

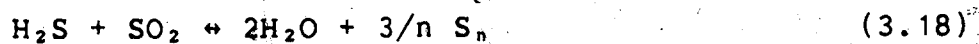
Method A, finds a composition which results in a lower free energy compared to that obtained by method B. However, this composition is not physically correct, because it predicts a much lower conversion even compared to the predicted conversion when the formation of liquid sulfur is neglected. Theoretically, it is expected that the formation of liquid sulfur would shift the equilibrium to higher levels of H_2S conversion. That is, method B provides the correct prediction.

Method A, with different initial feasible solution converges to the same conversion. Method A although logically right and results in a lower system free energy, is not suitable for the prediction of equilibrium conversion in the presence of liquid sulfur. The inaccuracy of method A is probably due to the flat nature of free energy surface. For example, data of Appendix A and table 3.2 show that although there is not much difference in the magnitude of free energy, there is a great difference in the predicted equilibrium composition and thus equilibrium conversion between methods A and B.

The error might also be due to the use of equation (3.8) rather than equation (3.10) for the expansion of $G(x)$. The error in the gas phase calculation was shown to be negligible (table 3.1), however this may not be true when sulfur condenses.

3.3 Claus Reaction as a Set of Parallel Reactions

Previous studies of Claus reaction (14, 23, 56, 57, 67, 135, 148, 169) have represented the Claus reaction as,

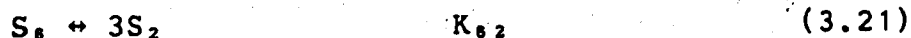


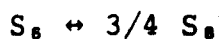
where n is the average number of atoms per molecule of sulfur vapor and ranges from 1 to 8 depending on the temperature and pressure of sulfur vapor. The number, n , is calculated from material balances as,

$$n = \frac{\sum_{i=1}^8 i x(S_i)}{\sum_{i=1}^8 x(S_i)} \quad (3.19)$$

where $x(S_i)$ is moles of sulfur species S_i in the sulfur vapor. Under the Claus catalytic convertor conditions, the value of n lies between 6 and 8. Reaction (3.18) then, represents the Claus reaction in terms of a sulfur polymer with a noninteger number of sulfur atoms, which is physically impossible.

In this study the catalytic chemistry of the Claus reaction is described by a set of parallel reactions. Reliable thermodynamic properties for odd-numbered sulfur species are unavailable (42). Also, the existing "best" thermodynamic properties predict that the contribution to the composition of the sulfur vapor by the odd-numbered sulfur species may be ignored at the Claus catalytic bed temperatures. Hence, in this study the sulfur vapor model of even-numbered species S_2 - S_4 - S_6 - S_8 has been employed. Then, in the absence of reactive gaseous impurities, the catalytic Claus reaction with even-numbered sulfur species model is represented as,




 K_{s_2}

(3.23)

The high temperature combustion of an acid gas in the furnace gives rise to the production of COS and CS₂, as was discussed in section 2.2. These sulfur compounds undergo partial hydrolysis in the catalytic convertors. This hydrolysis is most noticeable in the first convertor and becomes negligible in the following convertors (93). Typical feed to the catalytic Claus convertor contains about 0.3 % COS and 0.3 % CS₂ (93). In this study, the hydrolysis reactions of these species are neglected due to the lack of reliable kinetic rate expressions and their low concentrations compared to those of H₂S and SO₂ in the first convertor. Thus, COS and CS₂ are treated as non-reactive impurities and act as inerts towards Claus reactions.

The dynamics of formation and equilibration of the sulfur species is not fully known but is believed to be sufficiently rapid in the condensed phase (49) (on the catalyst surface) that S₈ and S₂ are already formed. In light of the above, the major assumption made is that reactions (3.21) to (3.23) are at equilibrium. The selection of S₈ in reaction (3.20) is arbitrary.

3.4 Sulfur Vapor Composition for Nonequilibrium Conversion Levels.

Using available thermodynamic properties and the free energy minimization approach, the equilibrium composition

attained for the combined reactions (3.20) to (3.23) may, in principle, be predicted. However, in the catalytic convertors, the conversion of H_2S varies as the gas moves down the bed. In the modelling of such a convertor, it is desired to know the concentration or partial pressure of all the species, including sulfur species, along the bed. The following is the analytical approach used to calculate the amount of the gas and sulfur species for any specified H_2S conversion level.

Let X be the conversion of H_2S relative to the H_2S content of a mole of inlet gas with composition of Y_1 , Y_2 , Y_3 , Y_{inert} . Mass balances under the constraint imposed by the stoichiometry of reaction (3.20) yields,

$$N_t = 1 - (1/2) Y_1 X + x(S_2) + x(S_4) + x(S_6) + x(S_8) \quad (3.24)$$

Performing a mass balance on the basis of atomic sulfur yields,

$$2x(S_2) + 4x(S_4) + 6x(S_6) + 8x(S_8) = (3/2) Y_1 X \quad (3.25)$$

For chemical reactions of ideal gases, $K = K_p$, hence

$$x(S_2)^2 = (K_{S_2})^{1/3} (N_t/\Pi)^{2/3} \{x(S_8)\}^{1/3} \quad (3.26)$$

$$x(S_4)^2 = (K_{S_4})^{2/3} (N_t/\Pi)^{1/3} \{x(S_8)\}^{2/3} \quad (3.27)$$

$$x(S_6)^2 = (K_{S_6})^{4/3} (\Pi/N_t)^{1/3} \{x(S_8)\}^{4/3} \quad (3.28)$$

Substituting (3.26) to (3.28) into (3.24) and (3.25) yields two non-linear algebraic equations in terms of two unknowns N_t and $x(S_2)$. The resulting two non-linear equations, their method of solution, and the program code are given in Appendix B.

The equilibrium constants of reactions (3.20) to (3.23) have been calculated from the standard free energy change associated with reactions (3.20) to (3.23). The equilibrium constants have been correlated with temperature, using Rau's (171) thermodynamic data for sulfur species and JANAF (193) data for all the other species,

$$\ln K = 11050/T - 11.56 \quad (3.29)$$

$$\ln K_{s_2} = -34173/T + 37.97 \quad (3.30)$$

$$\ln K_{s_4} = -13664/T + 12.60 \quad (3.31)$$

$$\ln K_{s_8} = 2932/T - 3.43 \quad (3.32)$$

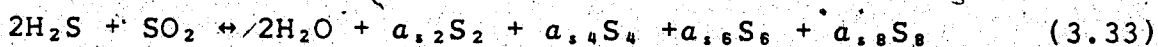
The program output for the calculation of the gas composition for different levels of conversions is given in table B.1, Appendix B.

3.5 Heat of Claus Reaction

The heat of reaction for equation (3.18) depends on the sulfur vapor composition and is usually given as a range of values (44,95,145). It is shown in section 3.4 and Appendix B, that the sulfur vapor equilibrium composition depends on the level of H_2S conversion at any specific temperature.

Subsequently, then, the heat of reaction should also depend on the local value of the H_2S conversion level at any given temperature.

To calculate the heat of the Claus reaction, the system of reactions (3.20) to (3.23) is represented as,



This form of an overall reaction is justified because it was assumed that the reactions (3.21) to (3.23) are at equilibrium (see section 3.3). The sulfur species stoichiometric coefficients $a_{.2}$ to $a_{.8}$ are required to satisfy,

$$2a_{.2} + 4a_{.4} + 6a_{.6} + 8a_{.8} = 3 \quad (3.34)$$

The stoichiometric coefficients are obtained from the values of $x(S_2)$ to $x(S_8)$ calculated by the method developed in section 3.4. Their relation is,

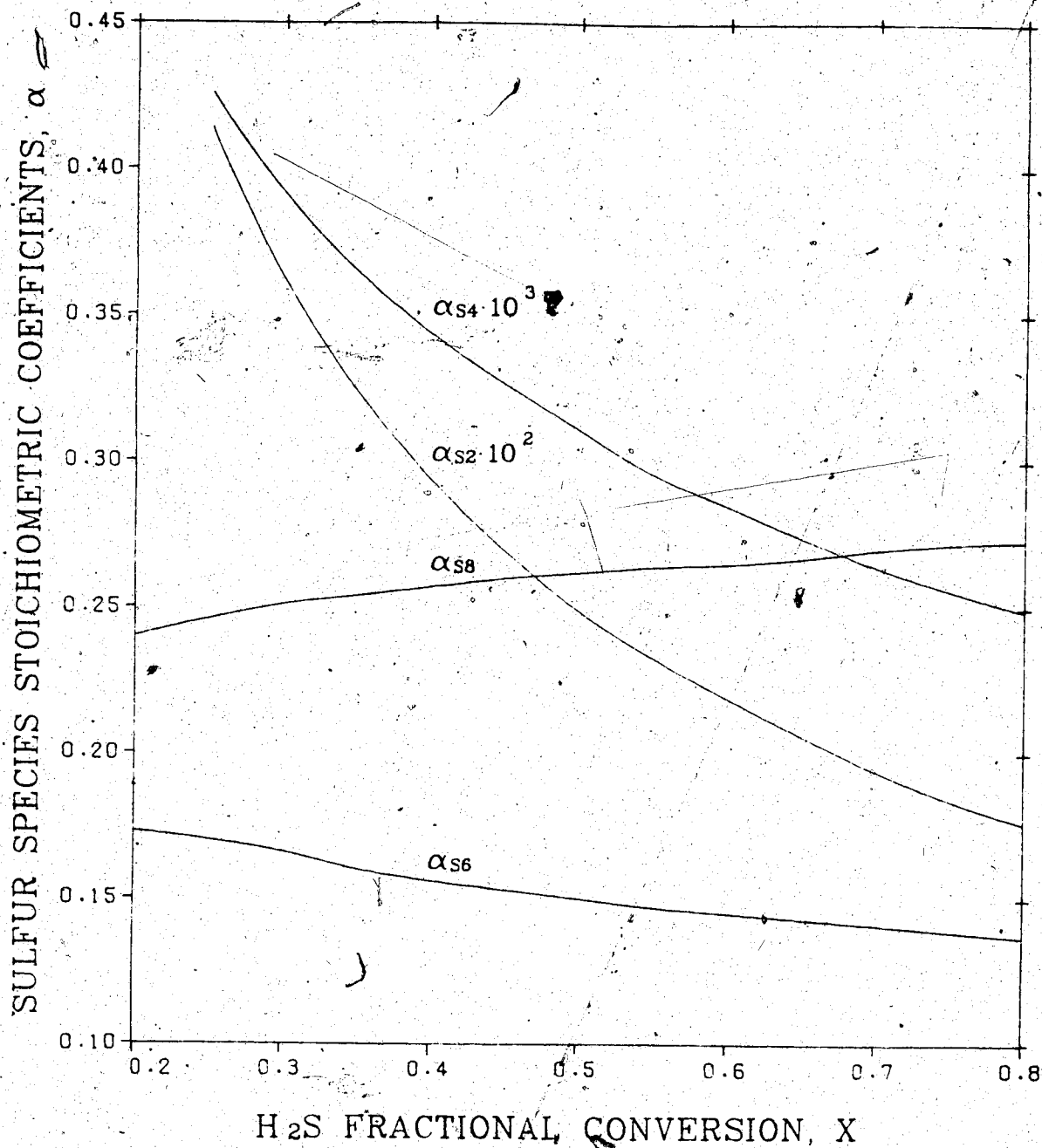
$$a_{.i} = 2 x(S_i) / (Y_1 X) \quad (3.35)$$

$i = 2, 4, 6, 8$

The stoichiometric coefficients and the thermodynamic properties can then be used to evaluate the heat of reaction by standard procedures (188).

Figure 3.1 shows how the stoichiometric coefficients of sulfur species in reaction (3.33) would change with the H_2S

Figure 3.1 Stoichiometric coefficients of sulfur species
 Inlet composition (mole fraction): $\text{H}_2\text{S} = 0.07$,
 $\text{SO}_2 = 0.035$, $\text{H}_2\text{O} = 0.25$, $\text{N}_2 = 0.645$
 Temperature = 550 K
 Pressure = 1 atm



conversion level at constant temperature of 550 K. The program output from which the data for the graph were obtained is given in table B.1.

The changes in conversion level imply changes in sulfur vapor partial pressure (P_s). Figure 3.1 would then also represent the variation of sulfur vapor composition due to the changes of P_s at the constant temperature of 550 K. This variation is shown in figure 3.2. The ordinate $Y(S_i)$ and P_s are defined as,

$$Y(S_i) = \frac{x(S_i)}{x(S_2) + x(S_4) + x(S_6) + x(S_8)}$$

$$= \frac{a_{s,i}}{a_{s,2} + a_{s,4} + a_{s,6} + a_{s,8}} \quad (3.36)$$

$$P_s = \{x(S_2) + x(S_4) + x(S_6) + x(S_8)\}P/Nt \quad (3.37)$$

The dependence of sulfur vapor composition upon its partial pressure has also been considered by McGregor (148), Liu (135), and Cho (44), in their analyses of material balance equations. They, however, expressed the Claus reaction as reaction (3.18). In order to evaluate n , the average number of atoms per molecule of sulfur vapor at different levels of H_2S conversion, they employed a trial and error method and used free energy minimization.

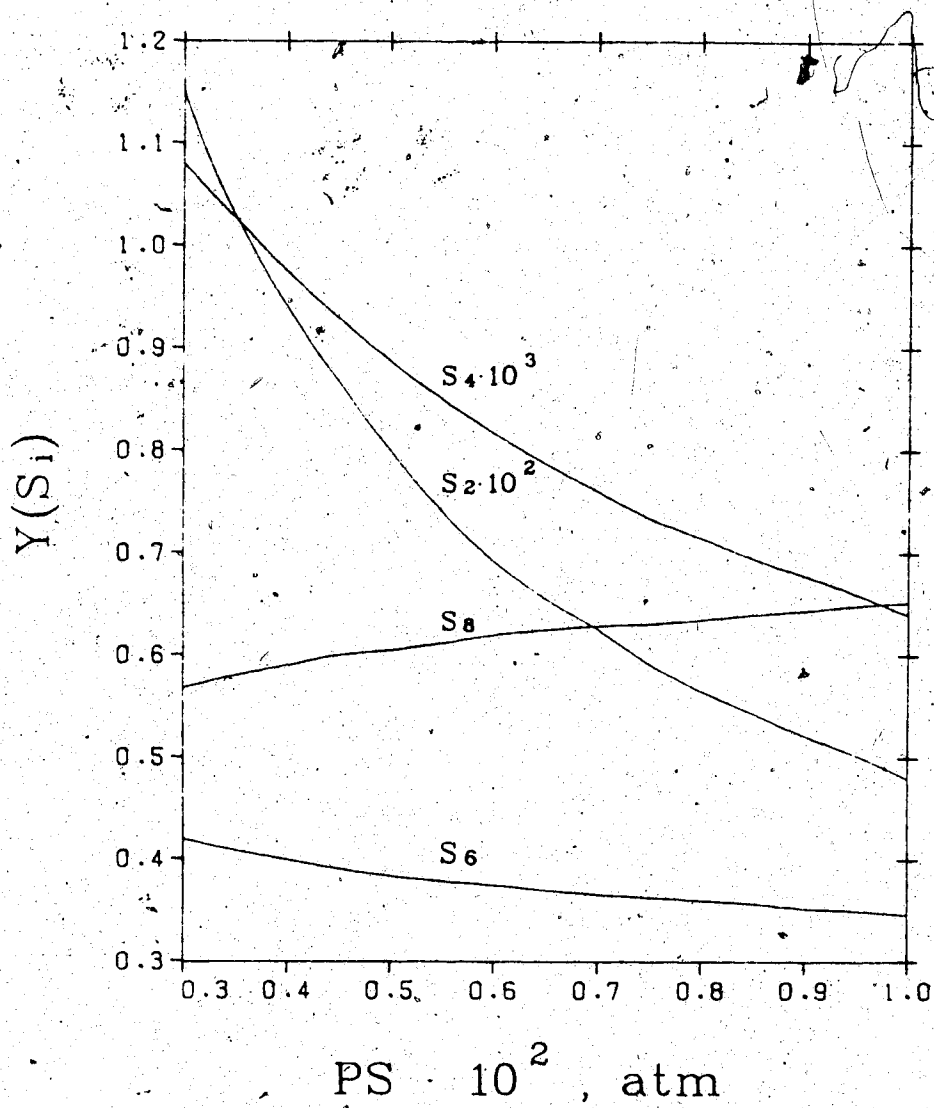
Their method was to assume a value of n and use it with the stoichiometric coefficients of reaction (3.18) to calculate the sulfur partial pressure P_s . Then the free

Figure 3.2 Sulfur vapor composition

Inlet composition (mole fraction): $\text{H}_2\text{S} = 0.07$, $\text{SO}_2 = 0.035$, $\text{H}_2\text{O} = 0.25$, $\text{N}_2 = 0.645$

Temperature = 550 K

Pressure = 1 atm



energy minimization routine, given the value of P_s was used to calculate the average molecular weight of sulfur and n . The latest value of n was compared to the assumed one and if the error exceeded 0.5%, the latest value of n was used for the next guess. Then the cycle continued until the error criterion was satisfied.

One of the major advantages of representing the Claus reaction by a set of four reactions (3.20) to (3.23), is the elimination of the lengthy trial and error and free energy minimization procedure. The method of section 3.4 could be used conveniently to calculate the concentration of the individual species for any level of H_2S conversion.

The heat of reaction as a function of H_2S conversion is shown in figure 3.3. Selected values are in table 3.3. In the low conversion region there is a sharp increase in the heat of reaction as the conversion increases.

The heat of reaction increases by 30% of its value at 0.001 conversion level, when the conversion increases by 0.1. However, as the conversion increases from 0.1 to 0.8, there is only a 2% increase in the heat of reaction compared to the value at the conversion level of 0.1.

3.6 Thermodynamically Consistent Claus Rate Expression

In the modelling of the catalytic Claus reaction, the correct intrinsic rate function should be used. The literature available on the Claus reaction rate expression has been summarized in table 2.1:

Figure 3.3 Heat of Claus reaction

Inlet composition (mole fraction): $\text{H}_2\text{S} = 0.07$, $\text{SO}_2 = 0.035$, $\text{H}_2\text{O} = 0.25$, $\text{N}_2 = 0.645$

Temperature = 550 K

Pressure = 1 atm

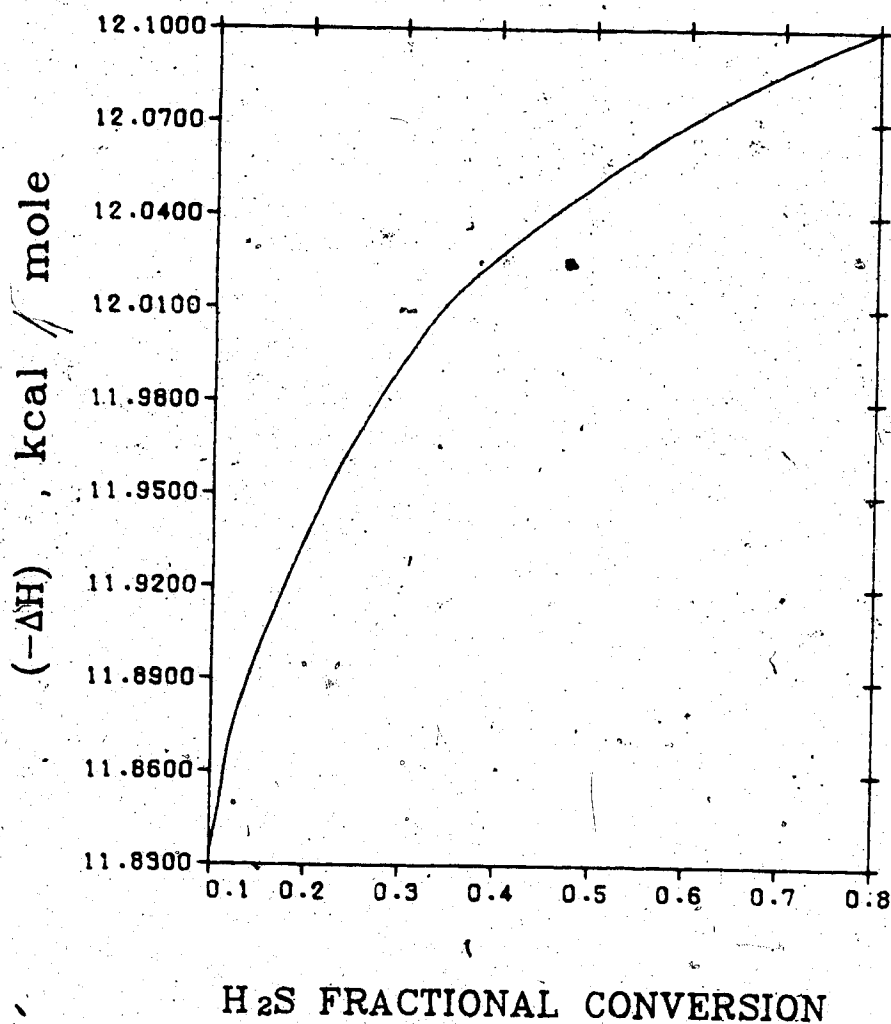


Table 3.3 Heat of Claus Reaction at 550 K¹

H ₂ S Conversion	-ΔH cal/mol H ₂ S
0.001	9072
0.01	11833
0.5	12051
0.8	12099
0.816(equilibrium)	12101

The most reliable forward rate expression is equation (2.10). This expression is believed to be free of inter-intra particle diffusional limitations. The similarity in form between equations (2.10) and (2.7), independently obtained for two different alumina-based catalysts in two different laboratory reactors, suggests that the same catalytic mechanism applies to both γ -alumina and bauxite catalysts. This generality and the intrinsic nature of equation (2.10) justifies incorporating this form of forward rate expression into more detailed fixed-bed reactor models.

The equation (2.10) is, however, expressed without the reverse reaction rate term. Liu (135) observed that the effect of the reverse reaction is negligible in magnitude compared to the forward reaction rate under industrial operation conditions.

¹ Initial composition (mole fraction): H₂S=0.07, SO₂=0.035, H₂O=0.25, N₂=0.645

The existence of a limiting equilibrium conversion in the set of reactions (3.20) to (3.23), would necessitate incorporation of a reverse reaction rate term, although its contribution to the concentration profile might not be significant.

The reverse reaction rate expression (2.13) was not used in this study because, the order of reaction with respect to sulfur is thermodynamically inconsistent. Furthermore, for non-elementary processes, it is not correct to estimate the net rate of disappearance of reactant by simply subtracting the initial rate equation of the reverse reaction from the initial rate expression of the forward reaction (189).

In this study, to extend the generality of the rate expression (2.10) to the reverse reaction, the principle of thermodynamic consistency (61) was employed to formulate the reverse rate expression. Based upon the forward rate expression (2.10), the following reverse rate expression for reaction (3.20) results (27,61),

$$R_{r1} = (k_f/K^m) (1 + 0.006 P_3)^{-2} (P_3^{2m} P_6^{0.5m} / P_1^{2m-1} P_2^{-0.5}) \quad (3.38)$$

Upon selecting $m=1/2$, a thermodynamically consistent overall rate expression would be,

$$-R_1 = k_f [P_1 \sqrt{P_2} - P_3 P_6^{0.25} / \sqrt{K}] [1 + 0.006 P_3]^{-2} \quad (3.39)$$

The temperature dependency of k_f is shown in equation (2.10) and that of the equilibrium constant, K , is predicted via thermodynamic analysis. Its method of determination is presented in Appendix B. Within the range of temperatures encountered in Claus convertors, the equilibrium constant for the adsorption of water vapor on alumina is relatively insensitive to temperature.

The correct equilibrium constant for use in equation (3.39) is K_p rather than K . It is shown in section A.2 that,

$$K_p = K/K\phi'' \quad (3.40)$$

For ideal gases where $K\phi''$ is unity, K_p is equal to K . The ideal gas law is inherent in the calculation procedure through out this thesis.

It is shown in section A.1 that at high furnace temperature, the Claus gas behaves ideally. At the reactor conditions the fugacity coefficient of all the species except sulfur is very close to unity. Hence, the error in assuming the Claus gas as an ideal gas is due to nonideality of sulfur species. The critical properties of sulfur as used in section A.1 for prediction of fugacity coefficient are mixture properties. The average number of sulfur atoms in the sulfur molecule at these critical conditions is 2.78, while at the reactor temperature S_8 and S_6 are dominant.

This makes the validity of using one set of critical properties for all the sulfur species to be questionable. However, using the mixture properties for S_8 , $K\phi''$ is estimated in section A.2 to have very low value of 0.0104 and 0.0672 at 450 and 550 K, respectively. Then by equation (3.40) K_p equals to 96K and 14.9K at 450 and 550 K.

These large values of K_p compared to K imply that the equilibrium of reaction (3.20) would shift to the right compared to the calculated equilibrium assuming ideal gas behaviour. This might be one of the reasons why the predicted equilibrium conversion of H_2S is reported to be less than the observed equilibrium conversion (section 2.3).

Equation (3.39) was employed in this study as the intrinsic overall rate of disappearance of H_2S .

4. MODELS OF CLAUS CATALYST PELLET

4.1 Introduction

Various kinds of mathematical models for a catalytic fixed bed reactor have already been discussed in the literature survey. The first step to be taken before choosing any proper model for the Claus catalytic convertor is to decide whether the catalyst pellet transport resistances are important.

It was shown in chapter 2, that the intra-particle transport limitation is frequently reduced to a lumped parameter, namely the effectiveness factor. The appropriate choice of a calculation method for the Claus catalyst effectiveness factor can reduce much of the computing time since the effectiveness factor should be repeatedly calculated along the reactor bed to obtain an accurate prediction of the reaction path through the bed.

It was shown in chapter 3, that the performance of the catalyst particles in the industrially important, modified Claus reaction introduces multiple reactions, sulfur vapor equilibria, nonlinear kinetics and limiting thermodynamic conversions into the calculation of local effectiveness factors. This chapter demonstrates a means for generating the local effectiveness factor, η , for the Claus pellets. A possible simplification of the effectiveness factor calculation for Claus catalyst pellets will also be presented.

The criteria suggested in the literature (36,146), for assuming particulate isothermality are based on the observations in the simple linear kinetic case. These criteria are based on the value of the Prater number which is a measure of the maximum possible internal temperature gradient. The Prater number ξ' is defined as,

$$\xi' = \frac{\Delta T_m}{T_s} = \frac{(-\Delta H) De C_s}{k_s T_s} \quad (4.1)$$

The parameter, ξ' , depends on the effective thermal conductivity k_s for which data are very limited. Smith, et al. (190) have shown that a modest value of ξ' , dramatically increases η for a certain Langmuir-Hinshelwood mechanism. However, in the simple linear kinetic case, the same value of the Prater number yields a value of η about identical to the isothermal value.

In light of the above, both nonisothermal and isothermal models of the Claus pellet will be considered in this study.

In a multicomponent system, the diffusional flux relationship for the various molecular species may become strongly coupled (6,191). However, they are uncoupled when Knudsen diffusion occurs in the pores. It was shown in Chapter 2, that the diffusional flux relationships could also be simplified by the use of an effective diffusivity parameter calculated at some average composition.

In this study the concept of an effective diffusivity has been used to express the diffusional flux of the various species. An average pore radius of about 8 nm has been determined for the alumina catalyst (46). In this pore size, the Knudsen diffusion is predominant. Hence, the use of an effective diffusivity for uncoupling of the diffusional fluxes is expected to introduce negligible error. The calculated values of the effective diffusivities of the different species are given in Appendix G.

In the typical Claus convertor, the pressure drop is estimated by Ergun equation to be of order 0.2% of the total pressure. Hence in the modelling of Claus pellet and convertors a constant total pressure is assumed. It is also assumed that the gases behave ideally.

4.2 Nonisothermal Claus Pellets

Using the criterion of McGreavy and Cresswell (146), that isothermal interiors occur when $\xi/\delta=4$, the Claus particles would be expected to exhibit isothermal interiors. However, as it was pointed out earlier, this criterion is based on the simple linear kinetics case. Here the effect of nonisothermality of the Claus particle will be studied parametrically. That is, it is desired to check mainly the conditions that could affect the temperature profile and consequently the effectiveness factor compared to the isothermal pellets.

To describe reactions (3.20) to (3.23) occurring within a spherical catalyst pellet, material balance equations are required for each independent species participating in the reaction. For reaction (3.20) specifying its four reactants is sufficient because the sulfur species other than S_6 are thermodynamically dependent upon the concentration of S_6 . At steady-state, differential material balances for H_2S , SO_2 , and H_2O are obtained,

$$\frac{d^2 C_i}{dr^2} + \frac{2}{r} \frac{dC_i}{dr} + \frac{a_i}{De_i} \rho_p R_c = 0 \quad (4.2)$$

and for conservation of the various sulfur species,

$$\begin{aligned} & (2 \frac{d^2 C_4}{dr^2} + 4 \frac{d^2 C_5}{dr^2} + 6 \frac{d^2 C_6}{dr^2} + 8 \frac{d^2 C_7}{dr^2}) \\ & + \frac{2}{r} (2 \frac{dC_4}{dr} + 4 \frac{dC_5}{dr} + 6 \frac{dC_6}{dr} + 8 \frac{dC_7}{dr}) + \\ & (6 a_6 / De_6) \rho_p R_c = 0 \end{aligned} \quad (4.3)$$

the steady state differential energy balance equation is,

$$\frac{d^2 T}{dr^2} + \frac{2}{r} \frac{dT}{dr} - (a_1 / k_s) \rho_p R_c (-\Delta H) = 0 \quad (4.4)$$

To satisfy the condition that reactions (3.19) to (3.21) represent the equilibrium conditions,

$$P_4 = (K_{62})^{1/3} P_6^{1/3} = a_1 P_6^{1/3} \quad (4.5)$$

$$P_5 = (K_{64})^{2/3} P_6^{2/3} = a_2 P_6^{2/3} \quad (4.6)$$

$$P_7 = (K_{68})^{4/3} P_6^{4/3} = a_3 P_6^{4/3} \quad (4.7)$$

To solve system of differential equations (4.2) to (4.4), C_4 , C_5 , C_7 have to be expressed in terms of C_6 . Set of equations (4.5) to (4.7) yields,

$$C_4 = (K_{62}/Rg^2)^{1/3} C_6^{1/3} / T^{2/3} \quad (4.8)$$

$$C_5 = (K_{64}/\sqrt{Rg})^{2/3} C_6^{2/3} / T^{1/3} \quad (4.9)$$

$$C_7 = (K_{68}Rg^{1/4})^{4/3} C_6^{4/3} T^{1/3} \quad (4.10)$$

Introduction of (4.8) to (4.10) into (4.3), yields a nonlinear differential equation which is highly coupled with the heat balance equation (4.4). The resulting differential equation, when only C_7 and C_6 are considered in equation (4.3) is shown in equation (C.5).

The solution of such a nonlinear, highly-coupled, differential equation is formidable if not impossible. At this point it is appropriate to assume that the stoichiometry of the reactions (3.20) to (3.23) would specify the composition profile of the different species relative to some reference species, for example H_2S . This assumption implies that the catalyst offers almost equal intra-particle mass transfer resistances for all of the species.

Invoking this simplifying assumption one obtains one mass balance differential equation for the reference species H_2S , and one differential equation for the heat balance. The

local values of concentration of the other species are then related to the corresponding values at the surface of the catalyst pellet and to the H_2S concentration by the stoichiometry of the reaction. In mathematical form these are expressed in dimensionless form as,

$$d^2\Psi_n/dy^2 + 2/y \, d\Psi_n/dy - 9 \, \phi_n^2 \, R_c/R_{c_s} = 0 \quad (4.11)$$

$$d^2t/dy^2 + 2/y \, dt/dy + 9 \, \phi_n^2 \, \xi (-\Delta H) R_c/R_{c_s} = 0 \quad (4.12)$$

where

$$\Psi_n = C_i/C_{i_s} \quad (4.13)$$

$$y = 2r/D_p \quad (4.14)$$

$$\phi_n^2 = (D_p^2/36) (2\rho_p R_{c_s}/C_{i_s} De_1) \quad (4.15)$$

$$\xi = De_1 C_{i_s}/k_s T_s \quad (4.16)$$

with the boundary conditions,

$$t = \Psi_n = 1 \quad \text{at } y=1 \quad (4.17)$$

$$dt/dy = d\Psi_n/dy = 0 \quad \text{at } y=0 \quad (4.18)$$

In the analysis of nonisothermal pellets (146,190,208), it is common to include the heat of reaction term in the definition of the parameter ξ (ξ' in equation 4.1) assuming it has a constant value within the limits of temperature encountered in the pellets. However, for the Claus reaction it was shown in chapter 3 that even for a constant

temperature, the heat of reaction is a function of extent of conversion.

By eliminating the rate term R_c/R_{c_s} between equations (4.11) and (4.12), and integrating twice between the limits of $y=0$ and $y=1$, the Prater's (82) relationship results,

$$\eta^2 = 1 + \xi(-\Delta H) (1-\psi_n) \quad (4.19)$$

For a spherical catalyst particle, the effectiveness factor becomes

$$\eta = 3 \int_0^1 R_c y^2 dy = \{1/(3 \phi_n^2)\} (d\psi_n/dy)_{y=1} \quad (4.20)$$

Using this analysis to calculate η , the boundary value problem, equations (4.11), (4.17), and (4.18) coupled with equation (4.19) must be solved, for a specified composition and temperature of the gas at the exterior surface of the catalyst particle.

4.2.1 Computational Scheme

In order to integrate equation (4.11) the rate of reaction R_c/R_{c_s} has to be specified at each node of the integration. The following describes the scheme for this calculation.

At a particular location in the catalyst bed, the flowing gas stream has achieved a given conversion of H_2S ,

X_s adjacent to the particular catalyst pellet. At a specified value of X_s and T_s , the composition of the gas is obtained by the method described in section 3.4, which then yields $N_{t,s}$ and $x(S_s)$. Then

$$P_{1,s} = (\Pi/N_{t,s}) Y_{H_2S} (1-X_s) \quad (4.21)$$

$$P_{2,s} = (\Pi/N_{t,s}) \{Y_{SO_2} - 0.5Y_{H_2S} X_s\} \quad (4.22)$$

$$P_{3,s} = (\Pi/N_{t,s}) \{Y_{H_2O} + Y_{H_2S} X_s\} \quad (4.23)$$

$$P_{6,s} = (\Pi/N_{t,s}) x(S_s) \quad (4.24)$$

The rate of the Claus reaction at the surface of the catalyst pellet ($R_{c,s}$) can then be calculated knowing T_s and $P_{1,s}$ to $P_{6,s}$.

Next, at the interior points of the catalyst pellet, the solution of the differential equation (4.11) starting from the initial point and a specific spatial step-size, yields Ψ_n at the subsequent point. The local value of conversion of H_2S is related to Ψ_n by,

$$X = 1 - \Psi_n (1 - X_s) t N_t / N_{t,s} \quad (4.25)$$

The composition of the gas at a specific point in the catalyst where Ψ_n is known, will be then calculated by the method of section 3.4 to evaluate N_t and $x(S_s)$, using equations (4.19) and (4.25) to specify the corresponding local values of temperature and conversion. Then,

$$P_2 = (\Pi/N_1) \{Y_{SO_2} - 0.5Y_{H_2S} X\} \quad (4.26)$$

$$P_3 = (\Pi/N_1) \{Y_{H_2O} + Y_{H_2S} X\} \quad (4.27)$$

$$P_6 = (\Pi/N_1) x(S_6) \quad (4.28)$$

The calculated local composition and temperature fixes the rate of reaction. The integration and the above procedure are continued to yield ψ_n and the gas composition at the subsequent spatial points of the catalyst pellet.

The Weisz and Hicks conventional method (208) was used to solve the two-point boundary value differential equation (4.11). In their method the boundary value problem is treated as an open-ended initial value problem; the detailed derivation of equations to apply the Weisz and Hicks method to this study is presented in Appendix C with the related flow chart and computer program.

The Weisz and Hicks method is a powerful procedure. This method is implicit in that an appropriate value of ϕ_n may be determined only after a solution is obtained. This point has been shown in figure C.1.

4.2.2 Nonisothermal Claus Pellet Modelling Results

In the numerical analysis of Claus pellets, different ϕ_n and ξ correspond to different Dp/\sqrt{De} and De/ks ratios, respectively, since in equations (4.15) and (4.16), all the other parameters or variables have been specified by choosing X_s and T_s .

In figure 4.1 a comparison is presented of the effectiveness factor curves of Claus pellets with different De/ks ratios when $T_s=500$ K and $X_s=0.2$. At this temperature and conversion, the calculated heat of reaction is 11.8 kcal/mol H_2S . The curve for $\xi=0.0$ illustrates the effectiveness factor curve of an isothermal Claus pellet since, by equation (4.19) this corresponds to $t=T/T_s=1$.

Figure 4.1 reveals that the effectiveness factor of Claus reaction can exceed unity when the ratio De/ks is large. However, when De/ks is equal to 100, the pellets behave practically isothermally.

The corresponding plot when $T_s=600$ K is shown in figure 4.2. The heat of the Claus reaction at this temperature range is of the order of 10.8 kcal/mole H_2S . Here the pellets show less sensitivity to the ratio of De/ks compared to figure 4.1. For example at $\phi_n=1.0$ and $\xi=0.00001$, the ratio of nonisothermal to isothermal effectiveness factor for $T_s=500$ K, is 1.14 compared to 1.04 for $T_s=600$ K. This effect is a direct result of the lower value of the heat of reaction at $T_s=600$ K compared to 500 K.

It is useful at this stage to consider the range of De/ks ratios that would be covered in physically realizable Claus systems. The upper bound to the magnitude of the diffusivity is the bulk gas-phase diffusivity, corrected for the fraction of void space in the solid (porosity), and for "tortuosity". The calculated value of this diffusivity, using the recommended values of tortuosity and porosity

Figure 4.1 Nonisothermal Claus pellet effectiveness factor
 Inlet composition (mole fraction): $\text{H}_2\text{S} = 0.1$
 $\text{SO}_2 = 0.05$, $\text{H}_2\text{O} = 0.2$, $\text{N}_2 = 0.65$
 Surface temperature = 500 K
 H_2S conversion at the surface = 0.2

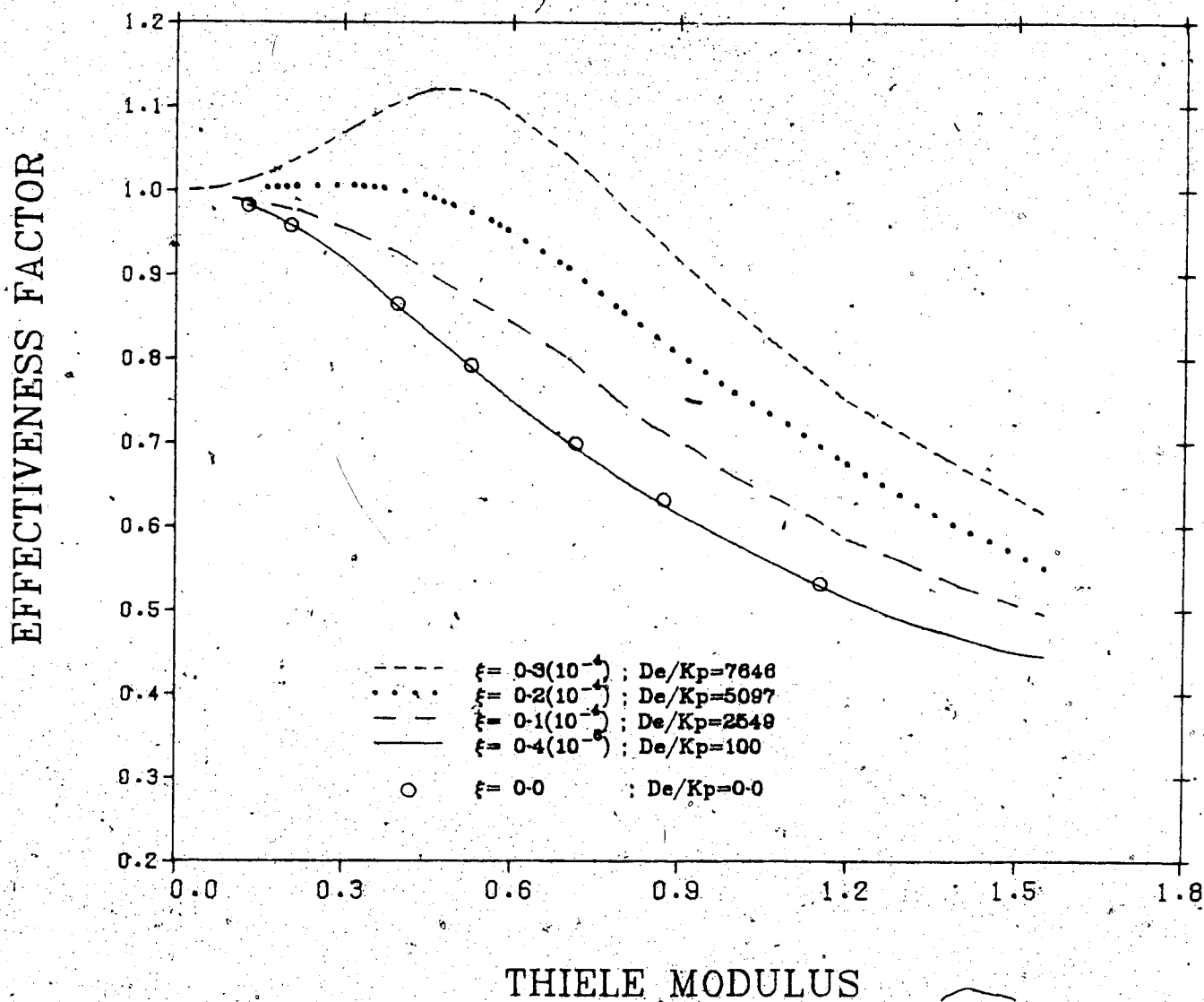
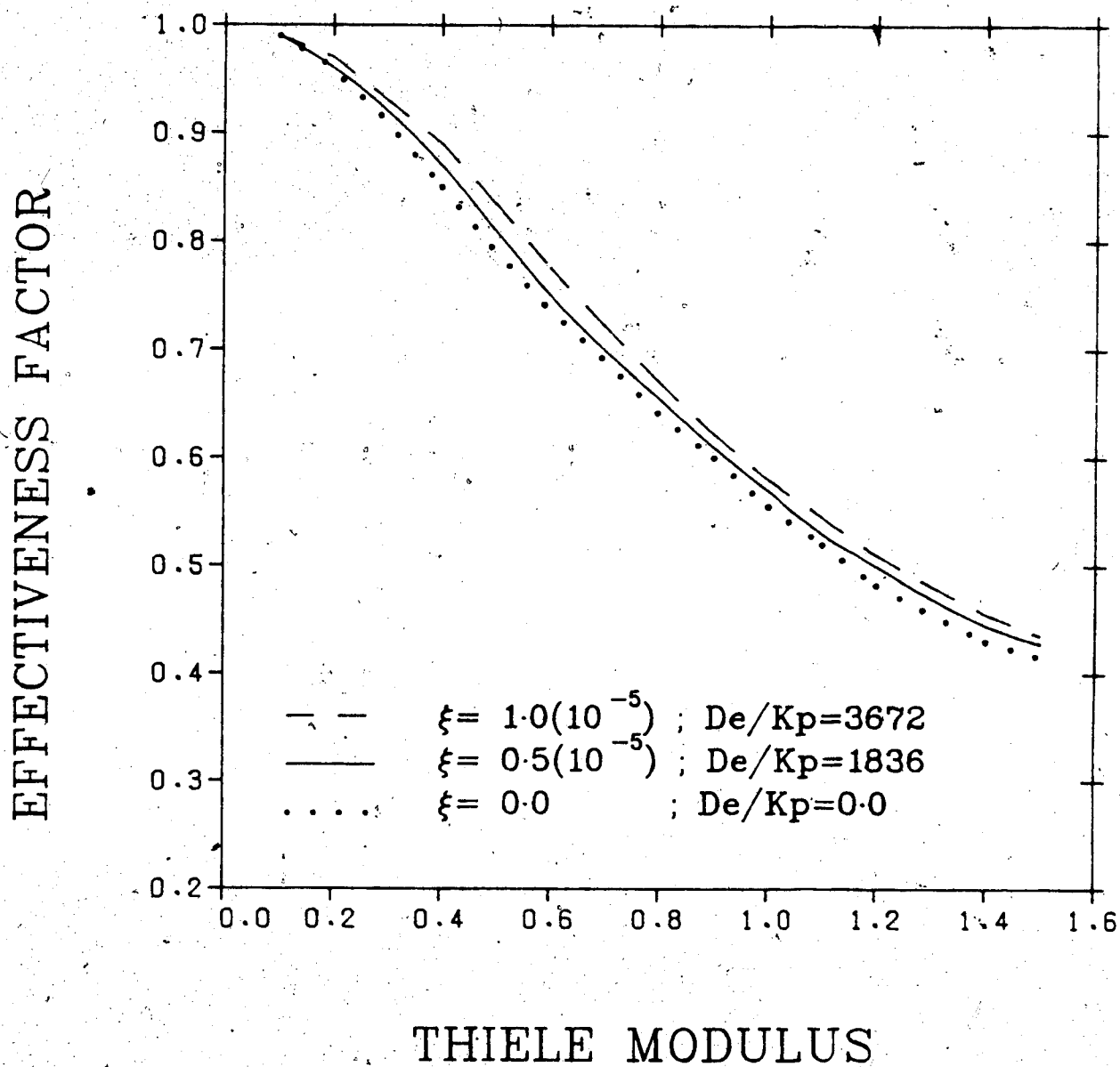


Figure 4.2 Nonisothermal Claus pellet effectiveness factor
 Inlet composition (mole fraction): $\text{H}_2\text{S} = 0.1$
 $\text{SO}_2 = 0.05$, $\text{H}_2\text{O} = 0.2$, $\text{N}_2 = 0.65$
 Surface temperature = 600 K
 H_2S conversion at the surface = 0.2



(180) is $0.056 \text{ cm}^2/\text{sec}$ as shown in Appendix G.

The minimum possible value of k_s corresponds to the thermal conductivity of insulators (208), and it is about $0.0001 \text{ cal/cm s K}$. Thus it is estimated that an upper-most limit of De/k_s to be encountered in Claus pellets, is 560. Figures 4.1 and 4.2 reveal that for this maximum ratio of De/k_s , the influence of pellets, nonisothermality is almost negligible for the Claus pellets.

The data obtained by Mischke and Smith (154) gave the value of k_s of alumina catalysts equal to $0.00034 \text{ cal/cm s K}$, when it was filled with air at 322 K. Furthermore, the calculated effective diffusivity using pore size distribution data of Chuang (46) is $0.00365 \text{ cm}^2/\text{s}$ as shown in Appendix G. Thus De/k_s for the Claus catalyst is of the order of 10.7.

In the light of the above analysis, the operation with Claus catalyst would therefore be expected to be free of thermal effects within the catalyst pellet and justifies neglecting these effects. Because of the absence of internal thermal effects, the energy balance equation within the catalyst pellet does not need to be considered when computing the effectiveness factor.

4.3 Isothermal Claus Pellets

The Claus pellets were shown in section 4.2.2 to behave isothermally. Thus when computing the effectiveness factor, the mass balance equations are the only equations to be

solved.

The material balance equations are required for each independent species participating in the reaction as was described in section 4.1. At steady state, different material balances for H_2S , SO_2 , and H_2O resulted in equation 4.1 and for conservation of the sulfur species in equation 4.2. The equations (4.1) and (4.2) can be transformed in terms of partial pressure in an isothermal pellets as,

$$\frac{d^2 P_i}{dr^2} + \frac{2}{r} \frac{dP_i}{dr} + \frac{a_i}{De_i} \rho_p R_g T_s R_c = 0 \quad (4.29)$$

$i=1,2,3$

$$\begin{aligned} & 2 \frac{d^2 P_4}{dr^2} + 4 \frac{d^2 P_5}{dr^2} + 6 \frac{d^2 P_6}{dr^2} + 8 \frac{d^2 P_7}{dr^2} \\ & + \left\{ 2 \frac{dP_4}{dr} + 4 \frac{dP_5}{dr} + 6 \frac{dP_6}{dr} + 8 \frac{dP_7}{dr} \right\} \\ & + \frac{6a_6}{De_6} \rho_p R_g T_s R_c = 0 \end{aligned} \quad (4.30)$$

Substituting (4.5) to (4.7) into (4.30) to eliminate P_4 , P_5 , and P_7 , yields,

$$\begin{aligned} & \left\{ \frac{2}{3} a_1 P_6^{2/3} + \frac{8}{3} a_2 P_6^{1/3} + 6 \right. \\ & + \left. \frac{32}{3} a_3 P_6^{1/3} \right\} (d^2 P_6 / dr^2) + \\ & \left\{ -\frac{4}{9} a_1 P_6^{5/3} - \frac{8}{9} a_2 P_6^{4/3} \right. \\ & + \left. \frac{32}{9} a_3 P_6^{2/3} \right\} (dP_6 / dr)^2 + \end{aligned}$$

$$\begin{aligned} & \{2/3 a_1 P_s^{2/3} + 8/3 a_2 P_s^{1/3} + 6 + 32/3 a_3 P_s^{1/3}\} \\ & (2/r)(dp_s/dr) \\ & + 6 a_s/De_s \rho p R_g T_s R_c = 0 \end{aligned} \quad (4.31)$$

Introducing a new variable, W, defined by

$$W = 2a_1 P_s^{1/3} + 4a_2 P_s^{2/3} + 6 P_s + 8a_3 P_s^{4/3} \quad (4.32)$$

simplifies equation (4.31) to

$$d^2W/dr^2 + 2/r dW/dr + 6a_s/De_s \rho p R_g T_s R_c = 0 \quad (4.33)$$

By choosing any two of the equation (4.29), and integrating twice between the limits $r=r$ to $r=D_p/2$ gives the following set of algebraic equations,

$$P_i = P_{i,s} + (a_i/a_1)(De_i/De_s)(P_1 - P_{1,s}) \quad (4.34)$$

$i=2,3$

Next, considering equation (4.33) and equation (4.29) for $i=1$, to eliminate the rate term, one finds

$$W = W_s + 6(a_s/a_1)(De_s/De_s)(P_1 - P_{1,s}) \quad (4.35)$$

or

$$\begin{aligned}
& 2a_1 P_{1,1}^{1/3} + 4a_2 P_{1,1}^{2/3} + 6P_{1,1} + 8a_3 P_{1,1}^{4/3} \\
& = 2a_1 P_{1,2}^{1/3} + 4a_2 P_{1,2}^{2/3} + 6P_{1,2} + 8a_3 P_{1,2}^{4/3} + \\
& 6(a_3/a_1)(De_1/De_2)(P_1 - P_{1,2})
\end{aligned} \tag{4.36}$$

Now the four differential equations (4.29) and (4.30) have been reduced to one differential mass conservation equation based upon reference species 1 (H_2S) and the two sets of algebraic equations (4.34) and (4.35).

To generalize the analysis, dimensionless variables are introduced:

$$\psi = P_1/P_{1,2}$$

and

$$y = 2r/Dp$$

which transforms equation (4.29) for the reference species 1 into,

$$d^2\psi/dy^2 + 2/y \, d\psi/dy - 9\phi^2 \, Rc/Rc_1 = 0 \tag{4.37}$$

where;

$$\phi = (Dp/6)\sqrt{(2 \rho_p R_g T_s Rc_1/De_1 P_{1,2})} \tag{4.38}$$

and the boundary conditions are

$$d\psi/dy = 0 \quad , \quad \text{at } y=0 \tag{4.39}$$

$$\psi = 1 \quad , \quad \text{at } y=1 \tag{4.40}$$

The effectiveness factor is calculated from equation 4.20 by replacing ϕ_n and ψ_n with ϕ and ψ .

Using this analysis to calculate the η , the boundary value problem, equations (4.37), (4.39) and (4.40) coupled with the equations (4.34) and (4.35) must be solved for a specified composition and temperature of the gas at the exterior surface of the catalyst particle.

4.3.1 Computational Scheme for Isothermal Claus Pellets

The first step to be taken is to specify the composition of the gas at the exterior surface of the catalyst particle. The computational method of section 4.2.1 which resulted in equations (4.21) to (4.24) is applicable here as well. The calculated partial pressures of the species and T_s defines R_c .

Solution of equation (4.37) gives the local values of ψ , or P_i , by which value, equations (4.34) and (4.35) may be solved to give the partial pressure of the other species. These partial pressures would then specify the local reaction rate.

Two different numerical schemes were employed for the solution of the boundary value problem equations (4.37), (4.39) and (4.40). The first method, the Weisz and Hicks method integrates the differential equation by the Runge-Kutta-Fehlberg (186) method and is a powerful but time-consuming numerical procedure which provides an accurate solution. The results of this method could be used

to estimate the accuracy of the second speedier method. As was mentioned in section 4.2.1, the Weisz and Hicks method is an implicit method in terms of ϕ .

The second method integrates equation (4.37) via the orthogonal collocation procedure. This method is considered explicit because the solution results for any specified value of the Thiele modulus, ϕ .

The detailed formulations of both methods have been presented in Appendix D.

4.3.2 Isothermal Claus Pellet Modelling Results

Figure 4.3 compares the two numerical procedures used to predict the partial pressure profile of component 1 (H_2S) at different ϕ . With increasing ϕ , the explicit method (orthogonal collocation) requires additional interior points for accurate results. Using six interior points with the explicit method, at $\phi=5.76$, the two methods predicted effectiveness factors differing by only 0.4%.

At large values of ϕ , the solution Ψ has a steep gradient near the pellet surface. Thus a large number of interior points are needed for accurate calculation of η (41,204). This would affect the efficiency of the collocation method. In this study the method of Paterson and Cresswell(162), using only one collocation point has been used for calculation of η when ϕ is large. The position of collocation point has been chosen according to the criterion developed by Villadsen and Michelsen (204). This method is

Figure 4.3 Comparison between Runge-Kutta-Fehlberg (RKF) and Orthogonal Collocation (OC) numerical methods.

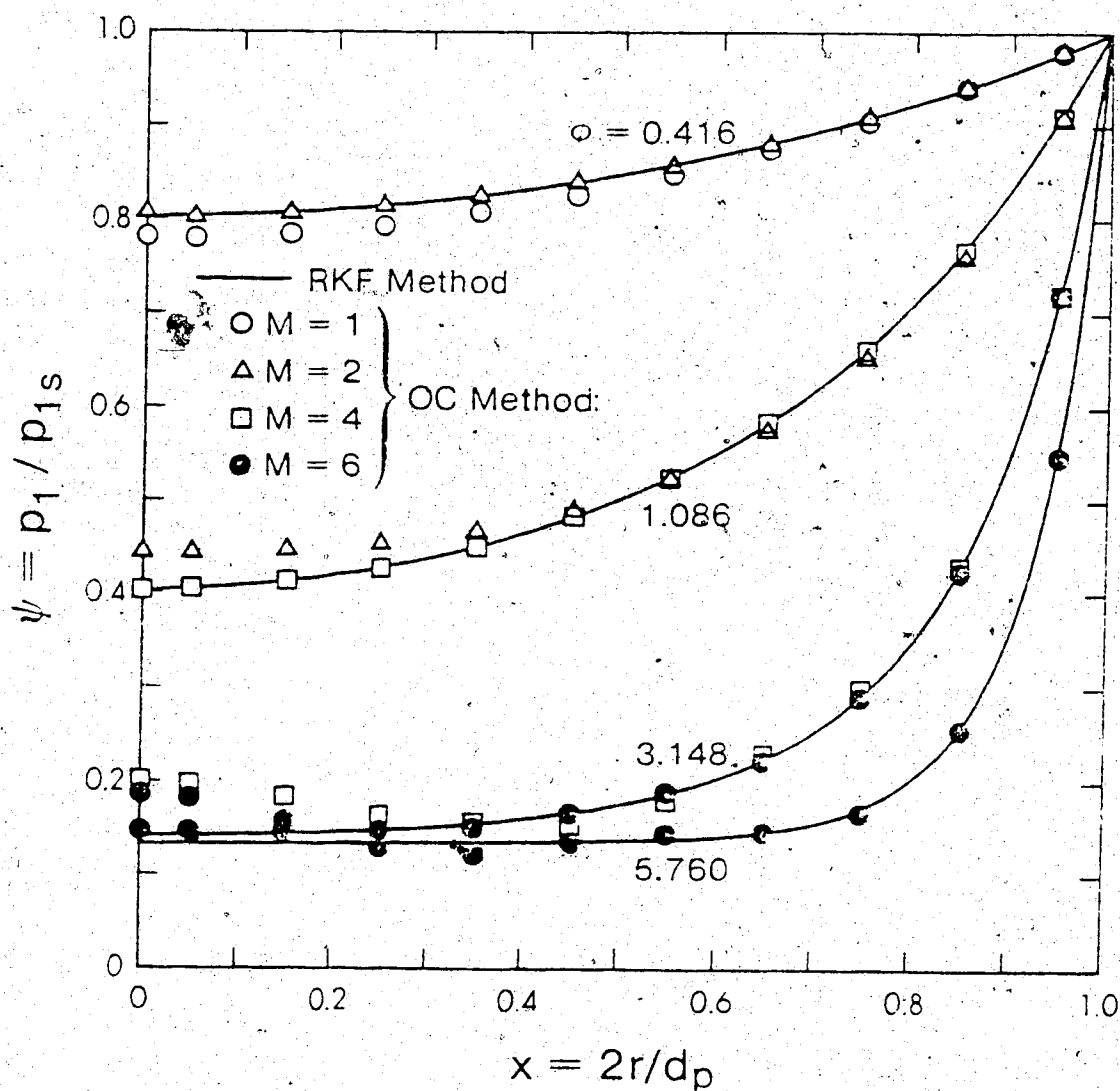
Inlet composition (mole fraction): $\text{H}_2\text{S} = 0.1$

$\text{SO}_2 = 0.05$, $\text{H}_2\text{O} = 0.2$, $\text{N}_2 = 0.65$

Surface temperature = 500 K

H_2S conversion at the surface = 0.5

M = number of interior points used in OC method.



discussed in section D.2.2.

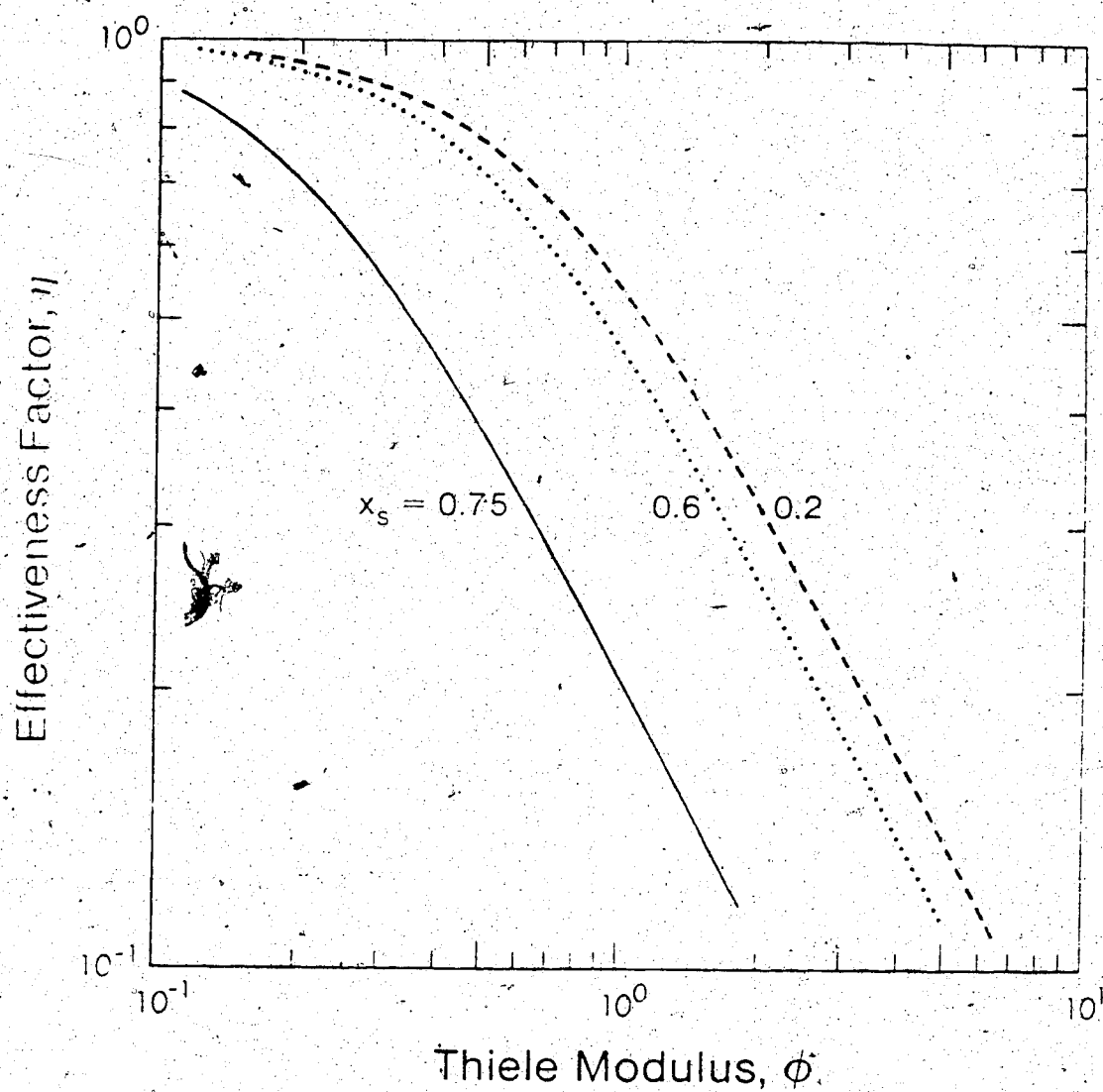
A typical catalyst particle of the type used in the modified Claus plants has $\phi \approx 6.0$ for a pellet of 0.6 cm in diameter, as shown in section D.3, thus about six interior points are required to obtain reasonably accurate composition profiles. The computer program for orthogonal collocation was written to permit adjustments in the number of interior points, depending upon the value of the Thiele modulus, thus reducing the number of computations.

Figure 4.3 shows that the efficient choice of the calculation method for the Claus catalyst effectiveness factor is orthogonal collocation, since it is efficient and is explicit in the value of ϕ . That is, the effectiveness factor can be directly calculated when the catalyst pellet surface conditions are specified.

Figure 4.4 illustrates the change in the effectiveness factor when the conversion at the surface is changed. In these calculated η - ϕ plots, parameters other than partial pressures were invariant. Operation of Claus reactors with non-stoichiometric feed compositions necessitates independent calculations for P_{2s}/P_{1s} , P_{3s}/P_{1s} , and P_{Ss}/P_{1s} , since all are changing quantities with X_s according to equations (4.21) to (4.24). When stoichiometric feed ratios are employed, P_{2s}/P_{1s} remains constant at 1/2 and only the other ratios vary when X_s is changed.

At a constant temperature, as was used in figure 4.4, sulfur might condense at high values of X_s . However, in the

Figure 4.4 Effectiveness factor versus Thiele modulus for spherical particle in modified Claus reaction, at varying conversion levels of H_2S at pellet exterior surface.



exothermic Claus reactor, there is a concomitant increase of temperature with conversion. Thus sulfur would not condense at high operating temperatures of the conventional Claus reactor.

In an isothermal reactor, the Thiele modulus of a first order reaction remains constant. In the Claus reactor, however, the Thiele modulus is proportional to $\sqrt{(P^{1.5}/P)}$ according to equations (3.39) and (4.38). Thus for a given pellet size, at a constant temperature the Thiele modulus decrease with conversion. This explains why the effectiveness factor is expected to increase with conversion although figure 4.4 shows that it decreases with conversion if the Thiele modulus remains constant. Figure 4.5 clarifies this point further. It shows how local values of the Thiele modulus decrease for a 0.8 cm Claus pellet in an adiabatic bed.

Figure 4.6 presents the change in effectiveness factor when the temperature is changed, while the conversion at the surface is invariant. The results of figures 4.4 and 4.6 imply that the Claus pellet effectiveness factor is a complex function of the pellet surface condition. This functional relationship apparently cannot be described by the Thiele modulus, ϕ .

Figure 4.5 Local Thiele modulus in the adiabatic catalytic Claus reactor.

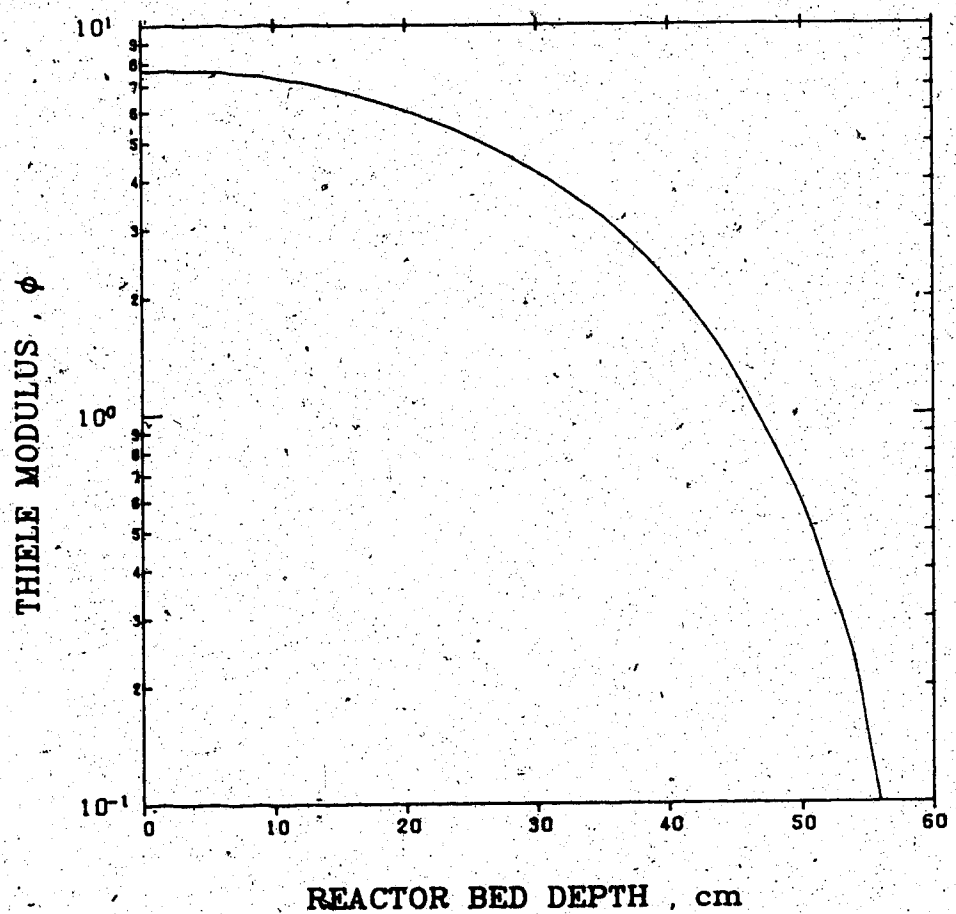
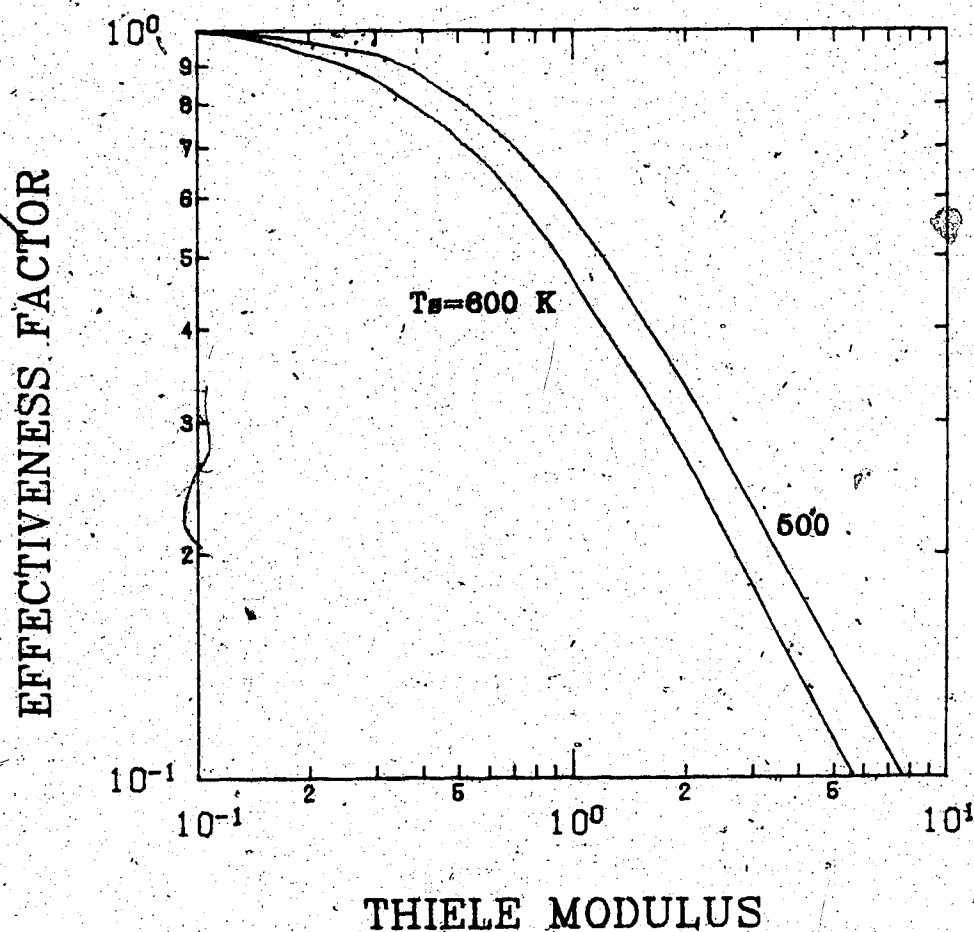


Figure 4.6 Effectiveness factor versus Thiele modulus for spherical particle in modified Claus reaction, at varying exterior surface temperatures.



4.4 Simplified Local Effectiveness Factor

It was shown in section 4.3 that, the effectiveness factor of the Claus pellets is function of surface condition as well as the Thiele modulus. At a given value of the Thiele modulus, the effectiveness factor, decreases as the conversion and temperature of the pellet surface increases. In the exothermic convertors X_s , and T_s are increasing function of the axial coordinate. The functional dependency of the Thiele modulus on axial coordinate depends on the variation of the $(T_s R_g)/P_1$, according to equation (4.38), for the specified catalyst pellet size. Thus the Thiele modulus might increase, remain constant or decrease with axial position, due to the complex interaction between the temperature, rate of reaction, and partial pressure.

In light of the above, the local values of η has to be calculated at each axial position to obtain an accurate prediction of the reaction rate through the bed. The calculation of a local effectiveness factor by the method of section 4.3 provides a model which is theoretically satisfactory, but perhaps too time-consuming to be useful for generating design alternatives. This section describes a method for simplification of the Claus effectiveness factor calculation.

Because the modified Claus reaction (3.20) is reversible, a limiting equilibrium conversion will be encountered for any specified T_s , X_s , and reactor feed composition. Thus the lower limit of Ψ in equation (4.37),

would correspond to the equilibrium value i.e. P_{e1}/P_{11} , when the Thiele modulus is large. The equilibrium composition within the catalyst particle is affected by the catalyst pellet surface condition.

To normalize Ψ in equation (4.37), it is appropriate to introduce a dimensionless variable θ , in terms of Ψ ,

$$\theta = (\Psi - \Psi_e) / (1 - \Psi_e) \quad (4.41)$$

where $\Psi_e = P_{e1}/P_{11}$. This type of parameter has been used previously by Kao and Satterfield (111) in evaluating η for a first-order reversible Langmuir-Hinshelwood type rate expression.

The boundary value problem (equation 4.37) is transformed to

$$\frac{d^2 \theta}{dy^2} + \frac{2}{y} \frac{d\theta}{dy} - \frac{9\phi^2}{(1 - \Psi_e)} R_c/R_{c1} = 0 \quad (4.42)$$

with

$$\theta = 1 \quad , \quad \text{at } y=1 \quad (4.43)$$

$$d\theta/dy = 0 \quad , \quad \text{at } y=0 \quad (4.44)$$

Because the composition within the catalyst particle are affected by the relative diffusivities of the different molecular species, the equilibrium composition, Ψ_e , must be evaluated at the conditions developing within the particle

interior. The equilibrium relation of the reaction (3.20), using equation (4.34) yields,

$$\begin{aligned} &Pe_8^{1/2} \{P_{3,} - De_1/De_3 (Pe_1 - P_{1,})\}^2 - \\ &K Pe_1 \{P_{2,} + De_1/2De_2 (Pe_1 - P_{1,})\} = 0 \end{aligned} \quad (4.45)$$

Simultaneous solution of equations (4.35) and (4.45) gives Pe_1 and Pe_8 .

Effectiveness factor plots in terms of a redefined Thiele modulus,

$$\Phi = \phi/\sqrt{(1-\psi_e)} \quad (4.46)$$

for differing values of X_s and T_s are shown in figures 4.7 and 4.8.

Figures 4.7 and 4.8 reveal that the influences of X_s and T_s upon η may be disguised, if not eliminated, by the use of ψ_e and the modified Thiele modulus, Φ . By specifying average values of X_s and T_s , figures 4.7 and 4.8 enable sufficiently reliable η to be predicted. Thus, it appears reasonable to use a single "average" plot of $\eta-\Phi$ to generate local values of η for use in reactor modelling.

In applying this approach to the modelling of the modified Claus process reactor, point values of $\eta-\Phi$ may be generated based upon a specified feed composition and some average X_s and T_s . Intermediate values of η could be obtained conveniently by using a natural spline

Figure 4.7 Effectiveness factor versus modified Thiele modulus for spherical particle in modified Claus reaction at varying conversion of H_2S at pellet exterior surface.
($T_s = 500\text{ K}$).

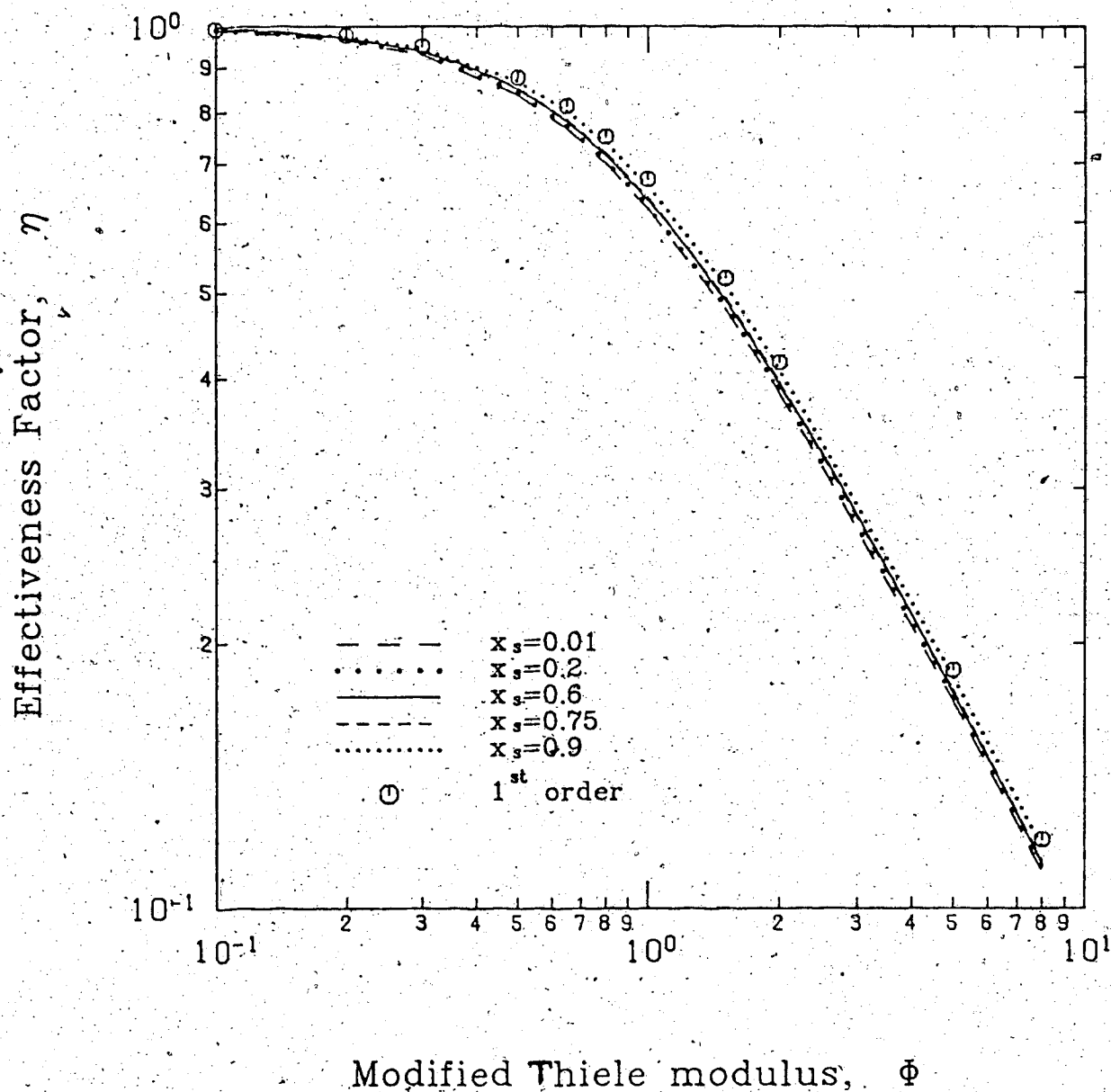
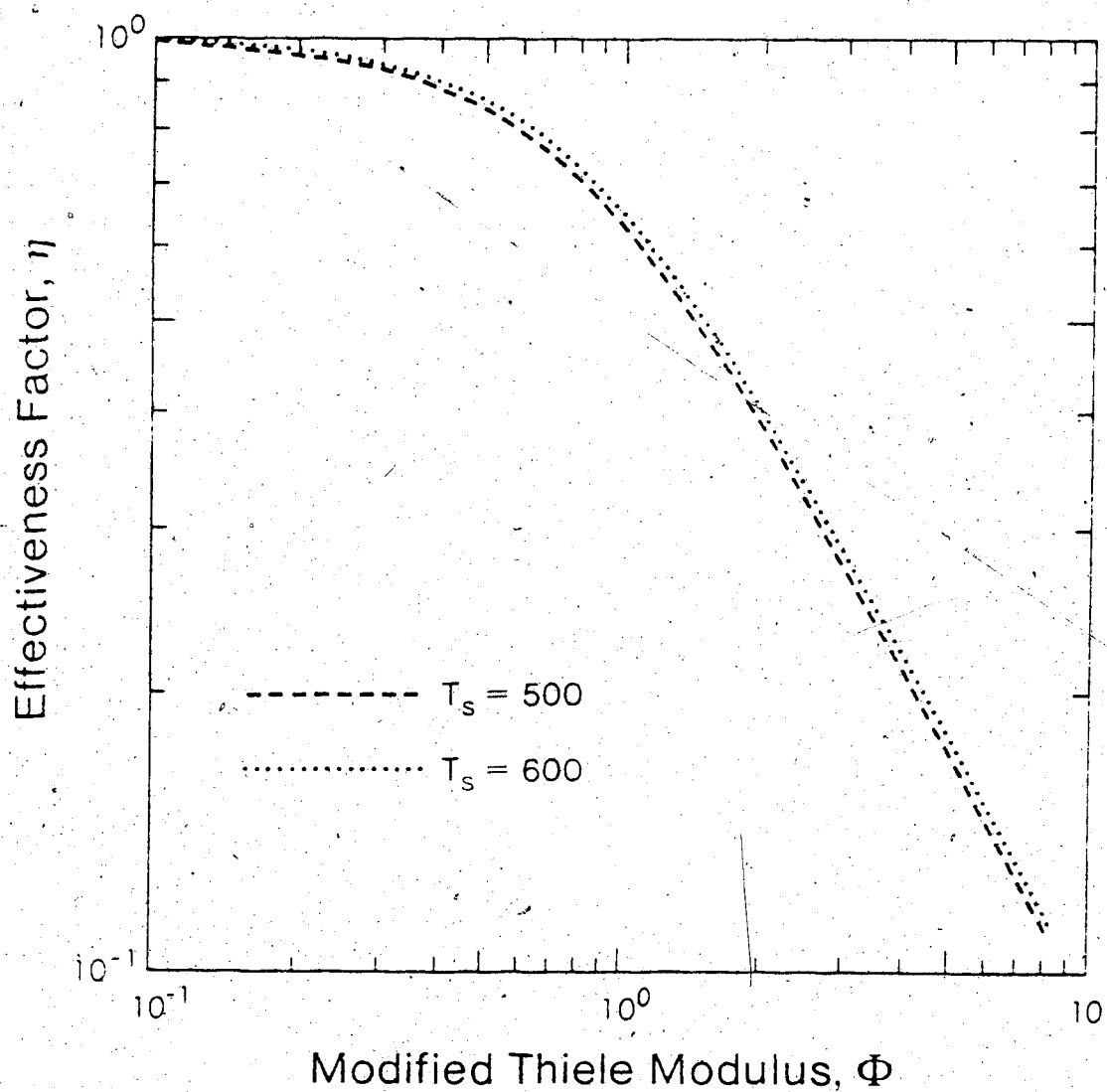


Figure 4.8 Effectiveness factor versus modified Thiele modulus for spherical particle in modified Claus reaction at varying surface temperatures. ($X_s = 0.5$).



interpolating formula (87). The algorithm for generating local effectiveness factor in a Claus convertor is described in section D.4.

The first order approximation of Claus process is shown by circles in figure 4.7. The ordinate, η , of these points were evaluated from the analytical solution of the effectiveness factor for first order reaction in a spherical pellet, that is:

$$\eta = (1/\Phi) \frac{(3 \Phi) \coth(3 \Phi) - 1}{3 \Phi} \quad (4.47)$$

The first order approximation, gives an upper limit of the Claus effectiveness factor at any given value of the modified Thiele modulus, Φ (defined by equation 4.46). The prediction is, however considered sufficiently reliable for routine calculation of the Claus pellet effectiveness factor. To obtain the first order approximation of η , equations (4.35) and (4.45) should still be solved for evaluation of Pe , and thus Φ at a given set of pellet surface conditions.

5. HIGH TEMPERATURE CLAUS REACTOR MODEL

5.1 Introduction

The literature on the design of the modified Claus process is sparse. The available design procedures (55,198) are based on the calculation of thermodynamic equilibrium conversion. Using available thermodynamic properties and a free energy minimization approach, the equilibrium conversion attained in each section of the Claus plant may, in principle, be predicted given the feed composition to that section. This approach has been used by Cho (44), Goar (89), and Truong (199) for evaluation of the effect of presence of impurities on the modified Claus process performance.

Dalla Lana et al. (55) described an attempt to provide thermodynamic equilibrium conversions by relating simple calculations involving graphical methods. The report purported to show that detailed calculation for 100% H_2S acid gas could within limitations be applied to acid gases of lower H_2S content. The basis for the method lay in regarding an acid gas of lower H_2S content as partially converted 100% H_2S acid gas, after removal of the elemental sulfur produced.

Truong (199) has modified the above graphical method, using reliable thermodynamic properties from JANAF tables and the values published by Rau et al. (171), to generate the equilibrium conversion versus temperature plots. She has

discussed the limitations and application procedures of the graphical approach. Truong (199) has compared the effects of CO_2 , N_2 and water vapor and concluded that, below 40% inert content the sulfur removal equivalent method of graphical approach gives the conversion within the accuracy of the graph.

The available literature on the modelling and design of the Claus catalytic convertors has been reviewed in section 2.7.4. This review indicates that the literature lacks studies on the fundamental processes involved in the Claus convertors.

The detailed investigation of the catalytic conversions of H_2S and SO_2 to elemental sulfur is justified, because they are required to go to completion, as far as possible, irrespective of the upstream furnace performance. An improved understanding of the operation of Claus catalytic beds could provide a basis for predicting the performance of such beds under a wide variety of operating conditions.

This chapter provides models of the Claus reactor bed in which the temperature is high enough that condensation of the product sulfur is not expected to occur within the catalyst pellet.

5.2 Model Development

The mathematical model for the Claus catalytic reactor was developed according to the scheme of table 5.1.

Table 5.1 Scheme for Development of Models for
High Temperature Claus Converter.

Stage 1	Chemical change stages adsorption / reaction / desorption
Stage 2	Transport processes inside the catalyst pellet heat / mass
Stage 3	Transport processes in a film layer heat / mass
Stage 4	Transport processes in a layer of catalyst bed heat / mass
Stage 5	Interaction with environment adiabatic / nonadiabatic

Stage 1 : The chemical changes of the Claus process take place according to the intrinsic reaction rate expression (3.39). The basis for such a choice has been discussed in section 3.6.

Stage 2 : The results of chapter 4 revealed that the Claus catalyst pellets would be expected to exhibit isothermal interiors. The mass transport processes inside the catalyst pellet will be presented as an effectiveness factor. The effectiveness factor is calculated as a function of modified Thiele modulus as was defined in equation (4.46) using the algorithm described in section D.4.

Stage 3 : Equation (2.18) has been employed to estimate the film layer mass and heat transfer processes. The physical properties of the gaseous mixtures for use in equation (2.18) have been evaluated in Appendix H.

Stage 4 : At this stage the question of axial dispersion of heat and mass have to be considered. In general, axial dispersion can be neglected whenever the bed is longer than 50 particle diameters (40,112). In the Claus reactor the catalyst diameter and the reactor length are in order of 0.6 cm and 100 cm, respectively. This justifies neglecting the axial dispersion of heat and mass.

Stage 5 : The Claus catalytic beds are wide and relatively

shallow insulated bedstas were discussed in section 2.6. These convertors are expected to operate adiabatically. Thus, the use of a one-dimensional reactor model provides a satisfactory description. However, in winter, the large temperature difference between the inside wall and the outside of the reactor may result in an appreciable heat loss and development of radial temperature, and consequently radial concentration, profiles. This non-adiabatic operation would then necessitate the use of a two-dimensional model.

5.3 Adiabatic 1-Dimensional Claus Process Model

The general steady-state transport and reaction processes in an adiabatic 1-dimensional, two-phase model for the Claus reaction are described by,

$$d (V_s C_{fj})/dz + A k_{mj} (C_{fj} - C_{sj}) = 0 \quad (5.1)$$

$$j = 1, 2, 3.$$

$$d (V_s \rho T_f)/dz - (Ah/C_p)(T_s - T_f) = 0 \quad (5.2)$$

with the coupling equations between catalyst and fluid phases,

$$A k_{mj} (C_{fj} - C_{sj}) = -a_j \rho b \eta R_c, \quad (5.3)$$

$$A h (T_s - T_f) = (-\Delta H) \rho b \eta R_c, \quad (5.4)$$

and for conservation of the various sulfur species,

$$d(V, Zf)/dz + A k_{ms} (Zf - Zs) = 0 \quad (5.5)$$

$$A k_{ms} (Zf - Zs) = -6 a_s \rho b \eta R_c \quad (5.6)$$

where,

$$Z = 2C_{s,2} + 4C_{s,4} + 6C_{s,6} + 8C_{s,8} \quad (5.7)$$

By combining any two of the equations in set of equations (5.3), to eliminate $(\rho b \eta R_c)$, the concentration of any species at the surface of the catalyst pellet can be expressed as a function of the corresponding value for the reference species (1). That is,

$$Cs_j = Cf_j - \left(\frac{k_{m1}}{k_{mj}} \right) \left(\frac{a_j}{a_1} \right) (Cf_1 - Cs_1) \quad (5.8)$$

$$j = 2, 3$$

Using the same procedure on equations (5.6) and (5.3) yields,

$$Zs = Zf - \left(\frac{k_{m1}}{k_{ms}} \right) \left(\frac{6a_s}{a_1} \right) (Cf_1 - Cs_1) \quad (5.9)$$

where by J-factor analysis (equation 2.18),

$$\frac{k_{m1}}{k_{mj}} = \left(\frac{Sc_1}{Sc_j} \right)^{2/3} = \left(\frac{Db_1}{Db_j} \right)^{2/3} \quad (5.10)$$

Combining any two equations in the relations (5.1), coupled with equation (5.3) yields,

$$d(V, Cf_j)/dz = (a_j/a_1) d(V, Cf_1)/dz \quad (5.11)$$

which upon integrating between the limits of $z=0$ (inlet to the reactor) to $z=z$ gives,

$$V, Cf_j = V, Cf_j^0 + (a_j/a_1)(V, Cf_1 - V, Cf_1^0) \quad (5.12)$$

$$j = 2, 3$$

Similar treatment for the sulfur species yields,

$$V, Zf = V, Zf^0 + (6a_s/a_1)(V, Cf_1 - V, Cf_1^0) \quad (5.13)$$

The equations (5.12) and (5.13) imply that the stoichiometry of the reaction defines the relation between the concentration of the different species in the bulk fluid phase, because there is no transport variable in these expressions. However, equations (5.8) and (5.9) show that the ratio of the transport variables (k_{m1}/k_{mj}) as well as the stoichiometry of the reaction (a_j/a_1) would affect the concentration of the different species on the catalyst surface relative to that of the reference species.

Next by combining equations (5.1) to (5.4), to eliminate the rate term, one finds:

$$d(V, \rho Tf)/dz - (-\Delta H/C_p a_1) d(V, Cf_1)/dz = 0 \quad (5.14)$$

The integration of (5.14) between the limits of $z=0$ to $z=z$

gives

$$V_1 \rho T_f = V_1^0 \rho^0 T^0 + (-\Delta H / C_p a_1) (V_1 C_{f1} - V_s^0 C_{f1}^0) \quad (5.15)$$

The above mathematical manipulation has reduced the system of the equations (5.1) to (5.6) to one differential mass conservation equation for the reference species (1) and the five sets of algebraic equations (5.8), (5.9), (5.12), (5.13), and (5.15).

The above sets of algebraic equations can be simplified by defining the concentrations in terms of conversion. The conversion of the reference species 1 is defined as,

$$\begin{aligned} x_f &= (C_{f1}^0 Q^0 - C_{f1} Q) / C_{f1}^0 Q^0 \\ &= (C_{f1}^0 V_1^0 - C_{f1} V_s) / C_{f1}^0 V_s^0 \end{aligned} \quad (5.16)$$

The volumetric flow rate (Q) or the superficial velocity of the gaseous mixture in a constant pressure reactor is a direct function of temperature and the total moles. The stoichiometry of reaction (3.33) may be used to express the volumetric expansion of the gaseous mixture as a function of conversion and temperature. Let

$$v = a_{1,2} + a_{1,4} + a_{1,6} + a_{1,8} \quad (5.17)$$

where $a_{1,i}$ are the stoichiometric coefficient in reaction

(3.33) defined in section 3.5. Then,

$$\begin{aligned}
 V_s/V_i^0 &= N_t T / N_t^0 T^0 \\
 &= \{ 1 - Y_i^0 (1-v) X_f/2 \} T/T^0 \\
 &= G T/T^0
 \end{aligned}
 \tag{5.18}$$

The equations (5.8), (5.9), (5.12) and (5.13) may be written in terms of conversion using equation (5.16) and (5.18),

$$C_{fj} = (T^0/T_f) (G)^{-1} \{ C_{fi}^0 - a_j/a_1 C_{fi}^0 X_f \} \tag{5.19}$$

$$Z_f = (T^0/T_f) (G)^{-1} \{ Z_f^0 - 6_s/a_1 C_{fi}^0 X_f \} \tag{5.20}$$

$$\begin{aligned}
 C_{sj} &= C_{fj} - (k_{m1}/k_{mj}) (a_j/a_1) (T^0 C_{fi}^0) (G)^{-1} \\
 &\quad [(1-X_f)/T_f - (1-X_s)/T_s] \\
 &= P_{js} / R_g T_s
 \end{aligned}
 \tag{5.21}$$

$$\begin{aligned}
 Z_s &= Z_f - (k_{m1}/k_{ms}) (6a_s/a_1) (T^0 C_{fi}^0) (G)^{-1} \\
 &\quad \{ (1-X_f)/T_f - (1-X_s)/T_s \} \\
 &= W_s / R_g T_s
 \end{aligned}
 \tag{5.22}$$

where W is defined by equations (4.32).

Next, equation (5.15) is expressed in terms of conversion by

$$T_f = G^{-1} \{ T^0 - (-\Delta H / C_p a_1) (C_{fi}^0 X_f / \rho^0) \} \tag{5.23}$$

The conservation equations (5.1) to (5.4) for the reference species 1 using equations (5.16) and (5.18) would result in,

$$d X_f / dz = -(a_1 \rho b / V_i^0 C_{fi}^0) \eta R_c \tag{5.24}$$

$$X_s = 1 - (a, h / -\Delta H)(G T_s / C_f (T^\circ k_{m1}))(T_s - T_f) - T_s / T_f (1 - X_f) \quad (5.25)$$

$$T_s = T_f + (-\Delta H \rho_b / A h) \eta R_c, \quad (5.26)$$

Using this analysis to obtain the reaction path through the bed, the differential equation (5.24) coupled with the equations (5.19) to (5.23) and (5.25) and (5.26) must be solved for a specified inlet composition, temperature, and flow to the bed.

5.3.1 Computational Scheme

By specifying X_f , the temperature in the bulk fluid phase is calculated from equation 5.23. Then X_s and T_s may be calculated through an iterative approach by solution of equations (5.25) and (5.26), while equations (5.21) and (5.22) are used for calculation of P_j , and thus R_c , and η through the approach discussed in section 4.3.

The converged solution of X_s and T_s specifies (ηR_c) and thus dX_f/dz by equation 5.24, which upon integration yields X_f at the next integration interval. The procedure is then repeated.

The Runge-Kutta-Fehlberg (186) and Newton-Raphson schemes were used for integration and iteration, respectively. The flow-chart of the program and the program code are presented in Appendix E.

5.3.2 Numerical Results of One-Dimensional Claus Model

The H_2S conversion profile along the catalyst bed is plotted in figure 5.1 for the first convertor at the feed temperature of 553 K and a space velocity of 1000 hr^{-1} . The corresponding temperature profile is presented in figure 5.2. These profiles indicate that a significant amount of reaction occurs at the entrance of the reactor bed and almost maximum conversion may be reached at the depth of about 40 cm. The maximum conversion is limited by the possible thermodynamic equilibrium value at the reactor outlet temperature. With this prediction it can be suggested that if the space velocity is increased to a higher level than 1000 hr^{-1} , a greater yield may be obtained without affecting the reactor efficiency.

The mass transfer coefficient $k_{m,j}$ of the species j , is a function of its bulk diffusivity by equation (5.10). Figure 5.1 shows that, the evaluation of $k_{m,j}$'s at an average value of bulk diffusivity would result only in minor error. This observation suggests that, the concentration of all the species at the surface of the catalyst pellet may be specified by using the stoichiometry of the reaction and the concentration of the reference species, as it is true for the bulk fluid phase (equation 5.12).

The point-value of the catalyst effectiveness factor is shown in figure 5.3. This profile indicates that the effectiveness factor decreases slowly in the initial section of reactor bed. It then increases slowly followed by a rapid

Figure 5.1 H_2S conversion profile along the catalyst bed depth
 Inlet composition (mole fraction): $\text{H}_2\text{S} = 0.07$,
 $\text{SO}_2 = 0.035$, $\text{H}_2\text{O} = 0.255$, $\text{N}_2 = 0.64$
 Inlet temperature = 553 K
 Pressure = 1 atm
 Space velocity = 1000 hr^{-1}

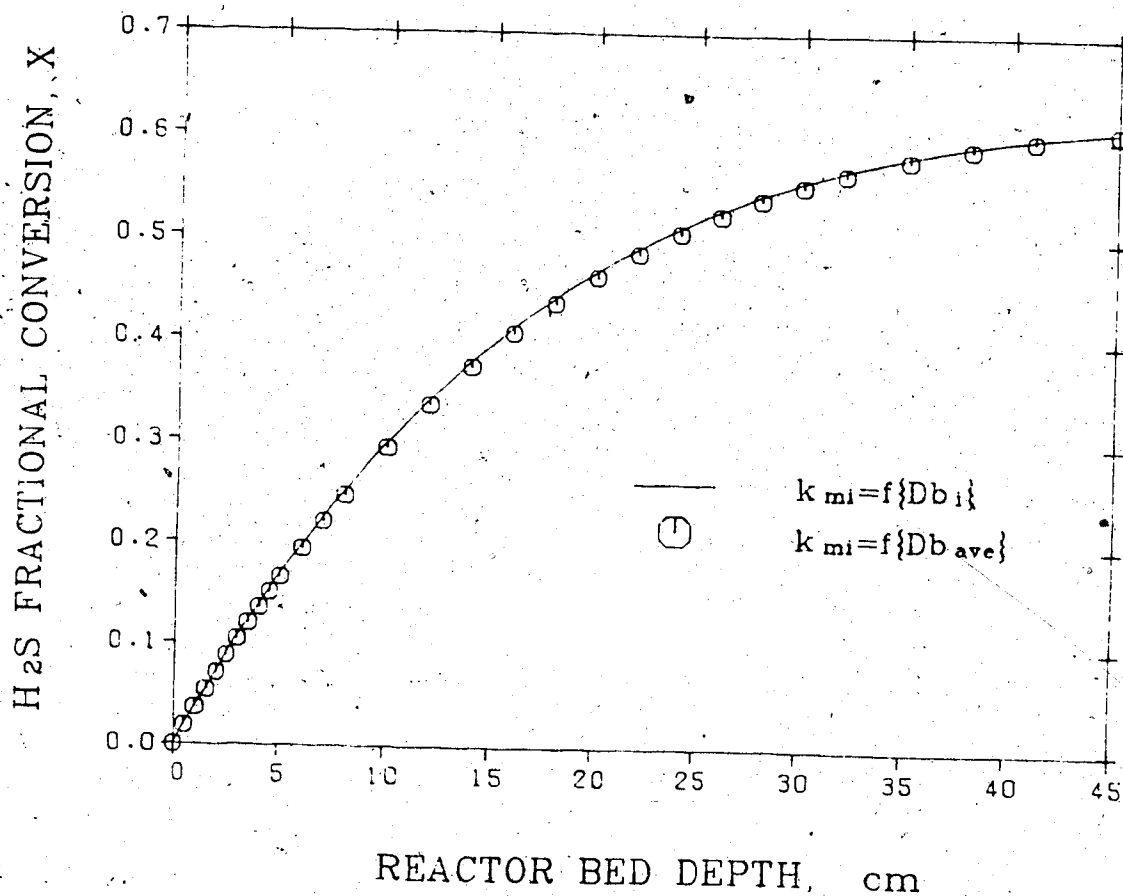


Figure 5.2 Temperature profile along the catalyst bed depth.
Inlet composition (mole fraction): $\text{H}_2\text{S} = 0.07$,
 $\text{SO}_2 = 0.035$, $\text{H}_2\text{O} = 0.255$, $\text{N}_2 = 0.64$
Inlet temperature = 553 K
Pressure = 1 atm
Space velocity = 1000 hr^{-1}

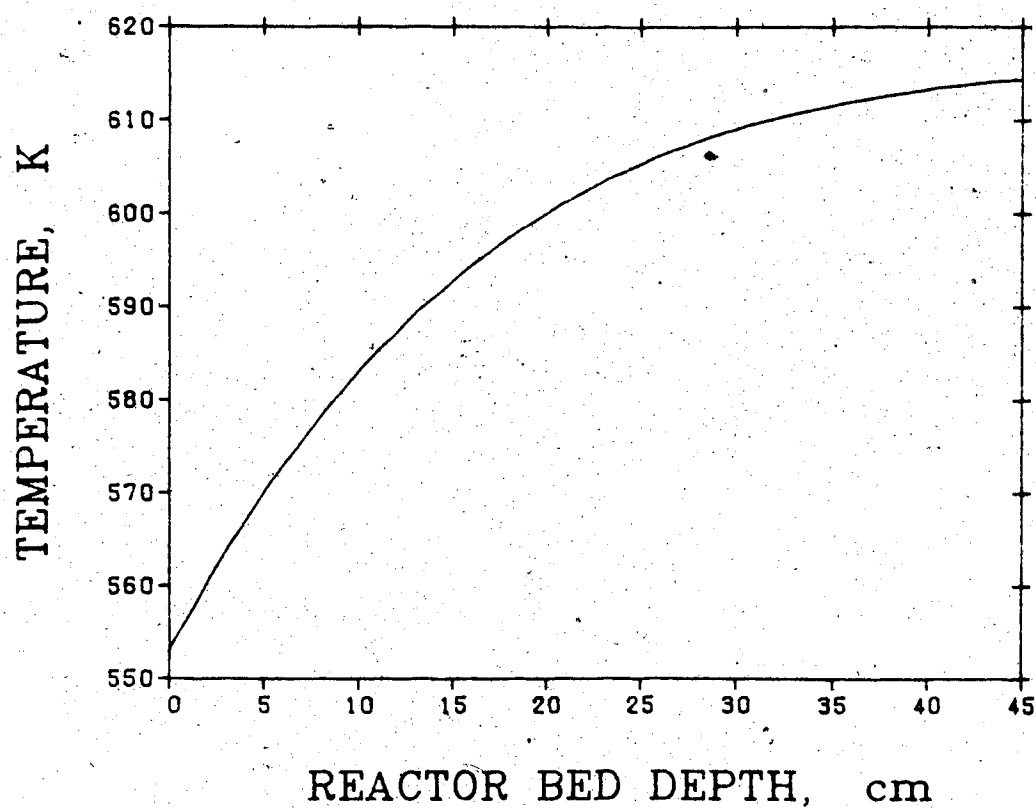
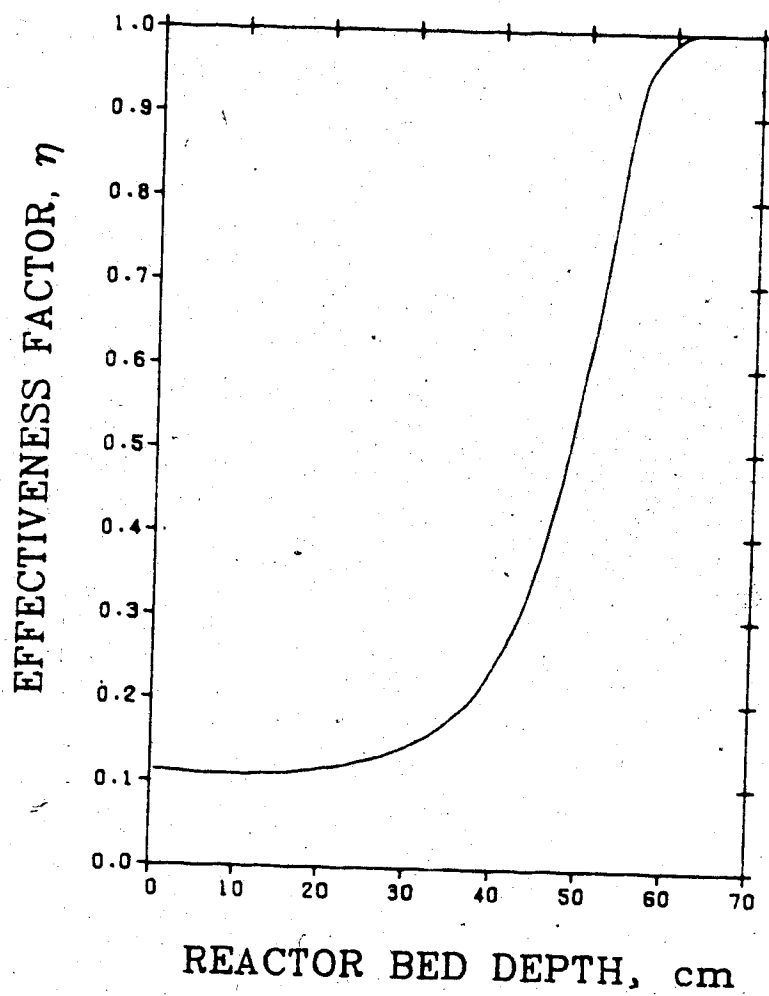


Figure 5.3 Local effectiveness factor in the catalytic Claus convertor.
Inlet composition (mole fraction): $\text{H}_2\text{S} = 0.07$,
 $\text{SO}_2 = 0.035$, $\text{H}_2\text{O} = 0.255$, $\text{N}_2 = 0.64$
Inlet temperature = 553 K
Pressure = 1 atm
Space velocity = 1000 hr^{-1}



increase to unity. In the entrance of the reactor bed where a significant reaction occurs up to the depth of 40 centimeters the effectiveness factor has a value of about 0.12.

In figures 5.4 and 5.5, the effect of the external mass and heat transfer resistances is shown, respectively, for the inlet section of the reactor since the inlet section can have the greatest gradient in temperature and concentration when significant reaction occurs at the inlet section. According to figure 5.4, the external diffusion effect results in the conversion difference of about 0.06. The external thermal resistance has caused a temperature difference of about 5 K as is shown in figure 5.5. In the Claus catalyst convertor, it is then predicted that external mass and heat transfer resistances are significant at the space velocity of 1000 hr^{-1} .

The state of knowledge concerning the thermodynamic properties for molecular sulfur vapor species is still uncertain as was discussed in section 2.3. Accordingly, the use of available thermodynamic properties for S_2 predicts conversions for reaction (3.20) lower than those experimentally observed. Thus the simulation results of figures 5.1 to 5.5 are conservative predictions.

Alternatively, the properties of S_2 to S_8 are frequently adjusted empirically to increase the predicted values for equilibrium conversion of reaction (3.20) as discussed in section 2.3. According to Yung (219), 10%, 15%,

Figure 5.4 Effect of film mass transport limitation in Claus catalytic convertor.
Inlet composition (mole fraction): $\text{H}_2\text{S} = 0.07$,
 $\text{SO}_2 = 0.035$, $\text{H}_2\text{O} = 0.255$, $\text{N}_2 = 0.64$
Inlet temperature = 553 K
Pressure = 1 atm
Space velocity = 1000 hr^{-1}

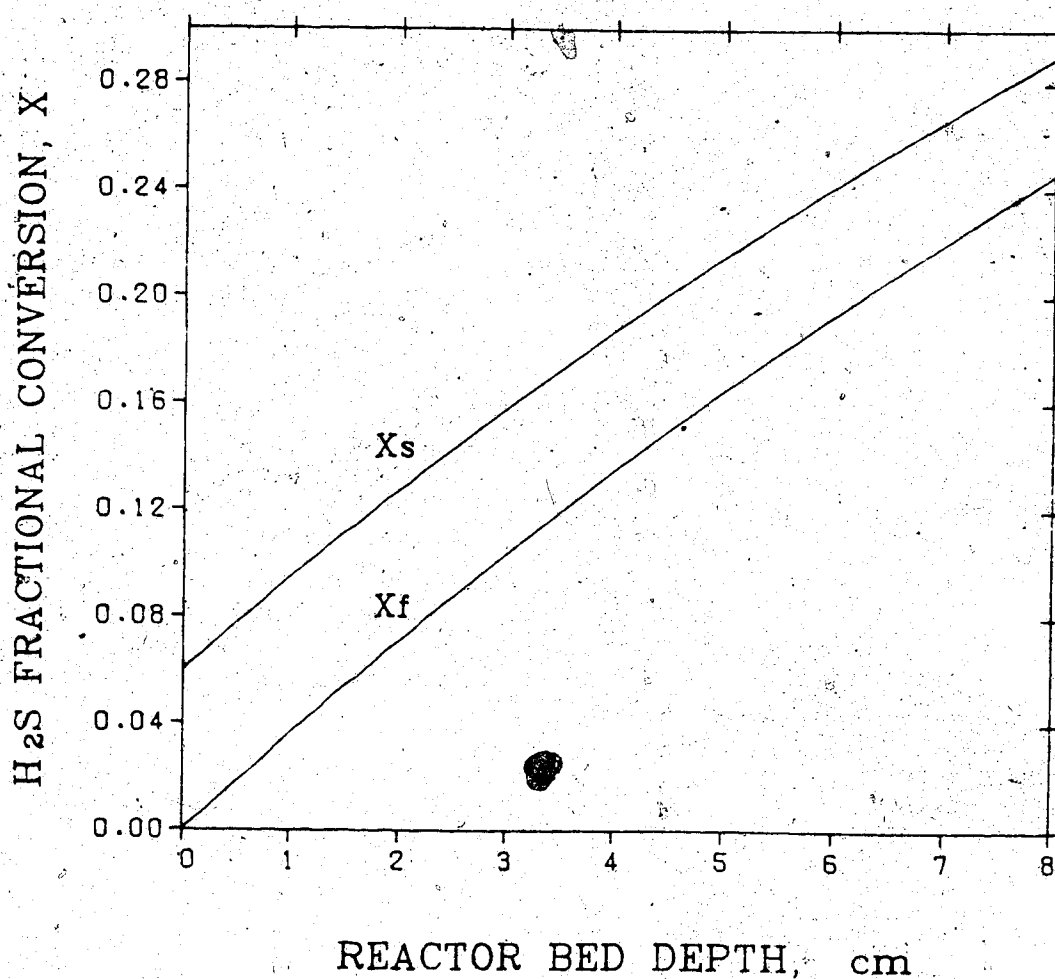
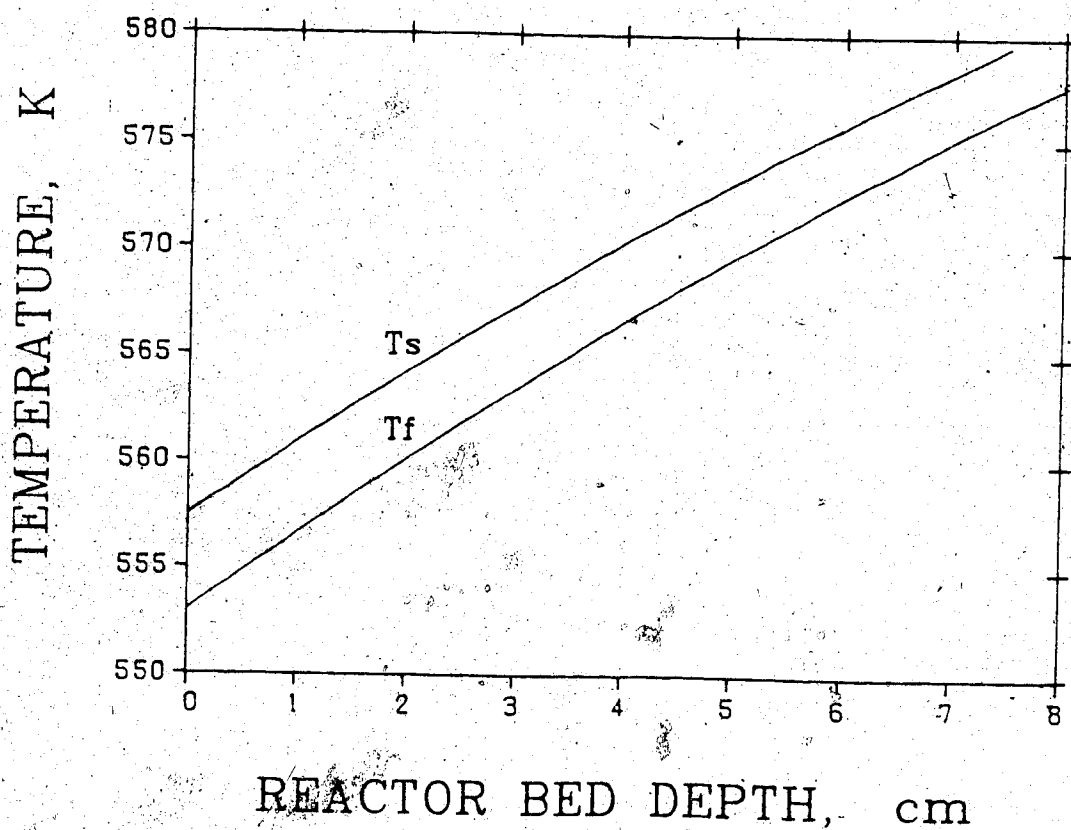


Figure 5.5 Effect of film heat transport limitation in Claus catalytic convertor.
Inlet composition (mole fraction): $\text{H}_2\text{S} = 0.07$,
 $\text{SO}_2 = 0.035$, $\text{H}_2\text{O} = 0.255$, $\text{N}_2 = 0.64$
Inlet temperature = 553 K
Pressure = 1 atm
Space velocity = 1000 hr^{-1}



and 20% increases in the absolute value of the free energies of S_2 , S_6 and S_8 respectively, give the best prediction of the experimental equilibrium H_2S conversion. Since the free energies are negative numbers, what Yung has meant was to reduce the free energies of the sulfur species. The fugacity coefficient of the sulfur species is low as shown in table A.2. Then, the ideal gas mixture approximation for the prediction of equilibrium H_2S conversion (equation 3.2) will introduce some error. Yung's results show that the g_i 's of S_2 , S_6 , and S_8 must be reduced by 10%, 15%, and 2 from its ideal value in equation (3.2) to eliminate the error of the ideal gas approximation and to get the correct equilibrium prediction. The equilibrium constants of reactions (3.20) to (3.23) were correlated with temperature using the suggested Yung's distorted free energy data. They are,

$$\ln K = 9891/T - 7.75 \quad (5.27)$$

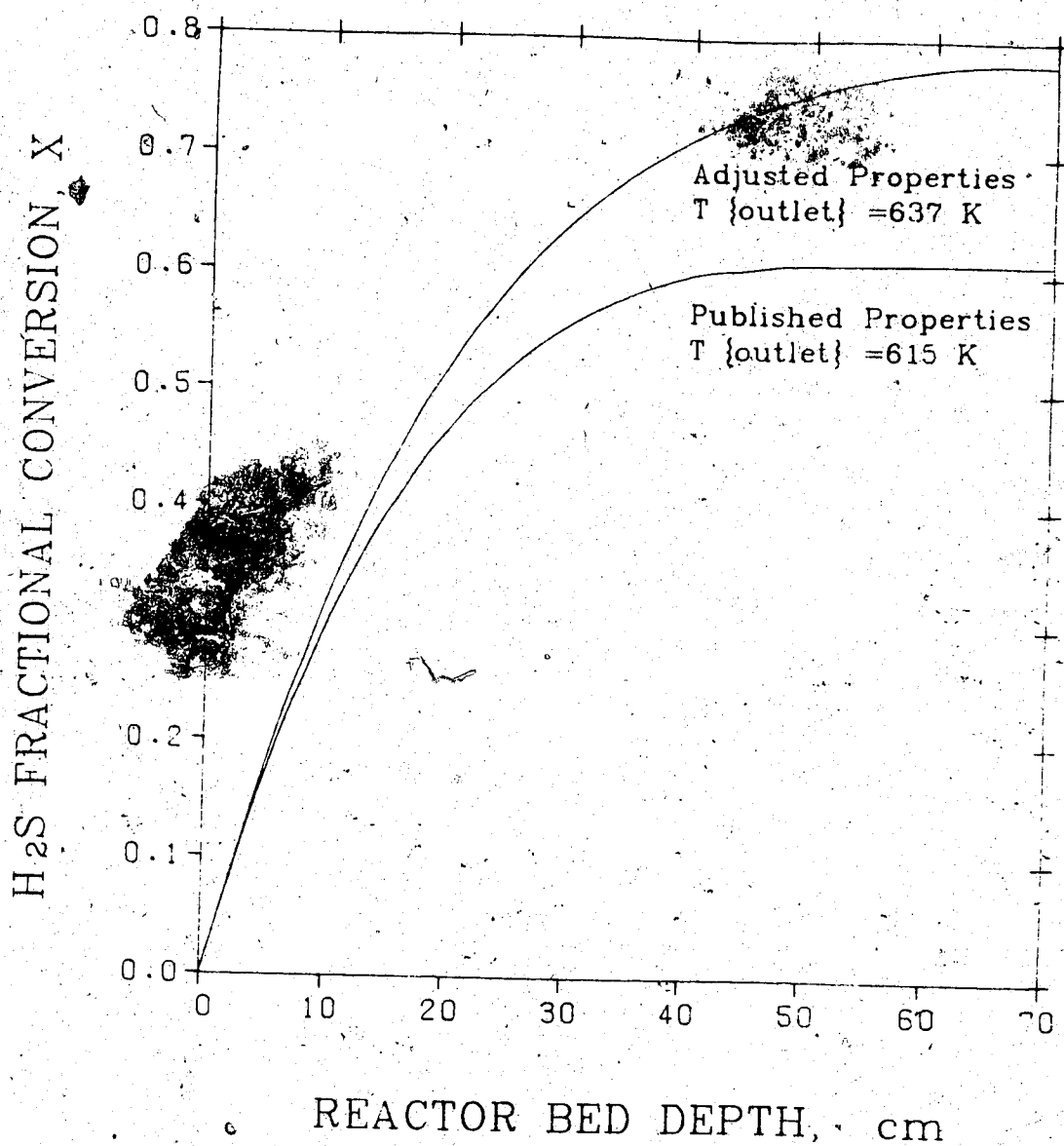
$$\ln K_{62} = -36904/T + 39.40 \quad (5.28)$$

$$\ln K_{64} = -11300/T + 4.91 \quad (5.29)$$

$$\ln K_{68} = 2738/T - 1.57 \quad (5.30)$$

Figure 5.6 presents the comparison of the conversion profiles using the published thermodynamic data and the adjusted data for the feed temperature of 553 K and space velocity of 1000 hr^{-1} . The two profiles show the same rate of fractional conversion increase at the inlet section of the bed. At the inlet section of the bed, the reverse

Figure 5.6 Effect of the thermodynamic properties of sulfur species on the predicted performance of Claus convertor.
 Inlet composition (mole fraction): $\text{H}_2\text{S} = 0.07$,
 $\text{SO}_2 = 0.035$, $\text{H}_2\text{O} = 0.255$, $\text{N}_2 = 0.64$
 Inlet temperature = 553 K
 Pressure = 1 atm
 Space velocity = 1000 hr^{-1}



reaction term does not contribute significantly and thus thermodynamic data of the sulfur species is not a decisive factor. In the vicinity of 25% fractional conversion of the convertor feed (see figure 5.6), the reverse reaction term contributes more significantly. The increased significance of the reverse reaction rate results in the dependence of both the equilibrium and the rate of increase of fractional conversion, on the thermodynamic data for sulfur species.

Figure 5.6 shows that the predicted equilibrium fractional conversion is increased from 0.61 to 0.78 by adjusting the free energy data of the sulfur species. Correspondingly the reactor outlet temperature is increased from 615 K to 637 K.

Figure 5.6 also reveals that, with the adjusted thermodynamic data, the maximum fractional conversion is reached at the depth of about 60 centimeteres compared to 40 centimeteres with the published data, for space velocity of 1000 hr^{-1} .

This result suggest that using the published thermodynamic data, the simulated results of the Claus reactor under varying space velocities have to be interpreted cautiously. That is, the simulation results using the published thermodynamic data, with space velocities higher than 1000 hr^{-1} might not predict the drop in the reactor efficiency and give the maximum possible conversion of 0.61. This conversion level would still be conservative compared to the model using the adjusted

thermodynamic data. However the predicted reactor bed depth might not be enough for obtaining the maximum reactor efficiency possible by use of adjusted thermodynamic data.

Figure 5.7 shows the effect of the feed temperature on the conversion profile along the reactor with a constant space velocity of 1000 hr^{-1} , using the adjusted thermodynamic properties of the sulfur species. The slopes of the profiles at the inlet section of the bed confirms that the high reaction rate can be achieved at the entrance of the catalyst bed by the increases of temperature. However, the high reaction rate at the inlet section, will be off-set by the lower equilibrium conversion at the outlet of the reactor as the feed temperature is increased. The asymptotes of the profiles in figure 5.7 shows that, the maximum possible H_2S fractional conversion of 0.72, 0.78, and 0.83, for the feed temperatures of 600, 553, and 500 K is approached at the depth of 50, 60, and 100 cm, respectively. Figure 5.7 also shows a very sluggish conversion profile for the feed temperature of 500 K compared to 553 and 600 K. This suggests that to have a balance between the maximum conversion and relatively high reaction rate the feed temperature should be between 500 and 553 K. The optimum choice depends on the economic factors and air pollution control policies.

Figure 5.8 has been plotted to evaluate the effect of the inlet temperature on the conversion-temperature plot with a space velocity of 1000 hr^{-1} . The slope of dx/dT is

Figure 5.7 Effect of inlet temperature on the performance of Claus convertor.

Inlet composition (mole fraction): $\text{H}_2\text{S} = 0.07$,
 $\text{SO}_2 = 0.035$, $\text{H}_2\text{O} = 0.255$, $\text{N}_2 = 0.64$
 Pressure = 1 atm
 Space velocity = 1000 hr^{-1}

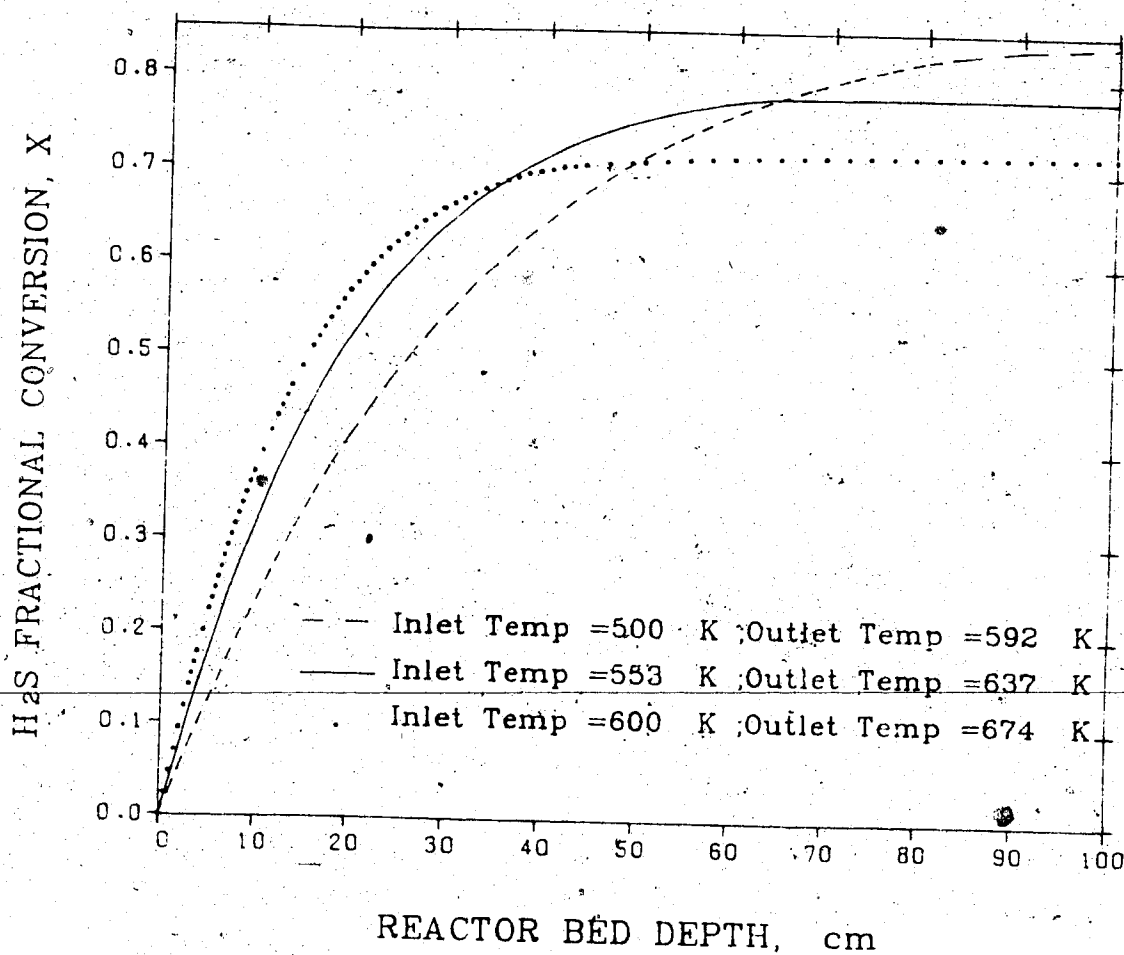
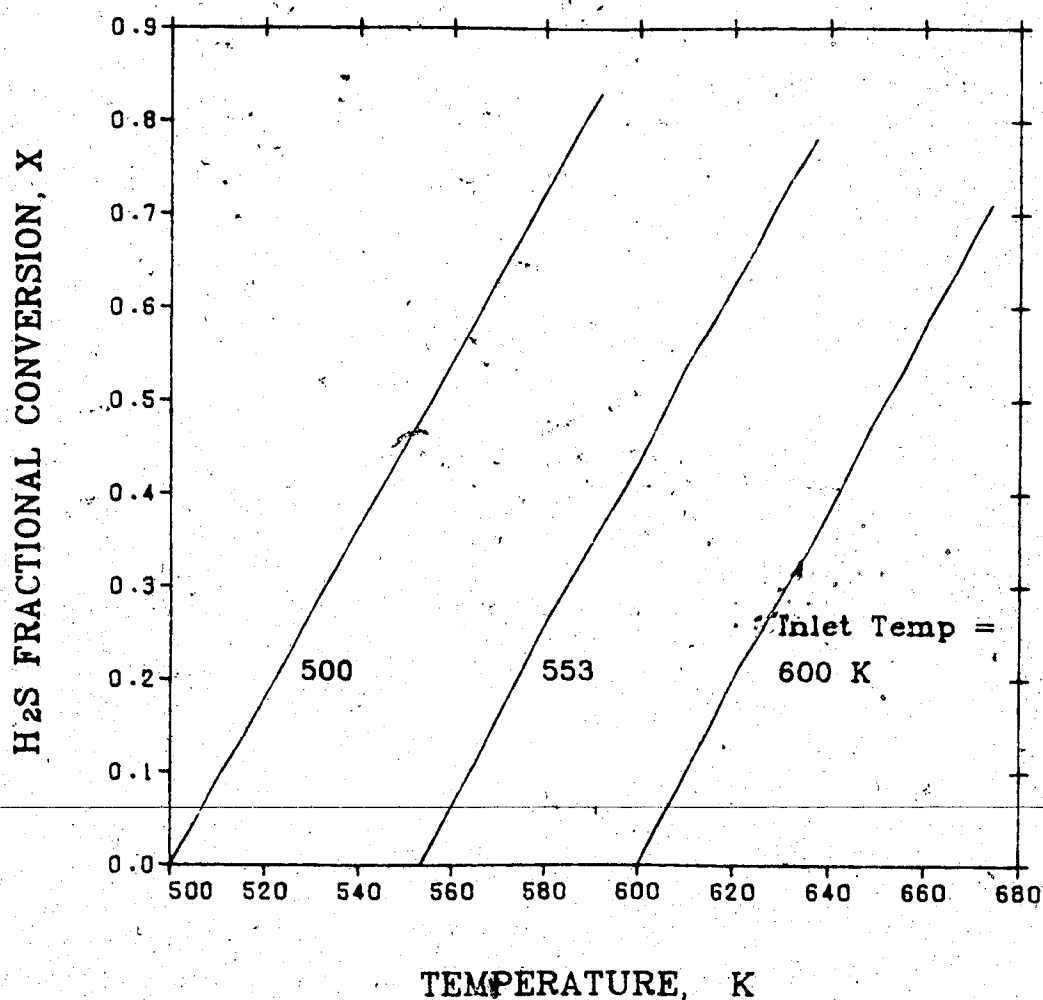


Figure 5.8 Effect of inlet temperature on the adiabatic reaction path.
Inlet composition (mole fraction): $\text{H}_2\text{S} = 0.07$,
 $\text{SO}_2 = 0.035$, $\text{H}_2\text{O} = 0.255$, $\text{N}_2 = 0.64$
Pressure = 1 atm
Space velocity = 1000 hr^{-1}



slightly decreased as the feed temperature is reduced.

The effect of the space velocity on the conversion profile at the fixed feed temperature of 553 K using the adjusted thermodynamic properties of sulfur species is shown in figure 5.9. The profiles indicate that one meter of the bed would not ensure the approach to the equilibrium when the space velocity is higher than 2000 hr⁻¹.

The Claus reactor simulation may advantageously be used to provide a basis for the evaluation of potential economic benefits of using catalysts differing in intrinsic catalytic activity, when subjected to identical operating conditions.

Cho (44) and Dalla Lana (54) have reported that "Cu" impregnated activated alumina (called novel catalyst) improves the H₂S/SO₂ activity and shows as much as a 50% improvement at the optimum content of 5 weight% of promoting agent. Figure 5.10 illustrates the comparison of the activities of the novel and activated alumina. These laboratory performance tests provide a measure of intrinsic catalytic activity via,

$$\{ \text{rate of reaction of H}_2\text{S} \} = \frac{d \{ \text{Frac. Conversion} \}}{d \{ \text{Space time} \}}$$

The ratio of the initial slopes of these H₂S conversion plots for the 5.4% Cu-promoted and γ-alumina catalysts is proportional to their intrinsic activity ratio. Thus when the rate expression (3.39) is multiplied by the activity ratio, it will show the rate enhancement by use of the novel

Figure 5.9 Effect of space velocity on the performance of Claus convertor.
Inlet composition (mole fraction): $\text{H}_2\text{S} = 0.07$,
 $\text{SO}_2 = 0.035$, $\text{H}_2\text{O} = 0.255$, $\text{N}_2 = 0.64$
Inlet temperature = 553 K
Pressure = 1 atm

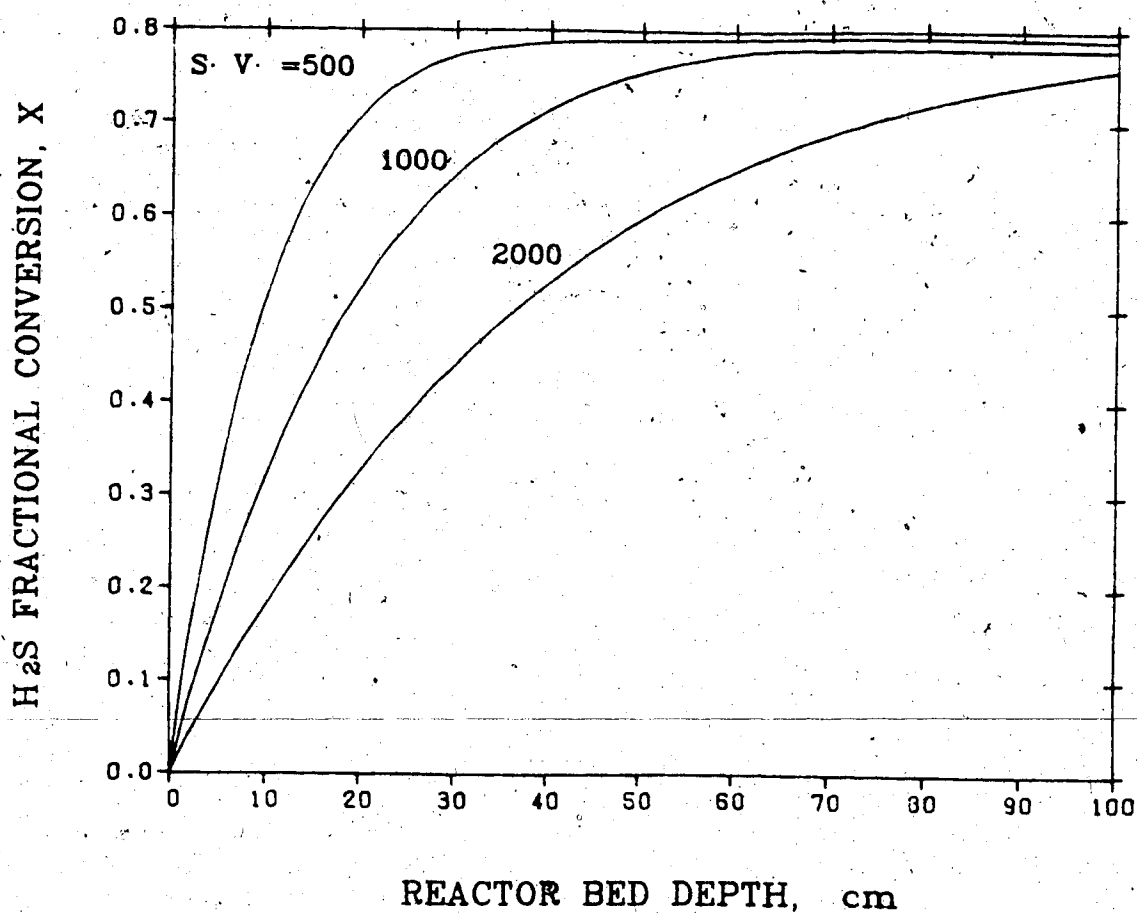
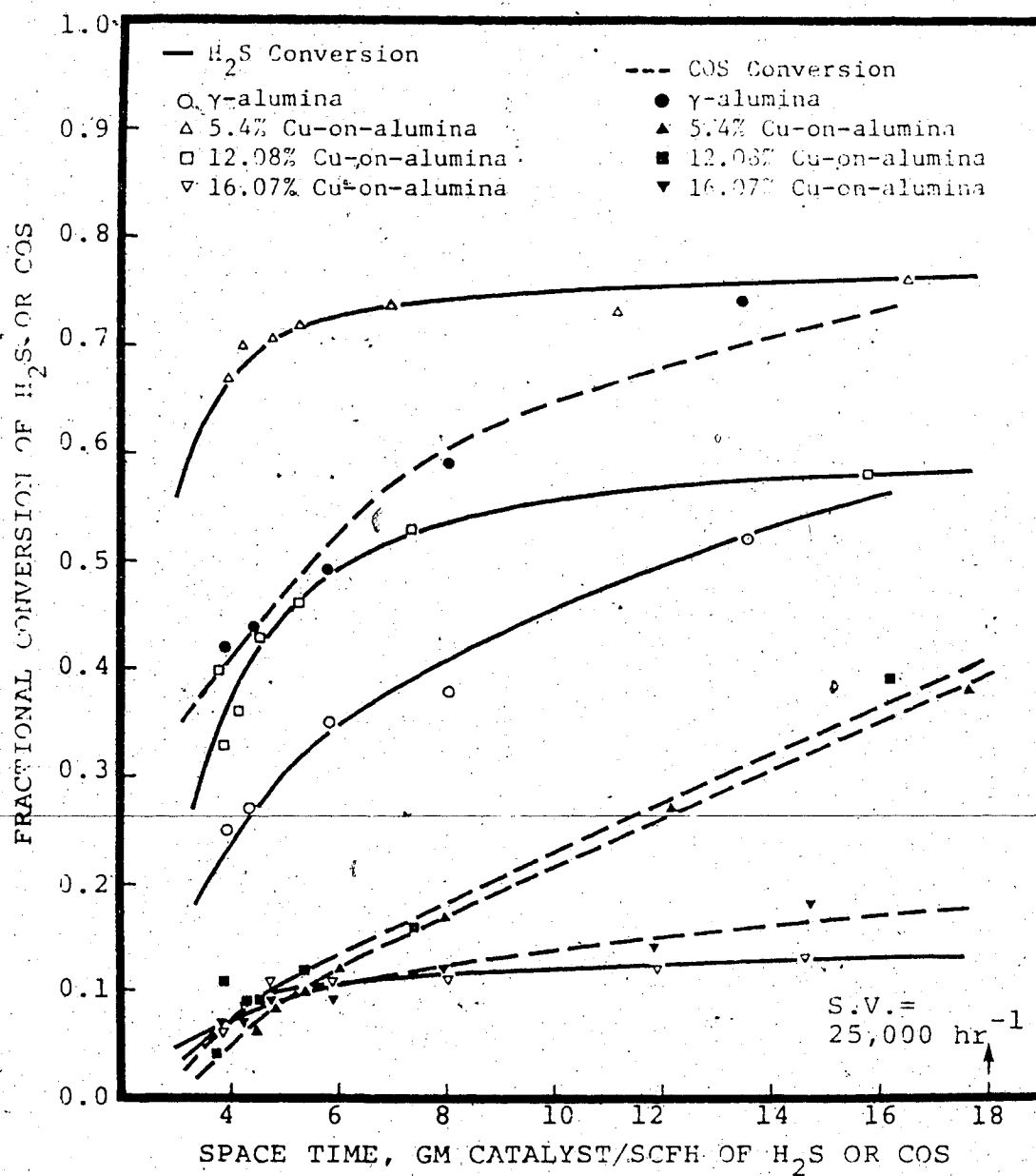


Figure 5.10 Comparison between novel catalyst and a commercial catalyst (44).



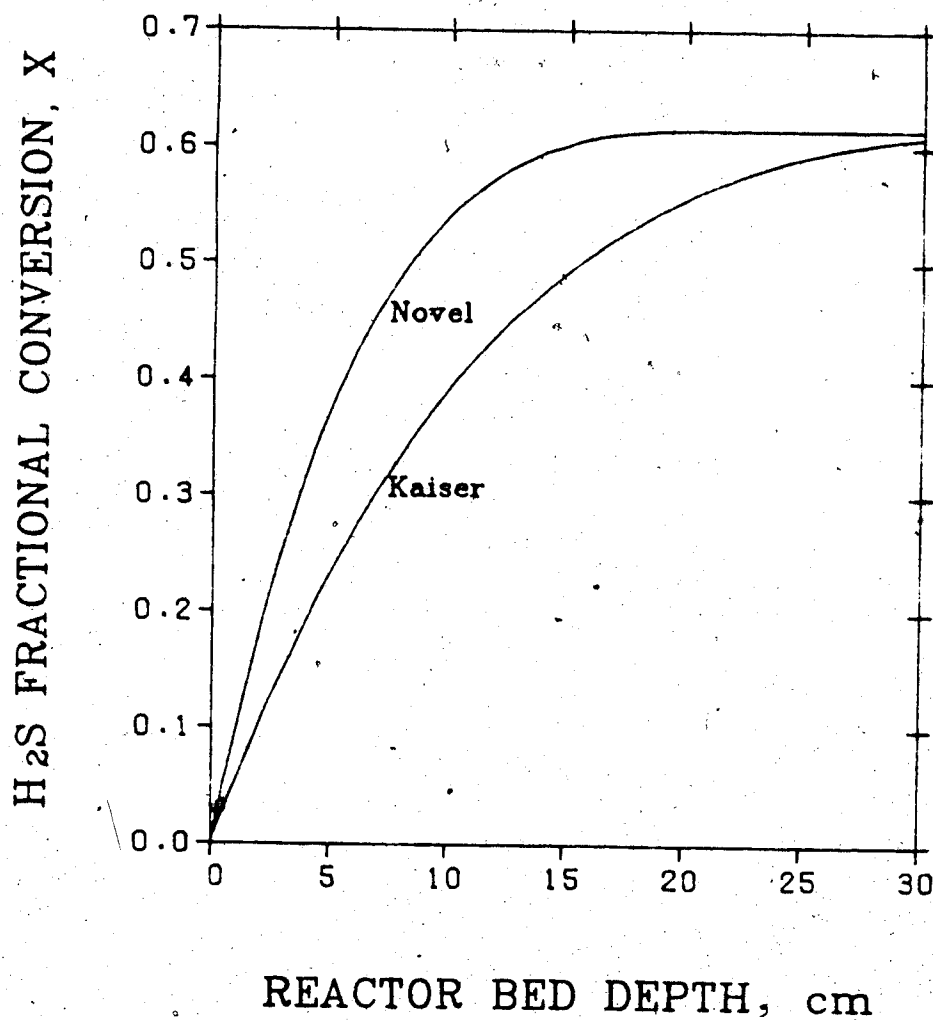
catalyst. The activity ratio, as measured from the initial slopes of the alumina and 5.4% Cu-promoted alumina profile in figure 5.10, is about 3.5.

The performance of Claus reactors employing activated alumina and novel catalyst will be compared using (kf) and $(3.5 kf)$ in the rate expression (3.39) for the rate expression of the two catalysts, respectively. In this simulation study the mass transfer coefficient and the effective diffusivity of all the species were taken equal to those for H_2S . The published thermodynamic data were used to specify the extent of equilibrium of reactions (3.20) to (3.23).

Figure 5.11 shows conversion rise as a function of distance along the bed axis. Equilibrium conversion is attained in about 15 cm for the novel catalyst versus about 30 cm for the activated alumina catalyst. Thus, 15 centimeteres bed depth reduction is possible without harm. Alternatively, one could observe that the novel catalyst extends the bed life.

The above result, 15 cm versus 30 cm implies that about $1/2$ of the bed depth is required for the novel catalyst compared to alumina. However, the intrinsic activity of the novel catalyst is 3.5 times that of alumina as was calculated from the initial slopes of the profiles in figure 5.10. This intrinsic activity ratio of 3.5 is not observed in the performance of the bed where the activity ratio was only about two. The reduced observed activity of the

Figure 5.11 H_2S conversion profile along novel and alumina catalysts bed depth.
Inlet composition (mole fraction): $\text{H}_2\text{S} = 0.07$,
 $\text{SO}_2 = 0.035$, $\text{H}_2\text{O} = 0.255$, $\text{N}_2 = 0.64$
Inlet temperature = 553 K
Pressure = 1 atm
Space velocity = 1000 hr^{-1}



converter is due to the lower effectiveness factor of the novel catalyst compared to that of the alumina catalyst. The effectiveness factor for the novel catalyst is about 0.09 compared to 0.16 for the alumina catalyst at the inlet section of the bed.

Figure 5.12 shows the performance of the novel catalyst at the same inlet conditions as figure 5.11 but at double the space velocity, 2000 hr^{-1} . The space velocity for the alumina catalyst was reduced below 2000 hr^{-1} until the alumina catalyst generated the same performance. This occurred at a space velocity of 1000 hr^{-1} . Thus, this prediction shows that the novel catalyst will maintain performance even if production is doubled (doubled feed gas flow rate). Alternatively, the capacity throughout is two times larger for the novel catalyst in an existing Claus converter.

Figure 5.13 shows that for a first stage converter of about 1 meter catalyst depth to be fully utilized, that is equilibrium conversion at the bed outlet (rather than within the bed), a space velocity of $10,000 \text{ hr}^{-1}$ would be needed for the novel catalyst versus 5000 hr^{-1} for an alumina catalyst. Published thermodynamic properties have been used in the simulation studies leading to figures 5.11 to 5.13. Thus, in reality a Claus first stage converter could not operate at the high levels of space velocities of 10,000 and 5000 because discussion of figure 5.6 revealed that using the adjusted thermodynamic properties of sulfur species

Figure 5.12 Efficiency of alumina and novel catalysts beds at different space velocities.
Inlet composition (mole fraction): $\text{H}_2\text{S} = 0.07$,
 $\text{SO}_2 = 0.035$, $\text{H}_2\text{O} = 0.255$, $\text{N}_2 = 0.64$
Inlet temperature = 553 K
Pressure = 1 atm,

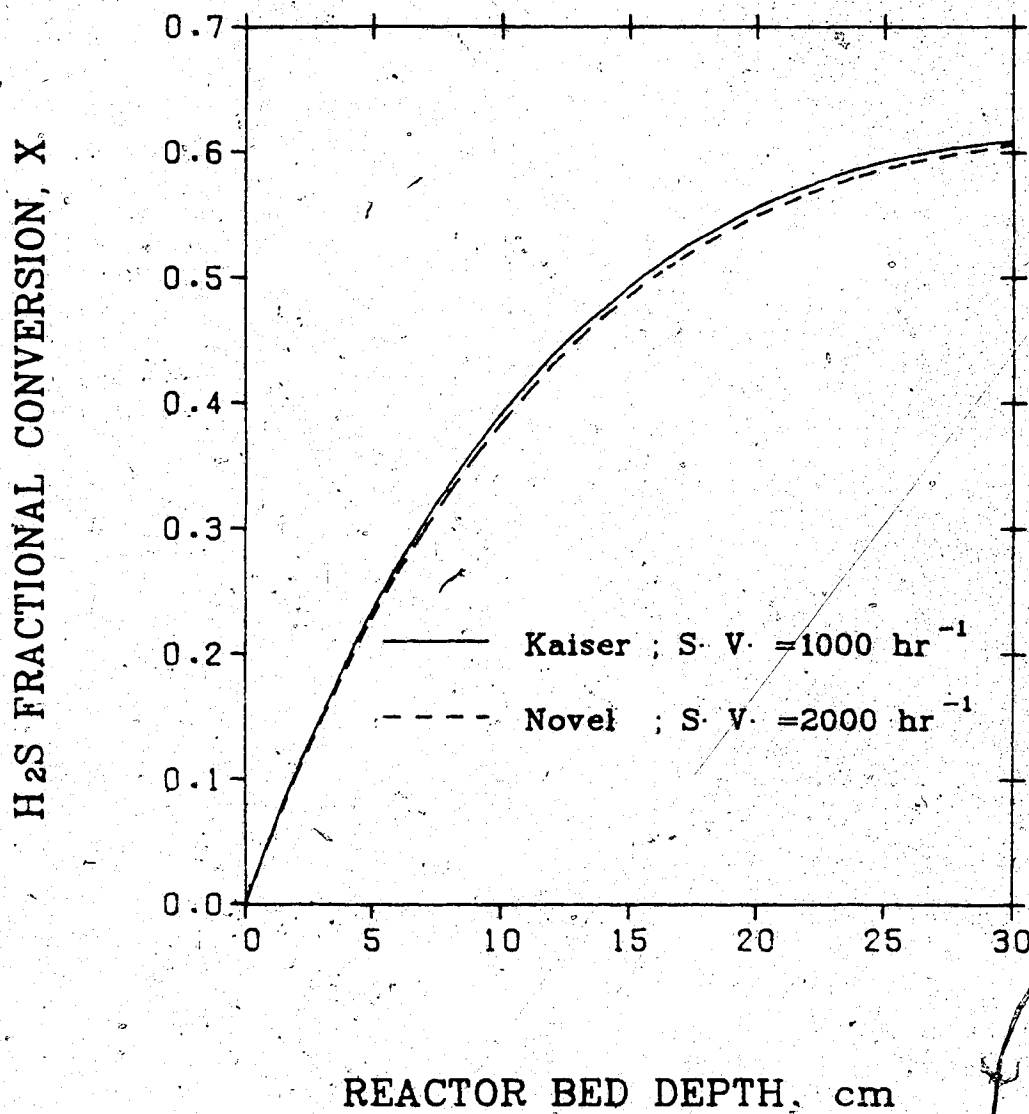
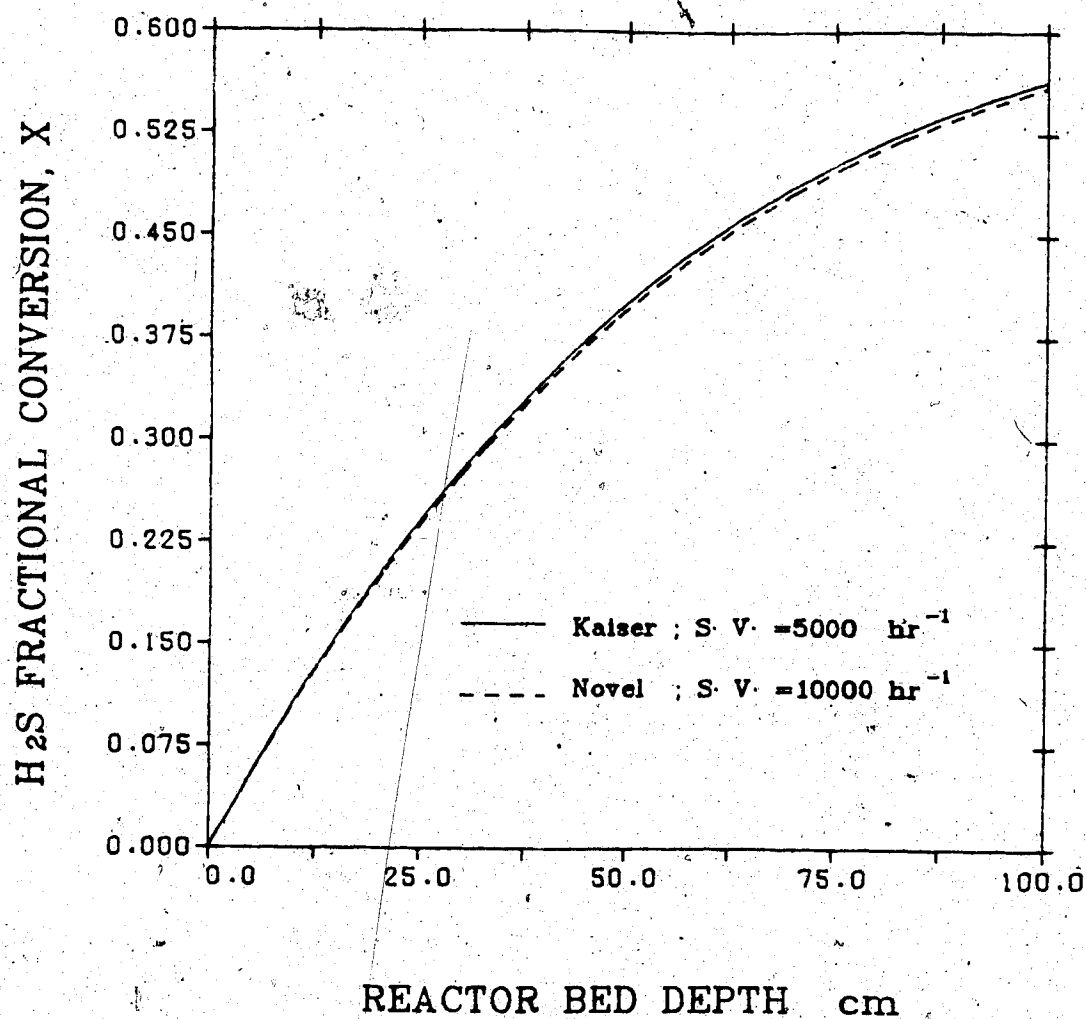


Figure 5.13 Space velocity for utilizing 1-meter depth of novel and alumina catalysts.
Inlet composition (mole fraction): $\text{H}_2\text{S} = 0.07$,
 $\text{SO}_2 = 0.035$, $\text{H}_2\text{O} = 0.255$, $\text{N}_2 = 0.64$
Inlet temperature = 553 K
Pressure = 1 atm



which is believed to be compatible with the observed equilibrium data, predicts longer bed or lower space velocity compared to the predicted values by published thermodynamic properties. Furthermore, if catalyst deactivation occurs, the outlet content of H_2S would gradually rise and shift the load down-stream to the second stage convertor, and beyond.

5.4 2-Dimensional Claus Process Model

5.4.1 Introduction

The accurate prediction of the Claus reactor behavior when the heat losses to the environment are appreciable, requires a model accounting for radial concentration and temperature gradients. The model then becomes 2-dimensional.

The 1-dimensional Claus reactor model revealed that the external mass and heat transfer resistances are not negligible at the typical space velocity of 1000 hr^{-1} . Thus a heterogeneous model which distinguishes between the solid and fluid is also required in the two-dimensional model of the Claus bed.

The difficulties encountered with 2-dimensional heterogeneous model arise from the heat transfer, which in contrast with mass transfer, occurs through the fluid and solid phase. Radial heat transport in the pseudo-homogeneous model which is based on a single lumped phase has been considered by many researchers (64,125,215,216). However,

the effective thermal conductivity in pseudo-homogeneous models does not distinguish explicitly between fluid and solid phase. De Wasch and Froment (63) used the mechanisms for heat transfer proposed by Yagi and Kunii (215) and developed separate effective radial thermal conductivity formula for solid and fluid phases in a fixed bed reactor. They grouped the heat transfer mechanisms according to the phases:

1. Solid phase

- a. conduction through the particle.
- b. conduction from particle to particle through the contact surfaces.
- c. conduction through the stagnant film surrounding the contact surfaces.
- d. radiation from particle to particle.

2. fluid phase

- a. conduction through the fluid.
- b. energy convection through the fluid
- c. transfer from fluid to solid
- d. radiation from void to void

By application of the methods used by Yagi and Kunii (215), De Wasch and Froment (63) derived the expression for effective heat conductivity for the fluid phase λ_f and for the solid phase λ_s as:

$$\lambda_f = \epsilon (k_g + \beta' D_p h_v + \rho C_p D_r) \quad (5.31)$$

$$\lambda_s = \frac{\beta' (1 - \epsilon)}{\{ (\gamma/k_s + 1/(kg/\phi')) + h_p D_p + D_p h_s \}} \quad (5.32)$$

These general equations may be simplified in many instances. For example, except at very low pressures the term for heat transfer through the contact surfaces ($h_p D_p$) can be neglected (215,216). For gaseous systems the radiation contribution h_v and h_s are negligible except for relatively large particles and high temperatures above 750 K (125).

Once the thermal conductivity of two phases are known, the material balance equations for the two-phase heterogeneous model may be developed.

5.4.2 Model Formulation

Based on the discussion in section 5.5.1, De Wasch and Froment (63) developed a heterogeneous two-dimensional model for a single reactant reaction in a fixed bed reactor. The general transport and reaction process for the Claus reaction using the De Wasch and Froment model may be described by the following equations:

for $j = 1, 2, 3$.

$$\partial (V_r C_{f,j}) / \partial z - D_{r,j} \nabla^2 C_{f,j} + k_{m,j} A (C_{f,j} - C_{s,j}) = 0 \quad (5.33)$$

$$k_{m,j} (C_{f,j} - C_{s,j}) = -a_j \rho_b \eta R_c \quad (5.34)$$

and for sulfur species,

$$\partial (V_z Z_f) / \partial z - D r_s \nabla^2 Z_f + k_{ms} A(Z_f - Z_s) = 0 \quad (5.35)$$

$$k_{ms}(Z_f - Z_s) = -6a_s \rho_b \eta R_c \quad (5.36)$$

with the energy balance equations,

$$C_p \partial (V_z \rho T_f) / \partial z - \lambda_f \nabla^2 T_f - h A(T_s - T_f) = 0 \quad (5.37)$$

$$\lambda_s \nabla^2 T_s + (-\Delta H) \rho_b \eta R_c - h A(T_s - T_f) = 0 \quad (5.38)$$

where,

$$\nabla^2 = 1/r \partial (r \partial / \partial r) / \partial r$$

If the radial diffusional and film transport resistances for all the species are equal, then the stoichiometry of the reaction will specify the concentration or amount of each species relative to the reference species 1 (H_2S), as was shown by the analytical solution in equation (5.12) and (5.13).

Wen and Fan (209) have summarized the available data on radial dispersion coefficient in packed beds and obtained the relationship

$$\frac{1}{P_{em}} = \frac{0.4}{(Re Sc)^{0.8}} + \frac{0.09}{\{ 1 + 10 / (Re Sc) \}} \quad (5.39)$$

The equation (5.39) gives the values of P_{em} 10.84, 10.86, 10.84 and 10.93 for H_2S , SO_2 , H_2O , and S_8 respectively at the space velocity of 1000 hr^{-1} . On the other hand, Froment (82) recommends P_{em} of 10 for all practical purposes.

Figure 5.1 revealed that the evaluation of k_m 's at an average value of bulk diffusivity results only in minor error.

To limit the complexities of solving four two-dimensional differential equation (5.33) and (5.35), k_m 's and P_{em} 's are taken equal, in the two-dimensional analysis of the Claus process. This simplification has also been considered by Ahmed (2) and Young (218) in the analysis of SO_2 oxidation reactor, although the authors have not mentioned it explicitly. The scatter of the data about the correlated equations for k_m and P_{em} , also justifies evaluation of single average k_m and Dr using an average value of Sc number.

Invoking the assumption of equal radial dispersion and film mass transfer coefficient, equation (5.33) have to be solved for the reference species 1 (H_2S). The corresponding local concentration of the other species would then be specified from the stoichiometry of the reaction.

The equations (5.33), (5.34), (5.37) and (5.38) have been developed in terms of conversion and different dimensionless groups in section E.2. The resulting equations are,

$$\begin{aligned} \partial X_f / \partial z' &= (a \text{ Pem})^{-1} \cdot [(1-s)(1-X_f) / (\tau f(1-s)+s)^2 \nabla^2 \tau f \\ &\quad + \nabla^2 X_f / (\tau f(1-s)+s)] \\ &\quad + \text{Dam } \eta \text{ Rc}_s / \text{Rc}^0 \end{aligned} \quad (5.40)$$

$$\partial \tau f / \partial z' = (a \text{ Peh})^{-1} \{ \nabla^2 \tau f + \gamma (\tau s - \tau f) \} \quad (5.41)$$

$$\begin{aligned} \nabla^2 \tau s &= - \{ \text{Dam } H' \text{ Peh } a \beta / (1-s) \} \eta \text{ Rc}_s / \text{Rc}^0 \\ &\quad + \gamma \beta (\tau s - \tau f) \end{aligned} \quad (5.42)$$

$$\frac{(1-X_f)}{\tau f(1-s)+s} - \frac{(1-X_s)}{\tau s(1-s)+s} = \text{Dam } \delta \eta \text{ Rc}_s / \text{Rc}^0 \quad (5.43)$$

The local values of SO_2 and H_2O are then specified by;

$$x(\text{SO}_2) = Y_{\text{SO}_2} - 0.5 Y_{\text{H}_2\text{S}} X \quad (5.44)$$

$$x(\text{H}_2\text{O}) = Y_{\text{H}_2\text{O}} + Y_{\text{H}_2\text{S}} X \quad (5.45)$$

The corresponding local values of total moles N_t , and S_s are obtained from the solution of equation (3.22) to (3.26) which led to the equations (B.1) and (B.2), as was explained in chapter 3. The boundary conditions for the equation, (5.33), (5.34), (5.37), (5.38) are,

$$C_{f1} = C_{f1}^0$$

$$\text{at } z=0 \quad (5.46)$$

$$T_f = T^0$$

$$\partial T_f / \partial z = \partial T_s / \partial z = \partial C_{f,1} / \partial z = 0 \quad \text{at } r=0 \quad (5.47)$$

$$\partial C_{f,1} / \partial z = 0 \quad \text{at } r=1 \quad (5.48)$$

$$U_f (T_f - T_a) = -\lambda_f \partial T_f / \partial r \quad \text{at } r=R_w \quad (5.49)$$

$$U_s (T_s - T_a) = -\lambda_s \partial T_s / \partial r \quad \text{at } r=R_w \quad (5.50)$$

where U_f and U_s are the overall heat transfer coefficients of fluid and catalyst pellet, respectively. They are obtained from the analysis of heat conduction through composite walls as,

$$U_f = R_w^{-1} (1/(R_w a_f) + U_0)^{-1} \quad (5.51)$$

$$U_s = R_w^{-1} (1/(R_w a_s) + U_0)^{-1} \quad (5.52)$$

where,

$$U_0 = \ln(R_{ins}/R_w)/K_{ins} + \ln(R_{sh}/R_{ins})/K_{sh} + 1/(R_0 h_a) \quad (5.53)$$

The boundary conditions (5.46) to (5.50) in terms of dimensionless variables will be,

$$x_f = 0 \quad \text{at } \hat{z}' = 0 \quad (5.54)$$

$$\tau_f = 1$$

$$\partial \tau_f / \partial r' = \partial \tau_s / \partial r' = \partial X_f / \partial r' = 0 \quad \text{at} \quad r' = 0 \quad (5.55)$$

$$\partial X_f / \partial r' = 0 \quad \text{at} \quad r' = 1 \quad (5.56)$$

$$B_{if} \tau_f + \partial \tau_f / \partial r' = 0 \quad \text{at} \quad r' = 1 \quad (5.57)$$

$$B_{is} \tau_s + \partial \tau_s / \partial r' = 0 \quad \text{at} \quad r' = 1 \quad (5.58)$$

Using this analysis to simulate the performance of the Claus two-dimensional model, the partial differential equations (5.40) to (5.42) and the algebraic equation (5.43) coupled with the boundary conditions (5.54) to (5.58) must be solved for a specified inlet composition, temperature and space velocity.

5.4.3 Computational Scheme

The partial differential equations (5.40) to (5.42) have been transformed into ordinary differential equations by application of orthogonal collocation in the radial direction. Section E.2 describes the method and presents the resulting equations and the computer code.

The analysis of section E.2, shows that in order to obtain the solution to the two-dimensional Claus model, $(2n_i+2)$ ordinary differential equations coupled with $(4n_i+4)$ nonlinear algebraic equations have to be solved, for a given

number of radial interior points (n_i) at each axial node.

The Runge-Kutta integration algorithm and the Newton-Raphson integration scheme were employed for integration and solution of the nonlinear algebraic equations, respectively. Five interior collocation points were used to represent the radial temperature and conversion profiles.

5.4.4 Numerical Results of Two-Dimensional Claus Model

The axial average temperature and conversion as defined by equation (E.52) and (E.53), along the catalyst beds of different diameter are plotted in figure 5.14 and 5.15, respectively. These profiles indicate that as the diameter of the reactor is increased, the effect of heat loss becomes less significant.

Figure 5.14 reveals that the heat loss has a pronounced effects on the average temperature profile in a bed of small diameter. The effect on the mean conversion, is however small, as figure 5.15 shows.

Figure 5.14 and 5.15 are obtained using constant inlet superficial velocity V_s of 40 cm/sec. This corresponds to a constant space velocity of 1440 hr^{-1} for the reactor beds of 1 meter depth. Figure 5.15 shows that at a given depth, the conversion is higher in a wider bed, for a constant space velocity. With this prediction, it is advisable to design large diameter Claus beds. In practice, the Claus catalytic convertors are actually designed as wide and shallow beds,

Figure 5.14 Axial profile of the radial mean temperature for Claus reactors with different diameter.
Inlet composition (mole fraction): $\text{H}_2\text{S} = 0.1$,
 $\text{SO}_2 = 0.05$, $\text{H}_2\text{O} = 0.2$, $\text{N}_2 = 0.65$
Inlet temperature = 500 K
 $T_a = 273$ K
Pressure = 1 atm
 $V_i = 40$ cm/sec

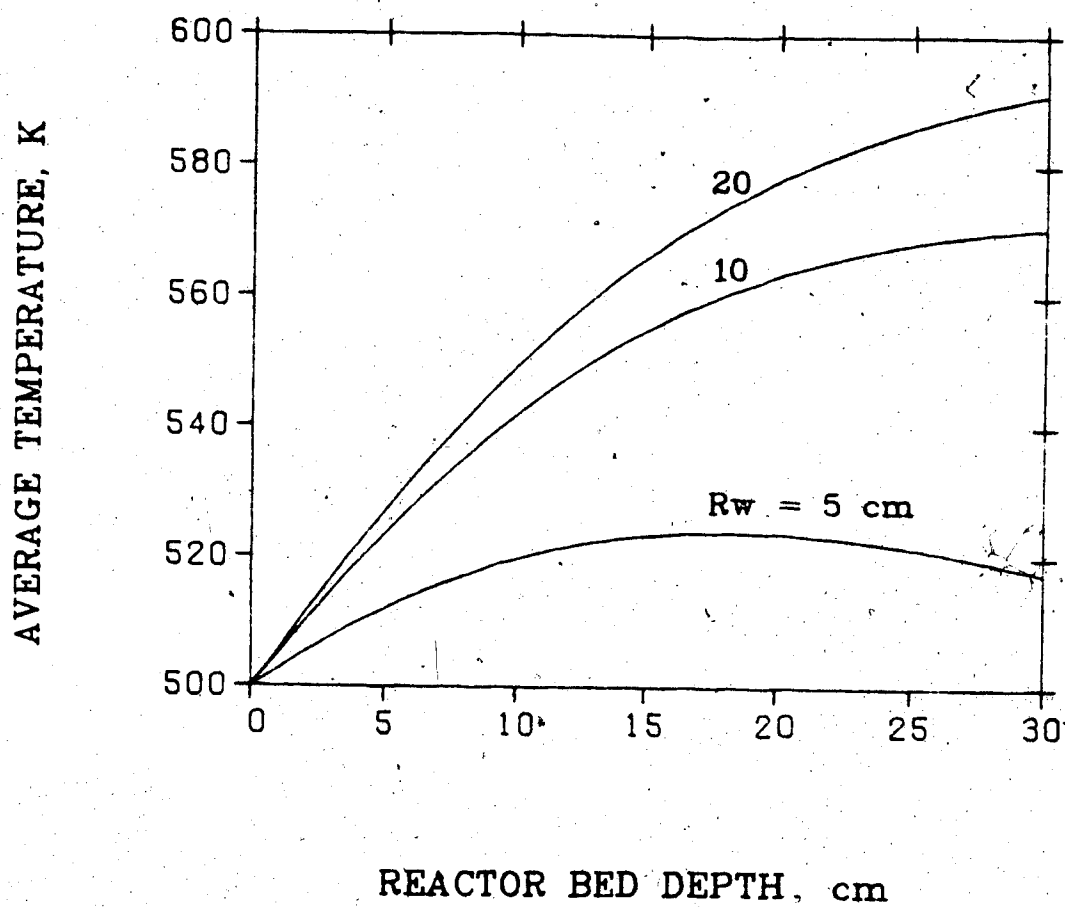
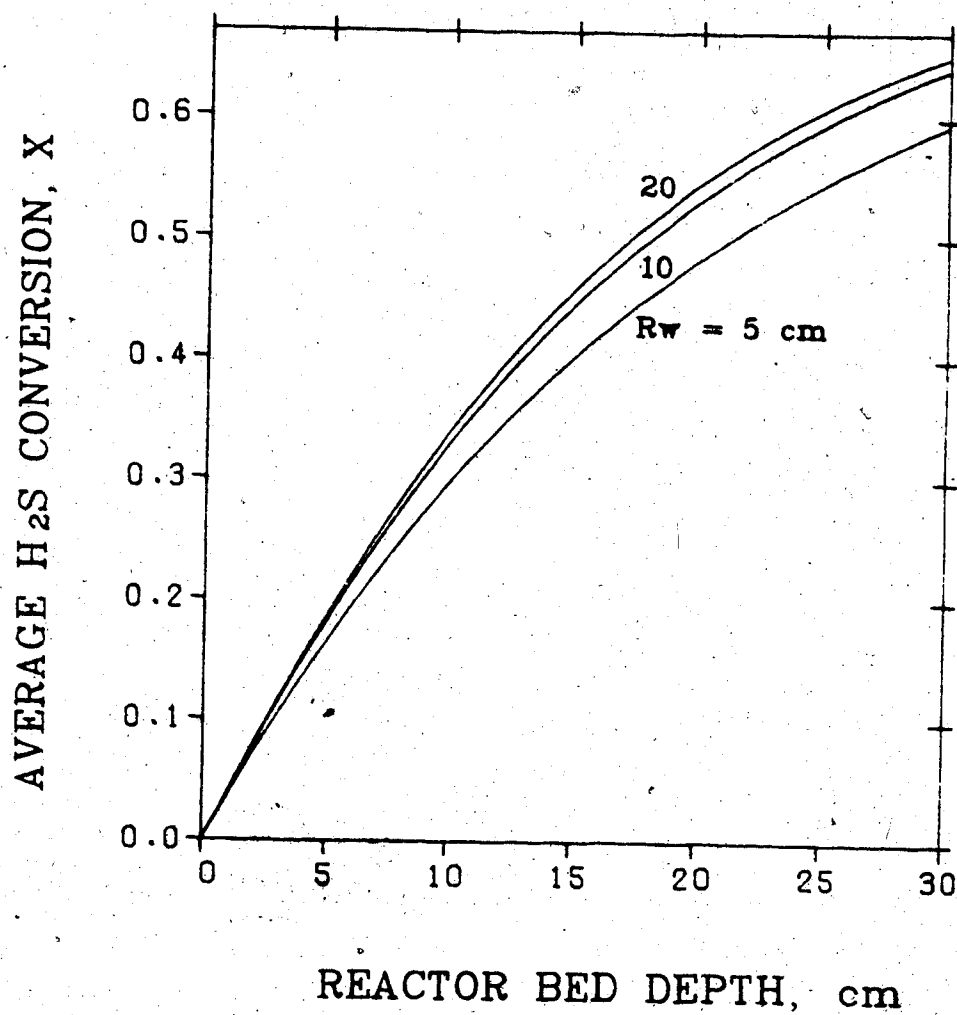


Figure 5.15 Axial profile of the radial mean conversion of H_2S for Claus reactors with different diameter.
 Inlet composition (mole fraction): $\text{H}_2\text{S} = 0.1$,
 $\text{SO}_2 = 0.05$, $\text{H}_2\text{O} = 0.2$, $\text{N}_2 = 0.65$
 Inlet temperature = 500 K
 $T_a = 273$ K
 Pressure = 1 atm
 $V_i = 40$ cm/sec



as was described in section 2.6.

The radial temperature and conversion profiles at the depth of 5 cm, are shown in figure 5.16 and 5.17, respectively. These profiles show that the heat loss affects the temperature and consequently the conversion profiles only in the vicinity of the wall.

5.5 Comparison of 1- and 2-Dimensional Models

Figure 5.18 presents the axial average temperature and the center line temperature profiles of a 30 centimeter diameter bed for a non-stoichiometric H_2S/SO_2 feed ratio. The temperature profile predicted by 1-dimensional model is also shown in figure 5.18. The corresponding conversion profiles are represented in figure 5.19. The average temperature profile in figure 5.18 shows a hot spot of about 500 K at an axial position of 60 centimeter. The hot spot is however, much lower than the corresponding predicted temperature (527 K) from the one-dimensional model.

The two-dimensional model predicts the centerline temperature close to the predicted temperature of the one-dimensional model. The centerline conversion profile is, however, much different from the one-dimensional model predicted value.

Figure 5.20 presents the radial temperature profiles as a function of axial position, for the conditions in figure 5.18 and 5.19. These profiles reveal that as the bed depth is increased, the non-uniformity of the temperature in the

Figure 5.16 Radial temperature profile in Claus converters with different diameter.
 Inlet composition (mole fraction): $\text{H}_2\text{S} = 0.1$,
 $\text{SO}_2 = 0.05$, $\text{H}_2\text{O} = 0.2$, $\text{N}_2 = 0.65$
 Inlet temperature = 500, K
 $T_a = 273$ K
 Pressure = 1 atm
 $V_i = 40$ cm/sec
 $z = 5$ cm

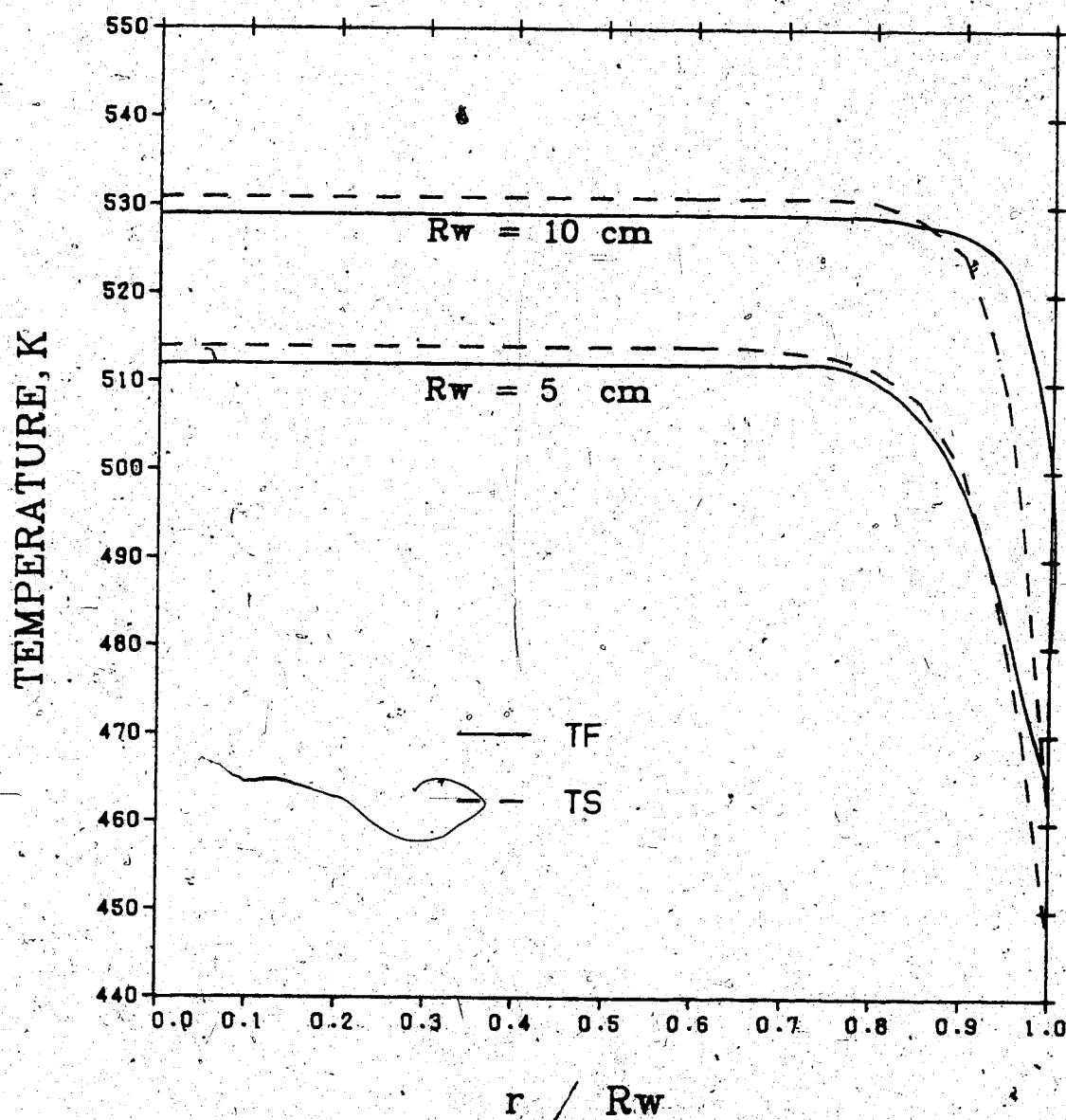


Figure 5. Radial H_2S conversion profile in Claus convertors with different diameter.

Inlet composition (mole fraction): $\text{H}_2\text{S} = 0.1$,
 $\text{SO}_2 = 0.05$, $\text{H}_2\text{O} = 0.2$, $\text{N}_2 = 0.65$

Inlet temperature = 500 K

$T_a = 273$ K

Pressure = 1 atm

$V_i = 40$ cm/sec

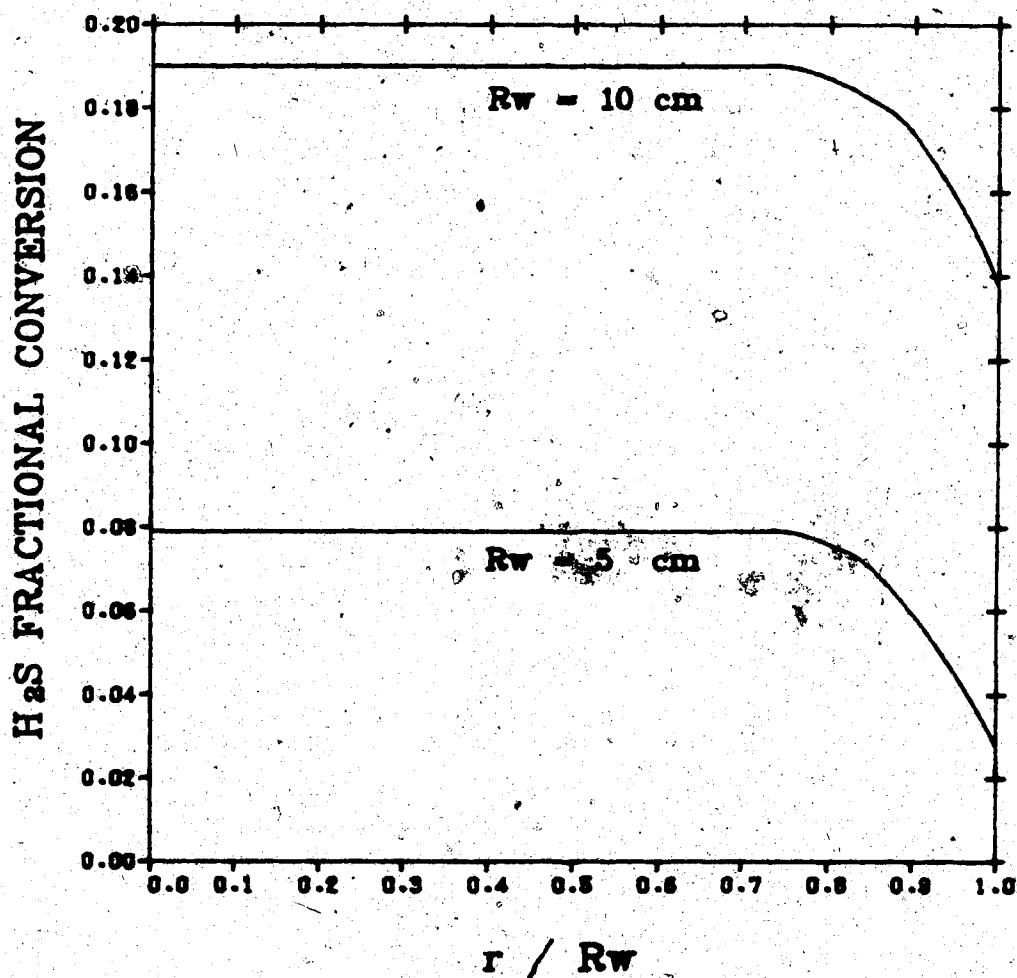


Figure 5.18 Temperature profile predictions by one and two dimensional models.
Inlet composition (mole fraction): $\text{H}_2\text{S} = 0.062$,
 $\text{SO}_2 = 0.021$, $\text{H}_2\text{O} = 0.231$, $\text{N}_2 = 0.686$
Inlet temperature = 463 K
 $T_a = 289$ K
Pressure = 1 atm
 $V_i = 38$ cm/sec
 $R_w = 15$ cm

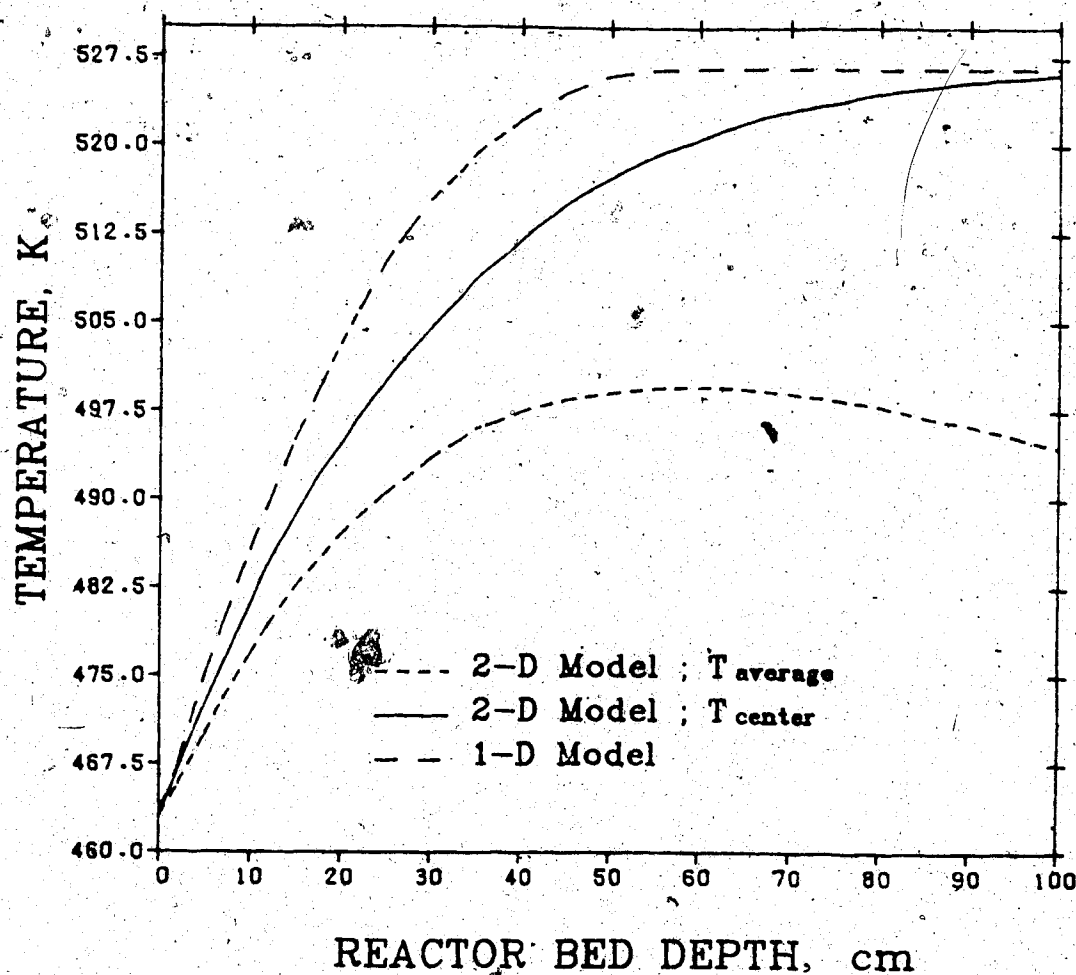


Figure 5.19 Conversion profile predictions by one and two dimensional models.
 Inlet composition (mole fraction): $\text{H}_2\text{S} = 0.062$,
 $\text{SO}_2 = 0.021$, $\text{H}_2\text{O} = 0.231$, $\text{N}_2 = 0.686$
 Inlet temperature = 463 K
 $T_a = 289$ K
 Pressure = 1 atm
 $V_i = 38$ cm/sec
 $R_w = 15$ cm

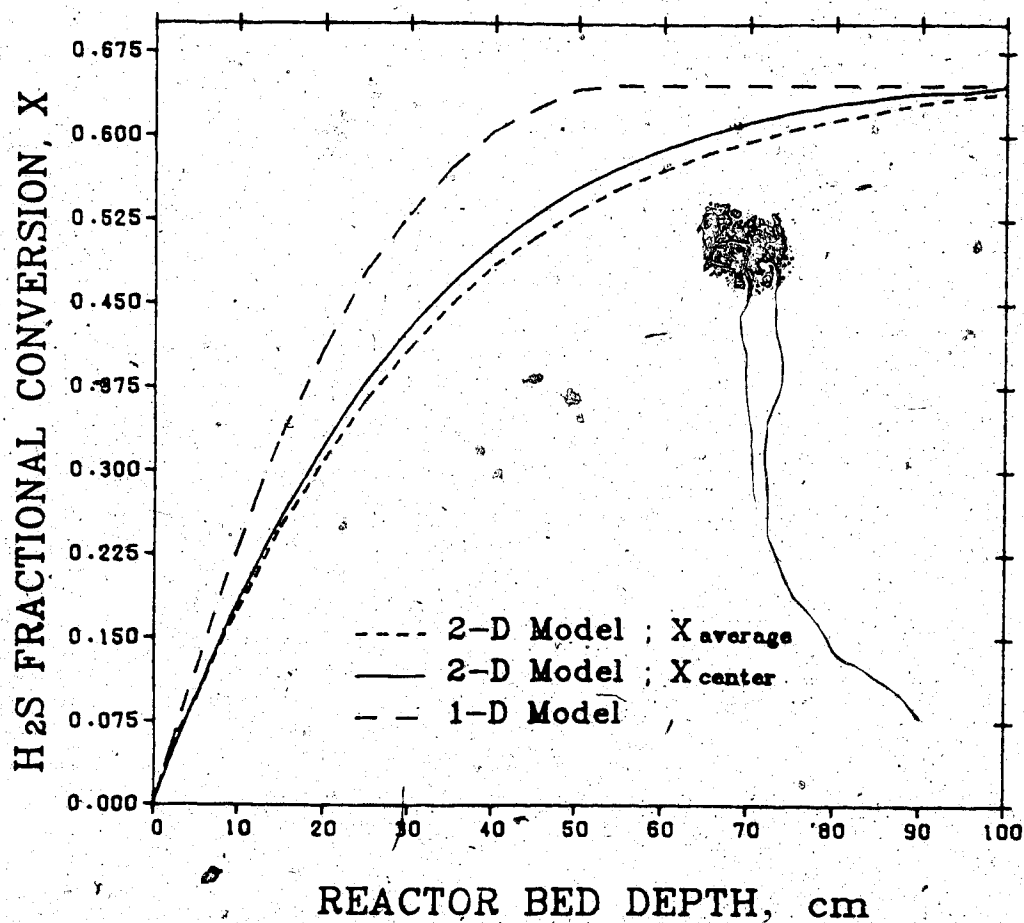
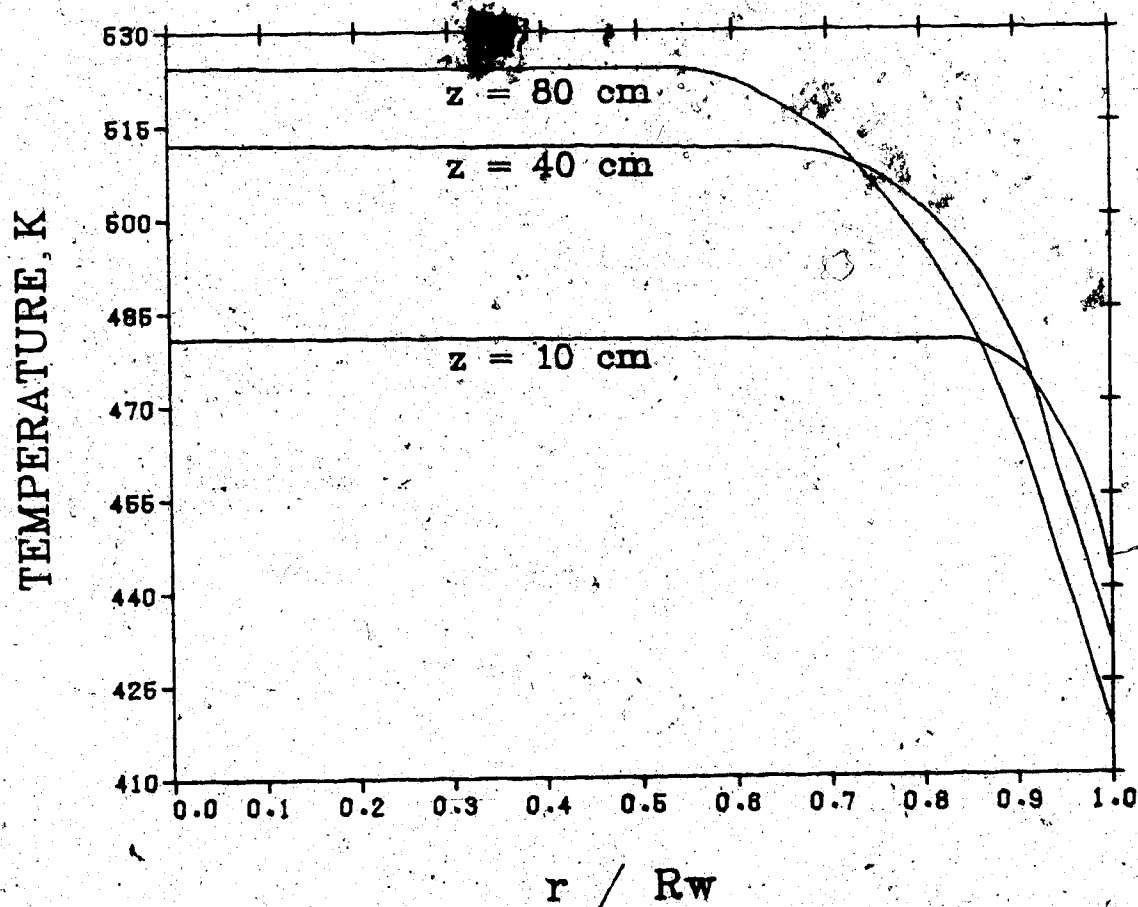


Figure 5.20 Radial temperature profile at different axial positions.
Inlet composition (mole fraction): $\text{H}_2\text{S} = 0.062$,
 $\text{SO}_2 = 0.021$, $\text{H}_2\text{O} = 0.231$, $\text{N}_2 = 0.686$
Inlet temperature = 463 K
 $T_a = 289$ K
Pressure = 1 atm
 $V_z = 38$ cm/sec
 $R_w = 15$ cm



radial direction is increased. This prediction confirms that a significant amount of reaction and heat production occurs at the entrance of the reactor bed where then the heat losses are relatively insignificant and affect only the immediate vicinity of the walls.

The predictions of 1- and 2-D models for a wide bed of 6 meters in diameter is shown in figures 5.21 and 5.22.

Figure 5.21 shows that, the average temperature predicted by the 2-D model is almost 5 degrees less than the temperature predicted by 1-D model at the outlet of the bed. This difference is however, less than the difference of 32 degrees predicted in figure 5.18 for a bed 10 centimeters in diameter.

Figure 5.22 reveals that the 2-D model predicts the same average and centerline conversion (the two lines are superimposed), although there is a difference between the predicted centerline and average temperature, as figure 5.21 shows. Thus, the few degree difference in the average and centerline temperatures seems to have negligible influence on conversion in wide beds. Furthermore, figure 5.22 also shows negligible difference between conversion predicted by 1- and 2-D models at the outlet section of the bed.

The complexity of the 2-D model is more than 1-D model in terms of model formulation, computer programming effort and computational time. It also offers a limited difference and accuracy compared to 1-D model for wide Claus reactors as figures 5.21 and 5.22 show. It seems that for all

Figure 5.21 Temperature profile predictions by one and two dimensional models in industrial size Claus reactor.
 Inlet composition (mole fraction): $\text{H}_2\text{S} = 0.07$,
 $\text{SO}_2 = 0.035$, $\text{H}_2\text{O} = 0.255$, $\text{N}_2 = 0.64$
 Inlet temperature = 553 K
 $T_a = 273$ K
 Pressure = 1 atm
 $V_i = 33$ cm/sec
 $R_w = 300$ cm

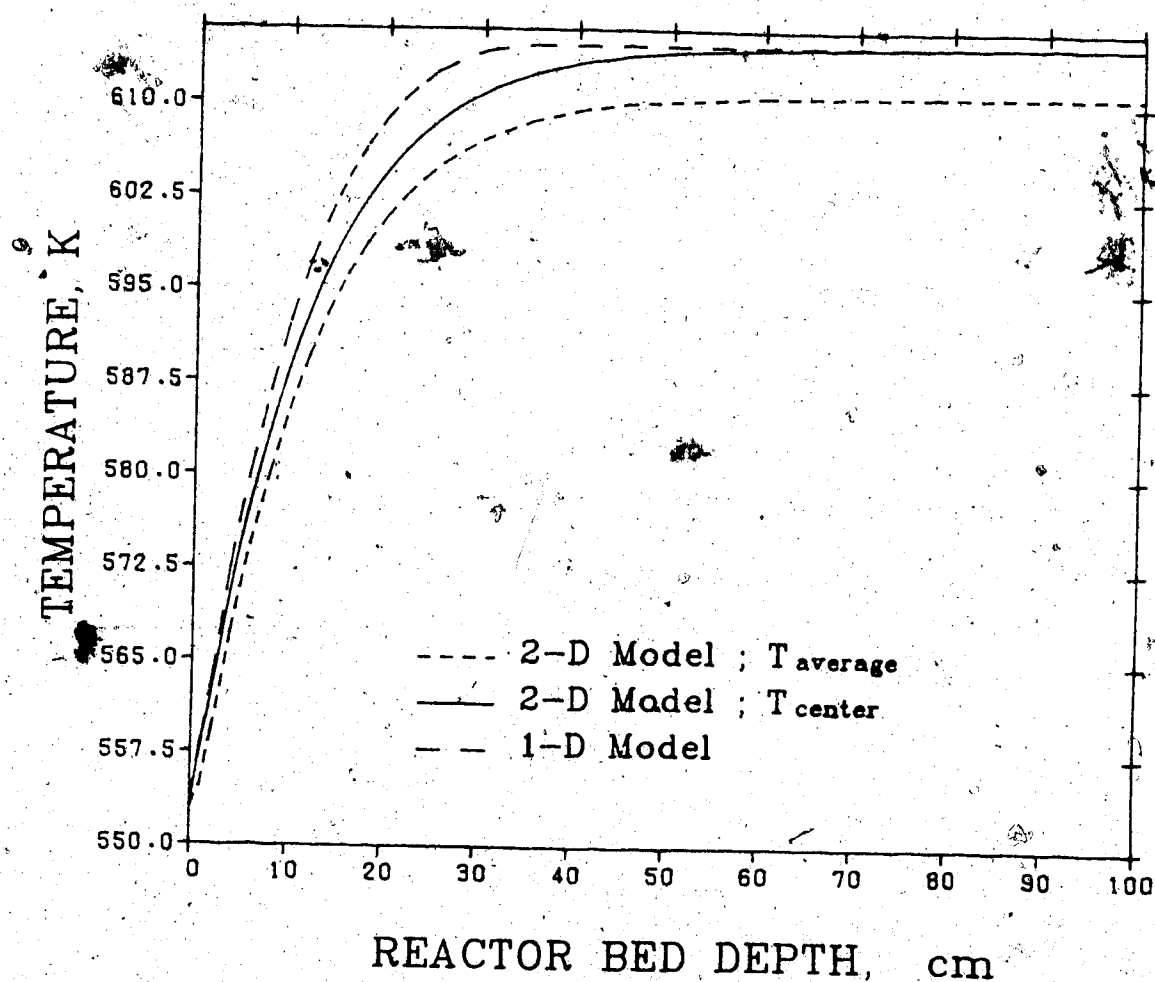


Figure 5.22 Conversion profile predictions by one and two dimensional models in industrial size Claus reactor.

Inlet composition (mole fraction): $\text{H}_2\text{S} = 0.07$,
 $\text{SO}_2 = 0.035$, $\text{H}_2\text{O} = 0.255$, $\text{N}_2 = 0.64$

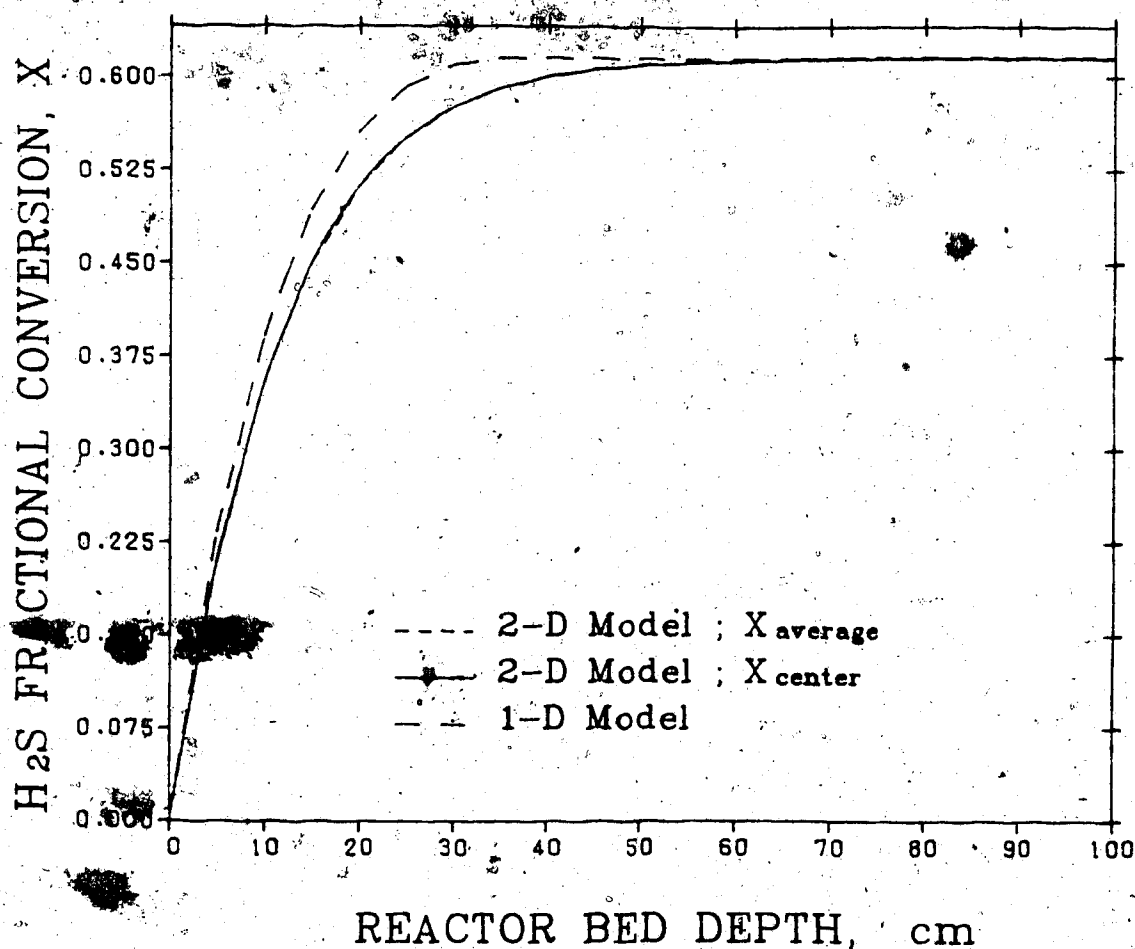
Inlet temperature = 553 K

$T_a = 273$ K

Pressure = 1 atm

$V_s = 33$ cm/sec

$R_w = 300$ cm



practical purposes the 1-D model is an appropriate choice for the modelling of the industrial size Claus reactor.

6. COLDBED CLAUS REACTOR MODEL

6.1 Introduction

The use of coldbed temperatures in Claus process catalytic reactors, discussed in section 2.6, enables attainment of very high conversions of H_2S to elemental sulfur because of removal of the product sulfur from the reaction phase and the favourable shift in the limiting equilibrium conversion.

Coldbed Claus reactors have been employed in the Sulfreen tailgas cleanup process, and more recently, in the Amoco CBA process (173) or in the MCRC (Mineral and Chemical Resource Co.) Process (99). The Amoco Process uses a coldbed 3rd stage whereas the MCRC process employs coldbed in both 2nd and 3rd stages. Figures 6.1 and 6.2 present process schematic diagrams of the MCRC and Amoco processes, respectively.

The elemental sulfur condensed on the catalyst due to low temperature operation of coldbed reactors also is a deactivating agent as was discussed in section 2.5. This condensation phenomenon results in a deactivation profile which moves along the bed axis, and which eventually breaks through the bed at large times on stream. A kinetic description of this deactivation process will be developed in this chapter.

The deactivation kinetics, discussed in section 2.8.1, may be represented by

Figure 6.1 Flow chart of MCRC process.

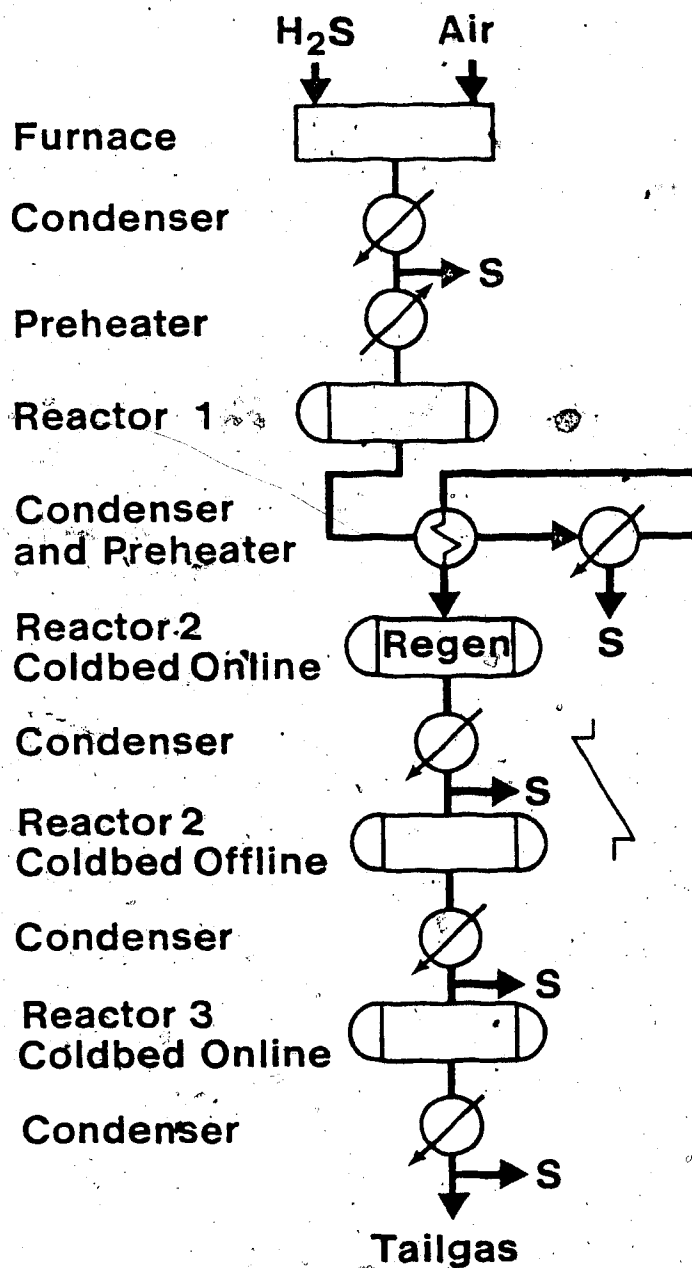
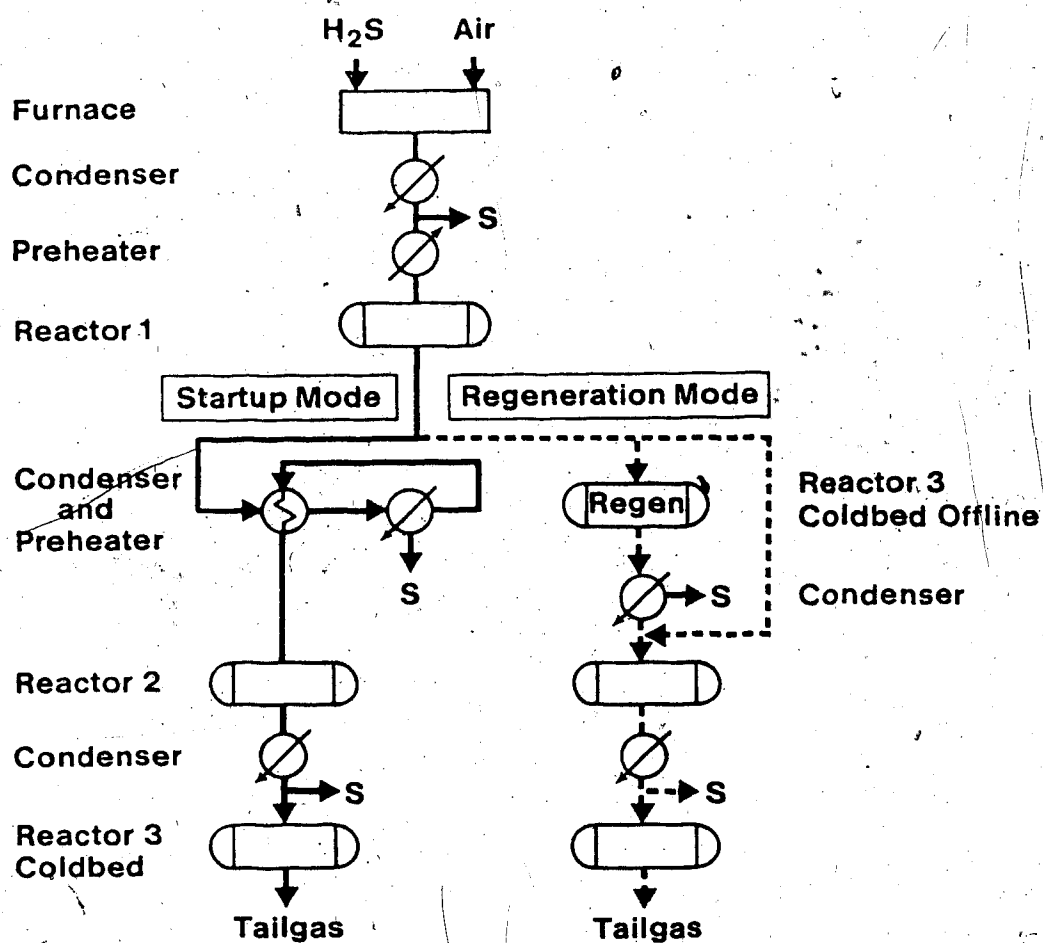


Figure 6.2 Flow chart of Amoco CBA process.



$$R_1 = k(1-\gamma)^{n_1} f_1 \{C_1, C_2, C_3, \dots, K_1, K_2, \dots\} \quad (6.1)$$

Equation (6.1) is valid when the deactivation process can be represented by "separable expression" and occurs by site coverage (section 2.8.1).

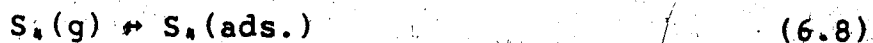
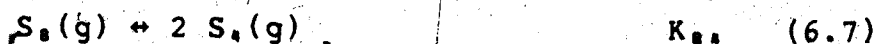
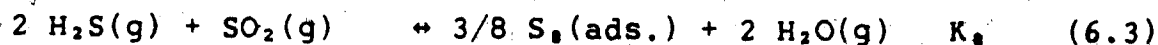
The analysis of the solid-catalyzed gas-phase deactivation reaction involving a first-order behavior coupled with pore diffusional limitations has been reported for several deactivation models as was discussed in section 2.8.2. This analysis, involving an arbitrary, non-negative order kinetics and an arbitrary spatial activity distribution function in the pellet, resulted in equation (2.43) for the flux of the reactant at the outer surface of the catalyst pellet. The global rate for the main reaction can then be obtained from equation (2.43) or,

$$R = Le^{-1} \{ 2 k_1 (1-\gamma_1) De \int_{C_0}^{C_f} g(C) dC \}^{1/2} \quad (6.2)$$

In the development of equation (6.2), a single-site reaction mechanism has been considered. That is, " n_1 " in equation (6.1) has been taken as unity. In this study the global rate expression (6.2) will be used for representation of the chemical reaction-deactivation-pore diffusion processes in the Claus coldbed process but it will be modified to accommodate the hypothetical Claus reaction mechanism.

6.2 Reaction Chemistry at Low Temperature

In the absence of reactive gaseous impurities, the overall Claus catalytic chemistry at low temperatures may be described by,



The species S_2 to S_8 , are assumed to equilibrate rapidly with S_8 both in the vapor phase and on the surface of the catalyst as was discussed in section 3.3. The selection of S_8 in reaction (6.3) although arbitrary, was chosen because S_8 is the dominant sulfur species at low temperatures.

Reactions (6.4) to (6.10) must meet the constraint that the sum of partial pressures of S_2 to S_8 must not exceed the vapor pressure, P_v . Meisen and Bennett (149) have correlated the sulfur vapor pressure data by the following expression,

$$\ln (P_v) = -1.61732 + 0.00542412T + 1439.83/T - 2208580/T^2 \quad (6.11)$$

where P_v and T are in units of atmosphere and Kelvin, respectively.

The sulfur vapor distribution under the operating conditions of the coldbed convertor may be predicted by the free energy minimization routine, specifying the pressure by equation (6.11), at any given temperature. Figure 6.3 represents such a distribution. It reveals that S_2 and S_8 are quantitatively insignificant at "coldbed" reactor conditions. Thus reactions (6.7) to (6.10) will be ignored in the modelling of coldbed Claus convertors.

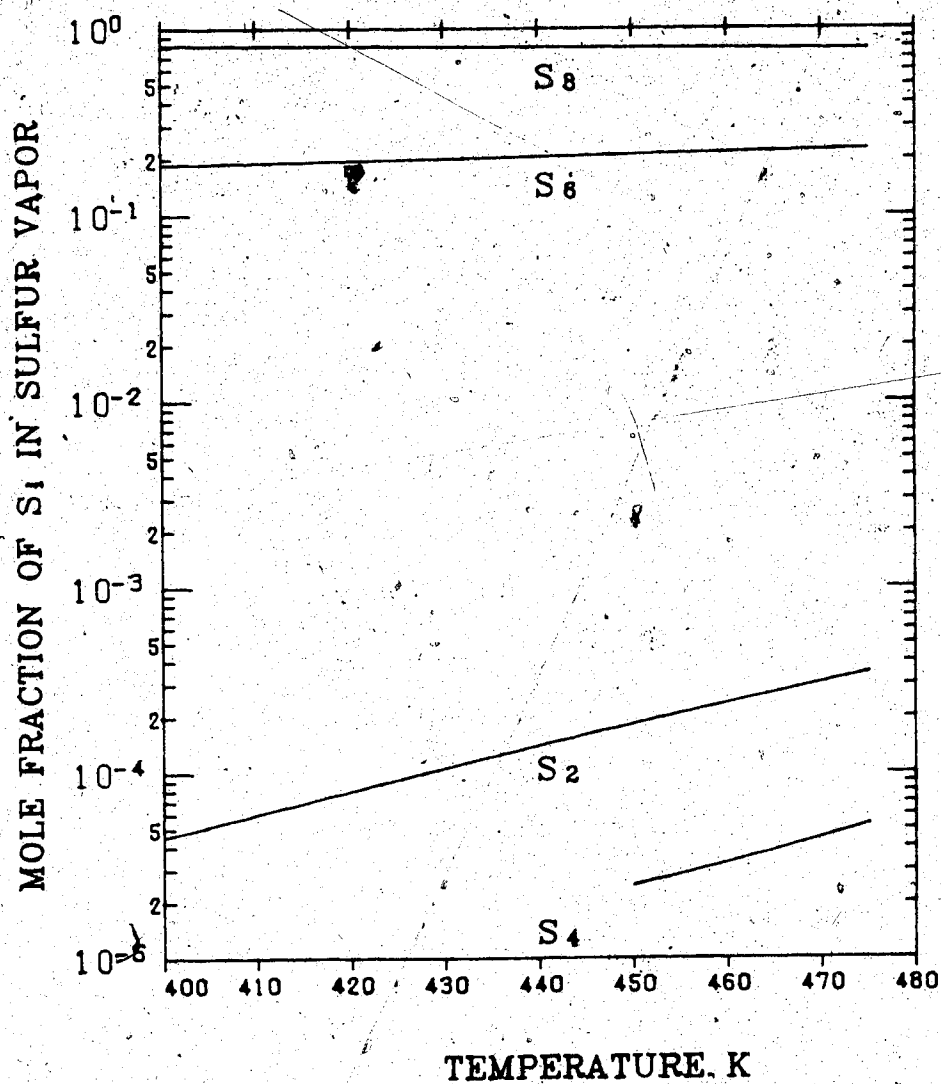
The thermodynamically consistent rate function (3.39), in terms of reaction (6.3) for fresh catalyst, is

$$-R_1 = k_f [P_1 \sqrt{P_2} - P_3 P_7^{1/6} / \sqrt{K_8}] [1 + 0.006P_3]^{-2} \quad (6.12)$$

Thermodynamic analysis using the thermodynamic data of JANAF(192) and Rau(171) predicts the temperature dependency of the equilibrium constants K_8 and K_{88} as,

$$\ln (K_8) = 12823/T - 13.9 \quad (6.13)$$

Figure 6.3 Sulfur vapor composition at its vapor pressure at different temperatures.



$$\ln (K_{s_6}) = -4030/T + 4.8 \quad (6.14)$$

The denominator term of equation (6.12) describes a second order inhibiting effect of the adsorbed water. From simple Langmuir-Hinshelwood kinetics, this implies a dual-site reaction mechanism or,

$$k_f \propto \{\text{total sites}\}^2 \quad (6.15)$$

That is "n1" assumes a value of 2 in equation (6.1). Thus the intrinsic kinetics of the deactivating Claus reaction becomes,

$$-R_1 = k_f (1-\gamma)^2 [P_1 \sqrt{P_2} - P_3 P_7^{1/2} / \sqrt{K_s}] [1 + 0.006 P_3]^{-2} \quad (6.16)$$

6.3 Analysis of Deactivation Rate

The quantitative modelling of the coldbed Claus reactor necessitates a knowledge of the rate of change of the catalytic activity $(1-\gamma)$. To present the rate of catalyst activity change, let A denote the reactants (H_2S and SO_2), N the total sulfur (adsorbed and in the gas phase), and P the adsorbed (deactivating agent) sulfur. Then the reactions (6.3) to (6.6) are represented as,



The stage 2 in reaction (6.17) is fast and considered to approach equilibrium as discussed in section 6.2. Thus, the rate of catalyst sulfur loading is assumed to equal the rate of production of total sulfur N.

Catalyst activity $(1-\gamma)$, in terms of fractional catalyst sulfur loading, q/Q , is

$$1 - \gamma = 1 - q/Q \quad (6.18)$$

where Q is of the order of 0.3 grams of sulfur per gram of alumina catalyst (98,117) for complete deactivation.

Equation (6.18) assumes a linear relationship between activity and sulfur loading and is widely used in the analysis of deactivating reactions (118, 120, 121, 130, 131, 142).

Differentiating (6.18) yields,

$$d\gamma/dt = 1/Q \, dq/dt \quad (6.19)$$

That is, the rate of change of catalyst sulfur loading would yield the rate of change of catalytic activity. Combining equation (6.19) with (6.16), and recalling that the rate of catalyst sulfur loading is the same as the rate of production of total sulfur, N , gives,

$$d\gamma/dt = (32.06/Q)(-1.5 R_1) \quad (6.20)$$

6.4 Coldbed Reactor Model

Since typical Claus catalyst beds are wide, shallow, and adiabatic, a one-dimensional model of a fixed-bed is appropriate. The 1-dimensional model also is justified by the results of the two-dimensional model of Claus beds at high temperatures in section 5.5. It was observed that even for small diameter beds the radial temperature and conversion profiles are flat except in the immediate vicinity of the walls.

The differential unsteady-state mass and energy conservation equations are developed in section (F.1). The mass balance equation for a component, i , in a constant-pressure reactor becomes

$$\partial C_{f,i} / \partial t = -w_1 \partial P_{f,i} / \partial z + w_2 \partial^2 P_{f,i} / \partial z^2 + a_i w_3 R \quad (6.21)$$

When the component is sulfur, the corresponding balance equation becomes,

$$\begin{aligned} (\partial / \partial t) \{ 8 C_{f_7} + 6 C_{f_8} \} = & -w_1 (\partial / \partial z) \{ 8 P_{f_7} + 6 P_{f_8} \} \\ & + w_2 (\partial^2 / \partial z^2) \{ 8 P_{f_7} + 6 P_{f_8} \} \\ & + 3 w_3 R \end{aligned} \quad (6.22)$$

valid for the condition, $(P_{f_7} + P_{f_8}) \leq P_v$. When the equality holds, the sulfur partial pressure equals its vapor pressure

and further sulfur produced will remain on the catalyst surface. The corresponding differential energy conservation equation is,

$$\partial T_f / \partial t = -V_1 \partial T_f / \partial z + V_2 \partial^2 T_f / \partial z^2 + V_3 R \quad (6.23)$$

The boundary conditions are,

at $z=0$

$$\partial P_{f1} / \partial z = (w_1 / w_2) (P_{f1} - P_i) \quad (6.24)$$

$$(\partial / \partial z) (8P_{f7} + 6P_{f8}) = (w_1 / w_2)$$

$$(8P_{f7} + 6P_{f8} - 8P_{f7} - 6P_{f8}) \quad (6.25)$$

at $z=1$

$$\partial P_{f1} / \partial z = \partial T / \partial z = 0 \quad (6.26)$$

The axial dispersion is of negligible importance for long beds. However, Eigenberger and Butt (70) recommend not to omit it entirely since the axial dispersion term has a smoothing influence upon their method of solution, which has been employed in this study. The Eigenberger-Butt solution method is discussed in section F.2.

6.4.1 Global Reaction Rate in Coldbed Reactor

The global rate of reaction for a single-site reaction mechanism (128,129) is given by equation (6.2) provided that certain conditions are met. The conditions placed on

equation 6.2 are that,

1. The external mass transfer resistance is negligible.
2. The catalyst pellet is isothermal
3. The activity of the exterior catalyst surface, $(1-\gamma)$, is not zero.
4. The differential of the activity $(1-\gamma)$ with respect to spatial coordinate in catalyst pellet, evaluated at the surface of the pellet is not steep, i.e. deactivation being considered is intermediate between uniform and shell-progressive deactivation.

The external mass transfer limitation in the Claus first-stage convertor at high temperature results in 0.06 difference between conversion in the bulk fluid and catalyst surface, at the inlet of the bed where significant reaction occurs (section 5.4.2). In the coldbed, the temperature is almost 100 K less than in the first-stage convertor. The concentration of H_2S is also less than in the first-stage convertor. The ratio of the rate constant, k_f , at coldbed reactor temperature, to k_f at the first-stage convertor temperature is then, approximately 0.1. Thus, the reaction rate in the coldbed being much lower than in the first-stage reactor justifies neglecting the external mass transfer limitation. The isothermality of the Claus pellet was shown in section 4.1.

The conditions (3) and (4) are valid for a series deactivation mechanism where the deactivation monotonically and smoothly increases toward the center of the catalyst

pellet (142). For a parallel deactivation mechanism, the deactivation increases smoothly toward the surface of the catalyst (142), thus condition (4) still applies. There is however the possibility of complete deactivation of the surface of the catalyst before deactivation of the interior, i.e. condition (3) may be violated.

The deactivation mechanism in coldbed reactors as shown in reaction (6.17) is a series deactivation. However, the rate of deactivation is proportional to the rate of disappearance of the reactants. In that respect the deactivation mechanism may be considered to be a parallel mechanism. The Kelvin equation (181) predicts the vapor pressure lowering for liquid sulfur wetting the walls within a cylindrical pore of given radius. Because the contact angle of liquid sulfur is about 60° (152). Thus, the pore mouth region will likely deactivate more readily than the external surface because of the higher probability of sulfur condensing. This suggests that the activity of the surface may not be neglected and condition (3) is met.

The above arguments justify the use of a global rate expression (6.2). This equation has to be modified for the dual-site mechanism. Equation (6.2) for the Claus process in terms of reference species 1, becomes

$$R = Le^{-1} \{ 2 k_f (1-\gamma_s)^2 De_1 \int_{C_{0,1}}^{C_{f,1}} g(C_1) dC_1 \}^{1/2} \quad (6.27)$$

or in terms of partial pressure for an isothermal pellet,

$$R = Le^{-1} [(2 kf_s (1-\gamma_s)^2 (De_1/Rg T_s) \int_{P_{01}}^{P_{f1}} g(P_1) dP_1]^{1/2} \quad (6.28)$$

whereby equation (6.16) becomes,

$$g(p) = [P_1/P_2 - P_3 P_7^{1/18}/\sqrt{K_s}] [1+0.006 P_3]^{-2} \quad (6.29)$$

and equations (4.34) and (4.35) becomes,

$$P_2 = Pf_2 + (De_1/2De_2)(P_1 - Pf_1) \quad (6.30)$$

$$P_3 = Pf_3 - (De_1/De_3)(P_1 - Pf_1) \quad (6.31)$$

$$8P_7 + 6P_8 = 8Pf_7 + 6Pf_7 - (3De_1/16De_7)(P_1 - Pf_1) \quad (6.32)$$

Equation (6.32) is valid if the partial pressure of the sulfur is less than the Kelvin vapor pressure at the cylindrical pore. Otherwise,

$$P_7 + P_8 = Pv_k \quad (6.33)$$

where from the equilibrium assumption of reaction (6.5),

$$P_8 = (K_{s8} P_7)^{3/4} \quad (6.34)$$

The partial pressure, P_{01} , of reference species 1, at the center of the catalyst pellet can be set equal to its

equilibrium value if the Thiele modulus is greater than 3. Otherwise, it can be approximated by the pressure corresponding to a pseudo-first-order reaction (127). The integrated value of $g(p)$ is not materially affected by an error in P_{01} , (127).

Next R has to be expressed in terms of the observable fluid temperature, T_f . Lee (127) has shown that the ratio of the rate constant, k_f , at bulk gas temperature, to $k_{f,}$ at the surface temperature, may be approximated by

$$(k_{f,}/k_f)^{1/2} = 1 + 1.2(E/(R_g T_f)) [Le(-\Delta H) R/(2h T_f)] \quad (6.35)$$

The ratio of the square root of the bulk fluid phase and catalyst surface temperature can be approximated by using the first order term in the Taylor series expansion.

$$(T_f/T_s)^{1/2} = 1.5 - 0.5 T_s/T_f \quad (6.36)$$

where, the ratio T_s/T_f by the coupling equation between solid and fluid phase is obtained via,

$$T_s/T_f = 1 + Le(-\Delta H) R/(h T_f) \quad (6.37)$$

Combining (6.28), (6.35), (6.36) and (6.37) yields,

$$R = Le^{-1} [(2k_f (1-\gamma_s)^2 De_1/(R_g T_f)) \int_{P_{01}}^{P_{f1}} g(P_1) dP_1]^{1/2} (T_f/T_s)^{1/2} (k_{f,}/k_f)^{1/2} \quad (6.38)$$

or,

$$R = q_1 \frac{[1 + 1.2(E/(R_g T_f)) \{Le(-\Delta H) R/(2h T_f)\}]}{[1 - Le(-\Delta H) R/(2h T_f)]} \quad (6.39)$$

resulting in a quadratic equation for the global reaction rate as,

$$q_1 q_2^2 q_3 R^2 + (1 + q_1 q_2 - q_1 q_2 q_3) R - q_1 = 0 \quad (6.40)$$

where

$$q_1 = Le^{-1} [(2 k_f(1-\gamma_s)^2 De_1/(R_g T_f)) \int_{P_{0,1}}^{P_{f,1}} g(P_1) dP_1]^{1/2} \quad (6.41)$$

$$q_2 = Le (-\Delta H)/(2h T_f) \quad (6.42)$$

$$q_3 = 1.2 E/(R_g T_f) \quad (6.43)$$

The solution of equation (6.40) gives one non-negative root for R in terms of the bulk fluid temperature and pressure by,

$$R = \frac{q_1 q_2 q_3 - 1 - q_1 q_2}{2 q_1 q_2^2 q_3} + \frac{[(1 + q_1 q_2 - q_1 q_2 q_3)^2 + 4 q_1 q_2^2 q_3]^{1/2}}{2 q_1 q_2^2 q_3} \quad (6.44)$$

6.4.2 Deactivation Rate in Coldbed Reactor

The rate of change of catalyst surface activity, $(1-\gamma_s)$, is obtained from equation (6.20) as,

$$\frac{\partial \gamma_s}{\partial t} = (48.09 \, k_f (1-\gamma_s)^2 / Q) \left[\frac{P_{f_1} \sqrt{P_{f_2}} - P_{f_3} P_{f_2}^{3/4} / \sqrt{K_s}}{[1+0.006 P_{f_1}]^{-2}} \right] \quad (6.45)$$

But from (6.35), (6.42), and (6.43),

$$k_{f_1} = k_f (1 + q_1 q_2 R)^2 \quad (6.46)$$

or

$$\frac{\partial \gamma_s}{\partial t} = (48.09 \, k_f (1-\gamma_s)^2 / Q_0) (1 + q_1 q_2 R)^2 \left[\frac{P_{f_1} \sqrt{P_{f_2}} - P_{f_3} P_{f_2}^{3/4} / \sqrt{K_s}}{[1+0.006 P_{f_1}]^{-2}} \right] \quad (6.47)$$

6.5 Computational Scheme

The system of partial differential equations, (6.21) to (6.23), were numerically integrated by a finite difference method with non-equidistant space steps, well suited for the solution of moving profiles - such as those for deactivating catalytic beds (70). This method, (Eigenberger-Butt-Method, "EBM") has been described in section F.2. The EBM can be interpreted as being a collocation method on a finite element in which each element is described by a second-order

collocation polynomial.

The EBM converts the partial differential equation into a system of ordinary differential equations (section F.2.2). The modified-Euler method was employed for the numerical integration of the resulting ordinary differential equations.

The source term R at each axial position was calculated from equation (6.44) for which, a three-point Gaussian quadrature formula (87) was employed for calculation of q_1 .

The computer program "COLDBED" based on the flowchart of figure F.1, presented in Appendix F performs the Claus coldbed simulation.

6.6 Numerical Results of Coldbed Simulation

Figure 6.4 shows the partial pressure of H_2S along the bed axis at 1.6 and 6.4 seconds. The axial temperature during this short period is predicted by the "COLDBED" program to stay constant at its initial value. The corresponding deactivation profile is presented in figure 6.5. The axial position of the spatial grid points are shown on the z (i.e. z/L) axis of figure 6.4. The position of the non-equidistant grid points show that the EBM numerical scheme locates fewer grid points in the region with a flat profile, thus a reduction in the total number of axial grid points can be achieved.

The rapid establishment of a pressure profile coupled with no temperature change has been observed by Billimoria

Figure 6.4 Axial profile of partial pressure of H_2S at short times after startup.

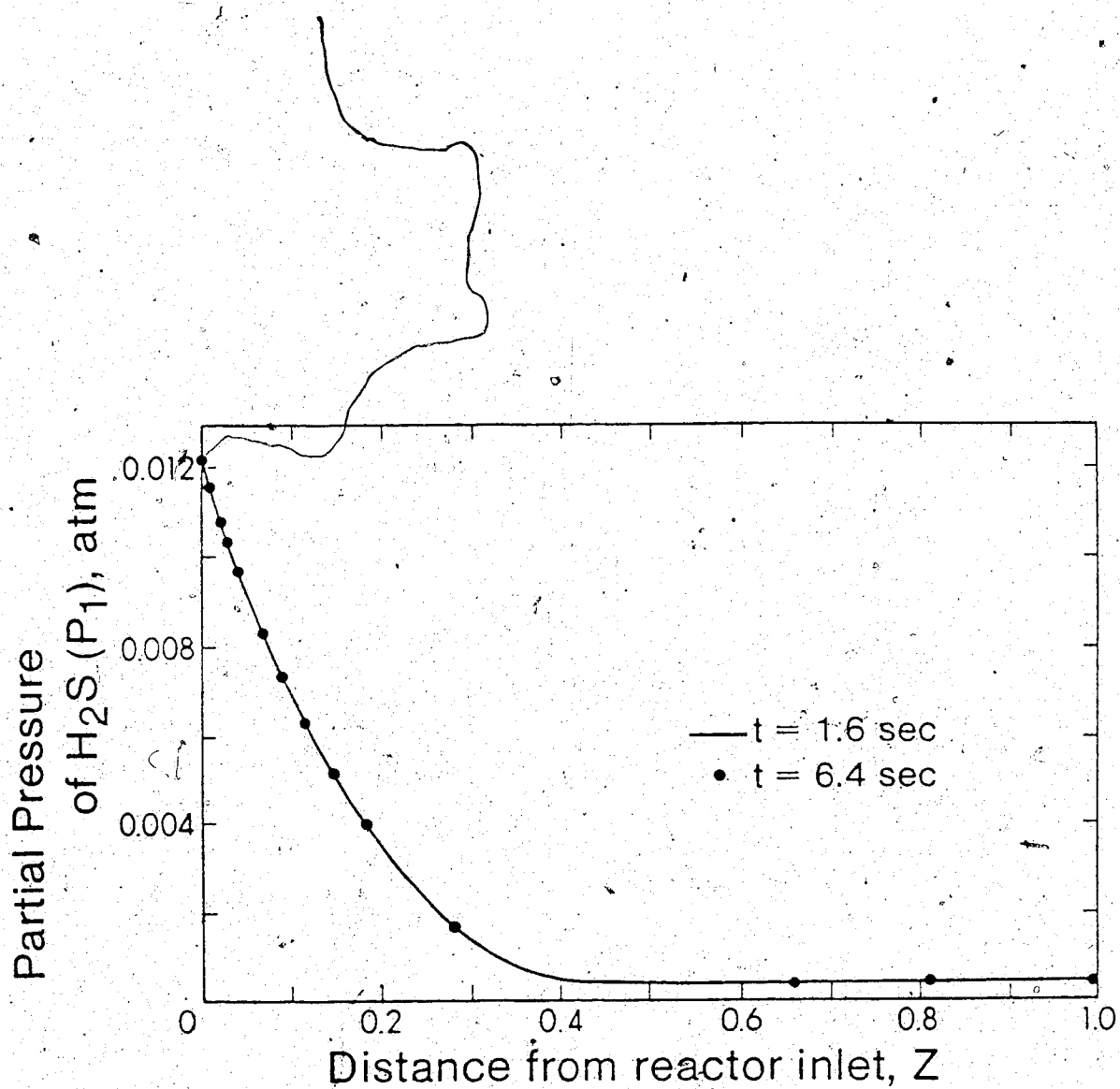
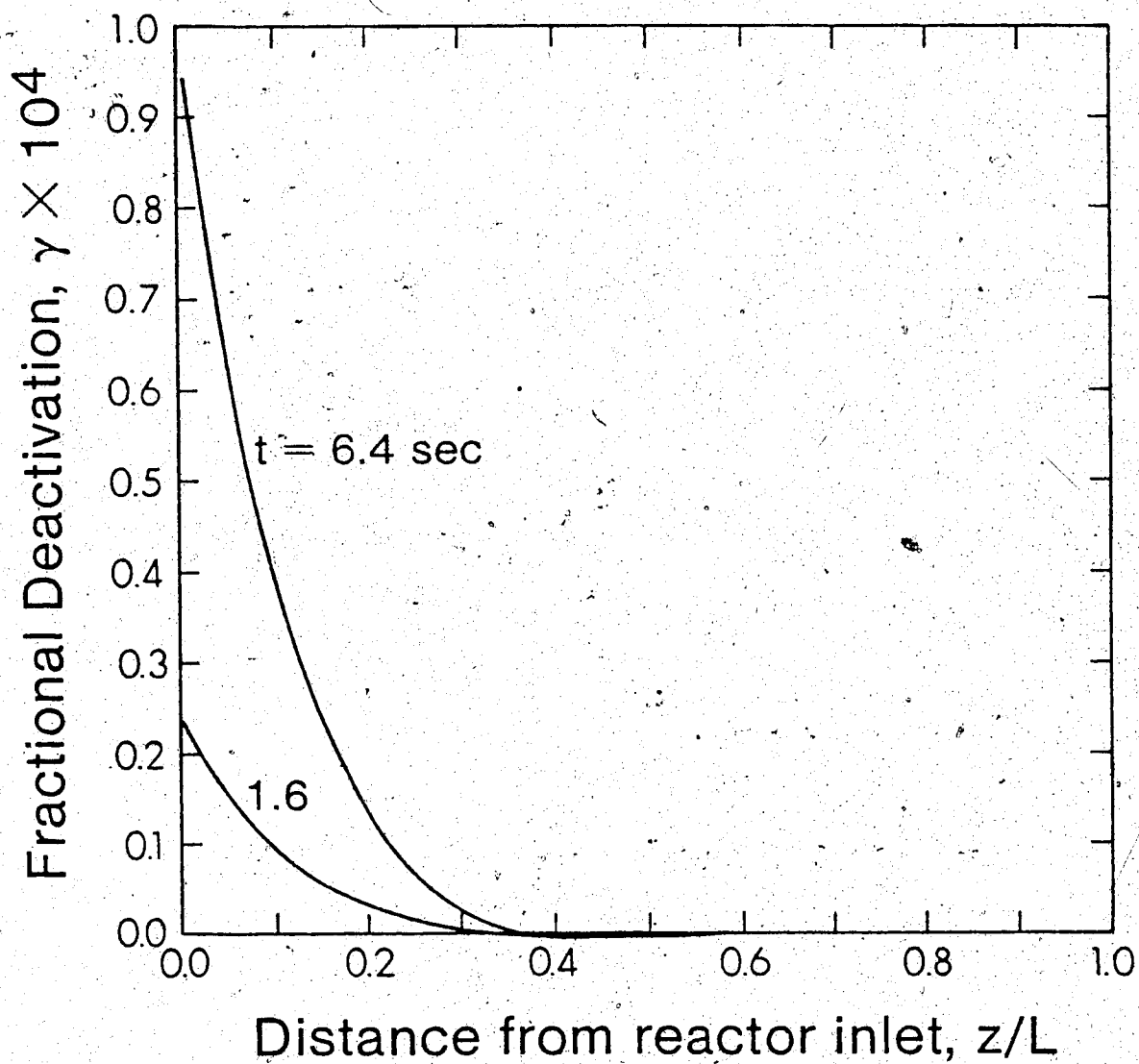


Figure 6.5 Deactivation of coldbed reactor at short times after startup.



and Butt (118) in the modelling of poisoning hydrogenation of benzene by thiophene as discussed in section 2.8.3. They termed this time zone at which rapid changes occur in the concentration profile, but with little change in the temperature profile, as the fast motion (FM) zone.

Figure 6.4 shows that the bed deactivation in the short time interval is relatively slow, such that its effect on the partial pressure profile is negligible. The assumption of a pseudosteady-state has been widely used under such circumstances for deactivating beds (16, 45, 70, 129, 130, 131, 142, 162). Neglecting the material transient and the axial dispersion term (dispersion being negligible when $L/D_p > 50$ (40, 112)), equations (6.21) to (6.23) simplify to

$$\partial P_{f1} / \partial z = a_1 w_3 / w_1 R \quad (6.48)$$

$$\partial T_f / \partial t = -V_1 (\partial T_f / \partial z) + V_3 R \quad (6.49)$$

Combining equations (6.48) for two components, 1 and j, to eliminate R yields

$$P_{fj} = (a_j / a_1) (P_{f1} - P_i) + P_i \quad (6.50)$$

Equation (6.50) implies that the stoichiometry of the reaction predicts the profile of the species j in terms of the profile of the reference species 1. Solutions of the pseudosteady-state model (equations (6.48) to (6.50)) were obtained by the finite difference scheme as described in section F.3.

6.7 Application of the Model to Coldbed Reactors

To simulate a Claus coldbed reactor, the calculations were based upon a modified Claus process sulfur recovery plant operating at 1 atm with an acid gas feed containing 100% H_2S and stoichiometric air. A 70% conversion in the front-end furnace was assumed; and this stream, after sulfur removal was fed into a first-stage adiabatic reactor at 553 K and a space velocity of 1000 hr^{-1} . Equilibrium conversion was predicted at the maximum first-stage adiabatic temperature.

The 2nd-stage adiabatic catalytic reactor was treated as a coldbed reactor with feed gas and bed both initially at 420 K. Figure 6.6 predicts the temperature profile in this 2nd-stage reactor at various times after startup. After one hour, a stable maximum temperature is reached within the bed.

Figure 6.7 presents the axial profile of the partial pressure of H_2S in the 2nd-stage reactor. The difference between the base of the profiles before and after one hour of operation is simply due to the effect of temperature upon equilibrium composition. Figure 6.6 shows that at early times ($t < 1$ hour) the outlet reactor temperature is 420 K while at later times it is at the maximum outlet temperature of 463 K.

Figure 6.8 predicts the establishment of the temperature profiles in the 2nd-stage coldbed reactor. The profiles in figures (6.7) and (6.8) reflect bed deactivation

Figure 6.6 Temperature profiles at times (< 1 hr) after startup in the 2nd-stage convertor.

Inlet Composition (mole fraction): $\text{H}_2\text{S} = 0.0276$,
 $\text{SO}_2 = 0.0138$, $\text{H}_2\text{O} = 0.3046$, $\text{N}_2 = 0.654$

Inlet temperature = 420 K

Pressure = 1 atm

Space Velocity = 1000 hr^{-1}

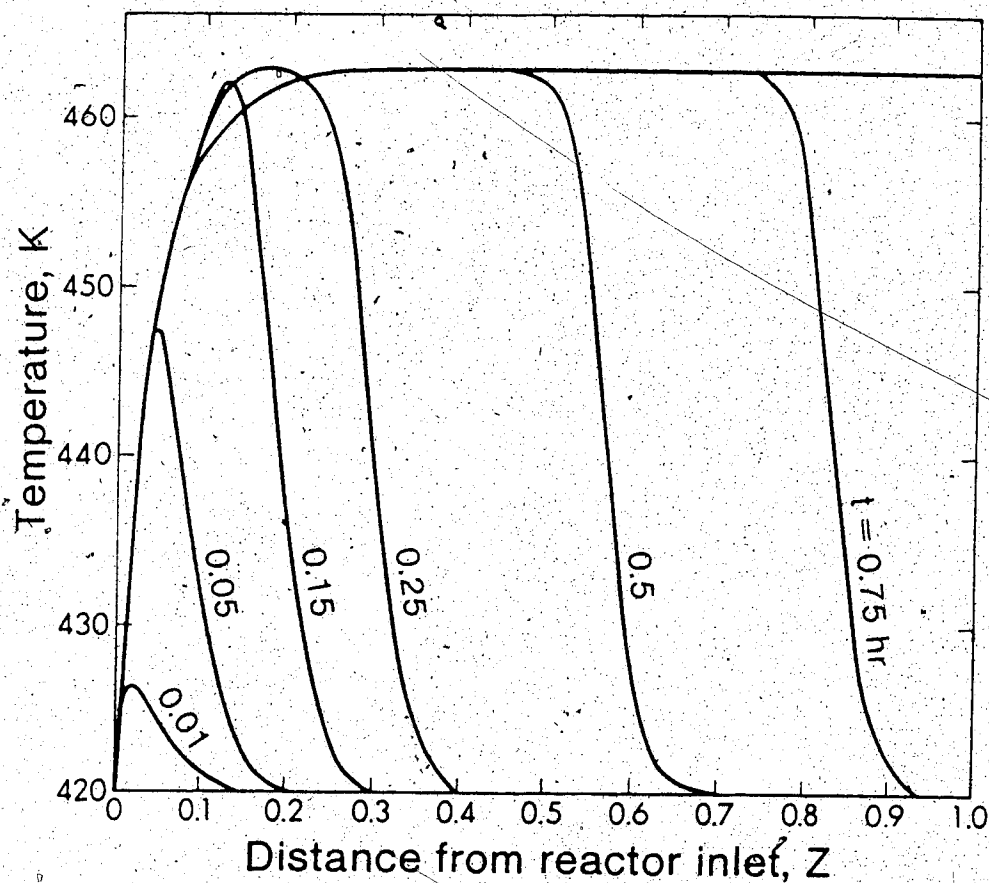


Figure 6.7 Axial profile of partial pressure of H_2S at various times after startup in the 2nd-stage convertor.
Inlet Composition (mole fraction): $\text{H}_2\text{S}=0.0276$,
 $\text{SO}_2=0.0138$, $\text{H}_2\text{O}=0.3046$, $\text{N}_2=0.654$
Inlet temperature = 420 K
Pressure = 1 atm
Space Velocity = 1000 hr^{-1}

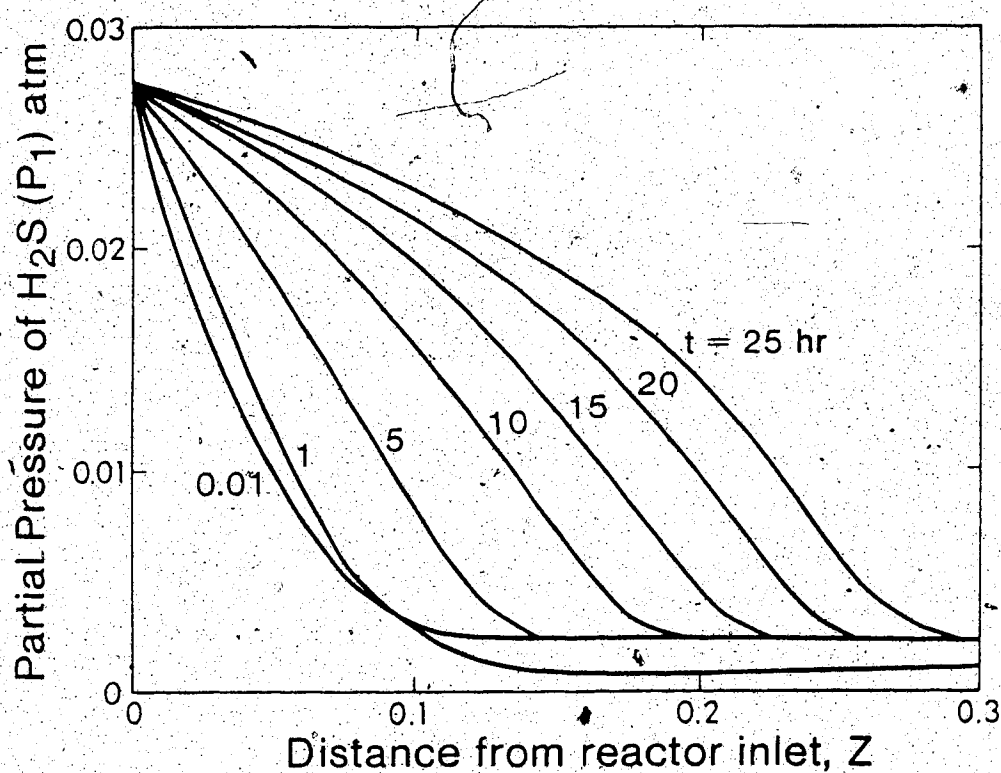
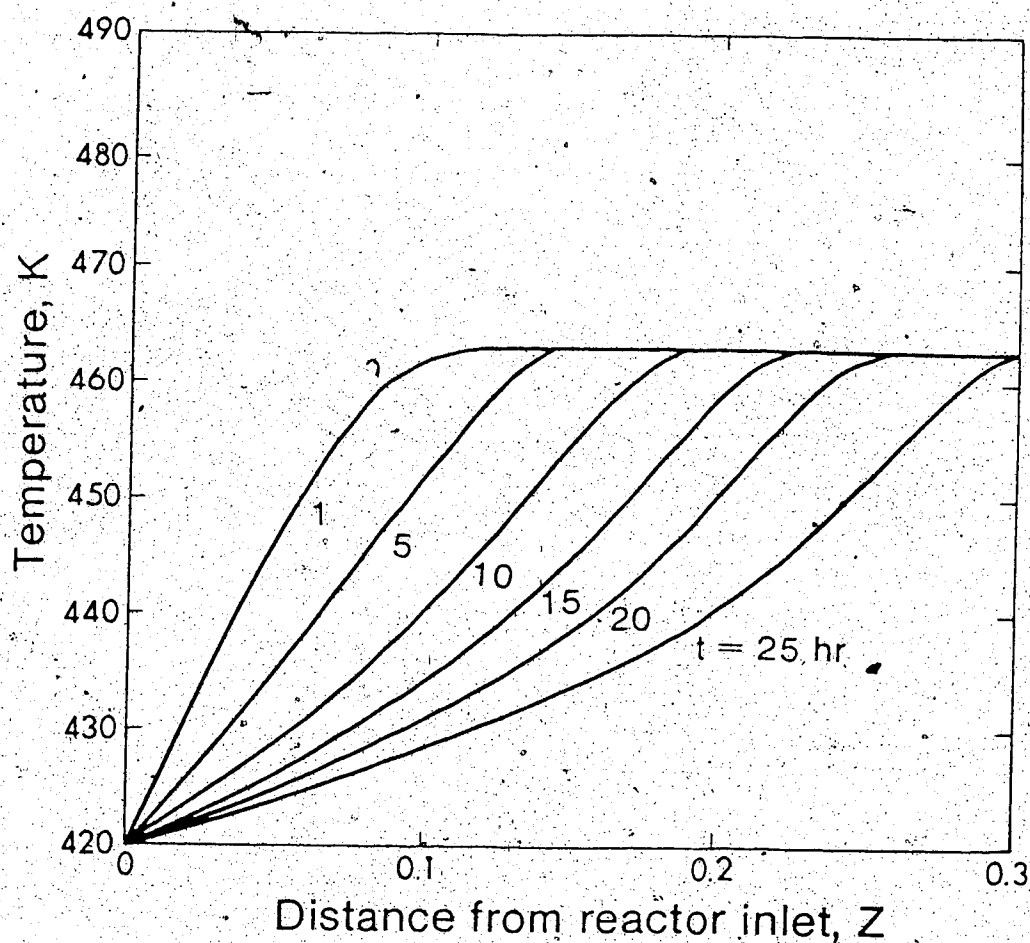


Figure 6.8 Temperature profiles at times (> 1 hr) after the startup in the 2nd-stage convertor.
Inlet Composition (mole fraction): $\text{H}_2\text{S}=0.0276$,
 $\text{SO}_2=0.0138$, $\text{H}_2\text{O}=0.3046$, $\text{N}_2=0.654$
Inlet temperature = 420 K
Pressure = 1 atm
Space Velocity = 1000 hr^{-1}



by retention of sulfur on the catalyst surface. The corresponding deactivation profiles are presented in figure 6.9.

In the MCRC process (figure 6.1), the "first sub-dew point" convertor (2nd-stage convertor) is reversed to operate as the "second sub-dew point" (3rd-stage) convertor after one day of operation (99). Figures (6.10) to (6.12) present the H_2S partial pressure, temperature, and the deactivation profiles in the "second sub-dew point convertor".

The Amoco process operates the 3rd-stage reactor at low temperatures. The simulation of the 3rd-stage coldbed reactor was obtained based upon a modified Claus process sulfur recovery plant operating at 1 atm with an acid gas feed containing 100% H_2S and stoichiometric air. A 70% conversion in the front-end furnace was assumed, and this stream after sulfur removal was fed into a first-stage adiabatic reactor at 553 K. The outlet of the first-stage reactor after sulfur removal, was fed into a 2nd-stage adiabatic reactor at 533 K. Equilibrium conversion was predicted at the maximum first and 2nd-stage adiabatic temperatures.

The simulation results for the 3rd-stage convertor are presented in figures (6.13) to (6.16) with the feed gas and bed both initially at 400 K. Similar to figure (6.6), figure (6.13) predicts that after one hour, a stable maximum temperature is reached within the bed.

Figure 6.9 The deactivation function at various times after the startup in the 2nd-stage convertor.

Inlet Composition (mole fraction): $\text{H}_2\text{S}=0.0276$,
 $\text{SO}_2=0.0138$, $\text{H}_2\text{O}=0.3046$, $\text{N}_2=0.654$
Inlet temperature = 420 K
Pressure = 1 atm
Space Velocity = 1000 hr^{-1}

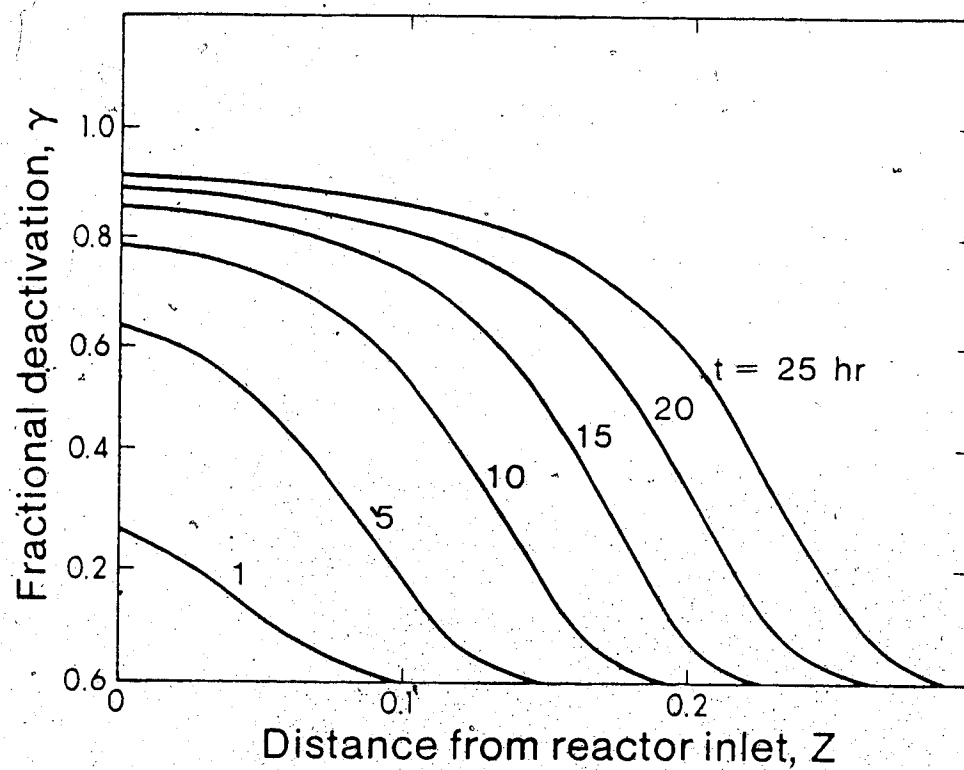


Figure 6.10 Axial profile of partial pressure of H_2S at various times after startup in the 3rd-stage convertor.
Inlet Composition (mole fraction): $\text{H}_2\text{S}=0.0025$,
 $\text{SO}_2=0.00125$, $\text{H}_2\text{O}=0.3297$, $\text{N}_2=0.6703$
Inlet temperature = 400 K
Pressure = 1 atm
Space Velocity = 1000 hr^{-1}

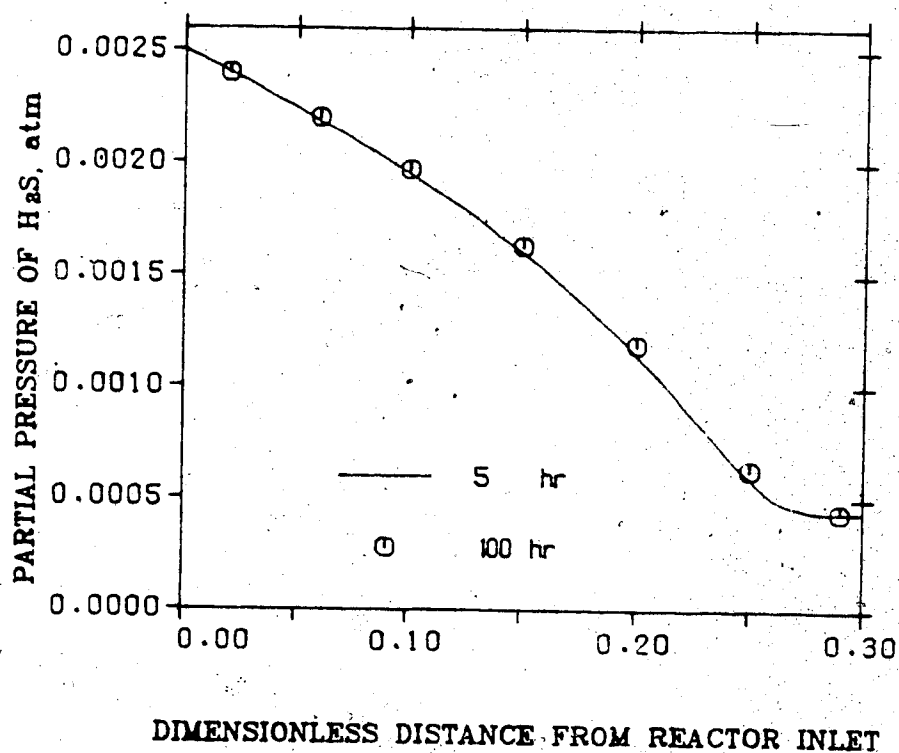


Figure 6.11 Temperature profiles at times (> 1 hr) after the startup in the 3rd-stage convertor.
Inlet Composition (mole fraction): $\text{H}_2\text{S}=0.0025$,
 $\text{SO}_2=0.00125$, $\text{H}_2\text{O}=0.3297$, $\text{N}_2=0.6703$
Inlet temperature = 400 K
Pressure = 1 atm
Space Velocity = 1000 hr^{-1}

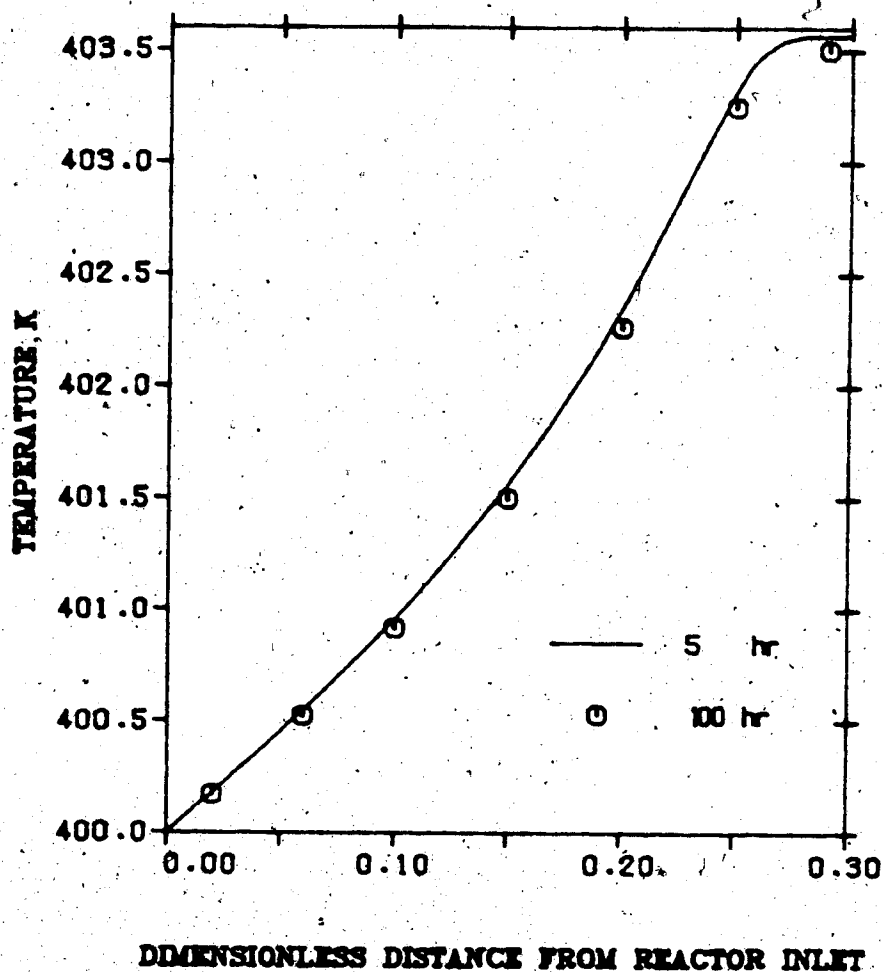


Figure 6.12 The deactivation function at various times after the startup in the 3rd-stage converter.

Inlet Composition (mole fraction): $\text{H}_2\text{S}=0.0025$,
 $\text{SO}_2=0.00125$, $\text{H}_2\text{O}=0.3297$, $\text{N}_2=0.6703$
Inlet temperature = 400 K
Pressure = 1 atm.
Space Velocity = 1000 hr^{-1}

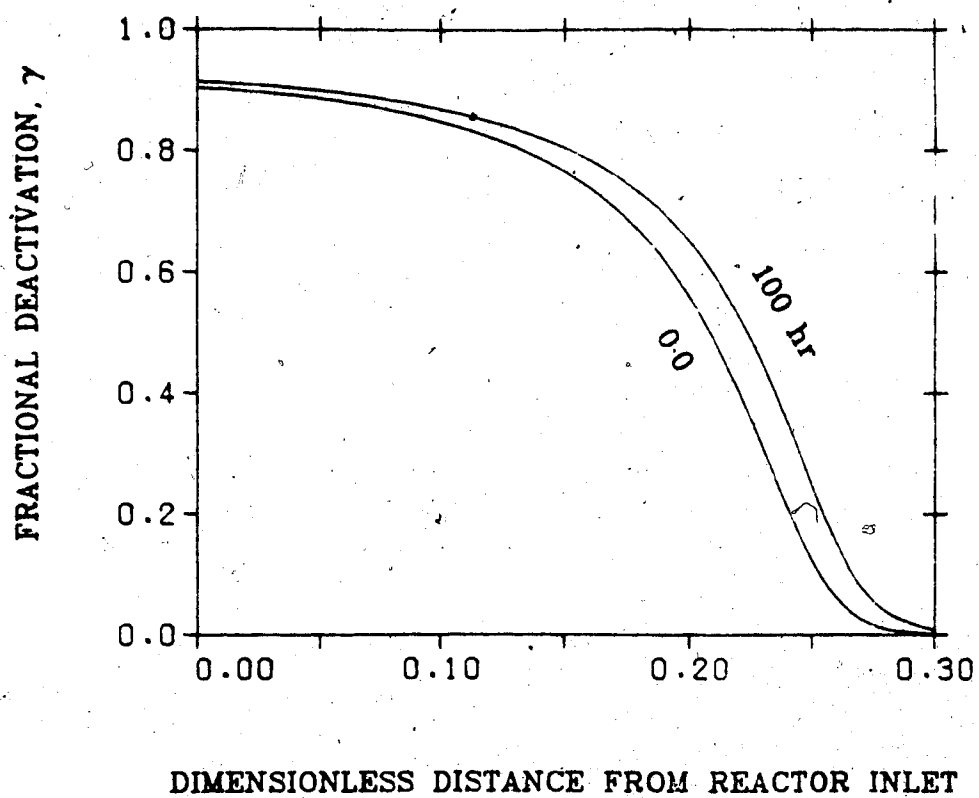


Figure 6.13 Temperature profiles at times (< 1 hr) after startup in the Amoco CBA reactor.
Inlet Composition (mole fraction): $\text{H}_2\text{S} = 0.0124$,
 $\text{SO}_2 = 0.0062$, $\text{H}_2\text{O} = 0.3224$, $\text{N}_2 = 0.6590$
Inlet temperature = 400 K
Pressure = 1 atm
Space Velocity = 1000 hr^{-1}

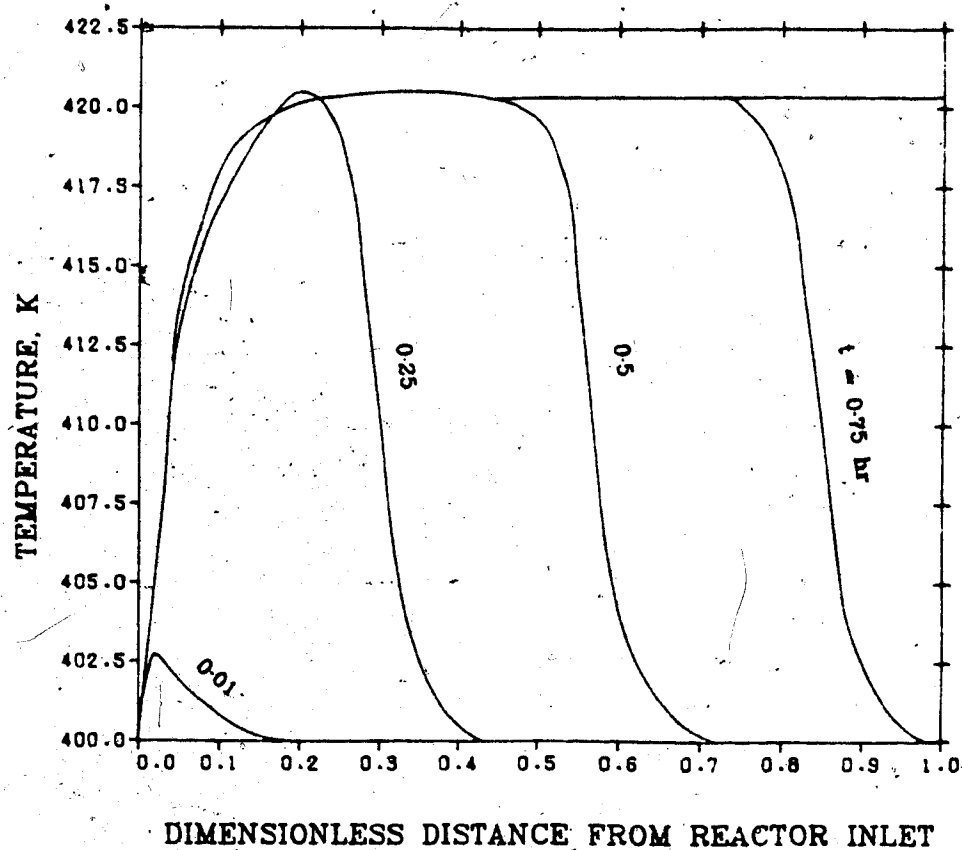


Figure 6.14 Axial profile of partial pressure of H_2S at various times after startup in the Amoco CBA convertor.
 Inlet Composition (mole fraction): $\text{H}_2\text{S}=0.0124$,
 $\text{SO}_2=0.0062$, $\text{H}_2\text{O}=0.3224$, $\text{N}_2=0.6590$
 Inlet temperature = 400 K
 Pressure = 1 atm
 Space Velocity = 1000 hr^{-1}

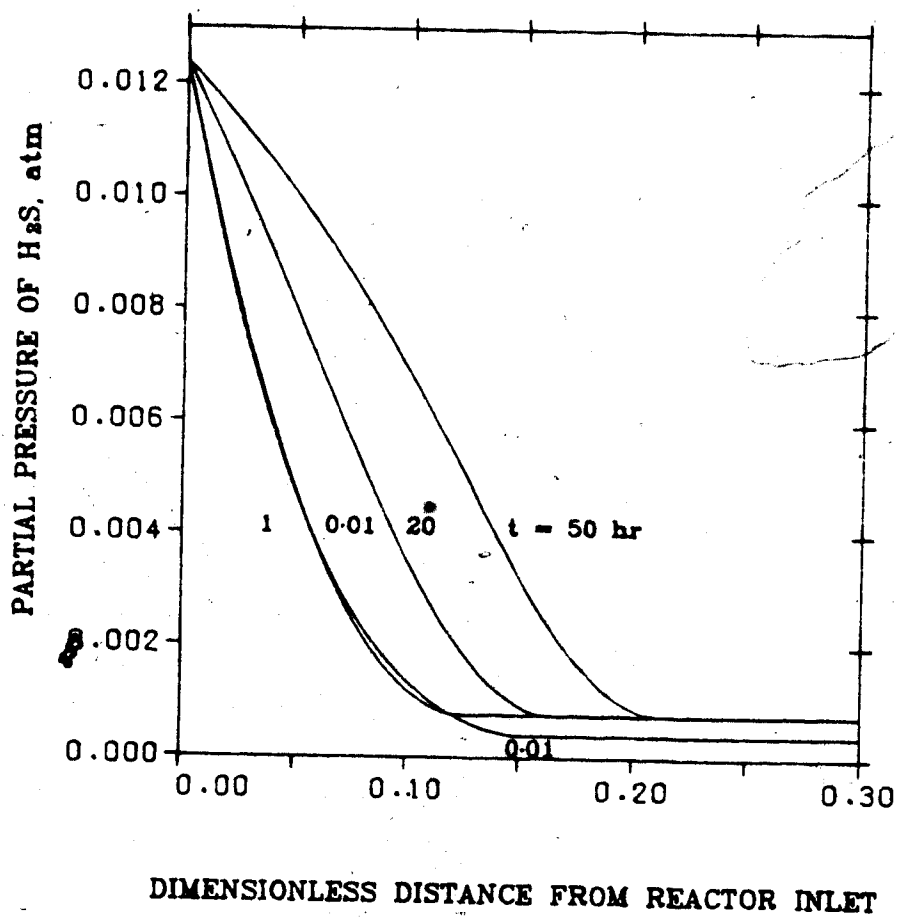


Figure 6.15 The deactivation function at various times in the Amoco CBA convertor.

Inlet Composition (mole fraction): $\text{H}_2\text{S}=0.0124$,
 $\text{SO}_2=0.0062$, $\text{H}_2\text{O}=0.3224$, $\text{N}_2=0.6590$

Inlet temperature = 400 K

Pressure = 1 atm

Space Velocity = 1000 hr^{-1}

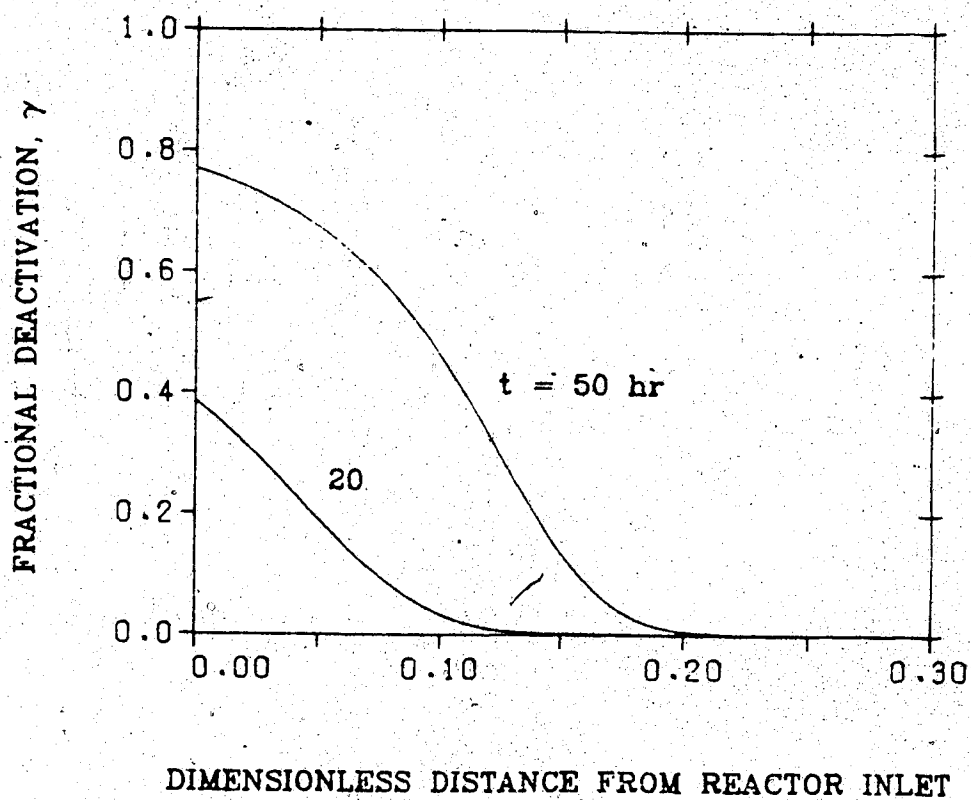
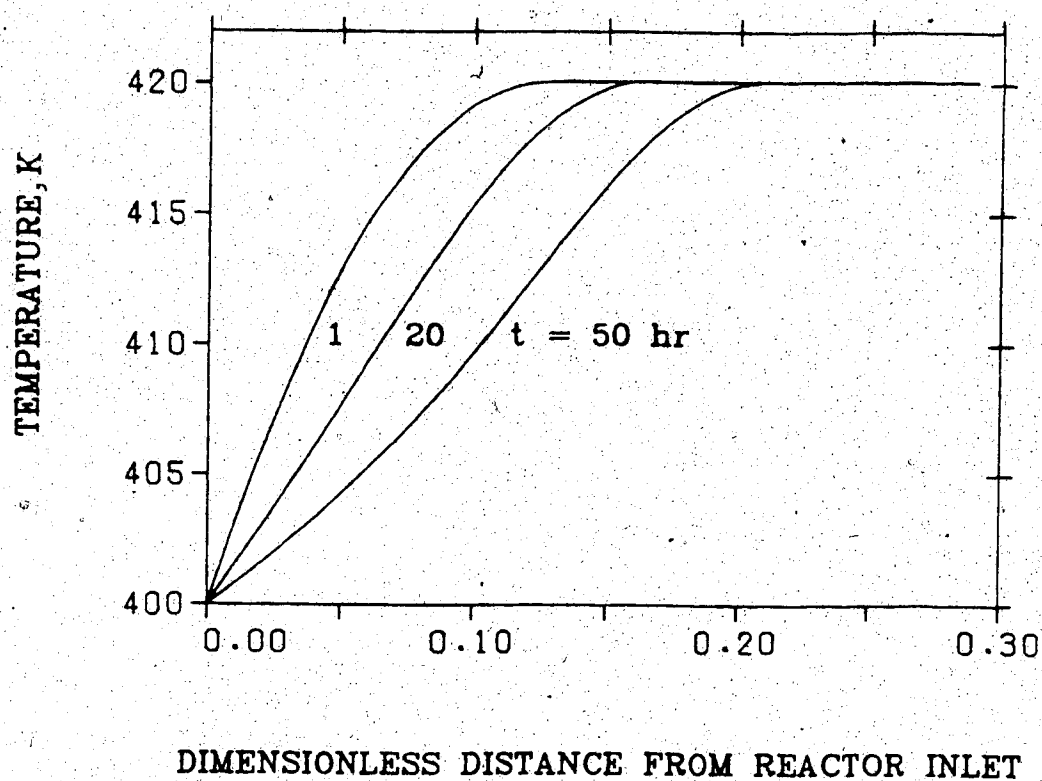


Figure 6.16 Temperature profiles at times (> 1 hr) after the startup in the Amoco CBA convertor.
Inlet Composition (mole fraction): $\text{H}_2\text{S}=0.0124$,
 $\text{SO}_2=0.0062$, $\text{H}_2\text{O}=0.3224$, $\text{N}_2=0.6590$
Inlet temperature = 400 K
Pressure = 1 atm
Space Velocity = 1000 hr^{-1}



Figures (6.7) and (6.14) show that the effect of deterioration of activity on the H_2S pressure profile, results in the movement of the fluid marked by a certain H_2S partial pressure through the bed at a relatively constant velocity. This velocity in the analysis of an adsorption column is called 'wave velocity'.

The wave velocities shown in figures (6.7) and (6.14) are much smaller than the superficial velocity (28 cm/sec) of the fluid through the reactor. The wave velocity depends on the inlet composition to the reactor and is larger for the 2nd-stage reactor than for the 3rd-stage reactor, because of the higher feed H_2S content.

The wave velocity is about 0.56 and 0.16 cm/hr for the coldbed 2nd-stage and the 3rd-stage reactors, respectively. These low values imply that the 2nd-stage coldbed reactor could be operated for about six days before H_2S break through in a convertor of one meter depth. Correspondingly, the third stage reactor could be operated for about twenty days.

Lee and Butt (131) have stated that deactivating catalytic beds are most likely regenerated when the average γ exceeds 0.3. On figures (6.7) and (6.14), this corresponds roughly to the 20-hour and six-day fronts, respectively.

In practice, the MCRC process switches the 2nd-stage convertor to operate as the 3rd-stage convertor after being on stream for one day (99). This corresponds to an average γ approaching 0.3. Thus this simulation predicts a

performance in reasonable agreement with that for an actual plant (99).

Figures (6.9) and (6.16) show that by the time the catalyst at the reactor entrance needs reactivation, the catalyst near the exit may still have a long life expectation before regeneration is required. A better operation is to reverse the direction of flow after a certain time period. In this way, the catalyst in the whole bed will reach the time for regeneration nearly simultaneously, and the catalyst service life before each reactivation will be prolonged.

The above alternative-reversal of flow direction, has been tested for the 2nd-stage convertor operated for one day with downward flow. The results are presented in figures (6.17) to (6.19). The bed initial temperature profile is the 25-hour front of figure (6.8).

Figure (6.17) shows that, initially the temperature in the front of the bed, the end of the bed in figure (6.8) becomes higher than the expected maximum adiabatic temperature of 463 K. The bed temperature at the front section of the bed is initially 463 K, thus further reaction increases its value. Figure (6.17) predicts that in about half an hour the temperature profile evolves to its final shape.

Figure (6.19) shows that the flow reversal results in the deactivation of the both ends of the reactor with the middle section still being active.

Figure 6.17 Temperature profiles at times (<1 hr) after the flow reversal in the 2nd-stage convertor.

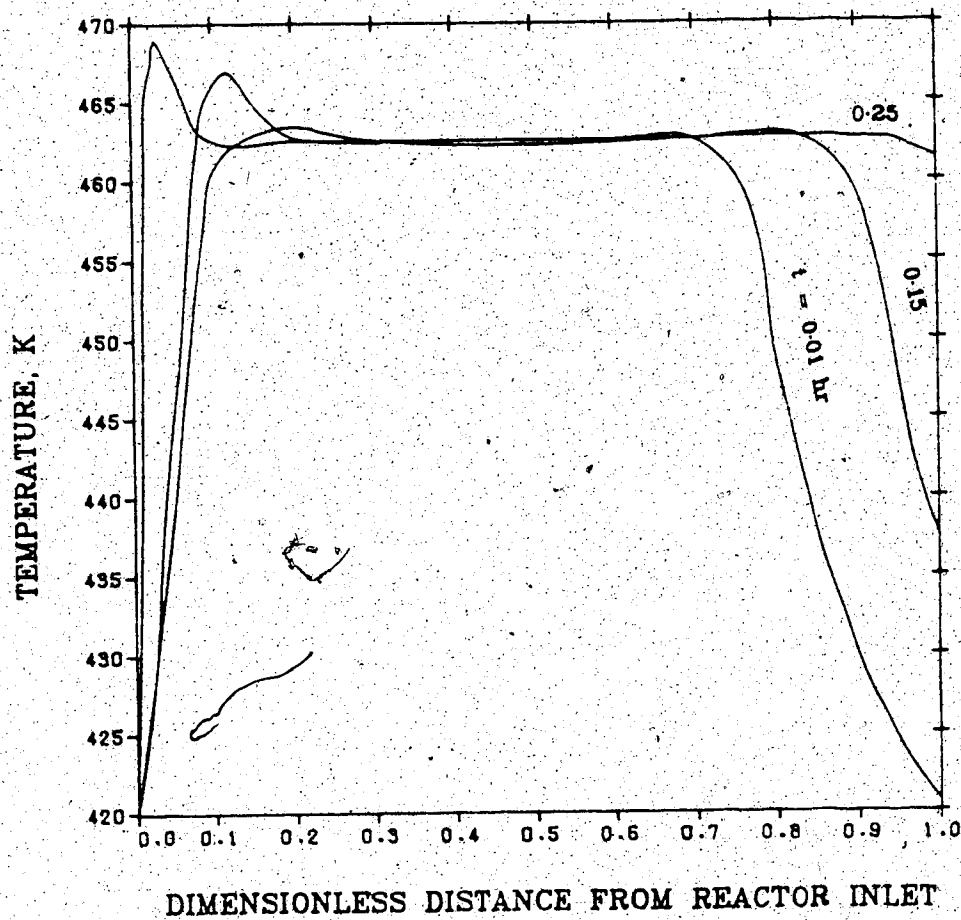


Figure 6.18 Axial profile of partial pressure of H_2S at various times after the flow reversal in the 2nd-stage convertor.

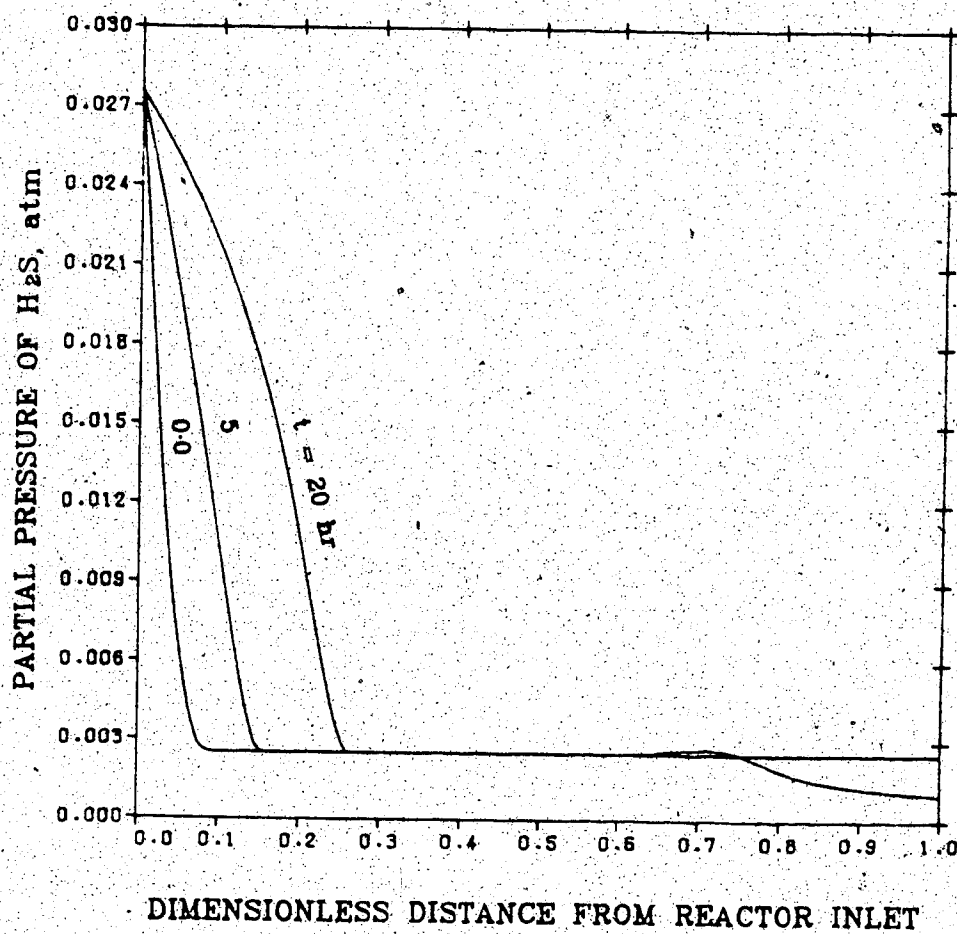
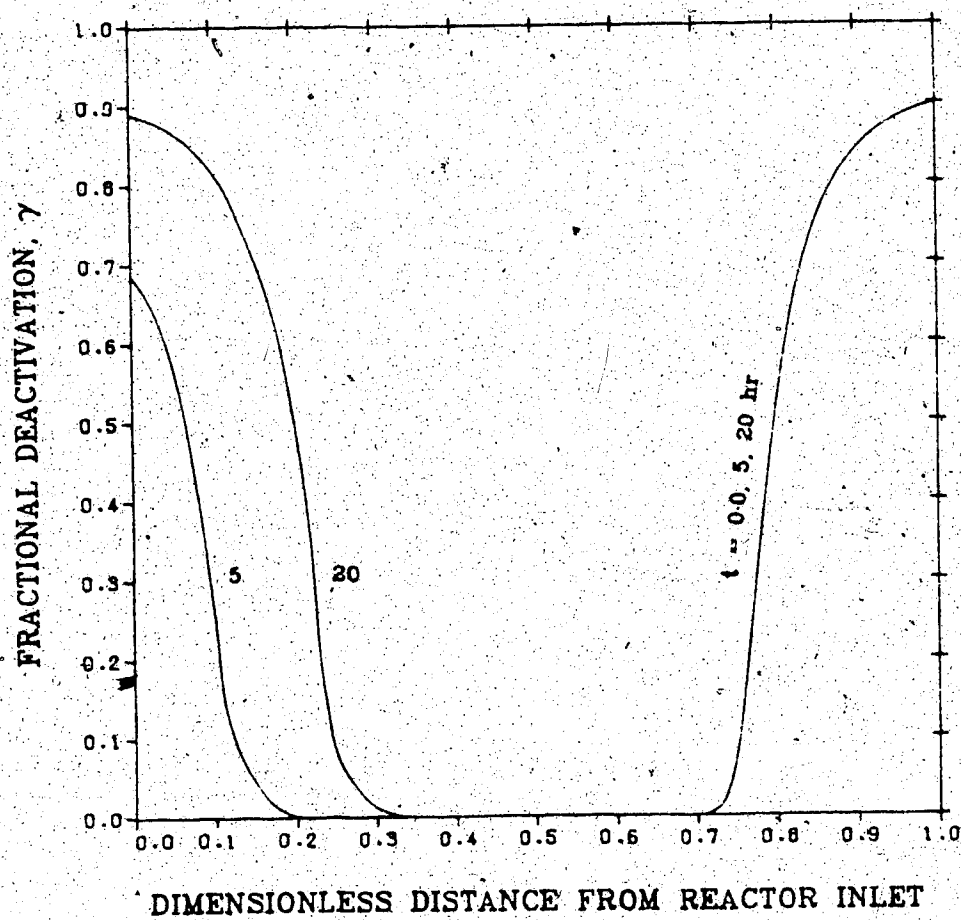


Figure 6.19 The deactivation function at various times after the flow reversal in the 2nd-stage convertor.



In general, the above simulation results show that the deactivation of Claus catalyst by adsorption of the product sulfur is a very slow process. However, a common concern is sulfate poisoning of the catalyst (section 2.5) that can occur at low temperatures and low H_2S concentration; conditions that are present in coldbed reactors. Thus, the wave velocity in the plant converters may, in fact, be greater than the predicted 0.56 and 0.16 cm/hr, due to the deactivation processes other than solely adsorption of the product sulfur.

The simulation analysis also depends upon crucial parameters such as maximum sulfur loading (Q) necessary to deactivate the catalyst, and upon the description of the kinetics. While published values for these are available (98,117), further laboratory experiments are needed to confirm their applicability at coldbed temperatures.

The linear relationship of activity deterioration with sulfur loading, equation (6.18), is based on the assumption of deactivation by site coverage. This assumption would fail if some of the pores are blocked due to the presence of condensed sulfur.

7. CONCLUSIONS AND RECOMMENDATIONS

7.1 Conclusions

The prediction of the performance of catalytic Claus convertors involves considerable complexities in the numerical computations. These complexities arise from,

1. multiple reaction steps in the system;
2. a nonlinear rate expression for the reversible exothermic reaction;
3. the calculation of an equilibrium distribution for the sulfur polymeric forms, S_2, \dots, S_8 ;
4. the existence of limiting equilibrium conversion.

On the basis of limited experimental data, the Claus reaction is assumed to control the kinetics whereas the sulfur polymerization steps are assumed to proceed very rapidly to their near-equilibrium composition distribution. The mathematical analysis of the Claus process depends upon the description of the kinetics of the reaction. In this study, to extend the generality of the published reliable intrinsic forward reaction rate (56), the principle of thermodynamic consistancy was employed to formulate the reverse rate expression. The visible rate of reverse Claus reaction is negligible compared to the forward rate at the conditions of Claus catalytic convertors (135, 44, 145). The existence of the limiting equilibrium conversion would, however, necessitate the consideration of the reverse reaction rate.

The Claus catalyst pellets offer major mass transfer resistance while exhibiting no heat transfer limitations. The mass transfer limitation was expressed by an effectiveness factor. The calculation of a local effectiveness factor for the Claus reaction depends upon the feed composition to the reactor, the extent of conversion and the temperature at the exterior of the catalyst pellet. Irrespective of such complexity, the use of a modified thiele modulus, Φ , enables a single η - Φ curve to be applicable for the given fixed-bed reactor design calculations.

The simulation of a Claus catalytic convertor employing an adiabatic one-dimensional heterogeneous model revealed that a significant amount of reaction occurs at the entrance of the reactor bed. At a space velocity of 1000 hr^{-1} and a feed temperature of 553 K, the external mass and heat transfer resistances were found to be significant in the entrance section of the convertors.

The reported experimentally measured H_2S conversion (44,83) is somewhat higher than the equilibrium value predicted based upon published thermodynamic data. Correspondingly, the reaction path predicted by the modelling of the Claus catalytic convertors were also terminated conservatively at the predicted equilibrium conversion using the published thermodynamic data. The use of adjusted sulfur species properties revealed an increase in the required depth of the catalyst bed compared to the

corresponding one when the published data were used. The adjusted data has further shown that, in a 1-meter catalyst bed, the maximum attainable H_2S conversion would be limited if a space velocity in excess of 2000 hr^{-1} is employed.

Due to mass transfer limitations, the intrinsic activity ratio of the novel to alumina catalyst is not experienced in the catalytic beds. The beds of novel catalysts were found to be twice as active as the beds of the alumina catalyst while their intrinsic activity ratio is 3.5.

The two-dimensional heterogeneous model of the Claus convertor showed that the heat losses affect the temperature and consequently the conversion profiles only in the immediate vicinity of the wall.

The modelling of a deactivating Claus coldbed reactor predicted that, a stable maximum temperature is reached within one hour after the startup. It also revealed that a Claus coldbed reactor would have low rates of deactivation with a breakthrough capacity of the order of several days. In the simulation study of the Claus coldbed, the rate expression which was developed for higher temperatures was extended to coldbed temperatures by adjustment of the rate constant.

The numerical techniques used in this study were orthogonal collocation (75), Weisze-Hick's method (207), Eigenberger-Butt (70) and Runge-Kutta-Fehlberg method (185).

In general this study showed that the simulation of normal or sub-dew point operation of Claus catalytic beds, or use of model for process design is feasible in spite of complexities in mathematical formulation. With a reliable kinetic expression (equation 3.37) in hand and information on physical and transport properties, the Claus reactor performance was modelled from which the effects of changing variables can be quickly ascertained for either normal or sub-dew temperatures.

The models and the computer programs developed in this study can be used to explore the effect of different design variables such as space velocity, reactor bed depth, feed composition and temperature. The modelling results can then be used as a preliminary test for determining the suitability of the design alternative before considering the more expensive pilot plant studies.

7.2 Recommendations

The models used in this study take into account the complex effect of transport limitations, nonlinear kinetics, and multiple reactions. Therefore, the numerical effort, computer programming and the computation times are immense. It would be appropriate to check the applicability of simplifying assumptions to reduce the numerical and computer programming effort.

In the analysis of the effectiveness factor (chapter 4), it was shown that the first-order approximation of the

Claus process could be considered sufficiently reliable for routine calculation of the Claus pellet effectiveness factor. The applicability of the simple first-order kinetic approximation of Claus kinetics should also be tested for the catalytic Claus beds.

The simulation of coldbed Claus convertors depends upon sulfur loading capacity, Q . While published values for Q are available (98,117), further experimental verification is needed.

NOMENCLATURE

a	intrinsic catalyst activity
a	global pellet activity
a _i	activity of the catalyst toward the deactivating reaction
a ₁ , a ₂ , a ₃	functions of the equilibrium constants, equations (4.5) to (4.7)
A	matrix used in orthogonal collocation method
A	effective film transfer area
B	matrix used in orthogonal collocation method
b _j	total number of atomic weigh element of j
C	concentration
C _s	catalyst surface concentration
C _f	bulk fluid concentration
C _p	fluid specific heat capacity
\bar{C}_t	average fluid concentration
C _{pa}	average bed specific heat capacity, eq ⁿ F.15
C _{pc}	catalyst specific heat capacity
D	combined bulk and Knudsen diffusivity
D _{am}	Damkohler number
D _z	axial diffusivity
D _b	bulk diffusivity
D _e	effective diffusivity
D _k	Knudsen diffusivity
D _p	pellet diameter
D _r	radial diffusivity

ΔH	heat of reaction
E	activation energy
G°	standard state free energy
G_i	parameter used in equation 5.18
g_i	dimensionless free energy of species i in the mixture
g_f	free energy parameter; equation (3.3)
h	film heat transfer coefficient
h_a	heat transfer coefficient from the reactor wall to atmosphere
h_p	heat transfer coefficient of catalyst contact point
h_s	radiation heat transfer coefficient from solid
h_v	radiation heat transfer coefficient from void
H'	$(-\Delta H) C_{fi} / \rho T^\circ C_p$
J_h	j -factor for heat transfer
J_m	j -factor for mass transfer
K	equilibrium constant for reaction 3.19
$K_{3.2}$	equilibrium constant for reaction 3.20
$K_{3.4}$	equilibrium constant for reaction 3.21
$K_{3.8}$	equilibrium constant for reaction 3.22
K_6	equilibrium constant for reaction 6.3
$K_{6.6}$	equilibrium constant for reaction 6.5
K_p	equilibrium constant based on pressure
K_ϕ	equilibrium constant based on activity coefficient
K_z	axial thermal conductivity

K_{ins}	thermal conductivity of insulation
K_r	radial thermal conductivity
K_{sh}	thermal conductivity of shield
k	rate constant for main reaction
k_d	rate constant for deactivation reaction
k_f	rate constant for forward reaction
k_g	thermal conductivity of the gas
k_m	film mass transfer coefficient
k_s	thermal conductivity of catalyst
L	reactor depth
Le	effective size of the catalyst pellet
N	total number of the species in the mixture
N_1	total number of the species excluding sulfur species
N_t	total moles of the gas
n	average number of S atoms in sulfur molecule
P	partial pressure
P_{eh}	heat Peclet number
P_{em}	mass Peclet number
Pr	Prandtl number
P_S	sulfur partial pressure, equation 3.36
P_v	sulfur vapor pressure
Q	maximum catalyst content of fouling substance
Q	volumetric flow rate
R	reaction rate
R_c	characteristic reaction rate, e.g. $R_1/2$
R_d	deactivation rate

Re	Reynolds number
R_g	universal gas constant
R_o	reactor outside radius
R_{sh}	shield radius
R_w	reactor radius
R	global reaction rate
r	radius
r'	r/R_w
Sc	Schmidt number
s	total number of catalyst sites
s	T_a/T°
T	temperature
T_a	atmospheric temperature
T_f	fluid temperature
T_s	catalyst temperature
t	T/T_s
t	time
U_f	overall fluid heat transfer coefficient, equation 5.49
U_o	overall wall heat transfer coefficient
U_s	overall solid heat transfer coefficient
V_s	superficial velocity
v	parameter defined by equation 5.17
v_1, v_2, v_3	parameters defined by equations F.12 to F.14
W	function of P_s defined by equation 4.32
w_1, w_2, w_3	parameters defined by equations F.7 to F.9
X	fractional conversion of H_2S

X_f	X in fluid phase
X_s	X in the catalyst surface
\bar{x}	total number of moles
x	moles of species
Y	mole fraction
$Y(S_i)$	parameter defined by equation 3.35
Y_I	effective reaction zone
Y_{H_2S}	mole fraction of H_2S in feed
Y_{SO_2}	mole fraction of SO_2 in feed
Y_{H_2O}	mole fraction of H_2O in feed
Y_{inert}	mole fraction of inerts in feed
\bar{y}	total number of moles; equation (3.7)
y	$2 \cdot r/D_p$
Z	parameter defined by equation 5.7
z	axial position
z'	z/R_w
z	z/L

Greek

α	R_w/D_p
a_i	stoichiometric coefficient of species i
α_f	wall fluid heat transfer coefficient
α_s	wall solid heat transfer coefficient
β	$(\Pi - P_v)/P_v$
β	λ_f/λ_s
β'	coefficient in equation 5.31

γ	$h A R w^2 / \lambda_f$
γ	fractional catalyst deactivation
δ	$V_i^0 / k_m A R w$
ϵ	porosity
η	catalyst effectiveness factor
θ	normalized pressure defined by 4.41
λ	Lagrange multiplier
λ_f	effective fluid radial thermal conductivity
λ_s	effective solid radial thermal conductivity
μ	viscosity
ξ	Prater number, equation 4.16
π	Lagrange multiplier
ρ	density of the gas
ρ_p	pellet density
τ	tortuosity factor
τ_f	dimensionless fluid temperature
τ_s	dimensionless solid temperature
ϕ	Thiele modulus for isothermal pellet eq ⁿ 4.38
ϕ_n	nonisothermal Thiele modulus, equation 4.15
ϕ'	coefficient in equation 5.32
ϕ''	fugacity coefficient
Π	total pressure
Φ	modified Thiele modulus, $\phi / \sqrt{(1 - \psi_e)}$
ψ	P_1 / P_{1s}
ψ_n	C_1 / C_{1s}

Subscripts

1	H_2S	2	SO_2
3	H_2O	4	S_2
5	S_4	6	S_8
7	S_8	8	inerts
i	species i		
s	partical surface		
0	center of the particle		

Superscripts

0	at reactor inlet
0	at time=0

BIBLIOGRAPHY

1. Abed, R., and Rinker, R.G., *AIChE J.*, 19:618, 1973.
2. Ahmed M., and Fahien, R.W., *Chem. Eng. Sci.*, 35:889, 1980a.
3. Ahmed M., and Fahien R.W., *Chem. Eng. Sci.*, 35:897, 1980b.
4. Anon, *Hydro. Proc.*, 57(1): 181, 1978.
5. Aris, R., *Chem. Eng. Sci.*, 6:262, 1957.
6. Aris, R., "The Mathematical Theory of Diffusion and Reaction in Permeable Catalysts", Clarendon Press, 1975.
7. Baddour, R.F., and Yoon, C.Y., *Chem. Eng. Prog. Symp. Ser.*, 57(32):35 1960.
8. Baehr, H., Megdah, H. : I.G. Farbenindustrie, Aktiengesellschaft U.S. Pat. 2092386, Sept. 7, 1937.
9. Bakshi, K.R., and Gavalas G.R., *AIChE J.*, 21:494, 1975
10. Baumeister, E.B., and Bennett, C.O., *AIChE J.*, 4:69, 1958.
11. Beeckman, J.W., and Froment, G.F., *Chem. Eng. Sci.*, 35:805, 1980.
12. Beneati, R.F., and Brosilow, C.B., *AIChE J.*, 8:359, 1962.
13. Bennett, H.A., Ph.D. Thesis, The University of British Columbia, Vancouver, B.C., 1979.

14. Bennett, H.A., and Meisen, A., Can. J. Chem. Eng., 59:532, 1981.
15. Berkowitz, J., J. Chem. Phys., 62:4074, 1975.
16. Bhatia, Q., and Hlavacek, V., in "Chemical and Catalytic Reactor Modelling", ACS Symp. Ser. 237, Dudukovic, M.P., and Mills, P.L., editors, 1984.
17. Bilous, O., and Amundson, N.R., AIChE J., 2:117, 1956.
18. Billimoria, R.M., and Butt, J.B., Chem. Eng. J., 22:71, 1981.
19. Birnbaum, I., and Lapidus, L., Chem. Eng. Sci., 33:443, 1978.
20. Bischoff, K.B., Chem. Eng. Sci., 16:131, 1961.
21. Bischoff, K.B., Can. J. Chem. Eng., 40:161, 1962.
22. Bischoff, B.K., AIChE J., 11:351, 1965.
23. Blanc, J.H., Tellier, J., Thibault, C., and Philardeau, B., Proc. 5th Can. Symp. on Catalysis, Calgary, 1977.
24. Boldingh, E., A Report in Chem. Eng. Dept., University of Alberta, Edmonton, Alberta, 1981.
25. Bonso, A.K., Ph.D. Thesis, The University of British Columbia, Vancouver, B.C., 1981.
26. Bosanquet, C.H., British TA Report BR-507, 1944.
27. Boudart, M., J. Phys. Chem., 80:2869, 1976.
28. Braune, H., and Steinbacher, E., Z. Naturf. Te.1A, 7:486, 1952.

29. Burns, R.A., Lippert, R.B., and Kerr, R.K., Hydro. Proc., :181, Nov. 1974.
30. Butler, J.R., Dew, J.E., and Zink, D.G., U.S. pat. 2724641, Nov. 22, 1955.
31. Butt, J.B., in "Progress in Catalyst Deactivation", Proc. NATO Adv. Study Inst., Figueiredo, J.L., editor, 1982.
32. Cairns, E.J., and Prausnitz, J.M., I&EC, 51:1441, 1959.
33. Calderbaur, P.H., and Pogorsky, L.A., Trans. Inst. Chem. Eng. (London); 35:195, 1957.
34. Cammeron, D.J., and Beavon, D.K., "Problems in the design of High Efficient Sulfur Plants", paper presented at the Feb., 1970 meeting of the Canadian Natural Gas Processing Association, Edmonton, Alberta.
35. Cappelli, A., Collina, A., and Renta, M., I&EC Proc. Des. Dev., 11:184, 1972.
36. Carberry, J.J., I&EC, 58:40, 1960.
37. Carberry, J.J., AIChE J., 7:350, 1961.
38. Carberry, J.J., I&EC Fundam., 14:129, 1975.
39. Carberry, J.J., and Gorring, R.L., J. Catal, 5:529, 1966.
40. Carberry, J.J., and Wendel, M., AIChE J., 9:132, 1963.
41. Carey, G.F., Finlayson, B.A., Chem. Eng. Sci., 30:587, 1975.
42. Chao, J., Hydro. Proc., 59(11):217, 1980.

43. Chilton, T.C., and Colburn, A.P., I&EC, 26:1183, 1934.
44. Cho, B.K., M.Sc. Thesis, University of Alberta, Edmonton, Alberta, 1975.
45. Chu, C., I&EC Fundam., 7:509, 1968.
46. Chuang, T.T., Ph.D. Thesis, Dept. of Chemical Engineering, Univ. of Alberta, 1971.
47. Claus, C.F., Brit. Pat. 5958, Dec. 31, 1883.
48. Coberly, C.A., and Marshall, W.R., Chem. Eng. Progr., 47:141, 1951.
49. Cocke, D.L., Abed, G., and Plack, J.H., J. Phys. Chem., 80:524, 1976.
50. Cormode, P.A., M.Sc. Thesis, University of Alberta, Edmonton, Alberta, 1965.
51. CRC Handbook of Chemistry and Physics, CRC Press, 61st Ed., 1980.
52. Crynes, B.L., Editor, "Chem. Reactions as a Means of Separation-Sulfur Removal", Marcel Dekker Inc., N.Y., 1977.
53. Cullis, C.F., and Mulcahy, M.F.R., Combust. Flame., 18:225, 1972.
54. Dalla Lana, I.G., Paper presented at CNGPA 3rd. Quarterly Meeting, Calgary, Sept., 1983.
55. Dalla Lana, I.G., Cho, B.K., and Liu, C.L., paper presented in CNGPA Research Seminar, Calgary, Nov., 1974.
56. Dalla Lana, I.G., Liu, C.L., and Cho, B.K., Proc. 6th Euro/4th Int. Symp. Chem. Reaction Eng., V-196, DECHEMA, 1976.

57. Dalla Lana, I.G., McGregor, D.E., Liu, C.L., and Cormode, A.E., Proc. 5th Euro/2nd Int. Symp. Chem. Reaction Eng., B2-9, Elsevier Publishing Co., 1972.
58. Danckwerts, P.V., Chem. Eng. Sci., 2:1, 1953.
59. Davis, J.C., Chem. Eng., 79:66, 1972.
60. De Acetis, J., and Thodos, G., I&EC, 52:1003, 1960.
61. Denbigh, K.G., "The Principles of Chemical Equilibrium", Cambridge Univ. Press, 3rd ed., 1972.
62. De Pauw, R., and Froment, G.F., Chem. Eng. Sci., 30:789, 1975.
63. Dewasch, A.P., and Froment, G.F., Chem. Eng. Sci., 26:629, 1971.
64. Dewasch, A.P., and Froment, G.F., Chem. Eng. Sci., 27:567, 1972.
65. Do, D.D., and Bailey, J.E., Chem. Eng. Sci., 37:545, 1982.
66. Dorweiler, V.P., and Fahien, R.W., AIChE J., 5:139, 1959.
67. Dupin, T., Hydro. Proc., 61(11):189, 1982.
68. Dwivedi, P.N., and Vpadhay, S.N., I&EC. Proc. Des. Dev., 16:157, 1977.
69. Eigenberger, G., Chem. Eng. Sci., 27:1909 & 1917, 1972.
70. Eigenberger, G., and Butt, J.B., Chem. Eng. Sci., 31:681, 1976.
71. Fahien, R.W., and Stankovich, F., Chem. Eng. Sci., 34:1350, 1979.

72. Fan, L.T., and Ahn, Y.K., I&EC. Proc. Des. Dev., 1:190, 1962.
73. Feick, J., and Quon, D., Can. J. Chem. Eng., 48:205, 1970.
74. Finlayson, B.A., Chem. Eng. Sci., 26:1081, 1971.
75. Finlayson, B.A., "The Method of Weighted Residuals and Variational Principles", Academic Press, 1972.
76. Finlayson, B.A., Cat. Rev.-Sci. Eng., 10:69, 1974.
77. Froment, G.F., Chem. Eng. Sci., 7:29, 1961.
78. Froment, G.F., I&EC, 59:18, 1967.
79. Froment, G.F., In "Chemical Reaction Engineering", Adv. in Chem. Ser. 109, Am. Chem. Soc., 1972.
80. Froment, G.F., in "Progress in Catalyst Deactivation", Proc. NATO Adv. Study Ins., Figuerido, J.L., editor, 1981.
81. Froment, G.F., and Bischoff, K.B., Chem. Eng. Sci., 16:189, 1961.
82. Froment, G.F., and Bischoff, K.B., "Chemical Reactor Analysis and Design", John Wiley & Sons Inc., 1979.
83. Gamson, B.W., and Elkins, E.H., Chem. Eng. Prog., 49(4):203, 1953.
84. Gas processing Handbook, Hydro. Proc., 61(4):85, 1982.
85. George, Z.M., J. Catal., 32:261, 1974.
86. George, Z.M., J. Catal., 35:218, 1974.

87. Gerald, C.F., "Applied Numerical Analysis", 2nd Ed., Addison-Wesley, 1978.
88. Goar, B.G., Hydro. Proc., 47(9):248, 1968.
89. Goar, B.G., Hydro. Proc., 53(7):129, 1974.
90. Goar, B.G., EP/Canada, 68(3):32, 1976.
91. Goddin, C.S., Hunt, E.B., and Palm, J.W., Hydro. Proc., 53(10):122, 1974.
92. Gottifredi, J.C., Gonzo, E.E., and Quiroga, O.D., Chem. Eng. Sci., 36:705;713, 1981.
93. Grancher, P., Alberta Sulfur Research Quarterly Bulletin, XIV(3):11, 1977.
94. Grancher, P., Hydro. Proc., 57(7):155, 1978.
95. Graulier, M., and Papee, D., EP/Canada, 66(4):32, 1974.
96. Hammer, B.G.G., Doktorsavhandling, Chalmers Tek. Hogskola, No 14:166, 1957.
97. Handley, D., and Heggs, P.J., Tran. Inst. Chem. Eng., 46:T251, 1968.
98. Heigold, R.E., Private Communication, 1983.
99. Heigold, R.E., and Berkeley, D.E., Oil & Gas J., 156, Sept. 1983.
100. Hlavacek, V., Marek, M., and Kubicek, M., Chem. Eng. Sci., 23:1083, 1968.
101. Hlavacek, V., Kubicek, M., and Marek, M., J. Catal., 15:31, 1969.

102. Hlavacek, V., and Kubicek, M., Chem. Eng. Sci., 25:1537, 1970.
103. Hlavacek, V., and Hofmann, H., Chem. Eng. Sci., 25:173, 1970a.
104. Hlavacek, V., and Hofmann, H., Chem. Eng. Sci., 25:187, 1970b.
105. Hlavacek, V., Hofmann, H., Votruba, J., and Kubicek, M., Chem. Eng. Sci., 28:1897, 1973.
106. Hlavacek, V., and Marek, M. Chem. Eng. Sci., 21:501, 1966.
107. Hugo, P., Chem. Eng. Sci., 25:1537, 1970.
108. Hyne, J.B., Canadian Gas J., 12: Mar.-Apr., 1972.
109. Hyne, J.B., and Ho, K.T., Alberta Sulfur Research Quarterly Bulletin, XV(3,4):49, Oct., 1978-Mar., 1979.
110. Johnson, M.F.L., and Stewert, W.E., J. Catal., 4:248, 1965.
111. Kao, H.S.P., and Satterfield, C.N., I&EC Fundam., 7: 665, 1968.
112. Karanth, W.G., and Hughes, R., Catal. Rev., 9:121, 1974.
113. Karren, B.L., M.Sc. Thesis, University of Alberta, Edmonton, Alberta, 1972.
114. Kaza, K.R., and Jackson, R., Chem. Eng. Sci., 35:1179, 1980.
115. Kaza, K.R., Villadsen, J., and Jackson, R., Chem. Eng. Sci., 35:17, 1980.

116. Kerr, R.K., Paskall, H.G., and Ballash, N., EP/Canada, 66-72, Sept.-Oct. 1976.
117. Kerr, R.K., Paskall, H.G., and Ballash, N., EP/Canada, 48, Jan.-Feb., 1977.
118. Khang, S.J., O. Levenspiel, I&EC Fundam., 12:185, 1973.
119. Kondalik, P., Horak, J., and Tesarova, J., I&EC Proc. Des. Dev., 7:951, 1968.
120. Krishnaswamy, S., and Kittrel, J.R., AIChE J., 27:120, 27:125, 1981.
121. Krishnaswamy, S., and Kittrell, J.R., I&EC Fundam., 21:95, 1982.
122. Kubota, H., Yamanaka, Y., and Dalla Lana, I.G., J. Chem. Eng. Japan, 2:71, 1969.
123. Kubie, J., Ph.D. Thesis, the University of Aston in Birmingham, 1974.
124. Kubota, H., Ikeda, M., and Nishimura, Y., Chem. Eng. (Japan), 4:59, 1966.
125. Kwong, S.S., and Smith, J.M., I&EC, 49:894, 1957.
126. Landau, M., and Molyneux, A., I. Chem. Eng. Symp. Series, No. 27, 1968.
127. Lee, H.H., AIChE J., 27:558, 1981.
128. Lee, H.H., Chem. Eng. Sci., 36:1921, 1981.
129. Lee, H.H., AIChE J., 29:340, 1983.
130. Lee, H.H., and Butt, J.B., AIChE J., 28:405, 1982.

131. Lee, H.H., and Butt, J.B., *AIChE J.*, 28:410, 1982b.
132. Lerou, J., and Froment, G.F., *Chem. Eng. Sci.*, 32:853, 1977.
133. Liu, S.L., and Amundson, N.R., *I&EC. Fundam.*, 2:183, 1963 a.
134. Liu, S.L., and Amundson, N.R., *I&EC Fundam.*, 1:200, 1962; 2:12, 1963 b.
135. Liu, C.L., Ph.D. Thesis, University of Alberta, Edmonton, Alberta, 1978.
136. Liu, C.L., Chuang, T.T., and Dalla Lana, I.G., *J. Catal.*, 26:474, 1972.
137. Livbjerg, H., and Villadsen, J., *Chem. Eng. Sci.*, 27:21, 1972.
138. Lovett, W.D., and Cunniff, F.T., *Chem. Eng. Progr.*, 70(5):43, 1974.
139. Lowe, A., *Chem. Eng. Sci.*, 37:944, 1982.
140. Maddox, R.N., "Gas and Liquid Sweetening", 2nd edition, Campbell Petroleum Series, 1974.
141. Marivoet, J., Teodoriu, P., and Waje, S., *Chem. Eng. Sci.*, 29:1836, 1974.
142. Masamune, S., and Smith, J.M., *AIChE J.*, 12:384, 1966.
143. Mason, E.A., Erans, R.B., and Watson, G.M., *J. Chem. Phys.*, 35:2076, 1961; 36:1894, 1962; 41:3815, 1964.
144. McBride, B. J., et al., "Thermodynamic Properties to 6000 K for 210 Substances Involving the First 18 Elements", NASA-SP-3001, Office of Scientific and Technical Information, NASA, Washington D.C., 1963.

145. McCulloch, N., M.Sc. Thesis, University of Alberta, Edmonton, Alberta, 1982.
146. McGreavy, C., and Cresswell, D.L., Can. J. Chem. Eng., 47:583, 1969.
147. McGreavy, C., and Turner, K., Can. J. Chem. Eng., 48:200, 1970.
148. McGregor, D.E., Ph.D. Thesis, University of Alberta, Edmonton, Alberta, 1971.
149. Meisen, A., and Bennett, H.A., Hydro. Proc., 58(12):131, 1979.
150. Menon, P.G., Speeramamurthy, R., Murti, P.S., Chem. Eng. Sci., 27:641, 1972.
151. Meyer, B., Chem. Rev., 76:367, 1976.
152. Meyer, B., "Sulfur, Energy, and Environment", Elsevier Sci. Pub. Co., 1977.
153. Mikus, O., Pour, V., Hlavacek, V., J. Catal., 69:140, 1981.
154. Mischke, R.A., and Smith, J.H., I&EC Fundam., 1(4):288, 1962.
155. Morales, M., Spinn, C.W., and Smith, J.M., I&EC, 43, 225, 1951.
156. Nabor, G.W., and Smith, J.M., I&EC, 45:1272, 1953.
157. Nobles, Palm, J.W., and Knudtson, D.K., Hydro. Proc., 56(7):143, 1977.
158. Olsen, J.H., I&EC Fundam., 7:185, 1968.
159. Oliver, R.C., Stephanou, S.E., and Baier, R.W., Chem.

Eng., 69:121, 1962.

160. Opekar, P.C., and Goar, B.C., Hydro. Proc., 45(6):181, 1966.

161. Paspek, S.C., and Verma, A., Chem. Eng. Sci., 35:33, 1980.

162. Paterson, W.R., and Cresswell, D.L., Chem. Eng. Sci., 26:605, 1971.

163. Petersen, E.P., Chem. Eng. Sci., 37:669, 1982.

164. Pearson, J.R.A., Chem. Eng. Sci., 10:281, 1959.

165. Pearson, M.J., Gas Processing, 241:22, May-June 1973a.

166. Pearson, M.J., Hydro. Proc., 52(2):81, Feb. 1973b.

167. Pearson, M.J., EP/Canada, 67(6):38, July-Aug. 1976.

168. Pillai, K.K., Chem. Eng. Sci., 32:59, 1977.

169. Preuner, G., and Schupp, W., Z. Phys. Chem., 68:129, 1909.

170. Quet, C., Teillier, J., and Voirin, R., "Cat. Deactivation Proceedings of the Int. Symp.", Antwerpen, Oct. 13-15, 1980.

171. Rau, H., Kutty, T.R.N., and Guedes de Carvalho, J.R.F., J. Chem. Thermodyn., 5:883, 1973.

172. Raymond, L.R., and Amundson, N.R., Can. J. Chem. Eng., 42:173, 1964.

173. Reed, R.L., Paper Presented at CGPA Quarterly Meeting, Calgary, Alberta, Sept. 14, 1983.

174. Rester, S., and Aris, R., Chem. Eng. Sci., 24:793, 1969.
175. Ridgway, K., and Tarbuck, K.J., Chem. Eng. Sci., 23:1147, 1968.
176. Roberts, G.W., and Satterfield, C.N., I&EC Fundam., 5:317, 1966.
177. Roblee, L.M., Baird, R.M., and Tireney, J.W., AIChE J., 4:460, 1958.
178. Ross, R.A., and Taylor, A.H., Proc. Brit. Ceram. Soc., 5:167, 1965.
179. Sabtier, P., and Reid, E.E., "Catalysis in Organic Chemistry", Princeton-Van Nostrand Co., N.Y., 1922.
180. Satterfield, C.N., "Mass Transfer in Heterogeneous Catalysis", MIT Press, 1970.
181. Satterfield, C.N., "Heterogeneous Catalysis in Practice", McGraw-Hill Inc., New York, 1980.
182. Schertz, W.W., and Bischoff, K.B., AIChE J., 15:597, 1969.
183. Schlunder, E.U., Chem. Ing. Tech., 38:967 & 1161, 1966.
184. Schuler, R.W., Stallings, V.P., and Smith, J.M., Chem. Eng. Prog. Symp. Ser., 48:19, 1952.
185. Schwartz, C.E., and Smith, J.M., I&EC, 45:1209, 1953.
186. Shampine, L.F., and Allen, J.R., "Numerical Computing: An Introduction", W.B. Saunders Comp., Toronto, 1973.
187. Sherwood, T.K., Pigford, R.L., and Wilke, C.R., "Mass Transfer", McGraw-Hill, New York, 1975.

188. Sinkule, J., Votruba, J., Hlavacek, V., and Hofmann, H., Chem. Eng. Sci., 31:23, 1976.
 189. Smith, J.M., "Chemical Engineering Kinetics", Third ed., McGraw-Hill, New York, 1981.
 190. Smith, T.G., Zahradnik, J., and Carberry, J.J., Chem. Eng. Sci., 30:763, 1975.
 191. Sorensen, J.P., and Stewart, W.E., Chem. Eng. Sci., 37:1103, 1982.
 192. Stecher, P.G., "Hydrogen Sulfide Removal Processes", Noyes Data Corporation, New Jersey, 1972.
 193. Stull, D.R., and Prophet, H., JANAF Thermochemical Tables, 2nd edition, NSRDS-NBS 37, 1971.
 194. Szepe, S., Levenspiel, O., "Proceedings of the 4th Euro. Symp. on Chemical Reaction Engineering", Pergamon, London, 265, 1968.
 195. Taylor, H.A., and Wesley W.A., J. Phys. Chem., 31:216, 1927.
 196. Thadani, M.C., and Peebles, F.N., I&EC Proc. Des. Dev., 5:267, 1966.
 197. Thiele, E.W., Reprinted in Chem. Eng. Fundam., 2(1):13, 1983.
-
198. Tinkler, J.D., Metzner, A.B., I&EC, 53:663, 1961.
 199. Truong, T.T.T., M.Sc. Thesis, University of Alberta, Edmonton, Alberta, 1982.
 200. Van Cauwenberghe, A.R., Chem. Eng. Sci., 21:203, 1966.
 201. Van Den Bosch, B., and Padmanabhan, Chem. Eng. Sci., 29:1217, 1974.

202. Van Welsenaere, R.J., and Froment; G.F., Chem. Eng. Sci., 25:1503, 1970.
 203. Villadsen, J.V., and Stewart, W.E., Chem. Eng. Sci., 22:1483, 1967.
 204. Villadsen, J.V., and Michelsen, M.L., "Solution of Differential Equation Models by Polynomial Approximation", Prentice-Hall, Inc., 1978.
 205. Votruba, J., Hlavacek, V., and Marek, M., Chem. Eng. Sci., 27:1845, 1972.
 206. Wakao, N., and Smith, J.M., Chem. Eng. Sci., 17:825, 1962.
 207. Wehner, J.F., and Wilhelm, R.H., Chem. Eng. Sci., 6:89, 1956.
 208. Weisz, P.B., and Hicks, J.S., Chem. Eng. Sci., 17:265, 1962.
 209. Wen, C.Y., and Fan, L.T., "Models for Flow Systems and Chemical Reactors", Marcel Dekker, Inc., 1975.
 210. Weng, H. S., Eigenberger, G., and Butt, J.B., Chem. Eng. Sci., 30:1341, 1975.
 211. Wheeler, A., "Advances in Catalysis", Vol III:249, Academic Press, Inc., 1951.
-
212. Whitaker, S., AIChE J., 18:361, 1972.
 213. White, W.B., Johnson, S.M., and Dantzig, G.B., J. Phys. Chem., 28:751, 1958.
 214. Wong, R.L., and Denny, V.E., Chem. Eng. Sci., 30:709, 1975.
 215. Yagi, S., and Kunii, D., AIChE J., 6:97, 1960.

216. Yagi, S., and Kunii, D., AIChE J., 3:373, 1957.
217. Yagi, S., Kunii, D., and Wakao, N., AIChE J., 6:543, 1960.
218. Young, L.C., and Finlayson, B.A., I&EC Fundam., 12:412, 1973.
219. Yung, B.K.Y., M.Eng. Report, University of Alberta, Chem. Eng. Dept., Edmonton, Alberta, 1983.
220. Zeldowitsch, J.B., Acta. Physicochim, USSR 10:583, 1939.

APPENDIX A: Claus Equilibria

Contents

1. Ideal Gas Approximation.
 2. Effect of nonideality of the Gas on Equilibrium Constant.
 3. Thermodynamic data file to be used with free energy minimization.
 4. "GEN" program: free energy minimization routine
 5. "CONDENSATION" program: free energy minimization routine in the presence of liquid sulfur; Method B.
 6. "SCONLB" program: free energy minimization routine in the presence of liquid sulfur; Method A.
 7. Results of "CONDENSATION " program.
 8. Results of "SCONLB" program.
-

A.1 Ideal Gas Approximation

The ideal gas law is inherent in the calculation procedure and the validity of its use will be considered here. To describe the behaviour of real gases, the thermodynamic property, the fugacity, f , is used. The fugacity is essentially a pseudo-pressure. When the fugacity is substituted for pressure, one can, in effect, use the same equations for real gases that one normally uses for ideal gases. Fugacity, f , is defined as

$$dG = Rg T d(\ln f) \quad (A.1)$$

with the requirement that as the pressure goes to zero,

$$\lim (f/P) = 1 \quad (A.2)$$

One method of determining pure component fugacity employs the Principle of Corresponding States and uses generalized charts to calculate the value of the fugacity coefficient, ϕ'' ,

$$\phi'' = f/P \quad (A.3)$$

The three parameter generalized fugacity coefficient tables² was used for determining ϕ'' for the components of interest at the operating conditions of the furnace, the

² Reid R.C. et al, "The Properties of Gases and Liquids", 3rd Ed., McGraw-Hill book company, 1977.

conventional Claus and the coldbed reactors. The critical properties and the Pitzer's acentric factor, w , of all the species except sulfur were obtained from Reid et al.³ The critical properties of sulfur is from Rau et al.⁴ The acentric factor of sulfur was obtained from

$$w = -\log P_{vr} \text{ (at } T_r=0.7) - 1.0 \quad (\text{A.4})$$

The critical properties and w of the Claus species are presented in table A.1.

Table A.2 shows that the fugacity coefficients of the different species at one atmosphere and typical temperatures of the coldbed reactor, conventional reactor and the furnace of the Claus process. It is apparent that at the conditions of the furnace the fugacity coefficients for all the species would be very close to unity and they behave ideally. Table A.2 also shows that the assumption of ideality is invalid for sulfur at the coldbed and conventional reactor conditions. The fugacity coefficients of the other species, however, is close to unity at the reactor conditions.

A.2 Effect of nonideality of the Gas on equilibrium Constant

The equilibrium constant based on activity is defined by

³ibid

⁴Rau H., et al, J. Chem. Thermodynamics, 5:291, 1973

Table A.1 Critical Properties of the Claus Species

Species	Tc(K)	Pc(atm)	w
H ₂ S	373.2	88.2	0.1
SO ₂	430.8	77.8	0.251
H ₂ O	647.3	217.6	0.344
N ₂	126.2	33.5	0.04
Sulfur (S ₂ , 78)	1313	179.7	0.247

Table A.2 Fugacity Coefficients* of Pure Species at One Atmosphere

T(K)	H ₂ S	SO ₂	H ₂ O	N ₂	Sulfur
450	0.9977	0.9968	0.9498	1.00005	0.00013
550	0.9989	0.9977	0.9682	1.0	0.0051
1500	1.000007	1.00004	1.0001	1.0	0.9977

*The fugacity coefficients were estimated from tables 5-6 and 5-7 of Reid et al.

$$\ln K = -\Delta G^\circ / (R_g T) \quad (A.5)$$

and is related to equilibrium constant based on partial pressure of the species involved in a reaction by

$$K = K_p K\phi'' \quad (A.6)$$

For ideal gases $K\phi''$ is unity and, $K=K_p$.

For reaction (3.20), $K\phi''$ is defined by,

$$K\phi'' = \frac{(\phi''_3)^2 (\phi''_6)^{0.5}}{(\phi''_1)^2 (\phi''_2)} \quad (A.7)$$

and its value is determined from data of table A.2 as,

P (atm)	T (K)	$K\phi''$
1.0	450	0.0104
1.0	550	0.0672
1.0	1500	0.9990

```

*****
*
* The data file to be used with "GEN" program. It contains*
* the species name, the mass balance atomic number in   *
* the order of H, N, O, S, C; and free energy coefficients*
* of the free energy function:                             *
*
*  $G/RT = C_1(1 - \ln T) - C_2T/2 - C_3T^2/6 - C_4T^3/12$       *
*  $- C_5T^4/20 + C_6/T + C_7 - C_8/T^2$                        *
*
* For example for H2, the first species in the file, the  *
* numbers 2.,0.,0.,0.,0., assign 2 H atoms and zero atoms *
* of N,O,S,C. The rest of the data for H2 are free       *
* energy coefficients in order of C1 to C8.                *
* The sulfur species free energy coefficients are from     *
* Rau (171). The coefficients for the rest of the species *
* were obtained from JANAF (193) tables. The method of    *
* the derivation of the free energy coefficients have      *
* been described in the references (51) and (144).         *
*
*****

```

H2

2.,0.,0.,0.,0.,
 3.116721,1.1458E-03,-9.04839E-07,3.096603E-10,
 0.,-9.722874E 02,-2.345249,0.,

N2

0.,2.,0.,0.,0.,
 3.4741,-1.811493E-04,9.56134E-07,-3.370366E-10,
 0.,-1035.053,3.268552,0.,

O2

0.,0.,2.,0.,0.,
 .3718994E 01,-.2516728E-02,.8583736E-05,-.8299872E-08,
 .2708218E-11,-.105767E 04,.39087E 01,0.,

CO

0.,0.,1.,0.,1.,
 3.428748,2.834611E-05,8.259018E-07,-3.157564E-10,
 0.,-1.433105E 04,4.19517,0.,

CO2

0.,0.,2.,0.,1.,
 2.680418,.007262,-4.308451E-06,9.25351E-10,
 0.,-4.844353E04,8.463569,0.,

H2O

2.,0.,1.,0.,0.,
 4.091473,-1.025776E-03,3.36041E-06,-1.485555E-09,
 0.,-30303.03,-0.42795,0.,

H2S

2.,0.,0.,1.,0.,
 3.679785,1.262427E-03,1.006445E-06,-4.756682E-10,
 0.,-.358756E 04,3.367966,0.,

SO2

0.,0.,2.,1.,0.,
 3.249204,6.48561E-03,-4.043923E-06,8.80362E-10,
 0.,-.36946E 05,9.58542,0.,

COS

0.,0.,1.,1.,1.,
 2.9492538,8.281002E-03,-5.6749E-06,1.358286E-09,
 0.,-.178558E 05,8.826578,0.,

CS2

0.,0.,0.,2.,1.,
 3.427127,8.29768E-03,-6.1069E-06,1.5126E-09,
 0.,.127498E 05,.687726E 01,0.,

CH4

4.,0.,0.,0.,1.,
 4.2497678,-6.9126562E-03,3.1602134E-05,-.29715432E-07,
 9.510358E-12,-1.0186632E 04,-9.1754991E-01,0.,

S1

0.,0.,0.,1.,0.,
 .2913725E 01,0.3129046E-03,-.2609251E-05,.3138244E-08,
 -.1170898E-11,.3256826E 05,.3568115E 01,0.,

S2

0.,0.,0.,2.,0.,
 4.300101,.000141,0.,0.,
 0.,.14289E 05,2.6277,-.19889E 05,

S3

0.,0.,0.,3.,0.,
 .64723E 01,.52367E-03,0.,0.,
 0.,.14810E 05,-5.048,-.39124E 05,

S4

0.,0.,0.,4.,0.,
 9.6133,.3943E-03,0.,0.,
 0.,.14169E 05,-18.3132,-.70997E 05,

S5

0.,0.,0.,5.,0.,
 .12869E 02,.127392E-03,0.,0.,
 0.,.86843E 04,-.37294E 02,-.9494E 05,

S6

0.,0.,0.,6.,0.,
 1.590131E 01,.00006,0.,0.,
 0.,.06781E 05,-.4926E 02,-.110775E 06,

S7

0.,0.,0.,7.,0.,
 .1864955E 02,.308661E-03,0.,0.,
 0.,.073115E 05,-.5863E 02,-.11891E 06,

S8

0.,0.,0.,8.,0.,
 2.14854E 01,.000433,0.,0.,
 0.,.049604E 05,-.7224E 02,-.12865E 06,

```

C *****
C *
C *
C *
C *
C * THIS PROGRAM CALCULATES EQUILIBRIUM COMPOSITIONS *
C * FOR COMPLEX REACTION SYSTEMS USING THE FREE ENERGY *
C * MINIMIZATION METHOD DEVELOPED BY WHITE *
C * COWORKERS. IT WILL HANDLE UP TO THIRTY DIFFERENT *
C * MOLECULAR SPECIES CONTAINING TEN DIFFERENT *
C * ELEMENTS. ANY NUMBER OF CASES CAN BE ATTEMPTED WITH *
C * AS MANY TEMPERATURES AND PRESSURES DESIRED. *
C *
C *
C * INPUT DATA *
C * M - NUMBER OF DIFFERENT ELEMENTS, H, C, O, S, N *
C * N - NUMBER OF GASEOUS SPECIES *
C * P - NUMBER OF CONDENSED SPECIE *
C * NPT - NUMBER OF TEMP. AND PRESS. CONDITIONS *
C * SNAM - THE NAMES OF THE SPECIES *
C * X - THE AMOUNT OF THIS SPECIE PRESENT IN *
C * THE STARTING CHEMICAL SYSTEM (EITHER *
C * NUMBER OF MOLES OR MOLE FRACTION). *
C * A - SPECIE ROW IN MASS BALANCE CONSTRAINT *
C * FRE - COEFFICIENTS FOR FREE ENERGY EXPRESSION *
C * PRESS - PRESSURE (ATMOSPHERES) *
C * T - TEMPERATURE (DEGREES KELVIN) *
C * IOPT=0 OR 1 , 0=NO DATA CHECK, 1=DATA CHECK *
C *
C * ISPN -SPECIES DATA FILE REFERENCE NUMBER *
C * FOR THE PURPOSE OF EQ.CONV. CALCULATION ALWAYS *
C * READ H2S AS THE FIRST SPECIES. *
C *
C * COMPOUND SPN , COMPOUND SPN *
C * H2 1 CH4 11 *
C * N2 2 S1 12 *
C * O2 3 S2 13 *
C * CO 4 S3 14 *
C * CO2 5 S4 15 *
C * H2O 6 S5 16 *
C * H2S 7 S6 17 *
C * SO2 8 S7 18 *
C * COS 9 S8 19 *
C * CS2 10 *
C *****
C *
C * INTEGER P *
C * DIMENSION SNAM(30 ),FRE(30,8),X(30),GA(30,30),GB(30) *
C * 1,F(30),A(30,30),Y(30),B(30),FRC(30),NG1(30),XX(30) *
C * U,GX(30),XORIG(30),ISPN(30),C(30),L(30),A1(30,30) *
C *****
C *
C * LOGICAL UNIT 4 REFERS THIS PROGRAM TO THE *
C * INPUT DATA FILE. THE FILE NAME IS *
C * "INPUTDATA". IF THE USER HAS A COMPLETE *
C * NEW SET OF PARAMETERS , HE HAS TO FIRST *
C * EMPTY THE "INPUTDATA" FILE AND THEN INSERT *
C * HIS SET OF PARAMETERS: *

```

```

C*      -FIRST LINE M,N,P,NPT      *
C*      -SECOND LINE IOPT          *
C*      -FROM THE THIRD LINE ON ,SPECIES REF.NO.,INT.CON *
C*      AFTER THE PROGRAM HAS BEEN RUN FOR THE SET OF *
C*      PARAMETERS IN THE INPUT DATA ; THE PROGRAM *
C*      WILL ASK THE USER IF HE WISHES TO CHANGE OR *
C*      ADD ANY VALUES FOR THE PARAMETERS. *
C*****
      READ(4,1) M, N,P,NPT
      1 FORMAT(5I5)
      READ(4,50) IOPT
      50 FORMAT(I2)
      N2=N+P
C
C *****
C
      IEEE=0
500    IF(IEEE.EQ.0)GO TO 511
      WRITE(6,502)
502    FORMAT(/,' TO EXIT, PLEASE TYPE 0 - TYPE 1
      # TO CONTINUE')
      CALL FREAD(5,'I:',IAAA)
      IF(IAAA.EQ.0)GO TO 501
      WRITE(6,503)
503    FORMAT('TO ALTER NUMBERS, TYPE 1')
      CALL FREAD(5,'I:',IBBB)
      IF(IBBB.NE.1)GO TO 504
      WRITE(6,505)
505    FORMAT('TYPE NEW NUMBERS LINE')
      CALL FREAD(5,'4I:',M,N,P,NPT)
      N2=N+P
504    CONTINUE
      WRITE(6,506)
506    FORMAT(/,'TO ALTER SPECIES, TYPE 1')
      CALL FREAD(5,'I:',ICCC)
      IF(ICCC.NE.1)GO TO 507
      WRITE(6,508)
508    FORMAT(/,'TYPE 1 IF LINE IS TO BE ALTERED')
      N2=N+P
      DO 509 IJK=1,N2
      WRITE(6,510)IJK
510    FORMAT('LINE NUMBER:',I5)
      CALL FREAD(5,'I:',IDDD)
      IF(IDDD.NE.1)GO TO 509
      CALL FREAD(5,'I,R:',ISPN(IJK),XORIG(IJK))
509    CONTINUE
507    CONTINUE
511    CONTINUE
C
C *****
C
      DO 2 I=1,N2
      IF(IEEE.NE.0)GO TO 515

```

```

      READ(4,3)   ISPN(I),XORIG(I)
3  FORMAT( I4,F15.10)
515  CONTINUE
C   *****
C   * LOGICAL UNIT 7 REFERS THIS PROGRAM TO *
C   * THE DATA FILE.WHEN RUNNING THE PROGRAM *
C   * ONE HAS TO SPECIFY"R -LOAD# 7=DATA2 *
C   * 4=INPUTDATA" . *
C   *****
      X(I)=XORIG(I)
      LINE=(ISPN(I)*4-3)*1000
      READ(7'LINE,40) SNAM(I)
40  FORMAT(A4)
      READ(7,41) (A1(I,J) ,J=1,5)
41  FORMAT(10F6.3)
C
C
C
C
C   IF FREE ENERGY EQUATION HAS MORE THAN EIGHT CONSTANTS ,
C   THEN THE LINE 132 AND THE THERMODYNAMIC DATA FILES HAVE
C   TO BE CHANGED ACCORDINGLY.
C
C
      READ(7,42) (FRE(I,K) ,K=1,8)
2  CONTINUE
      CALL REWIND(7)
42  FORMAT(4E15.7)
      WRITE(6,49)
49  FORMAT(//)
      IF(IOPT.EQ.0) GO TO 51
      WRITE(6,48)
48  FORMAT(50X,'DATA CHECK')
      DO 102 I=1,N2
      WRITE(6,43) SNAM(I) , X(I)
43  FORMAT(/,30X,A4 , 11X,'INITIAL AMOUNT=',F15.7)
      WRITE(6,44)
44  FORMAT(/,40X,'SPECIES ROW IN MASS BALANCE CONSTRAINT')
      WRITE(6,45) (A1(I,J) ,J=1,5)
45  FORMAT(34X,'NO.H=',F5.3,2X,'NO.N=',F5.3,2X,'NO.O='
      #,F5.3,2X,'NO.S=',F5.3,2X,'NO.C=',F5.3)
      WRITE(6,46)
46  FORMAT(/,40X,'COEFFICIENTS FOR FREE ENERGY
      #EXPRESSION')
      WRITE(6,47) (FRE(I,K) , K=1,8)
47  FORMAT(30X,4E17.7)
102 CONTINUE
C   *****
C   *
C   *REMOVING SINGULARITIES IN THE *
C   *MASS BALANCE MATRIX DUE TO THE*
C   *USE OF GENERAL DATA . *
C   *
C   *****

```

```

51 CONTINUE
  AL=0.
  DO 1001 I=1,5
    L(I)=I.
    DO 1002 J=1,N2
      AL=AL+ABS(A1(J,I))
1002 CONTINUE
    IF(AL.EQ.0.0) L(I)=0
    AL=0.0
1001 CONTINUE
    K=1.
    DO 1007 I=1,5
      DO 1003 J=1,N2
        IF(L(I).EQ.0) GO TO 1007
        A(J,K)=A1(J,I)
1003 CONTINUE
      K=K+1
1007 CONTINUE
1006 WRITE(6,1008)
1008 FORMAT(//,50X,'MASS BALANCE CONSTRAINT MATRIX')
    DO 1004 I=1,N2
      1004 WRITE(6,1005) (A(I,J) ; J=1,M)
1005 FORMAT(40X,5F10.2)
    DO 101 II=1,N2
      101 XX(II)=X(II)
      WRITE(6,7)
7 FORMAT(1H1,40X,'FREE ENERGY MINIMIZATION'///30X,
1,'MOLECULAR SPECIES',10X,'INITIAL MOLE NUMBERS',
110X,'INITIAL ','MOLE FRACTION',/)
      CALL DISTR(X,Y,B,N2,M,A)
      CALL MOFR(Y,FRC,N,P)
      DO 8 I=1,N2
        8 WRITE(6,9) SNAM(I),Y(I),FRC(I)
        9 FORMAT(30X,A4,20X,E15.7,15X,E15.7,/)
        JBI=2
        DO 10 NC=1,NPT
          WRITE(6,11)NC
11 FORMAT(/,'PRESSURE AND TEMPERATURE VALUES #:',15)
          CALL FREAD(5,'2R:',PRESS,T)
          DO 12 I=1,N2
            NG1(I)=0

```

C
C
C
C
C
C
C
C
C
C

IF THE HEAT CAPACITY FUNCTION IS SUCH THAT F/RT IS NOT DESCRIBED BY:

$$F/RT = A1(1-LNT) - A2T/2 - A3T^{**2}/6 - A4T^{**3}/12 - A5T^{**4}/20 + A6/T - A7 - A8/T/T$$

THEN THE LINES 213-215 SHOULD BE CHANGED ACCORDINGLY.

$$FRT = FRE(I,1) * (1.-ALOG(T)) - FRE(I,2) * T/2. - FRE(I,3) * T^{**2}/6. - FRE(I,4) * T^{**3}/12. - FRE(I,5) * T^{**4}/20. + FRE(I,6)$$


```

2/T-FRE(I,7)-FRE(I,8)/(T**2)
C(I)=FRT+ALOG(PRESS)
IF(I-N)12,12,13
13 C(I)=FRT
12 CONTINUE
DO 35 JB=1,JB1
DO 14 ITER=1,300
CALL FREN (Y,C,F,YBAR,N,P,NG1)
MG=M+P+1
CALL GSET (A,Y,GA,GB,B,F,P,M,MG,N)
CALL GAUSS(GA,GB,MG,GX)
IF(P)15,15,16
16 DO 17 I=1,P
II=I+1
IC=N+I
17 X(IC)=GX(II)
15 CONTINUE
DO 18 I=1,N
IF(NG1(I)) 19,19,18
19 X(I)=-Y(I)*((C(I)+ALOG(Y(I)/YBAR))-GX(1))
DO 21 J=1,M
IG=P+J+1
21 X(I)=X(I)+GX(IG)*A(I,J)*Y(I)
18 CONTINUE
3 CALL NEZE (X,Y,N2,NG1)
QUIT=1
DO 22 I=1,N2
IF(NG1(I)) 23,23,22
23 TEST=(X(I)-Y(I))/X(I)
IF(ABS(TEST)-0.1E-03) 22,22,24
24 QUIT=-1
22 CONTINUE
IF(QUIT) 25,25,26
25 DO 27 I=1,N2
27 Y(I)=X(I)
14 CONTINUE
26 DO 32 I=1,N2
NG1(I)=0
IF(X(I)) 33,33,34
34 Y(I)=X(I)
GO TO 32
33 Y(I)=0.000001
32 CONTINUE
35 CONTINUE
WRITE(6,28)T,PRESS
28 FORMAT(1H1,28X'TEMPERATURE (DEG K)=' ,F7.1,5X,
1,'PRESSURE'(ATM)=' ,E15.5/)
WRITE(6,29) ITER
29 FORMAT (1H0,30X,'NUMBER OF ITERATION =' ,I5///30X,
U'MOLECULAR SPECY'
U,8X,'EQUILIBRIUM MOLE NUMBERS',8X,'MOLE FRATION'//)
CALL MOFR (X,FRC,N,P)
GFREE=0.0
DO 30 I=1,N2

```

```

      GFREE=GFREE+F(I)
30  WRITE(6,31)  SNAM(I),X(I),FRC(I)
31  FORMAT (32X,A4,17X,E15.7,15X,E15.7,/)
      WRITE(6,69)  GFREE
69  FORMAT(10X,'SYSTEM FREE ENERGY=',E15.9)
      CALL COND (X,XX)
      PS=0.0
      PSI=0.0
      FS=0.
      DO 66 IJI=1,N
      IF(ISPNI(IJI)-11) 66,66,67
67  PS=PS+X(IJI)
      PSI=PSI+(ISPNI(IJI)-11)*X(IJI)
      FS=FS+FRC(IJI)
66  CONTINUE
      IF(PS.EQ.0.0) GO TO 10
      V=PSI/PS
C    IF(PSI.GT.0.0) WRITE(6,68) V
68  FORMAT(28X,'AVE. # OF S ATOMS IN SV=',F6.3)
      VV=3./V
C    EK=FS**VV*(FRC(3))**2
C    EK=EK/FRC(1)/FRC(1)/FRC(2)
C    EK=EK*PRESS**((VV-1.))
C    WRITE(6,71) EK
71  FORMAT(/,10X,'KE=',E12.6)
      JBI=1
10  CONTINUE
      IEEE=1
      GO TO 500
501  CONTINUE
      STOP
      END

C *****
C *
C *          SUBROUTINE GSET
C *
C * THIS SUBROUTINE SETS UP THE MATRIX EQUATION WHICH
C * CORRESPONDS TO EQUATION 2.13 IN THE REVIEW OF THE
C * METHOD, MCGERGOR (1971) THESIS.
C * THIS MATRIX EQUATION IS SOLVED USING
C * SUBROUTINE GAUSS.
C *
C *****
C SUBROUTINE GSET (A,Y,GA,GB,B,F,P,M,MG,N)
      INTEGER P
      DIMENSION A(30,30),Y(30),GA(30,30),GB(30),B(30),F(30)
      #,R(30,30)
      DO 1 K=1,M
      DO 1 J=1,K
      R(J,K)=0.0
      DO 2 I=1,N
2  R(J,K)=R(J,K)+A(I,J)*A(I,K)*Y(I)
1  R(K,J)=R(J,K)
      DO 3 I=1,MG

```

```

      DO 3 J=1,MG
3    GA(I,J)=0.0
      DO 4 IG=1,M
      DO 5 I=1,N
5    GA(IG,1)=GA(IG,1)+A(I,IG)*Y(I)
      IF(P)6,6,7
7    DO 8 I=1,P
      JG=I+1
      JGG=IG+P+1
      IGG=I+M+1
      II=N+I
      GA(IG,JG)=A(II,IG)
8    GA(IGG,JGG)=GA(IG,JG)
6    CONTINUE
      DO 9 J=1,M
      JG=J+P+1
9    GA(IG,JG)=R(IG,J)
      JG=P+IG+1
      IGG=M+1
4    GA(IGG,JG)=GA(IG,1)
      DO 10 J=1,M
      GB(J)=B(J)
      DO 10 I=1,N
10   GB(J)=GB(J)+A(I,J)*F(I)
      JGB=M+1
      GB(JGB)=0.0
      DO 11 I=1,N
11   GB(JGB)=GB(JGB)+F(I)
      IF(P)12,12,13
13   DO 14 I=1,P
      JGB=M+I+1
      II=N+I
14   GB(JGB)=F(II)
12  CONTINUE
      RETURN
      END

```

```

C *****
C *
C *          SUBROUTINE GAUSS
C *
C * THE FUNCTION OF THIS SUBROUTINE IS TO SOLVE THE
C * SET OF EQUATIONS A*X=B USING GAUSSIAN ELIMINATION
C * AND BACK SUBSTITUTION ROTATING ABOUT THE ELEMENT
C * OF MAXIMUM MODULUS.
C *
C *****

```

```

      SUBROUTINE GAUSS (A,R,N,X)
      DIMENSION A(30,30),R(30),X(30)
      M=N-1
      DO 11 J=1,M
      S=0.
      DO 12 I=J,N
      U= ABS(A(I,J))
      IF(U-S) 12,12,112

```

```

112 S=U
    L=I
12  CONTINUE
    IF(L-J) 119,19,119
119 DO 14 I=J,N
    S=A(L,I)
    A(L,I)=A(J,I)
14  A(J,I)=S
    S=R(L)
    R(L)=R(J)
    R(J)=S
19  IF(ABS(A(J,J))-1.E-30) 115,115,15
115 WRITE(6,3)
    3 FORMAT(1H,'MATRIX SINGULAR')
    RETURN
15  MM=J+1
    DO 11 I=MM,N
    IF(ABS(A(I,J))-1.E-30) 11,111,111
111 S=A(J,J)/A(I,J)
    A(I,J)=0.0
    DO 16 K=MM,N
16  A(I,K)=A(J,K)-S*A(I,K)
    R(I)=R(J)-S*R(I)
11  CONTINUE
    DO 17 K=1,N
    I=N+1-K
    S=0.0
    IF(I-N) 117,17,117
117 MM=I+1
    DO 18 J=MM,N
18  S=S+A(I,J)*X(J)
17  X(I)=(R(I)-S)/A(I,I)
    RETURN
    END
C *****
C *
C *          SUBROUTINE NEZE
C *
C * THIS SUBROUTINE TESTS FOR NEGATIVE OR ZERO AMOUNTS *
C * OF MOLECULAR SPECIES AND TAKES THE CORRECTIVE *
C * ACTION AS INDICATED IN THE METHOD REVIEW. *
C *
C *****
C SUBROUTINE NEZE (X,Y,N2,NG1)
C DIMENSION X(30),Y(30),NG1(30)
C TEST=1.0
C DO 1 I=1,N2
C IF(NG1(I)) 2,2,1
C 2 IF(X(I)) 3,3,1
C 3 SLAM=-0.99*Y(I)/(X(I)-Y(I))
C IF(SLAM-TEST)4,4,1
C 4 TEST=SLAM
C 1 CONTINUE
C DO 5 I=1,N2

```

```

IF(NG1(I))7,7,5
7 X(I)=Y(I)+TEST*(X(I)-Y(I))
  IF(X(I)-0.10E-10)6,6,5
6 X(I)=0.0
  NG1(I)=1
5 CONTINUE
  RETURN
  END
*****
*
*               SUBROUTINE FREN
*
* THIS SUBROUTINE CALCULATES THE FREE ENERGY
* CONTRIBUTION OF EACH SPECIE TO THE SYSTEM.
*
*****
SUBROUTINE FREN (Y,C,F,YBAR,N,P,NG1)
  INTEGER P
  DIMENSION Y(30),C(30),F(30),NG1(30)
  YBAR=0.0
  DO 1 I=1,N
1 YBAR=YBAR+Y(I)
  DO 2 I=1,N
    IF(NG1(I))3,3,4
3 F(I)=Y(I)*(C(I)+ALOG(Y(I)/YBAR))
    GO TO 2
2 F(I)=0.0
  CONTINUE
  IF(P)10,10,6
6 DO 7 I=1,P
  II=N+I
  IF(NG1(II))8,8,9
8 F(II)=Y(II)*C(II)
  GO TO 7
7 F(II)=0.0
  CONTINUE
10 CONTINUE
  RETURN
  END
*****
*
*               SUBROUTINE DISTR
*
* THIS SUBROUTINE IS USED TO GENERATE A POSITIVE SET
* OF MOLE NUMBERS FOR ALL SPECIES IN THE SYSTEM.
*
*****
SUBROUTINE DISTR(X,Y,B,N2,M,A)
  DIMENSION X(30),Y(30),B(30),A(30,30)
  DO 1 I=1,N2
    IF(X(I))2,2,1
2 X(I)=0.0000001
1 Y(I)=X(I)
  DO 3 J=1,M

```

```

      B(J)=0.0
      DO 3 I=1,N2
3     B(J)=B(J)+A(I,J)*Y(I)
      RETURN
      END

```

```

C *****
C *
C *               SUBROUTINE MOFR
C *
C * THIS PROGRAM CALCULATES THE MOLE FRACTION OF EACH
C * SPECIE IN THE MIXTURE
C *
C *****
      SUBROUTINE MOFR (Y,FRC,N,P)
      INTEGER P
      DIMENSION Y(30),FRC(30)
      DEN=0.0
      DO 1 I=1,N
1     DEN=DEN+Y(I)
      DO 2 I=1,N
2     FRC(I)=Y(I)/DEN
      IF(P) 7,7,8
8     DEN=0.0
      DO 3 I=1,P
      II=N+I
3     DEN=DEN+Y(II)
      DO 4 I=1,P
      II=N+I
4     FRC(II)=Y(II)/DEN
7     CONTINUE
      RETURN
      END

```

```

C *****
C *
C *               SUBROUTINE COND
C *
C * THIS PROGRAM CALCULATES THE PERCENTAGE OF
C * EQUILIBRIUM CONVERSION
C *
C *****
      SUBROUTINE COND(X,XX)
      DIMENSION X(30),XX(30)
      CONV=(XX(1)-X(1))/XX(1)
      WRITE(6,1) CONV
1     FORMAT(28X,'EQUILIBRIUM CONVERSION OF A (PCT)='',F6.3
      #,/)
      RETURN
      END

```

```

C *****
C *
C *                               MAINLINE CONDENSATION
C *
C * THIS PROGRAM CALCULATES EQUILIBRIUM COMPOSITIONS
C * FOR COMPLEX REACTION SYSTEMS USING THE FREE-ENERGY
C * MINIMIZATION METHOD DEVELOPED BY WHITE AND
C * COWORKERS. IT WILL HANDLE UP TO THIRTY DIFFERENT
C * MOLECULAR SPECIES CONTAINING TEN DIFFERENT
C * ELEMENTS. ANY NUMBER OF CASES CAN BE ATTEMPTED WITH
C * AS MANY TEMPERATURES AND PRESSURES DESIRED.
C * THE PROGRAM CHECKS THE PARTIAL PRESSURE OF THE
C * SULFUR SPECIES AND IF IT EXCEEDS THE VAPOUR
C * PRESSURE, THE PROGRAM MODIFIES THE MASS OF THE
C * SULFUR IN THE GASPHASE. IT THEN RECALCULATES
C * THE NEW EQUILIBRIA. THE PROCEDURE IS CONTINUED
C * UNTIL THE ERROR CRITERIA BETWEEN PARTIAL AND
C * VAPOR PRESSURE OF SULFUR IS MET.
C *
C * INPUT DATA
C *   M      - NUMBER OF DIFFERENT ELEMENTS, H,C,O,S,N
C *   N      - NUMBER OF GASEOUS SPECIES
C *   NS     - NUMBER OF SULFUR SPECIES
C *   P      - NUMBER OF CONDENSED SPECIE
C *   NPT    - NUMBER OF TEMP. AND PRESS. CONDITIONS
C *   SNAM   - THE NAMES OF THE SPECIES
C *   X      - THE AMOUNT OF THIS SPECIE PRESENT IN
C *             THE STARTING CHEMICAL SYSTEM (EITHER
C *             NUMBER OF MOLES OR MOLE FRACTION)
C *   A      - SPECIE ROW IN MASS BALANCE CONSTRAINT
C *   FRE    - COEFFICIENTS FOR FREE ENERGY EXPRESSION
C *   PRESS  - PRESSURE (ATMOSPHERES)
C *   T      - TEMPERATURE (DEGREES KELVIN)
C *   IOPT=0 OR 1 , 0=NO DATA CHECK, 1=DATA CHECK
C *
C *   ISPN -SPECIES DATA FILE REFERENCE NUMBER
C * FOR THE PURPOSE OF EQ.CONV. CALCULATION ALWAYS
C * READ H2S AS THE FIRST SPECIE.
C * READ THE SPECIES IN THE ORDER OF H2S,SO2,SULFUR
C * SPECIES, AND THEN THE REST OF THE SPECIES.
C * COMPOUND      SPN      ,      COMPOUND      SPN
C * H2             1          CH4             11
C * N2             2          S1              12
C * O2             3          S2              13
C * CO             4          S3              14
C * CO2            5          S4              15
C * H2O            6          S5              16
C * H2S            7          S6              17
C * SO2            8          S7              18
C * COS            9          S8              19
C * CS2           10
C *****
C   INTEGER P
C   COMMON /VAPOR/ BETA,BETA1,TSINPT

```

```

COMMON /NSUL/ NS
DIMENSION SNAM(30),FRE(30,8),X(30),GA(30,30),GB(30)
1,F(30),A(30,30),Y(30),B(30),FRC(30),NG1(30),XX(30)
U,GX(30),XORIG(30),ISPN(30),C(30),L(30),A1(30,30)

C
C*****
C      LOGICAL UNIT 4 REFERS THIS PRIGRAM TO THE      *
C*      INPUT DATA FILE. THE FILE NAME IS            *
C*      "INPUTDATA". IF THE USER HAS A COMPLETE      *
C*      NEW SET OF PARAMETERS , HE HAS TO FIRST      *
C*      EMPTY THE " INPUTDATA" FILE AND THEN INSERT  *
C*      HIS SET OF PARAMETERS:                        *
C*      -FIRST LINE M,N,P,NPT                        *
C*      -SECOND LINE IOPT                            *
C*      -FROM THE THIRD LINE ON ,SPECIES REF.NO.,INT.CON *
C*      AFTER THE PROGRAM HAS BEEN RUN FOR THE SET OF *
C*      PARAMETERS IN THE INPUT DATA ; THE PROGRAM   *
C*      WILL ASK THE USER IF HE WISHES TO CHANGE OR  *
C*      ADD ANY VALUES FOR THE PARAMETERS..         *
C*****
      READ(5,1) NS
      READ(4,1) M, N,P,NPT
      1 FORMAT(5I5)
      READ(4,50) IOPT
      50 FORMAT(I2)
      N2=N+P

C
C *****
C
C      IEEE=0
500   IF(IEEE.EQ.0)GO TO 511
      WRITE(6,502)
502   FORMAT(/,' TO EXIT, PLEASE TYPE 0 - TYPE 1
      #   TO CONTINUE')
      CALL FREAD(5,'I:',IAAA)
      IF(IAAA.EQ.0)GO TO 501
      WRITE(6,503)
503   FORMAT('TO ALTER NUMBERS, TYPE 1')
      CALL FREAD(5,'I:',IBBB)
      IF(IBBB.NE.1)GO TO 504
      WRITE(6,505)
505   FORMAT('TYPE NEW NUMBERS LINE')
      CALL FREAD(5,'4I:',M,N,P,NPT)
      N2=N+P
504   CONTINUE
      WRITE(6,506)
506   FORMAT(/,'TO ALTER SPECIES, TYPE 1')
      CALL FREAD(5,'I:',ICCC)
      IF(ICCC.NE.1)GO TO 507
      WRITE(6,508)
508   FORMAT(/,'TYPE 1 IF LINE IS TO BE ALTERED')
      N2=N+P
      DO 509 IJK=1,N2
      WRITE(6,510)IJK

```



```

510     FORMAT('LINE NUMBER:',I5)
      CALL FREAD(5,'I:',IDDD)
      IF(IDDD.NE.1)GO TO 509
      CALL FREAD(5,'I,R:',ISPN(IJK),XORIG(IJK))
509     CONTINUE
507     CONTINUE
511     CONTINUE
C
C *****
C

      DO 2 I=1,N2
        IF(IEEE.NE.0)GO TO 515
        READ(4,3) ISPN(I),XORIG(I)
3     FORMAT( I4,F15.10)
515     CONTINUE
C     *****
C     * LOGICAL UNIT 7 REFERS THIS PROGRAM TO *
C     * THE DATA FILE.WHEN RUNNING THE PROGRAM *
C     * ONE HAS TO SPECIFY"R -LOAD# 7=DATA1 *
C     * (OR DATA2)" 4=DATA INPUT" *
C     *****
      X(I)=XORIG(I)
      LINE=(ISPN(I)*4-3)*1000
      READ(7'LINE,40) SNAM(I)
40     FORMAT(A4)
      READ(7,41) (A1(I,J) ,J=1,5)
41     FORMAT(10F6.3)
C
C
C
C
C
C
C
C
      IF FREE ENERGY EQUATION HAS MORE THAN EIGHT CONSTANTS ,
      THEN THE LINE 62 AND THE THERMODYNAMIC DATA FILES HAVE
      TO BE CHANGED ACCORDINGLY.
C
C
C
      READ(7,42) (FRE(I,K) ,K=1,8)
2     CONTINUE
      CALL REWIND(7)
42     FORMAT(4E15.7)
      WRITE(6,49)
49     FORMAT(//)
      IF(IOPT.EQ.0) GO TO 51
      WRITE(6,48)
48     FORMAT(50X,'DATA CHECK')
      DO 102 I=1,N2
        WRITE(6,43) SNAM(I) , X(I)
43     FORMAT(/,30X,A4 , 11X,'INITIAL AMOUNT=',F15.7)
        WRITE(6,44)
44     FORMAT(/,40X,'SPECIE ROW IN MASS BALANCE CONSTRAINT')
        WRITE(6,45) (A1(I,J) ,J=1,5)
45     FORMAT(34X,'NO.H=',F5.3,2X,'NO.N=',F5.3,2X,'NO.O='
      ,F5.3,2X,'NO.S=',F5.3,2X,'NO.C=',F5.3)

```

```

      WRITE(6,46)
46  FORMAT(/,40X,'COEFFICIENTS FOR FREE ENERGY
      #EXPRESSION')
      WRITE(6,47) (FRE(I,K) , 'K=1,8)
47  FORMAT(30X,4E17.7)
102  CONTINUE
C    *****
C    *
C    *REMOVING SINGULARITIES IN THE *
C    *MASS BALANCE MATRIX DUE TO THE*
C    *USE OF GENERAL DATA .        *
C    *
C    *****
51  CONTINUE
      AL=0.
      DO 1001 I=1,5
        L(I)=I
        DO 1002 J=1,N2
          AL=AL+ABS(A1(J,I))
1002  CONTINUE
          IF(AL.EQ.0.0) L(I)=0
          AL=0.0
1001  CONTINUE
          K=1
          DO 1007 I=1,5
            DO 1003 J=1,N2
              IF(L(I).EQ.0) GO TO 1007
              A(J,K)=A1(J,I)
1003  CONTINUE
              K=K+1
1007  CONTINUE
1006  WRITE(6,1008)
1008  FORMAT(/,50X,'MASS BALANCE CONSTRAINT MATRIX')
      DO 1004 I=1,N2
1004  WRITE(6,1005) (A(I,J) , J=1,M)
1005  FORMAT(40X,5F10.2)
      DO 101 II=1,N2
101  XX(II)=X(II)
      WRITE(6,7)
7  FORMAT(1H1,40X,'FREE ENERGY MINIMIZATION'///30X,
1  'MOLECULAR SPECY',10X,'INITIAL MOLE NUMBERS',10X,
1  'INITIAL ', 'MOLE FRACTION',//)
      CALL DISTR(X,Y,B,N2,M,A)
C    TOTAL AMOUNT OF SULFUR TO THE SYSTEM IS B4
C
      TSINPT=B(4)
      CALL MOFR(Y,FRC,N,P)
      DO 8 I=1,N2
8  WRITE(6,9) SNAM(I),Y(I),FRC(I)
9  FORMAT(30X,A4,20X,E15.7,15X,E15.7,/)
      JBI=2
      DO 10 NC=1,NPT
        WRITE(6,11)NC
11  FORMAT(/,'PRESSURE AND TEMPERATURE VALUES #:',15)

```

```

      CALL FREAD(5,'2R:',PRESS,T)
C  EVALUTE THE VAPOR PRESSURE OF SULFUR
C
      PVLN=-1.61732+0.00542412*T+1439.83/T-2208580/T/T
      PV=EXP(PVLN)
      BETA=PV/(PRESS-PV)
C
      DO 12 I=1,N2
      NG1(I)=0
C
C
C
C
      IF THE HEAT CAPACITY FUNCTION IS SUCH THAT F/RT IS NOT
      DESCRIBED BY:
C
      F/RT=A1(1-LNT)-A2T/2-A3T**2/6-A4T**3/12
      -A5T**4/20+A6/T-A7-A8/T/T
C  THEN THE LINES 130-132 SHOULD BE CHANGED ACCORDINGLY:
C
      FRT=FRE(I,1)*(1.-ALOG(T))-FRE(I,2)*T/2.-FRE(I,3)*T
      1**2/6.-FRE(I,4)*T**3/12.-FRE(I,5)*T**4/20.+FRE(I,6)/T
      2-FRE(I,7)-FRE(I,8)/(T**2)
      C(I)=FRT+ALOG(PRESS)
      IF(I-N)12,12,13
13  C(I)=FRT
12  CONTINUE
C
      ICALL=1
      DO 58 JCON=1,50
C  WRITE(6,305) JCON,PV,BETA
305  FORMAT(/,10X,'JCON',5X,I5,2E14.7)
C
      DO 35 JB=1,JB1
      DO 14 ITER=1,30
      CALL FREN (Y,C,F,YBAR,N,P,NG1)
      MG=M+P+1
      CALL GSET (A,Y,GA,GB,B,F,P,M,MG,N)
      CALL GAUSS(GA,GB,MG,GX)
      IF(P)15,15,16
16  DO 17 I=1,P
      II=I+1
      IC=N+I
17  X(IC)=GX(II)
15  CONTINUE
      DO 18 I=1,N
      IF(NG1(I)) 19,19,18
19  X(I)=-Y(I)*((C(I)+ALOG(Y(I)/YBAR))-GX(1))
      DO 21 J=1,M
      IG=P+J+1
21  X(I)=X(I)+GX(IG)*A(I,J)*Y(I)
18  CONTINUE
      CALL NEZE (X,Y,N2,NG1)
      QUIT=1.

```

```

DO 22 I=1,N2
  IF(NG1(I)) 23,23,22
23 TEST=(X(I)-Y(I))/X(I)
  IF(ABS(TEST)-0.1E-06) 22,22,24
24 QUIT=-1.
22 CONTINUE
  IF(QUIT) 25,25,26
25 DO 27 I=1,N2
27 Y(I)=X(I)
14 CONTINUE
26 DO 32 I=1,N2
  NG1(I)=0
  IF(X(I)) 33,33,34
34 Y(I)=X(I)
  GO TO 32
33 Y(I)=0.0000001
32 CONTINUE
35 CONTINUE
  IF(JCON.GT.1) GO TO 63
  WRITE(6,64) ITER,(X(I),I=1,4)
64 FORMAT(/,5X,'WITHOUT CONSIDERING CONDENSATION THE
  #ANSWER IS ',/,10X,I5,10E15.6)
C
C : CHECK FOR THE CONDENSATION OF SULFUR
C
63 XBAR=GX(1)*YBAR
  CALL CHECKL(A,X,Y,N,M,ICALL,IFLAG,SL1,SL,XBAR,NG1)
  GO TO (300,301,302,303), IFLAG
300 WRITE(6,54)
54 FORMAT(/,5X,'THE VAPOR IS WITHIN THE DEW POINT
  # RANGE')
  GO TO 59
301 WRITE(6,55)
55 FORMAT(/,5X,'THERE IS NO POSSIBILITY OF CONDENSATION'
  #,'SULFUR < PV')
  GO TO 59
302 CONTINUE
  B(4)=TSINPT-SL
  C WRITE(6,306) SL1,SL,B(4)
306 FORMAT(/,'AFTER CHECK SL1,SL,B4',5X,3E14.7)
  GO TO 60
303 WRITE(6,56) SL
56 FORMAT(/,5X,'CONDENSATION OF SULFUR : ',5X,
  #'AMOUNT OF LIQUID FORMED=',E12.6)
  GO TO 59
60 CONTINUE
58 CONTINUE
  WRITE(6,61)
61 FORMAT(/,5X,'NO CONVERGENCE ON LIQUID SULFUR IN
  # 20 ITER')
  GO TO 62
59 WRITE(6,28)T,PRESS,PV,BETA
28 FORMAT(1H1,28X,'TEMPERATURE (DEG K)=',F7.1,5X,
  #'PRESSURE (ATM)=',E15.5,/,28X,'PV (ATM) =',

```

```

1E15.7,2X,'BETA =',E15.7,/)
WRITE(6,29) ITER
29 FORMAT (1H0,30X,'NUMBER OF ITERATION =',15///30X,
U'MOLECULAR SPECY'
U,8X,'EQUILIBRIUM MOLE NUMBERS',8X,'MOLE FRATION'//)
CALL MOFR (X,FRC,N,P)
GFREE=0.0
DO 30 I=1,N2
GFREE=GFREE+F(I)
30 WRITE(6,31) SNAM(I),X(I),FRC(I)
31 FORMAT (32X,A4,17X,E15.7,15X,E15.7,/)
WRITE(6,69) GFREE
69 FORMAT(10X,'SYSTEM FREE ENERGY=',E15.9)
CALL COND (X,XX)
PS=0.0
PSI=0.0
FS=0.
DO 66 IJI=1,N
IF(ISPNI(IJI)-11) 66,66,67
67 PS=PS+X(IJI)
PSI=PSI+(ISPNI(IJI)-11)*X(IJI)
FS=FS+FRC(IJI)
66 CONTINUE
IF(PS.EQ.0.0) GO TO 10
V=PSI/PS
C IF(PSI.GT.0.0) WRITE(6,68) V
68 FORMAT(28X,'AVE. # OF S ATOMS IN SV=',F6.3)
VV=3./V
JBI=1
10 CONTINUE
IEEE=1
GO TO 500
501 CONTINUE
62 STOP
END

```

```

C*****

```

```

C

```

```

C* SUBROUTINE CHECKL

```

```

C*

```

```

C* THIS SUBROUTINE FIRST CHECKS THE PARTIAL

```

```

C* PRESSURE OF SULFUR; IF IT EXCEEDS THE

```

```

C* VAPOR PRESSURE, THEN IT MODIFIES THE

```

```

C* VAPOR COMPOSITION AND AMOUNT OF LIQUID

```

```

C* SULFUR FOR THE NEXT ROUND OF ITERATIONS.

```

```

C*

```

```

C*****

```

```

C

```

```

SUBROUTINE CHECKL(A,X,Y,N,M,ICALL,IFLAG,SL1,SL,XBAR
#,NG1)

```

```

COMMON /VAPOR/ BETA,BETA1,TSINPT

```

```

COMMON /NSUL/ NS

```

```

DIMENSION X(30),NG1(30),Y(3),A(30,30),RATIO(10)

```

```

C

```

```

C

```

```

C ICALL=1 : FIRST CALL TO THE SUBROUTINE
C ICALL=2 : SUBSEQUENT CALLS
C
      J=2+NS
      GO TO (1,2), ICALL
1      SL1=0.0
2      S1=0.0
      DO 3 I=3,J
3      S1=S1+X(I)
      S2=XBAR-S1
C      WRITE(6,21) XBAR,S2
21     FORMAT(/,'CHECK XBAR',2E14.7)
      BETA2=S1/S2
C      WRITE(6,22) BETA,BETA2
22     FORMAT(/,'BETA',5X,2E14.7)
      TEST=(BETA2-BETA)/BETA
      GO TO (4,5),ICALL
4      IF(ABS(TEST).LE.0.005) IFLAG=1
      IF(TEST.LT.(-0.005)) IFLAG=2
      IF(TEST.GT.0.005) GO TO 6
C
C : IFLAG=1; DEW POINT, IFLAG=2; NO CONDENSATION.
C
      RETURN
5      IF(ABS(TEST)-0.005) 13,12,6
C
C : MODIFY THE VAPOR COMPOSITION
6      IFLAG=3
      SRATIO=0.0
      DO 7 I=3,J
      II=I-2
      RATIO(II)=X(I)/X(J)
7      SRATIO=SRATIO+RATIO(II)
      S8MOD=BETA*S2/SRATIO
      DO 8 I=3,J
      II=I-2
8      X(I)=S8MOD*RATIO(II)
      DO 9 I=1,N
      IF(X(I)) 20,20,9
20     NG1(I)=1
9      Y(I)=X(I)
      GO TO (10,12),ICALL
10     SUM=0.0
      DO 11 I=1,N
C      WRITE(6,26) X(I),A(I,4)
11     SUM=SUM+A(I,4)*X(I)
26     FORMAT(/,'CHECK X AND A(I,4)',2E14.7)
      BETA1=BETA2
C : THE FIRST ESTIMATE OF LIQUID FORMED
      SL=TSINPT-SUM
      ICALL=2
      RETURN
12     SLOPE=(SL-SL1)/(BETA2-BETA1)
      RINT=SL-SLOPE*BETA2

```

```

C : HERE THE NEXT ESTIMATE OF LIQUID SULFUR IS
C : FOUND BY INTERPOLATION BETWEEN THE LAST TWO
C : PREVIOUS ONES.
      SL1=SL
      BETA1=BETA2
      SL=SLOPE*BETA+RINT
      IF(SL-TSINPT) 15,16,16
16    SL=0.999999*TSINPT
15    RETURN
13    IFLAG=4
C : IFLAG=4; CONDENSATION AND CONVERGED SOLUTION WITHIN
C : 10 ITER.
      RETURN
      END

C *
C *          SUBROUTINE GSET
C * THIS SUBROUTINE IS LISTED IN "GEN".
C *
C *
C *          SUBROUTINE GAUSS
C * THIS SUBROUTINE IS LISTED IN "GEN".
C *
C *
C *          SUBROUTINE NEZ
C * THIS SUBROUTINE IS LISTED IN "GEN".
C *
C *
C *          SUBROUTINE FREE
C * THIS SUBROUTINE IS LISTED IN "GEN".
C *
C *
C *          SUBROUTINE DISTR
C * THIS SUBROUTINE IS LISTED IN "GEN".
C *
C *
C *          SUBROUTINE MOFR
C * THIS SUBROUTINE IS LISTED IN "GEN".
C *
C *
C *          SUBROUTINE COND
C * THIS SUBROUTINE IS LISTED IN "GEN".
C *

```

```

C*****
C*
C*          SCONLB
C*  THIS PROGRAM EVALUTES EQUILIBRIUM COMPOSITION OF
C*  MIXTURE OF N2,H2O,SO2,H2S,S1-S8 GIVEN TEMP &
C*  PRESSURE. IT ALSO EVALUTES THE POSSIBLE
C*  CONDENSATION OF SULFUR.
C*  HERE, FREE ENERGY IS MINIMIZED UNDER THE
C*  CONSTRAINT OF SULFUR PARTIAL PRESSURE BEING EQUAL
C*  TO VAPOR PRESSURE, USING LANDA*BETA AS ONE OF
C*  THE LAGRANGE MULTIPLIERS.
C*
C*****
      IMPLICIT REAL*8(A-H,O-Z)
      INTEGER P
      DIMENSION XINT(12),SNAM(12),A(12,4),FRE(12,8),X(12)
      #GB(12),FRC(12),F(12),Y(12),B(12),NG1(12),XX(12),GX(12)
      #,C(12),GA(5,5),ISPN(12)
      DO 1 I=1,4
      DO 1 J=1,12
1    A(J,I)=0
      A(1,1)=2
      A(2,2)=2
      A(2,3)=1
      A(3,3)=2
      A(3,4)=1
      A(4,2)=2
      A(4,4)=1
      DO 2 I=5,12
2    A(I,4)=I-4
      ISPN(1)=2
      ISPN(2)=6
      ISPN(3)=8
      ISPN(4)=7
      DO 5 I=5,12
      ISPN(I)=7+I
5    CONTINUE
      DO 6 I=1,12
      LINE=(ISPN(I)*4-1)*1000
      READ(7'LINE,42) (FRE(I,K),K=1,8)
6    CONTINUE
42   FORMAT(4D15.7)
C****READ THE INITIAL MOLE FRACTION IN THE SEQUENCE OF*****
C****  N2,H2O,SO2,H2S,S1-S8 *****
C
      READ(5,3) (XINT(I) ,I=1,12)
3    FORMAT(12F8.5)
      READ(5,4) PRESS,T
4    FORMAT(2F8.3)
      M=4
      N=12
      P=0
      PVLN=-1.61732+0.00542412*T+1439.83/T-2208580/T/T

```



```

VP=DEXP(PVLN)
WRITE(6,10) VP
10  FORMAT(10X,'VP=',F12.6,4X,'ATM')
DO 99 I=1,12
99  X(I)=XINT(I)
CALL EQCOM(T,X,PRESS,P,N,M,XINT,A,FRE,VP)
9   FORMAT(12F12.7)
IF (P.EQ.0) GO TO 7
CALL EQCOM(T,X,PRESS,P,N,M,XINT,A,FRE,VP)
7  STOP
END

C
C
SUBROUTINE EQCOM(T,X,PRESS,P,N,M,XINT,A,FRE,VP)
IMPLICIT REAL*8(A-H,O-Z)
INTEGER P
COMMON YH2S
DIMENSION XINT(12),SNAM(12),A(12,4),FRE(12,8),X(12),
#FRC(12),F(12),Y(12),B(12),NG1(12),X(12),GX(12),C(12)
#,GA(5,5),GB(12),RATIO(8),SCFAC(5)
DATA SNAM/'N2 ','H2O ','SO2 ','H2S ','S1 ','S2 ',
#'S3 ','S4 ','S5 ','S6 ','S7 ','S8 '/
IF(P.EQ.0) GO TO 101
C*****
C
C THE FOLLOWING 10 LINES DETERMINE THE INTIAL GUESS
C OF FEASIBLE SOLUTION .
C
C*****
BETA=VP/(PRESS-VP)
SRATIO=0.0D00
DO 70 I=1,8
II=I+4
RATIO(I)=X(II)/X(12)
SRATIO=SRATIO+RATIO(I)
70 CONTINUE
S8NEW=BETA*(X(1)+X(2)+X(3)+X(4))
S8NEW=S8NEW/SRATIO
DO 71 I=1,8
II=I+4
X(II)=RATIO(I)*S8NEW
71 CONTINUE
HL=0.0D00
DO 72 J=1,N
HL=HL+A(I,4)*X(I)
72 CONTINUE
HL =B(4)-HL
DO 42 I=1,12
42 Y(I)=X(I)
4  FORMAT(12E12.5)
WRITE(6,1007)
1007 FORMAT(/,15X,'INITIAL FEASIBLE MOLES',/)
WRITE(6,1008) (SNAM(I),X(I) , I=1,6)
WRITE(6,1008) (SNAM(I),X(I) , I=7,12)

```

```

1008  FORMAT(5X,6(A4,E14.6,',',',',2X))
      WRITE(6,43) HL
43    FORMAT(//,15X,'INITIAL FEASIBLE MOLE OF S CONDENSED'
      #,E14.6)
      IF(Y(5).LE.0.0D00) NG1(5)=1
      CALL FREN(Y,C,F,YBAR,N,P,NG1)
      GF=0.0D00
      DO 44 I=1,N
      GF=GF+F(I)
44    CONTINUE
      WRITE(6,2002) GF
101   IF(P-1) 1,2,2
      1  MM=M
      L=N
      GO TO 3
      2  MM=M-1
      L=4
      GO TO 11
3     CALL DISTR(X,Y,B,N,M,A)
5     FORMAT(4F10.5)
      CALL MOFR(Y,FRC,N)
      JBI=2
      DO 12 I=1,N
      FRT=FRE(I,1)*(1-DLOG(T))-FRE(I,2)*T/2.-FRE(I,3)*T
1**2/6.-FRE(I,4)*T**3/12.-FRE(I,5)*T**4/20.+FRE(I,6)/T
2-FRE(I,7)-FRE(I,8)/(T**2)
      C(I)=FRT+DLOG(PRESS)
12  CONTINUE
11   DO 17 I=1,N
17  NG1(I)=0
      IF(P.EQ.1) NG1(5)=1
993  FORMAT(12E12.4)
      DO 35 JB=1,JBI
      DO 14 ITER=1,300
      CALL FREN(Y,C,F,YBAR,N,P,NG1)
      MG=M+1
      CALL GSET(A,Y,A,GB,B,F,MM,M,MG,N,VP,P,PRESS)
      CALL SCALES(GA,MG,MG,SCFAC)
      DO 719 IS=1,MG
719  GB(IS)=GB(IS)*SCFAC(IS)
      CALL GAUSS(GA,GB,MG,GX)
991  FORMAT(F10.5)
      BETA=0.0
      IF(P.EQ.1) BETA=VP/(PRESS-VP)
900  DO 18 I=1,L
      IF(NG1(I)) 19,19,18
19   IF(P-1) 13,15,15
13   X(I)=-Y(I)*(C(I)+DLOG(Y(I)/YBAR)-GX(1))
      GO TO 16
15  X(I)=-Y(I)*((C(I)+DLOG(Y(I)/YBAR))-GX(1)+GX(5))
16  DO 21 J=1,MM
      IG=J+1
21  X(I)=X(I)+GX(IG)*A(I,J)*Y(I)
18  CONTINUE

```

```

      IF(P.EQ.0) GO TO 39
      DO 30 I=5,12
      IF(NG1(I)) 48,48,30
48    X(I)=Y(I)*(GX(5)/BETA+GX(1)-C(I)-DLOG(Y(I)/YBAR))
30    CONTINUE
108   HL1=0.0
      DO 997 I=1,N
997   HL1=HL1+A(I,4)*X(I)
      HL1=B(4)-HL1
992   FORMAT(12E10.3)
39    CALL NEZE (X,Y,N,NG1,P,VP,PRESS,HL1,HL)
      IF(P.EQ.0) GO TO 107
107   QUIT=1.
      DO 22 I=1,N
      IF(NG1(I)) 23,23,22
23    TEST=(X(I)-Y(I))/X(I)
      IF(DABS(TEST)-0.1D-06) 22,22,24
24    QUIT=-1.
22    CONTINUE
      IF(QUIT) 25,25,26
25    DO 27 I=1,N
27    Y(I)=X(I)
      IF(P.EQ.0) GO TO 14
      HL=0.0
      DO 998 I=1,N
998   HL=HL+A(I,4)*Y(I)
      HL=B(4)-HL
14    CONTINUE
26    IF(P.EQ.1) GO TO 37
      DO 32 I=1,N
      NG1(I)=0
      IF(X(I)) 33,33,34
34    Y(I)=X(I)
      GO TO 32
33    Y(I)=0.0000001
32    CONTINUE
35    CONTINUE
37    CALL MOFR(X,FRC,N)
      WRITE(6,141) ITER
      JBI=1
      GF=0.0
      DO 2001 I=1,N
2001  GF=GF+F(I)
      WRITE(6,2002) GF
2002  FORMAT(5X,'GIBBS FREE ENERGY=',E15.6)
      IF(P.EQ.1) GO TO 50
      SUM=0.
      DO 2000 I=5,12
2000  SUM=SUM+FRC(I)
      PS=PRESS*SUM
      IF(PS.LT.VP) GO TO 40
      P=1
      RETURN
50    WRITE(6,100)

```

```

100 FORMAT(//,10X,'CONDENSATION OF SULFUR SPECIES HAS
    #OCCURED')
    GO TO 45
40  WRITE(6,200)
200 FORMAT(/,10X,'CONDENSATION OF SULFUR HAS NOT OCCURED')
45  WRITE(6,300) PRESS, T
300 FORMAT(/,10X,'PRESS(ATM)=' ,F8.5,10X,'TEMP(K)=' ,F10.5)
    WRITE(6,400)
400 FORMAT(/,10X,'SPECIE' ,10X,'EQ.MOLE' ,10X,'EQ.MOLE '
    #,'FRACTION')
    DO 500 I=1,N
500  WRITE(6,600) SNAM(I),X(I),FRC(I)
600  FORMAT(10X,A4,9X,E14.7,5X,E14.7)
    IF (P.EQ.0) GO TO 1000
    B1=0
    DO 700 I=1,N
700  B1=B1+A(I,M)*X(I)
    SLIQ=B(M)-B1
    WRITE(6,800) SLIQ
800  FORMAT(//,10X,'MOLES OF SULFUR LIQUID FORMED PER '
    #,'MOLE OF INLET GAS=' ,3E12.5)
    SF=SLIQ/B(M)*100.
    WRITE(6,801) SF
801  FORMAT(/,10X,'PERCENTAGE OF INLET S CONVERTED TO'
    #,' LIQUID = ' ,E12.7,////)
1000 CONTINUE
    RETURN
    END

```

```

C
C
C *****
C *
C *          SUBROUTINE GSET
C *
C * THIS SUBROUTINE SETS UP THE MATRIX EQUATION WHICH
C * CORRESPONDS TO EQUATION 3.13 TO 3.15 IN THE REVIEW
C * OF THE METHOD ; CHAPTER 3.
C * THIS MATRIX EQUATION IS SOLVED USING
C * SUBROUTINE GAUSS.
C *
C *****
C SUBROUTINE GSET (A,Y,GA,GB,B,F,MM,M,MG,N,VP,P,PRESS)
  IMPLICIT REAL*8(A-H,O-Z)
  INTEGER P
  DIMENSION R(4,4),A(12,4),Y(12),GA(5,5),GB(5),B(5),
  #F(12),WKAREA(50),GAI(5,5),GII(5,5)
  IF(P.EQ.0) L=N
  IF(P.EQ.1) L=4
  DO 1 K=1,MM
  DO 1 J=1,K
  R(J,K)=0.0
  DO 2 I=1,L
2  R(J,K)=R(J,K)+A(I,J)*A(I,K)*Y(I)
1  R(K,J)=R(J,K)

```

```

      DO 3 I=1, MG
      DO 3 J=1, MG
3    GA(I, J)=0.0
      DO 4 IG=1, MM
      GA(IG, 1)=B(IG)
5    CONTINUE
6    CONTINUE
      DO 9 J=1, MM
      JG=J+1
9    GA(IG, JG)=R(IG, J)
      JG=IG+1
      IGG=M+1
4    GA(IGG, JG)=GA(IG, 1)
15   DO 10 J=1, MM
      GB(J)=B(J)
      DO 10 I=1, L
10   GB(J)=GB(J)+A(I, J)*F(I)
      JGB=M+1
      GB(JGB)=0.0
      DO 11 I=1, N
11   GB(JGB)=GB(JGB)+F(I)
      IF(P.EQ.0) GO TO 16
      BETA=VP/(PRESS-VP)
23   FORMAT(5E17.8)
      DO 19 I=1, MM
      GA(I, MG)=-GA(I, 1)
      II=I+1
19   GA(M, II)=GA(I, 1)
      GB(M)=0.0
      BB=0.0
      GAMA1=0.0
      GAMA2=0.0
      DO 20 I=5, 12
      GAMA1=GAMA1+Y(I)
20   GB(M)=GB(M)+F(I)
      DO 21 I=1, 4
      GAMA2=GAMA2+Y(I)
21   BB=BB+F(I)
      GA(M, MG)=-GAMA1/BETA/BETA-GAMA2
      GB(M)=-GB(M)/BETA+BB
16   RETURN
      END

```

```

C  *
C  *
C  *           SUBROUTINE GAUSS
C  * THIS SUBROUTINE IS LISTED IN "GEN".
C  *
C  * *****
C  *
C  *           SUBROUTINE NEZE
C  *
C  * THIS SUBROUTINE TESTS FOR NEGATIVE OR ZERO AMOUNTS
C  * OF MOLECULAR SPECIES .
C  *
C  * *****

```

```

SUBROUTINE NEZE (X,Y,N,NG1,P,VP,PRESS,HL1,HL)
IMPLICIT REAL*8(A-H,O-Z)
INTEGER P
COMMON YH2S
DIMENSION X(12),Y(12),NG1(12)
TEST=1.0
DO 1 I=1,N
  IF(NG1(I)) 2,2,1
2 IF(X(I)) 3,3,1
3 SLAM=-0.5*Y(I)/(X(I)-Y(I))
  IF(SLAM-TEST)4,4,1
4 TEST=SLAM
1 CONTINUE
  IF(P.EQ.0) GO TO 17
  IF(HL1.GT.0.0) GO TO 17
  SLAM=-0.5*HL/(HL1-HL)
  IF(SLAM-TEST)18,18,17
18 TEST=SLAM
  TEST=SLAM
17 DO 5 I=1,N
  IF(NG1(I))7,7,5
7 X(I)=Y(I)+TEST*(X(I)-Y(I))
  IF(X(I)-0.10E-10) 6,6,5
6 X(I)=0.0
  NG1(I)=1
5 CONTINUE
11 RETURN
END

C *****
C *
C *          SUBROUTINE FREN
C *
C * THIS SUBROUTINE CALCULATES THE FREE ENERGY
C * CONTRIBUTION OF EACH SPECIE TO THE SYSTEM.
C *
C *****
C SUBROUTINE FREN (Y,C,F,YBAR,N,P,NG1)
C IMPLICIT REAL*8(A-H,O-Z)
C INTEGER P
C DIMENSION Y(12),C(12),F(12),NG1(12)
C YBAR=0.0
C DO 1 I=1,N
C 1 YBAR=YBAR+Y(I)
C DO 2 I=1,N
C IF(NG1(I)) 3,3,4
C 3 F(I)=Y(I)*(C(I)+DLOG(Y(I)/YBAR))
C GO TO 2
C 4 F(I)=0.0
C 2 CONTINUE
C RETURN
C END

C *
C *          SUBROUTINE DISTR
C * THIS SUBROUTINE IS LISTED IN "GEN".

```

SUBROUTINE MOFR

* THIS PROGRAM CALCULATES THE MOLE FRACTION OF EACH
* SPECIE IN THE MIXTURE

```

SUBROUTINE MOFR (Y,FRC,N)
  IMPLICIT REAL*8(A-H,O-Z)
  INTEGER P
  DIMENSION Y(12),FRC(12)
  DEN=0.0
  DO 1 I=1,N
1  DEN=DEN+Y(I)
  DO 2 I=1,N
2  FRC(I)=Y(I)/DEN
  RETURN
END

```

* SUBROUTINE SCALE *

* SUBROUTINE SCALES (A,N,NDIM,SCFAC)
THIS SUBROUTINE SCALES THE VALUES IN AN N*N COEFFICIENT
MATRIX SO THAT THE LARGEST ELEMENT IN EACH ROW IS UNITY.
THE SCALED VALUES OF A ARE RETURNED IN THE A MATRIX AND
THE SCALE FACTOR FOR EACH ROW ARE RETURNED IN SCFAC
VECTOR. USE SCFAC TO SCALE THE ELEMENTS IN THE
B VECTOR (R.H.SIDES, BEFORE SOLVING THE SET OF
EQUATIONS AX=B.

A MATRIX OF COEFFICIENTS
N NUMBER OF EQUATIONS
NDIM FIRST DIMENSION OF A IN THE CALLING PROGRAM
SCFAC ARRAY TO HOLD THE SCALE FACTORS

```

  IMPLICIT REAL*8(A-H,O-Z,$)
  DIMENSION A(NDIM,NDIM),SCFAC(N)

```

FIND LARGEST VALUE IN EACH ROW. IF ANY ROW HAS ONLY
ZEROS, PRINT MESSAGE AND RETURN.

```

DO 20 I=1,N
  BIG=DABS(A(I,1))
  DO 10 J=2,N
    ANEXT=DABS(A(I,J))
    IF(ANEXT.GT.BIG) BIG=ANEXT
  CONTINUE
  IF (BIG.EQ.0) GO TO 99
  SCFAC(I)=1./BIG

```

```
20      CONTINUE
C / NOW SCALE THE A VALUES
      DO 40 I=1,N
      DO 50 J=1,N
      A(I,J)=A(I,J)*SCFAC(I)
50      CONTINUE
40      CONTINUE
      RETURN
C WE COME HERE WHEN ALL ELEMENTS IN ANY ROW ARE ZERO.
99      WRITE(6,200) I
200     FORMAT(//,21H ALL ELEMENTS IN ROW ,I3,9H ARE ZERO)
      RETURN
      END
```


Results of "CONDENSATION" program for calculation
of equilibrium in the presence of liquid sulfur

FREE ENERGY MINIMIZATION

MOLECULAR SPECY	INITIAL MOLE NUMBERS	INITIAL MOLE FRACTION
H2S	0.1000000E+00	0.1000000E+00
SO2	0.5000000E-01	0.5000000E-01
S1	0.9999997E-07	0.9999997E-07
S2	0.9999997E-07	0.9999997E-07
S3	0.9999997E-07	0.9999997E-07
S4	0.9999997E-07	0.9999997E-07
S5	0.9999997E-07	0.9999997E-07
S6	0.9999997E-07	0.9999997E-07
S7	0.9999997E-07	0.9999997E-07
S8	0.9999997E-07	0.9999997E-07
H2O	0.2000000E+00	0.2000000E+00
N2	0.6500000E+00	0.6500000E+00

PRESSURE AND TEMPERATURE VALUES # 1

CONDENSATION OF SULFUR : AMOUNT OF LIQUID FORMED=0.140074E+00

TEMPERATURE (DEG K) = 450.0 PRESSURE (ATM) = 0.10000E+01
 PV (ATM) = 0.1024647E-02 BETA = 0.1025698E-02

NUMBER OF ITERATION = 30

MOLECULAR SPECY	EQUILIBRIUM MOLE NUMBERS	MOLE FRACTION
H2S	0.1725014E-02	0.1812325E-02
SO2	0.8726758E-03	0.9168456E-03
S1	0.0	0.0
S2	0.1723365E-02	0.1810592E-06
S3	0.2589576E-07	0.2720646E-07
S4	0.2272924E-07	0.237967E-07
S5	0.5629088E-05	0.5914001E-05
S6	0.1886040E-03	0.1981501E-03
S7	0.9915489E-04	0.1041736E-03
S8	0.6846935E-03	0.7193487E-03
H2O	0.2982635E+00	0.3133600E+00
N2	0.6499814E+00	0.6828830E+00

SYSTEM FREE ENERGY = -420945587E+02
 EQUILIBRIUM CONVERSION OF A (PCT) = 0.983

*** THIS IS THE RESULTS OF "SCONLB" FOR THE CALCULATION OF THE LIQUID SULFUR *****
 VP= 0.001025 ATM

***** ITER ***** 14

***** FREE ENERGY OF THE SYSTEM WITHOUT THE CONSTRAINT OF VAPOR PRESSURE *****

GIBBS FREE ENERGY= -0.426360E+02

** EQ. COMPN. IGNORING CONDENSATION OF SULFUR

	N2	S1	S5	H2O	S2	S3	S6	S7	S8	H2S	S4	S8
	.650E+00	0.0	.398E-04	297E+00	128E-02	.843E-07	196E-02	152E-02	154E-01	256E-02	109E-06	

INITIAL FEASIBLE MOLES

	N2	S3	H2O	S4	S5	S6	S7	S8	H2S	S1	S2
	0.650000E+00	0.433789E-08	0.297438E+00	0.560740E-08	0.128100E-02	0.204511E-05	0.256199E-02	0.100915E-03	0.781337E-04	0.0	0.196021E-07

INITIAL FEASIBLE MOLE OF S CONDENSED 0.138641E+00

GIBBS FREE ENERGY= -0.420992E+02

***** ITER ***** 29

GIBBS FREE ENERGY= -0.422318E+02

CONDENSATION OF SULFUR SPECIES HAS OCCURRED

PRESS(ATM)= 1.00000 TEMP(K)= 450.00000

SPECIES	EQ. MOLE	EQ. MOLE FRACTION
N2	0.650000E+00	0.6527576E+00
H2O	0.2104898E+00	0.2113829E+00
S02	0.4475508E-01	0.4494495E-01
H2S	0.8951016E-01	0.8988991E-01
S1	0.0	0.0
S2	0.0	0.0
S3	0.0	0.0
S4	0.0	0.0
S5	0.0	0.0
S6	0.6950133E-07	0.6979619E-07
S7	0.2320810E-05	0.2330656E-05
S8	0.1017924E-02	0.1022242E-02

MOLES OF SULFUR LIQUID FORMED PER MOLE OF INLET GAS= 0.75783E-02

PERCENTAGE OF INLET S CONVERTED TO LIQUID = .5052089E+01

APPENDIX B: Gas Composition at a Given H_2S Conversion

Contents

1. Mathematical development of gas composition for a given H_2S conversion.
2. "S6" program: the program to calculate moles of S_8 and the total moles of the gas at a given level of H_2S conversion and temperature.
3. Results of "S6" program.

The analysis of section 3.4 led to the material balance equations (3.24) and (3.25), coupled with equilibrium relations (3.26) to (3.28). In this section these equations are reduced to two nonlinear algebraic equations whose solution would specify the amount of S_6 and total moles for specified level of H_2S conversion.

Substitution of equations (3.26) to (3.28) into (3.24) and (3.25) yields,

$$\begin{aligned} F_1(x(S_6), Nt) = & 1 - Nt - 0.5 Y_{H_2S} X + A Nt^{2/3} x(S_6)^{1/3} \\ & + x(S_6) + B Nt^{1/3} x(S_6)^{2/3} \\ & + C Nt^{-1/3} x(S_6)^{4/3} = 0 \end{aligned} \quad (B.1)$$

$$\begin{aligned} F_2(x(S_6), Nt) = & 3/2 Y_{H_2S} X - 2 A Nt^{2/3} x(S_6)^{1/3} \\ & - 4 B Nt^{1/3} x(S_6)^{2/3} - 6 x(S_6) \\ & - 8 C Nt^{-1/3} x(S_6)^{4/3} = 0 \end{aligned} \quad (B.2)$$

where,

$$A = (K_{62})^{1/3} (\Pi)^{-2/3} \quad (B.3)$$

$$B = (K_{64})^{2/3} (\Pi)^{-1/3} \quad (B.4)$$

$$C = (K_{68})^{4/3} (\Pi)^{1/3} \quad (B.5)$$

The two equations (B.1) and (B.2) are solved by the Newton-Raphson technique. This method requires the partial derivatives of the equations which are,

$$\begin{aligned} \partial F_1 / \partial x(S_6) = & 1/3 A Nt^{2/3} x(S_6)^{-2/3} + 1/3 B Nt^{1/3} x(S_6)^{-1/3} \\ & + 4/3 C Nt^{-1/3} x(S_6)^{1/3} \end{aligned} \quad (B.6)$$

$$\begin{aligned} \partial F_2 / \partial x(S_6) = & -2/3 A Nt^{2/3} x(S_6)^{-2/3} - 1/3 B Nt^{1/3} x(S_6)^{-1/3} \\ & - 6 - 32/3 C Nt^{-1/3} x(S_6)^{1/3} \end{aligned} \quad (B.7)$$

$$\begin{aligned} \partial F_1 / \partial Nt = & -1 + 2/3 A \{x(S_6)/Nt\}^{1/3} \\ & + 1/3 B \{x(S_6)/Nt\}^{2/3} - 1/3 C \{x(S_6)/Nt\}^{4/3} \end{aligned} \quad (B.8)$$

$$\begin{aligned} \partial F_2 / \partial Nt = & -4/3 A \{x(S_6)/Nt\}^{1/3} - 4/3 B \{x(S_6)/Nt\}^{2/3} \\ & + 8/3 C \{x(S_6)/Nt\}^{4/3} \end{aligned} \quad (B.9)$$

To solve equations (B.6) and (B.7), the equilibrium constants are evaluated from the Gibbs free energy change of reactions (3.20) to (3.23),

$$K = \text{Exp} (-\Delta G^\circ / (Rg T)) \quad (B.10)$$

$$K_{6,2} = \text{Exp} (-\Delta G_{6,2}^\circ / (Rg T)) \quad (B.11)$$

$$K_{6,4} = \text{Exp} (-\Delta G_{6,4}^\circ / (Rg T)) \quad (B.12)$$

$$K_{6,8} = \text{Exp} (-\Delta G_{6,8}^\circ / (Rf T)) \quad (B.13)$$

where,

$$\Delta G^\circ = 0.5 G^\circ S_6 + 2 G^\circ H_2O - G^\circ SO_2 - 2 G^\circ H_2S \quad (B.14)$$

$$\Delta G_{6,2}^\circ = 3 G^\circ S_2 - G^\circ S_6 \quad (B.15)$$

$$\Delta G_{6,4}^\circ = 1.5 G^\circ S_4 - G^\circ S_6 \quad (B.16)$$

$$\Delta G_{1,2}^{\circ} = 0.75 G^{\circ} S_1 - G^{\circ} S_2 \quad (B.17)$$

The Gibbs free energy of each species is calculated from the relationship,

$$G^{\circ}/(Rg T) = a_1 (1 - \ln T) - a_2/2 T - a_3/6 T^2 - a_4/12 T^3 - a_5/20 T^4 + a_6/T - a_7 \quad (B.18)$$

where T =temperature in Kelvin, and the constants a_1 are, the empirical constants which are function of the specific heat polynomials and the standard heat of formation and energy. The derivation of the equation (B.18) may be found in CRC handbook (51) and in reference (144). The data for use in equation (B.18) are from Rau (1973) for sulfur species and from JANAF (192) for the others. These data are stored in the data file as was presented in Appendix A.

At any specified value of T the Gibbs free energy change of reactions (3.20) to (3.23) specifies K to $K_{4,5}$ through equations (B.10) to (B.18). Alternatively, the equilibrium constants after being evaluated through use of equations (B.10) to (B.18) at several levels of temperature, may be correlated with temperature for more efficient processing. The equilibrium constant expressions are given in equations (3.29) to (3.32).

The "S6" program listed below, evaluates $x(S_i)$ and N_t using the above analysis. It will also evaluates the stoichiometric coefficients of reaction (3.31) and the heat

of Claus reaction by the method described in section 3.5.


```

C.....
C.....
C.....
C..... MAINLINE S6 .....
C..... THE PROGRAM TO CALCULATE S6 & N FOR ANY .....
C..... CONVERSION OF H2S USING THE METHOD OF .....
C..... CHAPTER 3 AND APPENDIX B .....
C.....
C.....
C.....

```

```

C
  IMPLICIT REAL*8 (A-H,O-Z,$)
  DIMENSION X(2),SNAM(8),RM(8),SC(8),CP(7),H298(7)
  #,PAR(4)
  DATA SNAM/'H2S ','SO2 ','H2O ','S2 ','S4 ','S6 '
  #,'S8 ','N2 '/
  DATA CP/8.9D00,11.1D00,8.4D00,8.4D00,18.4D00,
  #29.9D00,41.1/
  DATA H298/-4820D00,-70947D00,-57798D00,31200D00,
  #34810D00,24360D00,24320D00/
  EXTERNAL FUN,DF1,DF2
  READ(5,1) T,CONV,YH2S,P,YSO2,YH2O,YN2
1  FORMAT(4D15.5)
  READ(5,1) X(1),X(2),W
  WRITE(6,2)
2  FORMAT(////////,10X,'T',15X,'CONV',10X,'YH2S',12X,
  #'EST.S6',8X,'EST.N')
  WRITE(6,3) T,CONV,YH2S,X(1),X(2)
3  FORMAT(5D18.8)
  RLK62=-34173./T+37.9735
  RLK64=-13663.9/T+12.6028
  RLK68=2932./T-3.43174
  RK62=DEXP(RLK62)
  RK64=DEXP(RLK64)
  RK68=DEXP(RLK68)
  A=(RK62/P/P)**(1./3.)
  B=(RK64/DSQRT(P))**(2./3.)
  C=(RK68*(P**.25))**(4./3.)
  WRITE(6,100) A,B,C
100 FORMAT(//,5X,'A=',D15.7,2X,'B=',D15.7,2X,'C=',D15.7)
  PAR(1)=A
  PAR(2)=B
  PAR(3)=C
  PAR(4)=CONV*YH2S
  CALL SNLEQ(X,PAR,W)

```

```

C
C AMOUNT OF THE SPECIES
C

```

```

  RM(1)=YH2S*(1.-CONV)
  RM(2)=YSO2-YH2S*CONV/2.
  RM(3)=YH2O+YH2S*CONV
  RM(8)=YN2
  P1=(X(1)*X(2)*X(2))**(1./3)
  P2=(X(1)*X(1)*X(2))**(1./3.)
  P3=((X(1)**4)/X(2))**(1./3.)
  RM(4)=A*P1

```

```

RM(5)=B*P2
RM(6)=X(1)
RM(7)=C*P3

```

```

C
C   STOICHIOMETRIC COEFFICIENTS
C

```

```

DO 400 I=4,7
400 SC(I)=2.*RM(I)/YH2S/CONV
SC(1)=-2.
SC(2)=-1.
SC(3)=2.
SC(8)=0.0

```

```

C
C   HEAT OF REACTION
C

```

```

HR=0.0
DO 500 I=1,7
HR=HR+SC(I)*(H298(I)+CP(I)*(T-298.))
500 CONTINUE

```

```

C   THIS IS HEAT FOR 2 MOLES OF H2S
C   DIVIDE IT BY 2
C

```

```

HR=HR/2.

```

```

C
C   PRINT THE RESULTS
C

```

```

WRITE(6,200) CONV
200 FORMAT(//,5X,'H2S CONV = ',F6.2,5X,'SPECIES',10X,
#,'MOLES',17X,'STIO-COEF')
DO 220 K=1,8
WRITE(6,300) SNAM(K),RM(K),SC(K)
220 CONTINUE
300 FORMAT(/,26X,A4,6X,D18.7,5X,D18.7)
C

```

```

WRITE(6,510) HR
510 FORMAT(//,5X,'HEAT OF REACTION=',D14.5,2X,'CAL/
#,'MOLE H2S')
STOP
END

```

```

C
C   SUBROUTINE SNLEQ(X,PAR,W)
C   THIS SUBROUTINE SOLVES A SYSTEM OF TWO NONLINEAR
C   EQ'S BY NEWTONS'S METHOD.
      IMPLICIT REAL*8(A-H,O-Z,$)
      DIMENSION FSAVE(2),X(2),F(2,1),DF(2,2),WKAREA(12)
      &,XSAVE(2),PAR(4)
500 FORMAT(5D14.5)
      M=1
      N=2
      IA=2
      IDGT=0

```

```

MAXIT=100
FTOL=.1D-09
XTOL=.1D-08
DO 100 I=1,MAXIT
DO 10 J=1,2
10 XSAVE(J)=X(J)
F(1,1)=FUN(X,1,PAR)
F(2,1)=FUN(X,2,PAR)
ITEST=0
DO 20 J=1,2
IF(DABS(F(J,1)).GT.FTOL) ITEST=ITEST+1
FSAVE(J)=F(J,1)
F(J,1)=-F(J,1)
20 CONTINUE
IF(ITEST.NE.0) GO TO 30
WRITE(6,35) I,X(1),X(2),FSAVE(1),FSAVE(2)
35 FORMAT(///,2X,'FTOL MET AFTER ITER NO',I4,/,
# ,20X,'X & F VALUES ARE',2D16.6,/,36X,2D16.6)
RETURN
30 DF(1,1)=DF1(X,1,PAR)
DF(1,2)=DF2(X,1,PAR)
DF(2,1)=DF1(X,2,PAR)
DF(2,2)=DF2(X,2,PAR)
C
C LEQTF1 IS A SUBROUTINE IN IMSL LIB.
C
CALL LEQTF1(DF,M,N,IA,F,IDGT,WKAREA,IER)
X(1)=XSAVE(1)+W*F(1,1)
X(2)=XSAVE(2)+W*F(2,1)
ITEST=0
DO 50 JJ=1,2
IF(DABS(F(JJ,1)).GT.XTOL) ITEST=ITEST+1
50 CONTINUE
C IF XTOL MET PRINT THE RESULT
IF(ITEST.EQ.0) GO TO 200
100 CONTINUE
WRITE(6,400)
400 FORMAT(//,'CONVERGENCE WAS NOT ACHIEVED AFTER'
# , '50 ITER.')
RETURN
200 WRITE(6,300) I,X(1),X(2),FSAVE(1),FSAVE(2)
300 FORMAT(//,5X,'XTOL MET',5X,I4,2D18.7,/,10X,'F1='
# ,D16.7,10X,'F2=',D18.7)
RETURN
END
C
C
FUNCTION FUN(X,K,PAR)
IMPLICIT REAL*8(A-H,O-Z,$)
DIMENSION X(2),PAR(4)
COMMON /VAR/ P1,P2,P3,P4,P5,P6,P7
P1=(X(1)*X(2)*X(2))**(1./3)
P2=(X(1)*X(1)*X(2))**(1./3.)
P3=((X(1)**4)/X(2))**(1./3.)

```

```

P4=(X(2)/X(1))**(2./3.)
P5=DSQRT(P4)
P6=(X(1)/X(2))**(1./3.)
P7=P3/X(2)
GO TO (5,10) , K
5  FUN=1.-.5*PAR(4)+PAR(1)*P1+PAR(2)*P2+X(1)+PAR(3)
  **P3-X(2)
  RETURN
10  FUN=2.*PAR(1)*P1+4.*PAR(2)*P2+6.*X(1)+8.*PAR(3)
  **P3-1.5*PAR(4)
  RETURN
  END
C
C
FUNCTION DF1(X,K,PAR)
IMPLICIT REAL*8(A-H,O-Z,$)
DIMENSION X(2),PAR(4)
COMMON /VAR/ P1,P2,P3,P4,P5,P6,P7
GO TO (5,10) , K
5  DF1=PAR(1)*P4/3.+2.*PAR(2)*P5/3.+1.+4./3.*PAR(3)*P6
  RETURN
10  DF1=2./3.*PAR(1)*P4+8./3.*PAR(2)*P5+6.+32./3.
  **PAR(3)*P6
  RETURN
  END
C
C
FUNCTION DF2(X,K,PAR)
IMPLICIT REAL*8(A-H,O-Z,$)
DIMENSION X(2),PAR(4)
COMMON /VAR/ P1,P2,P3,P4,P5,P6,P7
GO TO (5,10) , K
5  DF2=2./3.*PAR(1)/P5+PAR(2)/3./P4-PAR(3)*P7/3.-1.
  RETURN
10  DF2=4./3.*PAR(1)/P5+4./3.*PAR(2)/P4-8.*PAR(3)*P7/3.
  RETURN
  END

```

T
 0.5500000E+03 CONV YH2S EST.S6 EST.N
 0.1000000E-02 0.7000000E-01 0.2000000E-02 0.1000000E+01

A= 0.3181216E-03 B= 0.2857383E-03 C= 0.1258147E+02

FTOL MET AFTER ITER NO 6
 X & F VALUES ARE

0.109642E-04 0.99986E+00
 -0.197306E-11 0.632297E-10

H2S CONV=	0.00	SPECIES	MOLES	STIO-COEF
		H2S	0.19993000E-01	-0.2000000E+01
		S02	0.3496500E-01	-0.1000000E+01
		H2O	0.2000700E+00	0.2000000E+01
		S2	0.7067210E-05	0.2019203E+00
		S4	0.1410210E-06	0.4029173E-02
		S6	0.1096418E-04	0.3132622E+00
		S8	0.3064562E-05	0.8755893E-01
		N2	0.6450000E+00	0.0

HEAT OF REACTION= -0.90721E+04 CAL/MOLE H2S

T	CONV	YH2S	EST.S6	EST.N
0.55000000E+03	0.10000000E+00	0.70000000E-01	0.20000000E-02	0.10000000E+01

A= 0.3181216E-03 B= 0.2857383E-03 C= 0.1258147E+02

XTOL MET 4 0.6985843E-03 0.9980094E+00
F1= 0.1674841E-08 F2= 0.1359825E-07

H2S CONV=	0.10	SPECIES	MOLES	STIO-COEFF
		H2S	0.6300000E-01	-0.2000000E+01
		S02	0.3150000E-01	-0.1000000E+01
		H2O	0.2070000E+00	0.2000000E+01
		S2	0.2818962E-04	0.8054178E-02
		S4	0.2248153E-05	0.643295E-03
		S6	0.6985843E-03	0.1995955E+00
		S8	0.7803903E-03	0.2229687E+00
		N2	0.6450000E+00	0.0

HEAT OF REACTION= -0.11833E+05 CAL/MOLE H2S

S6 PROGRAM
NONEQUILIBRIUM MIXTURE DISTRIBUTION

T CONV YH2S EST S6 EST N
0.5500000E+03 0.3000000E+00 0.7000000E-01 0.2000000E-02 0.1000000E+01

A= 0.3181216E-03 B= 0.2857383E-03 C= 0.1258147E+02

FTOL MET AFTER ITER NO 4
X & F VALUES ARE

0.173367E-02 0.993902E+00
-0.105471E-14 -0.506366E-14

H2S CONV=	0.30	SPECIES	MOLES	STIO-COEF
		H2S	0.4900000E-01	-0.2000000E+01
		S02	0.2450000E-01	-0.1000000E+01
		H2O	0.2710000E+00	0.2000000E+01
		S2	0.3806080E-04	0.3624839E-02
		S4	0.4115234E-05	0.3919271E-03
		S6	0.1733674E-02	0.1651118E+00
		S8	0.2625672E-02	0.2500640E+00
		N2	0.6450000E+00	0.0

HEAT OF REACTION= -0.11592E+05 CAL/MOLE H2S

T
 0.5500000E+03 0.4000000E+00 YH2S EST.S6 EST.N
 0.7000000E-01 0.2000000E-02 0.1000000E+01

A= 0.3181216E-03 B= 0.2857383E-03 C= 0.1258147E+00

XTOL MET 3 0.2192346E-02 0.9918313E+00
 F1= 0.1139099E-08 F2= 0.9163550E-08

H2S CONV=	0.40	SPECIES	MOLES	STIO-COEF
		H2S	0.4200000E-01	-0.2000000E+01
		SO2	0.2100000E-01	-0.1000000E+01
		H2O	0.2780000E+00	0.2000000E+01
		S2	0.4110123E-04	0.2935802E-02
		S4	0.4808990E-05	0.3434993E-03
		S6	0.2192346E-02	0.1565962E+00
		S8	0.3593060E-02	0.2566472E+00
		N2	0.6450000E+00	0.0

HEAT OF REACTION= -0.12026E+05 CAL/MOLE H2S

T
 $0.55000000E+03$ $CONV$ $0.50000000E+00$ $YH2S$ $EST.S6$ $EST.N$
 $0.70000000E-01$ $0.20000000E-02$ $0.10000000E+01$

$A=$ $0.3181216E-03$ $B=$ $0.2857383E-03$ $C=$ $0.1258147E+02$

FTOL MET AFTER ITER NO 4
 X & F VALUES ARE

$0.262780E-02$ $0.989755E+00$
 $0.814349E-13$ $0.749050E-12$

H2S CONV=	0.50	SPECIES	MOLES	STIO-COEF
H2S			$0.35000000E-01$	$-0.20000000E+01$
S02			$0.17500000E-01$	$-0.10000000E+01$
H2O			$0.28500000E+00$	$0.20000000E+01$
S2			$0.4359894E-04$	$0.2491368E-02$
S4			$0.5422582E-05$	$0.3098619E-03$
S6			$0.2627802E-02$	$0.1501601E+00$
S8			$0.4578037E-02$	$0.2616021E+00$
N2			$0.6450000E+00$	0.0

HEAT OF REACTION= $-0.12051E+05$ CAL/MOLE H2S

T
 0.5500000E+03 CONV 0.6000000E+00 YH2S EST S6 EST N
 0.7000000E-01 0.2000000E-02 0.1000000E+01

A= 0.3181216E-03 B= 0.2857383E-03 C= 0.1258147E+02

FTOL MET AFTER ITER NO 4
 X & F VALUES ARE

0.304531E-02 0.987674E+00
 0.356673E-11 0.292262E-10

H2S CONV= 0.60	SPECIES	MOLES	STIO-COEF
	H2S	0.2800000E-01	-0.2000000E+01
	S02	0.1400000E-01	-0.1000000E+01
	H2O	0.2920000E+00	0.2000000E+01
	S2	0.4573121E-04	0.2177677E-02
	S4	0.5978524E-05	0.2846916E-03
	S6	0.3045310E-02	0.1450148E+00
	S8	0.5576595E-02	0.2655522E+00
	N2	0.6450000E+00	0.0

HEAT OF REACTION= -0.12070E+05 CAL/MOLE H2S

118

APPENDIX C: Nonisothermal Claus Pellet

Contents

1. Sulfur species mass balance equation in nonisothermal pellet.
2. Numerical solution for the nonisothermal effectiveness factor: Weisz and Hick's method.
3. Flow chart of nonisothermal effectiveness factor calculation.
4. "NONISOEFF" program.

C.1 Sulfur Species Mass Balance Equation in Nonisothermal Pellet

Equation (4.2) is the steady state differential material balances for sulfur species. To show the complexity of this equation and its coupling effect with the heat balance equation, only C_6 and C_7 would be considered here. The generalization to include C_4 and C_5 will follow the same line.

Equation (4.2) neglecting C_5 and C_4 would yield,

$$6 \frac{d^2 C_6}{dr^2} + 8 \frac{d^2 C_7}{dr^2} + \frac{2}{r} \{ 6 \frac{dC_6}{dr} + 8 \frac{dC_7}{dr} \} + 6(a_6/De_6) \rho_p R_c = 0 \quad (C.1)$$

The differentials dC_7/dr and $d^2 C_7/dr^2$ are evaluated from equation (4.9) as follow,

$$C_7 = H C_6^{4/3} T^{1/3} \quad (4.9)$$

where,

$$H = (K_{68} R_g^{1/4})^{4/3} \quad (C.2)$$

$$\frac{dC_7}{dr} = \frac{4}{3} H C_6^{1/3} T^{1/3} \frac{dC_6}{dr} + \frac{1}{3} H C_6^{4/3} T^{-2/3} \frac{dT}{dr} \quad (C.3)$$

$$\begin{aligned} \frac{d^2 C_7}{dr^2} = & \frac{4}{9} H C_6^{-2/3} T^{1/3} \left(\frac{dC_6}{dr} \right)^2 \\ & + \frac{4}{3} H C_6^{1/3} T^{1/3} \frac{d^2 C_6}{dr^2} \\ & + \frac{8}{9} H C_6^{1/3} T^{-2/3} \left(\frac{dC_6}{dr} \right) \left(\frac{dT}{dr} \right) \\ & - \frac{2}{9} H C_6^{4/3} T^{-5/3} \left(\frac{dT}{dr} \right)^2 \\ & + \frac{1}{3} H C_6^{4/3} T^{-2/3} \frac{d^2 T}{dr^2} \end{aligned} \quad (C.4)$$

Substitution of (C.3) and (C.4) into (C.1) neglecting the terms $(dC_s/dr)^2$, $(dC_s/dr)(dT/dr)$, and $(dT/dr)^2$ yields,

$$\begin{aligned} & d^2C_s/dr^2 \{ 6 + 32/3 H C_s^{1/3} T^{1/3} \} \\ & + 2/r dC_s/dr \{ 6 + 32/3 H C_s^{1/3} T^{1/3} \} \\ & + 1/3 H C_s^{4/3} T^{-2/3} d^2T/dr^2 \\ & + 1/3 H C_s^{4/3} T^{-2/3} dT/dr \\ & + a (a_s/De_s) \rho_p R_c = 0 \end{aligned} \quad (C.5)$$

The equation (C.5) demonstrates the strong coupling of sulfur species mass balance and heat balance equations.

C.2 Numerical Solution of the Nonisothermal Effectiveness Factor: Weisz and Hick's Method

The steady state material and energy balances for a nonisothermal spherical Claus pellet resulted in,

$$d^2\psi_n/dy^2 + 2/y d\psi_n/dy - 9 \phi_n^2 R_c/R_{c_s} = 0 \quad (C.6)$$

$$t = 1 + \xi(-\Delta H) (1 - \psi_n) \quad (C.7)$$

$$X = 1 - \psi_n (1 - X_s) t N_t/N_{t_s} \quad (C.8)$$

The boundary conditions of the differential equation (C.6) are,

$$\psi_n = 1 \quad \text{at } y=1 \quad (C.9)$$

$$d\psi_n/dy = 0 \quad \text{at } y=0 \quad (C.10)$$

Equation (C.6) can be transformed by introducing a new variable,

$$z = y/d$$

Then equation (C.6) becomes,

$$\frac{d^2 \Psi_n}{dz^2} + \frac{2}{z} \frac{d\Psi_n}{dz} - 9 d^2 \phi_n^2 \frac{Rc}{Rc_0} = 0 \quad (C.11)$$

The computing procedures are:

1. Choose an arbitrary value of $(d\phi_n)$.
2. Specify an initial value of X_0 at $z=0$
3. Assume the temperature at the center of the pellet, t_0
4. Calculate $x(S_0)$ and Nt at X_0 and t_0
5. Calculate value of Ψ at the center Ψ_0 ,

$$\Psi_0 = \frac{1-X_0}{1-X_s} \frac{Nt_0}{Nt_0} \frac{1}{t_0}$$

6. Calculate heat of reaction.
7. Calculate t_0 from equation (C.7).
8. Compare t_0 from step 7 with the assumed one of step 3.
if, within the acceptable accuracy limit go to step 9
9. Calculate Rc_0 .
10. Integrate equation (C.9) up to $\Psi_n=1$ and get the value of X at that point.
11. Solve for $d = y/z = 1/z$ at $\Psi_n=1$ from the boundary

condition (C.9).

12. Solve for ϕ_n using step 1.

13. Solve for effectiveness factor by the relation

$$\begin{aligned}\eta &= (1/3\phi_n^2) (d\Psi_n/dy)_{y=1} \\ &= (1/3d\phi_n^2) (d\Psi_n/dz)_{z=1/d} \\ &= (z/3\phi_n^2) (d\Psi_n/dz)_{z=1/d}\end{aligned}\quad (C.12)$$

To integrate equation (C.9), it is transformed into two first order differential equations by letting,

$$d\Psi_n/dz = Y_1 \quad (C.13)$$

then

$$\frac{dY_1}{dz} + \frac{2}{z} Y_1 - 9(d^2 \phi_n^2) \frac{Rc}{Rc_s} = 0 \quad (C.14)$$

Equations (C.13) and (C.14) can be solved simultaneously using the Runge-Kutta-Fehlberg integration procedure (186).

To determine the value of the indeterminate form of $2Y_1/z$ at $z=0$ on the left hand side in equation (C.14), use can be made of the L'Hopital's rule at $z=0$,

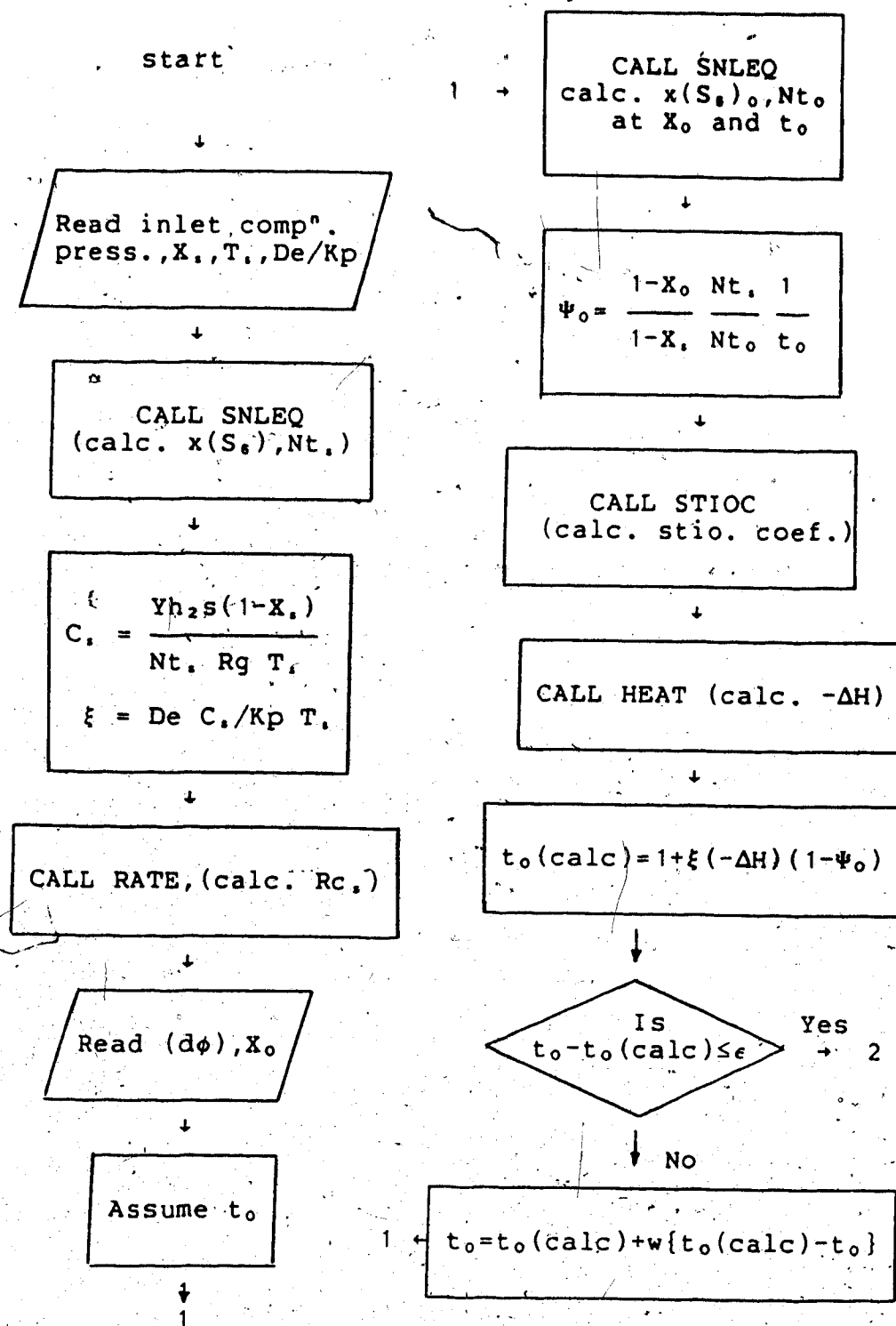
$$\lim_{z \rightarrow 0} 2 Y_1/z = 2 dY_1/dz \quad (C.15)$$

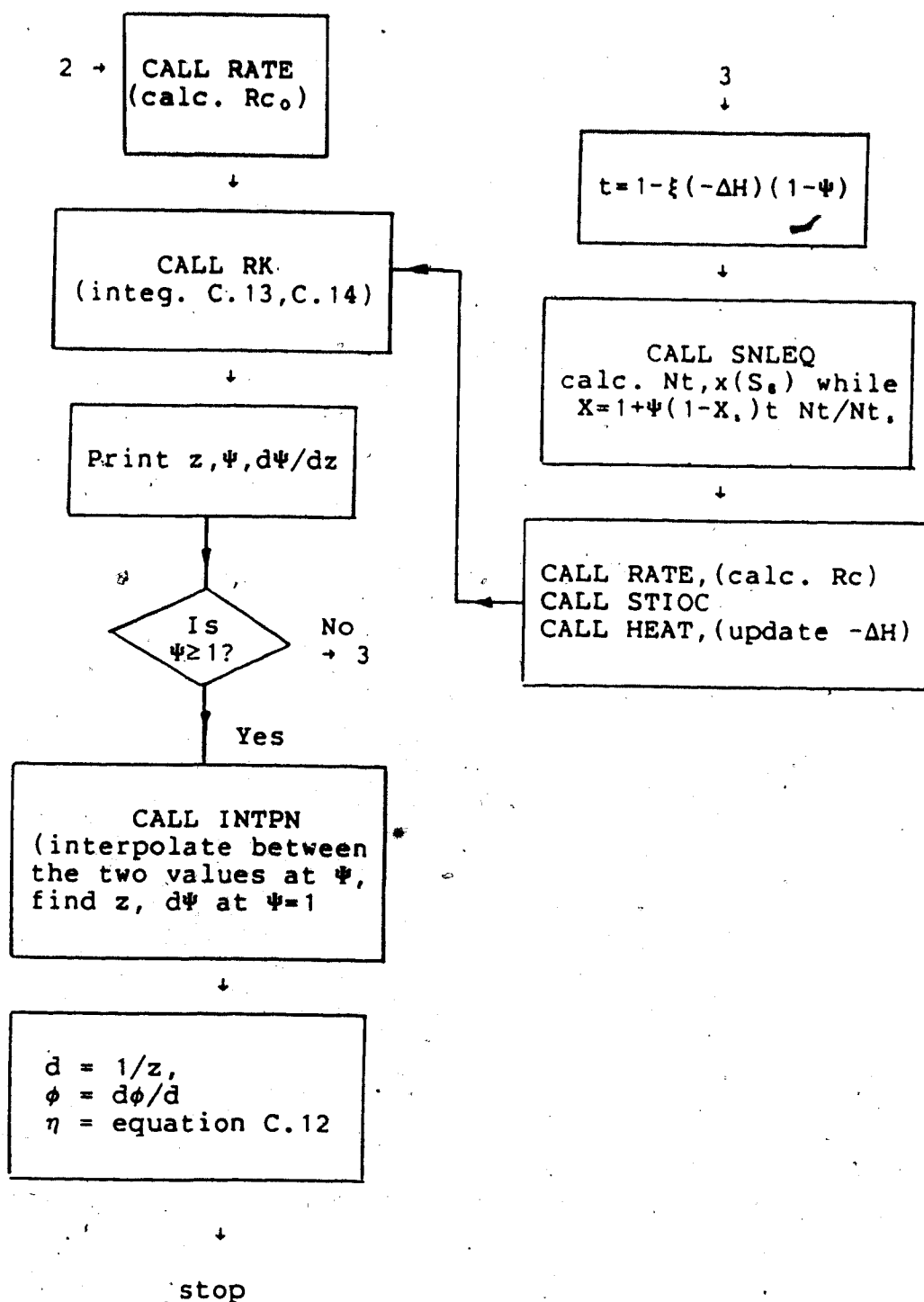
Now equation (C.1) at $z=0$ becomes,

$$3 \, dY_1/dz - 9(d^2 \phi_n^2) R_c/R_{c_s} = 0 \quad (C.16)$$

For points other than $z=0$, equation (C.14) still applies. The computer program "NONISOEFF" was used to calculate the nonisothermal effectiveness factor. The flow chart of this program is shown in figure C.1.

Figure C.1 Flow Chart of Nonisothermal Effectiveness Factor Calculation





```

C.....
C..
C..                                MAINLINE NONISOEFF
C..
C..THIS PROGRAM CALCULATES NON-ISOTHERMAL EFFECTIVENES..
C..FACTOR FOR CLAUS REACTION. IT USES CHANGE OF
C..VARIABLE TO CONVERT BOUNDARY VALUE PROBLEM TO
C..OPEN-ENDED INITIAL VALUE PROBLEM. INTEGRATION IS BY..
C..RUNG-KUTTA-FEHLBERG METHOD. MATHEMATICS OF THE
C..PROGRAM HAS BEEN DESCRIBED IN CHAPTER 4.
C..THE INPUTS ARE:
C..  YH2S= MOLE FRACTION OF H2S IN THE FEED
C..  YSO2= MOLE FRACTION OF SO2 IN THE FEED
C..  YH2O= MOLE FRACTION OF H2O IN THE FEED
C..  YN2 = MOLE FRACTION OF N2
C..  XS  = CONVERSION OF H2S AT THE SURFACE
C..  TS  = TEMP (K ) AT THE SURFACE
C..  NOPT= OPTION NUMBER ,1 ;SLAB ,2 ;SPHERICAL PELLET..
C..  AH  = ARBITRARY VALUE OF THIELE*A
C..  Y0  = CONVERSION OF H2S AT THE CENTER OF THE
C..  T0  = ESTIMATE OF TEMPRATURE AT THE CENTER
C..  BE  = THE NONISOTHERMAL FACTOR  $CS \cdot D / (K \cdot TS)$ 
C..        PELLET , ASSUMED VALUE
C..
C..THE OUTPUTS ARE:
C..
C..  Z   =Y/A WHERE Y IS THE DIMENSIONLESS LENGTH
C..  Y1  =C/CS WHERE C IS CONCENTRATION OF H2S
C..  Y2  =D(C/CS)/DZ
C..  THIELE MODULUS
C..  EFFECTIVENESS FACTOR
C..  NOTE: THE SUBROUTINE COTM CALLS IMSL LIB
C..        SUBROUTINE. HENCE ADD *IMSLDPLIB WHEN
C..  RUNNING THE PROGRAM. ALSO IT USES THERMODYNAMIC
C..  DATA FILE , SO ASSIGN 7=DATA2.
C..
C.....
C..  IMPLICIT REAL*8(A-H,O-Z,$)
C..  DIMENSION X(2),F(2,1),ISPN(7),SNAM(7),FRE(7,8),FRT(7)
C..  #,Y(2)
C..  COMMON W,A,B,C,RATE,RATES,YH2S,YSO2,YH2O,YN2,T,XS
C..  #,TMS,TM,X,CONV,RK12,AH,FRE,FRT,TS,S2,S4,S6,S8,HEAT,BE
C..  COMMON ICALL,NCALL,NOPT
C
C  FRE'S ARE THE COEFFICIENTS OF FREE ENERGY EQUATION.
C  FRT IS THE STANDARD FREE ENERGY OF SPECIE AT THE
C  TEMPERATURE OF THE SYSTEM.
C
C  EXTERNAL FUN
C  NCALL=1
C  ICALL=1
C  ISPN(1)=7
C  ISPN(2)=8
C  ISPN(3)=6

```

```

      ISPN(4)=13
      ISPN(5)=15
      ISPN(6)=17
      ISPN(7)=19
      DO 10 I=1,7
      LINE=(ISPN(I)*4-3)*1000
      READ(7'LINE,40) SNAM(I)
40  FORMAT(A4)
      READ(7,41) (FRE(I,K) , K=1,4)
41  FORMAT(/,4E15.7)
      READ(7,42) (FRE(I,K) ,K=5,8)
42  FORMAT(4E15.7)
10  CONTINUE
      WRITE(6,11)
11  FORMAT(5X,'TYPE OPTION : 1=SLAB ,.2=SPHERE')
      CALL FREAD(5,'I:',NOPT)
      WRITE(6,12)
12  FORMAT(5X,'TYPE TEMP')
      CALL FREAD(5,'R*8:',T)
      WRITE(6,13)
13  FORMAT(5X,'TYPE MOLE FRAC. OF H2S,SO2,H2O,N2',/,
#5X,' CONVERSION AND TEMPERATURE AT THE SURFACE ')
30  FORMAT(5E12.5)
      CALL FREAD(5,'7R*8:',YH2S,YSO2,YH2O,YN2,XS,TS)
C
C  CALL COTM TO CALCULATE S2 ,AND NT FOR CONDITION
C  AT THE SURFACE, AND RATES.
C  W IS THE RELAXATION FACTOR FOR N.R. METHOD
C
      W=.75
      CALL COTM(Y)
1  FORMAT(/,7X,'X/A=Z',11X,'Y(1)',14X,'Y(2)',17X,'T'
$,14X,'RATE',12X,'HEAT',/)
      WRITE(6,4)
4  FORMAT(/,5X,'TYPE THE STARTING POINT OF INTEGRATION
3,' FOR CONVERSIONS AT THE STARTING POINT LESS THAN
3,'EQUILIBRIUM OR EQUILIBRIUM LET Z=0.0 ;',/,5X,
#,' THIS WILL GIVE YOU THIELE MODULUS UP TO'
3,' ABOUT 4.5 ; FOR LARGER THIELE MODULUS',/,5X,
3,' THE CONVERSION REACHES EQUILIBRIUM AT LARGER'
#,' VALUE OF Z I.E. BEFORE THE CENTER OF CATALYST'
3,' ; HENCE LET Z BE SOME POSITIVE VALUE ',/,5X,
3,' AND LET THE CONVERSION AT THIS Z BE VERY NEAR',
3,' TO EQUILIBRIUM CONVERSION SUCH THAT THE RATE IS'
3,/,5X,'IN ORDER OF .1E-13 TO -14 OR SMALLER .'
3,' A SMALL POSITIVE NUMBER IS REQUIRED FOR START'
3' OF INTEGRATION.')
      DO 100 KK=1,50
      NCALL=2
      WRITE(6,401)
401 FORMAT(/,5X,'TYPE THE STARTING POINT OF'
#,'INTEGRATION')
      CALL FREAD(5,'R*8:',Z)
      WRITE(6,3)

```

```

3      FORMAT(5X, '//, 'TYPE A*THIELE,  CONVERSION AT INITIAL'
#,' POINT, MAX.INTG.STEP, ESTIMATE OF'
#,' TEMP AT INITIAL POINT AND BE')
      CALL FREAD(5, '5R*8:', AH, CONV, HMX, T, BE)

C
C
C      CALL TATC TO CALCULATE TEMPERATUR AT THE INITIAL POINT
C      CORRESPONDING TO THE CONVERSION AT INITIAL POINT
C      AND BE VALUE .
C
      WRITE(6, 409)
409    FORMAT(//, 5X, 'TYPE THE RELAXATION FACTOR AT '
#,' THE INITIAL POINT')
      CALL FREAD(5, 'R*8:', W)
      CALL TATC(Z)
      NCALL=3

C
C      CALCULATE Y1 AT THE INITIAL POINT :
C
      Y(1)=(1.-CONV)/(1.-XS)*TMS/TM*TS/T
      Y(2)=0.0
      H=.05
      WRITE(6, 300)
300    FORMAT(////, 5X, 'VALUES OF TEMP. , CONV. , Y(1) , '
#,' AND Y(2) AT THE INITIAL POINT ARE'
#,' RESPECTIVELY :', '/')
      WRITE(6, 200) T, CONV, Y(1), Y(2)
200    FORMAT(5X, 4D19.9, //)
      WRITE(6, 500) RATES, RATE, HEAT
500    FORMAT(1X, 'RATES=', D15.8, 5X, 'RATE AT INITIAL POINT='
%, D15.8, 5X, 'HEAT AT INITIAL POINT=', D15.8, //)
      WRITE(6, 1)
C      START THE INTEGRATION :
C
      W=.75
      CALL RKF(Z, Y, 2, FUN, 1.D3, H, HMX, .1D-04, .1D-04, IFLAG)
100    CONTINUE
      STOP
      END

C
C
C      THIS SUBROUTINE CALCULATES THE HEAT OF REACTION
C      ACCORDING TO THE STIOCHIOMETRIC COEFFICIENT
C      CALCULATED BY SUBROUTINE STIOC USING THE VALUES
C      OBTAINED IN SUBROUTINE COTM AT THE LOCAL CONDITION
C
      SUBROUTINE HEATR(ALFA, BETA, GAMA, DELTA)
      IMPLICIT REAL*8(A-H, O-Z, $)
      DIMENSION HFS(7), FRT(7), FRE(7, 8), X(2), CP(7, 5), H(7)
      COMMON W, A, B, C, RATE, RATES, YH2S, YSO2, YH2O, YN2, T, XS
#,' TMS, TM, X, CONV, RK12, AH, FRE, FRT, TS, S2, S4, S6, S8, HEAT, BE
      COMMON ICALL, NCALL, NOPT
      IF(ICALL.GT.1) GO TO 13
      R=1.986

```

```

HFS(1)=-4820.0
HFS(2)=-70947.0
HFS(3)=-57797.9
HFS(4)=31200.0
HFS(5)=34810.0
HFS(6)=24360.0
HFS(7)=24320.0

```

```

C
C THE COEFFICIENT OF FREE ENERGY EQUATION ARE CP/R . HENCE
C TO GET CP VALUES FROM FREE ENERGY COEFFICIENTS :
C

```

```

      DO 10 I=1,7
      DO 11 J=1,4
11    CP(I,J)=FRE(I,J)*R
10    CONTINUE
      DO 12 K=1,7
12    CP(K,5)=FRE(K,8)*2*R
13    TT=T-298.0
      DO 14 N=1,7
        H(N)=HFS(N)+CP(N,1)*TT+CP(N,2)/2.*TT**2
        #+CP(N,3)/3.*TT**3+CP(N,4)/4.*TT**4
        #-CP(N,5)/T+CP(N,5)/298.0
14    CONTINUE
        HEAT=H(3)+ALFA*H(4)+BETA*H(5)+GAMA*H(6)
        #+DELTA*H(7)-H(1)-.5*H(2)
      RETURN
      END

```

```

C
C
C THIS SUBROUTINE ITERATES THE VALUE OF T AT THE
C INITIAL POINT OF INTEGRATION TO GET T CORRESPONDING
C TO CONVERSION AND BE VALUE WITH
C ACCURACY IN T/TS WITHIN 0.00090000001 .
C

```

```

      SUBROUTINE TATC(Z)
      IMPLICIT REAL*8(A-H,O-Z,$)
      DIMENSION Y(2),X(2),FRE(7,8),FRT(7)
      COMMON W,A,B,C,RATE,RATES,YH2S,YO2,YH2O,YN2,T,XS
      #,TMS,TM,X,CONV,RK12,AH,FRE,FRT,TS,S2,S4,S6,S8,HEAT,BE
      COMMON ICALL,NCALL,NOPT

```

```

C
C TO GET S2 - S8 AND TOTAL MOLE CALL COTM
C

```

```

      CALL COTM(Y)

```

```

C
C TO GET STIOCHIOMETRIC COEFFICIENTS OF CLAUS REACTION
C

```

```

      CALL STIOC(S2,S4,S6,S8,ALFA,BETA,
      #GAMA,DELTA,YH2S,CONV)
      CALL HEATR(ALFA,BETA,GAMA,DELTA)
      ICALL=ICALL+1
      TRC=1.+BE*(-HEAT)*(1.-(1.-CONV)/(1.-XS)*TMS/TM*TS/T)
      TRA=T/TS
      IF(DABS(TRC-TRA).LT.0.1D-10) GO TO 2

```

```

      T=T+1.*(TRC*TS-T)
      GQ TO 1
2     IF(RATE) 9,9,6
6     RETURN
9     WRITE(6,7) RATE,T
7     FORMAT(//,5X,'RATE AT THE INTIAL POINT IS=',D16.8,
#5X,'T AT INITIAL POINT=',D16.8,/,
5X,'YOU HAVE PASSED EQUILIBRIUM .',
3/,5X,'TRY SMALLER CONVERSION AT INITIAL POINT',///)
      CALL EXIT
      END

```

```

C
C
C.. THIS SUBROUTINE CALCULATES THE STIOCHIOMETRIC ..
C.. COEFFICIENT. ..
C
C

```

```

      SUBROUTINE STIOC (S2,S4,S6,S8,ALFA,
#BETA,GAMA,DELTA,YH2S,CONV)
      IMPLICIT REAL*8(A-H,O-Z,$)
      ALFA=S2/YH2S/CONV
      BETA=S4/YH2S/CONV
      GAMA=S6/YH2S/CONV
      DELTA=S8/YH2S/CONV
      RETURN
      END

```

```

C
C
C.....
C... SUBROUTINE FUN. ....
C... THIS SUBROUTINE EVALUTES THE VALUE OF ....
C... DERIVATIVES TO BE USED BY RKF FOR INTEGRATION ....
C.....
C

```

```

      SUBROUTINE FUN(Z,Y,YP)
      IMPLICIT REAL*8(A-H,O-Z,$)
      DIMENSION Y(1),X(2),YP(1),FRT(7),FRE(7,8)
      COMMON W,A,B,C,RATE,RATES,YH2S,YO2,YH2O,YN2,T,XS
# ,TMS,TM,X,CONV,RK12,AH,FRE,FRT,TS,S2,S4,S6,S8,HEAT,BE
      COMMON ICALL,NCALL,NOPT
      IF(NCALL.EQ.3) GO TO 1
      CALL COTM(Y)
1     RATER=RATE/RATES
      NCALL=NCALL+1
      YP(1)=Y(2)
      IF(NOPT-1) 2,2,3
2     YP(2)=(AH**2)*RATER
      GO TO 6
3     IF(Z) 4,4,5
4     YP(2)=3.*(AH**2)*RATER
      GO TO 6
5     YP(2)=9.*(AH**2)*RATER-2./Z*Y(2)
6     CALL STIOC(S2,S4,S6,S8,ALFA,BETA,GAMA,DELTA,YH2S,CONV)
      CALL HEATR(ALFA,BETA,GAMA,DELTA)

```

RETURN
END

```

C
C
C.....
C.....          SUBROUTINE OUTP
C.....THIS SUBROUTINE CONTROLS THE INTEGRATION.....
C.....LENGTH BY CHECKING THE VALUE OF Y1 TO .....
C.....BE LESS THAN ONE.
C.....
C
C
SUBROUTINE OUTP(Z,Y,PAR)
IMPLICIT REAL*8(A-H,O-Z,$)
DIMENSION Y(2),X(2),FRE(7,8),FRT(7)
COMMON W,A,B,C,RATE,RATES,YH2S,YO2,YH2O,YN2,T,XS
#,TMS,TM,X,CONV,RK12,AH,FRE,FRT,TS,S2,S4,S6,S8,HEAT,BE
COMMON ICALL,NCALL,NOPT
IF(Y(2).LT.0.0) GO TO 9
IF(1.-Y(1)) 2,3,4
2 Y(2)=Y2+(Y(2)-Y2)*(1.-Y1)/(Y(1)-Y1)
Z=ZZ+(Z-ZZ)*(1.-Y1)/(Y(1)-Y1)
3 THIM=AH*Z
EFFEC=Z*Y(2)/THIM**2
IF(NOPT.GT.1) EFFEC=EFFEC/3.
WRITE(6,5) THIM,EFFEC
5 FORMAT(//,5X,'THIM=',D12.4,5X,'EFFEC=',D12.4,/)
PAR=1.
ZZ=0.
Y1=0.
Y2=0.
GO TO 6
4 ZZ=Z
Y1=Y(1)
Y2=Y(2)
6 RETURN
9 WRITE(6,10)
10 FORMAT(//,'THE RUN IS TERMINATED BECAUSE THE
#, 'INACCURACY IN THE NUMERICAL METHODS HAS
3, 'GIVEN THE WRONG COMBINATION OF CONVERSION AND
4,/, 'TEMPERATURE AT CENTER. THIS IS BECAUSE AT THE
%, 'THE CENTER YOUR ARE VERY CLOSE TO EQUILIBRIUM',/,
5, 'CORRESPONDINGLY THE RATE IS VERY SMALL NUMBER AND'
6, ' RELATIVE ERROR IS LARGE.',///)
CALL EXIT
END

```

```

C
C
C.....
C.....          SUBROUTINE COTM
C.....THIS SUBROUTINE CALCULATES MOLES OF S2 .....
C.....AND TOTAL MOLES FOR ANY CONVERSION OF .....
C.....H2S OR C/CS. THEN IT WOULD CALCULATES T .....
C..... THE RATE OS REACTION.
C.....

```



```

C      SUBROUTINE COTM(Y)
C      THIS SUBROUTINE SOLVES A SYSTEM OF TWO NONLINEAR
C      EQ S BY NEWTONS S METHOD.
      IMPLICIT REAL*8(A-H,O-Z,$)
      DIMENSION FSAVE(2),X(2),F(2,1),DF(2,2),WKAREA(12)
      #,XSAVE(2),Y(2),FRE(7,8),FRT(7)
      COMMON W,A,B,C,RATE,RATES,YH2S,YSO2,YH2O,YN2,T,XS
      #,TMS,TM,X,CONV,RK12,AH,FRE,FRT,TS,S2,S4,S6,S8,HEAT,BE
      COMMON ICALL,NCALL,NQPT
      M=1
      N=2
      IA=2
      IDGT=0
      MAXIT=100
      FTOL=.1D-09
      XTOL=.1D-08
      IF(NCALL-2) 57,55,56
57      T=TS
      GO TO 55
56      T=TS*(1.+BE*(-HEAT)*(1.-Y(1)))
55      DO 20 J=1,7
      FRT(J)=FRE(J,1)*(1.-DLOG(T))-FRE(J,2)*T/2.-FRE(J,3)
      #*T*T/6.-FRE(J,4)*(T**3)/12.-FRE(J,5)*(T**4)/20.
      #+FRE(J,6)/T-FRE(J,7)-FRE(J,8)/T/T
20      CONTINUE
      DFRT12=1.5*FRT(4)+2.*FRT(3)-2.*FRT(1)-FRT(2)
      DFRT14=0.75*FRT(5)+2.*FRT(3)-2.*FRT(1)-FRT(2)
      DFRT16=0.5*FRT(6)+2.*FRT(3)-2.*FRT(1)-FRT(2)
      DFRT18=0.375*FRT(7)+2.*FRT(3)-2.*FRT(1)-FRT(2)
      RK12=DEXP(-DFRT12)
      RK14=DEXP(-DFRT14)
      RK16=DEXP(-DFRT16)
      RK18=DEXP(-DFRT18)
      DFRT4=FRT(5)-2.*FRT(4)
      RK4=DEXP(-DFRT4)
      DFRT6=FRT(6)-3.*FRT(4)
      RK6=DEXP(-DFRT6)
      DFRT8=FRT(7)-4.*FRT(4)
      RK8=DEXP(-DFRT8)
      PRESS=1.0
      A=2.*RK4*PRESS
      B=3.*RK6*PRESS*PRESS
      C=4.*RK8*(PRESS**3)
      IF(NCALL.GT.2) GO TO 33
383      FORMAT(20X,I4)
C
C... THE FOLLOWING FEW LINES ARE TO RELATE THE INITIAL
C... GUESS OF S2 FORMED WITH TEMPERATURE
C
1000  IF(T-425.) 1001,1002,1002
1001  X(1)=.4D-08
      GO TO 111
1002  IF(T-450.) 1003,1004,1004

```

```

1003  X(1)=.4D-07
      GO TO 111
1004  IF(T-475.) 101,1008,1008
101    X(1)=.4D-06
      GO TO 111
1008  IF(T-500.0) 1009,102,102
1009  X(1)=.1D-05
      GO TO 111
102    IF(T-525.) 103,104,104
103    X(1)=.4D-05
      GO TO 111
104    IF(T-600.) 105,106,106
105    X(1)=.4D-04
      GO TO 111
106    IF(T-650.) 107,107,108
107    X(1)=.4D-03
      GO TO 111
108    IF(T-700.) 109,109,110
109    X(1)=.4D-02
      GO TO 111
110    X(1)=.008
111    CONTINUE
36    X(2)=.98D00
      IF(NCALL.EQ.1) CONV=XS
33    DO 100 I=1,MAXIT
      DO 10 J=1,2
10    XSAVE(J)=X(J)
      IF(NCALL.LE.3) GO TO 34
      CONV=1.0-Y(1)*(1.-XS)*X(2)/TMS*T/TS
34    D=.75*CONV*YH2S
      E=1.-.5*CONV*YH2S
      F(1,1)=X(1)*(X(2)**3)+A*(X(1)*X(2))**2
      #+B*(X(1)**3)*X(2)+C*(X(1)**4)-D*(X(2)**3)
      F(2,1)=(X(2)**4)-X(1)*(X(2)**3)-A/2*(X(1)*X(2))**2
      #-B/3.*(X(1)**3)*X(2)-C/4.*(X(1)**4)-E*(X(2)**3)
      ITEST=0
      DO 22 J=1,2
      IF(DABS(F(J,1)).GT.FTOL) ITEST=ITEST+1
      FSAVE(J)=F(J,1)
      F(J,1)=-F(J,1)
22    CONTINUE
      IF(ITEST.NE.0) GO TO 30
      GO TO 200
30    DF(1,1)=X(2)**3+2.*A*X(1)*(X(2)**2)
      #+3.*B*(X(1)**2)*X(2)+4.*C*(X(1)**3)
      DF(1,2)=3.*X(1)*(X(2)**2)+2.*A*(X(1)**2)*X(2)
      #+B*(X(1)**3)-3.*D*(X(2)**2)
      DF(2,1)=-X(2)**3-A*X(1)*(X(2)**2)
      #-B*(X(1)**2)*(X(2))-C*(X(1)**3)
      DF(2,2)=4.*(X(2)**3)-3.*X(1)*(X(2)**2)
      #-A*(X(1)**2)*X(2)-B/3.*(X(1)**3)-3.*E*(X(2)**2)
      IF(NCALL-3) 40,40,35
35    DF(1,2)=DF(1,2)+.75*YH2S*Y(1)/TMS*(1.-XS)*(X(2)**3)
      DF(2,2)=DF(2,2)-YH2S/2.*(X(2)**3)*Y(1)/TMS*(1.-XS)

```

```

C
C... THE FOLLOWING 6 LINES ARE TO SCALE THE COEFFICIENT
C... MATRIX TO INCREASE THE CONDITION OF THAT MATRIX .
C
40  DF(1,2)=DF(1,2)/DF(1,1)
    F(1,1)=F(1,1)/DF(1,1)
    DF(1,1)=DF(1,1)/DF(1,1)
    DF(2,2)=DF(2,2)/DF(2,1)
    F(2,1)=F(2,1)/DF(2,1)
    DF(2,1)=DF(2,1)/DF(2,1)
    CALL LEQTF(DF,M,N,IA,F,IDGT,WKAREA,IER)
C
C... W IS THE RELAXATION FACTOR USED
C
    X(1)=XSAVE(1)+W*F(1,1)
    X(2)=XSAVE(2)+W*F(2,1)
    ITEST=0
    DO 50 JJ=1,2
      IF(DABS(F(JJ,1)).GT.XTOL) ITEST=ITEST+1
50  CONTINUE
C  IF XTOL MET PRINT THE RESULT
    IF(ITEST.EQ.0) GO TO 200
100 CONTINUE
    WRITE(6,400)
400  FORMAT('/', 'CONVERGENCE WAS NOT ACHIEVED AFTER '
      #, '50 ITER.')
    RETURN
200  A1=2.56D-04*DEXP(-7350./1.986/T)
    A2=0.006D00
    TM=X(2)
    S2=X(1)
    S4=(S2**2)*RK4*PRESS/TM
    S6=(S2**3)*RK6*(PRESS/TM)**2
    S8=(S2**4)*RK8*(PRESS/TM)**3
C  WRITE(6,666) S2,S4,S6,S8
    H2S=YH2S*(1.-CONV)
    H2O=YH2O+YH2S*CONV
    SO2=YSO2-YH2S*CONV/2.
    RATE=A1/((1.+A2*H2O*760./TM)**2)
    RATE=RATE*(H2S*(760.**1.5)*DSQRT(SO2)*(TM**(-1.5))
      #-((X(1)*760.）**.75)*760.*
      #H2O*(TM**(-1.75))/DSQRT(RK12*SQRT(760.)))
    IF(NCALL.GT.1) GO TO 500
    TMS=TM
    RATES=RATE
2  FORMAT(5(D12.5,3X))
3  FORMAT(I10)
500 RETURN
    END
C
C
    SUBROUTINE RKF(A,Y,N,FUN,DA,H,HMX,ABSER,RELER,IFLAG)
C
C  THIS CODE INTEGRATES A SYSTEM OF FIRST ORDER ORDINARY

```

C DIFFERENTIAL EQUATIONS BY RUNGE-KUTTA-FEHLBERG
 C METHOD WITH AUTOMATIC ESTIMATION OF LOCAL ERROR
 C AND STEP SIZE ADJUSTMENT.

```

C      DOUBLE PRECISION PAR,Y(N),YTEMP(20),TEMP(20),R(20)
      DOUBLE PRECISION K1(20),K2(20),K3(20),K4(20),K5(20)
      #,K6(20)
      DOUBLE PRECISION U,RELER,ABSER,HMX,A,B,DA,HMAX,H
      #,HKEEP,ARG,RATIO
      DOUBLE PRECISION DABS,DMAX1,DMIN1,DSIGN,DSQRT,TR
      PAR=0.0
      U=1.0D-11
      IF(RELER.LT.0.0D0.OR.ABSER.LT.0.0D0) GO TO 18
      IF(RELER+ABSER.EQ.0.0D0) GO TO 18
      IF(HMX.LE.0.0D0) GO TO 18
      B=A+DA
      IF(DABS(DA).LE.13.0D0*U*DMAX1(DABS(A),DABS(B)))
      #GO TO 19
      HMAX=DMIN1(HMX,DABS(DA))
      IF(DABS(H).LE.13.0D0*U*DABS(A)) H=HMAX
      KOUNT=0
      IADJS=0
3     H=DSIGN(DMIN1(DABS(H),HMAX),DA)
      IF(DABS(B-A).GT.1.25D0*DABS(H)) GO TO 4
      HKEEP=H
      IADJS=1
      H=B-A
4     CALL FUN(A,Y,K1)
      KOUNT=KOUNT+1
5     CONTINUE
      DO 6 I=1,N
6     YTEMP(I)=Y(I)+0.25D0*H*K1(I)
      ARG=A+0.25D0*H
      CALL FUN(ARG,YTEMP,K2)
      DO 7 I=1,N
7     YTEMP(I)=Y(I)+H*(K1(I)*(3.0D0/32.0D0)+K2(I)*(9.0D0
      #/32.0D0))
      ARG=A+H*(3.0D0/8.0D0)
      CALL FUN(ARG,YTEMP,K3)
      DO 8 I=1,N
8     YTEMP(I)=Y(I)+H*(K1(I)*(1932.0D0/2197.0D0)-K2(I)*
      # (7200.0D0/2197.0D0)
      #+K3(I)*(7296.0D0/2197.0D0))
      ARG=A+H*(12.0D0/13.0D0)
      CALL FUN(ARG,YTEMP,K4)
      DO 9 I=1,N
9     YTEMP(I)=Y(I)+H*(K1(I)*(439.0D0/216.0D0)-8.0D0*K2(I)
      #+K3(I)*(3680.0D0/513.0D0)-K4(I)*(845.0D0/4104.0D0))
      ARG=A+H
      CALL FUN(ARG,YTEMP,K5)
      DO 10 I=1,N
10    YTEMP(I)=Y(I)+H*(-K1(I)*(8.0D0/27.0D0)+2.0D0*K2(I)
      #-K3(I)*3544.0D0/2565.0D0)
      #+K4(I)*(1859.0D0/4104.0D0)-K5(I)*(11.0D0/40.0D0))

```

```

ARG=A+0.5D0*H
CALL FUN(ARG,YTEMP,K6)
DO 11 I=1,N
TEMP(I)=K1(I)*(25.D0/216.D0)+K3(I)*(1408.D0/2565.D0)
**K4(I)*(2197.D0/4104.D0)-0.2D0*K5(I)
11 YTEMP(I)=Y(I)+H*TEMP(I)
DO 12 I=1,N
12 R(I)=K1(I)/360.D0-K3(I)*(128.D0/4275.D0)-K4(I)*
*(2197.D0/75240.D0)+K5(I)/50.D0+K6(I)*(2.D0/55.D0)
RATIO=0.0D0
DO 13 I=1,N
TR=DABS(R(I))/(RELER*DABS(YTEMP(I))+ABSER)
13 RATIO=DMAX1(RATIO,TR)
35 FORMAT(/,D12.5)
IF(RATIO.GT.1.D0) GO TO 15
DO 14 I=1,N
14 Y(I)=YTEMP(I)
A=A+H
CALL OUTP(A,Y,PAR)
IF(PAR) 21,20,21
20 IF(IADJS.EQ.1) GO TO 16
RATIO=DMAX1(RATIO,6,5536D-04)
15 RATIO=DMIN1(RATIO,4096.D0)
H=0.8D0*H/DSQRT(DSQRT(RATIO))
IF(DABS(H).LE.13.D0*U*DABS(A)) GO TO 19
KOUNT=KOUNT+5
IF(KOUNT.GE.31995) GO TO 17
IF(RATIO.LE.1.D0) GO TO 3
IADJS=0
GO TO 5
16 IFLAG=1
H=HKEEP
WRITE(6,25) IFLAG
25 FORMAT(/,5X,'IFLAG=',I5),
RETURN
17 IFLAG=2
WRITE(6,25) IFLAG
RETURN
18 IFLAG=3
WRITE(6,25) IFLAG
RETURN
19 IFLAG=4
WRITE(6,25) IFLAG
21 RETURN
END

```

APPENDIX D: Isothermal Claus Pellet

Contents

1. Isothermal effectiveness factor: Weisz and Hick's Method.
2. Isothermal effectiveness factor: Orthogonal Collocation Method.
3. Application of Orthogonal Collocation to Claus pellet.
4. Orthogonal Collocation for large ϕ .
5. Thiele modulus for the Claus reaction.
6. Estimation of the local effectiveness factor.
7. "ISOEFF" program: the program to calculate isothermal Claus effectiveness factor by Weisz and Hick's method.
8. "ORTHOGONAL" program; the program to evaluate A and B matrices.
9. Table D.2: output of the program "ORTHOGONAL",
10. Figure D.1: flow chart of the program "ORTEFF".
11. "ORTEFF" program: the program to calculate the isothermal Claus effectiveness factor by Orthogonal Collocation method.

D.1 Isothermal Effectiveness Factor - Weisz and Hick's Method

The steady state material balances for an isothermal spherical Claus pellet resulted in,

$$\frac{d^2\psi}{dy^2} + \frac{2}{y} \frac{d\psi}{dy} - 9 \phi^2 R_c = 0 \quad (D.1)$$

with

$$\psi = 1 \quad , \quad \text{at } y=1 \quad (D.2)$$

$$\frac{d\psi}{dy} = 0 \quad , \quad \text{at } y=0 \quad (D.3)$$

and

$$P_i = P_{s,i} + \frac{a_i}{a_1} \frac{De_1}{De_i} (P_1 - P_{s,1}) \quad (D.4)$$

$i = 2, 3$

$$W = W_s + 6 \left(\frac{a_s}{a_1} \right) \left(\frac{De_1}{De_s} \right) (P_1 - P_{s,1}) \quad (D.5)$$

Introducing $z=y/d$ as described in section C.2, yields

$$\frac{d^2\psi}{dz^2} + \frac{2}{z} \frac{d\psi}{dz} - 9 d^2 \phi^2 R = 0 \quad (D.6)$$

To integrate equation (D.6), it is transformed into two first order differential equations as shown in section C.2. The equations (C.3) to (C.6) are applicable when ψ_n and ϕ_n are replaced by ψ and ϕ respectively.

The computing procedure is:

1. Choose an arbitrary value of $(d\phi)$.

2. Specify an initial value of P_i at $z=0$.
3. Evaluate P_i , P_j , and P_k by solution of the equations (D.4) and (D.5).
4. Evaluate R_c .
5. Integrate equation (D.6) up to $\Psi=1$ and get the value of z at that point.
6. Solve for $d = y/z = 1/z$ at $\Psi=1$ from the boundary condition (D.2).
7. Solve for ϕ using step 1.
8. Evaluate the effectiveness factor from equation (C.12).

D.2 Isothermal Effectiveness Factor - Orthogonal Collocation Method

The method of orthogonal collocation has been well covered by Finlayson (75) and Villadsen and Michelsen (204). However, a brief description is presented in this section in order to facilitate the understanding of the method.

The collocation method is a special method of the general method of weighted residuals (MWR). The solution of the differential equations is expanded in a set of specified trial functions. The differential equation is satisfied exactly at n_i collocation points, " y_i ", and the residual at other points approaches zero in the limit as $n_i \rightarrow \infty$.

In the orthogonal collocation method the collocation points are taken as the roots to orthogonal polynomials. Villadsen and Stewart (203) choose the trial functions to be sets of orthogonal polynomials which satisfied the boundary

conditions and the roots to the polynomials gave the collocation points.

A brief description of the orthogonal collocation technique applicable to solution of equations (D.1) to (D.3) is presented below.

Let a function Ψ be approximated by a trial function,

$$\Psi\{y\} = 1 + (1-y^2) \sum_{i=1}^{n_i} a_i P_{i-1}\{y^2\} \quad (D.7)$$

The function $\Psi\{y\}$ defined by (D.7) is symmetric about $y=0$ and has the value of unity when $y=1$. That is, it automatically satisfies the boundary conditions (D.2) and (D.3). The parameter n_i is the total number of interior collocation points. The orthogonal polynomials in (D.7) are defined by,

$$\int_0^1 w\{y^2\} P_j\{y^2\} P_i\{y^2\} y^{m-1} dy = 0 \quad ; \quad j=1, \dots, i-1 \quad (D.8)$$

where $m=1,2,3$, for planar, cylindrical, or spherical geometry. Equation (D.7) can be substituted into the differential equation to form the residual, which is set equal to zero at the n_i interior collocation points y_j - the roots to the n_i -th polynomial.

Finlayson's approach is not to solve for the constants but for Ψ at the collocation point. Equation (D.7) can be written as,

$$\Psi(y) = \sum_{i=1}^{ni+1} d_i y^{2i-2} \quad (D.9)$$

where the $(ni+1)$ -th point is the boundary point. Taking the first and second derivative of this expression and evaluating them at the collocation points gives,

$$\Psi\{y_j\} = \sum_{i=1}^{ni+1} d_i y_j^{2i-2} \quad (D.10)$$

$$\frac{d\Psi}{dy} \{at\ y=y_j\} = \sum_{i=1}^{ni+1} (2i-2) y_j^{2i-3} d_i \quad (D.11)$$

$$\nabla^2 \Psi \{at\ y=y_j\} = \sum_{i=1}^{ni+1} d_i \nabla^2 \{y^{2i-2}\} \quad (D.12)$$

writing the above equation in the matrix notation yields,

$$\underline{\Psi} = \underline{Q} \underline{d} \quad (D.13)$$

$$d\underline{\Psi}/dy = \underline{C} \underline{d} \quad (D.14)$$

$$\nabla^2 \underline{\Psi} = \underline{D} \underline{d} \quad (D.15)$$

where

$$Q_{ji} = y_j^{2i-2} \quad (D.16)$$

$$C_{ji} = (2i-2) y_j^{2i-3} \quad (D.17)$$

$$D_{ji} = \nabla^2 (y^{2i-2}) \{at\ y=y_j\} \quad (D.18)$$

For spherical coordinates, where

$$\nabla^2 = 1/y^2 d/dy (y^2 d/dy)$$

D_{ji} becomes,

$$D_{ji} = (2i-2)(2i-1)y_j^{2i-4} \quad (D.19)$$

From equation (D.13)

$$\underline{d} = Q^{-1} \underline{\Psi} \quad (D.20)$$

substituting \underline{d} in equations (D.14) and (D.15) yields,

$$d\underline{\Psi}/dy = C Q^{-1} \underline{\Psi} \equiv A \underline{\Psi} \quad (D.21)$$

$$\nabla^2 \underline{\Psi} = D Q^{-1} \underline{\Psi} \equiv B \underline{\Psi} \quad (D.22)$$

As the collocation points y_j are known, matrices Q , C , and \underline{d} can be evaluated and hence A and B are determined. The derivatives in a differential equation whose solution is to be found can be replaced by equations (D.21) and (D.22). This treatment converts the differential equation into a set of algebraic equations whose solution provides Ψ at the collocation points. Thus equation (D.1) can be written as,

$$\sum_{i=1}^{n_i+1} B_{ji} \Psi_i - 9 \phi^2 R c_j \equiv 0 \quad (D.23)$$

$$j = 1, 2, \dots, n_i$$

Substitution of $d\Psi/dy$ in equation (4.20) yields the effectiveness factor as,

$$\eta = \left(1/3\phi^2 \right) \sum_{i=1}^{n_i+1} A_{n_i+1,i} \Psi_i \quad (D.24)$$

The "ORTHOGONAL" computer program evaluates the matrices A and B .

D.2.1 Application of Orthogonal Collocation to a Claus Pellet.

The following illustrates the method of orthogonal collocation when it is applied to the Claus reaction. For the purpose of illustration, only two interior points are considered. The computer program "ORTEFF" is however, written for an arbitrary number of interior points. Equation (D.23) for $n_i=2$ gives,

$$B_{11} \psi_1 + B_{12} \psi_2 + B_{13} \psi_3 - 9 \phi^2 R_{c1} = 0 \quad (D.25)$$

$$B_{21} \psi_1 + B_{22} \psi_2 + B_{23} \psi_3 - 9 \phi^2 R_{c2} = 0 \quad (D.26)$$

where ψ_3 by equation (D.2) is equal to unity. Thus,

$$B_{11} \psi_1 + B_{12} \psi_2 + B_{13} - 9 \phi^2 R_{c1} = 0 \quad (D.27)$$

$$B_{21} \psi_1 + B_{22} \psi_2 + B_{23} - 9 \phi^2 R_{c2} = 0 \quad (D.28)$$

To evaluate R_{c1} and R_{c2} , the partial pressures of different species involved in the rate expression should be specified at the interior points 1 and 2. Writing the equations (D.4) and (D.5) at the interior point $j=1,2$ yields,

$$P_i^j = P_{i,1}^j + (a_i/a_1)(De_1/De_i)(P_{1,1}^j - P_{i,1}^j) \quad (D.29)$$

$$i = 2,3$$

$$j = 1,2$$

$$W_i^j = W_{i,1}^j + 6(a_s/a_1)(De_1/De_s)(P_{1,1}^j - P_{i,1}^j) \quad (D.30)$$

where

$$P_i = P_{i,1} \Psi_i \quad (D.31)$$

and W_i is a function of P_i as given in equation (4.32).

The simultaneous solution of (D.27), (D.28), (D.29) and (D.30) yields Ψ_1 and Ψ_2 from which values the effectiveness factor can be calculated by equation (D.24).

D.2.2 Orthogonal Collocation For Large ϕ .

When the Thiele modulus is large, the solution Ψ has a steep gradient near the pellet surface, then a large number of collocation points is needed for accurate calculation of η .

For large values of ϕ , Paterson and Cresswell (162) developed the effective reaction zone method and applied the orthogonal collocation method. In their proposal, it was assumed that at some point within the catalyst pellet Y_I , the concentration of a reactant drops to a zero value for an irreversible reaction, or correspondingly to an equilibrium value for a reversible reaction.

The Paterson and Cresswell model is

$$\Psi \text{ given by (D.1)} \quad \text{for} \quad y > Y_I \quad (D.32)$$

$$\Psi = d\Psi/dy = 0 \quad \text{for} \quad y \leq Y_I \quad (D.33)$$

A new variable

$$x = \frac{y - YI}{1 - YI} \quad (D.34)$$

is introduced in the equation (D.1).

$$\frac{d^2\psi}{dx^2} + \frac{2(1-YI)}{YI + (1-YI)x} \frac{d\psi}{dx} - 9\phi^2(1-YI)^2 R_c = 0 \quad (D.35)$$

The appropriate boundary condition using (D.32) would be,

$$\psi = 1 \quad \text{at} \quad x = 1 \quad (D.36)$$

$$\psi = d\psi/dx = 0 \quad \text{at} \quad x = 0 \quad (D.37)$$

Paterson and Cresswell developed the equations for the orthogonal collocation method using an arbitrary n_i interior points. They, however used only one interior point to obtain the solution of equation (D.34).

It will be shown here, that the method of orthogonal collocation applied to the reaction interphase model of Paterson and Cresswell yields a real solution only when one interior point is considered. To illustrate this point a slab geometry with a first order reaction is considered. The material balance equation for such a system yields,

$$d^2\psi/dy^2 - \phi^2 \psi = 0 \quad (D.38)$$

which upon introduction of x yields,

$$d^2\Psi/dx^2 - \phi^2 (1 - YI)^2 \Psi = 0 \quad (D.39)$$

With two interior points, equation (D.9) using the boundary conditions (D.36) and (D.37) gives,

$$\Psi = d_2 (x^2 - x^4) + x^4 \quad (D.40)$$

Evaluation of the $d^2\Psi/dx^2$ from (D.40) at the interior points x_1 and x_2 and substitution into equation (D.39) yields,

$$\begin{aligned} d_2 (2 - 12x_j^2) + 12x_j^4 - \\ \phi^2 (1 - YI)^2 [x_j^4 + d_2 (x_j^2 - x_j^4)] = 0 \end{aligned} \quad (D.41)$$

$j = 1, 2$

Solution of the two equations in (D.41) yields,

$$a d_1^2 + b d_2 + c \equiv 0 \quad (D.42)$$

where

$$\begin{aligned} a &= (x_1^2 - x_2^2) (2 - 12x_2^2) - (2 - 12x_1^2) (x_2^2 - x_1^2) \\ b &= x_1^4 (2 - 12x_2^2) + 12x_2^4 (x_1^2 - x_1^4) - x_2^4 (2 - 12x_1^2) \\ &\quad - 12x_1^4 (x_2^2 - x_2^4) \\ c &= 12x_1^4 x_2^2 - 12x_1^2 x_2^4 \end{aligned}$$

Equation (D.42) has a real solution if

$$\Delta^2 = b^2 - 4ac \geq 0 \quad (D.43)$$

Table D.1 shows that Δ^2 is negative irrespective of the orthogonal polynomial chosen. Thus, there is no real solution when orthogonal collocation with more than one interior point is used with the reaction zone method. The reaction zone method of Paterson and Cresswell is only applicable with One-Point-Collocation.

Villadsen and Michelsen (204) have shown that reaction zone Collocation gives accurate results if the collocation point is correctly chosen. According to them, the collocation point should be chosen equal to $(n+1)^{-1/2}$ where n is the order of reaction - or increasing toward one when n increases from zero to infinity.

Equation (D.9) with one interior collocation point yields,

$$\Psi(x) = d_1 + d_2 x^2 \quad (D.44)$$

The coefficients d_1 and d_2 are determined from the boundary conditions (D.36) and (D.37) which gives,

$$\Psi(x) = x^2 \quad (D.45)$$

At the collocation point ξ_1 , equation (D.35)

Table D.1' Effective Reaction Zone With 2 interior points.

Orthogonal Polynomial	x_1, x_2	Δ^2
Legandre	0.33998, 0.86113	-2.073
Jacobi	0.28523, 0.76505	-0.9096
Chebyshev	0.45970, 0.88810	-4.00

using (D.45) yields,

$$2 + \frac{4(1-YI)\xi_1}{YI + (1+YI)\xi_1} - 9\phi^2(1-YI)^2 R = 0 \quad (D.46)$$

Equation (D.46) is a third-degree polynomial in YI which should be solved numerically. The effectiveness factor is found in the usual way from equation (4.20).

$$\begin{aligned} \eta &= \frac{1}{3\phi^2} \left(\frac{d\Psi}{dy} \right)_{y=1} \\ &= \frac{1}{3\phi^2 (1-YI)} \left[\frac{d\Psi}{dx} \right]_{x=1} \\ &= \frac{2}{3\phi^2 (1-YI)} \end{aligned} \quad (D.47)$$

When YI has been determined from (D.46), η is immediately available from (D.47).

The Claus reaction is not a simple n -th order reaction, thus the correct position of the collocation point is not known using the criterion of Villadsen and Michelsen (204).

The following computational procedure was used for calculating Claus reaction effectiveness factor for large ϕ using the explicit collocation method,

1. Choose ξ_1 = zero of Jacobi polynomial.
2. Calculate $\Psi\{\xi_1\} = \xi_1$.
3. Calculate P_2, P_3, P_4, P_1 from (D.29), (D.30), and (D.31).
4. Calculate $Rc\{\xi_1\}$ using the data from step (3).
5. Estimate the order of reaction (n) by using,

$$Rc\{\xi_1\} = \Psi^n\{\xi_1\}$$

6. Estimate optimum value of the collocation point from,

$$\xi\{\text{opt}\} = (n+1)^{-1/2}$$

7. Calculate $Rc\{\xi(\text{opt})\}$ using steps (2) to (4).
8. Evaluate YI by solution of (D.46).
9. Calculate effectiveness factor from (D.47).

The above scheme has been used in "ORTEFF" program for when the Thiele modulus is large. The flowchart of this program is shown in figure D.1.

D.3 Thiele Modulus of the Claus Reaction

The following, shows the typical value of ϕ calculated at the inlet condition of the first convertor. The rate of reverse reaction is neglected due to low sulfur pressure at the inlet of the bed. Thus from equation (2.10),

$$\begin{aligned}
 R_{c_1} &= R_1/2 \\
 &= (0.92/2) \text{ EXP } (-3700/535) \\
 &\quad * \frac{0.07 * \sqrt{0.035} * 760^{1.5}}{(1 + 0.006 * 0.255 * 760)^2} \quad (D.48) \\
 &= 0.027 \text{ mol/g h} \equiv 0.74 * 10^{-5} \text{ mol/g s}
 \end{aligned}$$

and ϕ from equation 4.35,

$$\begin{aligned}
 \phi &= 0.6/6 \sqrt{[2 * 1.53 * 82.06 * 535 * 0.74 * 10^{-5} / (0.00365 * 0.07)]} \\
 &= 6.25
 \end{aligned}$$

D.4 Local Effectiveness Factor Estimation

It was shown in section 4.3 that, the use of the modified Thiele modulus greatly reduces the variation of η with X_s and T_s . Thus a single η -plot may be used to calculate local values of η for the Claus catalytic bed.

The following algorithm is useful in estimating the point values of the Claus pellet effectiveness factor in the catalytic convertors,

1. Given the feed composition, generate plot of η vs Φ , assuming an average value of X_s and T_s .
2. Use natural spline (87), to specify the interpolating formula for plot of $\ln(\eta)$ vs $\ln(\Phi)$ - natural spline is used because the plot of $\ln(\eta)$ is linear at the low and high levels of $\ln(\Phi)$.
3. Calculate local values of Ψ_e , ϕ , and hence Φ in the Claus bed.

4. Calculate local value of η from the interpolation formula for the calculated local value of Φ .

```

C .....
C                               MAINLINE ISOEFF
C
C THIS PROGRAM CALCULATES THE ISOTHERMAL EFFECTIVENESS
C FACTOR FOR CLAUS REACTION. IT USES CHANGE OF VARIABLE
C
C TO CONVERT BOUNDARY VALUE PROBLEM TO OPEN-ENDED
C INITIAL VALUE PROBLEM. INTEGRATION IS BY RUNG-KUTTA
C -FEHLBERG METHOD. MATHEMATICS OF THE PROGRAM HAS
C DESCRIBED IN CHAPTER 4. THE INPUTS ARE:
C
C   T=TEMP( K)
C   YH2S= MOLE FRACTION OF H2S IN THE FEED
C   YSO2= MOLE FRACTION OF SO2 IN THE FEED
C   YH2O= MOLE FRACTION OF H2O IN THE FEED
C   YN2 = MOLE FRACTION OF N2
C   XS  =CONVERSION OF H2S AT THE SURFACE
C   NOPT= OPTION NUMBER , 1 ;SLAB , 2 ;SPHERICAL PELLET
C   AH  =ARBITRARY VALUE OF THIELE*A
C   Y0  =CONVERSION OF H2S AT THE CENTER OF THE
C         PELLET , , ASSUMED VALUE
C
C THE OUTPUTS ARE:
C
C   Z   =Y/A WHERE Y IS THE DIMENSIONLESS LENGTH
C   Y1  =C/CS WHERE C IS CONCENTRATION OF H2S
C   Y2  =D(C/CS)/DZ
C   THIELE MODULUS
C   EFFECTIVENESS FACTOR
C   NOTE: THE SUBROUTINE COTM CALLS IMSL LIB
C         SUBROUTINE. HENCE ADD +*IMSLDPLIB WHEN
C         RUNNING THE PROGRAM. ALSO IT USES THERMODYNAMIC
C         DATA FILE , SO ASSIGN 7=DATA2.
C .....
C   IMPLICIT REAL*8(A-H,O-Z,$)
C   DIMENSION X(2),Y(2),PARA(5),F(2,1)
C   COMMON RATE,RATES,YH2S,YSO2,YH2O,YN2,T,XS,XE
C   #,TMS,TM,X,CONV,AH,PRESS,PARA
C   COMMON NCALL,NOPT
C   EXTERNAL FUN,FUN1,DF1,DF2
C   NCALL=1
C   WRITE(6,11)
C   FORMAT(5X,'TYPE OPTION : 1=SLAB , 2=SPHERE')
C   CALL FREAD(5,'I:',NOPT)
C   WRITE(6,12)
C   FORMAT(5X,'TYPE TEMP , &PRESS')
C   CALL FREAD(5,'2R*8 :',T,PRESS)
C   WRITE(6,13)
C   FORMAT(5X,'TYPE MOLE FRAC. OF H2S,SO2,H2O,N2',/,
C   #5X,'AND CONVERSION AT THE SURFACE ')
C   FORMAT(5E12.5)
C   CALL FREAD(5,'6R*8:',YH2S,YSO2,YH2O,YN2,XS,XE)
C   RLK62=-34173./T+37.9735

```

```

RLK64=-13663.9/T+12.6028
RLK68=2932./T-3.43174
RLK=11050.1/T-11.5576
RK=DEXP(RLK)
RK62=DEXP(RLK62)
RK64=DEXP(RLK64)
RK68=DEXP(RLK68)
AA=(RK62/PRESS/PRESS)**(1./3.)
BB=(RK64/DSQRT(PRESS))**(2./3.)
CC=(RK68*(PRESS**.25))**(4./3.)
WRITE(8,110) AA,BB,CC
110 FORMAT(//,5X,'AA=',D15.7,2X,'BB=',D15.7,2X,'CC='
#,D15.7)
  PARA(1)=AA
  PARA(2)=BB
  PARA(3)=CC
  PARA(5)=RK
  CALL COTM(Y)
  WRITE(8,2)
2  FORMAT(//,2X,'TYPE STARTING POINT OF INTEGRATION ;'
#,' FOR CONVERSIONS AT THE STARTING POINT LESS THAN'
#,' EQUILIBRIUM OR EQUILIBRIUM LET Z=0.0 ;'
#,'/,2X,' THIS WILL GIVE YOU THIELE MODULUS UP TO'
#,' ABOUT 4.5 ; FOR LARGER THIELE MODULUS THE'
#,' CONVERSION REACHES EQUILIBRIUM AT',/,2X,
#,' LARGER VALUE OF Z I.E. BEYOND THE CENTER OF'
#,' CATALYST ; HENCE LET Z BE SOME POSITIVE VALUE'
#,' AND LET THE CONVERSION AT THIS',/,2X,
#,' Z BE VERY NEAR TO EQUILIBRIUM CONVERSION SUCH'
#,' THAT THE RATE IS IN ORDER OF .1E-13 OR LESS.'
#,'/,2X,' A SMALL POSITIVE NUMBER IS REQUIRED'
#,' FOR START OF INTEGRATION .')
1  FORMAT(//,7X,'X/A=Z',10X,'Y(1)',10X,'Y(2)',/,)
  DO 100 KK=1,20
  WRITE(6,4)
4  FORMAT(/,5X,'TYPE THE INITIAL POINT OF INTEGRATION ')
270 CALL FREAD(5,'R*8:',Z)
  NCALL=2
  WRITE(6,3)
3  FORMAT(5X,'TYPE A*THIELE, CONVERSION AT THE CENTER'
#,' AND MAX.INTG.STEP.')
  CALL FREAD(5,'3R*8:',AH,CONV,HMX)
  WRITE(8,4)
  WRITE(8,111) YH2S,YSO2,YH2O,YN2,XS,T,AH,CONV,Z
111 FORMAT(///,5X,'YH2S=',F7.3,5X,'YSO2=',F7.3,5X,'YH2O='
#,F7.3,5X,'YN2=',F7.3,
#,'/,5X,' XS =',F7.3,5X,' T =',F7.2,5X,' AH =',F7.3,
#5X,' CONV=',D18.9,/,5X,' Z INITIAL=',F9.5)
  WRITE(8,1)
  CALL COTM(Y)
  IF(RATE) 250,200,200
200 Y(1)=(1.-CONV)/(1.-XS)*TMS/TM
  Y(2)=0.0
  H=.1

```

```

100 CALL RKF(Z,Y,2,FUN,1.D3,H,HMX,.1D-06,.1D-06,IFLAG)
    CONTINUE
250 IF(KK.EQ.20) GO TO 280
    WRITE(6,260) CONV,RATE
260 FORMAT('/', ' RATE IS NEGATIVE , TRY DIFFERENT ',
# 'INITIAL VALUE',2D16.8)
    GO TO 270
280 STOP
    END

```

```

C
C
C.....
C..          SUBROUTINE FUN
C..  THIS SUBROUTINE EVALUTES THE VALUE OF
C.. DERIVATIVES TO BE USED BY RKF FOR INTEGRATION
C.....
C

```

```

SUBROUTINE FUN(Z,Y,YP)
  IMPLICIT REAL*8(A-H,O-Z,$)
  DIMENSION Y(1),PARA(5),X(2),YP(1)
  COMMON RATE,RATES,YH2S,YSO2,YH2O,YN2,T,XS,XE
  #,TMS,TM,X,CONV,AH,PRESS,PARA
  COMMON NCALL,NOPT
  IF(NCALL.EQ.2) GO TO 1
  CALL COTM(Y)
1  RATER=RATE/RATES
  NCALL=NCALL+1
  YP(1)=Y(2)
  IF(NOPT-1) 2,2,3
2  YP(2)=(AH**2)*RATER
  GO TO 6
3  IF(Z) 4,4,5
4  YP(2)=3.*(AH**2)*RATER
  GO TO 6
5  YP(2)=9.*(AH**2)*RATER-2./Z*Y(2)
6  RETURN
  END

```

```

C
C
C.....
C.....          SUBROUTINE OUTP
C..... THIS SUBROUTINE CONTROLS THE INTEGRATION
C..... LENGTH BY CHECKING THE VALUE OF Y1 TO
C..... BE LESS THAN ONE.
C.....
C

```

```

SUBROUTINE OUTP(Z,Y,PAR)
  IMPLICIT REAL*8(A-H,O-Z,$)
  DIMENSION Y(2),PARA(5),X(2)
  COMMON RATE,RATES,YH2S,YSO2,YH2O,YN2,T,XS,XE
  #,TMS,TM,X,CONV,AH,PRESS,PARA
  COMMON NCALL,NOPT
C  WRITE(8,1) Z,Y(1),Y(2)
1  FORMAT(5X,3(D12.5,3X))
  IF(1.-Y(1)) 2,3,4

```

```

2  Y(2)=Y2+(Y(2)-Y2)*(1.-Y1)/(Y(1)-Y1)
   Z=ZZ+(Z-ZZ)*(1.-Y1)/(Y(1)-Y1)
3  THIM=AH*Z
   EFFEC=Z*Y(2)/THIM**2
   IF(NOPT.GT.1) EFFEC=EFFEC/3.
   WRITE(8,5) THIM,EFFEC
5  FORMAT(/,5X,'THIM=',D14.7,5X,'EFFEC=',D14.7,/)
   PAR=1.
   ZZ=0.
   Y1=0.
   Y2=0.
   GO TO 6
4  ZZ=Z
   Y1=Y(1)
   Y2=Y(2)
6  RETURN
   END

C
C
C.....
C.....      SUBROUTINE COTM      ....
C.....  THIS SUBROUTINE CALCULATES MOLES OF S2      ....
C.....  AND TOTAL MOLES FOR ANY CONVERSION OF      ....
C.....  H2S OR C/CS. THEN IT WOULD CALCULATES T      ....
C.....  THE RATE OF REACTION.      ....
C.....
C
C      SUBROUTINE COTM(Y)
C      THIS SUBROUTINE SOLVES A SYSTEM OF TWO NONLINEAR
C      EQ S BY NEWTONS S METHOD.
      IMPLICIT REAL*8(A-H,O-Z,$)
      DIMENSION FSAVE(2),X(2),F(2,1),DF(2,2),WKAREA(12)
      #,XSAVE(2),Y(2),PARA(5)
      COMMON RATE,RATES,YH2S,YSO2,YH2O,YN2,T,XS,XE
      #,TMS,TM,X,CONV,AH,PRESS,PARA
      COMMON NCALL,NOPT
      M=1
      N=2
      IA=2
      IDGT=0
      MAXIT=50
      FTOL=.1D-11
      XTOL=.1D-11
      IF(NCALL.GT.2) GO TO 33
111  CONTINUE
      X(2)=.98D00
      X(1)=.02D00
      IF(NCALL.EQ.1) CONV=XS
33   DO 100 I=1,MAXIT
      DO 10 J=1,2
10   XSAVE(J)=X(J)
      IF(NCALL.LE.2) GO TO 34
      CONV=1.0-Y(1)*(1.-XS)*X(2)/TMS
1   FORMAT(45X,D12.5,3X,D12.5,2X,I5)

```



```

34  PARA(4)=YH2S*CONV
    F(1,1)=FUN1(X,1,PARA)
    F(2,1)=FUN1(X,2,PARA)
36  FORMAT(/,'FFFF',2D18.9)
    ITEST=0
    DO 20 J=1,2
      IF(DABS(F(J,1)).GT.FTOL) ITEST=ITEST+1
      FSAVE(J)=F(J,1)
      F(J,1)=-F(J,1)
20  CONTINUE
    IF(ITEST.NE.0) GO TO 30
    GO TO 200
30  DF(1,1)=DF1(X,1,PARA)
    DF(1,2)=DF2(X,1,PARA)
    DF(2,1)=DF1(X,2,PARA)
    DF(2,2)=DF2(X,2,PARA)
48  FORMAT(/,'DF',4D16.6)
49  FORMAT(/,'X F',4D16.6)
    IF(NCALL-2) 40,40,35
35  DF(1,2)=DF(1,2)+0.5*YH2S*Y(1)*(1.-XS)/TMS/X(2)/X(2)
    DF(2,2)=DF(2,2)+1.5*YH2S*Y(1)*(1.-XS)/TMS/X(2)/X(2)
40  DF(1,2)=DF(1,2)/DF(1,1)
    F(1,1)=F(1,1)/DF(1,1)
    DF(1,1)=DF(1,1)/DF(1,1)
    DF(2,2)=DF(2,2)/DF(2,1)
    F(2,1)=F(2,1)/DF(2,1)
    DF(2,1)=DF(2,1)/DF(2,1)
    CALL LEQT1F(DF,M,N,IA,F,IDGT,WKAREA,IER)
C
C... RELAXATION FACTOR OF .5 HAS BEEN USED TO INSURE
C... THE CONVERGENCE OF N-R METHOD TO CORRECT VALUES.
C
    X(1)=XSAVE(1)+1.*F(1,1)
    X(2)=XSAVE(2)+1.*F(2,1)
    ITEST=0
    DO 50 JJ=1,2
      IF(DABS(F(JJ,1)).GT.XTOL) ITEST=ITEST+1
50  CONTINUE
C  IF XTOL MET PRINT THE RESULT
    IF(ITEST.EQ.0) GO TO 200
100 CONTINUE
    WRITE(8,400)
400  FORMAT(/,'CONVERGENCE WAS NOT ACHIEVED AFTER '
      #,'50 ITER.')
```

```

200  A1=2.56D-04*DEHP(-7350./1.986/T)
    A2=0.006D00
    TM=X(2)
    H2S=YH2S*(1.-CONV)
    PPH2S=H2S/TM*PRESS*760.
    SO2=YSO2-YH2S*CONV/2.
    PPSO2=SO2*PRESS*760./TM
    H2O=YH2O+YH2S*CONV
    PPH2O=H2O*PRESS*760./TM
```

```

PPS6=X(1)/TM*PRESS*760.
EQK=PARA(5)/DSQRT(760.D00)
RATE=A1/((1.D00+A2*PPH20)**2)
RATE=RATE*(PPH2S*DSQRT(PPSO2)-PPH20/DSQRT(EQK)*
#(PPS6**.25))

```

```

C
C... IN THE ABOVE LINE SQRT(760.) HAS BEEN MULTIPLIED
C... BY RK12 ; BECAUSE PARTIAL PRESSURE IN THE RATE EQ'N
C... ARE IN MM HG WHILE RK12 IS IN UNITE OF (ATM)**.5
C

```

```

C      IF(NCALL.GT.1) GO TO 500
C      TMS=TM
C      RATES=RATE
2      FORMAT(5(D12.5,3X))
3      FORMAT(I10)
500     RETURN
C      END
C

```

```

C      SUBROUTINE RKF(A,Y,N,FUN,DA,H,HMX,ABSER,RELER,IFLAG)
C
C      THIS SUBROUTINE IS PRINTED IN "NONISOEFF".
C
C

```

```

C      FUNCTION FUN1(X,K,PARA)
C      IMPLICIT REAL*8(A-H,O-Z,$)
C      DIMENSION X(2),PARA(5)
C      COMMON /VAR/ P1,P2,P3,P4,P5,P6,P7
C      P1=(X(1)*X(2)*X(2))**(1./3.)
C      P2=(X(1)*X(1)*X(2))**(1./3.)
C      P3=((X(1)**4)*X(2))**(1./3.)
C      P4=(X(2)/X(1))**(2./3.)
C      P5=DSQRT(P4)
C      P6=(X(1)*X(2))**(1./3.)
C      P7=P3/X(2)
C      GO TO (5,10) , K
5      FUN1=1.-.5*PARA(4)+PARA(1)*P1+PARA(2)*P2+X(1)+
#PARA(3)*P3-X(2)
C      RETURN
10     FUN1=2.*PARA(1)*P1+4.*PARA(2)*P2+6.*X(1)+8.*
#PARA(3)*P3-1.5*PARA(4)
C      RETURN
C      END
C

```

```

C      FUNCTION DF1(X,K,PARA)
C      IMPLICIT REAL*8(A-H,O-Z,$)
C      DIMENSION X(2),PARA(5)
C      COMMON /VAR/ P1,P2,P3,P4,P5,P6,P7
C      GO TO (5,10) , K
5      DF1=PARA(1)*P4/3+2*PARA(2)*P5/3+1+4/3*PARA(3)*P6
C      RETURN
10     DF1=2/3*PARA(1)*P4+8/3*PARA(2)*P5+6+32/3*PARA(3)*P6
C      RETURN

```

END

C
C

FUNCTION DF2(X,K,PARA)
IMPLICIT REAL*8(A-H,O-Z,\$)
DIMENSION X(2),PARA(5)
COMMON /VAR/ P1,P2,P3,P4,P5,P6,P7
GO TO (5,10), K
5 DF2=2./3.*PARA(1)/P5+PARA(2)/3./P4+PARA(3)*P7/3.-1.
RETURN
10 DF2=4/3*PARA(1)/P5+4/3*PARA(2)/P4+8*PARA(3)*P7/3
RETURN
END

MAINLINE ORTHOGONAL

THIS PROGRAM CALCULATES THE A, B1, AND B MATRICES.
THIS CALCULATION IS DESCRIBED IN APPENDIX D.
B1 IS WHEN D/DX(D/DX) IS CALCULATED WHILE B
IS WHEN DIVERGENCE IS CALCULATED.

```

IMPLICIT REAL*8(A-H,O-Z,$)
DIMENSION A(10,10),B(10,10),C(10,10),D(10,10),Q(10,10)
$,QI(10,10),D1(10,10),B1(10,10),V(100),X(10)
#,WKAREA(130),FO(10),W(10)

```

```

CALL FREAD(5,'I:',N)

```

```

READ THE GEOMETRY SPECIFICATION,
S=1 SLAB, S=2 CYLINDRICAL, S=3 SPHERICAL

```

```

CALL FREAD(5,'R*8:',S)

```

```

READ X VECTOR , THE ZEROS OF LEGANDRE POLYNOMINAL.

```

```

N2=N+1
READ (5,170) (X(LL),LL=1,N2)
WRITE(6,100) N

```

```

CALCULATE THE Q,C,D MATRIXS

```

```

DO 20 I=1,N2
DO 20 J=1,N2
Q(J,I)=X(J)**(2*I-2)
C(J,I)=(2*I-2)*(X(J)**(2*I-3))
D(J,I)=(2*I-2)*(2*I-4+S)*(X(J)**(2*I-4))
D1(J,I)=(2*I-2)*(2*I-3)*(X(J)**(2*I-4))
CONTINUE

```

```

CALCULATE Q INVERSE USING IMSLLIB.

```

IN ORDER TO USE VARIABLE DIMENSION,
VECTOR NOTATION HAS BEEN USED IN THE FOLLOWINGS.

```

DO 30 I=1,N2
DO 30 J=1,N2
K=I+N2*(J-1)
V(K)=Q(I,J)
CONTINUE
CALL REC(Q,V,N2,QI)
DO 50 I=1,N2
DO 50 J=1,N2
K=I+N2*(J-1)
QI(I,J)=V(K)
CONTINUE

```

```

DO 51 I=1,N2
  ZI=2.*FLOAT(I)-2.+S
  FO(I)=1.D00/ZI
  WRITE(8,1) FO(I)
51 CONTINUE
C
DO 52 I=1,N2
  W(I)=0.0D00
  DO 52 K=1,N2
    W(I)=W(I)+FO(K)*QI(K,I)
52 CONTINUE
  CALL MMPL(C,QI,A,N2,N2,N2)
  WRITE(8,1) A(1,1)
1  FORMAT(D18.10)
  CALL MMPL(D,QI,B,N2,N2,N2)
  WRITE(8,1) B(1,1)
  CALL MMPL(D1,QI,B1,N2,N2,N2)
  WRITE(8,1) B1(1,1)
C
  WRITE(6,200)
200 FORMAT(//,5X,'COLLOCATION ABSCISSAS',/)
  WRITE(6,210) (X(MN),MN=1,N2)
210 FORMAT(10D18.10)
  WRITE(6,120)
  DO 60 I=1,N2
60  WRITE(6,150) (QI(I,J),J=1,N2)
  WRITE(6,130)
  DO 70 I=1,N2
70  WRITE(6,150) (A(I,J),J=1,N2)
  WRITE(6,140)
  DO 80 I=1,N2
80  WRITE(6,150) (B(I,J),J=1,N2)
  WRITE(6,160)
  DO 90 I=1,N2
90  WRITE(6,150) (B1(I,J),J=1,N2)
  WRITE(6,220)
  WRITE(6,210) (FO(I),I=1,N2)
  WRITE(6,230)
  WRITE(6,210) (W(I),I=1,N2)
  STOP
100 FORMAT(///,5X,'NUMBER OF INTERIOR POINTS=',I2)
120 FORMAT(///,5X,'MATRIX QINV',/)
130 FORMAT(///,5X,'MATRIX A',/)
140 FORMAT(///,5X,'MATRIX B',/)
150 FORMAT(10X,10D18.10)
160 FORMAT(///,5X,'MATRIX B1',/)
170 FORMAT(5D18.10)
220 FORMAT(///,5X,'F VECTOR')
230 FORMAT(///,5X,'W VECTOR')
END
C
SUBROUTINE MMPL(A,B,C,L,M,N)
  IMPLICIT REAL*8(A-H,O-Z,$)

```

```

      DIMENSION A(10,10),B(10,10),C(10,10)
      WRITE(8,1) (A(I,I),I=1,3)
1     FORMAT(3F10.5)
      DO 20 J=1,N
      DO 20 I=1,L
      C(I,J)=0.D00
      DO 10 K=1,M
      C(I,J)=C(I,J)+A(I,K)*B(K,J)
10    CONTINUE
20    CONTINUE
      RETURN
      END

C
C
      SUBROUTINE REC(F,V,N,FINV)
      IMPLICIT REAL*8(A-H,O-Z,$)
      DIMENSION F(N,N),V(30), FINV(N,N),WKAREA(100)
      DO 40 I=1,N
      DO 40 J=1,N
      K=I+N*(J-1)
40    F(I,J)=V(K)
      WRITE(6,100) N.
100   FORMAT(I5)
200   FORMAT(10 F10.4)
      IA=N
      IDGT=0
      CALL LINV2F(F,N,IA,FINV,IDGT,WKAREA,IER)
      DO 400 I=1,N
      DO 400 J=1,N
      K=I+N*(J-1)
400   V(K)=FINV(I,J)
      RETURN
      END

```

Table D-2 Output of "ORTHOGONAL" program for spherical coordinates using 1 to 6 interior points.

NUMBER OF INTERIOR POINTS= 1

COLLOCATION ABSCISSAS

0.7745966692E+00 0.1000000000E+01

MATRIX QINV

0.250000E+01	-0.150000E+01
-0.250000E+01	0.250000E+01

MATRIX A

-0.387298E+01	0.387298E+01
-0.500000E+01	0.500000E+01

MATRIX B

-0.150000E+02	0.150000E+02
-0.150000E+02	0.150000E+02

MATRIX B1

-0.500000E+01	0.500000E+01
-0.500000E+01	0.500000E+01

Table D.2 continued.

NUMBER OF INTERIOR POINTS= 2

COLLOCATION ABSCISSAS

0.5384693101E+00 0.9061798495E+00 0.1000000000E+01

MATRIX QINV

0.2177062574E+01 -0.3052062656E+01 0.1875000082E+01
 -0.4828260250E+01 0.1357826062E+02 -0.8750000367E+01
 0.2651197677E+01 -0.1052619796E+02 0.7875000284E+01

MATRIX A

-0.3544027272E+01 0.8049184963E+01 -0.4505157690E+01
 -0.8593033528E+00 -0.6722341582E+01 0.7581644935E+01
 0.9482702063E+00 -0.1494827061E+02 0.1400000040E+02

MATRIX B

-0.1359530870E+02 0.2042831058E+02 -0.6833001879E+01
 0.1457168997E+02 -0.9140469478E+02 0.7683300481E+02
 0.2405439203E+02 -0.1290543955E+03 0.1050000035E+03

MATRIX B1

-0.4319688219E+00 -0.9468230637E+01 0.9900199459E+01
 0.1646823038E+02 -0.7656803385E+02 0.6009980347E+02
 0.2215785162E+02 -0.9915785430E+02 0.7700000268E+02

Table D.2 continued

NUMBER OF INTERIOR POINTS= 3

COLLOCATION ABSCISSAS

0.4058451514E+00 0.7415311856E+00 0.9491079123E+00 0.1000000000E+01

MATRIX QINV

0.209160E+01	-0.243862E+01	0.353451E+01	-0.218750E+01
-0.821736E+01	0.19513E+02	-0.314214E+02	0.196875E+02
0.103484E+02	-0.339485E+02	0.669125E+02	-0.433125E+02
-0.422269E+01	0.164358E+02	-0.390256E+02	0.268125E+02

MATRIX A

-0.418186E+01	0.820264E+01	-0.101910E+02	0.617023E+01
-0.989277E+00	-0.367021E+01	0.100343E+02	-0.537484E+01
0.279030E+00	-0.227802E+01	-0.111486E+02	0.131476E+02
-0.377090E+00	0.272361E+01	-0.293465E+02	0.270000E+02

MATRIX B

-0.200257E+02	0.266019E+02	-0.125721E+02	0.599590E+01
0.108779E+02	-0.449190E+02	0.517498E+02	-0.177087E+02
-0.677872E+01	0.682366E+02	-0.313055E+03	0.251597E+03
-0.196883E+02	0.131043E+03	-0.489355E+03	0.378000E+03

MATRIX B1

0.582448E+00	-0.138206E+02	0.376490E+02	-0.244109E+02
0.135461E+02	-0.350200E+02	0.246860E+02	-0.321205E+01
-0.736671E+01	0.730370E+02	-0.289562E+03	0.223892E+03
-0.189342E+02	0.125596E+03	-0.430662E+03	0.324000E+03

Table D.2 continued.

NUMBER OF INTERIOR POINTS= 4				
COLLOCATION ABSCISSAS				
O. 3242534234E+00 O. 6133714327E+00 O. 8360311073E+00 O. 9681602395E+00 O. 1000000000E+01				
MATRIX QINV				
O. 205616E+01	-O. 224956E+01	O. 269595E+01	-O. 396349E+01	O. 246094E+01
-O. 126568E+02	O. 292638E+02	-O. 383794E+02	O. 578661E+02	-O. 360937E+02
O. 273890E+02	-O. 838855E+02	O. 138839E+03	-O. 223108E+03	O. 140766E+03
-O. 251303E+02	O. 895293E+02	-O. 175866E+03	O. 312561E+03	-O. 201094E+03
O. 834200E+01	-O. 326580E+02	O. 727111E+02	-O. 143356E+03	O. 949609E+02
MATRIX A				
-O. 498836E+01	O. 936546E+01	-O. 951917E+01	O. 133917E+02	-O. 824963E+01
-O. 115593E+01	-O. 342882E+01	O. 846320E+01	-O. 959694E+01	-O. 571849E+01
O. 323055E+00	-O. 232707E+01	-O. 457122E+01	O. 138289E+02	-O. 725362E+01
-O. 135396E+00	O. 786144E+00	-O. 411984E+01	-O. 169989E+02	O. 204680E+02
O. 196336E+00	-O. 110267E+01	O. 508680E+01	-O. 481805E+02	O. 440000E+02
MATRIX B				
-O. 293168E+02	O. 380222E+02	-O. 138935E+02	O. 111666E+02	-O. 597852E+01
O. 127352E+02	-O. 485888E+02	O. 476969E+02	-O. 230895E+02	O. 112462E+02
-O. 361360E+01	O. 370383E+02	-O. 110325E+03	O. 117187E+03	-O. 402871E+02
O. 481371E+01	-O. 297170E+02	O. 194228E+03	-O. 801769E+03	O. 632445E+03
O. 169890E+02	-O. 932721E+02	O. 395312E+03	-O. 130903E+04	O. 990000E+03
MATRIX B1				
O. 145148E+01	-O. 197440E+02	O. 448209E+02	-O. 771433E+02	O. 449053E+02
O. 165043E+02	-O. 374086E+02	O. 201012E+02	O. 820298E+01	-O. 739987E+01
-O. 438643E+01	O. 426053E+02	-O. 993894E+02	O. 841052E+02	-O. 229346E+02
O. 509340E+01	-O. 313410E+02	O. 202738E+03	-O. 766653E+03	O. 590163E+03
O. 165963E+02	-O. 910667E+02	O. 385138E+03	-O. 121267E+04	O. 902000E+03

Table D.2 continued.

NUMBER OF INTERIOR POINTS= 5

COLLOCATION ABSCISSAS

0.2695431560E+00 0.5190961292E+00 0.7301520056E+00 0.8870625998E+00 0.9782286581E+00 0.1000000000E+01

MATRIX QINV

0.2037997689E+01 -0.2162942475E+01 0.2418252007E+01 -0.2938712492E+01 0.4352436517E+01 -0.2707031246E+01
 -0.1814369689E+02 0.4099976770E+02 -0.5027769183E+02 0.6287617805E+02 -0.9410690068E+02 0.5865234366E+02
 0.5936720926E+02 -0.1758914200E+03 0.2724601707E+03 -0.3657990579E+03 0.5617771599E+03 -0.3519140619E+03
 -0.9123682786E+02 0.3113010627E+03 -0.5667840895E+03 0.8449534367E+03 -0.1352882018E+04 0.8546484361E+03
 0.6681580981E+02 -0.2484069398E+03 0.5062272476E+03 -0.8333290394E+03 0.1410821826E+04 -0.9021289047E+03
 -0.1884049201E+02 0.7416047190E+02 -0.1640438890E+03 0.2942371949E+03 -0.5299625040E+03 0.3444492182E+03

MATRIX A

-0.5855632247E+01 0.1078195199E+02 -0.1019356868E+02 0.1178766135E+02 -0.1714835592E+02 0.1062794350E+02
 -0.1340159180E+01 -0.3600203924E+01 0.8710020950E+01 -0.7960865357E+01 0.1079186162E+02 -0.660654105E+01
 0.3642298992E+00 -0.2503857150E+01 -0.3618269801E+01 0.1032192909E+02 -0.113160697E+02 0.6567573923E+01
 -0.1590533962E+00 0.8642046191E+00 -0.3897865306E+01 -0.5853243543E+01 0.1879109135E+02 -0.9745133722E+01
 0.7865543812E-01 -0.3982388650E+00 0.1428942490E+01 -0.6387677375E+01 -0.2424660309E+02 0.2952492140E+02
 -0.1179654968E+00 0.5894320507E+00 -0.2040146684E+01 0.8016379533E+01 -0.7144769931E+02 0.6499999991E+02

MATRIX B

-0.4103731989E+02 0.5279917004E+02 -0.1794218702E+02 0.1094184208E+02 -0.1093975563E+02 0.6178250415E+01
 0.1604368294E+02 -0.5950341591E+02 0.5621507711E+02 -0.2063322422E+02 0.172582737E+02 -0.9380397283E+01
 -0.3449437419E+01 0.3556712209E+02 -0.8728017341E+02 0.865140057E+02 -0.4189400961E+02 0.2054209779E+02
 0.2114217384E+01 -0.1312046772E+02 0.8695102543E+02 -0.2304844686E+03 0.2356634351E+03 -0.8112374157E+02
 -0.3921085439E+01 0.2035725188E+02 -0.7810479919E+02 0.4371512173E+03 -0.1716694619E+04 -0.1341212034E+04
 -0.1518058076E+02 0.7516708185E+02 -0.2538604543E+03 0.9157208630E+03 -0.2866846906E+04 0.2144999999E+04

MATRIX B1

0.2411249421E+01 -0.2720250505E+02 0.5769370619E+02 -0.7652215832E+02 0.1163003952E+03 -0.7268068749E+02
 0.2120711647E+02 -0.4563236690E+02 0.2265666486E+02 0.1003880321E+02 -0.2432115661E+02 0.1605093897E+02
 -0.4447119809E+01 0.4242557658E+02 -0.8736916920E+02 0.5824103005E+02 -0.1140280811E+02 0.2552490494E+01
 0.2472824311E+01 -0.1506883138E+02 0.9573927849E+02 -0.2172875566E+03 0.1932964334E+03 -0.5915204820E+02
 0.408497407E+01 0.2117145593E+02 -0.8102628892E+02 0.4502108988E+03 -0.1667122153E+04 0.1280847985E+04
 0.19446497E+02 0.7398821775E+02 -0.2497801610E+03 0.8996881040E+03 -0.2723951508E+04 0.2014999997E+04

Table D.2. continued.

NUMBER OF INTERIOR POINTS= 6

COLLOCATION ABSCISSAS

O. 2304583160E+00 O. 4484927510E+00 O. 6423493394E+00 O. 8015780907E+00 O. 9175983992E+00 O. 9841830547E+00 O. 1000000000E+01

MATRIX QINW

O. 2027435202E+01 -O. 2115320306E+01 O. 2284000012E+01 -O. 2584989134E+01 O. 3166680296E+01 -O. 4710423253E+01 O. 2932617182E+01
 -O. 2467697070E+02 O. 5505857339E+02 -O. 6526854264E+02 O. 7611150555E+02 -O. 9440612733E+02 O. 1411600742E+03 -O. 8797851545E+02
 O. 1131892149E+03 -O. 3291415177E+03 O. 4927564410E+03 -O. 618254741E+03 O. 7903808380E+03 -O. 1196736883E+04 O. 7478173814E+03
 -O. 2568483106E+03 O. 8552116692E+03 -O. 1495990863E+04 O. 2082508111E+04 -O. 2791187732E+04 O. 4312693839E+04 -O. 2706386714E+04
 O. 3092779601E+03 -O. 1116679287E+04 O. 2170811571E+04 -O. 3319213778E+04 O. 4721580526E+04 -O. 7501953742E+04 O. 4736176749E+04
 -O. 1895863831E+03 O. 7218703114E+03 -O. 1512584694E+04 O. 2500501881E+04 -O. 3783844533E+04 O. 6324809426E+04 -O. 3961166009E+04
 O. 4661705416E+02 -O. 1842044294E+03 O. 4079920874E+03 -O. 7190572563E+03 O. 1154310348E+04 -O. 1975262294E+04 O. 1269604490E+04

MATRIX A

-O. 6752153983E+01 O. 1230308598E+02 -O. 1122091882E+02 O. 1206198576E+02 -O. 1446743423E+02 O. 2133248694E+02 -O. 1325705165E+01
 -O. 1533439396E+01 -O. 3905955656E+01 -O. 9394953664E+01 -O. 7932946342E+01 -O. 8771171520E+01 -O. 1253280885E+02 O. 7739025059E+01
 O. 4083132648E+00 -O. 2742882185E+01 -O. 3428748235E+01 O. 9847957243E+01 -O. 8465180701E+01 O. 1118656366E+02 -O. 6806023042E+01
 -O. 1763335581E+00 O. 9304608803E+00 -O. 3956373142E+01 -O. 4113657191E+01 O. 1290269616E+02 -O. 1350520514E+02 O. 7918411995E+01
 O. 9394988512E+01 -O. 4569932474E+00 O. 1510691902E+01 -O. 7441802537E+01 -O. 2479990758E+02 -O. 1277424367E+02 -O. 4031300811E+02
 -O. 5074170923E+01 O. 2391770264E+00 -O. 7312320753E+00 O. 2197397519E+01 -O. 9083828567E+01 -O. 3288378031E+02 O. 4031300811E+02
 O. 7755455617E+01 -O. 3632403319E+00 O. 1094179855E+01 -O. 3168708606E+01 O. 1150776085E+02 -O. 9914754624E+02 O. 8999999999E+02

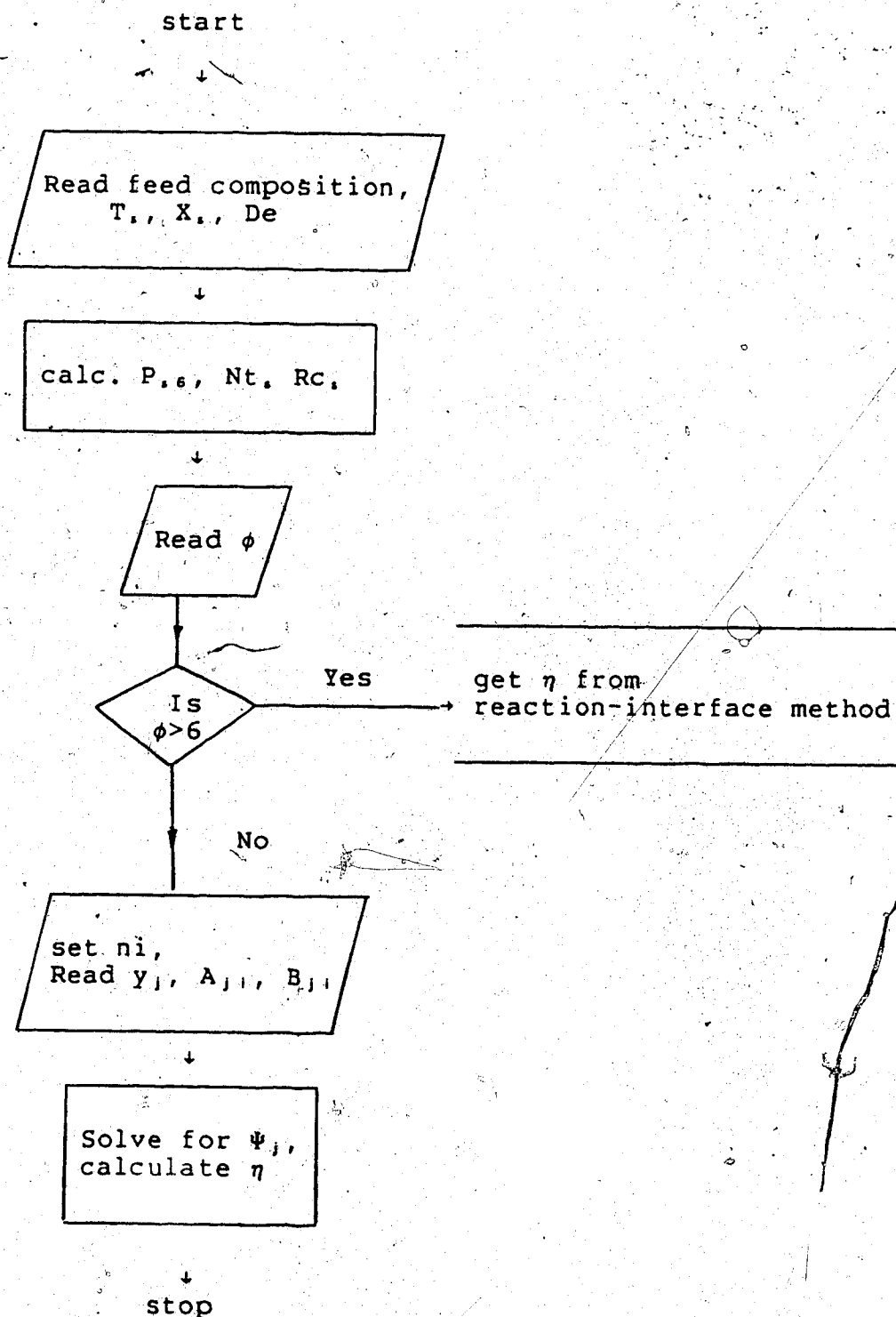
MATRIX B

-O. 5508623428E+02 O. 7062430421E+02 -O. 2331065319E+02 O. 1299325310E+02 -O. 9863476752E+01 O. 1109593470E+02 -O. 6453127793E+01
 O. 2030492025E+02 -O. 7429385755E+02 O. 6915267484E+02 -O. 2333558412E+02 O. 1470540228E+02 -O. 1522324257E+02 O. 8689686867E+01
 -O. 3811297897E+01 O. 3932605006E+02 -O. 1042324499E+03 O. 8851633380E+02 -O. 3214154348E+02 O. 2722862887E+02 -O. 1488572946E+02
 O. 1750023394E+01 -O. 1093184714E+02 O. 7291735731E+02 -O. 1765684587E+03 O. 1495463325E+03 -O. 7222498685E+02 O. 3551167951E+02
 -O. 1528272429E+01 O. 7925023357E+01 -O. 3045923740E+02 -O. 1720364854E+03 O. 4304131396E+03 O. 4308017736E+03 -O. 1483626330E+03
 O. 3400679533E+01 -O. 1622788305E+02 O. 5103981958E+02 -O. 1643475851E+03 O. 8521352744E+03 -O. 3254405863E+04 O. 252840558E+04
 O. 1386486539E+02 -O. 6465417415E+02 O. 1927837491E+03 -O. 5444168710E+03 O. 1814608812E+04 -O. 5507186377E+04 O. 4094999999E+04

MATRIX B1

O. 3511381977E+01 -O. 3614629264E+02 O. 7406850857E+02 -O. 9168498955E+02 O. 1156501112E+03 -O. 1740350452E+03 O. 1085963257E+03
 O. 2714311057E+02 -O. 5687571356E+02 O. 2725699808E+02 O. 1204044514E+02 -O. 2440859232E+02 O. 4066532562E+02 -O. 2582157353E+02
 -O. 5082610057E+01 O. 4786620731E+02 -O. 9355679230E+02 O. 5785402394E+02 -O. 5784605967E+01 -O. 7601526528E+01 O. 6305303597E+01
 O. 2189989407E+01 -O. 1325351978E+01 -O. 8278881759E+02 -O. 1653045625E+03 O. 1173530969E+03 -O. 3852844424E+02 O. 1575462256E+02
 -O. 1733045858E+01 O. 8921087098E+01 -O. 3375194563E+02 O. 1845289002E+03 -O. 4441929966E+03 O. 3767478267E+03 -O. 1205198562E+03
 O. 3503793905E+01 -O. 1671392480E+02 O. 5252578720E+02 -O. 1688130095E+03 O. 8705949066E+03 O. 3187581343E+04 O. 2446483789E+04
 O. 1370975628E+02 -O. 6392769348E+02 O. 1905953894E+03 -O. 5380794538E+03 O. 1791593291E+04 -O. 5308891284E+04 O. 3914999999E+04

Figure D.1 Flow Chart of Isothermal Effectiveness Factor
- Orthogonal Collocation



```

C*****
C*
C*          MAINLINE ORTEFF
C*
C* THIS PROGRAM EVALUTES THE ISOTHERMAL EFFECTIVE-
C* NESS FACTOR BY ORTHOGONAL COLLOCATION. IT USES
C* DIFFERENT INTERIOR POINTS DEPENDING ON THE
C* VALUE OF THE THIELE MODULUS. THE PROGRAM
C* ASSIGN UNIT 7 TO OR1 TO OR6 WHICH CONTAIN THE
C* OUTPUTS OF THE "ORTHOGONAL" PROGRAM. OR1 TO OR6
C* DEFINE THE NUMBER OF INTERIOR POINTS AND THE
C* A AND B WHICH WERE DESCRIBED IN APPENDIX D.
C* THE METHOD OF THE SOLUTION HAS BEEN
C* DESCRIBED IN CHAPTER 4 AND APPENDIX D
C*
C*****
C
C

```

```

      IMPLICIT REAL*8 (A-H,O-Z,$)
      DIMENSION X(30),RERATE(30),DF(30,30),B(11,11),
#B1(11,11),Y(3),Z(10),QINV(11,11),A(11,11),PAR(13)
      COMMON /COMP/ YH2S,YSO2,YH2O,YN2,DHS,DSO,DW,DS6
      COMMON /PARA/ S6SUR, FI,FIMOD,XS,RNS,RATES,C1
      COMMON /ORTH/ B,B1,A,X,QINV,Z
      COMMON /COND/ T,PRESS
      COMMON /CALL/ NCALL
      EXTERNAL FUN,FUNO,DF1,DF2,DF3,DF4,DF5,DF7,DF8,DF9,RATE
      WRITE(6,101)
101  FORMAT(/,2X,'PRESS,YH2S,YSO2,YH2O,YN2,DH2S,DSO2,
#,'DHWATER,DS6 ?')
      READ(5,1) PRESS,YH2S,YSO2,YH2O,YN2,DHS,DSO,DW,DS6
2    FORMAT(I5)
      WRITE(6,102)
102  FORMAT(/,2X,'CONVERSION AT THE SURFACE, TEMP ')
      READ(5,1) XS,T
1    FORMAT(9D15.5)
      RLK62=-34173./T+37.9735
      RLK64=-13663.9/T+12.6028
      RLK68=2932./T-3.43174
      RLK=11050.1/T-11.5576
      RK=DEXP(RLK)
      RK62=DEXP(RLK62)
      RK64=DEXP(RLK64)
      RK68=DEXP(RLK68)
      AA=(RK62/PRESS/PRESS)**(1./3.)
      BB=(RK64/DSQRT(PRESS))**(2./3.)
      CC=(RK68*(PRESS**.25))**(4./3.)
      WRITE(8,100) AA,BB,CC
100  FORMAT(//,5X,'A=',D15.7,2X,'B=',D15.7,2X,'C=',D15.7)
      PAR(1)=AA
      PAR(2)=BB
      PAR(3)=CC
      PAR(4)=YH2S*XS
      PAR(5)=RK

```

```

PAR(6)=YSO2
PAR(7)=YH2O
PAR(8)=PAR(5)*DSQRT(PRESS)
PAR(9)=DHS/DW
PAR(10)=DHS/DSO
PAR(13)=DHS/DS6
PAR(11)=YH2S
PAR(12)=YN2
NCALL=1
X(1)=.02
X(2)=.98
NEQ=2
CALL SNLEQ(RHS,X,PAR,1.D00,1,2,1,NI,YH2S,DF,NEQ)
S6SUR=X(1)
RNS=X(2)
RATES=RATE(PAR,XS,S6SUR,RNS)
WRITE(8,150)
150  FORMAT(////,10X,'XS',15X,'T',15X,'PRESS',15X,
# 'S6SUR',15X,'RNS',15X,'RATES')
WRITE(8,200) XS,T,PRESS,S6SUR,RNS,RATES
200  FORMAT(//,6D18.6,///)
C
C..NOW SNLEQ IS USED TO GET EQUILIBRIUM CONVERSION ..
C..HERE X(1) IS S6EQ, X(2) MOLE AT EQ, AND X(3) EQCONV..
C..NOW ICALL=2 AND NCALL=2 ..
C
NEQ=3
NCALL=2
WRITE(6,29)
29  FORMAT(/,'ESTIMATE OF S6 AT EQUILIBRIUM AND N,XEQ?')
READ(5,1) X(1),X(2),X(3)
CALL SNLEQ(RHS,X,PAR,0.5D00,1,3,2,NI,YH2S,DF,NEQ)
S6EQ=X(1)
RNE=X(2)
XEQ=X(3)
RATEEQ=RATE(PAR,XEQ,S6EQ,RNE)
WRITE(8,25) X(3),RATEEQ
25  FORMAT(//,10X,'XEQ=',F10.6,5X,'RATEEQ=',D15.9)
C
C C1 IS CEQ./C AT THE SURFACE
C
C1=(1.-XEQ)/(1.-XS)*RNS/RNE
C
DO 2000 II=1,20
WRITE(6,103)
103  FORMAT(//,2X,' FIMOD ?')
READ(5,1) FIMOD
FI=FIMOD*(DSQRT(1.-C1))
IF(FIMOD.LE..2D00) NI=1
IF(FIMOD.GT..2D00.AND.FIMOD.LE..5D00) NI=2
IF(FIMOD.GT..5D00.AND.FIMOD.LE.1.D00) NI=3
IF(FIMOD.GT.1.D00.AND.FIMOD.LE.3.5D00) NI=4
IF(FIMOD.GT.3.5D00.AND.FIMOD.LE.6.5D00) NI=5
IF(FIMOD.GT.6.5D00.AND.FIMOD.LE.9.0D00) NI=6

```

```

      IF(FIMOD.GT.9.0D00) GO TO 1110
      GO TO (11,12,13,14,15,16) , NI
11    CALL FTNCMD('ASSIGN 7=OR1',12)
      GO TO 17
12    CALL FTNCMD('ASSIGN 7=OR2',12)
      GO TO 17
13    CALL FTNCMD('ASSIGN 7=OR3',12)
      GO TO 17
14    CALL FTNCMD('ASSIGN 7=OR4',12)
      GO TO 17
15    CALL FTNCMD('ASSIGN 7=OR5',12)
      GO TO 17
16    CALL FTNCMD('ASSIGN 7=OR6',12)
17    N=3*NI
      M=1
      NM=NI+1
      LINE=(26+2*NM)*1000
      DO 300 I=1,NM
      READ(7'LINE,500) (B(I,J) , J=1,NM)
      LINE=LINE+1000
300   CONTINUE
      LINE=(21+NM)*1000
      DO 400 I=1,NM
      READ(7'LINE,500) (A(I,J) , J=1,NM)
      LINE=LINE+1000
400   CONTINUE
      LINE=(31+3*NM)*1000
      DO 450 I=1,NM
      READ(7'LINE,500) (B1(I,J),J=1,NM)
      LINE=LINE+1000
450   CONTINUE
      LINE=10*1000
      READ(7'LINE,545) (Z(I),I=1,NM)
500   FORMAT(10X,10D18.10)
545   FORMAT(10D18.10)
      LINE=16*1000
      DO 546 I=1,NM
      READ(7'LINE,500) (QINV(I,J) , J=1,NM)
      LINE=LINE+1000
546   CONTINUE
      SN=(RNS-RNE)/(XS-XEQ)
      BN=RNS-SN*XS
      SS6=(S6SUR-S6EQ)/(XS-XEQ)
      BS6=S6SUR-SS6*XS
      DO 602 J=1,NI
      SI=Z(J)*Z(J)
      JJ=J+2*(J-1)
      RHS=(SI*(1.D00-C1)+C1)*(1.D00-XS)/RNS
      X(JJ)=(1.D00-RHS*BN)/(1.D00+RHS*SN)
      X(JJ+1)=SS6*X(JJ)+BS6
      X(JJ+2)=SN*X(JJ)+BN
602   CONTINUE
      WRITE(8,700) (X(L), L=1,N)
700   FORMAT(/,5X,'INITIAL ESTIMATES ARE',5(6D15.6,/,27X))

```


525 NEQ=N

C

CALL SNLEQ(RHS,X,PAR,.75D00,M,N,3,NI,YH2S,DF,NEQ)
GO TO 1270

1110 CONTINUE

C

C IN THIS SECTION ONE POINT IS CONSIDERED FOR
C GETTING YI AND EFF.

C

WRITE(6,111)
111 FORMAT(5X,'TYPE IN RKISI ?')
CALL FREAD(5,'R*8:',RKISI)
SI=(RKISI)*(RKISI)
RHS=(SI*(1.D00-C1)+C1)*(1.D00-XS)/RNS
Y(3)=(1.D00-RHS*BN)/(1.D00+RHS*SN)
Y(1)=SS6*Y(3)+BS6
Y(2)=SN*Y(3)+BN

C

C NOW SNLEQ IS CALLED TO SOLVE FOR X,S6,AND N
C FOR SPECIFIED SI.

C

CALL SNLEQ(RHS,Y,PAR,1.D00,M,3,5,NI,YH2S,DF,3)
XRKISI=Y(3)
S6KISI=Y(1)
TMKISI=Y(2)
RRKISI=RATE(PAR,XRKISI,S6KISI,TMKISI)
WRITE(8,622) RRKISI

C

C NOW KISI OPTIMUM IS ESTIMATED

C

RRATIO=RATES/RRKISI
SIR=1.0D00/SI
POWER=DLOG(RRATIO)/DLOG(SIR)
OPKISI=(1.D00+POWER)**(.5D00/POWER)
OPKISI=1.D00/OPKISI
SI=OPKISI**2
RHS=(SI*(1.D00-C1)+C1)*(1.D00-XS)/RNS
Y(3)=(1.D00-RHS*BN)/(1.D00+RHS*SN)
Y(1)=SS6*Y(3)+BS6
Y(2)=SN*Y(3)+BN
CALL SNLEQ(RHS,Y,PAR,1.D00,M,3,5,NI,YH2S,DF,3)
XRKISI=Y(3)
S6KISI=Y(1)
TMKISI=Y(2)
RRKISI=RATE(PAR,XRKISI,S6KISI,TMKISI)
WRITE(8,622) RRKISI,POWER,OPKISI
622. FORMAT(//,'* RATIO OF RATE,N,KISI OPT.*',3D18.9)
AYI=9.D00*(FIMOD**2)*RRKISI/RATES
CALL SOLYI(YI,RKISI,AYI,NFLAG)
WRITE(8,560)
EFF=2./3./(FIMOD**2)/(1.-YI)
NI=1
WRITE(8,1300) NI,FI,FIMOD,EFF
GO TO 2000

```

1270 WRITE(8,535)
535  FORMAT(//,5X,'THE WHOLE PELLETT IS ACTIVE')
560  FORMAT(//,5X,'PORTION OF THE PELLETT IS INACTIVE')
580  DO 800 I=1,N,3
      RERATE(I)=RATE(PAR,X(I),X(I+1),X(I+2))
      RERATE(I)=RERATE(I)/RATES
800  CONTINUE
      WRITE(8,900)
900  FORMAT(/////5X,' COLLOCATION POINT',5X,' CONVERSION'
      #,8X,' RELRATE')
      K=1
      DO 1000 I=1,N,3
        WRITE(8,1100) K,X(I),RERATE(I)
        K=K+1
1000 CONTINUE
1100 FORMAT(10X,15,15X,F12.6,5X,D12.6)
      EFF=A(NM,NM)
      DO 1200 J=1,NI
        K=J+2*(J-1)
1150 EFF=EFF+A(NM,J)/(1.-C1)
      #*((1.-X(K))/(1.-XS)*RNS/X(K+2)-C1)
1200 CONTINUE
      EFF=EFF/3./FIMOD/FIMOD
      WRITE(8,1300)NI,FI,FIMOD,EFF
1300 FORMAT(//,5X,'NI=',I3,5X,'FI=',F10.6,5X,'FIMOD=',
      #F10.6,5X,'EFF=',F12.6)
2000 CONTINUE
      STOP
      END

C
C
      SUBROUTINE SNLEQ(RHS,X,PAR,W,M,N,ICALL,NI,YH2S,DF,NEQ)
C THIS SUBROUTINE SOLVES SYSTEM OF NONLINEAR
C EQ'S BY NEWTONS S METHOD.
C
      IMPLICIT REAL*8(A-H,O-Z,$)
      DIMENSION FSAVE(30),X(30),F(30,1),DF(NEQ,NEQ)
      #,WKAREA(1000),Z(10),XSAVE(30),PAR(13),Y(2)
500  FORMAT(5D14.5)
      IA=NEQ
      IDGT=0
      MAXIT=200
      FTOL=.1D-11
      XTOL=.1D-11
      NUM=N+1
      IF(NEQ.EQ.N) NUM=N
      DO 100 I=1,MAXIT
        DO 110 J=1,NUM
110  XSAVE(J)=X(J)
330  FORMAT(/,6D15.6)
C
C ICALL=1 FOR SURFACE , ICALL=2 FOR EQUILIBRIUM , AND
C ICALL=3 FOR PROFILE ESTIMATION.
C

```

```

      IF(ICALL.EQ.1) GO TO 70
      IF(ICALL.EQ.2) GO TO 75
C
C  ICALL=5 TO GET N,S6,X FOR GIVEN SI
C
      IF(ICALL.EQ.5) GO TO 900
      DO 30 II=1,N
      DO 30 J=1,N
30    DF(J,II)=0.0
      KK=1
      DO 10 KI=1,N,3
      F(KI,1)=FUNO(NI,N,KK,PAR)
      DF(KI,KI)=DF1(NI,KK,PAR)
      DF(KI,KI+1)=DF5(NI,KK,PAR)
      DF(KI,KI+2)=DF3(NI,KK,PAR)
      KK=KK+1
10    CONTINUE
      DO 20 KI=2,N,3
      PAR(4)=X(KI-1)
      Y(1)=X(KI)
      Y(2)=X(KI+1)
      F(KI,1)=FUN(Y,1,PAR)
      DF(KI,KI-1)=DF9(Y,1,PAR)
      F(KI+1,1)=FUN(Y,2,PAR)
      DF(KI,KI)=DF7(Y,1,PAR)
      DF(KI,KI+1)=DF8(Y,1,PAR)
      DF(KI+1,KI-1)=DF9(Y,2,PAR)
      DF(KI+1,KI)=DF7(Y,2,PAR)
      DF(KI+1,KI+1)=DF8(Y,2,PAR)
20    CONTINUE
21    IF (NI.EQ.1) GO TO 58
      KK=1
      DO 60 KI=1,N,3
      KKK=1
      DO 50 KJ=1,N,3
      IF(KI.EQ.KJ) GO TO 55
      DF(KI,KJ)=DF2(NI,KK,KKK)
      DF(KI,KJ+2)=DF4(KK,KKK,NI)
55    KKK=KKK+1
50    CONTINUE
      KK=KK+1
60    CONTINUE
58    CONTINUE
      GO TO 80
70    F(1,1)=FUN(X,1,PAR)
      F(2,1)=FUN(X,2,PAR)
      DF(1,1)=DF7(X,1,PAR)
      DF(1,2)=DF8(X,1,PAR)
      DF(2,1)=DF7(X,2,PAR)
      DF(2,2)=DF8(X,2,PAR)
2000  FORMAT(/,30D15.6)
3500  FORMAT(//,30D15.6)
      GO TO 80
75    PAR(4)=X(3)

```

```

F(1,1) = FUN(X,1,PAR)
F(2,1) = FUN(X,2,PAR)
F(3,1) = FUN(X,3,PAR)
DF(1,1) = DF7(X,1,PAR)
DF(1,2) = DF8(X,1,PAR)
DF(1,3) = DF9(X,1,PAR)
DF(2,1) = DF7(X,2,PAR)
DF(2,2) = DF8(X,2,PAR)
DF(2,3) = DF9(X,2,PAR)
DF(3,1) = DF7(X,3,PAR)
DF(3,2) = DF8(X,3,PAR)
DF(3,3) = DF9(X,3,PAR)
GO TO 80
900 PAR(4)=X(3)
F(1,1)=FUN(X,1,PAR)
F(2,1)=FUN(X,2,PAR)
F(3,1)=RHS-(1.D00-X(3))/X(2)
DF(1,1)=DF7(X,1,PAR)
DF(1,2)=DF8(X,1,PAR)
DF(1,3)=DF9(X,1,PAR)
DF(2,1)=DF7(X,2,PAR)
DF(2,2)=DF8(X,2,PAR)
DF(2,3)=DF9(X,2,PAR)
DF(3,1)=0.0D00
DF(3,2)=(1.D00-X(3))/X(2)/X(2)
DF(3,3)=1.D00/X(2)
80 ITEST=0
C
C SCALING THE JACOBIAN MATRIX
C
DO 92 ISS=1,NEQ
SCALE=DABS(DF(ISS,1))
DO 90 IS=1,NEQ
IF(DABS(DF(ISS,IS)).GT.SCALE) SCALE=DABS(DF(ISS,IS))
90 CONTINUE
DO 91 IS=1,NEQ
DF(ISS,IS)=DF(ISS,IS)/SCALE
91 CONTINUE
F(ISS,1)=F(ISS,1)/SCALE
92 CONTINUE
DO 220 J=1,NEQ
FSAVE(J)=F(J,1)
F(J,1)=-F(J,1)
220 CONTINUE
33 CALL LEQT1F(DF,M,NEQ,IA,F,IDGT,WKAREA,IER)
DO 1000 II=1,NEQ
X(II)=XSAVE(II)+W*F(II,1)
1000 CONTINUE
1001 DO 550 JJ=1,NEQ
IF(DABS(F(JJ,1)).GT.XTOL) ITEST=ITEST+1
IF(FSAVE(JJ).GT.FTOL) ITEST=ITEST+1
550 CONTINUE
C IF TOL MET PRINT THE RESULT
IF(ITEST.EQ.0) GO TO 200

```

```

100  CONTINUE
      WRITE(8,400)
400  FORMAT(//,'CONVERGENCE WAS NOT ACHIEVED AFTER '
      #,'100 ITER.')
      RETURN
200  CONTINUE
      WRITE(8,300) I,(X(L),L=1,NUM)
300  FORMAT(//,5X,'TOL MET',5X,I4,6(5D18.7,/))
      WRITE(8,36) (FSAVE(L),L=1,NUM)
36   FORMAT(/,22X,6(5D18.7,/))
350  RETURN
      END

```

C
C

```

      FUNCTION FUN(X,K,PAR)
      IMPLICIT REAL*8(A-H,O-Z,$)
      DIMENSION X(3),PAR(13)
      COMMON /VAR/ P1,P2,P3,P4,P5,P6,P7,P8,P9,PPH2O,PPH2S
      $,PPSO2,ZW,ZWS
      COMMON /PAR/ S6SUR, FI,FIMOD,XS,RNS,RATES,C1
      COMMON/CALL/NCALL
      P1=(X(1)*X(2)*X(2))**(1./3)
      P2=(X(1)*X(1)*X(2))**(1./3.)
      P3=((X(1)**4)/X(2))**(1./3.)
      P4=(X(2)/X(1))**(2./3.)
      P5=DSQRT(P4)
      P6=(X(1)/X(2))**(1./3.)
      P7=P3/X(2)
      IF(NCALL.LT.2) GO TO 30
      P8=(PAR(7)+PAR(11)*XS)/RNS
      P9=(PAR(6)-PAR(11)*XS/2.)/RNS
      ZWS=(S6SUR/RNS)**(1./3.)
      ZW=(X(1)/X(2))**(1./3.)
      ZSOVP=2.*PAR(1)*ZWS+4.*PAR(2)*ZWS**2+6.*S6SUR/RNS+
      $8.*PAR(3)*ZWS**4
      ZOVP=2.*PAR(1)*ZW+4.*PAR(2)*ZW**2+6.*X(1)/X(2)+
      #8.*PAR(3)*ZW**4
      A=(1.-XS)/RNS-(1.-PAR(4))/X(2)
      PPH2O=P8+PAR(9)*PAR(11)*A
      PPSO2=P9-PAR(10)*PAR(11)*A/2.
      GO TO (6,11,20),K
6     FUN=X(2)*(PPH2O+PPSO2-1.)+PAR(11)*(1.-PAR(4))
      #+PAR(1)*P1+PAR(2)*P2+X(1)+PAR(3)*P3+PAR(12)
      RETURN
11    FUN=ZOVP-ZSOVP-6./4.*PAR(13)*PAR(11)*A
      RETURN
20    PPH2S=PAR(11)*(1.-X(3))/X(2)
      FUN=PAR(8)*(PPH2S**2)*(PPSO2)
      FUN=FUN-(PPH2O**2)*DSQRT(X(1)/X(2))
      RETURN
30    GO TO (5,10),K
5     FUN=1.-.5*PAR(4)+PAR(1)*P1+PAR(2)*P2+X(1)+PAR(3)*
      #P3-X(2)
      RETURN

```

```

10  FUN=2.*PAR(1)*P1+4.*PAR(2)*P2+6.*X(1)+8.*PAR(3)*P3
    #-1.5*PAR(4)
    RETURN
    END
C
C
    FUNCTION DF7(X,K,PAR)
    IMPLICIT REAL*8(A-H,O-Z,$)
    DIMENSION X(3),PAR(13)
    COMMON /VAR/ P1,P2,P3,P4,P5,P6,P7,P8,P9,PPH20,PPH2S
    $,PPSO2,ZW,ZWS
    COMMON /PAR/ S6SUR, FI,FIMOD,XS,RNS,RATES,C1
    COMMON/CALL/NCALL
    GO TO (5,10,20) , K
5    DF7=PAR(1)*P4/3.+2.*PAR(2)*P5/3.+1.+4./3.*PAR(3)*P6
    RETURN
10   DF7=2./3.*PAR(1)/P2+8./3.*PAR(2)/P1+6./X(2)+32./3.
    #*PAR(3)*P6/X(2)
    RETURN
20   DF7=-0.5D00*(PPH20**2)/DSQRT(X(1)*X(2))
    RETURN
    END
C
C
    FUNCTION DF8(X,K,PAR)
    IMPLICIT REAL*8(A-H,O-Z,$)
    DIMENSION X(3),PAR(13)
    COMMON /VAR/ P1,P2,P3,P4,P5,P6,P7,P8,P9,PPH20,PPH2S
    $,PPSO2,ZW,ZWS
    COMMON /PAR/ S6SUR, FI,FIMOD,XS,RNS,RATES,C1
    COMMON/CALL/NCALL
    IF(NCALL.GT.1)-GO TO 50
    GO TO (5,10) , K
5    DF8=2./3.*PAR(1)/P5+PAR(2)/3./P4-PAR(3)*P7/3.-1.
    RETURN
10   DF8=4./3.*PAR(1)/P5+4./3.*PAR(2)/P4-8.*PAR(3)*P7/3.
    RETURN
50   GO TO (60,70,80) ,K
60   DF8=2/3*PAR(1)*P6+1/3*PAR(2)/P4-1/3*PAR(3)*P7-1
    DF8=DF8+PPH20+PPSO2+(PAR(9)-PAR(10)/2.)*PAR(11)
    #*(1.-PAR(4))/X(2)
    RETURN
70   DF8=-2./3.*PAR(1)*P6/X(2)-8./3.*PAR(2)/P4/X(2)-6.
    #*X(1)/X(2)/X(2)-32./3.*PAR(3)*P3/X(2)
    #/X(2)-6./4.*PAR(13)*PAR(11)*(1.-PAR(4))/X(2)/X(2)
    RETURN
80   DPH20=PAR(9)*PAR(11)*(1.-X(3))/(X(2)**2)
    DPSO2=-PAR(10)*PAR(11)*(1.-X(3))/(X(2)**2)
    DPH2S=-PAR(11)*(1.-X(3))/(X(2)**2)
    DF8=2.*PAR(8)*PPH2S*PPSO2*DPH2S
    DF8=DF8+PAR(8)*(PPH2S**2)*DPSO2
    DF8=DF8-2.*PPH20*DPH20*DSQRT(X(1)/X(2))
    DF8=DF8+.5*(PPH20**2)*DSQRT(X(1))*(X(2)**(-1.5))
    RETURN

```

END

C
C

FUNCTION DF9(X,K,PAR)

C THIS FUNCTION CALCULATES THE DIFFERENTIAL WITH RESPECT TO
C CONVERSION.

C

IMPLICIT REAL*8(A-H,O-Z,\$)

DIMENSION X(3),PAR(13)

COMMON /VAR/P1,P2,P3,P4,P5,P6,P7,P8,P9,PPH20,PPH2S
#,PPSO2,ZW,ZWS

COMMON /PAR/ S6SUR, FI,FIMOD,XS,RNS,RATES,C1

COMMON/CALL/NCALL

GO TO (5,10,20),K

5 DF9=PAR(11)*(PAR(9)-.3*PAR(10)-1.0)

RETURN

10 DF9=-6./4.*PAR(13)*PAR(11)/X(2)

RETURN

20 DPH20=PAR(9)*PAR(11)/X(2)

DPSO2=-PAR(10)*PAR(11)/2./X(2)

DPH2S=-PAR(11)/X(2)

DF9=2.*PAR(8)*PPH2S*PPSO2*DPH2S

DF9=DF9+PAR(8)*(PPH2S**2)*DPSO2

DF9=DF9-2.*PPH20*DPH20*DSQRT(X(1)/X(2))

RETURN

END

C
C

FUNCTION FUNO(NI,N,J,PAR)

IMPLICIT REAL*8(A-H,O-Z,\$)

DIMENSION X(30),B(11,11),B1(11,11),Z(10),A(11,11)
#,PAR(13),QINV(11,11)

COMMON /PAR/ S6SUR, FI,FIMOD,XS,RNS,RATES,C1

COMMON /ORTH/ B,B1,A,X,QINV,Z

FUNO=0.0

K=1

DO 10 I=1,N,3

5 FUNO=FUNO+B(J,K)*((1.-X(I))/(1.-XS)*RNS/X(I+2)

#-C1)/(1.D00-C1)

30 K=K+1

10 CONTINUE

M=J+2*(J-1)

R=RATE(PAR,X(M),X(M+1),X(M+2))

40 FUNO=FUNO+B(J,NI+1)-9.*FIMOD*FIMOD*R/RATES

60 RETURN

END

C
C
C

FUNCTION DF1(NI,J,PAR)

IMPLICIT REAL*8(A-H,O-Z,\$)

DIMENSION X(30),B(11,11),B1(11,11),Z(10),A(11,11)
#,PAR(13),QINV(11,11)

COMMON /PAR/ S6SUR, FI,FIMOD,XS,RNS,RATES,C1

```

COMMON /ORTH/ B,B1,A,X,QINV,Z
K=J+2*(J-1)
5 DF1=-B(J,J)/(1.-XS)*RNS/X(K+2)/(1.D00-C1)
20 R1=RATE(PAR,X(K),X(K+1),X(K+2))
CONV=X(K)+0.00001
R2=RATE(PAR,CONV,X(K+1),X(K+2))
DR=(R2-R1)/.00001
30 DF1=DF1-9.*FIMOD*FIMOD*DR/RATES
50 RETURN
END

```

C
C

```

FUNCTION DF2(NI,J,I)
IMPLICIT REAL*8(A-H,O-Z,$)
DIMENSION X(30),B(11,11),B1(11,11),Z(10),A(11,11)
#,PAR(13),QINV(11,11)
COMMON /PARA/ S6SUR, FI,FIMOD,XS,RNS,RATES,C1
COMMON /ORTH/ B,B1,A,X,QINV,Z
K=I+2*(I-1)
5 DF2=-B(J,I)*RNS/(1.-XS)/X(K+2)/(1.D00-C1)
20 RETURN
END

```

C
C

```

FUNCTION DF3(NI,J,PAR)
IMPLICIT REAL*8(A-H,O-Z,$)
DIMENSION X(30),B(11,11),B1(11,11),Z(10),A(11,11)
#,PAR(13),QINV(11,11)
COMMON /PARA/ S6SUR, FI,FIMOD,XS,RNS,RATES,C1
COMMON /ORTH/ B,B1,A,X,QINV,Z
K=J+2*(J-1)
5 DF3=-B(J,J)*(1.-X(K))/(1.-XS)*RNS/(X(K+2)**2)/
#(1.D00-C1)
20 R1=RATE(PAR,X(K),X(K+1),X(K+2)),
CM=X(K+2)+.00001
R2=RATE(PAR,X(K),X(K+1),CM)
DR=(R2-R1)/.00001
30 DF3=DF3-9.*FIMOD*FIMOD/RATES*DR
50 RETURN
END

```

C
C

```

FUNCTION DF4(J,I,NI)
IMPLICIT REAL*8(A-H,O-Z,$)
DIMENSION X(30),B(11,11),B1(11,11),Z(10),A(11,11)
#,PAR(13),QINV(11,11)
COMMON /PARA/ S6SUR, FI,FIMOD,XS,RNS,RATES,C1
COMMON /ORTH/ B,B1,A,X,QINV,Z
M=I+2*(I-1)
5 DF4=-B(J,I)*(1.-X(M))/(1.-XS)*RNS/(X(M+2)**2)/
#(1.D00-C1)
20 RETURN
END

```

C

C

```

      FUNCTION DF5(NI,J,PAR)
      IMPLICIT REAL*8(A-H,O-Z,$)
      DIMENSION X(30),B(11,11),B1(11,11),Z(10),A(11,11)
      #,PAR(13),QINV(11,11)
      COMMON /PARA/ S6SUR, FI,FIMOD,XS,RNS,RATES,C1
      COMMON /ORTH/ B,B1,A,X,QINV,Z
      K=J+2*(J-1)
      R1=RATE(PAR,X(K),X(K+1),X(K+2))
      CS6=X(K+1)+.00001
      R2=RATE(PAR,X(K),CS6,X(K+2))
      DR=(R2-R1)/.00001
10    DF5=-9.*FIMOD*FIMOD*DR/RATES
20    RETURN
      END

```

C

C

```

      FUNCTION RATE(PAR,Z1,S6,TM)
      IMPLICIT REAL*8(A-H,O-Z,$)
      DIMENSION PAR(8)
      COMMON /COMP/ YH2S,YSO2,YH2O,YN2,DHS,DSO,DW,DS6
      COMMON /PARA/ S6SUR, FI,FIMOD,XS,RNS,RATES,C1
      COMMON /COND/ T,PRESS
      EQK=PAR(5)/DSQRT(760.D00)
      PSO2=(YSO2-YH2S*XS/2.)/RNS-YH2S*DHS/DSO/2.
      #*((1.-XS)/RNS-(1.-Z1)/TM)
      PSO2=PSO2*PRESS*760.
      PH2O=(YH2O+YH2S*XS)/RNS+YH2S*DHS/DW
      #*((1.-XS)/RNS-(1.-Z1)/TM)
      PH2O=PH2O*PRESS*760.
      PH2S=YH2S*(1.-Z1)/TM*PRESS*760.
      PS6=S6/TM*760.*PRESS
      AB=2.56D-04*DEXP(-7350./1.986/T)
      RATE=AB/((1+.006D00*PH2O)**2)
      RATE=RATE*(PH2S*DSQRT(PSO2)-PH2O*DSQRT(DSQRT(PS6)
      #/EQK))
      RETURN
      END

```

C

C

```

      SUBROUTINE SOLYI(YI,RKISI,AYI,NFLAG)
      IMPLICIT REAL*8(A-H,O-Z,$)
      DIMENSION XX(3)
      PI=3.141592654D00
      B=(3.*RKISI-2.)/(1.-RKISI)
      C=(6.*RKISI+AYI-2.-3.*AYI*RKISI)/AYI/(1.-RKISI)
      DE=RKISI*(AYI-6.)/AYI/(1.-RKISI)
      P=C-B*B/3.
      Q=(2.*(B**3)-9.*B*C+27.*DE)/27.
      D=(P/3.)**3+(Q/2.)**2
70    FORMAT(//,'CUBIC',2(3D19.9))
      IF(D) 10,10,40
10    E=DABS(P)
      F=-Q/2./DSQRT((E**3)/27.)

```

```

ANGLE=DARCOS(F)
Y1=2.*DSQRT(E/3.)*DCOS(ANGLE/3.)
Y2=-2.*DSQRT(E/3.)*DCOS((ANGLE+PI)/3.)
Y3=-2.*DSQRT(E/3.)*DCOS((ANGLE-PI)/3.)
XX(1)=Y1-B/3.
XX(2)=Y2-B/3.
XX(3)=Y3-B/3.
YI=0.0D00
DO 15 I=1,3
IF(XX(I).GE.0.0D00.AND.XX(I).LE.(1.0D00)) YI=XX(I)
15 CONTINUE
IF(YI.GE.0.0D00) GO TO 30
WRITE(8,1) (XX(I),I=1,3)
1 FORMAT(//,5X,'NO SOLUTION FOR YI IN 0-1 RANGE',3D16.8)
NFLAG=-1
RETURN
-30 WRITE(8,2) Y1,Y2,Y3,(XX(I),I=1,3),YI
2 FORMAT(//,'SOLN OF CUBIC FUNCTION :',5X,3(3D15.8,))
NFLAG=1
RETURN
40 U=-Q/2.+DSQRT(D)
U=U**(1./3.)
V=-Q/2.-DSQRT(D)
V=V**(1./3.)
Y1=V+U
WRITE(8,70) U,V,Y1
XX(1)=Y1-B/3.
IF(XX(1).GE.0.0D00.AND.XX(1).LE.1.D00) GO TO 50
NFLAG=-1
WRITE(8,1) XX(1)
RETURN
50 YI=XX(1)
NFLAG=1
WRITE(8,2) Y1,XX(1),YI
RETURN
END

```

APPENDIX E: Claus Convertor Model

Contents

1. Development of the two dimensional model.
2. Solution of P.D.E. in two dimensional Claus reactor.
3. Flow chart of an adiabatic one dimensional Claus convertor.
4. "ADONEDIMBED" program
5. Table E.1: output of "ORTHOGONAL" program for cylindrical geometry.
6. Flow chart of two dimensional Claus convertor.
7. "BEDTWO" program

5.1 Development of the Two Dimensional Model.

The equations of the two dimensional model are presented in section 5.2 as,

$$\frac{\partial}{\partial z} (V_r C_{f1}) - D_r \nabla^2 C_{f1} + k_m A (C_{f1} - C_{s1}) = 0 \quad (E.1)$$

$$C_p \frac{\partial}{\partial z} (V_r \rho T_f) - \lambda_f \nabla^2 T_f - hA(T_s - T_f) = 0 \quad (E.2)$$

$$\lambda_s \nabla^2 T_s + (-a_1)(-\Delta H) \rho_b \eta R_c - hA(T_s - T_f) = 0 \quad (E.3)$$

$$k_m A (C_{f1} - C_{s1}) = -a_1 \eta \rho_b R_c \quad (E.4)$$

where in tubular reactor,

$$\nabla^2 = \frac{1}{r} \frac{\partial}{\partial r} \left(r \frac{\partial}{\partial r} \right)$$

The above equations will be simplified in terms of conversion by the following procedure.

Equation (5.18) expresses the velocity variation due to variations in temperature and amount of the gas as,

$$\begin{aligned} V_s/V_o &= \{ 1 - Y_1(1-v) X/2 \} T/T_o \\ &= G T/T_o \end{aligned} \quad (E.5)$$

where v is given by equation (5.17). At an average conversion of 0.5, the data of figure 3.2, shows that $v \approx 0.414$ which gives the value of 0.99 for G . Thus assuming unity for G , results in error of less than 1%. In the following development G is taken as unity. Then, conversion would be defined as:

$$\begin{aligned}
 X_f &= (C_{f1} V_1 - C_{f1} V_1) / C_{f1} V_1 \\
 &= 1 - (C_{f1}/C_{f1}) (T_f/T_0)
 \end{aligned}
 \quad (E.6)$$

then

$$\partial C_f / \partial r = -(C_{f0} T_0) \{ (1-X_f)/T_f^2 \partial T_f / \partial r - 1/T_f \partial X_f / \partial r \} \quad (E.7)$$

$$\begin{aligned}
 \partial^2 C_f / \partial r^2 &= -(C_{f0} T_0) \{ (1-X_f)/T_f^2 \partial^2 T_f / \partial r^2 + 1/T_f \partial^2 X_f / \partial r^2 \\
 &\quad - 2/T_f^2 (\partial T_f / \partial r) (\partial X_f / \partial r) - 2(1-X_f)/T_f^3 (\partial T_f / \partial r)^2 \}
 \end{aligned}
 \quad (E.8)$$

The terms $(\partial T_f / \partial r) (\partial X_f / \partial r)$ and $(\partial T_f / \partial r)^2$ are negligible, thus,

$$\begin{aligned}
 \partial^2 C_f / \partial r^2 &= -(C_{f0} T_0) \{ (1-X_f)/T_f^2 \partial^2 T_f / \partial r^2 \\
 &\quad + 1/T_f \partial^2 X_f / \partial r^2 \}
 \end{aligned}
 \quad (E.9)$$

and

$$\partial / \partial z (V_1 C_{f1}) = -C_{f1} V_1 \partial X_f / \partial z \quad (E.10)$$

Substitution of (E.7), (E.8), and (E.10) into (E.1) yields,

$$\begin{aligned}
 \partial X_f / \partial z &= D_r T_0 / V_1 \{ (1-X_f)/T_f^2 \nabla^2 T_f + 1/T_f \nabla^2 X_f \} \\
 &\quad + (1/C_{f1} V_1) k_m A (C_{f1} - C_{s1})
 \end{aligned}
 \quad (E.11)$$

Combination of (E.11) and (E.4) gives,

$$\frac{\partial X_f}{\partial z} = \frac{Dr}{V_i} T^0 \left\{ \frac{(1-X_f)}{T^2 f} \nabla^2 T_f + \frac{1}{T_f} \nabla^2 X_f \right\} + (-a_1 \rho b / C_f V_s^0) \eta R_c \quad (E.12)$$

To generalize, define the dimensionless variables,

$$z' = z/R_w$$

$$r' = r/R_w$$

$$\tau = \frac{T/T^0 - T_a/T^0}{1 - T_a/T^0} = \frac{T' - s}{1 - s}$$

$$P_{em} = V_i D_p / Dr$$

$$P_{eh} = M C_p D_p / \lambda f$$

$$D_{am} = -a_1 \rho b R_c^0 R_w / C_f V_s^0$$

$$H' = (-\Delta H) C_f / \rho^0 T^0 C_p$$

$$\alpha = R_w / D_p$$

$$\gamma = h A R_w^2 / \lambda f$$

$$\beta = \lambda f / \lambda s$$

$$\delta = V_i / k_m A R_w$$

Introduction of dimensionless variables into equation (E.12) gives,

$$\begin{aligned} \frac{\partial X_f}{R_w \partial z'} = & \frac{Dr}{V_i} T^0 \left[\left(\frac{T^0(1-s)}{R_w^2 T^0} \right) \left(\frac{1-X_f}{(\tau f (1-s)+s)^2} \right) \nabla^2 \tau f \right. \\ & + \left. \frac{1}{R_w^2 T^0 \tau f (1-s)+s} \nabla^2 X_f \right] \\ & - \frac{a_1 \rho b R_c^0}{C_f V_i} \frac{\eta R_c}{R_c^0} \end{aligned} \quad (E.13)$$

or

$$\frac{\partial Xf}{\partial z'} = (a \text{ Pem})^{-1} \left[\frac{(1-s)(1-Xf)}{(\tau f (1-s) + s)^2} \nabla^2 \tau f + \frac{\nabla^2 Xf}{(\tau f (1-s) + s)} \right] + \text{Dam } \eta \frac{Rc_s}{Rc^0} \quad (\text{E.14})$$

Equations (E.2), using the dimensionless variable is reduced to,

$$[C_p M T^0 (1-s)/Rw] \partial \tau f / \partial z' = (\lambda f T^0 (1-s)/Rw^2) \nabla^2 \tau f + h A T^0 (1-s) (\tau_s - \tau f)$$

or,

$$\partial \tau f / \partial z' = (a \text{ Pem})^{-1} [\nabla^2 \tau f + \gamma (\tau_s - \tau f)] \quad (\text{E.15})$$

Similarly equation (E.3) in dimensionless form would be

$$\lambda_s (1-s) T^0 / Rw^2 \nabla^2 \tau_s = a_1 (-\Delta H) \rho_b Rc^0 \eta Rc_s / Rc^0 + h A T^0 (1-s) (\tau_s - \tau f) \quad (\text{E.16})$$

or,

$$\nabla^2 \tau_s = [a_1 (-\Delta H) \rho_b Rc^0 Rw^2 / T^0 (1-s) \lambda_s] \eta Rc_s / Rc^0 + h A Rw^2 / \lambda_s (\tau_s - \tau f) \quad (\text{E.17})$$

that is,

$$\nabla^2 \tau_s = -[\text{Dam } H' \text{ Pem } a \beta / (1-s)] \eta Rc_s / Rc^0 + \gamma \beta (\tau_s - \tau f) \quad (\text{E.18})$$

Finally equation (E.4) using the definition of conversion, equation (E.6) is transformed to,

$$k_m A C_f T^0 [(1-X_f)/T_f - (1-X_s)/T_s] = -a_p b R_c^0 \eta R_{c_s}/R_c^0$$

or,

$$(1-X_f)/(\tau_f(1-s)+s) - (1-X_s)/(\tau_s(1-s)+s) = \text{Dam } \delta \eta R_{c_s}/R_c^0 \quad (\text{E.19})$$

E.2 Solution of Partial Differential Equations

Two-Dimensional Claus Reactor

An orthogonal collocation technique was used in the radial direction to convert the partial differential equation (5.40) to (5.42) into ordinary differential equations. As in the case of application of the orthogonal collocation to catalyst pellet effectiveness factor calculation (Section D.2), the symmetrical boundary conditions (5.65) at the center of tube ($r'=0$) are satisfied by trial function which is orthogonal polynomial in $(r')^2$. Thus, X_f , τ_f , and τ_s in the radial direction are described by,

$$X_f\{z', r'\} = \sum_{i=1}^{n_i+1} d_i (r')^{2i-2} \quad (\text{E.20})$$

$$\tau_f\{z', r'\} = \sum_{i=1}^{n_i+1} d_i (r')^{2i-2} \quad (\text{E.21})$$

$$\tau_s\{z', r'\} = \sum_{i=1}^{n_i+1} d_i (r')^{2i-2} \quad (\text{E.22})$$

The same mathematical manipulation described in section D.2 gives,

$$\nabla^2 \underline{Xf} = B \underline{Xf} \quad (\text{E.23})$$

$$\nabla^2 \underline{rf} = B \underline{rf} \quad (\text{E.24})$$

$$\nabla^2 \underline{rs} = B \underline{rs} \quad (\text{E.25})$$

$$\partial \underline{Xf} / \partial r' = A \underline{Xf} \quad (\text{E.26})$$

$$\partial \underline{rf} / \partial r' = A \underline{rf} \quad (\text{E.27})$$

$$\partial \underline{rs} / \partial r' = A \underline{rs} \quad (\text{E.28})$$

where the matrix B from equation (D.22) is,

$$B = D Q^{-1} \quad (\text{E.29})$$

and \underline{Xf} , \underline{rf} , and \underline{rs} are the vectors with the elements evaluated at the collocation points.

The elements of matrix D for cylindrical coordinates (tubular reactor), using equation (D.18)

$$D_{j,j} = \nabla^2 (r')^{2j-2} \quad (\text{at } r'=r'_j) \quad (\text{E.30})$$

and definition of ∇^2 in cylindrical coordinate (tubular reactor),

$$\nabla^2 = 1/r' \partial (r' \partial / \partial r') / \partial r' \quad (\text{E.31})$$

are obtained from,

$$D_{j,j} = (2i-2)^2 (r'_j)^{2i-4} \quad (E.32)$$

The elements of matrix Q are given by equation (D.16) as,

$$Q_{j,j} = (r'_j)^{2i-2} \quad (E.33)$$

The A matrix is given by equation (D.21) as,

$$A = C \cdot Q^{-1}$$

where,

$$C_{j,j} = (2i-2)(r'_j)^{2i-3} \quad (E.34)$$

The program "ORTHOGONAL" given in appendix D also calculates B and A for the cylindrical coordinates. Table E.1 lists the output of this program using interior points in cylindrical coordinates.

Substitution of (E.23) to (E.28) into (5.40) to (5.42) yields $(2 \cdot n_i)$ ordinary differential equations (n_i equations for X_f and n_i equations for rf), and n_i algebraic equations for rs where n_i is the number of interior points in the radial direction. The resulting ordinary differential and algebraic equations are,

$$\frac{dx_{f,j}}{dz'} = (aP_{em})^{-1} \left[\sum_{i=1}^{n_i+1} B_{j,i} \left(\frac{(1-s)(1-x_{f,j})}{(rf_j(1-s)+s)^2} rf_j \right) + \frac{1}{rf_j(1-s)+s} X_{f,j} \right] + \text{Dam } \eta_j \frac{Rc_{j,j}}{Rc^0} \quad (E.35)$$

$$\frac{drf_j}{dz'} = (a \text{ Peh})^{-1} \left[\sum_{i=1}^{ni+1} B_{ji} \tau f_i + \gamma (\tau s_j - \tau f_j) \right] \quad (\text{E.36})$$

$$\sum_{i=1}^{ni+1} B_{ji} \tau s_i = -[\text{Dam } H' \text{ Peh } a \beta / (1-s)] \eta_j \frac{Rc_{s,j}}{Rc^0} + \gamma \beta (\tau s_j - \tau f_j) \quad (\text{E.37})$$

where,

$$j = 1, 2, \dots, ni$$

and η_j , $Rc_{s,j}$ are the effectiveness factor and reaction rate at the catalyst surface condition at the j -th interior radial position. The equation (5.43) at the j -th interior radial position will be,

$$\frac{(1-Xf_j)}{\tau f_j (1-s) + s} - \frac{(1-Xs_j)}{\tau s_j (1-s) + s} = \text{Dam } \delta \eta_j \frac{Rc_{s,j}}{R^0 c} \quad (\text{E.38})$$

In the conventional orthogonal collocation method, there is no collocation point at the center ($r'=0$). Hence the temperature and conversion at the center of the tube might not be obtained accurately. To obtain a better estimate of the variables at the center, special equations which are based on using central differencing will be used as recommended by Ahmed and Fahien (2). These equations are obtained by simplifying equations (5.40) to (5.42) for the case $r' \rightarrow 0$.

Let G denotes Xf , τf , or τs . Then by boundary condition (5.55)

$$\partial G / \partial r' = 0 \quad \text{at } r' = 0 \quad (\text{E.39})$$

and hence $\nabla^2 G$ at $r' = 0$ will be,

$$\nabla^2 G = (1/r') \partial G / \partial r' + \partial^2 G / \partial r^2 = 0/0 + \partial^2 G / \partial r^2 \quad (\text{E.40})$$

which is indeterminate. Using L'Hopital's rule,

$$(1/r') \partial G / \partial r' = \partial^2 G / \partial r^2 \quad (\text{E.41})$$

and

$$\nabla^2 G = 2 \partial^2 G / \partial r^2 \quad \text{at } r' = 0 \quad (\text{E.42})$$

Next, using central differencing on (E.42) yields,

$$\nabla^2 G = 2(G_{-1} - 2G_0 + G_1) / (r'_1)^2, \quad \text{at } r' = 0 \quad (\text{E.43})$$

where the subscript on G denotes the grid point (location of interior points) and r'_1 is the first spatial interval.

However, by symmetry condition $G_1 = G_{-1}$, and

$$\nabla^2 G = 4 (G_1 - G_0) / (r'_1)^2 \quad (\text{E.44})$$

The use of (E.44) into the equations (5.40) to (5.43) converts them into the following equations,

$$\frac{dXf_0}{dz'} = (aPem)^{-1} (4/r_1'^2) \left[\frac{(1-s)(1-Xf_0)(\tau f_1 - \tau f_0)}{(\tau f_0(1-s) + s)^2} + \frac{Xf_1 - Xf_0}{\tau f_0(1+s) + s} \right] + \text{Dam } \eta_0 \text{ Rc}_{,0}/\text{Rc}^\circ \quad (\text{E.45})$$

$$\frac{drf_0}{dz'} = (aPeh)^{-1} \left[\frac{4(\tau f_1 - \tau f_0)}{(r_1')^2} + \gamma(\tau s_0 - \tau f_0) \right] \quad (\text{E.46})$$

$$4/(r_1')^2 (\tau s_1 - \tau s_0) = -[\text{Dam } H' \text{ Peh } a\beta/(1-s)] \eta_0 \text{ Rc}_{,0}/\text{Rc}^\circ + \gamma\beta (\tau s_0 - \tau f_0) \quad (\text{E.47})$$

$$\frac{(1-Xf_0)}{\tau f_0(1-s) + s} - \frac{(1-Xs_0)}{\tau s_0(1-s) + s} = \text{Dam } \delta \eta_0 \text{ Rc}_{,0}/\text{Rc}^\circ \quad (\text{E.48})$$

The above analysis has converted the partial differential and algebraic equations (5.40) to (5.43) into (2ni+2) ordinary differential equations - (E.35), (E.36), (E.45), and (E.46), and (2ni+2) algebraic equations - (E.37), (E.38), (E.47) and (E.48). The solution of these equations provides the conversion and temperature profiles as a function z' and r' .

In order to solve the system of equations (E.35) to (E.38) and (E.45) to (E.48), $x(S_e)$ and Nt have to be calculated at the radial points, '0' to 'ni' for the evaluation of $\eta_{j,0}$ and $\text{Rc}_{,j}$. Equations (B.1) and (B.2) relate $x(S_e)$ and Nt to the level of conversion and temperature. Thus these two equations have to be solved at every radial points '0' to 'ni'.

Next, the boundary conditions are considered. The boundary condition (5.55) is automatically satisfied because symmetrical orthogonal polynomials were chosen. The boundary conditions (5.56) to (5.58), using (E.26) to (E.28) are transformed to,

$$\sum_{i=1}^{ni+1} A_{ni+1,i} Xf_i = 0 \quad (E.49)$$

$$Bif \, rf_{ni+1} + \sum_{i=1}^{ni+1} A_{ni+1,i} rf_i = 0 \quad (E.50)$$

$$Bis \, rs_{ni+1} + \sum_{i=1}^{ni+1} A_{ni+1,i} rs_i = 0 \quad (E.51)$$

The equations (E.49) to (E.51) define Xf , rf , and rs at the $(ni+1)$ -th, that is at $r'=1$ in terms of the corresponding values at the interior points $i=1, \dots, ni$.

To summarize, the two dimensional model of claus reactor, involves solution of $(2ni+2)$ differential equations - (E.35), (E.36), (E.45), and (E.46); coupled with $(2ni+2)$ algebraic equations (E.37), (E.38), (E.47), and (E.48); and $(2ni+2)$ algebraic equations (B.1) and (B.2) to get $x(S_e)$, and Nt_e ; and the three equations (E.49) to (E.51).

The Runge-Kutta-Fehlberg integration algorithm and the Newton-Raphson method were used for integration of the ordinary differential equations and the algebraic equations, respectively. The computer program "BEDTWO" based on the

flowchart of figure E.2, evaluates the performance of the two-dimensional plaus model.

The average radial X_f , r_f , and r_s are obtained from,

$$\begin{aligned} \langle X_f \rangle &= 2 \int_0^{R_w} r X_f dr / R_w^2 \\ &= 2 \int_0^1 r' X_f dr' \end{aligned} \quad (E.52)$$

$$\langle r_f \rangle = 2 \int_0^1 r' r_f dr' \quad (E.53)$$

$$\langle r_s \rangle = 2 \int_0^1 r' r_s dr' \quad (E.54)$$

Finlayson (1972) has shown that the integrals of the form E.52 to E.54 can accurately be evaluated by,

$$\int_0^{n_i+1} G x dx = \sum_{j=1}^{n_i+1} W_j G_j \quad (E.55)$$

where,

$$\underline{W} = Q^{-1} \underline{f} \quad (E.56)$$

with Q given by (E.33) and vector \underline{f} by,

$$f_i = 1/2i \quad (E.57)$$

for cylindrical coordinates, Thus

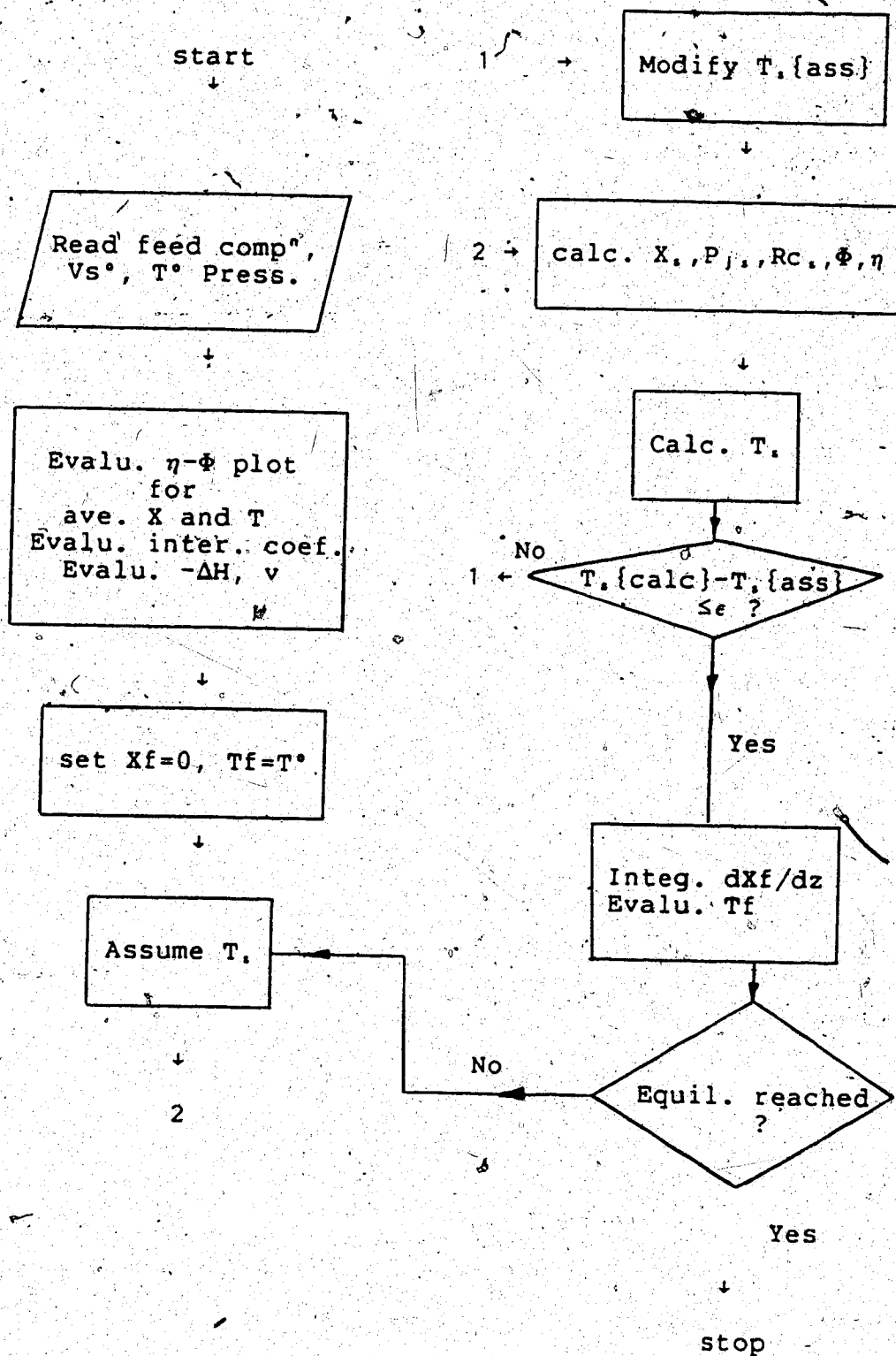
$$\langle Xf \rangle = 2 \sum_{j=1}^{ni+1} W_j Xf_j \quad (E.58)$$

$$\langle rf \rangle = 2 \sum_{j=1}^{ni+1} W_j rf_j \quad (E.59)$$

$$\langle rs \rangle = 2 \sum_{j=1}^{ni+1} W_j rs_j \quad (E.60)$$

The vector W is listed in table E.1, and is used in the program "BEDTWO" for the evaluation of the average radial properties.

Figure E.1 Flow Chart of an Adiabatic One-Dimensional Claus Convertor



```

C*****
C**
C**          MAINLINE ADONEDIMBED
C**
C** THIS PROGRAM SIMULATES THE AD. ONE DIM. MODEL OF
C** CLAUS CONVERTOR AS WAS DESCRIBED IN CHAPTER 5
C**
C*****
C
  IMPLICIT REAL*8(A-H,O-Z,$)
  DIMENSION U(11),V(11),AINT(11,4),GA1(11),GA2(11),
  #GA3(11),THIEM(11),EFF(11)
  DATA THIEM/.1,.2,.45,.6,.75,1.,1.5,2.,3.5,5.,8./
  COMMON/GAMA/GA1,GA2,GA3,U,V
  COMMON/COMP/YH2S,YSO2,YH2O,YN2,DHS,DSO,DW,DS6,DENP
  COMMON/RFCON/A1,A2,A3,A4,TF0,RNF,S6F,PRESS
  COMMON/RELK/RKH2O,RKSO2,CF0,DP
  COMMON/PARA/S6SUR,FI,FIMOD,XS,RNS,RATES,C1,CS
  #,ZCF,ZCF0,CDIF,RKS6,POVRT
  COMMON/SURRES/TS,ETA
  EXTERNAL SNLEQ,FUN,FUNO,DF1,DF2,DF3,DF4,DF5,DF7,DF8
  #,DF9,RATE,HEATR,RFCN,SEVAL
C
C  READ IN THE INPUTS TO THE PROGRAM
C
C***  FEED COMPOSITION, MOLE FRACTION
C
  CALL FREAD(5,'4R*8:',YH2S,YSO2,YH2O,YN2)
  CALL FREAD(5,'4R*8:',YS2,YS4,YS6,YS8)
C
C***  INLET TEMPERATURE AND PRESSURE
C
  CALL FREAD(5,'2R*8:',TF0,PRESS)
C
C  BULK DIFF. OF H2S,SO2,H2O,S6; VISCOSITY OF THE GAS;
C  THERMAL CONDUCTIVITY OF THE GAS.
C
  CALL FREAD(5,'6R*8:',DH2SM,DSO2M,DH2OM,DS6M,VIS,TCON)
C
C***  EFFECTIVE DIFFUSIVITIES IN THE CATALYST PELLET; H2S,
C***  SO2,H2O,S6.
C
  CALL FREAD(5,'4R*8:',DHS,DSO,DW,DS6)
C
C***  INLET SUPERSICIAL VELOCITY
C
  CALL FREAD(5,'R*8:',VS0)
C
C***  CATALYST PELLET DIAMETER, BED POROSITY, BED DENSITY,
C***  DENSITY OF THE PELLET
C
  CALL FREAD(5,'4R*8:',DP,EB,DENB,DENP)
C
C  WRITE THE INPUTS

```

```

C
100 WRITE(8,100)
    FORMAT(/,5X,'INPUTS TO THE PROGRAM ARE')
    WRITE(8,101) YH2S,YSO2,YH2O,YN2
    WRITE(8,101) TF0,PRESS
    WRITE(8,101) DH2SM,DSO2M,DH2OM,DS6M,VIS,TCON
    WRITE(8,101) DHS,DSO,DW,DS6
    WRITE(8,101) VS0
    WRITE(8,101) DP,EB,DENB,DENP
101  FORMAT(/,4X,6D15.5)
C  DEFINE THE VALUES OF REACTOR PARAMETERS
C
    CF0=YH2S*PRESS/TF0/82.06
    ZCF0=2*YS2+4*YS4+6*YS6+8*YS8
    ZCF0=ZCF0*PRESS/82.06/TF0
    RKH2O=(DH2OM/DH2SM)**(2./3.)
    RKS02=(DSO2M/DH2SM)**(2./3.)
    RKS6=(DS6M/DH2SM)**(2./3.)
    CPAVE=YH2O*8.126+YN2*6.9+YH2S*7.31+YSO2*6.453
    AMW=YH2O*18.+YH2S*34.+YSO2*64.+YN2*28
    CPAVE=CPAVE/AMW
    DEN0=AMW*PRESS/TF0/82.06
    GAVE=DEN0*VS0
    RE=DP*GAVE/VIS
    RJD=.458/EB*(RE**(-.407))
    RJH=RJD
    SCH2S=(VIS/DEN0/DH2SM)**(2./3.)
    CMT=RJD*GAVE/DEN0/SCH2S
    PRNO=(CPAVE*VIS/TCON)**(2./3.)
    CHT=RJH*CPAVE*GAVE/PRNO
    WRITE(8,6) RE,RJD,SCH2S,PRNO
6    FORMAT(/,5X,'RYNOLDS',4D15.6)
    WRITE(8,1) CMT,CHT
1    FORMAT(/,5X,'MASS TRAN.',2D15.6)
C
C  TO GET CURVE OF EFFECTIVENESS FACTOR VS MOD-THIELE
C  PARAMETER, USE TF0 AS THE TEMPERATURE AT THE SURFACE.
C  IT HAS BEEN SHOWN IN CHAPTER 4 THAT
C  EVEN 100 DEGREE DIFFERENCE DOES NOT HAVE ANY
C  EFFECT ON THE PLOT.
C
    TS=TF0+50.
    IF(YH2S.LT.0.05) TS=TF0
55  CALL EFFFAC(THIEM,EFF,TS,PRESS,HEAT)
C  READ(18,4) HEAT
C  READ(18,3) (THIEM(I),EFF(I),I=1,11)
    WRITE(8,4) HEAT
4    FORMAT(5X,'HEAT',D15.5)
C
C  USE THE EFFECTIVENESS FAC.-MOD THIELE DATA OBTAINED FOR
C  INTERPOLATION BY NATURAL SPLINE METHOD.
C
C
    WRITE(8,3) (THIEM(I),EFF(I), I=1,11)

```

```

3      FORMAT(/,4D15.8)
      DO 2 I=1,11
      U(I)=DLOG(THIEM(I))
      V(I)=DLOG(EFF(I))
2      CONTINUE
      CALL SPLN(U,V,11,AINT,GA1,GA2,GA3)
C
C      USING THE PARAMETERS OF THE SYSTEM, DEFINE THE CONSTANTS
C      OF EQUATIONS.
C
      A1=HEAT/CPAVE*YH2S/AMW
      A2=HEAT*CMT/CHT*CF0*TF0
      AH=6.*(1.-EB)/DP
      A3=HEAT*DENB/AH/CHT
      A4=DENB/VS0/CF0
      RNF=1.D00
      S6F=0.1D-03
C
C      NOW THE VARIABLES OF THE SYSTEM ARE DEFINED
C      START THE INTEGRATION.
C
      Z0=0.0D00
      X0=0.0D00
C
C*** INTEGRATION STEP SIZE
C
      CALL FREAD(5,'R:',H)
      WRITE(8,102)
102    FORMAT(/,2X,'Z',10X,'XF',12X,'XS',15X,'TF',10X,'TS'
      #,12X,'RATES',10X,'FIMOD',10X,'ETA',14X,'CS')
5      CALL RK4TH(RFUN,Z0,H,X0,XF)
      Z0=Z0+H
      TF=TF0+A1*XF
      WRITE(8,10) Z0,XF,XS,TF,TS,RATES,FIMOD,ETA,CS
      IF(DABS(XF-X0).LT..5D-03) GO TO 20
      X0=XF
      GO TO 5
10     FORMAT(F6.2,8D15.6)
20     STOP
      END
C
C
C
      SUBROUTINE RK4TH(FCN,T0,H,X0,X)
C      THIS SUBROUTINE ADVANCES THE SOLUTION OF A FIRST ORDER
C      DIFFERENTIAL EQUATION OF THE FORM  $DX/DT=F(X,T)$ , USING
C      THE RUNGE-KUTTA 4TH ORDER METHOD.
C      PARAMETERS ARE:
C      FCN  FUNCTION SUBPROGRAM TO COMPUTE  $DX/DT=F(X,T)$ 
C           THIS FUNCTION MUST BE DECLARED EXTERNAL BY THE
C           CALLING PROGRAM
C      X0& T0  VALUES OF X & T AT THE BEGINING OF THE INTERVAL
C      H      STEP SIZE
C      X      VALUE AT THE END OF INTERVAL

```

```

C
C
1  IMPLICIT REAL*8(A-H,O-Z,$)
    XK1=H*FCN(X0,T0)
    WRITE(8,1) X0,XK1
    FORMAT(/,5X,'RK4 ',2D15.5)
    XK2=H*FCN(X0+XK1/2.,T0+H/2.)
    XK3=H*FCN(X0+XK2/2.,T0+H/2.)
    XK4=H*FCN(X0+XK3,T0+H)
    X=X0+(XK1+2.*XK2+2.*XK3+XK4)/6.
    RETURN
    END

```

```

C
C
1  FUNCTION RFUN(XF,Z)
    IMPLICIT REAL*8(A-H,O-Z,$)
    DIMENSION PAR(13),DF(12,12),Y(2)
    COMMON/COMP/YH2S,YSO2,YH2O,YN2,DHS,DSO,DW,DS6,DENP
    COMMON/PARA/ S6SUR,FI,FIMOD,XS,RNS,RATES,C1,CS
    #,ZCF,ZCF0,CDIF,RKS6,POVRT
    COMMON/RFCON/A1,A2,A3,A4,TF0,RNF,S6F,PRESS
    COMMON/SURRES/TS,ETA
    WRITE(8,2) A1,A2,A3,A4,TF0,RNF,S6F,PRESS
    2  FORMAT(/,5X,'RFCON',8D15.5)
    TF=TF0+A1*XF
    IF(XF.LT.0.9D-06) GO TO 1
    NCALL=1
    ICALL=1
    NEQ=2
    C  CALL SNLEQ TO GET S6 , TOTAL MOLES CORRESPONDING TO
    C  THE FLUID CONDITION. FIRST GET THE EQUILIBRIUM CONSTANTS
    C  AT THE FLUID CONDITION.
    C
    CALL EQCTS(TF,PRESS,PAR)
    PAR(4)=YH2S*XF
    PAR(6)=YSO2
    PAR(7)=YH2O
    PAR(11)=YH2S
    PAR(12)=YN2
    Y(1)=S6F
    Y(2)=RNF
    C
    C  NOW CALCULATE TOTAL MOLES TO GET FLUID CONCENTRATION.
    C
    CALL SNLEQ(RHS,TF,PRESS,Y,PAR,1.D00,1,2,ICALL,NI
    #,YH2S,DF,NEQ)
    S6F=Y(1)
    RNF=Y(2)
    C
    C  NOW DEFINE THE PARAMETERS REQUIRED FOR GETTING TS & XS
    C
    1  U=PRESS/RNF/82.06/TF
    POVRT=U*RNF
    CFH2O=(YH2O+YH2S*XF)*U

```

```

CFSO2=(YSO2-.5*YH2S*XF)*U
ZCF=ZCF0+6./4.*YH2S*POVRT*XF
TS1=TF+1.D00
TS2=TF+3.0D00
CALL TEMS(TS1,TS2,TF,XF,CFH2O,CFSO2)

```

```

C
C NOW DEFINE THE DIFFERENTIAL
C

```

```

C WRITE(8,10) ETA
10 FORMAT(/,5X,'ETA IN RFUN SUBPROGRAM ',D15.5)
C RFUN=RATES*ETA*A4
C RETURN
C END

```

```

C
C SUBROUTINE EQCTS(T,PRESS,PAR)
C

```

```

C THIS SUBROUTINE EVALUTES THE EQUILIBRIUM CONSTANTS.
C PLEASE NOTE DIFFERENT EQUATIONS FOR K USING THE
C PUBLISHED AND ADJUSTED FREE ENERGY DATA.
C

```

```

C IMPLICIT REAL*8(A-H,O-Z,$)
C DIMENSION PAR(13)
C RLK62=-34173./T+37.9735

```

```

C DISTORTED DATA
C

```

```

C RLK62=-369044./T+39.3964
C DISTORTED FREE ENERGY DATA
C

```

```

C RLK64=-13663.9/T+12.6028
C RLK64=-11300.2/T+4.91264
C RLK68=2932./T-3.43174
C

```

```

C DISTORTED DATA
C

```

```

C RLK68=2737.72/T-1.56805
C RLK=11050.1/T-11.5576
C

```

```

C DISTORTED DATA
C

```

```

C RLK=9890.75/T-7.75403
C RK=DEXP(RLK)
C RK62=DEXP(RLK62)
C RK64=DEXP(RLK64)
C RK68=DEXP(RLK68)
C AA=(RK62/PRESS/PRESS)**(1./3.)
C BB=(RK64/DSQRT(PRESS))**(2./3.)
C CC=(RK68*(PRESS**.25))**(4./3.)
C PAR(1)=AA
C PAR(2)=BB
C PAR(3)=CC
C PAR(5)=RK

```

```

PAR(8)=PAR(5)*DSQRT(PRESS)
RETURN
END

```

C
C

```

SUBROUTINE TEMS(TS1,TS2,TF,XF,CFH2O,CF2O,
IMPLICIT REAL*8(A-H,O-Z,$)
DIMENSION F(100),T(100),GA1(11),GA2(11),GA3(11),
,X(3),U(11),V(11),PAR(13),DF(12),DHS,DSO,DW,DS6,DENP
COMMON/GAMA/GA1,GA2,GA3,U,V
COMMON/COMP/YH2S,YSO2,YH2O,YN2,DHS,DSO,DW,DS6,DENP
COMMON/RELK/RKH2O,RKSQ2,CF0,DP
COMMON/REFCON/A1,A2,A3,A4,TF0,RNF,S6F,PRESS
COMMON/PARA/ S6SUR,FI,FIMOD,XS,RNS,RATES,C1,CS
#,ZCF,ZCF0,CDIF,RKS6,POVRT
COMMON/SURRES/TS,ETA
COMMON/CALL/NCALL,NTYPE
PAR(6)=YH2S
PAR(7)=YH2O
PAR(9)=DHS/DW
PAR(10)=DHS/DSO
PAR(11)=YH2S
PAR(12)=YN2
PAR(13)=DHS/DS6
NCALL=0
NEQ=2
I=1
TS=TS1
5 XS=1.+TS/A2*(TS-TF)-TS/TF*(1.-XF)
CDIF=CF0*TF0*(1.-XS)/TS-(1.-XF)/TF
CSH2O=CFH2O-RKH2O*CDIF
CSSO2=CFSO2+.5*RKSQ2*CDIF
PSH2O=CSH2O*82.06*TS
PSSO2=CSSO2*82.06*TS
CALL EQCTS(TS,PRESS,PAR)
X(1)=S6F
X(2)=RNF
PAR(4)=YH2S*XS
CALL SNLEQ(RHS,TS,PRESS,X,PAR,,5D00,1,2,1,NI,YH2S,
#DF,NEQ)
S6SUR=X(1)
RNS=X(2)
18 NTYPE=2

```

```

RATES=RATE(PSH2O,PSSO2,NTYPE,TS,PRESS,PAR,XS,S6SUR,RNS)

```

```

C IF(I.GT.1) GO TO 10

```

```

CS=CF0*(1.-XS)*TF0/TS

```

```

C WRITE(8,41) CS,RATES

```

```

41 FORMAT(/,' CS , RATES (',2D15.5)

```

C

```

C IF RATES IS NEGATIVE,, THE ASSUMED TS IS TOO LARGE ,REDUCE

```

IT

C

```

IF(RATES) 40,45,45

```

```

40    TS=TF
      GO TO 5
45    FI=DP/6.*DSQRT(RATES/CS*DENP/DHS)
C     X(1)=S6SUR
      X(1)=0.006
      X(2)=1.0
      X(3)=0.75
C     X(2)=RNS
C     X(3)=.7D00
C
C     LET NCALL BE 2 TO GET CONDITION INSIDE THE PELLET.
C
      NCALL=2
      NEQ=3
      CALL SNLEQ(RHS,TS,PRESS,X,PAR,1.D00,-1,3,2,NI,YH2S,
#DF,NEQ)
C
C     RESET NCALL TO 1 AND NEQ TO 2 BECAUSE FROM NOW ON
C     ONLY SURFACE CONDITION IS CONSIDERED AT THIS VALUE
C     OF XF & TF .
C
      NCALL=0
      NEQ=2
      XEQ=X(3)
      RNE=X(2)
      C1=(1.-XEQ)/(1.-XS)*RNS/RNE
      FIMOD=FI/DSQRT(1.-C1)
      IF(FIMOD.LT..9D-01) GO TO 25
      FIM=DLOG(FIMOD)
      ETA=SEVAL(11,FIM,U,V,GA1,GA2,GA3)
      ETA=DEXP(ETA)
      GO TO 10
25    ETA=1.D00
C     WRITE(8,1) FIMOD,ETA
1     FORMAT(/,5X,'FIMOD-ETA',2D15.6)
C
10    F(I)=TS-TF-A3*RATES*ETA
      T(I)=TS
C     WRITE(8,50) I,TS,XS,RATES
50    FORMAT(/,5X,'ITER',2X,I5,3D18.5)
C     IF(I.GE.2) GO TO 20
      IF(I-2) 12,13,20
12    TS=TS2
      I=I+1
      GO TO 5
13    IF(DABS(T(2)-T(1)).GT..1D-10) GO TO 20
      TS=TF+.01
      I=2
      GO TO 5
20    DIFF=(F(I)-F(I-1))/(T(I)-T(I-1))
      TSC=TS-.75*F(I)/DIFF
C     WRITE(8,51) TS,TSC
51    FORMAT(/,5X,'TSC',2D18.5)
      IF(DABS(TSC-TS).LT.1.D-02) GO TO 30

```



```

      TS=TSC
      I=I+1
      GO TO 5
30    TS=TSC
      C      WRITE(8,2) I
      2      FORMAT(/,5X,'I=',I5)
      RETURN
      END

```

```

      C
      C
      C      FUNCTION HEATR(V1,V2,V3,V4,TS)
      C      IMPLICIT REAL*8(A-H,O-Z,$)
      C      DH298=-35008.8+V1*31200+V2*34810+V3*24360+V4*24320
      C      DCP=-4.818121+V1*8.54+V2*19.092+V3*31.58+V4*42.67
      C      HEATR=DH298+DCP*(TS-298)
      C      HEATR=-HEATR

```

```

      C
      C      THIS IS HEAT FOR 2 MOLES OF REACTED H2S. TO GET
      C      HEAT PER MOLE OF H2S DIVIDE BY 2.
      C

```

```

      C      HEATR=HEATR/2.
      C      RETURN
      C      END

```

```

      C
      C
      C      SUBROUTINE EFFFAC(THIEM,EFF,TS,PRESS,HEAT)
      C      IMPLICIT REAL*8 (A-H,O-Z,$)
      C      DIMENSION X(12),DF(12,12),B(5,5),B1(5,5),
      C      #THIEM(11),EFF(11),Y(3),Z(5),QINV(5,5),A(5,5),PAR(13)
      C      COMMON /COMP/ YH2S,YSO2,YH2O,YN2,DHS,DSO,DW,DS6,DENP
      C      COMMON /PARA/ S6SUR,FI,FIMOD,XS,RNS,RATES,C1,CS
      C      #,ZCF,ZCF0,CDIF,RKS6,POVRT
      C      COMMON /ORTH/ B,B1,A,X,QINV,Z
      C      COMMON /CALL/NCALL,NTYPE
      C      XS=.5D00
      C      IF(YH2S.LT.0.05) XS=0.1D00
      C      CALL EQCTS(TS,PRESS,PAR)
      C      PAR(4)=YH2S*XS
      C      PAR(6)=YSO2
      C      PAR(7)=YH2O
      C      PAR(9)=DHS/DW
      C      PAR(10)=DHS/DSO
      C      PAR(11)=YH2S
      C      PAR(12)=YN2
      C      PAR(13)=DHS/DS6
      C      NCALL=1
      C      X(1)=.02
      C      X(2)=.98
      C      NEQ=2
      C      CALL SNLEQ(RHS,TS,PRESS,X,PAR,1.D00,1,2,1,NI,YH2S,
      C      #DF,NEQ)
      C      S6SUR=X(1)
      C      RNS=X(2)
      C      NTYPE=1

```

```

      RATES=RATE(PSH2O,PSSO2,NTYPE,TS,PRESS,PAR,XS,S6SUR
# ,RNS)
C
C EVALUATE STIOCHIOMETRIC COEFFICIENTS FOR THIS AVERAGE
C CONVERSION AND FEED TEMPERATURE. ASSUME THIS IS CONSTANT
C WITH REGARD TO HEAT OF REACTION CALCULATION.
C
      S2=PAR(1)*((S6SUR*RNS*RNS)**(1./3.))
      S4=PAR(2)*((S6SUR*S6SUR*RNS)**(1./3.))
      S8=PAR(3)*(((S6SUR**4)/RNS)**(1./3.))
C REACTION: 2H2S+SO2=2H2O+V1 S2+V2 S4+V3 S6 V4 S8
C
      V1=2.*S2/YH2S/XS
      V2=2.*S4/YH2S/XS
      V3=2.*S6SUR/YH2S/XS
      V4=2.*S8/YH2S/XS
      HEAT=HEATR(V1,V2,V3,V4,TS)
C
C
C..NOW SNLEQ IS USED TO GET EQUILIBRIUM CONVERSION.
C..HERE X(1) IS S6EQ,X(2) MOLE AT EQ, AND X(3) EQCONV ..
C..NOW ICALL=2 AND NCALL=2 ..
C
      NEQ=3
      NCALL=2
      WRITE(6,1)
1  FORMAT('ESTIMATE OF S6,N AND XEQ AT THE CENTER OF'
# , ' THE PELLET ?')
      CALL FREAD(5,'3R*8:',X(1),X(2),X(3))
      CALL SNLEQ(RHS,TS,PRESS,X,PAR,.5D00,1,3,2,NI,YH2S
#DF,NEQ)
      S6EQ=X(1)
      RNE=X(2)
      XEQ=X(3)
C
C C1 IS CEQ./C AT THE SURFACE
C
      C1=(1.-XEQ)/(1.-XS)*RNS/RNE
      DO 2000 II=1,11
      FIMOD=THIEM(II)
      FI=FIMOD*(DSQRT(1.-C1))
      IF(II.EQ.1) NI=1
      IF(II.EQ.2) NI=2
      IF(II.EQ.3) GO TO 1109
      IF(II.EQ.4) NI=3
      IF(II.EQ.5.OR.II.EQ.6) GO TO 1109
      IF(II.EQ.7) NI=4
      IF(II.EQ.8.OR.II.EQ.9) GO TO 1109
      IF(II.EQ.10) GO TO 1110
      GO TO (11,12,13,14) , NI
11  CALL FTNCMD('ASSIGN 7=OR1',12)
      GO TO 17
12  CALL FTNCMD ('ASSIGN 7=OR2' ,12)
      GO TO 17

```

```

13  CALL FTNCMD('ASSIGN 7=OR3' ,12)
    GO TO 17
14  CALL FTNCMD ('ASSIGN 7=OR4' ,12)
17  N=3*NI
    M=1
    NM=NI+1
    LINE=(26+2*NM)*1000
    DO 300 I=1,NM
      READ(7'LINE,500) (B(I,J) , J=1,NM)
      LINE=LINE+1000
300  CONTINUE
    LINE=(21+NM)*1000
    DO 400 I=1,NM
      READ(7'LINE,500) (A(I,J) , J=1,NM)
      LINE=LINE+1000
400  CONTINUE
    LINE=(31+3*NM)*1000
    DO 450 I=1,NM
      READ(7'LINE,500) (B1(I,J),J=1,NM)
      LINE=LINE+1000
450  CONTINUE
    LINE=10*1000
    READ(7'LINE,545) (Z(I),I=1,NM)
500  FORMAT(10X,10D18.10)
545  FORMAT(10D18.10)
    LINE=16*1000
    DO 546 I=1,NM
      READ(7'LINE,500) (QINV(I,J) , J=1,NM)
      LINE=LINE+1000
546  CONTINUE
    SN=(RNS-RNE)/(XS-XEQ)
    BN=RNS-SN*XS
    SS6=(S6SUR-S6EQ)/(XS-XEQ)
    BS6=S6SUR-SS6*XS
    DO 602 J=1,NI
      SI=Z(J)*Z(J)
      JJ=J+2*(J-1)
      RHS=(SI*(1.D00-C1)+C1)*(1.D00-XS)/RNS
      X(JJ)=(1.D00-RHS*BN)/(1.D00+RHS*SN)
      X(JJ+1)=SS6*X(JJ)+BS6
      X(JJ+2)=SN*X(JJ)+BN
602  CONTINUE
525  NEQ=N
1109 CALL SNLEQ(RHS,TS,PRESS,X,PAR,.75D00,M,N,3,NI,YH2S
      #DF,NEQ)
    GO TO 1270
1110 CONTINUE

```

```

C
C  IN THIS SECTION ONE POINT IS CONSIDERED FOR
C  GETTING YI AND EFF.
C

```

```

    RKISI=.6546536707D00
    SI=(RKISI)*(RKISI)
    RHS=(SI*(1.D00-C1)+C1)*(1.D00-XS)/RNS

```

```

      Y(3)=(1.D00-RHS*BN)/(1.D00+RHS*SN)
      Y(1)=SS6*Y(3)+BS6
      Y(2)=SN*Y(3)+BN

```

```

C
C NOW SNLEQ IS CALLED TO SOLVE FOR X, S6, AND N
C FOR SPECIFIED SI.
C

```

```

      CALL SNLEQ
      (RHS, TS, PRESS, Y, PAR, 1.D00, M, 3, 5, NI, YH2S, DF, 3)
      XRKISI=Y(3)
      S6KISI=Y(1)
      TMKISI=Y(2)
      RRKISI=RATE(PSH20, PSSO2, NTYPE, TS, PRESS, PAR, XRKISI,
        #S6KISI, TMKISI)

```

```

C
C NOW KISI OPTIMUM IS ESTIMATED
C

```

```

      RRATIO=RATES/RRKISI
      SIR=1.0D00/SI
      POWER=DLOG(RRATIO)/DLOG(SIR)
      OPKISI=(1.D00+POWER)**(.5D00/POWER)
      OPKISI=1.D00/OPKISI
      SI=OPKISI**2
      RHS=(SI*(1.D00-C1)+C1)*(1.D00-XS)/RNS
      Y(3)=(1.D00-RHS*BN)/(1.D00+RHS*SN)
      Y(1)=SS6*Y(3)+BS6
      Y(2)=SN*Y(3)+BN
      CALL SNLEQ
      (RHS, TS, PRESS, Y, PAR, 1.D00, M, 3, 5, NI, YH2S, DF, 3)
      XRKISI=Y(3)
      S6KISI=Y(1)
      TMKISI=Y(2)
      RRKISI=RATE(PSH20, PSSO2, NTYPE, TS, PRESS, PAR, XRKISI,
        #S6KISI, TMKISI)
      AYI=9.D00*(FIMOD**2)*RRKISI/RATES
      CALL SOLYI(YI, RKISI, AYI, NFLAG)
      EFF(II)=2./3./(FIMOD**2)/(1.-YI)
      NI=1
      GO TO 2000
1270  EFF(II)=A(NM, NM)
      DO 1200 J=1, NI
      K=J+2*(J-1)
1150  EFF(II)=EFF(II)+A(NM, J)/(1.-C1)
      #((1.-X(K))/(1.-XS)*RNS/X(K+2)-C1)
1200  CONTINUE
      EFF(II)=EFF(II)/3./FIMOD/FIMOD
2000  CONTINUE
      RETURN
      END

```

```

C
C

```

```

      SUBROUTINE SNLEQ(RHS, TS, PRESS, X, PAR, W, M, N, ICALL, NI
        #, YH2S, DF, NEQ)
C THIS SUBROUTINE SOLVES SYSTEM OF NONLINEAR

```

C EQ S BY NEWTONS S METHOD.

C
IMPLICIT REAL*8(A-H,O-Z,S)
DIMENSION FSAVE(12),X(12),F(12,1),DF(NEQ,NEQ)
#,WKAREA(1000),Z(5),XSAVE(12),PAR(13),Y(2)

500 FORMAT(5D14.5)
IA=NEQ
IDGT=0
MAXIT=200
FTOL=.1D-11
XTOL=.1D-11
NUM=N+1
IF(NEQ.EQ.N) NUM=N
DO 100 I=1,MAXIT
DO 110 J=1,NUM
110 XSAVE(J)=X(J)
330 FORMAT(/,6D15.6)

C
C ICALL=1 FOR SURFACE , ICALL=2 FOR EQUILIBRIUM , AND
C ICALL=3 FOR PROFILE ESTIMATION.
C

IF(ICALL.EQ.1) GO TO 70

IF(ICALL.EQ.2) GO TO 75

C
C ICALL=5 TO GET N,S6,X FOR GIVEN SI
C

IF(ICALL.EQ.5) GO TO 900
DO 30 II=1,NEQ
DO 30 J=1,NEQ
30 DF(J,II)=0.0
KK=1
DO 10 KI=1,N,3
F(KI,1)=FUNO(TS,PRESS,NI,N,KK,PAR)
DF(KI,KI)=DF1(TS,PRESS,NI,KK,PAR)
DF(KI,KI+1)=DF5(TS,PRESS,NI,KK,PAR)
DF(KI,KI+2)=DF3(TS,PRESS,NI,KK,PAR)
KK=KK+1

10 CONTINUE
DO 20 KI=2,N,3
PAR(4)=X(KI-1)
Y(1)=X(KI)
Y(2)=X(KI+1)
F(KI,1)=FUN(Y,1,PAR)
DF(KI,KI-1)=DF9(Y,1,PAR)
F(KI+1,1)=FUN(Y,2,PAR)
DF(KI,KI)=DF7(Y,1,PAR)
DF(KI,KI+1)=DF8(Y,1,PAR)
DF(KI+1,KI-1)=DF9(Y,2,PAR)
DF(KI+1,KI)=DF7(Y,2,PAR)
DF(KI+1,KI+1)=DF8(Y,2,PAR)

20 CONTINUE
21 IF (NI.EQ.1) GO TO 58
KK=1
DO 60 KI=1,N,3

```

      KKK=1
      DO 50 KJ=1,N,3
      IF(KI.EQ.KJ) GO TO 55
      DF(KI,KJ)=DF2(NI,KK,KKK)
      DF(KI,KJ+2)=DF4(KK,KKK,NI)
55    KKK=KKK+1
50    CONTINUE
      KK=KK+1
60    CONTINUE
58    CONTINUE
      GO TO 80
70    F(1,1)=FUN(X,1,PAR)
      F(2,1)=FUN(X,2,PAR)
      DF(1,1)=DF7(X,1,PAR)
      DF(1,2)=DF8(X,1,PAR)
      DF(2,1)=DF7(X,2,PAR)
      DF(2,2)=DF8(X,2,PAR)
2000  FORMAT(/,30D15.6)
3500  FORMAT(//,30D15.6)
      GO TO 80
75    PAR(4)=X(3)
      F(1,1) = FUN(X,1,PAR)
      F(2,1) = FUN(X,2,PAR)
      F(3,1) = FUN(X,3,PAR)
      DF(1,1) = DF7(X,1,PAR)
      DF(1,2) = DF8(X,1,PAR)
      DF(1,3) = DF9(X,1,PAR)
      DF(2,1) = DF7(X,2,PAR)
      DF(2,2) = DF8(X,2,PAR)
      DF(2,3) = DF9(X,2,PAR)
      DF(3,1) = DF7(X,3,PAR)
      DF(3,2) = DF8(X,3,PAR)
      DF(3,3)=DF9(X,3,PAR)
      GO TO 80
900   PAR(4)=X(3)
      F(1,1)=FUN(X,1,PAR)
      F(2,1)=FUN(X,2,PAR)
      F(3,1)=RHS-(1.D00-X(3))/X(2)
      DF(1,1)=DF7(X,1,PAR)
      DF(1,2)=DF8(X,1,PAR)
      DF(1,3)=DF9(X,1,PAR)
      DF(2,1)=DF7(X,2,PAR)
      DF(2,2)=DF8(X,2,PAR)
      DF(2,3)=DF9(X,2,PAR)
      DF(3,1)=0.0D00
      DF(3,2)=(1.D00-X(3))/X(2)/X(2)
      DF(3,3)=1.D00/X(2)
80    ITEST=0
C
C    SCALING THE JACOBIAN MATRIX
C
      DO 92 ISS=1,NEQ
      SCALE=DABS(DF(ISS,1))
      DO 90 IS=1,NEQ

```

```

          IF(DABS(DF(ISS,IS)).GT.SCALE) SCALE=DABS(DF(ISS,IS))
90      CONTINUE
          DO 91 I=1,NEQ
          DF(ISS,IS)=DF(ISS,IS)/SCALE
91      CONTINUE
          F(ISS,1)=F(ISS,1)/SCALE
92      CONTINUE
          DO 220 J=1,NEQ
          FSAVE(J)=F(J,1)
          F(J,1)=-F(J,1)
220     CONTINUE
33      CALL LEQT1F(DF,M,NEQ,IA,F,IDGT,WKAREA,IER)
          DO 1000 II=1,NEQ
          X(II)=XSAVE(II)+W*F(II,1)
1000    CONTINUE
1001    DO 550 JJ=1,NEQ
          IF(DABS(F(JJ,1)).GT.XTOL) ITEST=ITEST+1
          IF(FSAVE(JJ).GT.FTOL) ITEST=ITEST+1
550     CONTINUE
C      IF TOL MET PRINT THE RESULT
          IF(ITEST.EQ.0) GO TO 200
100     CONTINUE
          WRITE(8,400)
400     FORMAT(/, 'CONVERGENCE WAS NOT ACHIEVED AFTER
          #, '100 ITER')
          RETURN
200     CONTINUE
350     RETURN
          END

```

```

C
FUNCTION FUN(X,K,PAR)
IMPLICIT REAL*8(A-H,O-Z,$)
DIMENSION X(3),PAR(13)
COMMON /VAR/ P1,P2,P3,P4,P5,P6,P7,P8,P9,PPH20,PPH2S
#,PPSO2,ZW,ZWS
COMMON /PAR/ S6SUR,FI,FIMOD,XS,RNS,RATES,C1,CS
#,ZCF,ZCF0,CDIF,RKS6,POVRT
COMMON/CALL/NCALL,NTYPE
P1=(X(1)*X(2)*X(2))**(1./3)
P2=(X(1)*X(1)*X(2))**(1./3.)
P3=((X(1)**4)/X(2))**(1./3.)
P4=(X(2)/X(1))**(2./3.)
P5=DSQRT(P4)
P6=(X(1)/X(2))**(1./3.)
P7=P3/X(2)
IF(NCALL.LT.2) GO TO 30
P8=(PAR(7)+PAR(11)*XS)/RNS
P9=(PAR(6)-PAR(11)*XS/2.)/RNS
A=(1.-XS)/RNS-(1.-PAR(4))/X(2)
PPH20=P8+PAR(9)*PAR(11)*A
PPSO2=P9-PAR(10)*PAR(11)*A/2.
ZWS=(S6SUR/RNS)**(1./3.)
ZW=(X(1)/X(2))**(1./3.)
ZSOVP=2.*PAR(1)*ZWS+4.*PAR(2)*ZWS*ZWS+6.*S6SUR/RNS+

```

```

#8.*PAR(3)*ZWS**4
ZOV=2.*PAR(1)*ZW+4.*PAR(2)*ZW*ZW+6.*X(1)/X(2)+
#8.*PAR(3)*ZW**4
GO TO (6,11,20) ,K
6 FUN=X(2)*(PPH2O+PPSO2-1.)+PAR(11)*(1.-PAR(4))
#+PAR(1)*P1+PAR(2)*P2+X(1)+PAR(3)*P3+PAR(12)
RETURN
11 FUN=ZOV-ZSOV-6./4.*PAR(13)*PAR(11)*A
RETURN
20 PPH2S=PAR(11)*(1.-X(3))/X(2)
FUN=PAR(8)*(PPH2S**2)*(PPSO2)
FUN=FUN-(PPH2O**2)*DSQRT(X(1)/X(2))
RETURN
30 GO TO (5,10) , K
5 FUN=1-.5*PAR(4)+PAR(1)*P1+PAR(2)*P2+X(1)+PAR(3)*P3
#-X(2)
RETURN
10 IF(NCALL.EQ.0) GO TO 12
FUN=2*PAR(1)*P1+4*PAR(2)*P2+6*X(1)+8*PAR(3)*P3
#-1.5*PAR(4)
RETURN
12 ZCS=POVRT*(2.*PAR(1)*P1+4.*PAR(2)*P2+6.*X(1)+8.
#*PAR(3)*P3)
FUN=ZCS-ZCF+6./4.*RKS6*CDIF
RETURN
END
C
C
FUNCTION DF7(X,K,PAR)
IMPLICIT REAL*8(A-H,O-Z,$)
DIMENSION X(3),PAR(13)
COMMON /VAR/ P1,P2,P3,P4,P5,P6,P7,P8,P9,PPH2O,PPH2S
#,PPSO2,ZW,ZWS
COMMON /PARA/ S6SUR, FI,FIMOD,XS,RNS,RATES,C1,CS
#,ZCF,ZCF0,CDIF,RKS6,POVRT
COMMON/CALL/NCALL,NTYPE
GO TO (5,10,20) , K
5 DF7=PAR(1)*P4/3.+2.*PAR(2)*P5/3.+1.+4./3.*PAR(3)*P6
RETURN
10 IF(NCALL.EQ.0) GO TO 11
DF7=2./3.*PAR(1)/P2+8./3.*PAR(2)/P1+6./X(2)+32./3.
#*PAR(3)*P6/X(2)
RETURN
11 DF7=POVRT*(2./3.*PAR(1)*P4+8./3.*PAR(2)/P6+6.+32./3.
#*PAR(3)*P6)
RETURN
20 DF7=-0.5D00*(PPH2O**2)/DSQRT(X(1)*X(2))
RETURN
END
C
C
FUNCTION DF8(X,K,PAR)
IMPLICIT REAL*8(A-H,O-Z,$)
DIMENSION X(3),PAR(13)

```



```

COMMON /VAR/ P1,P2,P3,P4,P5,P6,P7,P8,P9,PPH20,PPH2S
#,PPSO2,ZW,ZWS
COMMON /PAR/ S6SUR, FI,FIMOD,XS,RNS,RATES,C1,CS
#,ZCF,ZCF0,CDIF,RKS6,POVRT
COMMON/CALL/NCALL,NTYPE
IF(NCALL.GT.1) GO TO 50
GO TO (5,10) , K
5  DF8=2./3.*PAR(1)/P5+PAR(2)/3./P4-PAR(3)*P7/3.-1.
RETURN
10 DF8=4./3.*PAR(1)/P5+4./3.*PAR(2)/P4-8.*PAR(3)*P7/3.
IF(NCALL.EQ.0) DF8=DF8*POVRT
RETURN
50 GO TO (60,70,80) ,K
60 DF8=2/3*PAR(1)*P6+1/3.*PAR(2)/P4-1./3.*PAR(3)*P7-1.
DF8=DF8+PPH20+PPSO2+(PAR(9)-PAR(10)/2.)*PAR(11)
#*(1.-PAR(4))/X(2)
RETURN
70 DF8=-2./3.*PAR(1)*P6/X(2)-8./3.*PAR(2)/P4/X(2)-6.
#*X(1)/X(2)/X(2)-32./3.*PAR(3)*P3/X(2)/X(2)
-6./4.*PAR(13)*PAR(11)*(1.-PAR(4))/X(2)/X(2)
RETURN
80 DPH20=PAR(9)*PAR(11)*(1.-X(3))/(X(2)**2)
DPSO2=-PAR(10)*PAR(11)*(1.-X(3))/(X(2)**2)
DPH2S=-PAR(11)*(1.-X(3))/(X(2)**2)
DF8=2.*PAR(8)*PPH2S*PPSO2*DPH2S
DF8=DF8+PAR(8)*(PPH2S**2)*DPSO2
DF8=DF8-2.*PPH20*DPH20*DSQRT(X(1)/X(2))
DF8=DF8+.5*(PPH20**2)*DSQRT(X(1))*(X(2)**(-1.5))
RETURN
END

```

C
C

FUNCTION DF9(X,K,PAR)
C THIS FUNCTION CALCULATES THE DIFFERENTIAL WITH RESPECT
C TO CONVERSION.

C

```

IMPLICIT REAL*8(A-H,O-Z,$)
DIMENSION X(3),PAR(13)
COMMON /VAR/ P1,P2,P3,P4,P5,P6,P7,P8,P9,PPH20,PPH2S
#,PPSO2,ZW,ZWS
COMMON /PAR/ S6SUR, FI,FIMOD,XS,RNS,RATES,C1,CS
#,ZCF,ZCF0,CDIF,RKS6,POVRT
COMMON/CALL/NCALL,NTYPE
GO TO (5,10,20) ,K
5  DF9=PAR(11)*(PAR(9)-.5*PAR(10)-1.0)
RETURN
10 DF9=-6./4.*PAR(13)*PAR(11)/X(2)
RETURN
20 DPH20=PAR(9)*PAR(11)/X(2)
DPSO2=-PAR(10)*PAR(11)/2./X(2)
DPH2S=-PAR(11)/X(2)
DF9=2.*PAR(8)*PPH2S*PPSO2*DPH2S
DF9=DF9+PAR(8)*(PPH2S**2)*DPSO2
DF9=DF9-2.*PPH20*DPH20*DSQRT(X(1)/X(2))

```

RETURN
END

C
C

```

FUNCTION FUNO(TS,PRESS,NI,N,J,PAR)
IMPLICIT REAL*8(A-H,O-Z,$)
DIMENSION X(12),B(5,5),B1(5,5),Z(5),A(5,5),PAR(13),
#QINV(5,5)
COMMON /PARA/ S6SUR, FI,FIMOD,XS,RNS,RATES,C1,CS
#,ZCF,ZCF0,CDIF,RKS6,POVRT
COMMON /ORTH/ B,B1,A,X,QINV,Z
COMMON/CALL/NCALL,NTYPE
FUNO=0.0
K=1
DO 10 I=1,N,3
5 FUNO=FUNO+B(J,K)*((1.-X(I))/(1.-XS)*RNS/X(I+2)
#C1)/(1.D00-C1)
30 K=K+1
10 CONTINUE
M=J+2*(J-1)
R=RATE(PSH20,PSSO2,NTYPE,TS,PRESS,PAR,X(M),X(M+1)
#,X(M+2))
40 FUNO=FUNO+B(J,NI+1)-9.*FIMOD*FIMOD*R/RATES
60 RETURN
END

```

C
C

```

FUNCTION DF1(TS,PRESS,NI,J,PAR)
IMPLICIT REAL*8(A-H,O-Z,$)
DIMENSION X(12),B(5,5),B1(5,5),Z(5),A(5,5),PAR(13)
#,QINV(5,5)
COMMON /PARA/ S6SUR, FI,FIMOD,XS,RNS,RATES,C1,CS
#,ZCF,ZCF0,CDIF,RKS6,POVRT
COMMON /ORTH/ B,B1,A,X,QINV,Z
COMMON/CALL/NCALL,NTYPE
K=J+2*(J-1)
5 DF1=-B(J,J)/(1.-XS)*RNS/X(K+2)/(1.D00-C1)
20 R1=RATE(PSH20,PSSO2,NTYPE,TS,PRESS,PAR,X(K),X(K+1)
#,X(K+2))
CONV=X(K)+0.00001
R2=RATE(PSH20,PSSO2,NTYPE,TS,PRESS,PAR,CONV,X(K+1)
#,X(K+2))
DR=(R2-R1)/.00001
30 DF1=DF1-9.*FIMOD*FIMOD*DR/RATES
50 RETURN
END

```

C
C

```

FUNCTION DF2(NI,J,I)
IMPLICIT REAL*8(A-H,O-Z,$)
DIMENSION X(12),B(5,5),B1(5,5),Z(5),A(5,5),PAR(13)
#,QINV(5,5)
COMMON /PARA/ S6SUR, FI,FIMOD,XS,RNS,RATES,C1,CS
#,ZCF,ZCF0,CDIF,RKS6,POVRT

```

```

COMMON /ORTH/ B,B1,A,X,QINV,Z
K=I+2*(I-1)
5 DF2=-B(J,I)*RNS/(1.-XS)/X(K+2)/(1.D00-C1)
20 RETURN
END

```

C
C

```

FUNCTION DF3(TS,PRESS,NI,J,PAR)
IMPLICIT REAL*8(A-H,O-Z,$)
DIMENSION X(12),B(5,5),B1(5,5),Z(5),A(5,5),PAR(13)
#,QINV(5,5)
COMMON /PARA/ S6SUR, FI,FIMOD,XS,RNS,RATES,C1,CS
#,ZCF,ZCF0,CDIF,RKS6,POVRT
COMMON /ORTH/ B,B1,A,X,QINV,Z
COMMON/CALL/NCALL,NTYPE
K=J+2*(J-1)
5 DF3=-B(J,J)*(1.-X(K))/(1.-XS)*RNS/(X(K+2)**2)
#/(1.D00-C1)
20 R1=RATE(PSSH2O,PSSO2,NTYPE,TS,PRESS,PAR,X(K),X(K+1)
#,X(K+2))
CM=X(K+2)+.00001
R2=RATE(PSSH2O,PSSO2,NTYPE,TS,PRESS,PAR,X(K),X(K+1),CM)
DR=(R2-R1)/.00001
30 DF3=DF3-9.*FIMOD*FIMOD/RATES*DR
50 RETURN
END

```

C
C

```

FUNCTION DF4(J,I,NI)
IMPLICIT REAL*8(A-H,O-Z,$)
DIMENSION X(12),B(5,5),B1(5,5),Z(5),A(5,5),PAR(13)
#,QINV(5,5)
COMMON /PARA/ S6SUR, FI,FIMOD,XS,RNS,RATES,C1,CS
#,ZCF,ZCF0,CDIF,RKS6,POVRT
COMMON /ORTH/ B,B1,A,X,QINV,Z
M=I+2*(I-1)
5 DF4=-B(J,I)*(1.-X(M))/(1.-XS)*RNS/(X(M+2)**2)
#/(1.D00-C1)
20 RETURN
END

```

C
C

```

FUNCTION DF5(TS,PRESS,NI,J,PAR)
IMPLICIT REAL*8(A-H,O-Z,$)
DIMENSION X(12),B(5,5),B1(5,5),Z(5),A(5,5),PAR(13)
#,QINV(5,5)
COMMON /PARA/ S6SUR, FI,FIMOD,XS,RNS,RATES,C1,CS
#,ZCF,ZCF0,CDIF,RKS6,POVRT
COMMON /ORTH/ B,B1,A,X,QINV,Z
COMMON/CALL/NCALL,NTYPE
K=J+2*(J-1)
R1=RATE(PSSH2O,PSSO2,NTYPE,TS,PRESS,PAR,X(K)
#,X(K+1),X(K+2))
CS6=X(K+1)+.00001

```

```

R2=RATE(PSH2O,PSSO2,NTYPE,TS,PRESS,PAR,X(K),CS6
#,X(K+2))
DR=(R2-R1)/.00001
10 DF5=-9.*FIMOD*FIMOD*DR/RATES
20 RETURN
END

```

```

C
C
FUNCTION RATE(PSH2O,PSSO2,NTYPE,TS,PRESS,PAR,Z1,
#S6,TM)
IMPLICIT REAL*8(A-H,O-Z,$)
DIMENSION PAR(13)
COMMON /COMP/ YH2S,YSO2,YH2O,YN2,DHS,DSO,DW,DS6,DENP
COMMON /PARA/ S6$UR,FI,FIMOD,XS,RNS,RATES,C1,CS
#,ZCF,ZCF0,CDIF,RKS6,POVRT
EQK=PAR(5)/DSQRT(760.D00)
IF(NTYPE.EQ.2) GO TO 10
PSO2=(YSO2-YH2S*XS/2.)/RNS-YH2S*DHS/DSO/2.
#*((1.-XS)/RNS-(1.-Z1)/TM)
PSO2=PSO2*PRESS*760.
PH2O=(YH2O+YH2S*XS)/RNS+YH2S*DHS/DW
#*((1.-XS)/RNS-(1.-Z1)/TM)
PH2O=PH2O*PRESS*760.
GO TO 20
10 PSO2=PSSO2*760.
PH2O=PSH2O*760.
20 PH2S=YH2S*(1.-Z1)/TM*PRESS*760.
PS6=S6/TM*760.*PRESS
COEF=1.0
AB=COEF*2.56D-04*DEXP(-7350./1.986/TS)
RATE=AB/((1.+0.006D00*PH2O)**2)
RATE=RATE*(PH2S*DSQRT(PSO2)-PH2O*DSQRT(DSQRT(PS6)
#/EQK))
RETURN
END

```

```

C
C
SUBROUTINE SOLYI(YI,RKISI,AYI,NFLAG)
IMPLICIT REAL*8(A-H,O-Z,$)
DIMENSION XX(3)

```

```

C
PI=3.141592654D00
B=(3.*RKISI-2.)/(1.-RKISI)
C=(6.*RKISI+AYI-2.-3.*AYI*RKISI)/AYI/(1.-RKISI)
DE=RKISI*(AYI-6.)/AYI/(1.-RKISI)
P=C-B*B/3.
Q=(2.*(B**3)-9.*B*C+27.*DE)/27.
D=(P/3.）**3+(Q/2.）**2
70 FORMAT(//,'CUBIC',2(3D19.9))
IF(D) 10,10,40
10 E=DABS(P)
F=-Q/2./DSQRT((E**3)/27.)
ANGLE=DARCOS(F)
Y1=2.*DSQRT(E/3.)*DCOS(ANGLE/3.)

```

```

Y2=-2.*DSQRT(E/3.)*DCOS((ANGLE+PI)/3.)
Y3=-2.*DSQRT(E/3.)*DCOS((ANGLE-PI)/3.)
XX(1)=Y1-B/3.
XX(2)=Y2-B/3.
XX(3)=Y3-B/3.
  YI=0.0D00
  DO 15 I=1,3
  IF(XX(I).GE.0.0D00.AND.XX(I).LE.(1.0D00))  YI=XX(I)
15 CONTINUE
  IF(YI.GE.0.0D00) GO TO 30
  WRITE(8,1) (XX(I),I=1,3)
1  FORMAT(/,5X,'NO SOLUTION FOR YI IN 0-1 RANGE',3D16.8)
  NFLAG=-1
  RETURN
30 WRITE(8,2) YI
2  FORMAT(//,'REACTION INTERPHASE:',D15.8)
  NFLAG=1
  RETURN
40 U=-Q/2.+DSQRT(D)
  U=U**(1./3.)
  V=-Q/2.-DSQRT(D)
  V=V**(1./3.)
  Y1=V+U
  * XX(1)=Y1-B/3.
  IF(XX(1).GE.0.0D00.AND.XX(1).LE.1.D00) GO TO 50
  NFLAG=-1
  RETURN
50 YI=XX(1)
  NFLAG=1
  WRITE(8,2) YI
  RETURN
END

```

C
C

```

SUBROUTINE SPLN(X,Y,N,A,B,C,D)
  IMPLICIT REAL*8(A-H,O-Z,$)
  DIMENSION X(N),Y(N),A(N,4),B(N),C(N),D(N)
C  THIS SUBROUTINE COMPUTES THE MATRIX FOR FINDING THE
C  COEFFICIENTS OF A NATURAL CUBIC SPLINE THROUGH A
C  SET OF DATA.
C  PARAMETERS ARE:
C    X,Y  ARRAYS OF X&Y TO BE FITTED
C    X IN STRICTLY INCREASING ORDER
C    S    ARRAYS OF SECOND DERIVATIVES
C    N    NUMBER OF POINTS
C    A    AUGMENTED MATRIX OF COEFFICIENTS AND R.H.S
C    B,C,D ARRAYS OF POLYNOMIAL COEFFICIENTS
C

```

```

  IF(N.LT.3) GO TO 50
C
C  COMPUTE FOR THE N-2 ROWS
  NM2=N-2
  NM1=N-1
  DX1=X(2)-X(1)

```

```

D(1)=DX1
DY1=(Y(2)-Y(1))/DX1*6.
DO 10 I=1,NM2
  DX2=X(I+2)-X(I+1)
  D(I+1)=DX2
  DY2=(Y(I+2)-Y(I+1))/DX2*6.
  A(I,1)=DX1
  A(I,2)=2.*(DX1+DX2)
  A(I,3)=DX2
  A(I,4)=DY2-DY1
  DX1=DX2
  DY1=DY2
10 CONTINUE
C
C NOW SOLVE THE TRIANGULAR SYSTEM, FIRST REDUCE.
C
  DO 20 I=2,NM2
    A(I,2)=A(I,2)-A(I,1)/A(I-1,2)*A(I-1,3)
    A(I,4)=A(I,4)-A(I,1)/A(I-1,2)*A(I-1,4)
20 CONTINUE
C NOW BACK SUBSTITUE
C
  A(NM2,4)=A(NM2,4)/A(NM2,2)
  DO 30 I=2,NM2
    J=NM1-I
    A(J,4)=(A(J,4)-A(J,3)*A(J+1,4))/A(J,2)
30 CONTINUE
C
C NOW PUT THE VAULES IN TO SIGMA VECTOR OF
C FORSYTHE ETAL TEXT WHICH IS S VECTOR/6
C HERE C VECTOR IS SIGMA VECTOR
C
  DO 40 I=1,NM2
    C(I+1)=A(I,4)/6.
40 CONTINUE
C SIGMA(1)=SIGMA(N)=0. FOR NATURAL SPLINE
  C(1)=0.0D00
  C(N)=0.0D00
C NOW COMPUTE POLYNOMIAL COEFFICIENTS
C
  B(N)=(Y(N)-Y(NM1))/D(NM1)+D(NM1)*(C(NM1)+2.*C(N))
  DO 540 I = 1, NM1
    B(I)=(Y(I+1)-Y(I))/D(I)-D(I)*(C(I+1)+2.*C(I))
    D(I) = (C(I+1) - C(I))/D(I)
    C(I) = 3.*C(I)
540 CONTINUE
  C(N) = 3.*C(N)
  D(N) = D(N-1)
  RETURN
50 B(1) = (Y(2)-Y(1))/(X(2)-X(1))
  C(1) = 0.
  D(1) = 0.
  B(2) = B(1)
  C(2) = 0.

```

```

D(2) = 0.
RETURN
END

```

C
C

```

FUNCTION SEVAL(N,U,X,Y,B,C,D)
IMPLICIT REAL*8(A-H,O-Z,$)
DIMENSION X(N),Y(N),B(N),C(N),D(N)
DATA I/1/
IF ( I .GE. N ) I = 1
IF ( U .LT. X(I) ) GO TO 410
IF ( U .LE. X(I+1) ) GO TO 430
410 I = 1
J = N+1
420 K = (I+J)/2
IF ( U .LT. X (K) ) J = K
IF ( U .GE. X (K) ) I = K
IF ( J .GT. I + 1 ) GO TO 420
430 DX=U-X(I)
SEVAL = Y(I)+DX*(B(I)+DX*(C(I)+DX*D(I)))
DERIV=B(I)+DX*(2.0*C(I)+DX*(3.0*D(I)))
RETURN
END

```

Table E.1 Output of "ORTHOGONAL" program for cylindrical geometry
using 5 interior points.

NUMBER OF INTERIOR POINTS= 5

COLLOCATION ABSCISSAS

0.1995240765E+00 0.4449869862E+00 0.6617966532E+00 0.8339450062E+00 0.9494550617E+00 0.1000000000E+01

MATRIX QINV

0.1591191486E+01 -0.1026016477E+01 0.7711676089E+00 -0.5907336970E+00 0.4210577460E+00 -0.1666666668E+00
-0.1731310702E+02 0.3175504289E+02 -0.2600127599E+02 0.2041700395E+02 -0.1469099716E+02 0.5833333334E+01
0.6633033727E+02 -0.1628270532E+03 0.1835507385E+03 -0.1567237415E+03 0.1163363857E+03 -0.4666666666E+02
-0.115957297E+03 0.3268353239E+03 -0.4446180058E+03 0.4362704924E+03 -0.3425320808E+03 0.1400000000E+03
0.9461274676E+02 -0.2885995406E+03 0.4423387935E+03 -0.4891784127E+03 0.4158264130E+03 -0.1750000000E+03
-0.2926543880E+02 0.9386224352E+02 -0.1560414179E+03 0.1898053915E+03 -0.1753607784E+03 0.7699999999E+02

MATRIX A

-0.5011926475E+01 0.8089933306E+01 -0.5343762186E+01 0.3947333485E+01 -0.2775040260E+01 0.1093462130E+01
-0.1753982117E+01 -0.2247256731E+01 0.6165735494E+01 -0.3617804527E+01 0.2363658238E+01 -0.9103533569E+00
0.6234572566E+00 -0.3317907177E+01 -0.1511038159E+01 0.6252644789E+01 -0.3209273078E+01 0.1162116369E+01
-0.3922282884E+00 0.1658057593E+01 -0.5325241274E+01 -0.1199119840E+01 0.7480364432E+01 -0.2221832623E+01
0.3677846032E+00 -0.1444869814E+01 0.3645619740E+01 -0.9977274446E+01 -0.1053235732E+01 0.8461975649E+01
-0.7916570204E+00 0.3039926609E+01 -0.7211462964E+01 0.1618861020E+02 -0.4622541682E+02 0.3500000000E+02

MATRIX B

-0.3324382736E+02 0.4081463430E+02 -0.1071123110E+02 0.4804897452E+01 -0.2570343348E+01 0.9088700582E+00
0.1973404928E+02 -0.5648460023E+02 0.4573522480E+02 -0.1294499411E+02 0.5980779975E+01 -0.2020459722E+01
-0.4145035087E+01 0.3660221908E+02 -0.8388326710E+02 0.6428192203E+02 -0.1832950622E+02 0.5473667296E+01
0.1995544083E+01 -0.1111851622E+02 0.689858407E+02 -0.1566583827E+03 0.1211299642E+03 -0.2433719341E+02
-0.1621042897E+01 0.7800617181E+01 -0.2987206917E+02 0.1839406651E+03 -0.4863965892E+03 0.3261484190E+03
-0.5370138775E+02 0.2037127335E+03 -0.4679004953E+03 0.9529466203E+03 -0.1451724137E+04 0.8166666666E+03

Table E.1 continued.

MATRIX B1

```

-0.8624420405E+01  0.2654834427E+00  0.1607131204E+02  -0.1497884772E+02  0.1133795438E+02  -0.4571481733E+01
  0.2367569739E+02  -0.514343741E+02  0.3187923421E+02  -0.4814865274E+01  0.6690330900E+00  0.2533798716E-01
-0.5087102796E+01  0.4161570345E+02  -0.8160003077E+02  0.5483393712E+02  -0.1348017212E+02  0.3717665131E+01
  0.2465872804E+01  -0.1310572597E+02  0.7537418652E+02  -0.1552204943E+03  0.1121601108E+03  -0.2167294984E+02
-0.2008406784E+01  0.9322405702E+01  -0.3371176616E+02  0.1944490871E+03  -0.4852872837E+03  0.3172359638E+03
-0.5290973073E+02  0.2006728069E+03  -0.4606890323E+03  0.9367580101E+03  -0.1405498720E+04  0.7816666666E+03

```

F VECTOR

```

0.5000000000E+00  0.2500000000E+00  0.1666666667E+00  0.1250000000E+00  0.1000000000E+00  0.8333333333E-01

```

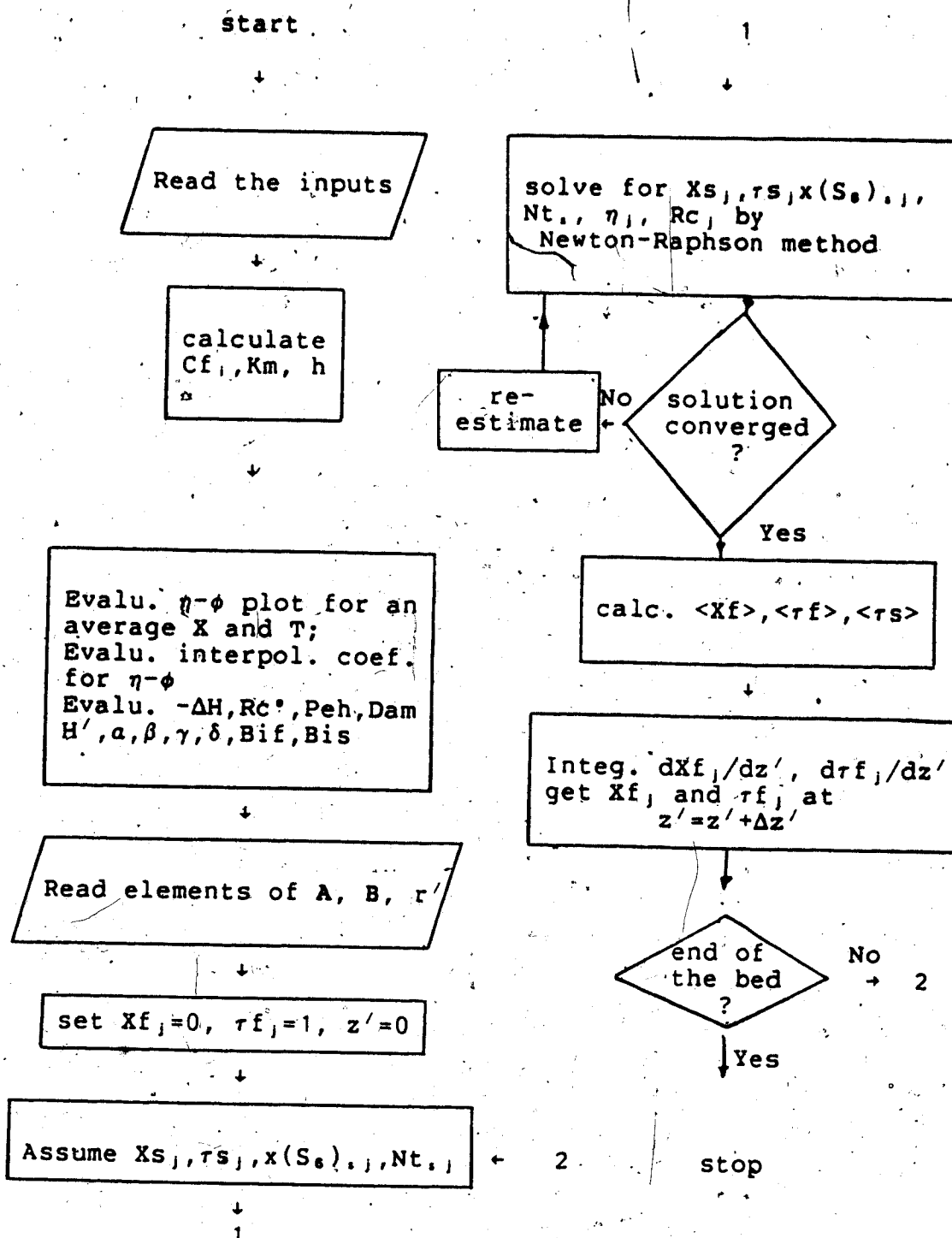
W VECTOR

```

0.5039709635E-01  0.1042253333E+00  0.1302316958E+00  0.1213467971E+00  0.7981018829E-01  0.1388888890E-01

```

Figure E.2 Flow Chart of Two-Dimensional Claus Reactor



```

C*****
C*                               MAINLINE BEDTWO                               *
C*                               *                                              *
C*THIS PROGRAM CALCULATES THE PERFORMANCE OF TWO                          *
C*DIMENSIONAL MODEL FOR CLAUS CONVERTOR AS WAS                             *
C*DESCRIBED IN CHAPTER 5 AND APPENDIX E.                                   *
C*HERE THE UNKNOWN IN RADIAL DIRECTION FOR ANY                            *
C*FLUID T AND X ARE XS,TS,S6, AND TOTAL MOLE. THAT IS XS*                  *
C*IS NOT EXPRESSED AS TS. FOR 5 INTERIOR POINTS IN THE                    *
C*RADIAL DIRECTION THEN, THERE ARE 20 EQUATIONS TO SOLVE.*
C*                                                                           *
C*****
      IMPLICIT REAL*8(A-H,O-Z,$)
      DIMENSION U(11),PAR(12),V(11),AINT(11,4),GA1(11)
      #,GA2(11),GA3(11),THIEM(11),SX(5),ST(5),
      #FT(5),ETA(5),TMOD(5),BJ(6,6),B1J(6,6),EFF(11)
      #,AJ(6,6),VECTOR(12),SULF(5),TMOL(5),RS(5),FX(5)
      #,YP(12),WGT(6)
      DATA THIEM/.1,.2,.45,.6,.75,1.,1.5,2.,3.5,5.,8./
      COMMON/GAM/GA1,GA2,GA3,U,V
      COMMON/COMP/YH2S,YSO2,YH2O,YN2,DHS,DSO,DW,DENP
      COMMON/PARA/FI,FIMOD,XS,RNS,RATES,C1,CS
      COMMON/CONST/DAM,RATE0,PRESS,C0,T0
      #,DP,FT0,ST0,FX0,SX0,STW,FTW,FXW,TA,PLAN
      #,A1,A2,A3,A4,A5,A6,A7,S,GAMA,XEQ,RNE,S6EQ
      COMMON/SPAR/PAR
      COMMON/CJAC/BJ,B1J,AJ,RSTAR
      COMMON/RADIAL/ETA0,TMOD0,RS0,FT,FX,SULF,TMOL,RS,
      #TMOD,ETA
      COMMON/SURT/ST,SX
      EXTERNAL SNLEQ,FUN,FUNO,DF1,DF2,DF3,DF4,DF5,DF7,
      #DF8,DF9,RATE
      #,HEATR,RFUN,ZFCN,SEVAL

C
C  READ IN THE INPUTS TO THE PROGRAM
C
C***  FEED COMPOSITION (MOLE FRACTION); H2S,SO2,H2O,N2
C
      CALL FREAD(5,'4R*8:',YH2S,YSO2,YH2O,YN2)
C
C  INLET TEMPERAURE K, AMBIENT TEMP. K, PRESSURE ATM.
C
      CALL FREAD(5,'3R*8:',T0,TA,PRESS)
C
C***  BULK DIFFUSIVITIES CM*CM/SEC; N2,H2S,SO2,H2O,S6;
C***  VISCOSITY OF THE GAS POISE; THERMAL CONDUCTIVITY
C***  OF THE GAS CAL/CM. SEC. K.
C
      CALL FREAD(5,'6R*8:',DN2M,DH2SM,DSO2M,DH2OM,VIS,TCON)
C
C***  EFFECTIVE DIFFUSIVITY IN THE PELLET;
C***  H2S,SO2,H2O.
C
      CALL FREAD(5,'3R*8:',DHS,DSO,DW)

```

```

C
C*** INLET SUPERFICIAL VELOCITY CM/SEC
C
  CALL FREAD(5,'R*8:',VS0)
C
C CATALYST DIA. CM; BED POROSITY; BED DENSITY G/CM*CM*CM;
C* REACTOR DIAMETER CM; REACTOR LENGTH CM.
C
  CALL FREAD(5,'6R*8:',DP,EB,DENB,DENP,RW,ZR)
C
C*** MASS PECKET NUMBER; LANDAF; LANDAS; ALFAF; ALFAS;
C*** U0; CAL/CM.CM.SEC.K
C
  CALL FREAD(5,'6R*8:',PEM,FLAN,SLAN,AF,AS,UO)
C
C WRITE THE INPUTS
C
  WRITE(8,100)
100  FORMAT(/,5X,'INPUTS TO THE PROGRAM ARE')
  WRITE(8,101) YH2S,YSO2,YH2O,YN2
  WRITE(8,101) T0,PRESS
  WRITE(8,101) DH2SM,DSO2M,DH2OM,VIS,TCON
  WRITE(8,101) DHS,DSO,DW
  WRITE(8,101) VS0
  WRITE(8,101) DP,EB,DENB,DENP
101  FORMAT(/,4X,5D15.5)
C
C DEFINE THE VALUES OF REACTOR PARAMETERS
C
  C0=YH2S*PRESS/T0/82.06
  CPAVE=YH2O*8.126+YN2*6.9+YH2S*7.31+YSO2*6.453
  AMW=YH2O*18.+YH2S*34.+YSO2*64.+YN2*28
  CPAVE=CPAVE/AMW
  DEN0=AMW*PRESS/T0/82.06
  GAVE=DEN0*VS0
  DAVE=YN2*DN2M+YH2S*DH2SM+YSO2*DSO2M+YH2O*DH2OM
  RE=DP*GAVE/VIS
  RJD=.458/EB*(RE*(-.407))
  RJH=RJD
  SC=(VIS/DEN0/DAVE)**(2./3.)
  CMT=RJD*GAVE/DEN0/SC
  PRNO=(CPAVE*VIS/TCON)**(2./3.)
  CHT=RJH*CPAVE*GAVE/PRNO
  WRITE(8,6) RE,RJD,SC,PRNO
6    FORMAT(/,5X,'RYNOLDS',4D15.6)
  WRITE(8,1) CMT,CHT
1    FORMAT(/,5X,'MASS TRAN.',2D15.6)
C
C TO GET CURVE OF EFF. FACTOR VS MOD-THIELE PARAMETER,
C USE TFO AS THE TEMP. AT THE SURFACE. IT HAS BEEN SHOWN
C PREVIOUSLY THAT EVEN 100 DEGREE DIFFERENCE DOES NOT
C HAVE ANY EFFECT ON THE PLOT.
C
  TS=T0+50.

```

```

      IF (YH2S.LT.0.05) TS=T0+10.0
55    CALL EFFFAC(THIEM,EFF,TS,PRESS,HEAT)
      WRITE(8,4) HEAT
4     FORMAT(/,5X,'HEAT',D15.5)
C
C USE THE EFF. FACTOR-MOD THIELE DATA OBTAINED FOR
C INTERPOLATION BY NATURAL SPLINE METHOD.
C
      WRITE(8,3) (THIEM(I),EFF(I), I=1,11)
3     FORMAT(/,4D15.8)
      DO 2 I=1,11
      U(I)=DLOG(THIEM(I))
      V(I)=DLOG(EFF(I))
2     CONTINUE
      CALL SPLN(U,V,11,AINT,GA1,GA2,GA3)
C
C EVALUATE RATE AT THE INLET COND. I.E. ZERO CONVERSION.
C
      CALL EQCTS(T0,PRESS,PAR)
      PAR(6)=YSO2
      PAR(7)=YH2O
      PAR(9)=DHS/DW
      PAR(10)=DHS/DSO
      PAR(11)=YH2S
      PAR(12)=YN2
      NTYPE=2
      RATE0=RATE(NTYPE,T0,PRESS,PAR,0.0D00,0.0D00,1.D00)
      WRITE(8,70) RATE0
70    FORMAT('MAIN RATE0',D15.5)
C
C READ JACOBI POLYNOMIAL PARAMETERS USED IN SPECIFYING
C THE RADIAL DISTRIBUTION.
C
      CALL FTNCMD('ASSIGN 7=JA5',12)
      NM=6
      LINE=(26+2*NM)*1000
      DO 300 I=1,NM
      READ(7'LINE,500) (BJ(I,J), J=1,NM)
      LINE=LINE+1000
300   CONTINUE
      LINE=(21+NM)*1000
      DO 400 I=1,NM
      READ(7'LINE,500) (AJ(I,J), J=1,NM)
      LINE=LINE+1000
400   CONTINUE
      LINE=(31+3*NM)*1000
      DO 450 I=1,NM
      READ(7'LINE,500) (B1J(I,J),J=1,NM)
      LINE=LINE+1000
450   CONTINUE
      LINE=10*1000
      READ(7'LINE,545) RSTAR
      RSTAR=RSTAR*RSTAR
      LINE=(40+4*NM)*1000

```

```

      READ(7,'LINE,545) (WGT(I),I=1,NM)
      WRITE(8,71) RSTAR
71    FORMAT('RSTAR MAIN',D17.7)
500   FORMAT(10X,10D18.10)
545   FORMAT(10D18.10)
C
C USING THE PARAMETERS OF THE SYSTEM, DEFINE THE CONSTANTS
C OF EQUATIONS.
C
      S=TA/T0
      RUS=1.D00/AS+RW*UO
      RUS=1.D00/RUS
      RUF=1.D00/AF+RW*UO
      RUF=1.D00/RUF
      BIS=RW*RUS/SLAN
      BIF=RW*RUF/FLAN
      A6=BIS+AJ(6,6)
      A7=BIF+AJ(6,6)
      A6=-1.D00/A6
      A7=-1.D00/A7
      DAM=DENB*RATE0/VS0*RW/CO
      ALFA=RW/DP
      PEH=DP*GAVE*CPAVE/FLAN
      BETA=FLAN/SLAN
      HST=HEAT*CO/DEN0/CPAVE/T0
      AH=6.*(1.-EB)/DP
      GAMA=CHT*AH*RW*RW/FLAN
      DELT=VS0/CMT/AH/RW
      A1=HST*DAM*PEH*ALFA*BETA/(1.-S)
      A2=GAMA*BETA
      A3=DAM*DELT
      A4=PEM*ALFA
      A5=PEH*ALFA
      WRITE(8,72) BIS,BIF,A6,A7
      WRITE(8,72) RATE0,DAM,HST,A1
      WRITE(8,72) A2,A3,A4,A5
      WRITE(8,72) PEH,ALFA,BETA
72    FORMAT('CONSTANTS ',4D12.4)
C
C DEFINE THE INLET CONDITION. NOTE VECTOR IS THE ARRAY
C TO BE INTEGRATED.
C
      DO 1000 I=2,6
      FX(I-1)=0.0D00
      SX(I-1)=.001D00+FX(I-1)
      FT(I-1)=1.D00
      VECTOR(I)=FX(I-1)
      VECTOR(I+6)=FT(I-1)
      SULF(I-1)=.2D-02
      TMOL(I-1)=.99D00
1000  CONTINUE
      FX0=0.0D00
      FT0=1.D00
      VECTOR(1)=0.0D00

```

VECTOR(7)=1.D00

C
C THE FIRST ESTIMATE OF TS AND TSO
C

```

      ST(1)=1.0123
      ST(2)=1.0122
      ST(3)=1.0121
      ST(4)=1.0120
      ST(5)=1.0119
      ST0=1.0124
      XEQ=0.768D00
      S6EQ=.0036D00
      RNE=.9335D00
      INT=12
      Y1=VECTOR(1)
      Z=0.0D00
      H=.2D00/RW
      HMAX=1.D00/RW
      DA=1.00D00/RW
      WRITE(8,1400)
      DO 1100 I=1,100
      CALL RKF(Z,VECTOR,INT,RFUN,DA,H,HMAX,1.D-02,0.0D00
      #,IFLAG)
      ZST=Z*RW
      WRITE(8,1300) Z,ZST,(VECTOR(II),II=1,6),FXW
      WRITE(8,1301) Z,ZST,(VECTOR(II),II=7,12),FTW
      CALL RFUN(Z,VECTOR,YP)
      AXF=WGT(6)*FXW
      ATF=WGT(6)*FTW
      ATS=WGT(6)*STW
      DO 1025 I1=1,5
      AXF=AXF+WGT(I1)*FX(I1)
      ATF=ATF+WGT(I1)*FT(I1)
      ATS=ATS+WGT(I1)*ST(I1)
1025  CONTINUE
      AXF=2.*AXF
      ATF=2.*ATF
      ATS=2.*ATS
      WRITE(8,1302) Z,ZST,ST0,(ST(II),II=1,5),STW
      WRITE(8,1303) AXF,ATF,ATS
      ATF=T0*(ATF*(1.-S)+S)
      ATS=T0*(ATS*(1.-S)+S)
      WRITE(8,1304) ATF,ATS
      WRITE(8,1305) ETA0,(ETA(L1),L1=1,5)
      IF(ZST.GE.ZR) GO TO 1200
      Y1=VECTOR(1)
1100  CONTINUE
C
1300  FORMAT(2D12.3,' FX ',7D15.6)
1301  FORMAT(2D12.3,' FT ',7D15.6)
1302  FORMAT(2D12.3,' ST ',7D15.6)
1303  FORMAT(5X,'AVERAGE XF, TF, TS ',3D15.6)
1304  FORMAT(5X,'AVERAGE TF AND TS IN DEGREE K ',2D15.6)
1305  FORMAT(5X,'EFFECTIVENESS FACTOR ',6D15.6)

```

```

1400  FORMAT(/,5X,'Z',10X,'ZST',/)
1200  STOP
      END

```

C
C

C SUBROUTINE ZFCN(SX,NI,ST,F,N,ZPAR,DIFF)
C THIS SUBPROGRAM IS USED TO EVALUATE
C F VECTOR=0. FVACTOR EXPRESSES SURFACE TEMP AND
C HENCE CONVERSION FOR ANY FLUID TEMP AND CONVERSION.
C

```

      IMPLICIT REAL*8(A-H,O-Z,$)
      DIMENSION ST(NI),DIFF(N,N),F(N),ZPAR(1),SX(NI),FT(5)
      #,FX(5),SUM(5),GA3(11),DF(3,3),CALX(5),RS(5),
      #SULF(5),TMOL(5),BJ(6,6),B1J(6,6),AJ(6,6),PAR(12),
      #Y(3),TMOD(5),ETA(5),U(11),V(11),GA1(11),GA2(11)
      COMMON/RADIAL/ETA0,TMOD0,RS0,FT,FX,SULF,TMOL,RS,
      #TMOD,ETA
      COMMON/CJAC/BJ,B1J,AJ,RSTAR
      COMMON/CONST/DAM,RATE0,PRESS,C0,T0
      #,DP,FT0,ST0,FX0,SX0,STW,FTW,FXW,TA,FLAN
      #,A1,A2,A3,A4,A5,A6,A7,S,GAMA,XEQ,RNE,S6EQ
      COMMON/GAM/GA1,GA2,GA3,U,V
      COMMON/COMP/YH2S,YSO2,YH2O,YN2,DHS,D6O,DW,DENP
      COMMON/CALL/NCALL,NTYPE
      COMMON/PARA/FI,FIMOD,XS,RNS,RATES,C1,CS
      COMMON/SPAR/PAR
      COMMON /VAR/ P1,P2,P3,P4,P5,P6,P7,P8,P9,PPH20,PPH2S
      #,PPSO2
      AP=34173.0D00
      BP=13663.9
      CP=-2932.0
      NTYPE=2
      M=NI+1
      DO 7 I=1,N
      DO 79 K=1,N
79  DIFF(I,K)=0.0D00
7   CONTINUE
5   STW=0.0D00
   DO 1 I=1,NI
   STW=STW+A6*AJ(M,I)*ST(I)
1   CONTINUE
   DO 10 J=1,NI
   SUM(J)=0.0D00
   DO 20 I=1,NI
   SUM(J)=SUM(J)+BJ(J,I)*ST(I)
20  CONTINUE
   SUM(J)=SUM(J)+STW*BJ(J,M)
10  CONTINUE
   DO 60 J=1,NI
   J1=J+NI
   J2=J+2*NI
   J3=J+3*NI
   TEMS=ST(J)*(1.-S)+S
   TEMF=FT(J)*(1.-S)+S

```



```

TEMP=TEMS*T0
CALL EQCTS(TEMP,PRESS,PAR)
RATES=RATE(NTYPE,TEMP,PRESS,PAR,SX(J),SULF(J),TMOL(J))
RS(J)=RATES/RATE0
CS=C0*(1.D00-SX(J))/TEMS
C IF RATES<0 THE ASSUMED ST IS TOO LARGE
C
IF(RATES) 30,40,40
30 DO 35 K=1,NI
ST(K)=FT(K)
35 CONTINUE
GO TO 5
40 FI=DP/6.*DSQRT(RATES/CS*DENP/DHS)
C
C GET CEQ/CS TO GET FIMOD
C
NCALL=2
NEQ=3
ICALL=2
Y(1)=S6EQ
Y(2)=RNE
Y(3)=XEQ
XS=SX(J)
RNS=TMOL(J)
CALL SNLEQ(RHS,TEMP,PRESS,Y,PAR,1.D00,1,3,ICALL,NI
#,YH2S,DF,NEQ)
XEQ=Y(3)
RNE=Y(2)
C1=(1.D00-XEQ)/(1.D00-SX(J))*TMOL(J)/RNE
TMOD(J)=FI/DSQRT(1.D00-C1)
IF(TMOD(J).LT..9D-01) GO TO 45
FIM=DLOG(TMOD(J))
ETA(J)=SEVAL(11,FIM,U,V,GA1,GA2,GA3)
ETA(J)=DEXP(ETA(J))
GO TO 50
45 ETA(J)=1.D00
50 F(J)=SUM(J)+ETA(J)*RS(J)*A1-A2*(ST(J)-FT(J))
F(J1)=(1.-FX(J))/TEMF-(1.-SX(J))/TEMS-A3*ETA(J)*RS(J)
NCALL=1
Y(1)=SULF(J)
Y(2)=TMOL(J)
PAR(4)=YH2S*SX(J)
F(J2)=FUN(Y,1,PAR)
F(J3)=FUN(Y,2,PAR)
DIFF(J2,J1)=-.5*YH2S
DIFF(J3,J1)=-1.5*YH2S
DIFF(J2,J2)=DF7(Y,1,PAR)
DIFF(J2,J3)=DF8(Y,1,PAR)
DIFF(J3,J2)=DF7(Y,2,PAR)
DIFF(J3,J3)=DF8(Y,2,PAR)
C
C DIFF OF FUNCTION FUN W.R.T.TEMPERATURE
C
DPAR1=P1*AP*PAR(1)/3.

```

```

DPAR2=P2*BP*PAR(2)*2./3.
DPAR3=P3*CP*PAR(3)*4./3.
DIFF(J2,J)=(1.-S)/(TEMP**2)*T0*(DPAR1+DPAR2+DPAR3)
DIFF(J3,J)=(1.-S)/(TEMP**2)*T0*(2.*DPAR1+4.*DPAR2
#+8.*DPAR3)

```

```

C
C DIFF OF RATE W.R.T. SX
C

```

```

CONV=SX(J)+.0001D00
R2=RATE(NTYPE,TEMP,PRESS,PAR,CONV,SULF(J),TMOL(J))
R2=R2/RATE0
DIF=(R2-RS(J))/0.0001D00
DIFF(J1,J1)=1./TEMS-A3*ETA(J)*DIF
DIFF(J,J1)=A1*ETA(J)*DIF

```

```

C
C DIFF W.R.T SULF
C

```

```

DSUL=SULF(J)+.0001
R3=RATE(NTYPE,TEMP,PRESS,PAR,SX(J),DSUL,TMOL(J))
R3=R3/RATE0
DIF=(R3-RS(J))/0.0001
DIFF(J,J2)=A1*ETA(J)*DIF
DIFF(J1,J2)=-A3*ETA(J)*DIF

```

```

C
C DIFF W.R.T TMOL
C

```

```

DMOL=TMOL(J)+.0001
R4=RATE(NTYPE,TEMP,PRESS,PAR,SX(J),SULF(J),DMOL)
R4=R4/RATE0
DIF=(R4-RS(J))/0.0001
DIFF(J,J3)=A1*ETA(J)*DIF
DIFF(J1,J3)=-A3*ETA(J)*DIF

```

```

C
C DIFF OF RATE W.R.T. THO=T-TA/T0-TA

```

```

TMPY=ST(J)+.0001
TEMS=TMPY*(1.-S)+S
TEMP=TEMS*T0
CALL EQCTS(TEMP,PRESS,PAR)
R1=RATE(NTYPE,TEMP,PRESS,PAR,SX(J),SULF(J),TMOL(J))
R1=R1/RATE0
DIF=(R1-RS(J))/0.0001
DIFF(J,J)=BJ(J,J)+A6*BJ(J,M)*AJ(M,J)-A2+A1*ETA(J)*DIF
DIFF(J1,J)=(1.-S)*(1.-SX(J))/(((1.-S)*ST(J)+S)**2)
#-A3*ETA(J)*DIF

```

```

DO 2 I=1,NI
IF(J.EQ.I) GO TO 2
DIFF(J,I)=BJ(J,I)+A6*BJ(J,M)*AJ(M,I)
CONTINUE
CONTINUE
RETURN
END

```

```

C
C
SUBROUTINE RFUN(Z,VECTOR,YP)

```

C THIS SUBROUTINE EVALUATES THE DIFFERENTIALS

C

```

      IMPLICIT REAL*8(A-H,O-Z,$)
      DIMENSION VECTOR(1),YP(1),ST(5),FT(5),SX(5),FX(5),
      #RS(5),ETA(5),
      #BJ(6,6),SULF(5),TMOL(5),TMOD(5),B1J(6,6),AJ(6,6)
      #,WKAREA(500),DIFF(20,20),B(20,1),ZPAR(1),VST(5),F(20)
      COMMON/CONST/DAM,RATE0,PRESS,C0,T0
      #,DP,FT0,ST0,FX0,SX0,STW,FTW,FXW,TA,FLAN
      #,A1,A2,A3,A4,A5,A6,A7,S,GAMA,XEQ,RNE,S6EQ
      COMMON/RADIAL/ETA0,TMOD0,RS0,FT,FX,SULF,TMOL,RS,
      #TMOD,ETA
      COMMON/SURT/ST,SX
      COMMON/CJAC/BJ,B1J,AJ,RSTAR

```

C

C REDEFINE FT AND FX VECTOR

C

```

      DO 1 I=2,6
      FX(I-1)=VECTOR(I)
      FT(I-1)=VECTOR(I+6)
1    CONTINUE
      FX0=VECTOR(1)
      FT0=VECTOR(7)
      ITMAX=100
      N=20
      NI=5
      M=NI+1

```

C

C THE ESTIMATE OF ST FOR THE FIRST TIME COMES FROM MAIN
 C PROGRAM THROUGH COMMON BLOCK. AFTER FIRST CONVERGENCE
 C THE CONVERGED VALUE OF ST IS USED AS THE ESTIMATE OF
 C THE NEXT STEP.

C

```

      DO 10 K=1,ITMAX
      CALL ZFCN(SX,NI,ST,F,N,ZPAR,DIFF)
      ITEST=0
      DO 2 I=1,N
      B(I,1)=-F(I)
2    CONTINUE

```

C#####

C SCALING THE JACOBIAN MATRIX

C#####

```

      DO 21 ISS=1,N
      SCALE=DABS(DIFF(ISS,1))
      DO 22 IS=1,N
      IF(DABS(DIFF(ISS,IS)).GT.SCALE) SCALE
      #=DABS(DIFF(ISS,IS))

```

22 CONTINUE

```

      DO 23 IS=1,N
      DIFF(ISS,IS)=DIFF(ISS,IS)/SCALE

```

23 CONTINUE

```

      B(ISS,1)=B(ISS,1)/SCALE

```

21 CONTINUE

```

      CALL LEQTF(DIFF,1,N,N,B,0,WKAREA,IER)

```

```

DO 3 I=1,N
IF(DABS(B(I,1)).GT..1D-06) ITEST=ITEST+1
IF(DABS(F(I)).GT..1D-06) ITEST=ITEST+1
3 CONTINUE
DO 8 L=1,NI
L1=L+NI
L2=L+2*NI
L3=L+3*NI
ST(L)=ST(L)+B(L,1)
SX(L)=SX(L)+B(L1,1)
SULF(L)=SULF(L)+B(L2,1)
TMOL(L)=TMOL(L)+B(L3,1)
8 CONTINUE
IF(ITEST.EQ.0) GO TO 4
10 CONTINUE
C
C NOW ST AND SX ARE KNOWN.
C GET THE FLUID TEMP AT THE WALL
C IF Z=0 THEN FTW=1. AND FXW=0.0
C
4 IF(Z-.0001D00) 80,81,81
80 FTW=1.0D00
FXW=0.0D00
GO TO 82
81 FTW=0.0D00
DO 5 I=1,NI
FTW=FTW+A7*AJ(M,I)*FT(I)
5 CONTINUE
C
C DEFINE THE DIFFERENTIALS.
C NOTE THAT YP1=DX0/DZS, YP2-YP6=DXJ/DZS
C , YP7=DT0/DZS, AND YP8-YP12=DTJ/DZS
C
C DEFINE FXW
C
FXW=0.0D00
DO 6 IN=1,5
FXW=FXW+AJ(M,IN)*FX(IN)
6 CONTINUE
FXW=-FXW/AJ(M,M)
82 DO 40 J=1,5
S2=BJ(J,6)*FXW
S1=BJ(J,6)*FTW
DO 30 I=1,5
S2=S2+BJ(J,I)*FX(I)
S1=S1+BJ(J,I)*FT(I)
30 CONTINUE
TEMP=FT(J)*(1.-S)+S
YP(J+1)=S2/TEMP+(1.-FX(J))*(1.-S)*S1/(TEMP**2)
VST(J)=1.D00
YP(J+1)=YP(J+1)/A4/VST(J)+DAM/VST(J)*ETA(J)*RS(J)
YP(J+7)=(S1+GAMA*(ST(J)-FT(J)))/A5
40 CONTINUE
C

```

C CALL TEMO TO GET TANDX AT THE CENTER FOR THE SOLID
C CORRESPONDING TO THE FLUID.

C

TS1=ST(1)

TS2=ST(1)+.01

CALL TEMO(TS1,TS2)

C

WRITE(1,71) Z,ST0,SX0

71

FORMAT(5X,'RFUN Z ,ST0,SX0 ',3D15.5)

C

C DEFINE YP1 AND YP7

C

VST0=1.D00

TM0=FT0*(1.-S)+S

YP(1)=(FX(1)-FX0)/TM0+(FT(1)-FT0)*(1.-FX0)*(1.-S)
#/(TM0**2)

YP(1)=YP(1)*4./RSTAR/VST0/A4+ETA0/VST0*RS0*DAM

YP(7)=(4./RSTAR*(FT(1)-FT0)+GAMA*(ST0-FT0))/A5

RETURN

END

C

C

SUBROUTINE EQCTS(T,PRESS,PAR)

IMPLICIT REAL*8(A-H,O-Z,\$)

DIMENSION PAR(12)

RLK62=-34173./T+37.9735

RLK64=-13663.9/T+12.6028

RLK68=2932./T-3.43174

RLK=11050.1/T-11.5576

RK=DEXP(RLK)

RK62=DEXP(RLK62)

RK64=DEXP(RLK64)

RK68=DEXP(RLK68)

AA=(RK62/PRESS/PRESS)**(1./3.)

BB=(RK64/DSQRT(PRESS))**(2./3.)

CC=(RK68*(PRESS**.25))**(4./3.)

PAR(1)=AA

PAR(2)=BB

PAR(3)=CC

PAR(5)=RK

PAR(8)=PAR(5)*DSQRT(PRESS)

RETURN

END

C

C

SUBROUTINE TEMO(TS1,TS2)

IMPLICIT REAL*8(A-H,O-Z,\$)

DIMENSION F(100),T(100),GA1(11),GA2(11),GA3(11),X(3)
\$,V(11),ST(5),FT(5),SX(5),FX(5),PAR(12),DF(12,12)

\$,U(11),SULF(5),RS(5),TMOL(5),TMOD(5),ETA(5)

#,BJ(6,6),B1J(6,6),AJ(6,6)

COMMON/GAM/GA1,GA2,GA3,U,V

COMMON/COMP/YH2S,YSO2,YH2O,YN2,DHS,DSO,DW,DENP

COMMON/CONST/DAM,RATE0,PRESS,C0,T0

#,DP,FT0,ST0,FX0,SX0,STW,FTW,FXW,TA,FLAN

```

# , A1, A2, A3, A4, A5, A6, A7, S, GAMA, XEQ, RNE, S6EQ
COMMON/RADIAL/ETA0, TMO0, RS0, FT, FX, SULF, TMOL, RS,
#TMO0, ETA
COMMON/SURT/ST, SX
COMMON/PARA/FI, FIMOD, XS, RNS, RATES, C1, CS
COMMON/CALL/NCALL, NTYPE
COMMON/CJAC/BJ, B1J, AJ, RSTAR
COMMON/SPAR/PAR
NCALL=1
NEQ=2
I=1
ST0=TS1
5  ERO=A2*(ST0-FT0)-4./RSTAR*(ST(1)-ST0)
   ERO=ERO/A1
   TMO=ST0*(1.-S)+S
   SX0=1.+A3*ERO*TMO-(1.-FX0)*TMO/(FT0*(1.-S)+S)
   TEMP=TMO*T0
   CALL EQCTS(TEMP, PRESS, PAR)
   X(1)=SULF(1)
   X(2)=TMOL(1)
   PAR(4)=YH2S*SX0
   CALL SNLEQ(RHS, TEMP, PRESS, X, PAR, 1.D00, 1, 2, 1, NI
# , YH2S, DF, NEQ)
   SULF0=X(1)
   TMO0=X(2)
18  NTYPE=2
   RATES0=RATE(NTYPE, TEMP, PRESS, PAR, SX0, SULF0, TMO0)
   RS0=RATES0/RATE0
   CS=C0*(1.-SX0)/TMO
C
C IF RATES IS NEG., THE ASSUMED TS IS TOO LARGE ,REDUCE IT
C
   IF(RATES0) 40,45,45
40  ST0=FT0+.0001D00
   GO TO 5
45  FI=DP/6.*DSQRT(RATES0/CS*DENP/DHS)
   X(1)=S6EQ
   X(2)=RNE
   X(3)=XEQ
   XS=SX0
   RNS=TMOL0
C
C LET NCALL BE 2 TO GET CONDITION INSIDE THE PELLET.
C
   NCALL=2
   NEQ=3
   CALL SNLEQ(RHS, TEMP, PRESS, X, PAR, 1.D00, 1, 3, 2, NI
# , YH2S, DF, NEQ)
C
C RESET NCALL TO 1 AND NEQ TO 2
C
   NCALL=1
   NEQ=2
   XEQ=X(3)

```

```

RNE=X(2)
C1=(1.-XEQ)/(1.-SX0)*TMOLO/RNE
TMOD0=FI/DSQRT(1.-C1)
IF(TMOD0.LT..9D-01) GO TO 25
FIM=DLOG(TMOD0)
ETA0=SEVAL(11,FIM,U,V,GA1,GA2,GA3)
ETA0=DEXP(ETA0)
GO TO 10
25 ETA0=1.D00
10 F(I)=4./(RSTAR)*(ST(1)-ST0)+ETA0*RS0*A1-A2*(ST0-FT0)
T(I)=ST0
IF(I-2) 12,13,20
12 ST0=TS2
I=I+1
GO TO 5
13 IF(DABS(T(2)-T(1)).GT..1D-10) GO TO 20
ST0=FT0+.00001D00
I=2
GO TO 5
20 DIFF=(F(I)-F(I-1))/(T(I)-T(I-1))
TSC=ST0-.75*F(I)/DIFF
IF(DABS(TSC-ST0).LT.1D-06) GO TO 30
ST0=TSC
I=I+1
GO TO 5
30 ST0=TSC
RETURN
END

```

C
C

```

FUNCTION HEATR(V1,V2,V3,V4,TS)
IMPLICIT REAL*8(A-H,O-Z,$)
DH298=-35008.8+V1*31200+V2*34810+V3*24360+V4*24320
DCP=-4.818121+V1*8.54+V2*19.092+V3*31.58+V4*42.67
HEATR=DH298+DCP*(TS-298)
HEATR=-HEATR

```

C
C
C
C

THIS IS HEAT FOR 2 MOLES OF REACTED H2S. TO GET
HEAT PER MOLE OF H2S DIVIDE BY 2.

```

HEATR=HEATR/2.
RETURN
END

```

C
C

```

SUBROUTINE EFFFAC(THIEM,EFF,TS,PRESS,HEAT)
IMPLICIT REAL*8 (A-H,O-Z,$)
DIMENSION X(12),DF(12,12),B(5,5),B1(5,5),
#THIEM(11),EFF(11),Y(3),Z(5),QINV(5,5),A(5,5),PAR(12)
COMMON /COMP/ YH2S,YSO2,YH2O,YN2,DHS,DSO,DW,DENP
COMMON /PARA/ FI,FIMOD,XS,RNS,RATES,C1,CS
COMMON /ORTH/ B,B1,A,X,QINV,Z
COMMON /CALL/NCALL,NTYPE
XS=.5D00

```

```

CALL EQCTS(TS,PRESS,PAR)
PAR(4)=YH2S*XS
PAR(6)=YSO2
PAR(7)=YH2O
PAR(9)=DHS/DW
PAR(10)=DHS/DSO
PAR(11)=YH2S
PAR(12)=YN2
NCALL=1
X(1)=.02
X(2)=.98
NEQ=2
CALL SNLEQ(RHS,TS,PRESS,X,PAR,1.D00,1,2,1,NI
#,YH2S,DF,NEQ)
S6SUR=X(1)
RNS=X(2)
NTYPE=1
RATES=RATE(NTYPE,TS,PRESS,PAR,XS,S6SUR,RNS)
C
C EVAL. STOI. COEF. FOR THIS AVERAGE CONVERSION AND
C FEED TEMP.. ASSUME THIS IS CONSTANT THROUGH THE BED WITH
C REGARD TO HEAT OF REACTION CALCULATION.
C
      S2=PAR(1)*(S6SUR*RNS*RNS)**(1./3.)
      S4=PAR(2)*(S6SUR*S6SUR*RNS)**(1./3.)
      S8=PAR(3)*((S6SUR**4)/RNS)**(1./3.)
C
C REACTION: 2H2S+SO2=2H2O+V1 S2+V2 S4+V3 S6 V4 S8
C
      V1=2.*S2/YH2S/XS
      V2=2.*S4/YH2S/XS
      V3=2.*S6SUR/YH2S/XS
      V4=2.*S8/YH2S/XS
      HEAT=HEATR(V1,V2,V3,V4,TS)
C
C NOW SNLEQ IS USED TO GET EQUILIBRIUM CONVERSION
C HERE X(1) IS S6EQ , X(2) MOLE AT EQ, AND X(3) EQCONV.
C NOW ICALL=2 AND NCALL=2
C
      NEQ=3
      NCALL=2
      X(3)=.8
      CALL SNLEQ(RHS,TS,PRESS,X,PAR,1.D00,1,3,2,NI
#,YH2S,DF,NEQ)
      S6EQ=X(1)
      RNE=X(2)
      XEQ=X(3)
C
C C1 IS CEQ./C AT THE SURFACE
C
      C1=(1.-XEQ)/(1.-XS)*RNS/RNE
      DO 2000 II=1,11
      FIMOD=THIEM(II)
      FI=FIMOD*(DSQRT(1.-C1))

```



```

IF(II.EQ.1) NI=1
IF(II.EQ.2) NI=2
IF(II.EQ.3) GO TO 1109
IF(II.EQ.4) NI=3
IF(II.EQ.5.OR.II.EQ.6) GO TO 1109
IF(II.EQ.7) NI=4
IF(II.EQ.8.OR.II.EQ.9) GO TO 1109
IF(II.GE.10) GO TO 1110
GO TO (11,12,13,14) , NI
11 CALL FTNCMD('ASSIGN 7=OR1',12)
GO TO 17
12 CALL FTNCMD ('ASSIGN 7=OR2' ,12)
GO TO 17
13 CALL FTNCMD('ASSIGN 7=OR3' ,12)
GO TO 17
14 CALL FTNCMD ('ASSIGN 7=OR4' ,12)
17 N=3*NI
M=1
NM=NI+1
LINE=(26+2*NM)*1000
DO 300 I=1,NM.
READ(7'LINE,500) (B(I,J) , J=1,NM)
LINE=LINE+1000
300 CONTINUE
LINE=(21+NM)*1000
DO 400 I=1,NM
READ(7'LINE,500) (A(I,J) , J=1,NM)
LINE=LINE+1000
400 CONTINUE
LINE=(31+3*NM)*1000
DO 450 I=1,NM
READ(7'LINE,500) (B1(I,J),J=1,NM)
LINE=LINE+1000
450 CONTINUE
LINE=10*1000
READ(7'LINE,545) (Z(I),I=1,NM)
500 FORMAT(10X,10D18.10)
545 FORMAT(10D18.10)
LINE=16*1000
DO 546 I=1,NM
READ(7'LINE,500) (QINV(I,J) , J=1,NM)
LINE=LINE+1000
546 CONTINUE
SN=(RNS-RNE)/(XS-XEQ)
BN=RNS-SN*XS
SS6=(S6SUR-S6EQ)/(XS-XEQ)
BS6=S6SUR-SS6*XS
DO 602 J=1,NI
SI=Z(J)*Z(J)
JJ=J+2*(J-1)
RHS=(SI*(1.D00-C1)+C1)*(1.D00-XS)/RNS
X(JJ)=(1.D00-RHS*BN)/(1.D00+RHS*SN)
X(JJ+1)=SS6*X(JJ)+BS6
X(JJ+2)=SN*X(JJ)+BN

```

```

602  CONTINUE
525  NEQ=N
1109 CALL SNLEQ(RHS,TS,PRESS,X,PAR,.75D00,M,N,3,NI
      #,YH2S,DF,NEQ)
      GO TO 1270
1110 CONTINUE
C
C IN THIS SECTION ONE POINT IS CONSIDERED FOR
C GETTING YI AND EFF.
C
      RKISI=.6546536707D00
      SI=(RKISI)*(RKISI)
      RHS=(SI*(1.D00-C1)+C1)*(1.D00-XS)/RNS
      Y(3)=(1.D00-RHS*BN)/(1.D00+RHS*SN)
      Y(1)=SS6*Y(3)+BS6
      Y(2)=SN*Y(3)+BN
C
C NOW SNLEQ IS CALLED TO SOLVE FOR X,S6,AND N
C FOR SPECIFIED SI.
C
      CALL SNLEQ(RHS,TS,PRESS,Y,PAR,1.D0,M,3,5,NI,YH2S,DF,3)
      XRKISI=Y(3)
      S6KISI=Y(1)
      TMKISI=Y(2)
      RRKISI=RATE(NTYPE,TS,PRESS,PAR,XRKISI,S6KISI,TMKISI)
C
C NOW KISI OPTIMUM IS ESTIMATED
C
      RRATIO=RATES/RRKISI
      SIR=1.0D00/SI
      POWER=DLOG(RRATIO)/DLOG(SIR)
      OPKISI=(1.D00+POWER)**(.5D00/POWER)
      OPKISI=1.D00/OPKISI
      SI=OPKISI**2
      RHS=(SI*(1.D00-C1)+C1)*(1.D00-XS)/RNS
      Y(3)=(1.D00-RHS*BN)/(1.D00+RHS*SN)
      Y(1)=SS6*Y(3)+BS6
      Y(2)=SN*Y(3)+BN
      CALL SNLEQ(RHS,TS,PRESS,Y,PAR,1.D0,M,3,5,NI,YH2S,DF,3)
      XRKISI=Y(3)
      S6KISI=Y(1)
      TMKISI=Y(2)
      RRKISI=RATE(NTYPE,TS,PRESS,PAR,XRKISI,S6KISI,TMKISI)
      AYI=9.D00*(FIMOD**2)*RRKISI/RATES
      CALL SOLYI(YI,RKISI,AYI,NFLAG)
      EFF(II)=2./3./((FIMOD**2)/(1.-YI))
      NI=1
      GO TO 2000
1270 EFF(II)=A(NM,NM)
      DO 1200 J=1,NI
      K=J+2*(J-1)
1150 EFF(II)=EFF(II)+A(NM,J)/(1.-C1)
      #*((1.-X(K))/(1.-XS)*RNS/X(K+2)-C1)
1200 CONTINUE

```

```

2000 EFF(11)=EFF(11)/3./FIMOD/FIMOD
      CONTINUE
      RETURN
      END

```

C
C

```

      SUBROUTINE SNLEQ(RHS,TS,PRESS,X,PAR,W,M,N,ICALL,NI
      #,YH2S,DF,NEQ)
C THIS SUBROUTINE IS LISTED IN "ADONEDIMBED".
C
C

```

```

      FUNCTION FUN(X,K,PAR)
      IMPLICIT REAL*8(A-H,O-Z,$)
      DIMENSION X(3),PAR(12)
      COMMON /VAR/ P1,P2,P3,P4,P5,P6,P7,P8,P9,PPH20,PPH2S
      #,PPSO2
      COMMON /PARA/ FI,FIMOD,XS,RNS,RATES,C1,CS
      COMMON/CALL/NCALL,NTYPE
      P1=(X(1)*X(2)*X(2))**(1./3.)
      P2=(X(1)*X(1)*X(2))**(1./3.)
      P3=((X(1)**4)*X(2))**(1./3.)
      P4=(X(2)/X(1))**(2./3.)
      P5=DSQRT(P4)
      P6=(X(1)*X(2))**(1./3.)
      P7=P3/X(2)
      IF(NCALL.LT.2) GO TO 30
      P8=(PAR(7)+PAR(11)*XS)/RNS
      P9=(PAR(6)-PAR(11)*XS/2.)/RNS
      A=(1.-XS)/RNS-(1.-PAR(4))/X(2)
      PPH20=P8+PAR(9)*PAR(11)*A
      PPSO2=P9+PAR(10)*PAR(11)*A/2.
      GO TO (6,11,20),K
6      FUN=X(2)*(PPH20+PPSO2-1.)+PAR(11)*(1.-PAR(4))
      #+PAR(1)*P1+PAR(2)*P2+X(1)+PAR(3)*P3+PAR(12)
      RETURN
11     FUN=PPSO2*X(2)+PAR(11)*(1.-PAR(4))+2.*PAR(1)*P1
      #+4.*PAR(2)*P2+6.*X(1)+8*PAR(3)*P3-PAR(6)
      FUN=FUN-PAR(11)
      RETURN
20     PPH2S=PAR(11)*(1.-X(3))/X(2)
      FUN=PAR(8)*(PPH2S**2)*(PPSO2)
      FUN=FUN-(PPH20**2)*DSQRT(X(1)/X(2))
      RETURN
30     GO TO (5,10),K
5      FUN
      =1-.5*PAR(4)+PAR(1)*P1+PAR(2)*P2+X(1)+PAR(3)*P3-X(2)
      RETURN
10     FUN=2*PAR(1)*P1+4*PAR(2)*P2+6*X(1)+8*PAR(3)*P3
      #-1.5*PAR(4)
      RETURN
      END

```

C
C

```

      FUNCTION DF7(X,K,PAR)

```

```

      IMPLICIT REAL*8(A-H,O-Z,$)
      DIMENSION X(3),PAR(12)
      COMMON /VAR/ P1,P2,P3,P4,P5,P6,P7,P8,P9,PPH2O,PPH2S
      #,PPSO2
      COMMON /PAR/ FI,FIMOD,XS,RNS,RATES,C1,CS
      COMMON/CALL/NCALL,NTYPE
      GO TO (5,10,20) , K
5      DF7=PAR(1)*P4/3.+2.*PAR(2)*P5/3.+1.+4./3.*PAR(3)*P6
      RETURN
10     DF7=2/3*PAR(1)*P4+8/3*PAR(2)*P5+6.+32./3.*PAR(3)*P6
      RETURN
20     DF7=-0.5D00*(PPH2O**2)/DSQRT(X(1)*X(2))
      RETURN
      END

```

C
C

```

      FUNCTION DF8(X,K,PAR)
      IMPLICIT REAL*8(A-H,O-Z,$)
      DIMENSION X(3),PAR(12)
      COMMON /VAR/ P1,P2,P3,P4,P5,P6,P7,P8,P9,PPH2O,PPH2S
      #,PPSO2
      COMMON /PAR/ FI,FIMOD,XS,RNS,RATES,C1,CS
      COMMON/CALL/NCALL,NTYPE
      IF(NCALL.GT.1) GO TO 50
      GO TO (5,10) , K
5      DF8=2./3.*PAR(1)/P5+PAR(2)/3./P4+PAR(3)*P7/3.-1.
      RETURN
10     DF8=4./3.*PAR(1)/P5+4./3.*PAR(2)/P4+8.*PAR(3)*P7/3.
      RETURN
50     GO TO (60,70,80) , K
60     DF8=-1.D00+PPH2O+PPSO2+(1.-PAR(4))/X(2)*PAR(11)*(PAR
      # (9)-PAR(10)/2)+2/3*PAR(1)/P5+PAR(2)/3/P4+PAR(3)/3*P7
      RETURN
70     DF8=PPSO2-(1.-PAR(4))/X(2)*PAR(10)*PAR(11)/2.
      #+4./3.*PAR(1)/P5+4./3.*PAR(2)/P4+8./3.*PAR(3)*P7
      RETURN
80     DPH2O=PAR(9)*PAR(11)*(1.-X(3))/(X(2)**2)
      DPSO2=-PAR(10)*PAR(11)*(1.-X(3))/(X(2)**2)
      DPH2S=-PAR(11)*(1.-X(3))/(X(2)**2)
      DF8=2.*PAR(8)*PPH2S*PPSO2*DEH2S
      DF8=DF8+PAR(8)*(PPH2S**2)*DPSO2
      DF8=DF8-2.*PPH2O*DPH2O*DSQRT(X(1)/X(2))
      DF8=DF8+.5*(PPH2O**2)*DSQRT(X(1))*(X(2)**(-1.5))
      RETURN
      END

```

C
C

```

      FUNCTION DF9(X,K,PAR)
C THIS FUNCTION CALC. THE DIFF. WITH RESPECT TO CONV.
C

```

```

      IMPLICIT REAL*8(A-H,O-Z,$)
      DIMENSION X(3),PAR(12)
      COMMON /VAR/ P1,P2,P3,P4,P5,P6,P7,P8,P9,PPH2O,PPH2S
      #,PPSO2

```

```

COMMON /PARA/ FI,FIMOD,XS,RNS,RATES,C1,CS
COMMON/CALL/NCALL,NTYPE
GO TO (5,10,20),K
5  DF9=PAR(11)*(PAR(9)-.5*PAR(10)-1.0)
   RETURN
10  DF9=-PAR(11)*(1+.5*PAR(10))
   RETURN
20  DPH2O=PAR(9)*PAR(11)/X(2)
   DPSO2=-PAR(10)*PAR(11)/2./X(2)
   DPH2S=-PAR(11)/X(2)
   DF9=2.*PAR(8)*PPH2S*PPSO2*DPH2S
   DF9=DF9+PAR(8)*(PPH2S**2)*DPSO2
   DF9=DF9-2.*PPH2O*DPH2O*DSQRT(X(1)/X(2))
   RETURN
END

```

C
C

```

FUNCTION FUNO(TS,PRESS,NI,N,J,PAR)
IMPLICIT REAL*8(A-H,O-Z,$)
DIMENSION X(12),B(5,5),B1(5,5),Z(5),A(5,5),PAR(12),
#QINV(5,5)
COMMON /PARA/ FI,FIMOD,XS,RNS,RATES,C1,CS
COMMON /ORTH/ B,B1,A,X,QINV,Z
COMMON/CALL/NCALL,NTYPE
FUNO=0.0
K=1
DO 10 I=1,N,3
5  FUNO=FUNO+B(J,K)*((1.-X(I))/(1.-XS)*RNS/X(I+2)
  #-C1)/(1.D00-C1)
30  K=K+1
10  CONTINUE
   M=J+2*(J-1)
   R=RATE(NTYPE,TS,PRESS,PAR,X(M),X(M+1),X(M+2))
40  FUNO=FUNO+B(J,NI+1)-9.*FIMOD*FIMOD*R/RATES
60  RETURN
END

```

C
C

```

FUNCTION DF1(TS,PRESS,NI,J,PAR)
IMPLICIT REAL*8(A-H,O-Z,$)
DIMENSION X(12),B(5,5),B1(5,5),Z(5),A(5,5),PAR(12)
#,QINV(5,5)
COMMON /PARA/ FI,FIMOD,XS,RNS,RATES,C1,CS
COMMON /ORTH/ B,B1,A,X,QINV,Z
COMMON/CALL/NCALL,NTYPE
K=J+2*(J-1)
5  DF1=-B(J,J)/(1.-XS)*RNS/X(K+2)/(1.D00-C1)
20  R1=RATE(NTYPE,TS,PRESS,PAR,X(K),X(K+1),X(K+2))
   CONV=X(K)+0.00001
   R2=RATE(NTYPE,TS,PRESS,PAR,CONV,X(K+1),X(K+2))
   DR=(R2-R1)/.00001
30  DF1=DF1-9.*FIMOD*FIMOD*DR/RATES
50  RETURN
END

```

C
C

```

FUNCTION DF2(NI,J,I)
IMPLICIT REAL*8(A-H,O-Z,$)
DIMENSION X(12),B(5,5),B1(5,5),Z(5),A(5,5),PAR(12)
#,QINV(5,5)
COMMON /PARA/ FI,FIMOD,XS,RNS,RATES,C1,CS
COMMON /ORTH/ B,B1,A,X,QINV,Z
K=I+2*(I-1)
5 DF2=-B(J,I)*RNS/((1.-XS)/X(K+2)/(1.D00-C1)
20 RETURN
END

```

C
C

```

FUNCTION DF3(TS,PRESS,NI,J,PAR)
IMPLICIT REAL*8(A-H,O-Z,$)
DIMENSION X(12),B(5,5),B1(5,5),Z(5),A(5,5),PAR(12)
#,QINV(5,5)
COMMON /PARA/ FI,FIMOD,XS,RNS,RATES,C1,CS
COMMON /ORTH/ B,B1,A,X,QINV,Z
COMMON/CALL/NCALL,NTYPE
K=J+2*(J-1)
5 DF3=-B(J,J)*(1.-X(K))/(1.-XS)*RNS/(X(K+2)**2)/(1.-C1)
20 R1=RATE(NTYPE,TS,PRESS,PAR,X(K),X(K+1),X(K+2))
CM=X(K+2)+.00001
R2=RATE(NTYPE,TS,PRESS,PAR,X(K),X(K+1),CM)
DR=(R2-R1)/.00001
30 DF3=DF3-9.*FIMOD*FIMOD/RATES*DR
50 RETURN
END

```

C
C

```

FUNCTION DF4(J,I,NI)
IMPLICIT REAL*8(A-H,O-Z,$)
DIMENSION X(12),B(5,5),B1(5,5),Z(5),A(5,5),PAR(12)
#,QINV(5,5)
COMMON /PARA/ FI,FIMOD,XS,RNS,RATES,C1,CS
COMMON /ORTH/ B,B1,A,X,QINV,Z
M=I+2*(I-1)
5 DF4=-B(J,I)*(1.-X(M))/(1.-XS)*RNS/(X(M+2)**2)/(1.-C1)
20 RETURN
END

```

C
C

```

FUNCTION DF5(TS,PRESS,NI,J,PAR)
IMPLICIT REAL*8(A-H,O-Z,$)
DIMENSION X(12),B(5,5),B1(5,5),Z(5),A(5,5),PAR(12)
#,QINV(5,5)
COMMON /PARA/ FI,FIMOD,XS,RNS,RATES,C1,CS
COMMON /ORTH/ B,B1,A,X,QINV,Z
COMMON/CALL/NCALL,NTYPE
K=J+2*(J-1)
R1=RATE(NTYPE,TS,PRESS,PAR,X(K),X(K+1),X(K+2))
CS6=X(K+1)+.00001

```

```

      R2=RATE(NTYPE,TS,PRESS,PAR,X(K),CS6,X(K+2))
      DR=(R2-R1)/.00001
10    DF5=-9.*FIMOD*FIMOD*DR/RATES
20    RETURN
      END

```

C
C

```

      FUNCTION RATE(NTYPE,TS,PRESS,PAR,Z1,S6,TM)
      IMPLICIT REAL*8(A-H,O-Z,$)
      DIMENSION PAR(12)
      COMMON /COMP/ YH2S,YSO2,YH2O,YN2,DHS,DSO,DW,DENP
      COMMON /PARA/ F1,FIMOD,XS,RNS,RATES,C1,CS
      EQK=PAR(5)/DSQRT(760.D00)
      IF(NTYPE.EQ.2) GO TO 10
      PSO2=(YSO2-YH2S*XS/2.)/RNS-YH2S*DHS/DSO/2.
      #*((1.-XS)/RNS-(1.-Z1)/TM)
      PSO2=PSO2*PRESS*760.
      PH2O=(YH2O+YH2S*XS)/RNS+YH2S*DHS/DW
      #*((1.-XS)/RNS-(1.-Z1)/TM)
      PH2O=PH2O*PRESS*760.
      GO TO 20
10    PSO2=(YSO2-YH2S*Z1/2.)/TM*PRESS*760.D00
      PH2O=(YH2O+YH2S*Z1)/TM*PRESS*760.D00
20    PH2S=YH2S*(1.-Z1)/TM*PRESS*760.
      PS6=S6/TM*760.*PRESS
      AB=2.56D-04*DEXP(-7350./1.986/TS)
      RATE=AB/(1.+0.006D00*PH2O)**2)
      RATE=RATE*(PH2S*DSQRT(PSO2)-PH2O*DSQRT(DSQRT(PS6)
      #/EQK))
      RETURN
      END

```

C
C

```

      SUBROUTINE SOLYI(YI,RKISI,AYI,NFLAG)

```

C
C
C
C
C

```

      THIS SUBROUTINE IS LISTED IN "ADONEDIMBED".

```

C
C

```

      SUBROUTINE SPLN(X,Y,N,A,B,C,D)

```

C
C
C
C

```

      THIS SUBROUTINE HAS BEEN PRINTED IN THE "ADONEDIMBED".

```

C
C

```

      FUNCTION SEVAL(N,U,X,Y,B,C,D)

```

C
C
C
C

```

      THIS FUNC. IS PRINTED IN "ADONEDIMBED".

```

C
C

```

      SUBROUTINE RKF(A,Y,N,FUN,DA,H,HMX,ABSER,RELER,IFLAG)

```

C

```

      THIS SUBROUTINE IS PRINTED IN "NONISOEFF".

```

APPENDIX F: Coldbed Reactor

Contents

1. Development of the coldbed reactor model.
2. Numerical method for coldbed reactor model.
3. Eigenberger-Butt algorithm.
4. Adjustment of spatial grid points.
5. Solution of the O.D.E.
6. Flow chart of coldbed reactor.
7. Numerical method of pseudosteady-state coldbed reactor.
8. "COLDBED" program.
9. "CBSSTEADY" program.

F.1 Development of Coldbed Reactor Model

The general unsteady state mass transport and reaction processes in the one dimensional adiabatic reactor including axial dispersion is described by

$$\epsilon \frac{\partial C_{f1}}{\partial t} = -\frac{\partial}{\partial z}(V_s C_{f1}) + (D_z \epsilon \bar{C}_t / \Pi) \frac{\partial^2 C_{f1}}{\partial z^2} + a_1 R_{C1} (\rho_b / \rho_p) \quad (F.1)$$

The superficial velocity in a constant pressure reactor is given by equation (5.18) as,

$$V_s / V_0 = \{ 1 - Y_1 (1 - v) X_f / 2 \} = G T_f / T^0 \quad (F.2)$$

where v as given by equation (5.17) for the condition of the coldbed reactor becomes,

$$v = a_{s,s} + a_{s,s} \quad (F.3)$$

because the formation of S_2 and S_4 species have been neglected (section 6.2).

Data of figure 6.3 shows that, over 400 to 450 K, $x(S_6)/x(S_8)$ changes from 0.23 to 0.244. Thus, the ratio $a_{s,s}/a_{s,s}$ in the operating condition of the coldbed reactor on the average is

$$a_{s,s}/a_{s,s} = x(S_6)/x(S_8) \cong 0.24 \quad (F.4)$$

Combining equations (F.4) and (3.35) gives, $a_{1,8} = 0.318$ and $a_{1,8} = 0.076$. Thus v will be equal to 0.394.

G for an average H_2S conversion of 0.5 and for a feed composition to the second stage convertor will be,

$$G = 1 - 0.028 (1-0.394)(0.5/2) = 0.996$$

To avoid excessive complexity G will be taken as unity. This introduces the error of about 0.4% in V_1/V_1^0 . Taking V_1/V_1^0 equal to T_f/T^0 yields,

$$V_1 C_{f1} = V_1^0 T_f C_{f1}/T^0 = V_1^0 P_{f1}/R_g T^0 \quad (F.5)$$

Combining equation (F.1) with (F.5) and introducing the dimensionless length z ($=z/L$) gives,

$$\partial C_{f1}/\partial t = -w_1 \partial P_{f1}/\partial z + w_2 \partial^2 P_{f1}/\partial z^2 + a_1 w_3 R \quad (F.6)$$

where,

$$w_1 = V_1^0 / R_g T^0 \epsilon L \quad (F.7)$$

$$w_2 = Dz \bar{C}_t / \Pi L^2 \quad (F.8)$$

$$w_3 = \rho b / \rho p \epsilon \quad (F.9)$$

The corresponding balance equation, when the component is sulfur becomes,

$$\begin{aligned} \partial[8Cf_7+6Cf_8]/\partial t = & -w_1 \partial [8Pf_7+6Pf_8]/\partial z \\ & + w_2 \partial^2/\partial z^2 [8Pf_7+6Pf_8] + 3w_3 R \end{aligned} \quad (F.10)$$

valid for the condition, $(Pf_7+Pf_8) \leq P_v$. When the equality holds, the sulfur partial pressure equals to its vapor pressure and further sulfur produced will remain on the catalyst surface.

The energy conservation balance gives,

$$\partial Tf/\partial t = -v_1 \partial Tf/\partial z + v_2 \partial^2 Tf/\partial z^2 + v_3 R \quad (F.11)$$

where,

$$v_1 = \bar{C}_t V_i C_p / C_{pa} L \quad (F.12)$$

$$v_2 = Kz / C_{pa} L^2 \quad (F.13)$$

$$v_3 = (-\Delta H) \rho_b / \rho_p C_{pa} \quad (F.14)$$

$$C_{pa} = \epsilon C_p \bar{C}_t + \rho_b C_{pc} \quad (F.15)$$

The boundary conditions for equations (F.1), (F.10) and (F.11) (199) are,

at $z=0$

$$\begin{aligned} \partial Pf_1/\partial z = & V_i L/\epsilon Dz (Pf_1 - P_i^*) \\ \equiv & w_1/w_2 (Pf_1 - P_i^*) \end{aligned} \quad (F.16)$$

$$\partial(8Pf_7+6Pf_8)/\partial z = w_1/w_2 (8Pf_7+6Pf_8-8P_i^*-6P_i^*) \quad (F.17)$$

$$\begin{aligned}\partial T_f / \partial z &= \bar{C}_t V_1 C_p L / K z (T_f - T^0) \\ &\equiv v_1 / v_2 (T_f - T^0)\end{aligned}\quad (F.18)$$

and at $z=1$

$$\partial P f_1 / \partial z = \partial T_f / \partial z = 0 \quad (F.19)$$

F.2 Numerical Method of Coldbed Reactor Model

The system of partial differential equation (F.6), (F.10), and (F.11) subject to the boundary conditions (F.16) to (F.19) were solved by the method of Eigenberger and Butt (70). This method is a finite difference method with non-equidistant space steps. Its prime feature is the automatic positioning of axial grid points at required positions. The authors have claimed that the method is well suited for the solution of moving profiles such as those for deactivating catalytic beds.

Their method converts the partial differential equation to an ordinary differential equation by assuming that, the profiles of dependent variables in the spatial coordinate can be piecewise approximated by second order parabolas. The followings briefly describes the method of Eigenberger and Butt as applied to Claus coldbed reactor.

F.2.2 Eigenberger-Butt Algorithm

During the calculation, the dependent variable P_f and T_f will be evaluated at certain nonequidistant grid points z_m , $m=1,2,\dots,mn$. The solution profile in the interval z_{m-1} to z_{m+1} is then approximated by a parabola and the difference approximation is evaluated for the middle of the element at

$$z = \frac{(z_{m-1} + 2z_m + z_{m+1})}{4} \quad (F.20)$$

Here, the derivation of the equations will be shown for equation (F.11).

At any spatial interval, the temperature profile will be represented by,

$$T_f = a + b z + c z^2 \quad (F.21)$$

The coefficient a to c are evaluated by the solution at the grid points z_{m-1} , z_m , and z_{m+1} as,

$$c = \frac{DZM(T_{f_{m+1}} - T_{f_m}) - DZP(T_{f_m} - T_{f_{m-1}})}{DZP * DZM * (DZP + DZM)} \quad (F.22)$$

$$b = (T_{f_m} - T_{f_{m-1}}) / DZM - c(z_m + z_{m-1}) \quad (F.23)$$

$$a = T_{f_{m-1}} + b z_{m-1} + c(z_{m-1})^2 \quad (F.24)$$

where,

$$DZM\{m\} = z_m - z_{m-1} \quad (F.25)$$

$$DZP\{m\} = z_{m+1} - z_m \quad (F.26)$$

The parabola approximation (F.21) gives the spatial derivatives of equation (F.11) as,

$$-v_1 \partial Tf / \partial z + v_2 \partial^2 Tf / \partial z^2 = -v_1 (b + 2cz) + 2cv_2 \quad (F.27)$$

Substituting for b and c from (F.22) and (F.23) and evaluating (F.27) at point z (middle of the element, equation (F.20)) yields,

$$-v_1 \partial Tf / \partial z + v_2 \partial^2 Tf / \partial z^2 = C\{m,1\}Tf_{m-1} + C\{m,2\}Tf_m + C\{m,3\}Tf_{m+1} \quad (F.28)$$

where for $m=2$ to $mn-1$,

$$C\{m,1\} = (2v_2 + 0.5 v_1 \text{ SUM}) / DZM * \text{SUM} \quad (F.29)$$

$$C\{m,2\} = -\{2 v_2 + 0.5 v_1 (DZP - DZM)\} / DZM * DZP \quad (F.30)$$

$$C\{m,3\} = -(C\{m,1\} + C\{m,2\}) \quad (F.31)$$

$$\text{SUM} = DZM\{m\} + DZP\{m\} \quad (F.32)$$

The approximation of (F.27) by (F.28) is the same for all elements except the first and the last one. The difference approximation for the last element is evaluated at (70),

$$z = z_{mn} - DZM\{mn\}/4 \quad (F.33)$$

The parabola coefficients of equation (F.21) using the boundary condition (F.19) are,

$$c = (Tf_{mn-1} - Tf_{mn})/DZM^2\{mn\} \quad (F.34)$$

$$b = -2c z_{mn} \quad (F.35)$$

Next equation (F.27) is evaluated at the middle point z in equation (F.33), using equations (F.34) and (F.35) which for the last element yields,

$$-v_1 \partial Tf / \partial z + v_2 \partial^2 Tf / \partial z^2 = C\{mn,1\} Tf_{mn-1} + C\{mn,2\} Tf_{mn} \quad (F.36)$$

where,

$$\begin{aligned} C\{mn,1\} &= -C\{mn,2\} \\ &= 2v_2/DZM^2\{mn\} + 0.5v_1/DZM\{mn\} \end{aligned} \quad (F.37)$$

Eigenberger and Butt recommend that for small values of v_2 (large axial pellet numbers), a satisfactory

approximation can be obtained by writing the balance equations for the first element. The energy balance equation for the first element is,

$$\begin{aligned} (DZP\{1\} L C_{pa}/2) \cdot dT_{f1}/dt = & \bar{C}_t v_1 C_p \{T^0 - (T_{f1} + T_{f2})/2\} \\ & + K_z (T_{f2} - T_{f1})/L DZP\{1\} \\ & + [L \rho_b DZP\{1\} (-\Delta H)/2\rho_p] R\{1\} \end{aligned} \quad (F.38)$$

which simplifies to,

$$\begin{aligned} dT_{f1}/dt = & (2v_1/DZP\{1\})T^0 - (v_1/DZP\{1\} + 2v_2/DZP^2\{1\})T_{f1} \\ & + (2v_2/DZP^2\{1\} - v_1/DZP\{1\})T_{f2} + v_3 R\{1\} \end{aligned} \quad (F.39)$$

The original partial differential equation (F.11) with the boundary conditions (F.18) and (F.19) are now using equation (F.27) and (F.36) have been reduced to the ordinary differential equations;

for $m=2, mn-1$

$$\begin{aligned} dT_{fm}/dt = & C\{m,1\}T_{f_{m-1}} + C\{m,2\}T_{fm} + C\{m,3\}T_{f_{m-1}} \\ & + v_2 R_m \end{aligned} \quad (F.40)$$

for $m=mn$

$$dT_{f_{mn}}/dt = C\{mn,1\}T_{f_{mn-1}} + C\{mn,2\}T_{f_{mn}} + v_2 R_{mn} \quad (F.41)$$

The integration of the resulting system of ordinary differential equations - (E.39), (F.40) and (F.41), will give the temperature profile as a function of time for the specified number of axial points (mn) and spatial intervals. The same approach should be followed to reduce the partial differential equations (F.6) and (F.10) to the corresponding ordinary differential equations.

The source term $R\{P_f, T_f, z\}$ can be calculated only at the grid point. In order to evaluate the mean value of the source term R_m in a non-equidistant interval, Eigenberger and Butt recommended, to assume that the variation of the source term within the interval is approximated by a parabola and take the integral value of R for the element. The result (199) is,

$$R_m = B\{m,1\} R_{m-1} + B\{m,2\} R_m + B\{m,3\} R_{m+1} \quad (F.42)$$

where, for $m=2, mn-1$,

$$B\{m,1\} = \frac{3(DZP\{m\})^2(DZM\{m\})^2 - 2(DZP\{m\})^4 + (DZM\{m\})^3 DZP\{m\}}{DEN} \quad (F.43)$$

$$B\{m,3\} = \frac{3(DZP\{m\})^2(DZM\{m\})^2 - 2(DZM\{m\})^4 + (DZP\{m\})^3 DZM\{m\}}{DEN} \quad (F.44)$$

$$DEN = 12 DZP\{m\} DZM\{m\} [DZM\{m\} + DZP\{m\}]^2 \quad (F.45)$$

and, for first and last element,

$$\begin{aligned} B\{1,1\} &= 0 & ; & \quad B\{1,3\} = 0.25 \\ B\{mn,1\} &= 1/12 & ; & \quad B\{mn,3\} = 0 \end{aligned}$$

$B\{m,2\}$ for all the elements is given by,

$$B\{m,2\} = 1 - B\{m,1\} - B\{m,3\} \quad (F.46)$$

F.2.3 Adjustment of Spatial Grid Points

After the integration of the ordinary differential equations for one step, the result is checked for spatial accuracy. The decision whether an additional grid points has to be inserted or an existing grid point can be omitted depends upon the error E of the approximation of the parabola in an interval. This error is defined as the difference between two adjacent parabola-approximation, halfway between the grid points:

$$E\{m\} = YHM\{m+1\} - YHP\{m\} \quad (F.47)$$

Where, the "halfway" YHM, YHP have to be calculated for each grid point. The parabola approximation gives

$$\begin{aligned} YHM\{m\} &= Tf \left[at \left(z_{m-1} + z_m \right) / 2 \right] \\ &= HM\{m,1\} Tf_{m-1} + HM\{m,2\} Tf_m + HM\{m,3\} Tf_{m+1} \quad (F.48) \end{aligned}$$

$$YHP\{m\} = Tf \left\{ at(z_m + z_{m+1}) / 2 \right\}$$

$$= \text{HP}\{m,1\} \text{Tf}_{m-1} + \text{HP}\{m,2\} \text{Tf}_m + \text{HP}\{m,3\} \text{Tf}_{m+1} \quad (\text{F.49})$$

where, HM and HP for $m=2, mn$ are,

$$\text{HM}\{m,1\} = \text{NUM} / 4 \text{DZM}\{m\} \text{DZP}\{m\} \{\text{DZM}\{m\} + \text{DZP}\{m\}\} \quad (\text{F.50})$$

$$\text{HM}\{m,2\} = \text{NUM} / 4 \text{DZM}\{m\} \text{DZP}\{m\} \quad (\text{F.51})$$

$$\text{HP}\{m,1\} = -(\text{DZP}\{m\})^2 / 4 \text{DZM}\{m\} [\text{DZM}\{m\} + \text{DZP}\{m\}] \quad (\text{F.52})$$

$$\text{HP}\{m,2\} = \text{DZP}\{m\} [2 \text{DZM}\{m\} + \text{DZP}\{m\}] / 4 \text{DZM}\{m\} \text{DZP}\{m\} \quad (\text{F.53})$$

$$\text{HM}\{m,3\} = 1 - \text{HM}\{m,1\} - \text{HM}\{m,2\} \quad (\text{F.54})$$

$$\text{HP}\{m,3\} = 1 - \text{HP}\{m,1\} - \text{HP}\{m,2\} \quad (\text{F.55})$$

$$\text{DZM}\{m\} [2 \text{DZP}\{m\} + \text{DZM}\{m\}] \quad (\text{F.56})$$

Using the boundary conditions at $z=0$ and $z=1$ the half value for the entrance and exit (70) are,

$$\begin{aligned} \text{YHP}\{1\} &= \text{Tf} \{ \text{at } (z_1 + z_2) / 2 \} \\ &= v_1 \text{DZP}(1) / 4v_2 \text{T}^\circ + (3/4 + v_1 \text{DZP}(1) / 4v_2) \text{Tf}_1 \\ &\quad + 1/4 \text{Tf}_2 \end{aligned} \quad (\text{F.57})$$

$$\begin{aligned} \text{YHM}\{mn\} &= \text{Tf} \{ \text{at } (z_{mn-1} + z_{mn}) / 2 \} \\ &= 3/4 \text{Tf}_{mn} + 1/4 \text{Tf}_{mn-1} \end{aligned} \quad (\text{F.58})$$

Now if the relative value of $E\{m\}$ is larger than a specified limit E_{mx} a new grid point at $(z_m + z_{m+1})/2$ should be inserted. The value of the variable at this point is set to be the mean between $YHP(m)$ and $YHM(m+1)$:

$$Tf \{at (z_m + z_{m+1})/2\} = [YHP(m) + YHM(m+1)] / 2 \quad (F.59)$$

However, if the two successive errors are below another specified value E_{min} , the grid point in the middle will be omitted. To avoid halving and doubling of the same interval in successive time steps, the condition

$$E_{mx} \cong 0.1 E_{min}$$

has been recommended (70).

F.2.4 Solution of the O.D.E.

The system of O.D.E. (F.39) to (F.41) and the corresponding equations which are obtained by transformation of P.D.E. (F.6) and (F.10) are solved by the Modified Euler Method (87).

Eigenberger and Butt (70) have, recommended using trapazoidal rule. However, for trapazoidal method, since the source term is nonlinear, the resulting equations have to be solved iteratively. This approach was initially used for the solution of the O.D.E., but did not result in convergence. Thus the modified Euler method was employed.

To evaluate the source term at the grid points R from equation (6.44), the integral function q_i was evaluated by three-point Gaussian quadrature formula (87).

F.2.6 Flow chart for Coldbed Reactor

Figure F.1 present the flowchart based on Eigenberger-Butt method, for solution of the unsteady state partial differential equations (F.6), (F.10), and (F.11) coupled with the deactivation equation (6.45) and the global rate expression (6.44).

F.3 Numerical Method for Pseudosteady-state Coldbed Reactor

The classical explicit finite difference method was employed for the solution of the pseudosteady-state coldbed model, equations (6.44), (6.45), and (6.46) to (6.48). The followings are the mathematical steps involved in this method.

To solve the differential equations, the z axis is divided to N equispaced points. Let ' k ' represent the spatial grid point and ' j ' represent the time grid.

The integration of equation (6.48) for the reference species by Euler method yields,

$$Pf|_{k+1} = Pf|_k - 2w_3/w_1 R_k \quad (F.60)$$

where, R_k is the global rate of reaction evaluated at the conditions of the k 'th grid point at time j .

Next, the equation (6.49) is replaced by a forward and central difference (87) approximation in time and z axis, respectively. Thus,

$$\begin{aligned} (Tf_k^{j+1} - Tf_k^j) / \Delta t = & -(v_1/2\Delta z)(Tf_{k+1}^j - Tf_{k-1}^j) \\ & + (v_3/2)(R_k^j + R_k^{j+1}) \end{aligned} \quad (F.61)$$

In the equation (F.61), the source term R_k has been taken as the average of it's value at time j and $j+1$. The global rate ratio from equation (6.37) is,

$$R_k^{j+1}/R_k^j = [(kf/Tf)_k^{j+1} / (kf/Tf)_k^j]^{1/2} = \text{RATIO} \quad (F.62)$$

The first order term in the Taylor series expansion of $(kf/Tf)^{1/2}$ gives,

$$\begin{aligned} \text{RATIO} &= 1 + (1/2)[(E/Rg Tf_k^j) - 1][(Tf_k^{j+1}/Tf_k^j) - 1] \\ &\equiv 1 + A1 [Tf_k^{j+1}/Tf_k^j - 1] \end{aligned} \quad (F.63)$$

Thus,

$$\begin{aligned} R_k^j + R_k^{j+1} &= R_k^j (1 + \text{RATIO}) \\ &\equiv R_k^j [2 + A1 (Tf_k^{j+1}/Tf_k^j - 1)] \\ &\equiv A2 + A3 Tf_k^{j+1} \end{aligned} \quad (F.64)$$

where,

$$A2 = (2-A1) R_k \quad (F.65)$$

$$A3 = A1 R_k / Tf_k \quad (F.66)$$

Combining equations (F.61) and (F.64) gives:

$$\begin{aligned} Tf_{k,j+1} - Tf_k &= -(v_1 \Delta t / 2 \Delta z) (Tf_{k,j+1} - Tf_{k,j-1}) \\ &+ (v_3 \Delta t / 2) (A2 + A3 Tf_{k,j+1}) \end{aligned} \quad (F.67)$$

Rearranging equation (F.67) gives the predicted value of Tf at time $j+1$ as,

$$\begin{aligned} Tf_{k,j+1} &= Tf_k / A4 - (v_1 \Delta t / 2 \Delta z A4) (Tf_{k,j+1} - Tf_{k,j-1}) \\ &+ v_3 \Delta t A2 / 2 A4 \end{aligned} \quad (F.68)$$

where,

$$A4 = 1 - v_3 A3 \Delta t / 2 \quad (F.69)$$

Next The deactivation equation, equation (6.47) is solved by Euler formula

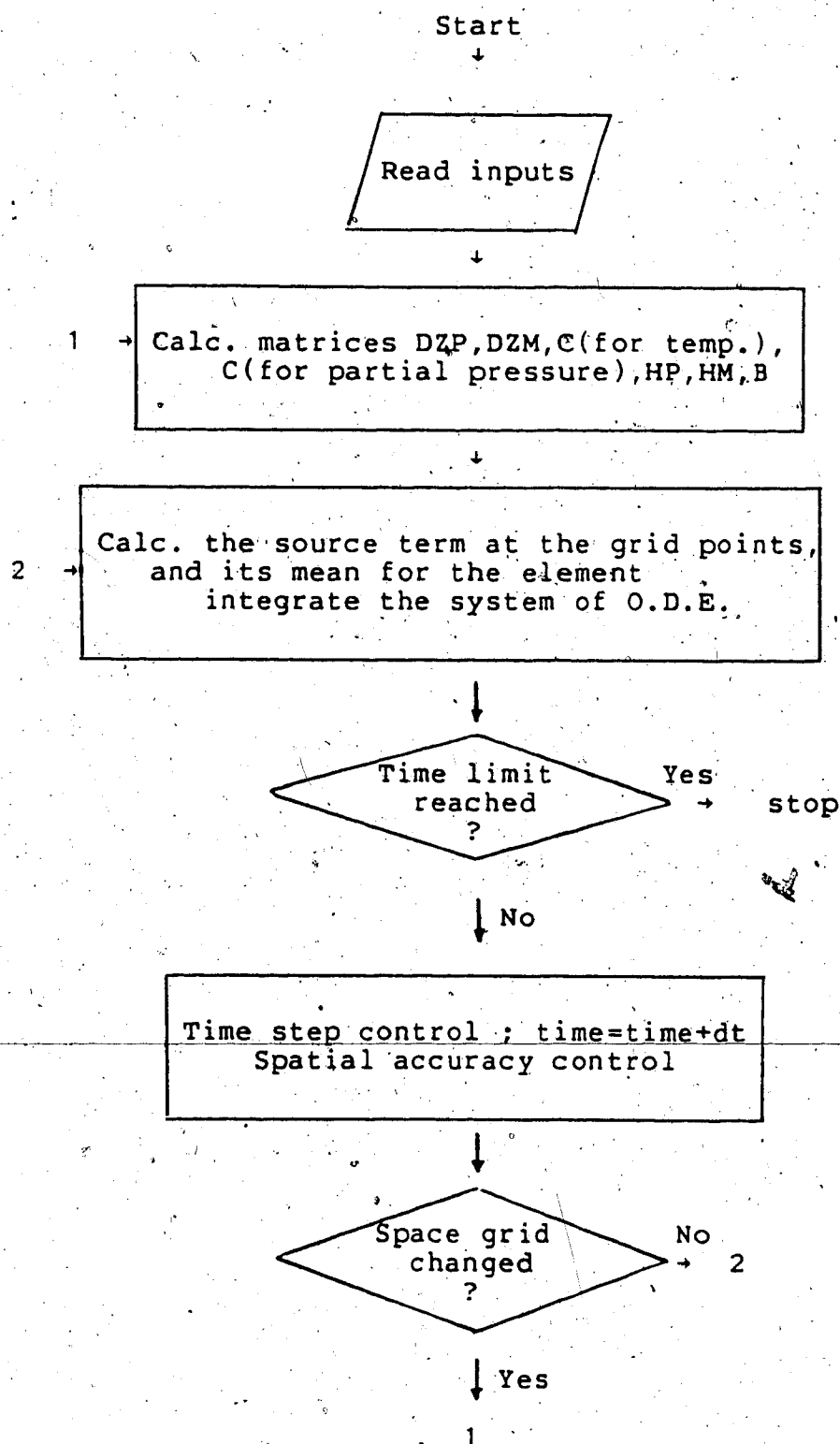
$$\gamma_{s,k,j+1} = \gamma_{s,k,j} + A5 \quad (F.70)$$

where, $A5$ is the right side equation (6.47) evaluated at grid point k and time j .

The above analysis shows that the pseudosteady-state solution of the coldbed reactor will be obtained by the

solution of the equations (F.60), (F.68) and (F.70). The computer program "CBPSSTEADY" performs the above computations of the pseudosteady-state Claus reactor.

Figure F.1 Flowchart for Computation of Unsteady State Coldbed Reactor Model.



```

C.....
C      COLDBED
C
C  A COMPUTER PROGRAM TO PERFORM COLDBED SIMULATION FOR
C  UNSTEADYSTATE MATERIAL & ENERGY BALANCE EQ. OF CHAP. 6.
C
C  INPUTS TO THE PROGRAM:
C    T0 = FEED TEMPERATURE K
C    TIN = BED INITIAL TEMPERATURE K
C    PRESS = TOTAL PRESSURE ATM
C    YI = MOLE FRACTION OF SPECIES I IN THE FEED
C    CP = GAS HEAT CAPACITY CAL/MOLE K
C    U0 = INLET SUPERFICIAL VELOCITY CM/SEC
C    EB = BED POROSITY
C    DP = CATALYST PELLET DIAMETER CM
C    ROB = BED DENSITY
C    ROP = PELLET DENSITY GR/CM**3
C    HTC = FILM HEAT TRANSFER COEFFICIENT CAL/SEC K CM
C    DI = EFFECTIVE DIFFUSIVITY OF SPECIES I
C    DAX = AXIAL DISPERSION
C    AXLN = AXIAL THERMAL CONDUCTIVITY
C    AMW = AVERAGE MOLECULAR WEIGHT OF THE GAS
C    CPCAT = CATALYST HEAT CAPACITY
C    DTIME = TIME INTERVAL
C    EMAX = MAX ERROR BOUND
C    EMIN = MIN ERROR BOUND
C    LM = NUMBER OF GRID POINTS
C    IOPT = OPTION FLAG
C  1 : INITIALLY THE CONC. IN THE BED IS CLOSE TO ZERO
C      (AFTER REGENARTION)
C  2 : SPECIFY TIME, LM, GRID POINTS LOCATION, TEMP.
C      PARTIAL PRESSURE AND RATES AT THE GRID POINTS.
C
C  " ALL THE UNITS ARE IN CM, K, SEC, GR, AND CALORI "
C.....
C    COMMON/PINT/P10,P20,P30,P50,PRESS,T0,YH2S,YSO2,YH2O,YS8
C    COMMON/QPAR/Q1,Q2,V1,V2,V3,W1,W2,W3,G1,G2,RK0,EFFL,DHS
C    #,RO0,ROP,ROB,DAX,AXLN,DP,CPCAT,AMW,EB,DSO,DHO,DS8,U0
C    #,BL,CP,HTC,HEAT
C    COMMON/STIOS/ALFA,BETA
C    COMMON/ERRPAR/EMAX,EMIN
C    DIMENSION PAR(9),W(100),G(100),S(100),Z(100),T(100),
C    #DZP(100),DZM(100),P1(100),P2(100),P3(100),P5(100),
C    #GA(100)
C    COMMON/PARA/PAR
C    READ(5,1) T0,TIN,PRESS
C    READ(5,1) YH2S,YSO2,YN2,YH2O,YS8
C    READ(5,1) CP,U0,EB,DP,BL,ROB,ROP,HTC
C    READ(5,1) DHS,DSO,DHO,DS8
C    READ(5,1) DAX,AXLN,AMW,CPCAT
C    READ(5,2) DTIME,EMAX,EMIN,LM,IOPT
C    WRITE(6,10) DTIME,EMAX,EMIN,LM
10  FORMAT(/,'DTIME=',F10.5,2X,'EMAX=',F10.5,2X,'EMIN='

```

```

      #,F10.5,2X,'LM=',I5)
      ICASE=2
      GO TO (3,4), IOPT
3     TIME=0.0
      Z(1)=0.0
C
C INITIALLY THE BED IS AT TIN, EXCEPT THE FEED WHICH IS
C T0. ALSO THE CONC. OF H2S IS ZERO EVERYWHERE EXCEPT
C AT THE INLET WHICH IS CN0
C
192 DO 11 I=1,LM
      T(I)=TIN
      P1(I)=0.0
      P2(I)=0.0
      P3(I)=0.0
      P5(I)=0.0
      GA(I)=0.0
11 CONTINUE
      IDACT=2
198 DO 20 I=1,LM
C
C INITIALLY THE WHOLE BED IS ACTIVE
C
      G(I)=0.0
      S(I)=0.0
20 W(I)=0.0
C
      DZPI=1.0
      LMMM=LM-2
      DO 18/L=1,LMMM
      EXPT=FLOAT(L)/2.
18 DZPI=DZPI+(1.5**EXPT)
      DZP(1)=1./DZPI
      LMM=LM-1
      DO 21 L=2,LM
      DZM(L)=DZP(L-1)
      DZP(L)=DZM(L)*SQRT(1.5)
21 Z(L)=DZM(L)+Z(L-1)
      GO TO 6


---


4 READ(8,81) TIME,LM
  READ(8,56) (Z(II),II=1,LM)
  READ(8,50) (T(II),II=1,LM)
  READ(8,51) (P1(II),II=1,LM)
  READ(8,54) (P2(II),II=1,LM)
  READ(8,58) (P3(II),II=1,LM)
  READ(8,53) (P5(II),II=1,LM)
  READ(8,52) (GA(II),II=1,LM)
  READ(8,57) (W(II),II=1,LM)
  READ(8,59) (S(II),II=1,LM)
  READ(8,60) (G(II),II=1,LM)
  LMM=LM-1
  LMMM=LM-2
C
6 CALL PARAM

```

```

        WRITE(8,62)
62  FORMAT(/,'THE PARAMETERS ARE:',/)
        WRITE(8,63) ALFA,BETA,V1,V2,V3
        WRITE(8,63) W1,W2,W3,G1,G2,HEAT
        MAXI=50
        INDT=0
100  CALL ARPRO(LM,Z,P1,P2,P3,P5,T,GA,S,W,G,TIME,DTIME,MAXI
        #,INDT,JCONV,ICASE)
        WRITE(8,81) TIME,LM,INDT,JCONV
        WRITE(8,56) (Z(II),II=1,LM)
        WRITE(8,50) (T(II),II=1,LM)
        WRITE(8,51) (P1(II),II=1,LM)
        WRITE(8,54) (P2(II),II=1,LM)
        WRITE(8,58) (P3(II),II=1,LM)
        WRITE(8,55) (P5(II),II=1,LM)
        WRITE(8,52) (GA(II),II=1,LM)
        WRITE(8,57) (W(II),II=1,LM)
        WRITE(8,59) (S(II),II=1,LM)
        WRITE(8,60) (G(II),II=1,LM)
        WRITE(8,61)
81  FORMAT(E15.7,2X,3I6)
61  FORMAT(/)
        IF(TIME.LE.5.0) GO TO 100
1   FORMAT(10E12.5)
2   FORMAT(3E12.5,2I5)
50  FORMAT('TEMP',7E15.7)
51  FORMAT('P1',7E15.7)
52  FORMAT('GAMA',7E15.7)
53  FORMAT('P5',7E15.7)
58  FORMAT('P3',7E15.7)
54  FORMAT('P2',7E15.7)
55  FORMAT('P5',7E15.7)
56  FORMAT('Z',7E15.7)
57  FORMAT('W',7E15.7)
59  FORMAT('S',7E15.7)
60  FORMAT('G',7E15.7)
65  FORMAT(/,'THE SOL. HAS NOT CONV. AT TIME= ',E10.4)
63  FORMAT(7E15.7)
200 STOP
    END

```

C
C

```

SUBROUTINE SAGE(Z1,Z2,Z3,Y1,Y2,Y3)
T1=Y1-Y2
T2=Y3-Y2
T3=T1*T2
IF(T3) 2,2,1
1  SLOPE=(Y1-Y3)/(Z1-Z3)
   RINT=Y1-SLOPE*Z1
   Y2=SLOPE*Z2+RINT
2  RETURN
END

```

C
C

```

SUBROUTINE SOURCE(IDACT, ICASE, PAR, T, GA, PV, S, W, G, P1
#, P2, P3, P5)
COMMON/PINT/P10, P20, P30, P50, PRESS, T0, YH2S, YSO2, YH2O, YS8
COMMON/QPAR/Q1, Q2, V1, V2, V3, W1, W2, W3, G1, G2, RK0, EFFL, DHS
#, RO0, ROP, ROB, DAX, AXLN, DP, CPCAT, AMW, EB, DSO, DHO, DS8, U0
#, BL, CP, HTC, HEAT
COMMON/STIOS/ALFA, BETA
DIMENSION PAR(9)
IDACT=2
PAR(1)=EQCTS(T, 1)
PAR(5)=EQCTS(T, 2)
IF(P1) 4, 4, 1
C TEST IF VAPOR PRESSURE HAS EXCEEDED
1 PAR(7)=VAPPR(T)
IF(P5.LT.0.0) P5=0.0
TEST=P5*(1.+BETA/ALFA)
5 IF(TEST.LT.PAR(7)) GO TO 3
2 P5=PAR(7)/(1.0+BETA/ALFA)
IDACT=1
3 CALL GLOBAL(ICASE, PAR, T, GA, GR, G, IDACT, P1, P2, P3, P5)
S=V2*GR
W=W2*GR
RETURN
4 P2=0.0
P3=0.0
P5=0.0
W=0.0
S=0.0
G=0.0
RETURN
END

```

```

SUBROUTINE GLOBAL(ICASE, PAR, T, GAMA, GLOBR,
#DACT, IDACT, P1, P2, P3, P5)

```

THIS SUBROUTINE CALCULATES THE GLOBAL RATE
AT THE SPATIAL COORDINATES.

```

COMMON/PINT/P10, P20, P30, P50, PRESS, T0, YH2S, YSO2, YH2O, YS8
COMMON/QPAR/Q1, Q2, V1, V2, V3, W1, W2, W3, G1, G2, RK0, EFFL, DHS
#, RO0, ROP, ROB, DAX, AXLN, DP, CPCAT, AMW, EB, DSO, DHO, DS8, U0
#, BL, CP, HTC, HEAT
COMMON/STIOS/ALFA, BETA
DIMENSION PAR(9)
GO TO(1, 2), ICASE
2 IF(P2.LT.0.0) GO TO 7
FPB=P1*SQRT(P2)-P3/PAR(5)*(P5**(3./16.))
IF(FPB.LT.0.0) GO TO 7
FPB=FPB/((1.+4.56*P3)**2)
RK=RK0*EXP(-3675./T)
F1B=EFFL*SQRT(RK*FPB*82.06*T/P1/DHS)
F1S=F1B*(1.005)*(1.+22.05/T)
IF(F1S.LE.0.1) GO TO 8

```

```

      IF(F1S.GT.3.0) GO TO 1
      PL=P1/COSH(F1S)
      GO TO 3
1     PL=0.05*P1
C
C     CALL QINT TO INTEGRATE THE RATE FUNCTION.
C
3     PU=P1
      CALL QINT(PU,PL,PAR,RINT,P1,P2,P3,P5)
      Q=2.*RK/82.06*(1.-GAMA)/T*DHS*RINT
      F1=Q1/T*SQRT(Q)
      F2=T/Q2
      F3=EFFL*2.*F2+F1*(F2-2)
      F4=F3*F3+8.*F2*F1*F1
      Q3=2.*F1*Q1/T
      GLOBR=-F3/Q3+SQRT(F4)/Q3
      GO TO (4,5),IDACT
4     DACT=RK*FPB*(1.-GAMA)*(G1+G2*GLOBR/T/T)
      GO TO 6
5     DACT=0.0
6     RETURN
7     GLOBR=0.0
      DACT=0.0
      RETURN
8     GLOBR=RK*(1.-GAMA)*FPB
      GO TO (9,10),IDACT
9     DACT=GLOBR*G1
      RETURN
10    DACT=0.0
      RETURN
      END
C
C
      SUBROUTINE QINT(PU,PL,PAR,RINT,P1,P2,P3,P5)
      COMMON/PINT/P10,P20,P30,P50,PRESS,T0,YH2S,YSO2,YH2O,YS8
      DIMENSION Z(3),Y(3),PAR(9),X1(3),X2(3),X3(3),GP(3)
      COMMON/STIOS/ALFA,BETA
      PAR(9)=8.*P5+PAR(1)*(P5**(0.75))
      Z(1)=-SQRT(0.6)
      Z(2)=0.0
      Z(3)=-Z(1)
      DO 1 I=1,3
      X1(I)=((PU-PL)*Z(I)+PU+PL)/2.
      PAR(6)=X1(I)-P1
      X2(I)=P2+0.5*PAR(2)*(X1(I)-P1)
      X3(I)=P3-PAR(3)*(X1(I)-P1)
      S=PAR(9)-3./16.*PAR(4)*PAR(6)
      Y(I)=S/(8.0+6.0*BETA/ALFA)
C  HERE PAR(7) IS PV. CHECK IF INTERNAL VALUES OF (P6+P5)
C  EXCEEDS KELVIN VAPOR PRESSURE OF SULFUR.
C
      PORVP=0.4*PAR(7)
      P6POR=(Y(I)**.75)*PAR(1)/6.0
      TEST=P6POR+Y(I)

```

```

      IF (TEST.LT.PORVP) GO TO 1
      Y(I)=PORVP/(1.+BETA/ALFA)
1     CONTINUE
      DO 2 I=1,3
      IF(X2(I)) 15,16,16
15    GP(I)=0.0
      GO TO 2
16    GP(I)=X1(I)*SQRT(X2(I))-X3(I)*(Y(I)**(3./16.))/P
      GP(I)=GP(I)/(1.+4.56*X3(I))**2
2     CONTINUE
      RINT=5./9.*GP(1)+8./9.*GP(2)+5./9.*GP(3)
      RETURN
      END

```

C
C

```

      FUNCTION EQCTS(T,I)
      GO TO (1,2),I
1     EQCTS=EXP(-4030.2/T+4.825)
      EQCTS=EQCTS**0.75
      EQCTS=EQCTS*6.
      RETURN
2     EQCTS=EXP(12823./T-13.91)
      EQCTS=SQRT(EQCTS)
      RETURN
      END

```

C
C

```

      SUBROUTINE NEWTN(IND,X,FTOL,XTOL,NLIM,I,PAR)
C     THIS SUBROUTINE IS LISTED IN "CBSSTEADY".
C
C
C

```

```

      FUNCTION EQF(X,PAR)
      DIMENSION PAR(9)
      A=PAR(6)+0.5*PAR(2)*X
      B=PAR(9)-PAR(3)*X
      EQF=X*PAR(5)*SQRT(A)-B*(PAR(8)**3./16.)
      RETURN
      END

```

C
C

```

      FUNCTION DEQFN(X,PAR)
      DIMENSION PAR(9)
      A=PAR(6)+0.5*PAR(2)*X
      B=PAR(9)-PAR(3)*X
      DA=0.5*PAR(2)
      DB=-PAR(3)
      DEQFN=PAR(5)*SQRT(A)+0.5*X*PAR(5)*DA/SQRT(A)
      #-(PAR(8)**3./16.)*DB
      RETURN
      END

```

C
C

```

      FUNCTION VAPPR(T)

```

```

PVLN=-1.61732+0.542412E-02*T+143983.E-02/T-2208580.0
#/(T**2)
VAPPR=EXP(PVLN)
RETURN
END

```

C
C

```

FUNCTION VLEQ(X,PAR)
COMMON/STIOS/ALFA,BETA
DIMENSION PAR(9)
VLEQ=X+PAR(1)/6.0*(X**0.75)-PAR(7)
RETURN
END

```

C
C

```

FUNCTION VLEQD(X,PAR)
DIMENSION PAR(9)
VLEQD=1.0+.75/6.0*PAR(1)*(X**(-0.25))
RETURN
END

```

C
C

```

SUBROUTINE ADSUPT(ALFA,BETA,LM,Z,E1,E2,NADD,NSUB,EMAX
#,EMIN,Y1,Y2,Y3,P2,P3,P5,S,W,G,PAR,DZP)
DIMENSION Z(100),YT1(100),Y1(100),ZT(100),E1(100)
#,Y3(100),E2(100),Y2(100),YT2(100),
#YT3(100),G(100),GT(100),DZP(100),S(100),PAR(9),
#E3(100),TT(100),T(100),YY(2),W(100),ST(100),WT(100)
#,P2(100),P2T(100),P3(100),P3T(100),P5T(100),P5(100)
LMM=LM-1
LMMM=LMM-1
NADD=0
NSUB=0

```

C ADD PIONTS; IF APPLICABLE

```

14 DO 1 I=1,LMM
  IF(DZP(I).LT.0.0001) GO TO 1
  IF(ABS(E1(I)).LT.EMAX.AND.ABS(E2(I)).LT.EMAX) GO TO 1
200 NADD=NADD+1
  KKK=LM+NADD
  Z(KKK)=(Z(I+1)+Z(I))/2.0
  Y1(KKK)=(Y1(I+1)+Y1(I))/2.0
  Y2(KKK)=(Y2(I+1)+Y2(I))/2.0
  Y3(KKK)=(Y3(I)+Y3(I+1))/2.
  P2(KKK)=(P2(I+1)+P2(I))/2.
  P3(KKK)=(P3(I+1)+P3(I))/2.
  P5(KKK)=(P5(I+1)+P5(I))/2.

```

C

C IF PTS ARE ADDED, SOURCE TERMS SHOULD BE CALCULATED FOR THE NEW PTS.

C

```

  S(KKK)=(S(I+1)+S(I))/2.0
  W(KKK)=(W(I+1)+W(I))/2.0
  G(KKK)=(G(I+1)+G(I))/2.0
1 CONTINUE

```



```

13  K=1
    ZT(1)=Z(1)
    YT1(1)=Y1(1)
    YT2(1)=Y2(1)
    YT3(1)=Y3(1)
    P2T(1)=P2(1)
    P3T(1)=P3(1)
    P5T(1)=P5(1)
    ST(1)=S(1)
    WT(1)=W(1)
    GT(1)=G(1)
    DO 2 I=1,LMMM,2
    T1=ABS(E1(I))+ABS(E1(I+1))
    T2=ABS(E2(I))+ABS(E2(I+1))
    IF(T1.LT.EMIN.AND.T2.LT.EMIN) GO TO 5
    ZT(K+1)=Z(I+1)
    YT1(K+1)=Y1(I+1)
    YT2(K+1)=Y2(I+1)
    YT3(K+1)=Y3(I+1)
    P2T(K+1)=P2(I+1)
    P3T(K+1)=P3(I+1)
    P5T(K+1)=P5(I+1)
    ST(K+1)=S(I+1)
    WT(K+1)=W(I+1)
    GT(K+1)=G(I+1)
    ZT(K+2)=Z(I+2)
    YT1(K+2)=Y1(I+2)
    YT2(K+2)=Y2(I+2)
    YT3(K+2)=Y3(I+2)
    P2T(K+2)=P2(I+2)
    P3T(K+2)=P3(I+2)
    P5T(K+2)=P5(I+2)
    ST(K+2)=S(I+2)
    WT(K+2)=W(I+2)
    GT(K+2)=G(I+2)
    K=K+2
    GO TO 2
5   NSUB=NSUB+1
    ZT(K+1)=Z(I+2)
    YT1(K+1)=Y1(I+2)
    YT2(K+1)=Y2(I+2)
    YT3(K+1)=Y3(I+2)
    P2T(K+1)=P2(I+2)
    P3T(K+1)=P3(I+2)
    P5T(K+1)=P5(I+2)
    WT(K+1)=W(I+2)
    ST(K+1)=S(I+2)
    GT(K+1)=G(I+2)
    K=K+1
2   CONTINUE
    IF(NADD.EQ.0.AND.NSUB.EQ.0) GO TO 7
    N=LM-NSUB
    ZT(N)=Z(LM)
    YT1(N)=Y1(LM)

```

```

      YT2(N)=Y2(LM)
      YT3(N)=Y3(LM)
      P2T(N)=P2(LM)
      P3T(N)=P3(LM)
      P5T(N)=P5(LM)
      ST(N)=S(LM)
      WT(N)=W(LM)
      GT(N)=G(LM)
      IF(NADD.EQ.0) GO TO 6
8     DO 3 I=1,NADD
      YT1(N+I)=Y1(LM+I)
      YT2(N+I)=Y2(LM+I)
      YT3(N+I)=Y2(LM+I)
      P2T(N+I)=P2(LM+I)
      P3T(N+I)=P2(LM+I)
      P5T(N+I)=P5(LM+I)
      ST(N+I)=S(LM+I)
      WT(N+I)=W(LM+I)
      GT(N+I)=G(LM+I)
3     ZT(N+I)=Z(LM+I)
6     LM=N+NADD
      CALL DSORD(ZT,LM,YT1,YT2,YT3,P2T,P3T,P5T,ST,WT,GT)
      DO 4 I=1,LM
      Y1(I)=YT1(I)
      Y2(I)=YT2(I)
      Y3(I)=YT3(I)
      P2(I)=P2T(I)
      P3(I)=P3T(I)
      P5(I)=P5T(I)
      S(I)=ST(I)
      W(I)=WT(I)
      G(I)=GT(I)
4     Z(I)=ZT(I)
7     RETURN
      END

```

C
C

```

      SUBROUTINE DSORD(A,N,B,C,D,E,F,G,H,O,P)
      DIMENSION A(100),F(100),G(100),E(100),D(100),C(100)
      #,B(100),H(100),O(100),P(100)
      NA=N-1
      DO 3 J=1,NA
      M=J
      MA=J+1
      DO 2 I=MA,N
2     IF(A(I).LT.A(M)) M=I
      TEMP=A(J)
      TEMP1=B(J)
      TEMP2=C(J)
      TEMP3=D(J)
      TEMP4=E(J)
      TEMP5=F(J)
      TEMP6=G(J)
      TEMP7=H(J)

```

```

TEMP8=O(J)
TEMP9=P(J)
B(J)=B(M)
B(M)=TEMP1
C(J)=C(M)
C(M)=TEMP2
D(J)=D(M)
D(M)=TEMP3
F(J)=F(M)
F(M)=TEMP5
G(J)=G(M)
G(M)=TEMP6
H(J)=H(M)
H(M)=TEMP7
O(J)=O(M)
O(M)=TEMP8
P(J)=P(M)
P(M)=TEMP9
E(J)=E(M)
E(M)=TEMP4
A(J)=A(M)
A(M)=TEMP
RETURN
END.

```

3

C

C

```

FUNCTION HEATR(A1,A2,T)
DH298=-35008.8+A2*24360+A1*24320
DCP=-4.818121+A2*31.58+A1*42.67
HEATR=DH298+DCP*(T-298)
HEATR=-HEATR

```

C

C

C

C

```

THIS IS HEAT FOR 2 MOLES OF REACTED H2S. TO GET
HEAT PER MOLE OF H2S DIVIDE BY 2.

```

```

HEATR=HEATR/2.
RETURN
END

```

C

C

```

SUBROUTINE PARAM
DIMENSION PAR(9),A(3)
COMMON/PINT/P10,P20,P30,P50,PRESS,T0,YH2S,YSO2,YH2O,YS8
COMMON/QPAR/Q1,Q2,V1,V2,V3,W1,W2,W3,G1,G2,RK0,EFFL,DHS
#,RO0,ROP,ROB,DAX,AXLN,DP,CPCAT,AMW,EB,DSO,DHO,DS8,UO
#,BL,CP,HTC,HEAT
COMMON/STIOS/ALFA,BETA
COMMON/PARA/PAR
KFLAG=1
PAR(2)=DHS/DSO
PAR(3)=DHS/DHO
PAR(4)=DHS/DS8
P10=YH2S*PRESS
P20=YSO2*PRESS

```

```

P30=YH20*PRESS
P50=YS8*PRESS
EFFL=DP/6.
RO0=AMW*PRESS/82.06/T0
CTA=RO0/AMW
CPA=EB*CP*CTA+ROB*CPCAT
RK0=5.364*ROP
FMASS=RO0*U0
NLIM=20
FTOL=0.1E-09
XTOL=0.1E-09
IND=1
T1=T0
DO 1 I=1,3
PAR(1)=EQCTS(T1,1)
PV=VAPPR(T1)
PAR(7)=PV
S8=PV*7.0/8.0
CALL NEWTN(IND,S8,FTOL,XTOL,NLIM,KFLAG,PAR)
S6=PV-S8
A(I)=S8/S6
T1=T1+10.0
CONTINUE
AVE=A(1)+A(2)+A(3)
AVE=AVE/3.0
BETA=3.0/(8.0*AVE+6.0)
ALFA=AVE*BETA
V1=CTA*U0*CP/CPA/BL
HEAT=HEATR(ALFA,BETA,T0)
Q1=EFFL*HEAT/HTC
Q2=0.6*7350/1.986
V2=ROB*HEAT/ROP/CPA
W1=U0/EB/BL
W2=-ROB*82.06*T0/EB/ROP
W3=DAX/BL/BL
V3=AXLN/BL/BL/CPA
C COEFFICIENTS IN THE DEACTIVATION FUNCTION
G1=(4*ALFA+3.*BETA)*32.16/0.3/ROP
G2=1.2*7350.*Q1*G1/1.986
RETURN
END
C
C
SUBROUTINE SPTS(LM,Z,DZM,DZP,C,CPM,HM,HP)
DIMENSION Z(100),DZM(100),DZP(100),C(100,3),CPM(100,3)
#,HM(100,3),HP(100,3)
COMMON/PINT/P10,P20,P30,P50,PRESS,T0,YH2S,YSO2,YH2O,YS8
COMMON/QPAR/Q1,Q2,V1,V2,V3,W1,W2,W3,G1,G2,RK0,EFFL,DHS
#,RO0,ROP,ROB,DAX,AXLN,DP,CPCAT,AMW,EB,DSO,DHO,DS8,U0
#,BL,CP,HTC,HEAT
LMM=LM-1
1000 DO 19 L=2,LMM
DZM(L)=Z(L)-Z(L-1)
DZP(L)=Z(L+1)-Z(L)

```

```

DZDIFF=DZM(L)-DZP(L)
DZSUM=DZM(L)+DZP(L)
C(L,1)=(0.5*V1*DZSUM+2.*V3)/DZSUM/DZM(L)
CPM(L,1)=(0.5*W1*DZSUM+2.*W3)/DZSUM/DZM(L)
C(L,2)=(0.5*V1*DZDIFF-2.*V3)/DZM(L)/DZP(L)
CPM(L,2)=(0.5*W1*DZDIFF-2.*W3)/DZM(L)/DZP(L)
C(L,3)=-(C(L,1)+C(L,2))
CPM(L,3)=-(CPM(L,1)+CPM(L,2))
REALN=2.0*DZP(L)+DZM(L)
HM(L,1)=REALN/4./DZSUM
HM(L,2)=REALN/4./DZP(L)
HM(L,3)=1.-HM(L,1)-HM(L,2)
HP(L,1)=-(DZP(L)**2)/4./DZM(L)/DZSUM
HP(L,2)=DZP(L)*(2.*DZM(L)+DZP(L))/4./DZM(L)/DZP(L)
HP(L,3)=1-HP(L,1)-HP(L,2)

```

19 CONTINUE

```

DZM(LM)=Z(LM)-Z(LM-1)
DZP(LM)=Z(LM)-Z(LM-1)
C(LM,1)=0.5*V1/DZM(LM)+2.*V3/(DZM(LM)**2)
CPM(LM,1)=2.*W3/(DZM(LM)**2)+W1/2./DZM(LM)
C(LM,2)=-C(LM,1)
CPM(LM,2)=-CPM(LM,1)
C(LM,3)=0.0
CPM(LM,3)=0.0
C(1,1)=0.0
CPM(1,1)=0.0
F1=1./DZP(1)
F2=F1*F1
C(1,2)=-V1*F1-2.*V3*F2
C(1,3)=-V1*F1+2.*V3*F2
CPM(1,2)=-W1*F1-2.*W3*F2
CPM(1,3)=-W1*F1+2.*W3*F2
RETURN
END

```

C
C

```

SUBROUTINE ARPRO(LM,Z,P1,P2,P3,P5,T,GA,S,W,G,TIME,DTIME
# ,MAXI,INDT,JCONV,ICASE)
  DIMENSION P1(100),P2(100),P3(100),P5(100),GA(100)
# ,TC(100),G(100),S(100),SPR(100),
# WPR(100),GPR(100),P1PR(100),P2PR(100),P3PR(100),
# TPR(100),GAPR(100),P1C(100),P2C(100),P3C(100),P5C(100)
# ,DZM(100),DZP(100),C(100,3),CPM(100,3),HM(100,3)
# ,HP(100,3),YHP(100),YHM(100),YHPP1(100),YHMP1(100)
# ,DT(100),DP1(100),DP2(100),DP3(100),DP5(100),DGA(100)
# ,T(100),Z(100),W(100),P5PR(100),GAC(100),B(100,3)
# ,PAR(9),ERRY(100),ERRP(100)
  COMMON/PINT/P10,P20,P30,P50,PRESS,T0,YH2S,YSO2,YH2O,YS8
  COMMON/QPAR/Q1,Q2,V1,V2,V3,W1,W2,W3,G1,G2,RK0,EFFL,DHS
# ,RO0,ROP,ROB,DAX,AXLN,DP,CPCAT,AMW,EB,DSO,DHO,DS8,U0
# ,BL,CP,HTC,HEAT
  COMMON/STIOS/ALFA,BETA
  COMMON/PARA/PAR
  COMMON/ERRPAR/EMAX,EMIN

```

```

      ISTEP=1
1000 CALL SPTS(LM,Z,DZM,DZP,C,CPM,HM,HP)
      LMM=LM-1
      P1(LM+1)=0.0
      P2(LM+1)=0.0
      P3(LM+1)=0.0
      T(LM+1)=0.0
      P5(LM+1)=0.0
500 DO 102 ITER=1,2
      DO 90 L=1,LM
      DT(L)=S(L)
      DP1(L)=W(L)
      DGA(L)=G(L)
      IF(L.EQ.1) GO TO 60
      DO 31 KK=1,3
      KKK=L-2+KK
      DT(L)=DT(L)+C(L,KK)*T(KKK)
      DP1(L)=DP1(L)+CPM(L,KK)*P1(KKK)
31 CONTINUE
      DP2(L)=0.5*DP1(L)
      DP3(L)=-DP1(L)
      DP5(L)=-1.5/(8.0+6.0*BETA/ALFA)*DP1(L)
      DO 32 KK=1,3
      KKK=L+KK-2
      DP2(L)=DP2(L)+CPM(L,KK)*(P2(KKK)-0.5*P1(KKK))
      DP3(L)=DP3(L)+CPM(L,KK)*(P3(KKK)+P1(KKK))
      DP5(L)=DP5(L)+CPM(L,KK)*(P5(KKK)+1.5/(8.0+6.0*BETA/ALFA)
      #*P1(KKK))
32 CONTINUE
      GO TO 61
C
C COMPUTE FOR THE INLET
C
60 DET=-T0*(C(1,2)+C(1,3))
      DEP1=-P10*(CPM(1,2)+CPM(1,3))
      DEP2=DEP1*P20/P10
      DEP3=DEP1*P30/P10
      DEP5=DEP1*P50/P10
      DT(1)=DT(1)+DET+C(1,2)*T(1)+C(1,3)*T(2)
      DP1(1)=DP1(1)+DEP1+CPM(1,2)*P1(1)+CPM(1,3)*P1(2)
      DP2(1)=DEP2+0.5*W(1)+CPM(1,2)*P2(1)+CPM(1,3)*P2(2)
      DP3(1)=DEP3-W(1)+CPM(1,2)*P3(1)+CPM(1,3)*P3(2)
      DP5(1)=-1.5/(8.0+6.0*BETA/ALFA)*W(1)
      DP5(1)=DP5(1)+(CPM(1,2)*P5(1)+CPM(1,3)*P5(2))
      DP5(1)=DP5(1)+DEP5
61 TPR(L)=T(L)+DTIME*DT(L)
      P1PR(L)=P1(L)+DTIME*DP1(L)
      P2PR(L)=P2(L)+DTIME*DP2(L)
      P3PR(L)=P3(L)+DTIME*DP3(L)
      P5PR(L)=P5(L)+DTIME*DP5(L)
      GAPR(L)=GA(L)+DTIME*DGA(L)
90 CONTINUE
C
C CHECK FOR SAGE EFFECT.

```

```

C
DO 41 L=2,LMM,2
CALL SAGE(Z(L-1),Z(L),Z(L+1),TPR(L-1),TPR(L),TPR(L+1))
CALL SAGE(Z(L-1),Z(L),Z(L+1),P1PR(L-1),P1PR(L),
#P1PR(L+1))
CALL SAGE(Z(L-1),Z(L),Z(L+1),P2PR(L-1),P2PR(L),
#P2PR(L+1))
CALL SAGE(Z(L-1),Z(L),Z(L+1),P3PR(L-1),P3PR(L),
#P3PR(L+1))
CALL SAGE(Z(L-1),Z(L),Z(L+1),P5PR(L-1),P5PR(L),
#P5PR(L+1))
CALL SAGE(Z(L-1),Z(L),Z(L+1),GAPR(L-1),GAPR(L),
#GAPR(L+1))
41 CONTINUE
C
C NOW CORRECT. REPEAT CORRECTION UP TO 8 TIMES.
C
DO 96 J=1,10
C
C COMPUTE THE SOURCE TERMS FOR THE PREDICTED VALUES
C
JCONV=J
DO 23 I=1,LM
214 CALL SOURCE(IDACT,ICASE,PAR,TPR(I),GAPR(I),PV,SPR(I),
#WPR(I),GPR(I),P1PR(I),P2PR(I),P3PR(I),P5PR(I))
23 CONTINUE
P1PR(LM+1)=0.0
P2PR(LM+1)=0.0
P3PR(LM+1)=0.0
TPR(LM+1)=0.0
P5PR(LM+1)=0.0
C
C CORRECT THE SOLUTION
C
DO 91 L=1,LM
DTCR=SPR(L)
DP1C=WPR(L)
DGAC=GPR(L)
IF(L.EQ.1) GO TO 62
DO 33 KK=1,3
KKK=L+KK-2
DTCR=DTCR+C(L,KK)*TPR(KKK)
DP1C=DP1C+CPM(L,KK)*P1PR(KKK)
33 CONTINUE
DP2C=0.5*DP1C
DP3C=-DP1C
DP5C=-1.5/(8.0+6.0*BETA/ALFA)*DP1C
DO 34 KK=1,3
KKK=L+KK-2
DP2C=DP2C+CPM(L,KK)*(P2PR(KKK)-0.5*P1PR(KKK))
DP3C=DP3C+CPM(L,KK)*(P3PR(KKK)+P1PR(KKK))
DP5C=DP5C+CPM(L,KK)*(P5PR(KKK)+
#1.5/(8.0+6.0*BETA/ALFA)*P1PR(KKK))
34 CONTINUE

```

```

GO TO 63
62  DTCR=DTCR+DET+C(1,2)*TPR(1)+C(1,3)*TPR(2)
    DP1C=DP1C+DEP1+CPM(1,2)*P1PR(1)+CPM(1,3)*P1PR(2)
    DP2C=DEP2+CPM(1,2)*P2PR(1)+CPM(1,3)*P2PR(2)+0.5*WPR(1)
    DP3C=DEP3+CPM(1,2)*P3PR(1)+CPM(1,3)*P3PR(2)-WPR(1)
    DP5C=DEP5+(CPM(1,2)*P5PR(1)+CPM(1,3)*P5PR(2))-1.5
    #/(8.0+6.0*BETA/ALFA)*WPR(1)
63  TC(L)=T(L)+DTIME*(DT(L)+DTCR)/2.
    P1C(L)=P1(L)+DTIME*(DP1(L)+DP1C)/2.
    P2C(L)=P2(L)+DTIME*(DP2(L)+DP2C)/2.
    P3C(L)=P3(L)+DTIME*(DP3(L)+DP3C)/2.
    P5C(L)=P5(L)+DTIME*(DP5(L)+DP5C)/2.
    GAC(L)=GA(L)+DTIME*(DGA(L)+DGAC)/2.
91  CONTINUE
C
C  CHECK FOR SAGE EFFECT
C
    DO 42 L=2,LMM,2
    CALL SAGE(Z(L-1),Z(L),Z(L+1),TC(L-1),TC(L),TC(L+1))
    CALL SAGE(Z(L-1),Z(L),Z(L+1),P1C(L-1),P1C(L),P1C(L+1))
    CALL SAGE(Z(L-1),Z(L),Z(L+1),P2C(L-1),P2C(L),P2C(L+1))
    CALL SAGE(Z(L-1),Z(L),Z(L+1),P3C(L-1),P3C(L),P3C(L+1))
    CALL SAGE(Z(L-1),Z(L),Z(L+1),P5C(L-1),P5C(L),P5C(L+1))
    CALL SAGE(Z(L-1),Z(L),Z(L+1),GAC(L-1),GAC(L),GAC(L+1))
42  CONTINUE
C  TEST FOR CONVERGENCE
C
    ITEST=0
    DO 94 JJ=1,LM
    IF(P1C(JJ)) 94,94,101
101  TEST=ABS(P1PR(JJ)-P1C(JJ))/P1C(JJ)
    IF(TEST.GT.0.1) ITEST=ITEST+1
94  CONTINUE
    IF(ITEST.LE.0) GO TO 98
    DO 95 JJ=1,LM
    TPR(JJ)=TC(JJ)
    P1PR(JJ)=P1C(JJ)
    P2PR(JJ)=P2C(JJ)
    P3PR(JJ)=P3C(JJ)
    P5PR(JJ)=P5C(JJ)
    GAPR(JJ)=GAC(JJ)
95  CONTINUE
96  CONTINUE
98  TIME=TIME+DTIME
    DO 92 L=1,LM
    T(L)=TPR(L)
    P1(L)=P1PR(L)
    P2(L)=P2PR(L)
    P3(L)=P3PR(L)
    P5(L)=P5PR(L)
    GA(L)=GAPR(L)
    S(L)=SPR(L)
    W(L)=WPR(L)
    G(L)=GPR(L)

```



```

92  CONTINUE
25  CONTINUE
102 CONTINUE
4000 DO 37 L=2,LMM
    YHM(L)=HM(L,1)*T(L-1)+HM(L,2)*T(L)+HM(L,3)*T(L+1)
    YHP(L)=HP(L,1)*T(L-1)+HP(L,2)*T(L)+HP(L,3)*T(L+1)
    YHMP1(L)=HM(L,1)*P1(L-1)+HM(L,2)*P1(L)+HM(L,3)*P1(L+1)
    YHPP1(L)=HP(L,1)*P1(L-1)+HP(L,2)*P1(L)+HP(L,3)*P1(L+1)
37  CONTINUE
    FACT=0.25*V1/V3*DZP(1)
    YHP(1)=-FACT*T0+(0.75+FACT)*T(1)+0.25*T(2)
    FACT=0.25*W1/W3*DZP(1)
    YHPP1(1)=-FACT*P10+(0.75+FACT)*P1(1)+0.25*P1(2)
    YHM(LM)=3./4.*T(LM)+1./4.*T(LM-1)
    YHMP1(LM)=3./4.*P1(LM)+1./4.*P1(LM-1)
    DO 38 I=1,LMM
        ERRY(I)=YHM(I+1)-YHP(I)
        ERRP(I)=YHMP1(I+1)-YHPP1(I)
38  CONTINUE
    CALL ADSUPT(ALFA,BETA,LM,Z,ERRY,ERRP,NADD,NSUB,EMAX
    #,EMIN,T,P1,GA,P2,P3,P5,S,W,G,PAR,DZP)
    ISTEP=ISTEP+1
    IF(ISTEP.GT.MAXI) GO TO 400
    IF(NADD.EQ.0.AND.NSUB.EQ.0) GO TO 500
    GO TO 1000
400  RETURN
    END

```

.....

CBPSSTEADY

A COMPUTER PROGRAM TO PERFORM SIMULATION OF
PSEUDOSTEADY STATE COLDBED REACTOR.

INPUTS ARE :

PI0 = PARTIAL PRESSURE OF H2S, SO2, H2O, INERTS
T0 = FEED TEMPERATURE
PRESS = TOTAL PRESSURE
U = SUPERFICIAL VELOCITY
TIMEMX = MAX INTEGRATION TIME IN HR
DT = TIME INTERVAL IN HR
DI = EFFECTIVE DIFFUSIVITIES
ROB = BED DENSITY
ROP = PELLET DENSITY
DP = PELLET DIAMETER
BL = BED DEPTH
CPG = GAS HEAT CAPACITY PER MOLE
N = NUMBER OF AXIAL POINTS
IOPT : 1 = NO AXIAL DISPERSION IN HEAT BALANCE
 2 = HEAT BALANCE WITH AXIAL DISPERSION
ICHOIC : 1 = FLOW DOWNWARD; BED AFTER REGENERATION
 2 = FLOW UPWARD; AFTER THE BED HAS PARTLY DEACT.
 BY DOWNWARD FLOW. READ THE INITIAL TEMP. AND
 DEACTIVATION PROFILES FROM UNIT 98
NPRINT = PRINTING STEPS

" ALL THE UNITS ARE IN GR, CM, SEC, K, ATM, AND CALORI "

.....

COMMON/PRINT/P10,P20,P30,PRESS
DIMENSION PAR(20),GR(200),ICASE(200),P1(200),Z(200)
#,GA(200),T(200),TO(200)
READ(5,1) P10,P20,P30,P40,P50
READ(5,1) T0,PRESS,U

TIME IS IN HR

READ(5,1) TIMEMX,DT
READ(5,1) DMS,DSO,DHO,DS8
READ(5,1) ROB,ROP,DP,BL,CPG
READ(5,2) N,IOPT,ICHOIC,NPRINT

CT=PRESS/82.06/T0
CPA=0.2

QP IS THE SULFUR CAPACITY OF THE CATALYST.

QP=0.3

CALCULATE ALFA & BETA
TMEXP=T0+12000.*P10/CPG/PRESS



```

TAVE=(T0+TMEXP)/2.
PAR(1)=EQCTS(TAVE,1)
PV=VAPPR(TAVE)
PAR(7)=PV
S8=PV*7.0/8.0
KFLAG=1
XTOL=0.1E-09
FTOL=0.1E-09
NLIM=20
IND=1
CALL NEWTN(IND,S8,FTOL,XTOL,NLIM,KFLAG,PAR)
S6=PV-S8
A=S8/S6
BETA=3.0/(8.0*A+6.0)
ALFA=A*BETA
P50=PV/(1.0+BETA/ALFA)

```

C
C CALCULATE THE HEAT OF REACTION
C

```

HEAT=HEATR(ALFA,BETA,TAVE)
PAR(2)=DHS/DSO
PAR(3)=DHS/DHO
PAR(4)=DHS/DS8
PAR(5)=EQCTS(T0,2)
EFFL=DP/6.0
PAR(6)=SQRT(2.0*DHS/82.06)/EFFL
PAR(8)=1.5/(8.0+6.0*BETA/ALFA)
PAR(9)=(PV/(1.+BETA/ALFA))**(3./16.)
PAR(10)=P20-P10/2.0
PAR(11)=P10+P30
PAR(12)=0.9354*EFFL*SQRT(82.06/DHS)
PAR(13)=-(ROB/ROP)*(BL/U)*82.06*T0
PAR(14)=PAR(8)*P10+P50
PAR(15)=1.0+BETA/ALFA
PAR(16)=(4.*ALFA+3.*BETA)*32.0/ROP/QP

```

C
C PAR(16) IS IN 1/SEC, MULTIPLY BY 3600 TO GET 1/HR
C

```

PAR(16)=PAR(16)*3600.0
PAR(17)=HEAT*ROB*BL/ROP/CT/U/CPG
PAR(18)=5.364*ROP
PAR(19)=CT*U*CPG/CPA/BL
PAR(20)=HEAT*ROB/ROP/CPA
PAR(1)=EQCTS(T0,1)
PAR(7)=VAPPR(T0)
AXL=0.003
V3=AXL/CPA/BL/BL

```

C CALCULATE EQUILIBRIUM PRESSURE OF H2S
IND=2

```

CONV=0.97
CALL NEWTN(IND,CONV,FTOL,XTOL,NLIM,KFLAG,PAR)
TM=(1.0-P10*CONV/2.0)/(1.0-PV/PRESS)
P1E=P10*(1.-CONV)*PRESS/TM

```

C

C START INTEG. ASSUMING PSEUDOSTEADY STATE FOR PRESSURE.

C
 TIME=0.0
 DZ=1.0/FLOAT(N-1)
 P1(1)=P10
 T(1)=T0
 WRITE(6,7) CONV,P1E,DZ
 DO 10 I=1,N
 Z(I)=(I-1)*DZ
 ICASE(I)=0
 GO TO (1101,10) , ICHOIC
 1101 T(I)=T0
 TO(I)=T0
 10 GA(I)=0.0
 WRITE(6,4) (Z(I),I=1,N)
 GO TO (1118,1119) , ICHOIC

C
 C READ THE INITIAL TEMPERATURE AND DEACTIVATION PROFILE
 C

1119 READ(98,99) (TO(I),I=1,201)
 READ(98,99) (GA(I),I=1,201)
 DO 96 I=2,N
 96 T(I)=TO(I)
 99 FORMAT(10F10.4)
 1118 DO 11 I=2,N
 IEND=I
 CALL SOURCE(PAR,P1(I-1),TO(I-1),ICASE(I-1),GA(I-1)
 #,GR(I-1),P1E)
 P1(I)=P1(I-1)+DZ*PAR(13)*GR(I-1)
 CHECK=P1(I-1)-P1(I)
 GO TO (128,11) , ICHOIC
 128 IF(CHECK.LE.0.1E-06.AND.GA(IEND).LT.0.001) GO TO 12
 11 CONTINUE
 12 K=IEND+1
 CALL SOURCE(PAR,P1(IEND),TO(IEND),ICASE(IEND),GA(IEND)
 #,GR(IEND),P1E)
 DO 13 I=K,N
 GR(I)=GR(I-1)
 13 P1(I)=P1(I-1)
 WRITE(6,3) TIME,IEND
 WRITE(6,5) (P(I),I=1,IEND)
 WRITE(6,8) (T(I),I=1,IEND)
 WRITE(6,6) (GA(I),I=1,IEND)
 WRITE(6,9) (GR(I),I=1,IEND)
 100 DO 21 KP=1,NPRINT
 IF(IEND.GT.N) IEND=N
 17 DO 15 I=1,IEND
 IF(I.EQ.N) GO TO 20
 27 AVEG=0.25*GR(I+1)*(7350./1.986/TO(I+1)-1.0).
 DENOM=1.0-AVEG*PAR(20)*DT*3600.0/TO(I+1)
 GO TO (18,19) , IOPT
 18 IF(I.EQ.(N-1)) GO TO 29
 T(I+1)=-PAR(19)*DT*3600./2.0/DZ*(TO(I+2)-TO(I))+
 #PAR(20)*DT*3600.*(GR(I+1)-AVEG)+TO(I+1)

```

      T(I+1)=T(I+1)/DENOM
      GO TO 20
29  T(I+1)=-PAR(19)*DT*3600./2.0/DZ*(TO(I-1)-4.*TO(I)+3.
    #*TO(I+1))+PAR(20)*DT*3600.0*(GR(I+1)-AVEG)+TO(I+1)
      T(I+1)=T(I+1)/DENOM
      GO TO 20
19  IF(I.EQ.(N-2)) GO TO 30
      IF(I.GT.1) GO TO 31
      AVEG1=0.25*GR(1)*(7350./1.986/TO(1)-1.0)
      DENOM1=1.0-AVEG*PAR(20)*DT*3600.0/TO(1)
      T(1)=-PAR(19)/V3*PAR(19)*DT*3600.0*(TO(1)-T0)
    #+V3/2./DZ*DT*3600.0*(4.*TO(2)-TO(3)-3.0*TO(1))
    #+PAR(20)*DT*3600.0*(GR(1)-AVEG1)+TO(1)
      T(1)=T(1)/DENOM1
31  T(I+1)=-PAR(19)*DT*3600./2.0/DZ*(TO(I+2)-TO(I))+
    #PAR(20)*DT*3600.0*(GR(I+1)-AVEG)+TO(I+1)
    #+V3*DT*3600.0*(TO(I)-2.0*TO(I+1)+TO(I+2))/DZ/DZ
      T(I+1)=T(I+1)/DENOM
      GO TO 20
30  T(I+1)=PAR(20)*DT*3600.0*(GR(I+1)-AVEG)+TO(I+1)
    #+V3*DT*3600.0/2./DZ*(TO(I-1)-4.0*TO(I)+3.0*TO(I+1))
      T(I+1)=T(I+1)/DENOM
20  PAR(7)=VAPPR(T(I))
      PAR(5)=EQCTS(T(I),2)
      PAR(9)=(PAR(7)/(1.+BETA/ALFA))**(3./16.)
      IF(ICASE(I).EQ.0) GO TO 15
14  FP=FPB(P1(I),PAR)
      RK=PAR(18)*EXP(-7350./1.986/T(I))
      DGA=PAR(16)*RK*((1.-GA(I))**2)*FP
      IF(DGA.LT.0.0) DGA=0.0
      GA(I)=GA(I)+DT*DGA
15  CONTINUE
      K=IEND+1
      IF(ABS(T(K)-T0).GT.0.0001) IEND=K
      K=K+2
      IF(K.GT.N) K=N
      DO 22 I=2,K
      IF(GA(I-1).GE.0.9995) GO TO 22
26  CALL SOURCE(PAR,P1(I-1),T(I-1),ICASE(I-1),GA(I-1)
    #,GR(I-1),P1E)
      P1(I)=P1(I-1)+DZ*PAR(13)*GR(I-1)
22  CONTINUE
      TIME=TIME+DT
      DO 121 JJ=1,K
      TO(JJ)=T(JJ)
121 CONTINUE
21  CONTINUE
      WRITE(6,3) TIME,IEND
      WRITE(6,5) (P1(I),I=1,K)
      WRITE(6,8) (T(I),I=1,K)
      WRITE(6,6) (GA(I),I=1,K)
      IF(TIME.LT.0.99) GO TO 100

```

C

C AFTER THE FIRST HR , TEMP & PRESSURE ROFILES BEHAVE

C IN PSEUDOSTEADY STATE.

C

```

1117 DT=1.0
909 FORMAT(8F9.4)
522 FORMAT(8F9.5)
116 DO 111 I=1,N
    IF(I.EQ.1) GO TO 117
    IEND=I
    CALL SOURCE(PAR,P1(I-1),T(I-1),ICASE(I-1),GA(I-1)
    #,GR(I-1),P1E)
    P1(I)=P1(I-1)+DZ*PAR(13)*GR(I-1)
    T(I)=T(I-1)+DZ*PAR(17)*GR(I-1)
117 PAR(7)=VAPPR(T(I))
    PAR(5)=EQCTS(T(I),2)
    PAR(9)=(PAR(7)/(1.+BETA/ALFA))**(3./16.)
114 FP=FPB(P1(I),PAR)
    RK=PAR(18)*EXP(-7350./1.986/T(I))
    DGA=PAR(16)*RK*((1.-GA(I))**2)*FP
    IF (DGA.LT.0.0) DGA=0.0
    GA(I)=GA(I)+DT*DGA
115 CONTINUE
    IF(I.EQ.1) GO TO 111
    CHECK=P1(I-1)-P1(I)
    IF(CHECK.LE.0.1E-06.AND.GA(IEND).LT.0.1) GO TO 112
111 CONTINUE
112 K=IEND+1
    CALL SOURCE(PAR,P1(IEND),T(IEND),ICASE(IEND),GA(IEND),
    #GR(IEND),P1E)
    DO 113 I=K,N
        GR(I)=GR(I-1)
        T(I)=T(I-1)
113 P1(I)=P1(I-1)
    TIME=TIME+DT
    WRITE(6,3) TIME,IEND
    WRITE(6,5) (P1(I),I=1,IEND)
    WRITE(6,8) (T(I),I=1,IEND)
    WRITE(6,6) (GA(I),I=1,IEND)
    IF(TIME.LT.TIMEMX) GO TO 116
    STOP
1  FORMAT(5F10.5)
2  FORMAT(4I5)
3  FORMAT(/,'TIME (HR) =',F9.5,5X,'IEND=',I5)
4  FORMAT(/,' Z ',8F9.5)
5  FORMAT(' P1 ',8F9.5)
6  FORMAT(' GA ',8F9.5)
7  FORMAT('EQ.CONV.=',F9.5,3X,'P1E=',E10.5,2X,'DZ=',F9.5)
8  FORMAT(' T ',8F11.5)
9  FORMAT(' GR ',8E11.5)
51 FORMAT(I5,F10.5)
    END

```

C

C

SUBROUTINE NEWTN(IND,X,FTOL,XTOL,NLIM,I,PAR)
 C SUBROUTINE FOR ROOT FINDING BY NEWTON'S METHOD

```

C  PARAMETERS ARE C  FCN  FUNCTION THAT COMPUTES F(X)
C  FDER  FUNCTION THAT COMPUTES THE DERIVATIVE OF F
C  BOTH FUNCTION MUST BE DECLARED EXTERNAL
C  I      A SIGNAL FOR HOW ROUTINE TERMINATED.
C      I=1  MEETS TOLERANCE FOR X
C      I=2  MEETS TOLERANCE FOR F(X)
C      I=-1  NLIM EXCEEDED
C
C  WHEN THE SUBROUTINE IS CALLED THE VALUE OF I INDICATES
C  WHETHER TO PRINT EACH VALUE OR NOT. I=0 MEANS PRINT,
C  NE.0 MEANS DON'T.
C

```

```

C      DIMENSION PAR(20)
C      GO TO (1,2), IND
1     FX=VLEQ(X,PAR)
C     FDER=VLEQD(X,PAR)
C     GO TO 3
2     FX=EQF(X,PAR)
C     FDER=DEQFN(X,PAR)
3     DO 20 J=1,NLIM
C     DELX=FX/FDER
C     X=X-DELX
C     GO TO (6,7), IND
6     FX=VLEQ(X,PAR)
C     FDER=VLEQD(X,PAR)
C     GO TO 5
7     FX=EQF(X,PAR)
C     FDER=DEQFN(X,PAR)
5     IF(ABS(DELX).LE.XTOL) GO TO 60
C     IF(ABS(FX).LE.FTOL) GO TO 70
20    CONTINUE
C  WHEN LOOP NORMALLY COMPLETED, NLIM IS EXCEEDED.
C     I=-1
C     RETURN
60    I=1
C     RETURN
70    I=2
C     RETURN
C     END
C
C

```

```

C  FUNCTION VLEQ(X,PAR)
C  COMMON/STIOS/ALFA,BETA
C  DIMENSION PAR(20)
C  VLEQ=X+PAR(1)/6.0*(X**0.75)-PAR(7)
C  RETURN
C  END
C
C

```

```

C  FUNCTION VLEQD(X,PAR)
C  DIMENSION PAR(20)
C  VLEQD=1.0+.75/6.0*PAR(1)*(X**(-0.25))
C  RETURN
C  END

```

```

C
C
SUBROUTINE SOURCE(PAR,P1,T,ICASE,GA,R,P1E)
  DIMENSION PAR(20)
C THIS SUBROUTINE SETS UP THE COND. NECESSARY FOR EVAL.
C OF THE GLOBAL RATE.
C FIG IS THE GENERALIZED THIELE MODULUS FOR CLAUS REACTION;
C ASSUMING RATE AS 1.5 ORDER W.R.T. H2S.
C

```

```

  PAR(5)=EQCTS(T,2)
  PAR(7)=VAPPR(T)
  RK=PAR(18)*EXP(-7350./1.986/T)
  FIG=PAR(12)*RK*(P1**0.25-P1E**0.25)
  IF(FIG-3.0) 1,1,2
1  PL=P1/COSH(FIG)
  IF(PL.LT.P1E) PL=P1E
  PU=P1
  IF(PL.GT.PU) PL=PU
  GO TO 3
2  PL=P1E
  PU=P1
3  P2=P1/2.+PAR(10)
  P3=PAR(11)-PAR(10)
  P5=PAR(14)-PAR(8)*P1
  TEST=P5*PAR(15)
  TEST=TEST-PAR(7)
  IF(TEST+0.5E-08) 5,4,4
4  P5=PAR(7)/PAR(15)
  ICASE=1
5  CALL RATE(PU,PL,PAR,RINT,P1,P2,P3,P5)
  R=PAR(6)*SQRT(RK/T*(1.-GA)*(1-GA)*RINT)
  RETURN
END

```

```

C
C
SUBROUTINE RATE(PU,PL,PAR,RINT,P1,P2,P3,P5)
C
C GAUSSION QUADRATURE FORMULA IS USED FOR CALCULATION
C OF THE INTEGRAL IN THE GLOBAL RATE EXPRESSION.
C

```

```

  DIMENSION Z(3),X5(3),PAR(20),X1(3),X2(3),X3(3),GP(3)
  Z(1)=-SQRT(0.6)
  Z(2)=0.0
  Z(3)=-Z(1)
  DO 1 I=1,3
    X1(I)=((PU-PL)*Z(I)+PU+PL)/2.
    X2(I)=P2+0.5*PAR(2)*(X1(I)-P1)
    X3(I)=P3-PAR(3)*(X1(I)-P1)
    X5(I)=P5*PAR(15)-1.5*PAR(4)*(X1(I)-P1)
    TEST=PAR(15)*X5(I)

```

```

C HERE PAR(7) IS PV. CHECK IF INTERNAL VALUES OF (P6+P5)
C EXCEEDS KELVIN VAPOR PRESSURE OF SULFUR.
C

```

```

  PORVP=0.8*PAR(7)

```



```

      IF (TEST.LE.PORVP) GO TO 2
      X5(I)=PORVP/PAR(15)
2     GP(I)=X1(I)*SQRT(X2(I))-X3(I)*(X5(I)**(3./16.))/PAR(5)
      GP(I)=GP(I)/(1.+4.56*X3(I))**2
      IF(GP(I).LT.0.0) GP(I)=0.0
1     CONTINUE
      RINT=5./9.*GP(1)+8./9.*GP(2)+5./9.*GP(3)
      RETURN
      END

```

C
C

```

      FUNCTION EQCTS(T,I)
      GO TO (1,2),I
1     EQCTS=EXP(-4030.2/T+4.825)
      EQCTS=EQCTS**0.75
      EQCTS=EQCTS*6.
      RETURN
2     EQCTS=EXP(12823./T-13.91)
      EQCTS=SQRT(EQCTS)
      RETURN
      END

```

C
C

```

      FUNCTION EQF(X,PAR)
C THIS FUNC. SUBPROGRAM DEFINES THE EQUILIBRIUM CONDITION
      COMMON/PRINT/P10,P20,P30,PRESS
      DIMENSION PAR(20)
      A=(PRESS-PAR(7))/(1.0-0.5*P10*X)
      H2S=P10*(1.-X)*A
      SO2=(P20-0.5*P10*X)*A
      H2O=(P30+P10*X)*A
      EQF=PAR(5)*H2S*SQRT(SO2)-PAR(9)*H2O
      RETURN
      END

```

C
C

```

      FUNCTION DEQFN(X,PAR)
C THIS FUNC. DEFINES THE DERIVATIVE OF 'EQF' W.R.T. X
      COMMON/PRINT/P10,P20,P30,PRESS
      DIMENSION PAR(20)
      A=(PRESS-PAR(7))/(1.0-0.5*P10*X)
      H2S=P10*(1.-X)*A
      SO2=(P20-0.5*P10*X)*A
      H2O=(P30+P10*X)*A
      DA=0.5*P10*(PRESS-PAR(7))/((1.0-0.5*P10*X)**2)
      DHS=-P10*A+P10*(1.-X)*DA
      DSO=-0.5*P10*A+(P20-0.5*P10*X)*DA
      DHO=P10*A+(P30+P10*X)*DA
      DEQFN=PAR(5)*SQRT(SO2)*DHS+PAR(5)*H2S*0.5*DSO/SO2
      #-PAR(9)*DHO
      RETURN
      END

```

C
C

```

      FUNCTION FPB(P1,PAR)
C THIS FUNCTION DEFINES THE PRESSURE FUNCTION OF THE RATE
C EXPRESSION.

```

```

      DIMENSION PAR(20)
      P2=P1+PAR(10)
      P3=PAR(11)-P1
      FPB=P1*SQRT(P2)-P3*PAR(9)/PAR(5)
      FPB=FPB/((1.+4.56*P3)**2)
      RETURN
      END

```

```

C
C

```

```

      FUNCTION VAPPR(T)
      PVLN=-1.61732+0.542412E-02*T+143983.E-02/T-2208580.0
      #/(T**2)
      VAPPR=EXP(PVLN)
      RETURN
      END

```

```

C

```

```

      FUNCTION HEATR(A1,A2,T)
      DH298=-35008.8+A2*24360+A1*24320
      DCP=-4.818121+A2*31.58+A1*42.67
      HEATR=DH298+DCP*(T-298)
      HEATR=-HEATR

```

```

C
C
C
C

```

```

      THIS IS HEAT FOR 2 MOLES OF REACTED H2S. TO GET
      HEAT PER MOLE OF H2S DIVIDE BY 2.

```

```

      HEATR=HEATR/2.
      RETURN
      END

```

APPENDIX G: Physical Properties of Claus Catalytic Process.

G.1 Molecular Diffusivity

To estimate the molecular diffusivity of the species in the Claus process, the *Chapman-Enskog formula* (188) is used. The equation is (for the binary gas mixture 1,2)

$$D_{b,1,2} = \frac{0.001858 T^{3/2} \{ (M_1 + M_2) / (M_1 M_2) \}^{1/2}}{\Pi \sigma_{1,2}^2 \Omega} \quad (G.1)$$

where

M_1, M_2 = molecular weights of the species 1 and 2
 $\sigma_{1,2}, \epsilon_{1,2}$ = constants in the Lennard-Jones potential energy function for the molecular pair 1 and 2; σ is in Å

Ω = collision integral; function of $KB T/\epsilon_{1,2}$

Let species H_2S , SO_2 , H_2O , S_8 and N_2 be denoted by 1 to 5, respectively. Then equation (G.1) for $T=550$ K and $\Pi=1$ atm gives, the binary bulk diffusivities in cm^2/sec as,

$$\begin{aligned} D_{b,1,2} &= 0.302, & D_{b,1,3} &= 0.521, & D_{b,1,4} &= 0.104, & D_{b,1,5} &= 0.419 \\ D_{b,2,1} &= 0.302, & D_{b,2,3} &= 0.406, & D_{b,2,4} &= 0.074, & D_{b,2,5} &= 0.320 \\ D_{b,3,1} &= 0.521, & D_{b,3,2} &= 0.406, & D_{b,3,4} &= 0.131, & D_{b,3,5} &= 0.566 \\ D_{b,4,1} &= 0.104, & D_{b,4,2} &= 0.074, & D_{b,4,3} &= 0.131, & D_{b,4,5} &= 0.146 \end{aligned}$$

G.2 Multicomponent Diffusivity

The effective diffusivity for species j diffusing through the mixture for a chemical reaction is found (82) by,

$$\frac{1}{Db_{jm}} = \frac{\sum (1/Db_{jk}) (y_k - y_j a_k / a_j)}{1 - y_j \sum a_k / a_j} \quad (G.2)$$

Froment (82) recommends using a constant mean composition for the evaluation of multicomponent bulk diffusivity. Equation (G.2) at mean composition of 10% H₂S, 5% SO₂, 20% H₂O, and 65% N₂ gives the multicomponent diffusivities of the Claus species as,

$$Db_{1m}=0.447, \quad Db_{2m}=0.342, \quad Db_{3m}=0.430$$

$$Db_{4m}=0.131, \quad Db_{5m}=0.229$$

G.3 Knudsen Diffusivity

The Knudsen diffusivity of the Claus species are calculated from (189),

$$Dk_j = 9.7(10)^3 \text{ } r_p (M_j)^{1/2} \quad (G.3)$$

where r_p = average radius of a pore
= 8nm from the data of Chuang (46)

then, at T=550 K

$$Dk_1=0.0312, \quad Dk_2=0.0227, \quad Dk_3=0.0429$$

$$Dk_4=0.0125, \quad Dk_5=0.0344$$

G.4 Effective Diffusivity in Catalyst Pores

Equation (2.22) gives the combined diffusivity of the species j within a catalyst pore as,

$$1/D_j = 1/D_{b,j} + 1/D_{k,j} \quad (G.4)$$

Thus substituting for D_b and D_k in equation (G.4) yields,

$$D_1=0.0292 \quad , \quad D_2=0.0213 \quad , \quad D_3=0.0390$$

$$D_4=0.0114 \quad , \quad D_5=0.0299$$

Next, to evaluate the effective diffusivity of the species in the Claus catalyst pellet Wheeler's model is used,

$$De_j = (\epsilon/\tau) D_j \quad (G.5)$$

where ϵ = catalyst porosity

τ = catalyst tortuosity factor

Substituting the recommended values (180,181) of $\epsilon=0.4$ and $\tau=4$ in equation (G.5) gives,

$$De_1=0.00292 \quad , \quad De_2=0.00213 \quad , \quad De_3=0.0039$$

$$De_4=0.00114 \quad , \quad De_5=0.00299$$

G.5 Viscosity of the Gas Mixture

The viscosity of a gaseous mixture is calculated from,

$$\mu_m = \sum \mu_i / \{ 1 + \sum \phi_{ij} (y_j/y_i) \} \quad (G.6)$$

where

$$\phi_{ij} = \frac{\{ 1 + (\mu_i/\mu_j)^{1/2} (M_i/M_j)^{1/4} \}^2}{\sqrt{8} \{ 1 + M_i/M_j \}^{1/2}} \quad (G.7)$$

$$\phi_{ji} = (\mu_j/\mu_i) (M_i/M_j) \phi_{ij} \quad (G.8)$$

The viscosity (poise) of the different species at 550 K (51, °) is,

$$\mu_1=0.000225, \mu_2=0.000238, \mu_3=0.000192, \mu_5=0.000272$$

Thus equation (G.6) and (G.7) yields

$$\begin{aligned} \phi_{12}=1.307, \phi_{21}=0.735, \phi_{13}=0.767, \phi_{31}=1.244 \\ \phi_{15}=0.826, \phi_{51}=1.218, \phi_{23}=0.542, \phi_{32}=1.563 \\ \phi_{25}=0.604, \phi_{52}=1.583, \phi_{35}=1.037, \phi_{53}=0.943 \end{aligned}$$

Next for a Claus gas with an average composition of 10% H₂S, 5% SO₂, 20% H₂O, and 65% N₂, equation (G.5) gives the mixture viscosity as,

$$\mu_m = 0.000225 / [1 + \sum \phi_{ij} y_j / 0.1]$$

Reid, R.C., Prausnitz, J.M., and Sherwood, T.K., "The Properties of Gases and Liquids", 3rd Ed., McGraw-Hill Book Co., 1977.
'and ibid

$$\begin{aligned}
& +0.000238/[1 + \sum \phi_2, y_i/0.05] \\
& +0.000192/[1 + \sum \phi_3, y_i/0.2] \\
& +0.000272/[1 + \sum \phi_4, y_i/0.65] \\
& = 0.000252 \text{ poise}
\end{aligned}$$

G.6 Thermal Conductivity of the Gas Mixture

The thermal conductivity of a gas mixture is usually not a linear function of composition⁸. If the constituents differ in polarity, the mixture conductivity is larger than would be predicted from a mole fraction average. The recommended correlation⁹ is

$$k_g = \sum K_i / \{1 + \sum A_{ij} y_j/y_i\} \quad (\text{G.9})$$

where

K_i = thermal conductivity of the species

$$A_{ij} = a/4 \{1 + \mu_i/\mu_j (M_j/M_i)^{3/4} b\}^2 \quad (\text{G.10})$$

$$a = (1 + S_{ij}/T) / (1 + S_i/T)$$

$$b = \{(1 + S_i/T) / (1 + S_j/T)\}^2$$

$$S_i = 1.5 \cdot T b_i$$

$$S_{ij} = S_{ji} = C(S_i S_j)^{1/2}$$

$$C \approx 1.0$$

The thermal conductivity (cal/cm s K) of the different

ibid

ibid

species at 550 K is,

$$\begin{aligned} K_1 &= 7.24(10)^{-5} & K_2 &= 5.33(10)^{-5} \\ K_3 &= 9.82(10)^{-5} & K_4 &= 9.89(10)^{-5} \end{aligned}$$

Substituting the species viscosities given in section G.5 into equation (G.10) yields,

$$\begin{aligned} A_{11} &= 1.0 & A_{12} &= 1.239 & A_{13} &= 0.059 & A_{14} &= 0.024 \\ A_{21} &= 0.015 & A_{22} &= 1.0 & A_{23} &= 0.723 & A_{24} &= 0.666 \\ A_{31} &= 1.100 & A_{32} &= 1.511 & A_{33} &= 1.0 & A_{34} &= 0.944 \\ A_{41} &= 1.156 & A_{42} &= 1.420 & A_{43} &= 0.957 & A_{44} &= 1.0 \end{aligned}$$

Next, equation (G.9) gives,

$$\begin{aligned} k_g &= 7.24(10)^{-5} / \{1 + \sum A_{1j} y_j / 0.1\} \\ &+ 5.33(10)^{-5} / \{1 + \sum A_{2j} y_j / 0.05\} \\ &+ 9.82(10)^{-5} / \{1 + \sum A_{3j} y_j / 0.2\} \\ &+ 9.89(10)^{-5} / \{1 + \sum A_{4j} y_j / 0.65\} \\ &= 9.41(10)^{-5} \text{ cal/cm s K} \end{aligned}$$

G.7 Heat Transfer Parameters of the Claus Two-Dimensional Model

In chapter 5 it was shown that the effective radial fluid and solid thermal conductivities neglecting radiation and surface contact heat transfer, are given by:

$$\lambda_f = e (k_g + \rho C_p D_r) \quad (G.11)$$

$$\lambda_s = \beta' (1-e) / \{\gamma/k_s + \phi'/k_g\} \quad (G.12)$$

where

$$k_s = 0.00034 \text{ cal/cm}^2 \text{ s K}$$

$$\gamma = 1.0$$

$$\phi' = \phi_2 + (\phi_1 - \phi_2)(e - 0.26)/(0.476 - 0.26)$$

$$\phi_1 = F(k_s/k_g) = F(0.00034/0.0000941) = 0.325$$

$$\phi_2 = F(k_s/k_g) = F(0.00034/0.0000941) = 0.1$$

thus

$$\begin{aligned} \phi' &= 0.1 + (0.325 - 0.1)(0.4 - 0.26)/(0.476 - 0.26) \\ &= 0.246 \end{aligned}$$

$$\begin{aligned} \lambda_s &= (1 - 0.4) / \{2/(3 \times 0.00034) + 0.246/0.0000941\} \\ &= 1.311(10)^{-4} \text{ cal/cm}^2 \text{ s K} \end{aligned}$$

$$\begin{aligned} \lambda_f &= 0.4 \{9.41(10)^{-5} + 0.2216(10)^{-4} \times 7.164 \times 2.4\} \\ &= 1.9(10)^{-4} \text{ cal/cm}^2 \text{ s K} \end{aligned}$$

Next, to evaluate the catalyst phase wall heat transfer coefficient, α_s , Olbrich¹³ suggests that

$$\alpha_s = 2.12 \lambda_s / D_p \quad (G.13)$$

¹¹Michke, R.A., and Smith, J.H., I&Ec Fundam., 1(4):288, 1962

¹²Froment, G.F., and Bischoff, K.B., "Chemical Reactor Analysis and Design", John Wiley & Sons Inc., 1979.

¹³ibid

¹⁴Olbrich, W.E., and Potter, O.E., Chem. Eng. Sci., 27(9), 1723, 1972

$$2.12 * 1.311(10)^{-4} / 0.6 = 4.63(10)^{-4} \text{ cal/cm s K}$$

The gas phase wall heat transfer coefficient, a_f , is given by (63),

$$a_f = a_w \lambda_f / \lambda_e \quad (G.14)$$

where, the effective wall heat transfer coefficient, a_w , is given by Yagi and Kunii (215) as,

$$a_w = k_g / D_p \{0.5 + 0.054 \text{ Pr Re}\} \quad (G.15)$$

Thus for the Claus system where

$$\begin{aligned} \text{Pr} &= C_p \mu_m / k_g \\ &= (7.164 / 28.4) (0.000252) / 9.41(10)^{-5} \\ &= 0.68 \end{aligned}$$

$$\begin{aligned} \text{Re} &= \rho V_s D_p / \mu_m \\ &= (0.000221 * 28.4) (40) (0.6) / 0.000252 \\ &= 60 \end{aligned}$$

a_w is calculated as,

$$\begin{aligned} a_w &= \{9.41(10)^{-5} / 0.6\} \{5.0 + 0.054(60)(0.68)\} \\ &= 1.13(10)^{-3} \text{ cal/cm}^2 \text{ sec K} \end{aligned}$$

According to De Wasch and Froment (64), λ_e (kcal/m h K) is given by,

$$\lambda_e = \lambda_e^0 + 0.0025 Re / \{1 + 46(D_p/2R_w)^2\} \quad (G.16)$$

where

$$\begin{aligned} \lambda_e^0 &= kg\{\epsilon + \beta'(1-\epsilon)/(\phi' + \gamma kg/ks)\} \quad (G.17) \\ &= 9.41(10)^{-5} \{0.4 + (1-0.4)/(0.246 + 2/3(0.0000941/0.00034))\} \\ &= 1.69(10)^{-4} \text{ cal/cm s K} \\ &\equiv 6.084(10)^{-2} \text{ kcal/m h K} \end{aligned}$$

Thus for a Claus converter with diameter of, 30 cm,

$$\begin{aligned} \lambda_e &= 6.084(10)^{-2} + 0.0025(60)/\{1 + 46(0.6/30)^2\} \\ &= 0.208 \text{ kcal/m h K} \\ &= 5.78(10)^{-4} \text{ cal/cm s K} \end{aligned}$$

Then a_f from equation (G.14) is calculated as,

$$\begin{aligned} a_f &= (0.00113)(0.00019) / 0.000578 \\ &= 6.64(10)^{-4} \text{ cal/cm s K} \end{aligned}$$